AVERTISSEMENT

Ce document est le fruit d'un long travail approuvé par le jury de soutenance et mis à disposition de l'ensemble de la communauté universitaire élargie.

Il est soumis à la propriété intellectuelle de l'auteur. Ceci implique une obligation de citation et de référencement lors de l'utilisation de ce document.

D'autre part, toute contrefaçon, plagiat, reproduction illicite encourt une poursuite pénale.

Contact : ddoc-theses-contact@univ-lorraine.fr

LIENS

Code de la Propriété Intellectuelle. articles L 122. 4
Code de la Propriété Intellectuelle. articles L 335.2- L 335.10
http://www.cfcopies.com/V2/leg/leg_droi.php
http://www.culture.gouv.fr/culture/infos-pratiques/droits/protection.htm

Ecole Doctorale SIReNa
(Sciences et Ingénierie des Ressources Naturelles)

Thèse

Présentée et soutenue publiquement pour l'obtention du titre de

DOCTEUR DE L'UNIVERSITE DE LORRAINE

Mention : « Ecotoxicologie, Biodiversité, Ecosystèmes »

par **Nicolas GROSJEAN**

Etude des gènes de réponse aux terres rares chez des organismes modèles

Study of rare earth element responsive genes in model organisms

Soutenance publique le 26 juin 2019

Membres du jury :
Rapporteurs :

Mme Catherine CURIE	DR, BPMP, CNRS, Montpellier - France
M. Markus TAMÁS	Prof., University of Gothenburg, Gothenburg - Sweden

Examinateurs :

M. Damien BLAUDEZ	MCF, LIEC, Université de Lorraine, Nancy - France ***(Co-encadrant)***
M. Michel CHALOT	Prof., LCE, Université de Bourgogne Franche-Comté, Montbéliard - France
Mme Elisabeth Maria GROSS	Prof., LIEC, Université de Lorraine, Metz - France ***(Directrice de thèse)***
Mme Marie LE JEAN	MCF, LIEC, Université de Lorraine, Metz - France ***(Co-directrice de thèse)***
M. Adam SCHIKORA	Priv.-Doz., Julius Kühn Institute, Braunschweig – Germany
M. Sébastien THOMINE	DR, I2BC, CNRS, Gif-sur-Yvette - France

Laboratoire Interdisciplinaire des Environnements Continentaux (LIEC)
UMR 7360 CNRS – Université de Lorraine

Remerciements

Travailler 3 années sur un projet est l'occasion de rencontrer de nombreuses personnes qui rendent tous ce voyage beaucoup plus agréable et enrichissant ;

My first thanks will go to Dr. **Catherine Curie** and Pr. **Markus Tamàs** for reviewing this PhD work, and to the three examinators Dr. **Sébastien Thomine**, Dr. **Adam Schikora** and Pr. **Michel Chalot** for taking part in the jury. Merci plus particulièrement à ces deux derniers pour vos encouragements et pour avoir participé à l'évolution de ce travail de thèse au cours des différents comités de thèses !

Je tiens à remercier le LabEx Ressources 21 qui a permis d'effectuer cette thèse dont je suis particulièrement fier. Merci également à la direction du LIEC, nouvelle et ancienne (**Laure Giamberini**, **Christian Mustin** et **Fabien Thomas**), pour m'avoir permis d'effectuer mes travaux dans les locaux du LIEC principalement à Aiguillettes, et quelques visites à Bridoux. Mes remerciements vont également au GISFI. Un grand merci à **Nadia Crini** pour toutes ces analyses ICP réalisées, dont les résultats ont permis de développer nombre de nos hypothèses !

Mes plus grands remerciements et ma reconnaissance vont à mes encadrants de thèse ; **Elisabeth Gross**, mais surtout **Marie Le Jean** et **Damien Blaudez**. Vous m'avez fait confiance depuis le 1er Octobre 2015 quand cette thèse a débuté, et un tout nouveau monde était à découvrir. Un monde dans lequel ces terres rares pas si rares nous ont tout de même forcées à nous creuser sérieusement la tête. **Marie** et **Damien**, votre investissement dans cette thèse a été incroyable du premier au dernier jour, je vous en remercie. J'ai énormément appris et évolué à tous niveaux grâce à vous. C'est gratifiant de se sentir épaulé, de pouvoir avancer en sachant qu'on me faisait confiance, et surtout de se sentir chercheur et non pas simple étudiant. Derrière toutes ces réunions, questionnements, indécisions, doutes etc. du point de vue professionnel, j'ai pu rencontrer deux personnes assez différentes mais qui se complètent/balancent plutôt bien. Vous êtes un mélange explosif de curiosité, de dynamisme, d'implication, de blagues (Damien, il faudra s'améliorer un peu), d'énergie, d'envie et de bonne humeur même le matin au café à l'hôtel avant une conf. J'aurais toujours comme souvenir ces voyages en congrès où on a pu discuter de choses et d'autres, visité de sacré belles villes, et appris qu'il fallait faire la gueule dans les pays de l'est. Malgré ce jour de Mars 2017 où le ciel m'est tombé sur la tête (ou plutôt l'ordi s'est fait la malle), j'espère avoir atteint les objectifs que vous aviez imaginé, et que ce travail fait honneur à l'investissement et la confiance que vous m'avez donné. Passer trois ans et demi avec de vraies personnes humaines et non pas de simples chefs fait la différence. Merci pour votre disponibilité, merci pour tout, merci !

Christine et **Cécile**, sans qui nous serions tous perdus, vous êtes les piliers du site Aiguillettes ! **Christine** tu es la maitresse de ces lieux, où l'emplacement du moindre cône est référencés dans un coin de ta tête. J'ai énormément apprécié ces différentes discussions, blagues, et toute cette bonne humeur quotidienne. **Cécile**, tu es indispensable de par ton efficacité et ta rapidité d'exécution, mais surtout pour ta gentillesse, ton sourire et tes petites attentions constantes ! **Thierry**, la référence cycliste, tu es la bonne humeur et le bon humour du laboratoire. Merci pour ton don de nous faire sourire. Merci à tous les autres membres du LIEC Aiguillettes sans exception ; **Aurélie** (couronnée reine pâtissière 2018 !), **Asfaw**, **David**, **Patrick**, **Anne**, **Sylvie**, **Coralie**, **Géraldine**, **Alexis**, **Hervé** et notamment à **Emmanuelle** et **Didier** avec qui j'ai pu collaborer ! Vous êtes tous responsables de la bonne humeur au labo !

Sans une bonne ambiance, on ne travaille pas aussi bien et on peut se perdre rapidement. Alors un vrai grand merci à tous les plus « jeunes » que j'ai pu rencontrer pendant ces différentes années, chacun avec sa personnalité et son petit grain particulier ! **Céline Gaullier**, tu m'as fait rire au possible durant ces 3+ années, je n'aurais pu espérer une meilleure collègue de bureau ! L'avocatier en est la preuve, la bonne humeur est un bon engrais. **Roro** (Romain Présent) Merci ! Malgré ton cœur d'alsacien, tu es un sacré monsieur et un excellent ami. Certes coriace, tu es toujours plein de joie de vivre et toujours prêt à rire, discuter et aller prendre un bon bol d'air (ou une bonne bière on ne va pas se le cacher). **Kévin** (guitariste adepte des joggings et de boutades en tout genre), **Yuyu** (**yum-yum** you are that incredible mix of friendship, craziness, happiness and lust for living life to the fullest. Never change, only good things can happen), **Andrea** (Porco dio! One of the smartest man I met who doesn't take himself too seriously), **Emna** (6 mois d'une Californienne de Sfax qui crée ses tuto beauté), **Maxime** (ce grand bonhomme très cultivé et amical qui a grimpé quelques étages de plus pour nous rejoindre. C'est toujours un plaisir de passer du temps avec toi), **Axel** (Crossfitter pro en devenir, et surtout copain de rando pour les périples monoprix-labo journaliers), **Justine** (pour ces battle de dance et ces innovations gastronomiques de pizzaiolo), **Renaud** (un Charmoisien extrêmement sympathique, fier de sa région et pas non plus le dernier pour aller prendre un verre), **Florian** (hopla, mon binôme de cuvée thèse 2015, l'alsacien qui a le cœur sur la main mais qui devrait faire (beaucoup) plus confiance en ses capacités), **Clotilde** (notre Suédoise qui garde toujours le sourire), **Camille**, **Elise** et **Fatima** (pour ton addiction aux mi-cho-ko). Mais aussi aux différents stagiaires que j'ai eu l'occasion de co-

encadrer, **Nicolas**, **Felix** et surtout **Jordan** le monsieur à la blague facile, toi qui ne voulait apparemment pas quitter le LIEC, mais avec qui j'ai beaucoup ri pendant ces nombreux mois ! Merci pour les pauses dans le bureau qui permettent de se vider la tête dans les périodes de rush ! Le trio du LSE **Anne**, **Clémentine**, et **Séverine** vous avez cette folie chacune à votre niveau, et ça fait du bien d'avoir pu rire avec vous.

A tous les « anciens » qui sont partis au fur et à mesure, mais avec qui je garderai de (très) bon souvenirs ; **Charlotte** (ma grande demi-sœur du même papa haha ! Merci de m'avoir guidé dans mes premiers pas au LIEC pour mon M1, tu es une fine scientifique qui carbure à cent à l'heure), **Quentin** (mon compatriote végétarien, fin statisticien et adepte de bonnes blagues), **Amélia** (l'expatriée à Cologne, toujours de bon conseil et de bonne humeur), et **Johanne** (le chameau québécois qui sait faire rire et qui sait écouter). J'ai adoré tous ces rires, compétitions culinaires, verres et échanges que l'on a pu avoir ensemble.

Un énorme clin d'oeil à **Dafné** et surtout **Anne Vicente** pour notre aventure Pint of Science qui a vu le jour en Lorraine en 2017. C'était pour moi un projet qui me tenait à cœur, et de le faire avec vous a été un véritable plaisir. Le résultat était encore plus gratifiant que je ne l'imaginais !

Une pensée très particulière pour **Fadi Hajj**, un collègue, un ami. Merci pour tout ce que tu représentais et représente maintenant pour moi. Ton état d'esprit sera toujours dans un coin de ma tête, et je garderai ce souvenir de toi à jamais.

Les amis sont aussi ceux qui permettent de déconnecter du train-train quotidien. **Julie**, **Lucie W**., **Lucie L**., **Floriane, Arthur**, **Guillaume**, **Pablo**, et **Camille,** merci à vous tous pour toujours être là (depuis plus ou moins 10 ans !) sans concession et pour nos réunions toujours à rigoler. Vous êtes les principaux acteurs qui m'ont permis de terminer avec cette motivation et cette bonne humeur. Je vous dois énormément pour votre amitié sans limite. **Anaïs** et **Marie**, vous m'avez fait rire depuis que je suis arrivé à la fac jusqu'à mon arrivée en thèse, merci de continuer d'être aussi attachantes. **Andrew** le français de cœur, je te serai éternellement reconnaissant pour tout le soutien, l'amitié et la confiance en moi que tu m'as apporté. Je suis incroyablement chanceux d'avoir rencontré un ami comme toi.

Charline, **Charles**, et surtout **Maman**, cette thèse est pour vous. Un simple Merci semble peu comparé à tout ce que vous avez et ce que vous continuez à faire pour moi. **Charline** tu es une perle et tu aides et donnes sans rien n'attendre en retour. Je t'admire pour tout ce que tu entreprends et réussi, je ne serais pas capable d'en faire la moitié. **Charles,** mon frangin colocataire qui était prêt à me cuire des pâtes quand je rentrais tard le soir, je sais que tu as l'envie de réussir, que tu vas réussir et faire ce que tu veux. Derrière ta pseudo nonchalance se cache un jeune homme incroyable avec le cœur sur la main. **Maman** tous ces sacrifices et tout ce que tu as porté sur tes épaules m'ont permis de réaliser ce que j'ai toujours voulu atteindre. Tu es la femme la plus forte, dévouée, altruiste et aimante que je connaisse. Merci d'être là quoi qu'il arrive, et j'espère que ce petit succès te rend fière et heureuse. J'ai beaucoup appris de vous trois et je vous admire vraiment. Ce travail est autant mon accomplissement que le vôtre.

List of abbreviations

ANOVA	Analysis of variance
BF	Bioaccumulation factor
BNS	Basal nutrient solution
BP	Biological pathway
CAT	Catalase
CC	Cellular component
CDF	Cation diffusion facilitator
CME	Clathrin mediated endocytosis
CNGCs	Cyclic nucleotide-gated channels
CPZ	Chlorpromazine
DEG	Differentially expressed gene
DEP	Differentially expressed protein
DHS	Dihydrosphingosines
DW	Dry weight
EC_{10}	10% effect concentration
EC_{50}	50% effect concentration
ESCRT	Endosomal sorting complexes required for transport
EXAFS	Extended X-ray absorption fine structure spectrometry
FC	Fold change
FCR	Ferric-chelate reductase
GARP	Golgi-associated retrograde protein
GM	Germination medium
GO	Gene ontology
GPx	Glutathione peroxidase
GSH	Glutathione
GSL	Glycosphingolipid
GST	Glutathione-S-transferase
HIPP	Heavy metal-associated isoprenylated plant proteins
HREEs	Heavy rare earth elements
IAC	Ion-adsorption clay
ICP-AES	Inductively coupled plasma atomic emission spectroscopy
ICP-MS	Inductively coupled plasma mass spectrometry
IPC	Inositol phosphorylceramide
ITS	Internal transcribed spacer
K.O.	Knock out
LCB	Long chain base
LD_{50}	Half-lethal doses
LREEs	Light rare earth elements
MAPK	Mitogen-activated protein kinase
MDA	Malondialdehyde
MDH	Methanol dehydrogenase
MF	Molecular function
MIPC	Mannosyl-inositol phosphorylceramide
MIPS	Munich Information Center for Protein Sequences
MRI	Magnetic resonance imaging
MT	Metallothioneins
MVB	Multi vesicular body
NA	Nicotianamine
NBI	Nitrogen balance index
NRAMP	Natural resistance-associated macrophage proteins
OMIM	Online Mendelian Inheritance in Man
ORF	Open reading frame
PC	Phytochelatins
PCA	Principal component analysis
PGP	Plant growth promoting
PHC	Phytoceramides
PHS	Phytosphingosines
POD	Peroxidase
ppm	parts per million
PVC	Prevacuolar compartment
REEs	Rare earth elements
REO	Rare earth oxides
ROS	Reactive oxygen species
SNARE	Soluble N-ethylmaleimide-sensitive factor Attachment Protein Receptor
SOD	Superoxide dismutase
TAC	Total antioxidant capacity
TCE	Technology-critical element
TF	Translocation factor
TPCK	Tosyl phenylalanyl chloromethyl ketone
US EPA	United States environmental protection agency
VMA	Vacuolar membrane atpase
YNB	Yeast nitrogen base
YPD - YPG	Yeast peptone dextrose - galactose
ZIP	Zn-regulated transporter (ZRT) Fe-regulated transporter (IRT)-like proteins
ZRT	Zn-regulated transporter

Table of Contents

State of the art **1**

I. The Rare Earth Elements (REEs) **3**

I.1. What are the Rare Earth Elements? 3

I.2. Are they actually Rare? 5

I.3. REE concentrations in soils 7

I.4. What parameters influence their bioavailability? 12

II. REE demand, production, use and recyclability **13**

II.1. Demand and Production 13

II.2. Uses 16

II.2.a. REE usage in technology 16

II.2.b. REE usage in natural environments and agriculture 18

II.3. Recyclability 21

II.4. Bibliometric analysis on REE effects on biota 23

III. Transfer and effects of REEs on organisms **25**

III.1. Introduction 25

III.1.a. REE transfer to organisms 25

III.1.b. REE interaction with bio-molecules 27

III.2. REEs and microorganisms 28

III.2.a. REE accumulation by microorganisms 29

III.2.b. Positive effects 30

III.2.c. Toxic effects 32

III.3. REEs and plants 33

III.3.a. REE-content in non-accumulating plants 33

III.3.b. REE-hyperaccumulating plants 34

III.3.c. Use of REEs for Growth promotion 37

III.3.d. Toxicity of REEs in plant 38

IV. REE effects in animals and human health **40**

V. The use of model organisms to study REE toxicity **44**

V.1. Metal transport in yeast and plant cells 45

V.2. Modes of action of metal toxicity 46

V.3. How organisms cope with toxic metals 48

V.4. The usefulness of ‘omic’ analyses to study metal homeostasis 49

Context of the thesis **51**

Objectives **53**

Part I – The use of genome-wide analyses in the eukaryotic model *Saccharomyces cerevisiae* to identify key mechanisms of REE toxicity and tolerance in eukaryotic cells **57**

Introduction **59**

Chapter I.1 – Global deletome profile of *Saccharomyces cerevisiae* exposed to the technology-critical element yttrium (**published**) **63**

Chapter I.2 – A genome-wide deletion mutant screen identifies specific pathways affected by light and heavy lanthanides in *Saccharomyces cerevisiae* **79**

Chapter I.3 – Omic approaches reveal response and uptake discrepancies between light and heavy rare earth elements in *Saccharomyces cerevisiae* **115**

Part II – Investigation of REE toxicity, resistance and transfer mechanisms in plants **141**
Introduction **143**
Chapter II.1 - Transcriptomic identification of rare earth element responsive genes in *Arabidopsis thaliana*: the root architecture and ion homeostasis at stake **149**
Chapter II.2 - Heavy for the shoots: rare earth element accumulation and fractionation are conserved traits in the *Phytolacca* genus **171**
Chapter II.3 - Searching for new hardy ferns accumulating rare earth elements **189**
Discussions, conclusions and perspectives **205**
Part I - The use of genome-wide analyses in the eukaryotic model *Saccharomyces cerevisiae* to identify key mechanisms of REE toxicity and tolerance in eukaryotic cells 207
Part II - Investigation of the REE toxicity, resistance and transfer mechanisms in plants, being more complex eukaryotes 211
General discussion 219
Outcomes of the thesis 225
General conclusion **230**
References **231**
Extended Abstract (Fr) **243**

State of the art

I. The Rare Earth Elements (REEs)

I.1. What are the Rare Earth Elements?

The group of the REEs gather 17 elements with close chemical and physical characteristics. This set of REEs includes Yttrium (Y), Scandium (Sc) and the 15 so-called lanthanides (Ln) (Figure 1). Despite not being part of the Ln, Y and Sc are also considered as REEs since they share the same chemical properties and are often found in the same ores and rocks as Ln (Cotton, 2006).

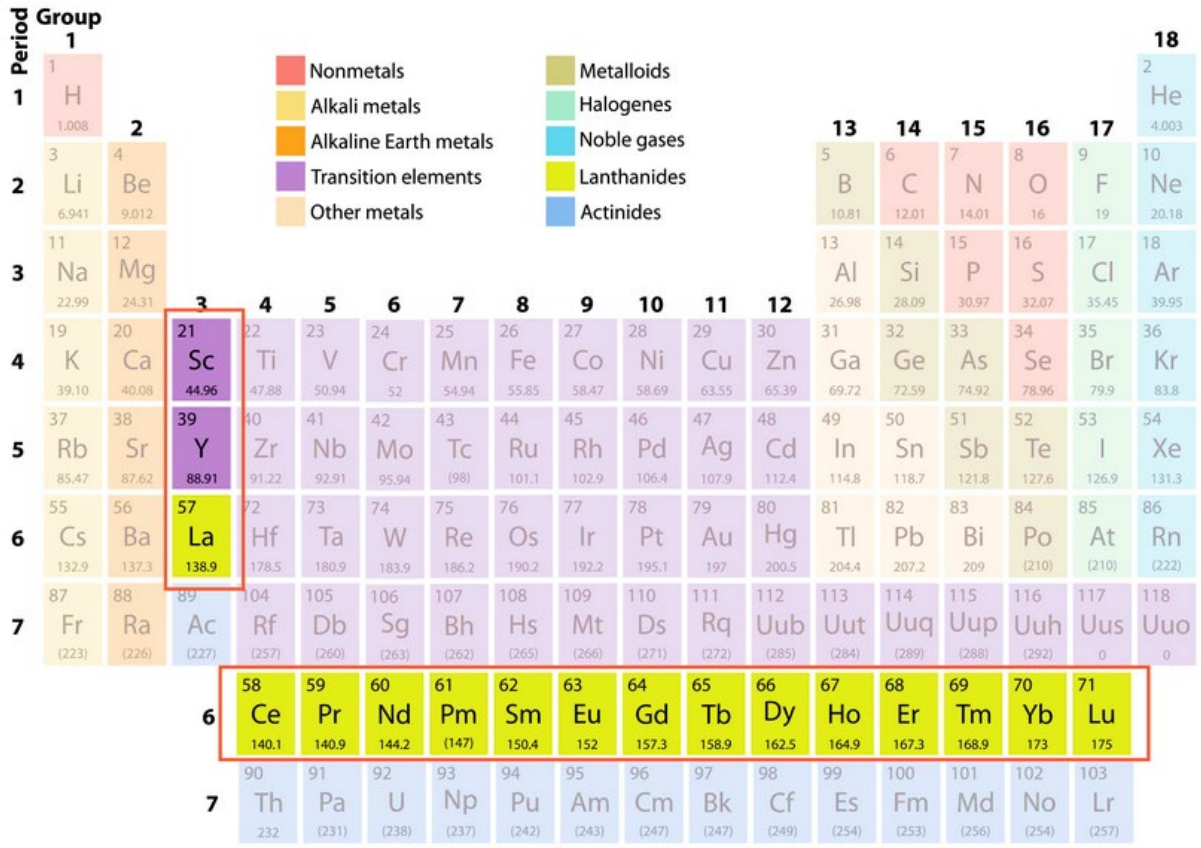

Figure 1: Periodic table of elements with the rare earth elements highlighted by the red boxes.
From http://www.rareelementresources.com/rare-earth-elements

The first REEs discovered and described were Y (ytterbite or dadolinite minerals) and Cerium (Ce) (cerite mineral), in 1794 and 1903 respectively (Figure 2). Afterwards, it was found that these minerals were actually made of several elements as shown in Figure 2. The last REE described, Promethium (Pm) in 1947, is extremely rare on Earth and all of its isotopes are radioactive.

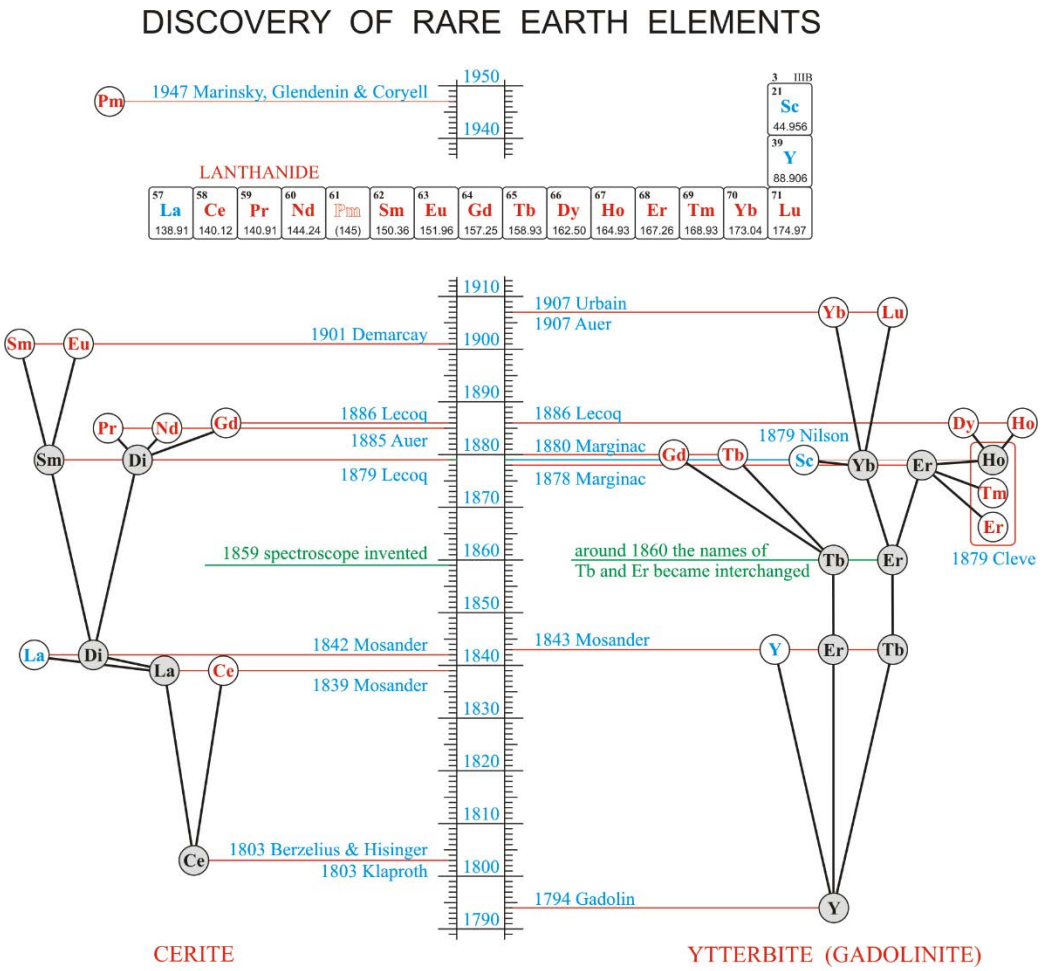

Figure 2: Discovery of the REEs, 150 years of rare earths history. The complex compositions of the two starting minerals cerite and gadolinite (ytterbite) are revealed in the flow chart of discoveries of the elements. Elements in red or blue are the actual known pure elements. In black are the elements previously thought to be in pure form. (Di = didymium). From https://www.periodni.com/history_of_rare_earth_elements.html

Among the 15 Ln, two to three groups, relying on their ionic radius, can be distinguished. The light REEs (LREEs) gather Lanthanum (La), Cerium (Ce), Praseodymium (Pr), Neodymium (Nd), Promethium (Pm), Samarium (Sm), and Europium (Eu), while the heavy REEs (HREEs) gather Gadolinium (Gd), Terbium (Tb), Dysprosium (Dy), Holmium (Ho), Erbium (Er), Thulium (Tm), Ytterbium (Yb), and Lutetium (Lu), but also the non-Ln element Y. The Ln are very close in term of physical and chemical properties. Indeed, the series of 15 Ln are characterized by the so-called Ln contraction (Cotton, 2006). This consists of a decrease of the ionic radius, ranging from 1.22 Å for La to 0.99 Å for Lu, with the increase of the atomic number, from 57 for La, to 71 for Lu (Table 1). Y is associated to the HREEs because its chemical reactivity is similar to that of Tb and Dy (Cotton, 2006). The ionic radius of Y is also close to that of Dy and Ho, and thus, Y can be ranked between these two, regarding the ionic

radius. However, there is no strict definition of LREEs and HREEs, and is not consistent among different authors (Zepf, 2013).

Most of the REEs are mainly found at a trivalent oxidation state in aqueous solution, although some of the REEs can be found at a divalent or tetravalent state (Table 1). Furthermore, they prefer anionic ligands with highly electronegative donor atoms, such as O or F (Cotton, 2006).

Table 1: Properties of rare earth elements. Modified from (Hirano and Suzuki, 1996).

REE	Atomic number	Electron configuration	Valence	Radius of REE^{3+} (Å)	Clarke number
Sc	21	$3d^1 4s^2$	+3	0.83	5×10^{-4}
Y	39	$4d^1 5s^2$	+3	1.06	3×10^{-3}
La	57	$5d^1 6s^2$	+3	1.22	1.8×10^{-3}
Ce	58	$4f^2 6s^2$	+3, +4	1.18	4.5×10^{-3}
Pr	59	$4f^3 6s^2$	+3, +4	1.16	5×10^{-4}
Nd	60	$4f^4 6s^2$	+3, +5	1.15	2.2×10^{-3}
Pm	61	$4f^5 6s^2$	+3	-	-
Sm	62	$4f^6 6s^2$	+2, +3	1.13	6×10^{-4}
Eu	63	$4f^7 6s^2$	+2, +3	1.13	1×10^{-4}
Gd	64	$4f^7 5d^1 6s^2$	+3	1.11	6×10^{-4}
Tb	65	$4f^9 6s^2$	+3, +4	1.09	8×10^{-5}
Dy	66	$4f^{10} 6s^2$	+3, +4	1.07	4×10^{-4}
Ho	67	$4f^{11} 6s^2$	+3	1.05	1×10^{-4}
Er	68	$4f^{12} 6s^2$	+3	1.04	2×10^{-4}
Tm	69	$4f^{13} 6s^2$	+2, +3	1.04	2×10^{-5}
Yb	70	$4f^{14} 6s^2$	+2, +3	1.00	2.5×10^{-4}
Lu	71	$4f^{14} 5d^1 6s^2$	+3	0.99	7×10^{-5}

I.2. Are they actually Rare?

Unlike their name, the rare earth elements are not so rare in the Earth's crust and in soils. The term 'rare earth' comes from chemists of the metal industry from the 1940s because of the inability to extract these elements in pure form from 'earth', which meant ores back in the time. Furthermore, the REEs were not abundant enough for an economical and profitable mining operation. The lightest Ln are the most abundant in the Earth's crust compared to the heaviest. Additionally, the REEs follow the Oddo-Harkins rule, meaning that elements with even atomic number are more abundant than elements with odd atomic number, because of a higher stability of their nuclei (Cotton, 2006).

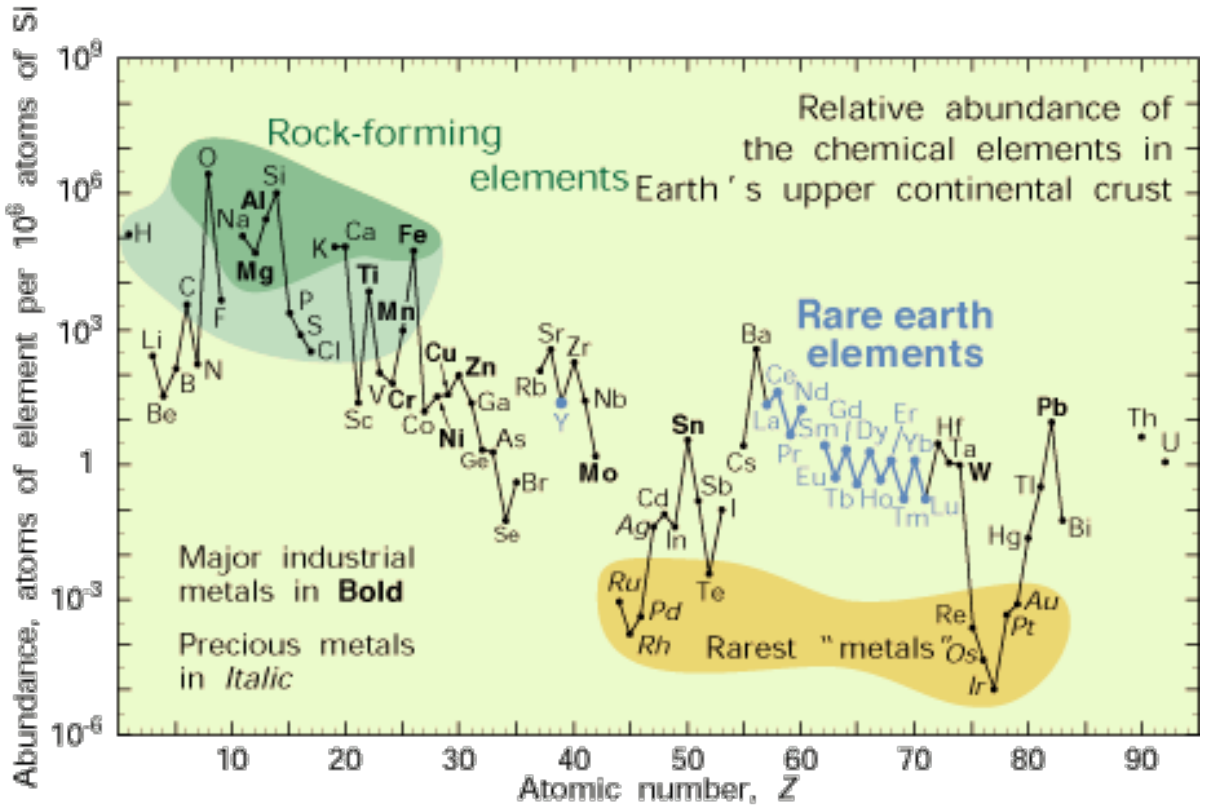

Figure 3: Abundance of chemical elements in the upper layer of the continental crust as a function of the atomic number. Many elements are grouped into categories: (i) Rock-forming elements (major elements in dark green, minor in light green); (ii) Rare Earth (Lanthanides La-Lu and Y, in blue); (iii) Major industrial metals (total production> 3x107 kg / year, in bold); (iv) precious metals (italic); and (v) the nine rarest metals - the six elements of the platinum group (Platinum group metals) plus Au, Re and Te (in orange). From https://pubs.usgs.gov/fs/2002/fs087-02/

The most abundant REEs in the Earth's crust are Ce, Nd, La, and Y, with a concentration of 66, 40, 35, and 31 ppm respectively. To compare with other well-known elements, their content in the Earth's crust are as high as of Cr, Cu, Ni, Mo, Sn, or Pb (Figure 3). Additionally, Ce is the 25th most abundant element in the Earth's crust. Although Tm and Lu are the least abundant of the REEs in the Earth's crust, they are 200 times more abundant than Au and other elements of the platinum group, and more abundant than Cd, Hg, and Se (Figure 3). REEs occur usually in ore minerals such as monazites, bastnaesites, xenotimes, and lateritic ion-adsorption clays (IAC). Rocks bearing these minerals are the most exploited REE-containing ores, for instance pegmatites, granites and related metamorphic igneous rocks.

Monazite (phosphates) and bastnaesite (fluorocarbonates or hydroxides) contain essentially LREEs, but also Y in the case of bastnaesite. These are two different minerals, with general formula $CePO_4$, and $Ce(CO_3)F$, respectively, where Ce can be replaced by other LREEs (Voncken, 2016).

Regarding HREEs, they can be extracted from xenotimes and lateritic ion-adsorption clays. Xenotime with YPO_4 as a general formula, contains generally Y but also appreciable amounts of HREEs (Voncken, 2016). Lateritic IAC from south China (Jiangxi province) are the main source of HREEs, where 90-60% of the REEs are absorbed on clay minerals, like kaolinite [$Al_2Si_2O_5(OH)_4$], halloysite [$Al(OH)_6Si_2O_5(OH)_3$] or muscovite [$KAl_2(AlSi_3O_{10})(OH)_2$]. Despite the low content in REEs, these materials are economically interesting because of the easy extraction of REEs with weak acids (Voßenkaul *et al.*, 2013).

I.3. REE concentrations in soils

The concentration of REEs in soils is usually dependent on the parent material underneath, but also on different parameters such as clay mineral, and organic matter contents (Tyler, 2004b). Therefore, their concentration can vary between different locations (Table 2) (Ramos *et al.*, 2016). Nevertheless, the overall relative soil concentration for the different REEs is usually consistent with their concentration in the Earth's crust, with more LREEs than HREEs, and still following the Oddo-Harkins rule (Table 2). As shown in Table 2, concentrations can vary from 34 ppm in Denmark, to more than 200 ppm in Bhutan, Croatia, Cape Verde, and Uganda (Ramos *et al.*, 2016). One hundred and nineteen French soils analyzed in a study showed a mean concentration of 160 ppm (Table 2) (Ramos *et al.*, 2016). Overall, out of the 2814 analyses of soils collected from 33 different countries, the relative mean REE concentration is of 155 ppm.

Table 2: Concentrations of REE (in ppm) reported for soils worldwide. Adapted from (Silvio J Ramos et al., 2016)

Country	Method	n	REE	La	Ce	Pr
Albania	HNO3, HF, HClO4, alkaline fusion/ICP-MS	3	138.5	19–31 (25)	38–59 (52)	4.4–7.3 (5.9)
Germany	HNO3, HF, HClO4, alkaline fusion/ICP-MS, ICP-AES	79	118.0	3.7–57 (23)	7.4–115 (48)	0.8–13 (5.5)
Austria	HNO3, HF, HClO4, alkaline fusion/ICP-MS	18	154.3	4.0–56 (29)	8.7–106 (59)	0.9–13 (7.0)
Australia	HCl, HNO3/ICP-MS	9	109.8	2.7–24 (15)	21–120 (60)	0.8–6.8 (4.1)
Belgium	HNO3, HF, HClO4, alkaline	5	164.3	29–34 (31)	62–70 (64)	6.5–7.9 (7.3)
Brazil	HCl,HNO3,HF/ICP-MS, INAA	79	159.9	3.0–62 (20)	15–286 (82)	–
Bhutan	INAA	6	214.2	41–60 (51)	82–133 (106)	–
Cape Verde	INAA	63	346.2	39–413 (74)	76–685 (156)	–
China	HNO3, HF, HClO4/ICP-MS, ICP-AES, INAA	852	190.2	8.0–57 (30)	18–122 (67)	1.7–12 (6.6)
Croatia	HNO3, HF, HClO4, alkaline fusion/ICP-MS	13	228.6	27–52 (43)	55–128 (91)	6.5–12 (10)
Denmark	HNO3, HF, HClO4, alkaline fusion/ICP-MS	5	34.4	2.6–12 (6.6)	5–23 (13)	0.5–2.7 (1.5)
Slovakia	HNO3, HF, HClO4, alkaline fusion/ICP-MS	15	160.1	6.5–41 (31)	13–84 (63)	1.5–9.6 (7.1)
Spain	HNO3, HF, HClO4, alkaline fusion/ICP-MS	100	165.6	5.3–128 (33)	11–246 (63)	1.3–32 (7.7)
United States	HNO3, HF, HClO/INAA, RNAA, ICP-MS	2	183.1	7.5–176 (33)	15–350 (67)	7.0–8.4 (7.7)
Estonia	HNO3, HF, HClO4, alkaline fusion/ICP-MS	11	131.8	5.5–37 (26)	9.6–71 (50)	1.2–9.7 (6.1)
Finland	HNO3, HF, HClO4, Alkaline Fusion/ICP-MS, ICP-AES	319	77.9	4.8–45 (15)	8.5–90 (28)	1.0–10 (3.3)
France	HNO3, HF, HClO4, alkaline fusion/ICP-MS	119	159.7	2.6–66 (31)	5.5–159 (63)	0.51–4.4 (7.3)
Greece	HNO3, HF, HClO4, alkaline fusion/ICP-MS	41	155.8	13–64 (29)	23–102 (57)	2.9–14 (6.8)
Netherlands	HNO3, HF, HClO4, alkaline fusion/ICP-MS	8	69.5	5.6–22 (13)	12–43 (27)	1.3–5.1 (3.1)
Hungary	HNO3, HF, HClO4, alkaline fusion/ICP-MS	14	142.4	7.5–42 (27)	15–87 (55)	1.7–10 (6.4)
Ireland	HNO3, HF, HClO4, alkaline fusion/ICP-MS	11	102.5	12–36 (20)	23–78 (39)	2.5–9.1 (4.6)
Italy	HNO3, HF, HClO4, alkaline fusion/ICP-MS	51	194.1	6.9–143 (40)	14–267 (78)	1.3–29 (8.8)
Japan	HNO3, HF, HClO4/ICP-MS	653	132.1	0.9–120 (19)	1.1–150 (43)	0.2–31 (4.6)
Latvia	HNO3, HF, HClO4, alkaline fusion/ICP-MS	7	108.7	11–31 (21)	21–67 (44)	2.3–8.1 (4.9)
Lithuania	HNO3, HF, HClO4, alkaline fusion/ICP-MS	16	90.8	7.9–28 (18)	15–59 (36)	1.7–7.0 (4.1)
Norway	HNO3, HF, HClO4, alkaline fusion/ICP-MS	58	123.0	2.9–101 (21)	5.7–253 (48)	0.7–23 (5.2)
Poland	HNO3, HF, HClO4, alkaline fusion/ICP-MS, XRF	64	88.8	2.7–35 (13)	5.5–72 (27)	0.7–8.0 (3.0)
Portugal	HNO3, HF, HClO4, alkaline fusion/ICP-MS	19	186.1	19–74 (38)	38–151 (77)	4.7–18 (9.0)
UK	HNO3, HF, HClO4, alkaline fusion/ICP-MS	60	126.3	1.1–103 (23)	2.5–206 (48)	0.3–30 (5.6)
Czech Republic	HNO3, HF, HClO4, alkaline fusion/ICP-MS	10	144.3	15–35 (26)	32–80 (57)	3.3–8.6 (6.3)
Sweden	HNO3, HF, HClO4, alkaline fusion/ICP-MS	85	105.6	1.4–34 (17)	2.1–83 (37)	0.4–14 (4.2)
Switzerland	HNO3, HF, HClO4, alkaline fusion/ICP-MS	10	134.6	1.7–85 (27)	3.2–117 (50)	0.4–16 (6.0)
Uganda	Alkaline fusion	9	484.0	77–134 (123)	216–291 (273)	–

Table 2: (Continued)

Country	Nd	Sm	Eu	Gd	Tb	Dy	Ho
Albania	18–27 (22)	3.6–5.3 (4.5)	0.8–1.0 (0.9)	3.6–5.3 (4.3)	0.6–0.8 (0.7)	3.8–4.8 (4.2)	0.7–0.9 (0.8)
Germany	3.2–55 (20)	0.5–8.7 (3.8)	0.1–1.6 (0.7)	0.5–7.8 (3.8)	0.1–1.1 (0.6)	0.5–6.0 (3.1)	0.1–1.2 (0.6)
Austria	3.5–50 (26)	0.7–10 (5.2)	0.1–2.0 (1.0)	0.8–9.5 (4.8)	0.08–1.3 (0.71)	0.6–7.4 (3.9)	0.1–1.3 (0.8)
Australia	2.8–24 (15)	0.4–4.6 (2.8)	0.1–1.6 (0.6)	0.6–4.3 (2.6)	0.1–0.7 (0.48)	0.3–3.2 (2.1)	0.1–0.4 (0.3)
Belgium	23–31 (28)	4.3–5.7 (5.2)	0.8–1.2 (1.0)	3.9–5.6 (5.1)	0.6–0.9 (0.8)	3.6–5.0 (4.5)	0.7–1.2 (0.9)
Brazil	6.0–116 (25)	0.4–6.7 (3.5)	–	–	0.2–1.2 (0.7)	–	–
Bhutan	31–44 (37)	6.4–12 (8.4)	0.9–3.2 (1.4)	–	0.8–1.2 (1.0)	4.2–7.8 (5.4)	–
Cape Verde	44–211 (68)	7.5–25 (11)	2.2–7.5 (3.5)	–	0.8–2.1 (1.3)	4.5–13 (7.1)	–
China	6.2–41 (26)	1.2–7.8 (5.2)	0.2–2.4 (1.2)	1.6–7.1 (5.0)	0.3–1.2 (0.7)	2.0–6.3 (3.9)	0.3–1.2 (0.8)
Croatia	24–45 (39)	5.0–8.9 (7.6)	1.0–1.8 (1.5)	4.8–8.5 (7.2)	0.7–1.3 (1.0)	3.8–7.0 (6.0)	0.8–1.4 (1.2)
Denmark	2.0–10 (5.5)	0.4–1.8 (1.0)	0.1–0.4 (0.2)	0.5–1.9 (1.1)	0.1–0.3 (0.2)	0.5–2.2 (1.1)	0.1–0.4 (0.2)
Slovakia	5.6–36 (27)	1.0–7.0 (5.0)	0.2–1.3 (0.9)	0.9–6.6 (4.7)	0.2–1.1 (0.73)	1.1–5.9 (4.2)	0.2–1.2 (0.9)
Spain	4.6–132 (28)	0.9–23 (5.9)	0.2–7.0 (1.1)	0.9–24 (5.4)	0.1–3.7 (0.8)	0.7–23 (4.4)	0.1–4.8 (0.9)
United States	29–35 (30)	5.2–6.6 (5.9)	0.5–1.6 (1.0)	4.0–6.2 (5.1)	0.6–1.0 (0.7)	–	0.9–1.5 (1.2)
Estonia	3.5–38 (23)	0.9–8.4 (4.5)	0.2–1.6 (0.9)	0.7–9.3 (4.6)	0.1–1.3 (0.6)	0.7–7.2 (4.0)	0.2–1.3 (0.8)
Finland	3.4–41 (13)	0.6–6.8 (2.3)	0.3–1.3 (0.6)	0.6–6.4 (2.3)	0.07–0.9 (0.3)	0.5–4.8 (2.0)	0.1–1.1 (0.4)
France	2.1–54 (27)	0.4–11 (5.1)	0.1–2.2 (1.0)	0.4–11 (5.0)	0.05–1.5 (0.7)	0.3–8.6 (4.2)	0.04–1.8 (0.8)
Greece	11–53 (26)	2.1–10 (5.1)	0.5–2.4 (1.1)	2.2–11 (5.2)	0.4–1.6 (0.7)	2.1–9.2 (4.5)	0.4–1.9 (0.9)
Netherlands	4.7–19 (12)	0.8–3.7 (2.2)	0.2–0.8 (0.5)	0.9–3.8 (2.3)	0.1–0.5 (0.3)	0.6–3.0 (1.9)	0.1–0.6 (0.4)
Hungary	6.4–37 (24)	1.2–7.5 (4.6)	0.3–1.4 (0.9)	1.2–7.2 (4.8)	0.2–1.1 (0.7)	1.1–5.8 (3.9)	0.2–1.2 (0.8)
Ireland	9.0–35 (17)	1.4–6.6 (3.3)	0.2–1.3 (0.7)	1.4–6.4 (3.2)	0.23–1.0 (0.5)	1.3–5.8 (3.1)	0.3–1.2 (0.6)
Italy	5.4–94 (32)	1.0–16 (5.9)	0.2–3.2 (1.2)	0.9–13 (5.6)	0.2–1.7 (0.8)	0.9–8.9 (4.5)	0.2–1.7 (0.9)
Japan	0.8–120 (18)	0.2–30 (3.8)	0.04–8.1 (1.0)	0.2–27 (3.7)	0.02–3.8 (0.6)	0.1–25 (3.4)	0.02–4.3 (0.7)
Latvia	5.5–28 (18)	1.2–5.5 (3.3)	0.3–1.1 (0.6)	1.8–5.4 (3.2)	0.2–0.9 (0.4)	1.4–5.1 (2.9)	0.3–1.0 (0.6)
Lithuania	5.9–24 (15)	1.2–5.4 (3.0)	0.2–0.9 (0.5)	1.0–4.6 (2.9)	0.2–0.7 (0.4)	1.1–4.6 (2.6)	0.2–0.8 (0.5)
Norway	2.8–80 (20)	0.5–13 (3.7)	0.1–4.3 (0.9)	0.6–11 (3.7)	0.1–1.7 (0.5)	0.8–9.0 (3.4)	0.9–1.8 (0.7)
Poland	2.3–30 (12)	0.4–5.5 (2.3)	0.1–1.0 (0.3	0.4–5.6 (1.9)	0.05–0.8 (0.3)	0.4–5.1 (1.8)	0.1–1.0 (0.4)
Portugal	16–63 (32)	2.9–10 (5.8)	0.4–2.0 (0.9)	2.8–9.3 (5.2)	0.4–1.4 (0.7)	1.8–7.1 (3.7)	0.3–1.3 (0.7)
UK	1.1–112 (21)	0.2–30 (4.0)3	0.7–1.7 (0.8)	0.2–36 (4.1)	0.03–7.0 (0.6)	0.2–45 (3.8)	0.03–9.2 (0.8)
Czech Republic	13–33 (23)	2.2–6.0 (4.6)	0.4–1.2 (0.8)	2.1–5.6 (4.4)	0.3–0.9 (0.7)	1.9–5.1 (4.1)	0.4–1.0 (0.8)
Sweden	1.0–53 (15)	0.2–6.0 (3.0)	0.03–1.5 (0.6)	0.2–6.4 (3.0)	0.04–1.2 (0.5)	0.9–6.2 (2.9)	0.03–1.3 (0.6)
Switzerland	1.5–65 (23)	0.3–13 (4.4)	0.1–2.9 (0.9)	0.2–15 (4.5)	0.04–2.1 (0.6)	0.2–13 (3.8)	0.1–2.7 (0.8)
Uganda	51–98 (88)	–	–	–	–	–	–

Table 2: (Continued)

Country	Er	Tm	Yb	Lu	Sc	Y	References
Albania	2.1–2.8 (2.4)	0.3–0.4 (0.4)	2–2.6 (2.1)	0.2–0.4 (0.3)	10–15 (13)	–	(El-Ramady, 2010)
Germany	0.3–3.5 (1.8)	0.1–0.2 (0.13)	0.1–1.5 (0.5)	0.1–0.6 (0.4)	0.8–15 (6.1)	–	(Markert, 1987; Markert and De Li, 1991; Salminen, 2005; El-Ramady, 2010; Loell *et al.*, 2011)
Austria	0.3–3.7 (2.2)	0.06–0.5 (0.3)	0.3–3.3 (2.1)	0.04–0.5 (0.3)	1.3–21 (12)	–	(El-Ramady, 2010)
Australia	0.2–1.6 (0.8)	0.1–0.2 (0.13)	0.1–1.5 (0.5)	0.1–0.2 (0.1)	–	0.6–12 (5.3)	(Diatloff *et al.*, 1996)
Belgium	2.1–3.3 (2.8)	0.3–0.5 (0.4)	2.1–3.5 (2.9)	0.3–0.6 (0.4)	7.8–14 (10)	–	(El-Ramady, 2010)
Brazil	–	–	1.5–4.3 (2.9)	–	6.6–30 (18)	4.0–16 (7.8)	(Moreira *et al.*, 2011; Smidt, 2011; Oliveira *et al.*, 2012)
Bhutan	–	–	2.9–4.4 (3.5)	0.4–0.6 (0.5)	–	–	(Caspari, 2006)
Cape Verde	–	–	–	0.1–0.9 (0.3)	6.0–44 (25)	–	(Marques *et al.*, 2012)
China	0.8–3.1 (2.2)	0.1–0.4 (0.2)	0.6–2.7 (2.1)	0.1–0.4 (0.3)	11–13 (12)	14–35 (27)	(Wang *et al.*, 2004; Miao *et al.*, 2008; Zhang *et al.*, 2008; CHENG *et al.*, 2012; Li *et al.*, 2013)
Croatia	2.3–4.2 (3.6)	0.3–0.6 (0.5)	2.1–4.0 (3.5)	0.3–0.6 (0.5)	7.7–16 (13)	–	(El-Ramady, 2010)
Denmark	0.3–1.3 (0.7)	0.05–0.2 (0.1)	0.4–1.5 (0.9)	0.05–0.2 (0.1)	0.9–3.9 (2.2)	–	(El-Ramady, 2010)
Slovakia	0.7–3.4 (2.5)	0.1–0.5 (0.3)	0.8–3.3 (2.4)	0.1–0.5 (0.4)	2.0–15 (10)	–	(El-Ramady, 2010)
Spain	0.3–14 (2.5)	0.04–2.1 (0.3)	0.4–13 (2.3)	0.03–2.0 (0.3)	1.3–54 (10)	–	(El-Ramady, 2010)
United States	1.5–2.2 (1.9)	0.3–0.6 (0.4)	2.3–3.5 (2.9)	0.3–0.5 (0.4)	2.8–17 (9.9)	3.8–169 (16)	(Laul *et al.*, 1979)
Estonia	0.5–3.8 (2.2)	0.07–0.5 (0.3)	0.6–3.2 (2.1)	0.1–0.5 (0.3)	1.3–10 (6.4)	–	(El-Ramady, 2010)
Finland	0.3–3.2 (1.2)	0.05–0.5 (0.1)	0.4–3.4 (1.2)	0.04–0.5 (0.1)	2.0–21 (8.1)	–	(El-Ramady, 2010)
France	0.2–5.0 (2.4)	0.02–0.71 (0.3)	0.2–4.5 (2.3)	0.01–0.7 (0.3)	0.3–29 (9.3)	–	(El-Ramady, 2010)
Greece	1.2–5.3 (2.5)	0.2–0.7 (0.3)	0.8–5.0 (2.4)	0.1–0.7 (0.3)	4.4–23 (14)	–	(El-Ramady, 2010)
Netherlands	0.4–1.8 (1.1)	0.09–0.3 (0.2)	0.3–1.9 (1.1)	0.08–0.3 (0.1)	0.9–9.5 (4.3)	–	(El-Ramady, 2010)
Hungary	0.8–3.7 (2.4)	0.1–0.5 (0.3)	0.8–3.4 (2.3)	0.1–0.5 (0.3)	2.9–17 (9.0)	–	(El-Ramady, 2010)
Ireland	0.8–3.1 (1.8)	0.1–0.5 (0.2)	0.9–3.0 (1.7)	0.2–0.4 (0.3)	3.2–12 (6.5)	–	(El-Ramady, 2010)
Italy	0.6–4.9 (2.5)	0.1–0.7 (0.3)	0.7–4.1 (2.3)	0.1–0.6 (0.3)	5.5–21 (11)	–	(El-Ramady, 2010)
Japan	0.1–13 (2.0)	0.01–1.5 (0.2)	0.06–12 (1.9)	0.01–1.5 (0.2)	0.4–56 (17)	3.2–28 (13)	(Yoshida *et al.*, 1998; Takeda *et al.*, 2004; Uchida *et al.*, 2007)
Latvia	0.9–2.7 (1.6)	0.1–0.4 (0.3)	0.9–2.9 (1.8)	0.2–0.4 (0.3)	1.8–11 (5.8)	–	(El-Ramady, 2010)
Lithuania	0.8–2.2 (1.5)	0.1–0.4 (0.2)	0.8–2.6 (1.6)	0.1–0.3 (0.2)	1.8–7.6 (4.3)	–	(El-Ramady, 2010)
Norway	0.6–5.0 (2.1)	0.09–0.8 (0.3)	0.6–5.8 (2.2)	0.1–0.8 (0.3)	2.5–33 (11)	–	(El-Ramady, 2010)
Poland	0.3–3.1 (1.2)	0.05–0.5 (0.1)	0.3–3.4 (1.2)	0.05–0.5 (0.2)	0.7–12 (3.4)	14–30 (21)	(Chojnicki, 2000; Salminen, 2005)
Portugal	0.9–3.6 (2.0)	0.1–0.6 (0.3)	0.7–3.5 (1.9)	0.1–0.5 (0.2)	1.9–20 (8.7)	–	(El-Ramady, 2010)
UK	0.1–26 (2.3)	0.01–4.0 (0.3)	0.09–25 (2.3)	0.02–3.2 (0.3)	0.7–23 (9.4)	–	(El-Ramady, 2010)
Czech Republic	1.1–3.3 (2.5)	0.2–0.5 (0.3)	1.2–3.2 (2.5)	0.2–0.5 (0.3)	3.6–28 (11)	–	(El-Ramady, 2010)
Sweden	0.1–4.0 (1.8)	0.09–0.6 (0.2)	0.07–4.2 (1.9)	0.09–0.6 (0.3)	0.9–16 (7.6)	3.5–27 (10)	(Markert and De Li, 1991; Öhlander *et al.*, 1996; Tyler and Olsson, 2002; Salminen, 2005; Sadeghi *et al.*, 2013)
Switzerland	0.1–7.9 (2.2)	0.02–1.1 (0.3)	0.1–7.1 (2.0)	0.02–1.0 (0.3)	0.7–15 (8.8)	–	(El-Ramady, 2010)
Uganda	–	–	–	–	–	–	(Smith *et al.*, 2000)

Range of concentrations and average values – inside brackets – obtained via different analytical methods. n number of observations. Method: Sample preparation/Sample analysis

However, as for many mined metals, much higher concentrations can be found in soils surrounding mining areas. While the world average REE concentration in soil is of more than 150 ppm, several studies reported concentrations that can reach 10 times more (Table 3). In China, soils from the Jiangxi REE mining area (lateritic IAC) can display REE concentrations from 542 ppm to 2,373 ppm (Zhenggui *et al.*, 2001; Liang *et al.*, 2014). In the Baotou area (inner Mongolia, China), a REE concentration in the soil of more than 27,000 ppm has even been reported (Liang *et al.*, 2014) (Table 3). Such high concentrations in soils can thus have an important impact on the ecosystem, and interactions of REEs with the biota have to be monitored.

Table 3: pH and REE concentrations (ppm) in soils from REE mining areas from China. Adapted from (Zhenggui et al., 2001; Liang et al., 2014).

	Jiangxi REE mining areas			**South-Jiangxi REE mining areas**				**Baotou REE mining areas**		**China average**	**World average**
pH	**–**	**5.26**	**3.69**	**4.13**	**4.82**	**4.8**	**4.3**	**7.02**	**7.02**	**–**	**–**
La	208	62.3	110	492	381	112	30	6,905	55.0	37.4	50
Ce	351	85.2	44.2	630	861	303	49	12,170	133	64.7	7
Pr	46.9	–	31.3	166	102	23	11	1,614	12.0	6.67	35
Nd	159	97.0	154	411	375	81	39	5,727	42.9	25.1	4.5
Sm	25.0	39.0	49.1	127	78	18	21	492	6.7	4.94	1
Eu	2.36	1.50	3.99	12	7	2	1	96.9	1.25	0.98	4
Gd	21.7	–	42.3	106	71	24	21	329	5.43	4.38	0.7
Tb	2.54	10.2	6.64	13	18	4	4	38.1	0.76	0.58	5
Dy	11.1	–	37.4	42	58	19	21	54.6	4.37	3.93	0.6
Ho	1.97	–	7.28	16	17	6	7	–	0.91	0.83	2
Er	5.47	–	19.7	33	36	14	17	–	2.54	2.42	0.6
Tm	2.87	–	2.45	7	5	2	3	–	0.38	0.35	3
Yb	4.58	36.7	15.9	27	29	18	20	–	2.53	2.32	0.4
Lu	0.68	5.60	1.91	6	4	3	3	–	0.4	0.35	40
Y	51.2	–	–	226	330	152	148	–	–	–	–
ΣREE	870	542	688	2314	2373	783	396	27,550	280	177	194
ref.	(Zhu *et al.*, 2002)	(Gao *et al.*, 2001)	(Yu *et al.*, 2009)	(Zhenggui *et al.*, 2001)	(Zhenggui *et al.*, 2001)	(Zhenggui *et al.*, 2001)	(Zhenggui *et al.*, 2001)	(Y. X. Li *et al.*, 2010)	(Zhang *et al.*, 2012)	(Wei F. S. Zheng C. J., 1991)	(Wang *et al.*, 1989)

I.4. What parameters influence their bioavailability?

As for any other element found in soils, the behavior, and the resulting bioavailability of REEs, is governed by several factors (Figure 4). Among these factors, pH, redox potential, cationic exchange capacity (CEC), organic matter content, and mineral phases can be mentioned.

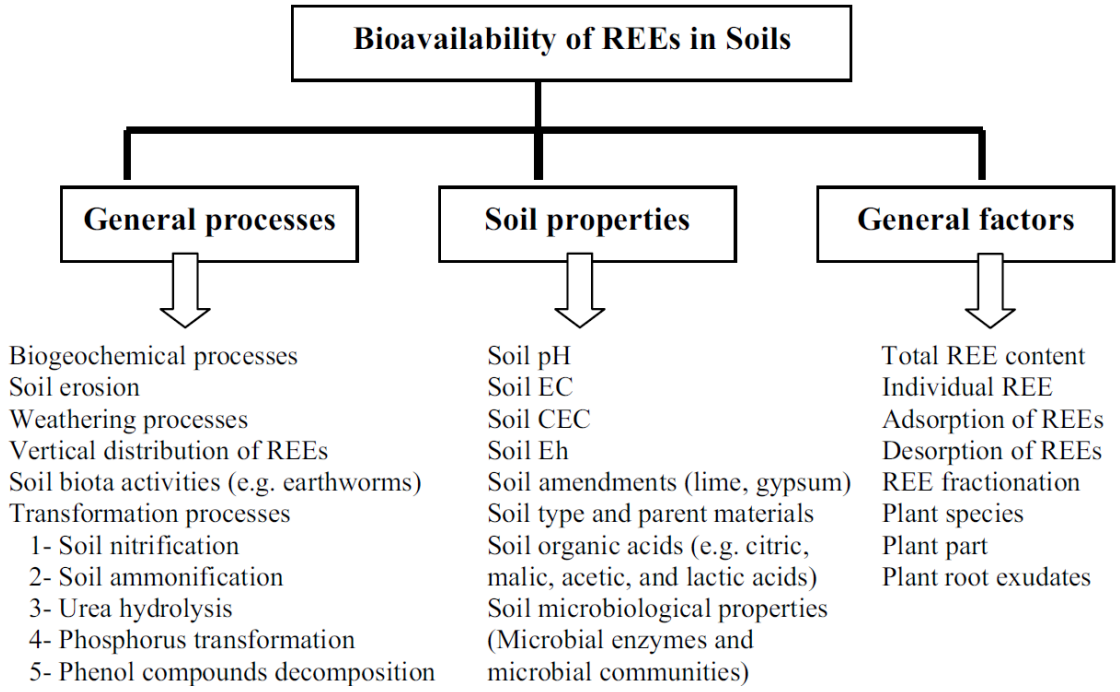

Figure 4: Factors affecting the bioavailability of REEs in soils. From (El-Ramady, 2008).

Organic matter contained in soils have many negatively charged groups, and thus have a very important ability to adsorb or chelate cations, among which, REEs. Therefore, organic matter is very important in the stabilization and sequestration of REEs in soils (Tyler, 2004a). Additionally, high content of clay minerals, phosphates or sulfates in soil solution, but also amount and lability of Fe-Mn-hydroxy coumpounds are of high importance in the complexation of REEs in either the soil solution or soil particles (Tyler, 2004a).

Another parameter of high influence on REE availability in soils is pH. It has been experimentally shown that when decreasing the pH of a soil from 7.5 to 3.5, the release of La, Ce, Gd, and Y was greatly increased (Tyler, 2004a). The opposite reaction occurred when the pH was increased. Indeed, this study showed that less REEs were found in the soil solution (Tyler, 2004a). Along with pH, the redox potential is also of high influence on REE bioavailability in soils. A decrease in redox potential favors the release and availability of REEs. These two parameters, pH and redox potential combined enable the dissolution of Fe-Mn oxyhydroxides which thus release REEs (Hu *et al.*, 2006).

The mobility, solubility and reactivity of REEs in soils is also highly governed by organic acids. Therefore, plants can strongly influence the mobility and bioavailability of REEs in soils. Plants indeed produce root exudates that locally decrease pH, chelate REE ions, or dissolve them in the soil solution. Root exudates can be carbohydrates, amino acids, enzymes, indole compounds or organic acids (Hayat *et al.*, 2017). Specifically organic acids, such as citric acid, have been shown to chelate REEs (S. Ding *et al.*, 2005).

II. REE demand, production, use and recyclability

II.1. Demand and Production

Since REEs are mainly found in bastnaesite, monazite, and IAC minerals, deposits from China, Australia, and the USA are the largest world's resources of REEs, followed by deposits from Brazil, India, Malaysia, South Africa, Sri Lanka, Thailand, and the USA (Long *et al.*, 2010; Dutta *et al.*, 2016) (Figure 5).

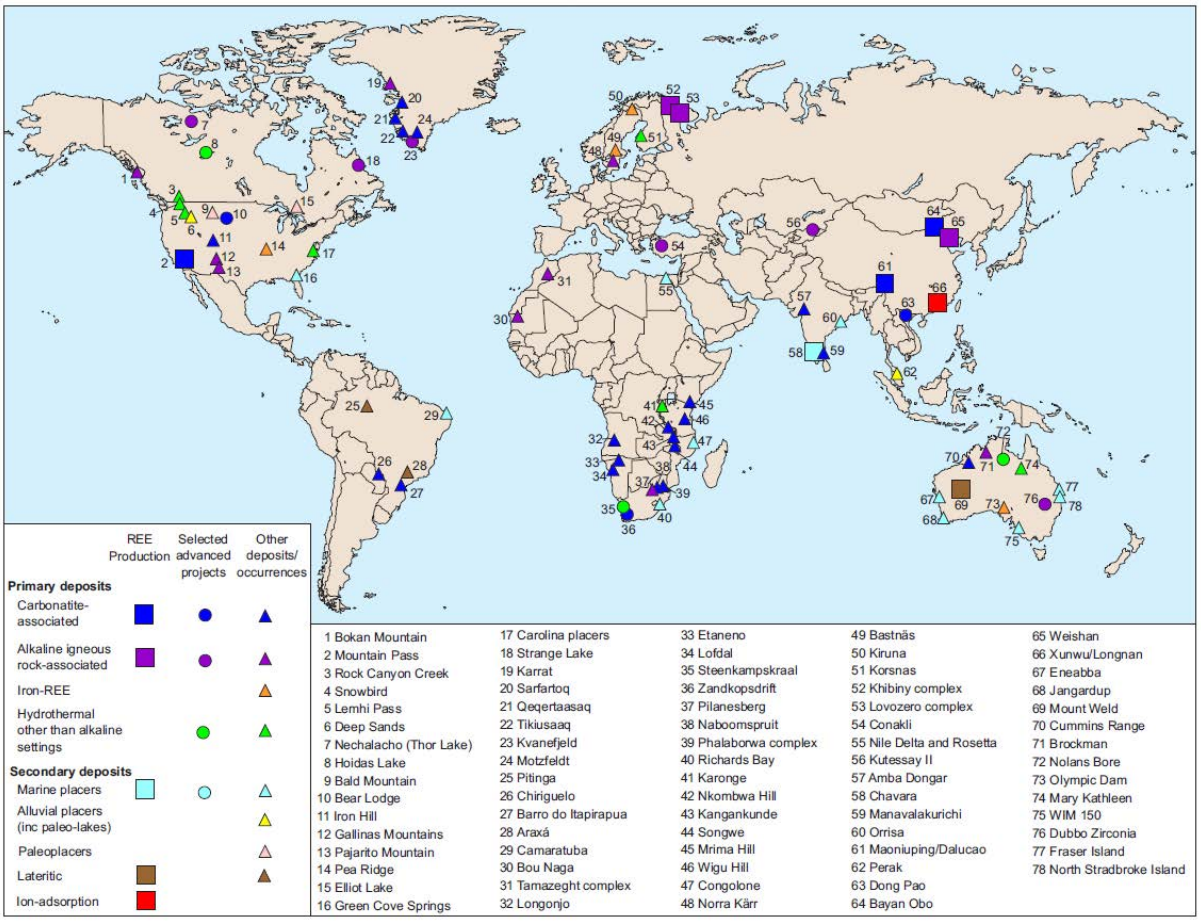

Figure 5: World map of REE deposits. From (Walter et al., 2011)

Starting in 1952, the USA were the biggest producers of REEs with the exploitation of Mountain Pass in California. China started to govern the REE market since the early 1990s,

when Mountain Pass production declined. Indeed, China produced high amounts of REE and sold them at such low prices that other mines around the world were unable to economically compete (Figure 6 & 7).

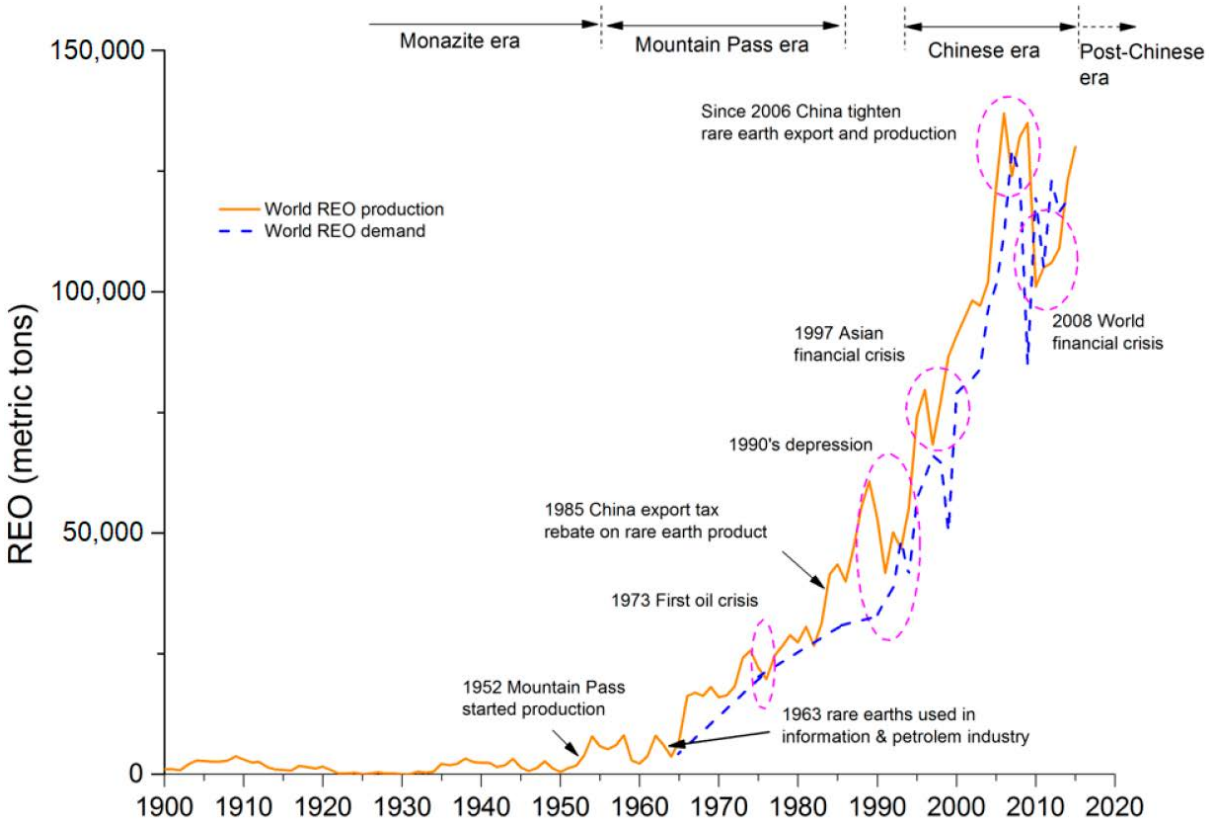

Figure 6: Global rare earth oxides (REO) production (orange line) and demand (dashed blue line). Main events that occurred in the history of REO production and demand are circled by pink dashed circles. From (Zhou et al., 2017).

In the past fifty years, a substantial increase in REE production was observed. In 1970, the world REE production was less than 20,000 metric tons of rare earth oxides (REO), while in 2017, 130,000 metric tons of REO were produced (Gambogi, 2018) (Table 4). China is still the biggest REO producer, with 105,000 metric tons produced annually (in 2017). More recently, Australia began to increase its REE production, with slightly more than 2,000 metric tons in 2011, to 20,000 metric tons in 2017. Russia and India are secondary producers with respectively 3,000 and 1,500 metric tons produced in 2017 (Gambogi, 2018) (Table 4 & Figure 7).

Table 4: Rare earths: estimated world mine production by country[1, 2] (Metric tons of rare-earth oxide equivalent). Modified From (United States Geological Survey, 2016; Gambogi, 2018)

Country[3]	2011	2012	2013	2014	2015	2016	2017	Reserves
Australia	2,188 [4]	3,222 [4]	3,000	8,000	12,000	15,000	20,000	3,400,000
Brazil	140	1,620 [r]	330	--	880	2,200	2,000	22,000,000
China	93,800	93,800	93,800 [5]	105,000 [5]	105,000 [5]	105,000	105,000	44,000,000
India[6]	1,700	1,700	1,700	1,700	1,700	1,500	1,500	6,900,000
Malaysia	410	100	180	240	310	300	300	30,000
Russia	2,500	2,200 [r]	2,500	2,600	2,800	2,800	3,000	18,000,000
Thailand[7]	3,100	120	130	1,900	760	1,600	1,600	NA
United states	--	3,000	5,500	5,400	5,900	--	--	1,400,000
Vietnam[7]	200	200	100	--	250	220	100	22,000,000
World Total (Rounded)	104,000	106,000 [r]	107,000	125,000	130,000	129,000	130,000	120,000,000

[r]revised. -- Zero. NA Not Available
[1]totals and estimated data are rounded to no more than three significant digits; may not add to totals shown.
[2]Includes data available through December 13, 2017.
[3]In addition to the countries listed, rare-earth minerals were thought to have been produced in Indonesia, Nigeria, North Korea, and some Commonwealth of Independent states countries, but information was inadequate to make reliable estimates of output.
[4]reported figure.
[5]Official production quota. Illegal production could not be quantified.
[6]India's Department of atomic energy did not disclose monazite production data.
[7]Rare-earth oxide content of exports.

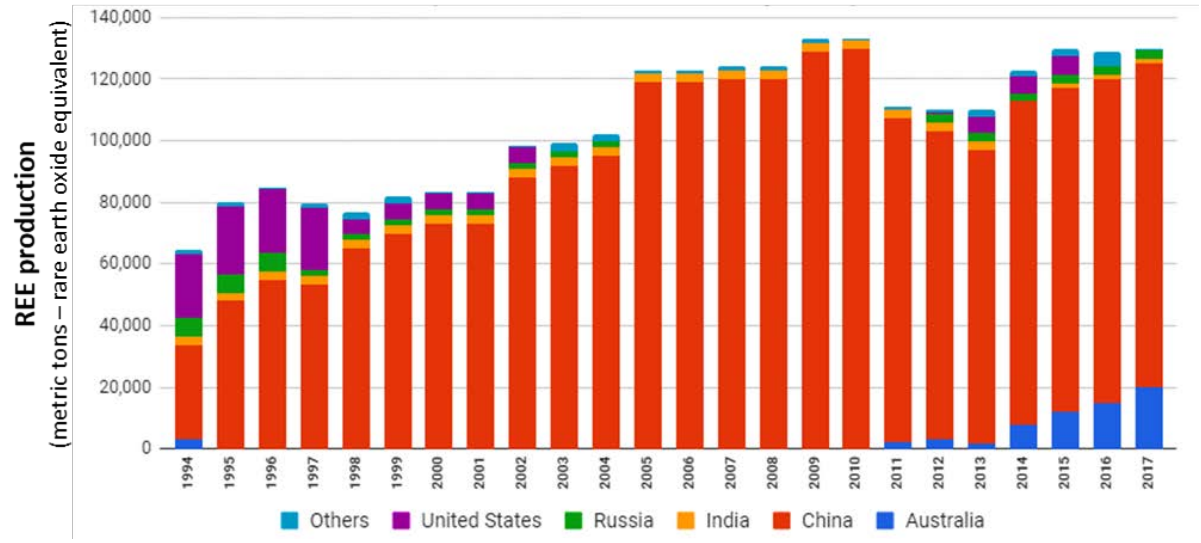

Figure 7: Contribution of different countries to the global REE production. This chart shows China's dominance in the production of rare earth elements between 1994 and 2017. The United States were a significant producer through the 1990s, but low-priced materials being sold by China forced mines in the United States and other countries out of operation. As China limited exports, and prices increased rapidly in 2009 and 2010, mines in Australia and the United States became active again. Graph by Geology.com using data from the United States Geological Survey. From https://geology.com/articles/rare-earth-elements/

II.2. Uses

II.2.a. REE usage in technology

Called the technology metals by the US EPA (United States Environmental Protection Agency), the group of REEs are key elements in the recent technological advances. The REEs display a wide range of properties that make them crucial for many domains.

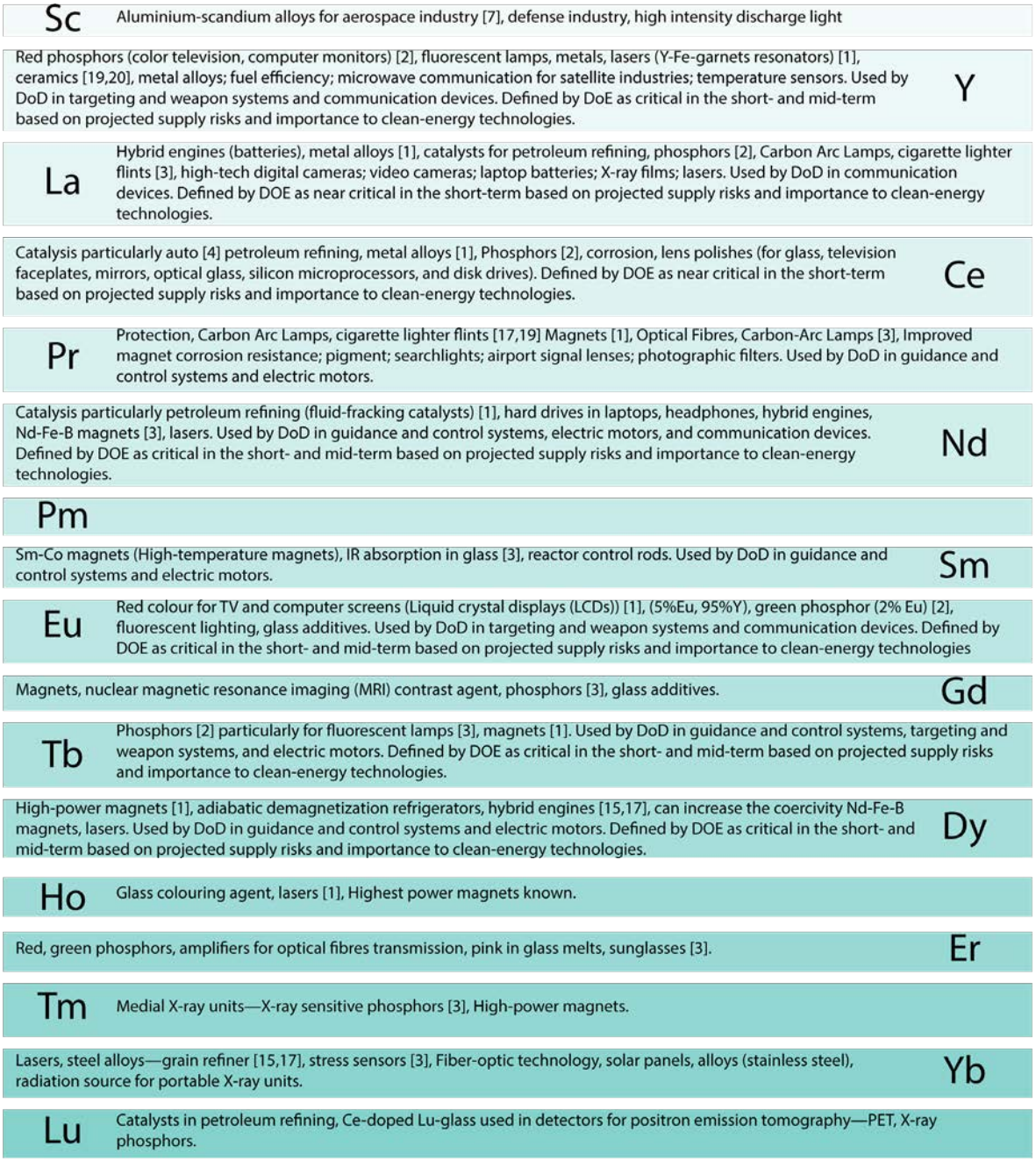

Figure 8: Abundance, resources, production and uses of the rare earths. DoD - US Department of Defense, DoE - US Department of Environment. [1] (Humphries, 2012), [2] GE, Lighting. Available online: http://www.gelighting.com, [3] (Hurst, 2010), [4] (United States Geological Survey, 2016), [5] MMTA. Minor Metals Trade Association. Available online: http://www.mmta.co.uk/metals/Ce, [6] (Hughes, 1995), [7] (Ahmad, 2003). Modified from (Haque et al., 2014) and (Reisman et al., 2013).

They allowed the miniaturization of electronic devices, the development of green energies and medical technologies, but they are also essential components for defense and telecommunication systems (Figure 8). REE are mainly used as catalysts (24%) and magnets (23%), but are also important for diverse domains such as polishing (12%), metallurgy (8%) as additives in alloys, in batteries, in glass and ceramic (7 & 6%), phosphors (lights) and pigments (3%), among others (Figure 9).

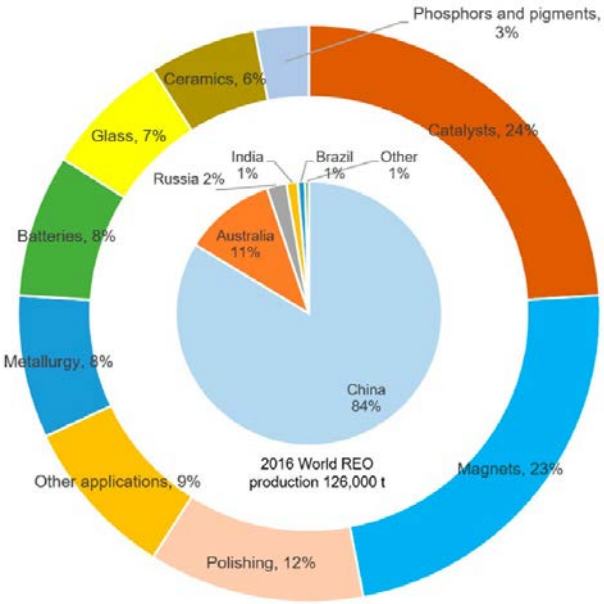

Figure 9: The distribution of global rare earth production and consumption in 2015. From (Zhou et al., 2017).

Their unequaled magnetic properties allow them to be used in magnetic resonance imaging (MRI), strong permanent magnets, such as motors in cordless tools, and in hard disk drives. Such magnets can be mainly of two kinds, either NdFeB magnets or Sm-Co magnets. Dy can be also used in combination to Nd in these magnets. REEs can be found in numerous high-tech objects of daily use, such as laptop screens, smartphones, hard drives, cameras, cigarette lighters, and headphones. They are also key components of the green energy transition by their use in hybrid and electric cars (REE-Ni batteries) and in wind turbines. Hybrid electric cars with nickel metal hybrid batteries can use up to 4.5 kg of REEs (Alonso *et al.*, 2012), while 2 MW wind turbine generators can contain more than 350 kg of Nd and 50 kg of Dy. Additionally, to their use as magnets in medical technologies, Gd is also used as a MRI contrast agent, when chelated (Figure 8) (Reisman *et al.*, 2013). Alternatives to REEs exist, however the use of other elements for these different applications is less efficient.

II.2.b. REE usage in natural environments and agriculture

The high affinity of REEs with phosphates can turn out to be an advantage in certain circumstances. REEs, and especially La, can be used to remediate the eutrophication of water bodies, by precipitating phosphates. Indeed, lanthanum modified bentonite (LMB), commercially known as Phoslock®, has been applied to about 200 water bodies across the world (about 50% in Europe, 30% in Australia and New Zealand, 13% in North America, 2% in Asia and 1% in Africa and South America) (Copetti *et al.*, 2016). In a review of total La (TLa) and filterable La (FLa) concentrations measured in the surface and bottom waters of 16 treated lakes, the maximum surface water of TLa and FLa concentrations ranged between 0.026 $mg.L^{-1}$ and 2.30 $mg.L^{-1}$ and 0.002 $mg.L^{-1}$ to 0.14 $mg.L^{-1}$, respectively (Spears *et al.*, 2013).

Besides their main uses for their physical properties, they have been extensively used in agriculture in China, Brazil and other countries. In the early 1970s, China started to pay attention at REEs as a potential fertilizer in agriculture. Indeed, when applied at low concentrations (up to 0.23 $kg.ha^{-1}.y^{-1}$) REEs promoted the growth and yield of crop plants. Several field trials were carried out on plants such as rice, wheat, soybean, peanut, tobacco, sugarcane, watermelon, beet, among others. Since the 1980's, the fertilizer NONGLE, a mix of both soluble chloride and oxide forms of REEs was used. Later on, the first commercialized fertilizer was called CHANGLE-REEs, which was composed of light REE nitrates. These fertilizers were enriched in the LREEs La, Ce, Pr, and Nd. For instance, the composition of CHANGLE-REEs, was 25-28% of La_2O_3, 49-51% CeO_2, 5-6% Pr_6O_{11}, and 15-17% Nd_2O_3. In the following years, new REE-fertilizers were commercialized. They were composed of ammonium bicarbonate and REEs. The MAR fertilizer, composed of a mixture of LREEs and amino-acids, was also created (Hu *et al.*, 2004).

Despite the intentional use of REEs in agriculture, their indirect and involuntary dissemination is an unknown factor in environmental risk assessment. A high reactivity of REEs with phosphate in particular, is also responsible for the emission of REEs by the production and the use of phosphate fertilizers. Table 5 gathers REE concentrations in different phosphate fertilizers used in Pakistan, Egypt, Bulgaria, USA and Brazil. A concentration of 2.6 g REEs is reported per kilogram of superphosphate produced, therefore a normal fertilization of 300 $kg.ha^{-1}.year^{-1}$ of phosphate provides more REEs in the form of impurities than intentional input into Chinese agriculture (Tyler, 2004a). As reported by Ramos et al. (2016), Brazil is a major phosphate fertilizer consumer (Ramos *et al.*, 2016). Only in 2014, about 4.2 million tons of monoammonium phosphate, 5.2 million tons of single superphosphate, and 1.8 million tons of

triple superphosphate, were used. Taking the concentrations of REEs in these fertilizers into account Brazil spread 23,800 t of REEs on their soils in 2014 (Ramos *et al.*, 2016) (Table 5). However, depending on the country of production, the REE content in phosphate fertilizer can vary greatly. For instance, in single superphosphate (SSP) from Pakistan, a total of 61 ppm can be found, while in the same product from Brazil, more than 3000 ppm of REEs have been measured (Ramos *et al.*, 2016).

Table 5: Worldwide contents of selected REE reported for major phosphate fertilizers and other particular agricultural inputs (mg/kg). Adapted from (Silvio J. Ramos et al., 2016).

Product	REE	La	Ce	Nd	Sm	Eu	Tb	Sc	Country	References
Single superphosphate (SSP)	61.3	18.4	40.2	–	2	0.4	0.3	–	Pakistan	(Waheed, 2011)
NPK (08:23:18)	235	90	129	–	12	3	1.5	–		
Limestone	31.9	19.5	10.4	–	1.6	0.2	–	0.2	Egypt	(Abdel-Haleem, 2001)
Superphosphate	30.7	18	8.5	–		0.3	–	3.9		
Superphosphate	75.5	17	35	23.5	–	–	–	–	Bulgaria	(Todorovsky, 1997)
NPK (12:12:17)	1327	500	600	181	33.2	9.9	3	–	Spain	(Otero *et al.*, 2005)
NPK (4:14:08)	2400	534	1181	571	77	17.1	4.5	15.2	Brazil	(Turra, 2011)
SSP	3129	674	1499	770	122	32.5	6.5	24.6		
Thermophosphate	3240	755	1575	748	105	24.5	8.3	23.9		
Phosphoric acid	62.9	18.7	16.5	14.2	0.9	0.8	2.5	9.3	USA	(Al-Thyabat and Zhang, 2015)
Phosphate rock	9831	2319	5468	1720	245	67	12	–	Brazil	(Leonardo, 2014)
Phosphogypsum	5662	1484	3015	970	150	37	6	–		
Monoammonium phosphate (MAP)	925	177	449	234	43	13.6	8.7	–	Brazil	(Dinali, 2014)
Triple superphosphate (TSP)	2746	727	1332	556	89	29	13.7	–		
Apatite concentrate	7802	1514	4204	1738	293	24.5	28.9	–	Iran	(Jorjani and Shahbazi, 2016)
Fertilizer enriched with REEs	3326	15,400	24,100	1100	2000	200	25.8	–	China	(Xu *et al.*, 2002)

Historically, France, Spain, and the UK are major users of phosphate fertilizers in Europe. Thus, one may hypothesize that increased content of REEs in soils was expected. However, similar REE concentrations in soils from different European countries were observed. Additionally, in order to know if there was an influence of the use of fertilizers on the natural REE signature of soils, authors normalized the data to concentrations in chondrites (Ramos *et al.*, 2016). They observed that the signature of European soils was different from that of apatite of sedimentary

origin from Morocco, which is a large exporter of phosphate fertilizers. This shows that the wide use of phosphate fertilizers containing REEs has not yet affected REE concentrations in European soils (Ramos *et al.*, 2016).

Table 6: Chinese feeding studies with REEs. From (Rambeck and Wehr, 2005).

Species	REE dosage	Effects	References
laying hen	200 - 800 mg / kg	+ 3.9 to 8.85 % EY + 0.5 to 1.33 g EW	(Wu *et al.*, 1994)
broiler	300 mg / kg	+ 20.3 % WG	(Zhang and Shao, 1995)
	400 mg / kg	+18.6 % WG	
	500 mg / kg	+ 6.6 % WG	
broiler	65 mg / kg	+ 6.3 % WG	(Xie and Wang, 1998)
	130 mg / kg	+ 10.71 % WG	
	195 mg / kg	- 0.09% WG	
pig	100 mg / kg	+ 8 % WG & - 8 % FC	(Chen, 1997)
	130 mg / kg	+ 25 % WG & - 19 % FC	
pig	200 mg / kg	+ 3.97 % WG & - 1.66 % FC	(Hu *et al.*, 1999)
	400 mg / kg	+ 8.93 % WG & - 4.65 % FC	
	600 mg / kg	+ 32.34 % WG & - 11.29 FC	
pig	50 mg / kg	+ 6-12% WG & - 4 to - 10% FC	(Xia and He, 1997)
	100 mg / kg	+ 13% WG & - 6 to - 7% FC	
	150 mg / kg	+ 6-12% WG & - 4 to - 10% FC	
piglets	300 mg / kg	+ 12% WG & - 11% FC	(Shen, 1991)
	600 mg / kg	+ 14% WG & - 14% FC	
	900 mg / kg	+ 7% WG & - 6% FC	
piglets	48 mg / kg	+ 11-19% WG & - 9 to - 19% FC	(Yuan, 1994)
piglets	75 mg / kg	+ 13-20% WG & - 5 to - 8% FC	(He and Xia, 1998)
pig	100 mg / kg	+ 13.26 % WG & - 8.50 % FC	(Xu *et al.*, 1999)
pig	100 mg / kg	+13.06 % WG & - 6.53 % FC	(Wang and Xu, 2003)

WG = weight gain, FC = feed conversion, EY = egg yield, EW = egg weight.

REEs are also used in meat production. Studies about the effect of REEs on meat production were first conducted in China, and showed positive results. In 2000, He and Rambeck, two German researchers demonstrated that after 8 weeks of REE treatment, an increase of 19% of the body weight of piglets was obtained (He and Rambeck, 2000). In a second paper, they indicated the possibility of using REEs as a sage and inexpensive alternative performance enhancers for pig production (He *et al.*, 2001). The effects of REEs reported by the different feeding studies both from China (Table 6) and under "Western conditions" are shown in Table 7 (Rambeck and Wehr, 2005). Pig, piglets and broilers have been used in those studies (Table 6, 7). Taken together, these results showed the efficiency of REEs to be used in meat production in both Asian and European conditions. However, the underlying mechanisms responsible for these positive effects are still unknown.

Table 7: Feeding studies with REE under 'western conditions'. From (Rambeck and Wehr, 2005).

Species	REE	REE dosage	Effects	References
piglets	REE-chloride	75 mg / kg	+ 2 % WG - 4 to - 5 % FC	(Rambeck *et al.*, 2000)
		150 mg / kg	+ 0 to + 5 % WG - 3 to - 7 % FC	
broiler	REE-chloride	150 mg / kg	no effects on WG, FC, EY or EW	(Schuller *et al.*, 2002)
	REE-chloride	300 mg / kg	no effects on WG, FC, EY or EW	
Japanese quails	REE-chloride	75 mg / kg	no effects on WG, FC, EY or EW	(Schuller *et al.*, 2002)
	REE-chloride	150 mg / kg	no effects on WG, FC, EY or EW	
	REE-chloride	300 mg / kg	no effects on WG, FC, EY or EW	
broiler	REE-chloride	100 mg / kg	+ 5 % WG	(Halle *et al.*, 2002)
	REE-nitrate	100 mg / kg	+2 % WG	
	REE-ascorbate	100 mg / kg	+7 % WG	
	REE-citrate	100 mg / kg	+ 6.5 % WG	
fattening pigs	REE-chloride	100 mg / kg	- 3.6 % WG	(Böhme *et al.*, 2002)
	REE-nitrate	100 mg / kg	- 3.6 % WG	
	REE-ascorbate	100 mg / kg	- 3.4 % WG	
	REE-citrate	100 mg / kg	- 1.1 % WG	
piglets	REE-chloride	150 mg / kg	+ 19 % WG - 11 % FC	(Borger, 2003)
fattening pigs	REE-chloride	150 mg / kg	+ 12 % WG - 3 % FC	
piglets	REE-chloride	300 mg / kg	+ 4 to + 5 % WG	(Eisele, 2003)
fattening pigs	REE-chloride	200 mg / kg	+ 3 to + 10 % WG - 2 to - 9 % FC	
fattening pigs	REE-chloride	200 mg / kg	+ 8.8 % WG - 3.6 % FC	(Kessler, 2004)

WG = weight gain, FC = feed conversion

II.3. Recyclability

REE recycling has recently gained interest for several reasons. The main drivers are the increasing demand for REEs, together with concerns on the continued and affordable supplies for these elements, their cost, but also new policies implemented by some countries on REE recycling (Reisman *et al.*, 2013). As shown in Figure 10, the recycled proportions of economically important metals, numerous REEs as well as other strategic metals, are very low (Ciacci *et al.*, 2015). This is the case for Y (non-Ln rare earth), La, Ce, Eu, Gd (LREEs), and Tb, Yb, Tm (HREEs). Yet, some other REE such as Ho, and Er show complete unrecyclability.

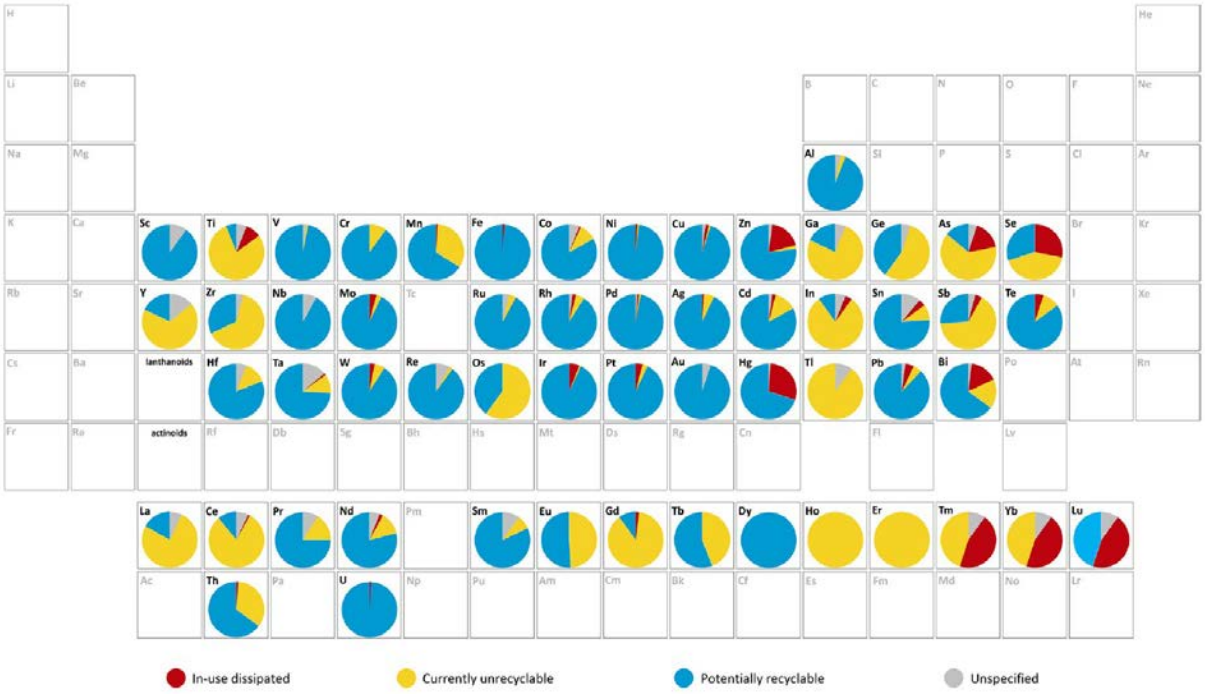

Figure 10: Percent distribution of elements among the four material stream. From (Ciacci et al., 2015)

Table 8 shows studies demonstrating the efficiency of REE recycling from several end-of-life products and the percentage of recovery. Several programs exist in order to recycle some of these REEs (Pr, Nd, Sm, Eu, Tb, and Dy) from magnets, phosphors, and hybrid car batteries, but most are at the R&D stage. Indeed, a COST (European cooperation in science and technology) action, called ReCreew (COST action ES1407) has been launched in 2016. It is a European network for innovative recovery strategies of rare earth and other critical metals from electric and electronic waste (COST, 2016). Another example of REE recycling project is the RECUP'TR developed by CNRS researchers in France, which aims at the extraction and recycling of REEs contained in magnets (https://www.recup-tr.com/).

Table 8: List of studies from 2016 on recycling of REEs from end-of-life products. From (Dutta et al., 2016).

Recycle	REE	Method used	% Recovery	References
Motors	Nd, Pr, Dy	Hydrometallurgy	82 (99% purity)	(Bandara *et al.*, 2016)
Permanent magnet	Nd, Pr	Vacuum Induction melting, hydrolysis & magnetic separation	93 (99.7% purity)	(Bian *et al.*, 2016)
Fuel cell catalyst	Pt	Hydrometallurgy	76	(Duclos *et al.*, 2016)
Phosphor (lamps)	Eu, Y	Hydrometallurgy	100 (99.9% purity)	(Dupont and Binnemans, 2015)
Oil refining catalyst	La, Ce	Hydrometallurgy	NA	(Ferella *et al.*, 2016)
NiMH magnets	Nd, Sm, Pr	Hydrometallurgy	98.1 (Nd), 95.5 (Sm), 95.5 (Pr)	(Meshram *et al.*, 2016)
NiMH magnets	Ce La, Nd	Hydrometallurgy	89.4 (Ce) NA	(Sinha *et al.*, 2016)
Permanent magnet	REEs	Hydro & pyrometallurgy	NA	(Sun *et al.*, 2016)
Phosphor (lamps)	Tb, Eu, Y	Mechanical activation & leaching	89.4 (Tb), 93.1 (Eu), 94.6 (Eu)	(Tan *et al.*, 2016)
Fluorescent lamp	Eu, Y	Hydrometallurgy	99.9	(Tunsu *et al.*, 2015)

NA = Not available

The contamination context of soils around mining areas, the application of REE fertilizers in agriculture, as well as the worldwide use of REE-bearing phosphate fertilizers, result in their widespread release in soils. Additionally, the increasing demand production, utilization and the current recycling inabilities, make these elements to be considered as emerging contaminants. While most of the efforts are made to find sustainable solutions for REE production in order to fulfil the demand, relatively few information currently exists on their environmental impact. US EPA has reviewed the human health toxicity for a few REEs in its Integrated Risk Information System (IRIS) and Provisional Peer-Reviewed Toxicity Values (PPRTV) programs between 2007 and 2009 (Reisman *et al.*, 2013). Therefore, a concern arises regarding the becoming of REEs in ecosystems, and their effects on organisms.

II.4. Bibliometric analysis on REE effects on biota

The use of bibliometric analyses gives a rapid overview of the research evolution concerning specific topics. In the case of REEs, a survey of the Web of Science database on the scientific literature from the last 40 years was made (Figure 11). When using the key words “rare earth elements”, a total of 21792 results came out. When associating the key words “rare earth elements” AND “*toxic*”, hundred times less results came out, with a total of 540 scientific contributions. When replacing “*toxic*” by “plant*”, it resulted in a total of 896 outputs (Figure 11). However, it is important to keep in mind that the term “plant” can refer not only to plant organisms, but also to industrial plants. When combining the key words “rare earth elements” AND “*toxic*” AND “plant*”, we obtained 148 results. A last search was carried out with the

key words “rare earth elements” AND “microorganism*”, which ended up with a total of 96 results. The results obtained with the different key words above, were mostly scientific contributions from China, the USA, Germany, Japan, Russia, France, Canada, and Brazil (Figure 11).

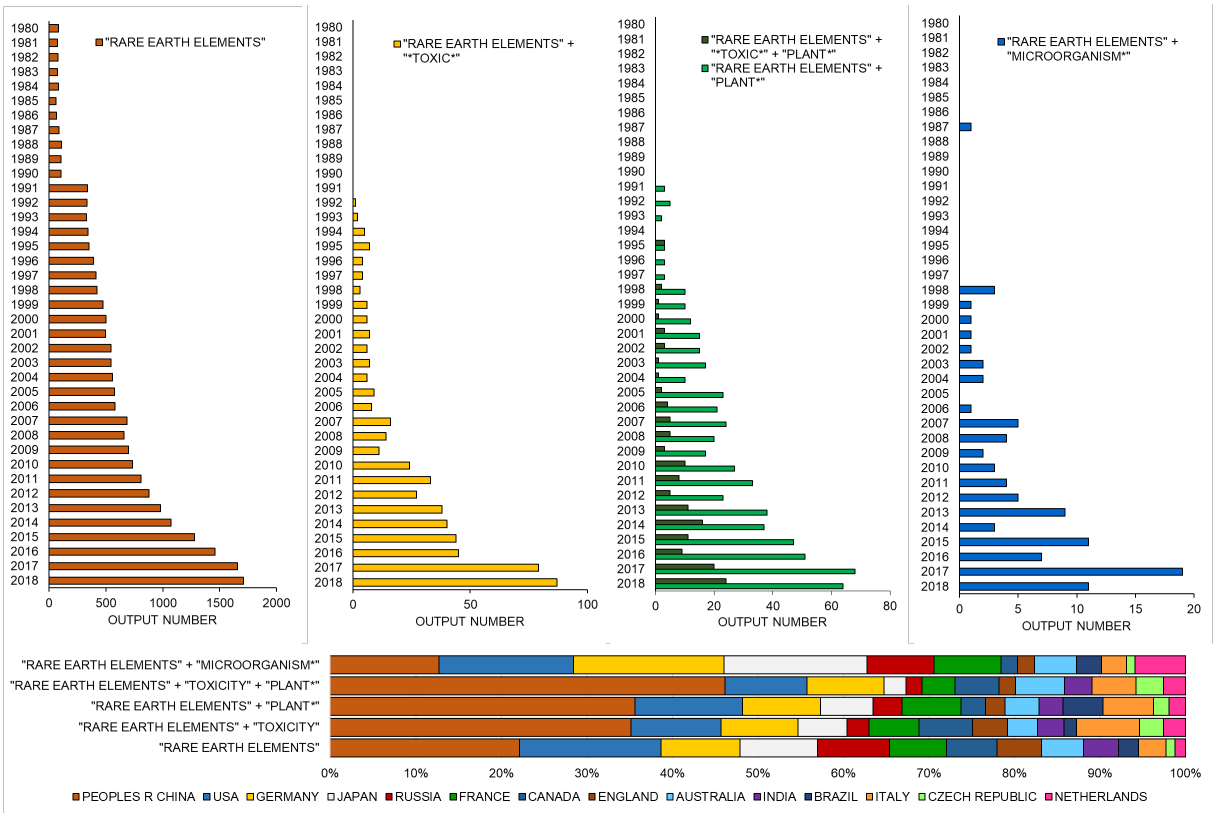

Figure 11: Bibliometric analysis using Web of Science on queries related to the rare earth elements. The top graphs represent the evolution of the number of scientific contributions (as number of outputs resulting from the query), from 1980 to 2018. The bottom graph represents the output affiliations to countries (as percentage of the total) by using different queries. Analysis carried out in January 2019.

As shown in figure 11, fifty percent of these results were from the last 5 or 10 years. Furthermore, an increasing number of scientific contributions on this topic is observed each year, supporting the rising interest for REEs. In conclusion, the effects of REEs on organisms (e.g. plants and microorganisms) is still poorly documented. Finally, the relatively low number of results when adding the key word “*toxic*” supports the lack of knowledge about the toxicological effect of REEs on organisms.

III. Transfer and effects of REEs on organisms

III.1. Introduction

III.1.a. REE transfer to organisms

It is only recently that the uptake of REEs in organisms was more in depth investigated. In plants, REE uptake was first thought to be stopped at the Casparian strip (Nagahashi *et al.*, 1974). Moreover, the strong valence of REEs is responsible for the strong affinity of these elements to the plant cell wall. Though, REE uptake appears to be possible in many living organisms such as plants, fungi and prokaryotes. The similar ion radius between several Ln and Ca, allow the blocking of Ca-channels by Ln ions (Klusenerl *et al.*, 1995). This characteristic made that REEs were previously used for studies of plant physiology and biochemistry, not to study the effect of REE on plants, but as tools to study Ca homeostasis. Indeed, their properties of Ca-channel inhibitor coupled to their fluorescence make them effective tools for the study of these carriers, especially in plants (Lansman, 1990; Lewis and Spalding, 1998). Later on, a study showed that La and Eu could enter into plant cells through artificial Ca-channels (Gao *et al.*, 2003).

Quite recently, Ene *et al.*, (2015) demonstrated an adsorption of Ln ions on the cell wall of *S. cerevisiae* as well as an inhibition of Ca channels (Cch1p-Mid1p) by Ln. Furthermore, they suggested their accumulation in yeast via these proteins. Indeed, the authors demonstrated that La accumulation was two times less important in ΔCch1 and ΔMid1 mutants. This difference was much less marked for Gd (Figure 12), which could suggest that there might not exist a single and common way of entry for all REEs. They observed that the inhibitory effect would be concentration-dependent and especially in function of the ionic radius; the lower the ionic radius (when the molecular weight increases), the more these ions could fit in the transporter and block the entry of Ca ions (Ene *et al.*, 2015a). In the same manner, it has been observed

that Ln ions could block Ca channels in human and animal cells. Also, Dy^{3+} and La^{3+} blocked Ca-ATPase and Mg-ATPase (Palasz and Czekaj, 2000).

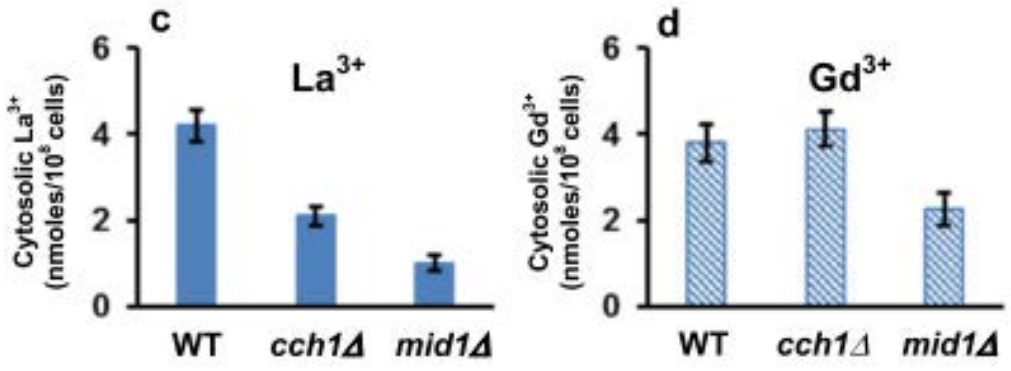

Figure 12: Cytosolic uptake of La (left) or Gd (right) in wild type (WT) strain of *Saccharomyces cerevisiae*, or when deleted for a subunit of the Ca channel Cch1 - Mid1. From (Ene et al., 2015b).

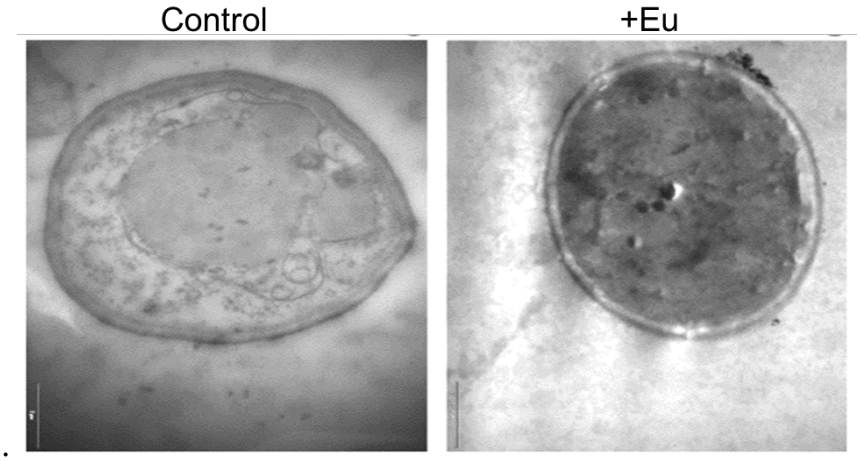

Figure 13: Europium accumulation (right) in *Saccharomyces cerevisiae* observed by transmission electronic microscopy. From (Roy et al., 2008).

In *S. cerevisiae*, Roy, Sinha, & Lahiri, (2008) visually observed using transmission electron microscopy that Eu could be taken up inside yeast cells (Figure 13). Furthermore, they hypothesized that the Eu uptake mechanism was different from transition elements (e.g. Co, Cu, Ni). Macdiarmid and Gardner (1998) observed that when Alr1p and Alr2p, the two plasmalemma Mg transporters in *S. cerevisiae*, were overexpressed in yeast cells, the strains were getting more sensitive to divalent toxic ions such as Zn^{2+}, Mn^{2+}, Ni^{2+}, but also to La^{3+} (MacDiarmid and Gardner, 1998). This observation was the only clue of the putative involvement of these Mg transporters as a way of entry of Ln in yeast cells. These examples support the hypothesis of a non-specific way of entry of REEs into cells through broad specificity cation transporters. However, the transport of REEs through their cationic state is not the only considered pathway. Many studies showed the presence of REEs in the roots of

plants and their translocation to the aerial part. To further support a putative different behavior of the different REEs, their fractionation in plants depending on their ionic radius has been reported. It has been postulated that a passive apoplastic and/or symplastic diffusion was preferential for LREEs (ionic form), whereas the HREEs would be complexed and then absorbed (Brioschi *et al.*, 2013). These two mechanisms would allow the translocation of REEs to the aerial parts of plants. In *Phytolacca americana*, asparagine, glutamate, and histidine could be involved in the transfer of La and Y in the xylem (Wu *et al.*, 2013). Similarly, Yuan *et al.* (2017) showed the important role of citrate in REE translocation in the same plant (Yuan *et al.*, 2017). In tomato, glutamate could also play this role (Wu *et al.*, 2009, 2013), while in wheat, this would be ensured by citrate, malate, and oxalate in the xylem sap (S. M. Ding *et al.*, 2005; Ding *et al.*, 2006). In these different studies, a range of several micromolar concentrations (0-0.2-1-5-25 µM for wheat, 0-1-10-50-100-250 µM for *P. americana*) of a mixture of the 14 REEs were applied under hydroponic conditions. Organic acids have been shown to be essential for both transport of nutrients in plants (e.g. Fe) (Álvarez-fernández *et al.*, 2014), and to toxic metal absorption by plant roots, long distance translocation in the xylem and storage in the vacuole of leaf cells (e.g. Al) (Kobayashi *et al.*, 2013). Altogether, these data suggest the high importance of several organic acids in REE translocation in plants. Furthermore, correlations were found between the contents of REEs and essential ions absorption in plants. Positive correlation of REEs with Fe, Al, Mg, K and P have been reported by Brioschi *et al.* (2012) in beech, spruce, and oak (Brioschi *et al.*, 2013). Increased absorption of macro- (Mg) and micro-elements (Fe, and Zn) was also reported in the fungus *Ganoderma lucidum*, when amended with REEs (Zhang *et al.*, 2013). Putative shared entry pathways in the roots between REEs and Ca but also Al ions have been hypothesized in *P. americana*, but no direct evidence was shown in this study (Yuan *et al.*, 2017). However, those observations may suggest common but non-specific uptake or translocation mechanisms within plant tissues for REEs and essential elements.

III.1.b. REE interaction with bio-molecules

REEs and phosphates are highly reactive (high affinity with anionic ligands and highly electronegative donor atoms, such as O) and thus form a precipitate. As shown previously, this affinity of REEs for phosphates, which is an essential element for plant growth, can lead to phosphate deficiency, which then cause an indirect effect on the plant (Ruiz-Herrera *et al.*, 2012). However, thanks to their particular characteristics, REEs are well suited as potential cofactors in certain metabolically relevant enzymes. While Mn, Fe, and Cu are intermediate

Lewis acids, REEs are considered as hard Lewis acids, like essential elements such as Zn, Ca, and Mg. Moreover, REEs display high coordination numbers, exhibit fast ligand exchange rate characteristics, and have relatively inaccessible redox chemistry. Many metalloenzymes, especially hydrolytic enzymes, require hard Lewis acids (e.g. Ca, Mg, and Zn) for activation of key elemental bonds requiring cleavage (e.g. phosphate ester bonds) (Franklin, 2001). Therefore, Franklin (2010) demonstrated that Ln can be remarkably effective catalysts for such biochemical processes.

Furthermore, REEs have an ionic radius close to that of Ca. Thanks to this similarity, Ln can replace (with a lower affinity) Ca in certain enzymes without inhibiting the activity. To illustrate this, a study demonstrated that Ln had a higher affinity than Ca (up to 17 times more) for the α-type Phospholipase D of cabbage (Dressler *et al.*, 2014). It has also been shown that Tb ions could directly interact with an horseradish peroxidase (Lihong Wang *et al.*, 2014). As demonstrated by the replacement of Ca by REEs in some molecules, there is a possible replacement of other elements by REEs. In *Dicranopteris dichotoma*, an REE-hyperaccumulating fern species, but also in spinach, Mg of chlorophyll can be substituted by Ce which would stimulate growth, chlorophyll concentration and photosynthetic efficiency in these plants (Tao *et al.*, 2001). To further support the possible interactions of REEs with biomolecules, two low molecular weight LREE-binding peptides that are thought to be involved in REE transport in plants have been found (Wang *et al.*, 2003; Lai *et al.*, 2006). In the same manner, Yang et al. (2016) demonstrated the interaction of La with a vitronectin-like protein, in *A. thaliana* leaves (Yang *et al.*, 2016).

It can be postulated that REEs are the natural binding ions of some proteins. In a recent study, the Protein Data Bank was screened to determine if some proteins potentially bind REEs. Using this computational analysis, it appeared that a hundred proteins have a possible binding site for the use of Ln as cofactor (Djinovic-Carugo and Carugo, 2015). All these results strongly suggest that REEs can interact with many biological molecules, and thus being either beneficial (cofactors), or deleterious to living organisms, impairing essential biochemical processes, but also that some mechanisms may exist in organisms to cope with these elements.

III.2. REEs and microorganisms

As shown by the bibliometric analysis (Figure 11), most of the studies regarding the effects and interactions of REEs with microorganisms emerged only recently. The studies carried out were mainly based on experiments with pure cultures of fungal or bacterial microorganisms.

III.2.a. REE accumulation by microorganisms

Several early studies reported that microorganisms could accumulate REEs. These observations support a possible transfer of these elements into living organisms and thus putative interactions with the cellular components. In 1998, Kamijo *et al*. screened 465 oligotrophic bacterial strains for their ability to reduce concentrations of Y in the culture medium (Kamijo *et al.*, 1998). Two species, namely *Variovorax paradoxus* and *Comamonas acidovorans*, were the most effective species. These bacteria could also reduce concentrations of most of the LREEs, but also that of some HREEs (Tb, Dy, Ho, and Er). However, they could not reduce concentrations of the heaviest REEs such as Tm, Yb, and Lu. This reduction of the REE concentration was associated to a decrease of the concentration of other trivalent ions (Fe^{3+} and Cr^{3+}) in the medium only when Y was present. Moreover, no reduction of the concentration of divalent ions (Mn^{2+}, Cu^{2+}, and Fe^{2+}) could be formed in the medium (Kamijo *et al.*, 1998). The same authors also observed the production of extracellular materials under Y exposure. A siderophore-producing *Arthrobacter luteolus* strain, isolated from REE-enriched environment in India, was also able to accumulate Sm and Sc (Emmanuel *et al.*, 2012). A total of 76 strains from 69 species (42 bacteria, including 20 actinomycetes, and18 fungi, including 16 yeasts) were tested for their REE removal capabilities from the culture medium (Tsuruta, 2007). Slightly different abilities between the strains were observed but generally, the accumulation was nearly identical for the various REEs and organisms tested (Tsuruta, 2007). As shown above, there was also an affinity towards different REEs according to the bacterial strains, marked by a selective accumulation when several REEs were present in the medium. For example, in *Actinomycetes* and Gram-positive bacteria, the concentration of Eu was greater than that of Gd (Tsuruta, 2007). Unlike as observed for other bacterial strains by Kamijo et al. (1998), the two bacteria *Arthrobacter nicotianae* and *Streptomyces albus* accumulated preferentially HREEs relatively to LREEs (Kamijo *et al.*, 1998; Tsuruta, 2006). Some fungal species also accumulated REEs, confirming some of the findings of Kamijo et al. (1998). For instance, a *Penidiella* strain isolated from an abandoned mine, accumulated Dy on the cell surface but also other REEs (Horiike and Yamashita, 2015). Additionally, It has been observed that some strains of *Trichoderma*, could accumulate REEs intracellularly (d'Aquino *et al.*, 2009).

Andrès, Texier, and Le Cloirec (2003) compiled published works on the sorption of REEs by microorganisms and the different bacterial and fungal biosorption capacities for several REEs. It has been argued that REEs would be adsorbed efficiently on microbial cell wall, mainly on carboxyl and phosphate functional groups (Andrès *et al.*, 2003). Extended X-ray absorption

fine structure spectrometry (EXAFS) were later used to study the biosorption of REEs on bacteria (*Pantoea agglomerans* and *Bacillus subtilis*). This approach helped at demonstrating the preferential binding of LREEs onto phosphate groups while HREEs would bind equally well on both phosphate and carboxyl groups (Ngwenya *et al.*, 2009; Takahashi *et al.*, 2010; Moriwaki and Yamamoto, 2013). Similar findings were found in *Saccharomyces cerevisiae* using the same methods (Jiang *et al.*, 2010, 2012).

Altogether, these results suggest the existence of accumulation mechanisms for REEs by microorganisms, but also that specific pathways are brought into play for the different REEs. Indeed, differential accumulation of REEs in living organisms could be modulated by both specific adsorption of cell membrane or cell wall, but also by non-specific uptake systems.

III.2.b. Positive effects

As for other elements such as Cu, Zn or Mn, REEs display hormetic effects towards a wide range of organisms, such as bacteria. Indeed, the studies presented below reported positive effects on the growth of bacteria at low concentrations, while at higher concentrations, toxic effects were observed.

Regarding the cellular response, some positive effects or even the need of REEs in some bacteria and fungi have been highlighted. Despite not being considered as essential elements, REEs appear to actually play a role in some cellular processes and therefore can influence communities at the ecological scale. For instance, the fact that REE contamination could impact microbial communities and thus modify community functions is of particular interest.

It has been observed that some strains of *Trichoderma* sp., together with REE accumulation, exhibited an increase in the dry mass of 170% to 240% after adding 0.1 to 1 mM of La in the culture medium. Additionally, 50-150 µg/mL of La^{3+} stimulated the growth of *E. coli* (Wenhua *et al.*, 2003). These results suggest that REEs could be essential for certain microorganisms but also at lower concentrations (d'Aquino *et al.*, 2009). Indeed, REEs would be particularly involved in gene regulation in bacteria as exemplified below.

In *Streptomyces*, cryptic genes of secondary metabolism (i.e. silent genes under laboratory conditions) were activated when REEs were added in the culture medium (100-500 µM $ScCl_3$, 1,700-2,500 µM $LaCl_3$). Among these, genes encoding for antibiotics, pigments (actinorhodine), cytochromes P450, siderophores, and transcriptional regulators, among others can be found (Ochi, 1987; Kamijo *et al.*, 1999; Kawai *et al.*, 2007; Tanaka *et al.*, 2010; Ochi *et al.*, 2014).

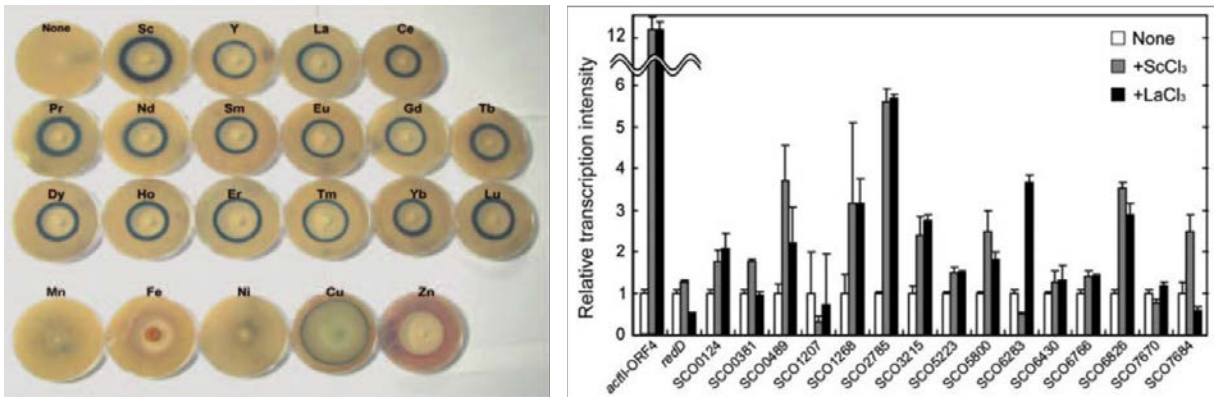

Figure 14: Effect of REEs on the production of secondary metabolites in *Streptomyces coelicolor*. Left, cultures of Streptomyces on growth medium supplemented with different metals. A blue halo (actinorhodin) is formed specifically when REEs are in the growth medium. On the right, relative expression of genes of *Streptomyces* in the presence of La, or Sc. From (Tanaka et al., 2010).

One very visual example reported in the literature was the production of the pigment actinorhodin by *Streptomyces coelicolor*, characterized by a blue halo, when REEs were added in the culture medium (Figure 14) (Tanaka *et al.*, 2010). It is however noteworthy that, as observed in Figure 14, no actinorhodin was produced in the absence of REEs, but also when other metals were used (Mn, Fe, Ni, Cu, Zn). Additionally, the transcription of several genes increased after exposure to either Sc or La (Figure 14) (Tanaka *et al.*, 2010). In *Bacillus* these 'revival' effects of cryptic genes have also been identified (Inaoka and Ochi, 2012). As a consequence, the production of secondary metabolites possibly, as for *Streptomyces*, influence the structure of soil microbial communities (Bontemps *et al.*, 2013). Thus, these data provide some clues about the putative impact of abiotic factors such as REEs, on ecological niches of microorganism communities.



Figure 15: Living on rare earth elements. The backsides of leaves obtained from plants were pressed onto an ammonium mineral salts medium (ATCC medium: 784 AMS) that either lacked (left side) or contained (right side) 20 µM LaCl3. The addition of La^{3+} allowed more methanol-using bacteria (pink) to grow. From (Skovran and Martinez-Gomez, 2015).

Recently, several bacteria were reported to use REEs for their growth, with the example of *Methylacidiphilum fumariolicum*, isolated from volcanic mud, which displayed a better growth when Ce^{3+} was added to the culture medium (5 to 320 nM Ce (III)) (Pol *et al.*, 2014). A striking example of the need of REE for some bacteria to grow was brought by Skovran and Martinez-Gomez in 2015. Indeed, some methylotrophic bacteria were isolated from the phyllosphere of trees by the addition of La in the growth medium (Figure 15) (Skovran and Martinez-Gomez, 2015). These different bacteria synthesize several methanol dehydrogenase (MDH) enzymes allowing them to use single-carbon chemicals released from plant leaves for their growth. First, it has been hypothesized for a long time that REEs (La, and Ce) might replace Ca ions as enzymatic cofactors. However, Ln-dependent enzymes have recently been identified (Fitriyanto *et al.*, 2011; Hibi *et al.*, 2011; Nakagawa *et al.*, 2012; Haque *et al.*, 2015). It is the case of the MDH XoxF from the model *Methylobacterium extorquens*, also widely present in other methylotrophic bacteria, unlike the MDH MxaF, which is Ca dependent. Indeed, XoxF from several *Methylobacterium* species were present and active only when La^{3+} was added to the culture medium (Hibi *et al.*, 2011). Furthermore, the XoxF from *M. fumariolicum* has different catalytic properties from other XoxF enzymes. This example where specific enzymes use Ln as cofactors suggests that Ln could be important in other essential enzymes (Hibi *et al.*, 2011; Pol *et al.*, 2014). Wehrmann et al. (2017, 2018) recently demonstrated that other alcohol dehydrogenase enzymes of the non-methylotrophic bacterium *Pseudomonas putida* can use Ln as cofactors. In their studies, two redundant ethanol dehydrogenases, PedE and PedH, used Ca and Ln ions as cofactors, respectively (Wehrmann *et al.*, 2017, 2018). This result is consistent with those obtained on methylotrophic bacteria that possess the two MDH MxaF and XoxF. These results emphasize the potential use of REEs as essential ions in several biochemical process, and therefore raise an increasing interest for the role played by REEs in living organisms.

III.2.c. Toxic effects

In opposition to the beneficial effects of REEs, at higher concentrations these elements induced toxic effects on microorganisms. In 2005, it has been demonstrated that La also has an effect on viruses. Indeed, some alterations induced by La in the RNA replication complex of flaviviruses were shown (Koschinski *et al.*, 2005). But this was the only example available of the effect of REEs on viruses. However, on bacteria and fungi, REEs showed marked toxicological effects at high concentrations (1-100 mM), and thus have been proposed as potential antibacterial and antifungal agents.

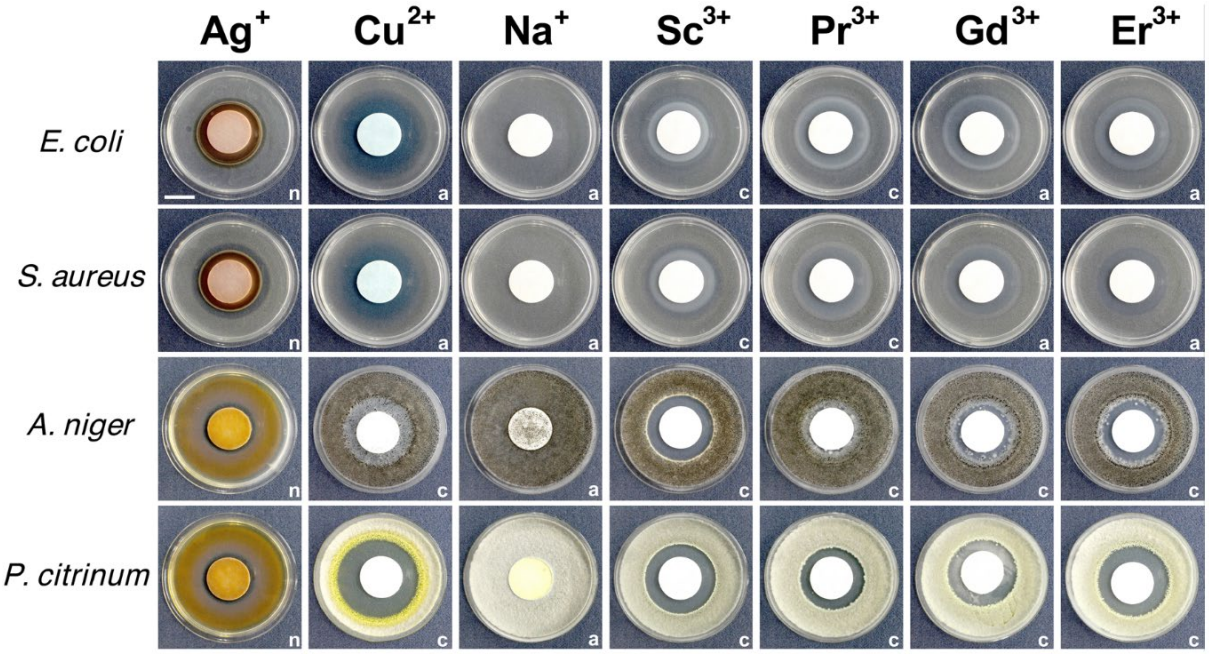

Figure 16: Rare earth ions have antibacterial and antifungal activity. Antibacterial activity of REE ions against Gram-negative (*Escherichia coli*) and gram-positive (*Staphylococcus aureus*) bacteria and antifungal activity of these ions against common fungi (*Aspergillus niger, Penicillium citrinum*) assayed by the paper-disc diffusion method. Paper discs were soaked in 100 mM metal solutions and placed at the center of the Petri dishes. Plates were incubated for 24 h for bacteria and 7 days for fungi. The counter-anion species used are acetate (a), chloride (c) and nitrate (n) (scale bar: 2 cm). Note that in sodium salt, no inhibitory zone was found. From (Wakabayashi et al., 2016).

The bacteria responsible for many nosocomial diseases, *Staphylococcus aureus*, and potentially other Gram-positive bacteria, but also *Escherichia coli* were sensitive when exposed to REEs (EC_{50} > 10 mM) (Figure 16). Such REE antibacterial activity was similar to that of Cu^{2+} and Ag^{2+} ions (Wakabayashi *et al.*, 2016). In fungi, the antifungal activity of REEs towards *Aspergillus niger* and *Penicillium citrinum* was also shown *(*Figure 16). La toxicity was also characterized by a highly impacted hyphal structure in strains of *Fusarium* sp. and *Pythium* sp. among other pathogenic fungi and oomycetes (EC_{50} > 130 mg/L) (Xiuqin and Wenji, 2006). Many studies investigated the beneficial and essential functions of REEs in bacteria, especially at identifying the molecular actors. However, the relatively few data dealing with REE toxicity are mostly restricted to growth inhibition tests, to identify antibacterial and antifungal concentration.

III.3. REEs and plants

III.3.a. REE-content in non-accumulating plants

Early reports demonstrated REE accumulation in plants even under not polluted conditions. In the literature, many plants were analyzed for their REE content, especially crop plants either from field studies or pots experiments. Under conditions of normal REE concentrations in soils,

REEs are present in a limited quantity within plants. It is estimated that the presence of REEs in leaves is between 0.0011 (Lu) and 0.33 ppm (Ce) (Djingova *et al.*, 2001) or even up to 5 ppm (Ozaki *et al.*, 1997). Yet, REE content in plants greatly depends on the soil and REE bioavailability, but also on the plant compartment analyzed. Usually, concentrations are higher in roots, followed by those of leaves, and finally stems. To have an average, the content of REEs in leaves is usually below 10 ppm dry weight. Moreover, Ozaki et al. (2000) measured the content of REEs in several fern species grown on non-contaminated soils. In the non-accumulating species, the content in La and Ce were in the range of 0.003-2.7 and 0.076-3.6 ppm dry weight, respectively (Ozaki, Shuichi Enomoto, *et al.*, 2000). Relatively low transfer ratios, from 0.04 to 0.09 of REEs from soil to plants, were usually measured (Tyler, 2004b).

III.3.b. REE-hyperaccumulating plants

Conversely, and as for many elements (Zn, Cd, As, Ni, etc.), some plants have the capacity to hyperaccumulate REEs. To date, up to 22 plant species, that have been identified through either field investigation or collection screening based on REE content, are known to accumulate or hyperaccumulate REEs (C. Liu *et al.*, 2017) (Table 9).

Two ferns display the highest accumulation rates; *Dicranopteris dichotoma* (or *D. linearis* syn.) at 3,000 ppm of its dry mass in LREEs (Zhenggui, 2001; Shan *et al.*, 2003) and *Pronephrium simplex* able to accumulate up to 1,200 ppm dry weight (Lai *et al.*, 2005, 2006). *Dicranopteris dichotoma* grows well around REE mining areas in China, and tolerates high concentrations of REEs in soils. This fern species was the most studied one, not only for its high REE accumulation ability, but also because it is a fast growing, high-biomass producer widely distributed in sub-tropical climatic zones (C. Liu *et al.*, 2017). Liu et al. (2017) reviewed and gathered the different concentration and fractionation parameters of REEs in samples of *D. dichotoma* from different sites reported in the literature. They observed that this species accumulated between 225 and 2,649 ppm, together with a high bioaccumulation factor of more than one (2 to 75), which support its hyperaccumulation trait. Other ferns have also this ability to accumulate REEs, but to a lesser extent such as *Dryopteris erythrosora* (Ozaki *et al.*, 1997), *Blechnum orientale* (Zhang *et al.*, 2002) or *Athyrium yokoscense* (Ichihashi *et al.*, 1991). Additionally, it was interesting to observe the higher accumulation of LREEs compared to HREEs in ferns. However, in the reported studies, ferns were grown under natural conditions. In such conditions, LREEs are over-represented relatively to LREEs, and the different LREEs (e.g. La, Ce, Pr, Nd) are found at very different concentrations in soils, so that it is impossible to properly compare the preferential transfer of these different REEs in plant tissues.

Table 9: Rare earth element (REE) hyperaccumulator and potential hyperaccumulator species reported. Modified from (C. Liu *et al.*, 2017). BF Bioaccumulation factor

Family	Species	Accumulation characteristics in foliage	Distribution	References
Juglandaceae	*Carya tomentosa*	∑REE in foliage: 1350 ppm (ash)	America	(Thomas, 1975)
Juglandaceae	*Carya cathayensis*	∑REE in foliage: 2296 ppm	America	(Robinson, 1943)
Juglandaceae	*Carya aquatica*	∑REE in foliage: 84 ppm	America	(Wood and Grauke, 2011)
Juglandaceae	*Carya cordiformis*	∑REE in foliage: 692 ppm	America	(Wood and Grauke, 2011)
Juglandaceae	*Carya floridana*	∑REE in foliage: 531 ppm	America	(Wood and Grauke, 2011)
Juglandaceae	*Carya glabra*	∑REE in foliage: 787 ppm	America	(Wood and Grauke, 2011)
Juglandaceae	*Carya illinoinensis*	∑REE in foliage: 190 ppm	America	(Wood and Grauke, 2011)
Juglandaceae	*Carya laciniosa*	∑REE in foliage: 512 ppm	America	(Wood and Grauke, 2011)
Juglandaceae	*Carya myristiciformis*	∑REE in foliage: 166 ppm	America	(Wood and Grauke, 2011)
Juglandaceae	*Carya ovata*	∑REE in foliage: 488 ppm	America	(Wood and Grauke, 2011)
Juglandaceae	*Carya pallida*	∑REE in foliage: 598 ppm	America	(Wood and Grauke, 2011)
Juglandaceae	*Carya septentrionalis*	∑REE in foliage: 632 ppm	America	(Wood and Grauke, 2011)
Juglandaceae	*Carya texana*	∑REE in foliage: 335 ppm	America	(Wood and Grauke, 2011)
Juglandaceae	*Carya tomentosa*	∑REE in foliage: 859 ppm	America	(Wood and Grauke, 2011)
Gleicheniaceae	*Dicranopteris dicthotoma*	∑REE in foliage: 3358 ppm	China	(Wang *et al.*, 1997)
Blechnaceae	*Blechnum orientale*	∑REE in foliage: 1022 ppm	China	(Xiao *et al.*, 2003)
Thelypteridaceae	*Pronephrium simplex*	∑REE in foliage: 1234 ppm	China	(Ying Lai *et al.*, 2005)
Thelypteridaceae	*Pronephrium triphyllum*	∑REE in foliage: 1027 ppm	China	(Xue, 2009)
Euphorbiaceae	*Glochidion triandrum*	–	–	(Koyama *et al.*, 1987)
Phytolaccaceae	*Phytolacca americana*	∑REE in foliage: 623 ppm	Japan	(Ichihashi *et al.*, 1992)
Athyriaceae	*Athyrium yokoscence*	∑REE in foliage: 202 ppm	Japan	(Ichihashi *et al.*, 1992)
Lindsaeaceae	*Stenoloma chusana*	∑REE in foliage: 725 ppm	China	(Xiao *et al.*, 2003)
Blechnaceae	*Woodwardia japonica*	∑REE in foliage: 367 ppm	China	(Xiao *et al.*, 2003)
Dryopteridaceae	*Dryopteris erythrosora*	BF of La >1	Japan	(Ozaki, Shuichi Enomoto, *et al.*, 2000)
Dryopteridaceae	*Dryopteris fuscipes*	BF of La >1	Japan	(Ozaki, Shuichi Enomoto, *et al.*, 2000)
Aspleniaceae	*Asplenium filipes*	BF of La >1	Japan	(Ozaki, Shuichi Enomoto, *et al.*, 2000)
Aspleniaceae	*Asplenium hondoense*	BF of La >1	Japan	(Ozaki, Shuichi Enomoto, *et al.*, 2000)
Aspleniaceae	*Asplenium ruprechtii*	BF of La >1	Japan	(Ozaki, Shuichi Enomoto, *et al.*, 2000)
Aspleniaceae	*Asplenium ritoense*	BF of La >1	Japan	(Ozaki, Shuichi Enomoto, *et al.*, 2000)
Aspleniaceae	*Asplenium subnomale*	BF of La >1	Japan	(Ozaki, Shuichi Enomoto, *et al.*, 2000)
Aspleniaceae	*Asplenium trichomanes*	BF of La >1	Japan	(Ozaki, Shuichi Enomoto, *et al.*, 2000)
Parkeriaceae	*Adiantum monochlamys*	BF of La >1	Japan	(Ozaki, Shuichi Enomoto, *et al.*, 2000)
Blechnaceae	*Blechnum subnomale*	BF of La >1	Japan	(Ozaki, Shuichi Enomoto, *et al.*, 2000)
Gleicheniaceae	*Dicranopteris strigose*	BF of La >1	Japan	(Ozaki, Shuichi Enomoto, *et al.*, 2000)

Although an over-representation of ferns as accumulators is currently observed (Table 9), a few Angiosperms also display this capacity. The pecan nut tree *Carya tomentosa* has been reported to accumulate high concentrations of REEs in its shoots, even when grown in non-contaminated areas (Wood and Grauke, 2011). Early reports from Robinson (1943) and Thomas (1975) have shown that *C. tomentosa* trees were able to accumulate 2,296 and 1,350 ppm in their leaves, respectively, on non-contamination soil (Robinson, 1943; Thomas, 1975). Wood and Grauke (2011) also demonstrated that all species of *Carya* were able to accumulate REEs, suggesting a rather conserved mechanism of either absorption or detoxification. They however observed a few discrepancies among the genus, depending on the ploidy level of the different species. Indeed, they observed that tetraploid species accumulated the greatest amount of REEs, (e.g. *C. tomentosa* with 859 ppm), compared to diploid species (e.g. 84 ppm in *C. aquatica)* (Wood and Grauke, 2011). According to the authors, these results provided evidence that REEs confer an adaptive advantage to tetraploid taxa for adapting to relatively xeric habitats. Still, this study was the only reporting the conservation of a REE accumulation trait among different species of a single genus.

Another angiosperm has been studied for its high REE accumulation. *Phytolacca americana* was at first well-known for its ability to hyperaccumulate Mn (Peng *et al.*, 2008). Yet, *P. americana* was found around REE mining areas in China, where it accumulated relatively high concentrations of REEs (Ichihashi *et al.*, 1991). Particularly, this species was found at a REE mining site in the South Jiangxi Province in China, with an average REE concentration of around 250 ppm in leaves, reaching up to 1,040 ppm (Yuan *et al.*, 2018). Recently, several studies investigated REE translocation and fractionation in *P. americana* (Yuan *et al.*, 2017, 2018). Unlike observed in ferns, *P. americana* revealed a higher translocation of HREEs to the leaves relatively to LREEs, while more LREEs were accumulated in roots. Organic or amino acids were suggested to complex REEs and take part into the long-distance transport of these elements in *P. americana* (Wu *et al.*, 2013; Yuan *et al.*, 2017). It exists several other species in the genus *Phytolacca*, among which another recognized Mn hyperaccumulator, *P. acinosa* (Xu *et al.*, 2009; Xue *et al.*, 2010). Nevertheless, unlike for *Carya* species, their REE accumulation ability is still unknown.

III.3.c. Use of REEs for Growth promotion

Recent field experiments have shown that the use of La caused a production increase in rice. Several parameters increased as illustrated by an overall increase in yield at a La addition of 0.05-1.5 mg/L, in the root dry weight at 0.05-0.75 mg/L and in the number of grains at 0.05-6 mg/L. Other parameters such as a greater tolerance to drought or an increased germination rate can be obtained through soil amendment, foliar spraying, or seed coating of a mixture of REEs (Tyler, 2004b). Hu et al. (2004) reported yield increases after REE applications to different crops in studies that were carried out either in Bulgaria, Australia, but more generally in China (Table 10). In consequence to REE applications, the yield increase ranged from 4 % relatively to the control for rapeseed, to 103 % for corn (Hu *et al.*, 2004).

Table 10: Yield increases (relative to control) observed after REE applications to different crops. From (Hu et al., 2004)

Crop	Country	Yield increase (%)
Sugar beet	Bulgaria	17-24
Sugar beet	China	7
Wheat	China	6-17
Rape	China	4-48
Potato	China	5-6
Soybean	China	8-9
Cotton	China	5-12
Rice	China	7
Corn	China	9-103
Barley	Australia	18-19
Peanut	China	8-12
Tobacco	China	8-10
Rubber	China	8-10
Sugarcane	China	10-15
Cabbage	China	10-20
Litschi	China	14-17
Grape	China	8-12

Under laboratory conditions, beneficial effects have also been highlighted. In *A. thaliana*, Ce and La promoted floral initiation and reproductive growth together with a significant increase of the height, dry weight and average number of flowers compared to the control condition (He and Loh, 2000). Additionally, the addition of La and Ce nitrate in the culture medium (0.5 to 10 µM) significantly increased the length of primary roots during vegetative growth (He and Loh, 2000). Ce^{3+} also stimulated the growth and the amount of chlorophylls in plants. In corn

and mung bean, an increase of root growth by 36 and 21%, respectively, was measured after La addition (Diatloff *et al.*, 1995). In the fern *Dryopteris erythrosora*, a growth improvement by La exceeded that by Ca. This indicated that the beneficial effect of La was therefore due to its intrinsic nature and not a function of "super Ca ion" (Ozaki, Schuichi Enomoto, *et al.*, 2000).

Several molecular and cellular effects in response to REEs have also been shown in other plants. In the fern *Dicranopteris dichotoma* but also in spinach, Mg of chlorophyll can be substituted by Ce, which would stimulate growth, chlorophyll concentration and photosynthetic efficiency in these plants (Tao *et al.*, 2001). In other examples, the addition of REEs in the culture medium increased the production of secondary metabolites, such as taxol in *Taxus* sp. cells (Wu *et al.*, 2001; Zhang *et al.*, 2013). More amazing still, Wang et al. (2014) have demonstrated the activation of endocytosis by REEs (La and Tb) in protoplasts of foliar cells of *Armoracia rusticana*.

Combined together, these numerous positive effects of REEs on plants, from increased seed germination, photosynthesis efficiency, drought tolerance, root length, growth, yield, quality, and production lead to their vast utilization as fertilizers in agriculture.

III.3.d. Toxicity of REEs in plant

In contrast to the effects described above, various works reported that the presence of REEs can also induce a stress, even a toxicity. However, toxic effects can be indirectly caused by the presence of REEs.

For instance, hormesis effects was observed on *Arabidopsis thaliana* exposed to different concentrations of Ce (Wang *et al.*, 2011). Indeed, low concentrations (0.5 µM) stimulated the primary root elongation, chlorophyll content, and rosette diameter of the plants, while higher concentrations (50-500 µM) had the opposite effects (Wang *et al.*, 2011). Ce was mainly distributed on the root cell wall but could also enter and destroy the ultrastructure of cells and disturb the intrinsic balance of nutrients (Wang *et al.*, 2011). Similarly, the application of Ce to wheat seedling culture medium had negative effects; elongation of the primary root was inhibited, root and aerial dry weight decreased, together with a decrease of Ca, Mg, K, Cu and Zn contents (Hu *et al.*, 2002).

Still in *A. thaliana*, several other studies demonstrated that REEs affected the root system architecture and morphogenesis (Figure 17).

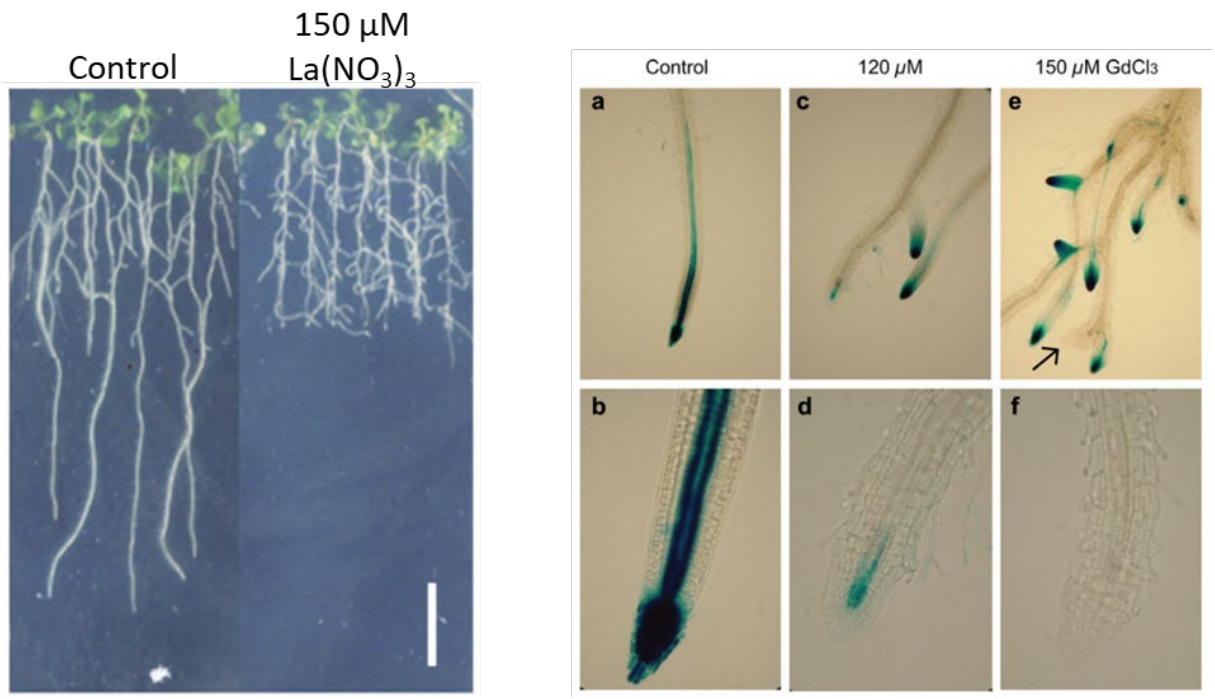

Figure 17: REE effect on *Arabidopsis thaliana* root architecture. Left, root growth inhibition caused by La (bar = 1cm) Right, Effect of Gd on auxin-inducible gene expression in *Arabidopsis* transgenic seedlings expressing the auxin-inducible marker DR5:uidA. Microscope photographs were taken at 10X (a, c, e) or 40X (b, d, f) magnification. Notice that Gd decreases GUS expression in the primary root tip region (d and f), matching with differentiation events such as root hair formation and lateral root formation close to the apex zone (c – f). Arrow (e) indicates the primary root tip. From (Liu et al., 2016) and (Ruiz-Herrera et al., 2012).

In 2007, Kobayashi et al. (2007) observed that the La tolerance of root growth was not correlated with tolerance to either Al or Cu, but with tolerance towards verapamil, a Ca channel blocker. Thus, it was hypothesized that the major La toxicity on the root growth of *A. thaliana* may involve its action as a Ca channel antagonist (Kobayashi *et al.*, 2007). Conversely, and due to the high reactivity of REE ions with phosphates, La and Gd indirectly induced low-P adaptive responses by inducing phosphorus deficiency through phosphate precipitation in the growth medium (Ruiz-Herrera *et al.*, 2012). This was characterized by the inhibition of the primary root growth together with an increased development of root hairs and lateral roots (Ruiz-Herrera *et al.*, 2012). The low-P phenotype was further confirmed with the increased expression of the phosphate transporters AtPT1 and AtPT2 in the roots under Gd exposure (Ruiz-Herrera *et al.*, 2012). Also it was showed that the reduction of cell proliferation was caused by the reduction of the number of meristematic cells and mitotic activity.

Furthermore, the same authors also revealed the involvement of auxin signaling in lateral root formation in response to Gd, by increasing the expression of the auxin-responsive gene marker DR5 (Figure 17) (Ruiz-Herrera *et al.*, 2012). Liu et al. (2017) demonstrated that the inhibition of the primary root growth by La in *A. thaliana* was caused by the repression of auxin carrier

abundance in the primary root tip (AtAUX1, and AtPIN1/2/4/7). Therefore, impairing auxin distribution in roots was responsible for the observed phenotype (Y. Liu *et al.*, 2017). Liu, Kilaru, and Hasenstein (2007) and Wang et al. (2014) also showed the involvement of another plant hormone, abscisic acid (ABA), in REE response (Liu *et al.*, 2007; J. Wang *et al.*, 2014). The former authors demonstrated in *Zea mays* that 1 mM of La doubled the ABA content in intact roots but decreased ABA content in root protoplasts. They also concluded that Ca and La actions were partially independent of each other (Liu *et al.*, 2007). In *A. thaliana*, REEs interacted with ABA, in the regulation of seed germination and root growth. It was suggested that La could interact with ABA upstream of H_2O_2 generation, thus regulating H_2O_2 signaling in root cells (J. Wang *et al.*, 2014). Additionally, in *A. thaliana*, primary root growth inhibition, by increasing cell death in the root tip and subsequent loss of meristematic cell division potential, was caused by La exposure (Liu *et al.*, 2016). La induced ROS over-accumulation in the tip, possibly causing cell death, auxin redistribution and ultimately the remodeling of the root system architecture (Liu *et al.*, 2016).

Toxicity of REEs to different plants was often linked to oxidative stress, such as an increased production of GSH, as shown in various publications since the 2010s. More generally, some REEs (Y, La, Ce, Nd, Gd, Tb, and Yb) induced reactive oxygen species (ROS) formation, and lipid peroxidation. For instance, the formation of ROS including an accumulation of H_2O_2 and lipid peroxidation in *Glycine max* and *Oryza sativa* was noted (Pagano *et al.*, 2015a). REEs could also modulate the activity of antioxidants such as superoxide dismutase (SOD), catalase (CAT), and glutathione peroxidase (GPx) (Pagano *et al.*, 2015a). Additionally, genotoxic effects were also observed (Table 11), characterized in plants by the increase of micronuclei formation induced by Ce, Er, Y, Sm and Eu in *Zea mais* and in *Vicia faba*, as well as chromosome and mitotic aberrations (Pagano *et al.*, 2015b).

A recent growing effort has been made at understanding the molecular and cellular mechanisms involved in the toxic effects of REEs in plants, especially on the root architecture. However, a more detailed picture regarding the toxic effects, REE uptake and translocation mechanisms is still lacking. Furthermore, the molecular actors underlying these mechanisms have not been identified yet.

IV. REE effects in animals and human health

Similarly to plants, genotoxic and oxidative stress-related effects were reported in different other organisms, such fish, rats, mice or animal cells (Pagano *et al.*, 2015b) (Table 11). In

addition, several studies, gathered in a review by Rim, Koo and Park, (2013) aimed at investigating REE toxicity towards human and animals (Rim *et al.*, 2013) (Figure 18). Most of the data currently available report the half-lethal doses (LD50) of some REEs (Sc, La, Ce, Nd, Eu) on rats, and lack more in depth investigation of the toxic effects on other animals and humans.

Table 11: Oxidative-stress and genotoxic effects reported after REE exposure in plants. From (Pagano *et al.*, 2015b).

REE	Test models	[REE]	Findings	References
Multiple	*Zea mais*		(↑) Micronuclei by Ce(III) ≤ 25 mg/L, Er(III) ≤ 5 mg/L, Y(III) ≤ 5 mg/L, Sm(III) ≤ 125 mg/L, and Eu(III) ≤ 125 mg/L; no significant effect by La(III)	(Huang *et al.*, 2007)
Y	*Nymphoides peltata*	0-5 mg/L	↑↓ Superoxide dismutase (SOD) and glutathione (GSH)	(Fu *et al.*, 2014)
La	Soybean (*Glycine max*)	0-0.85 mM	↓ Catalase (CAT) and glutathione peroxidase (GPx); ↑ H2O2 accumulation and lipid peroxidation	(Liang and Wang, 2013)
Ce	*Oryza sativa*	0-500 mg/L	↑ H2O2 and lipid peroxidation	(Rico *et al.*, 2013)
Pr(III) & Nd(III)	*Vicia faba*	0-0.5 %	(↑) Micronuclei; mitotic & chromosomal aberrations	(Jha and Singh, 1994)
Tb	Horseradish (*Armoracia rusticana*)	0-0.2 mM	↑ ROS and lipid peroxidation	(Jiang *et al.*, 2011)
Ho(III)	*Vicia faba*		(↑↓) Micronuclei; chromosomal aberrations and mitotic index	(Qu *et al.*, 2004)

Sc	Elemental Sc is considered non-toxic, and little animal testing of Sc compounds has been done. The half lethal dose (LD50) levels for Sc (III) chloride for rats have been determined as 4 mg/kg for intraperitoneal, and 755 mg/kg for oral administration.
Y	Water soluble compounds of Y are considered mildly toxic, while its insoluble compounds are non-toxic. In experiments on animals, Y and its compounds caused lung and liver damage. In rats, inhalation of Y citrate caused pulmonary edema and dyspnea, while inhalation of Y chloride caused liver edema, pleural effusions, and pulmonary hyperemia. Exposure to Y compounds in humans may cause lung disease.
La	In animals, the injection of La solutions produces hyperglycaemia, low blood pressure, degeneration of the spleen and hepatic alterations. La oxide (1312-81-8) LD50 in rat oral (> 8,500 mg/kg), mouse intraperitoneal (i.p.) (530 mg/kg).
Ce	Ce is a strong reducing agent, and ignites spontaneously in air at 65°C to 80°C. Fumes from Ce fires are toxic. Animals injected with large doses of Ce have died due to cardiovascular collapse. Ce (IV) oxide is a powerful oxidizing agent at high temperatures, and will react with combustible organic materials. Ceric oxide (1306-38-3) LD50 in rat oral (5,000 mg/kg), dermal (1,000-2,000 mg/kg), inhalation dust (5.05 mg/L)."
Pr	Pr is of low to moderate toxicity
Nd	Nd compounds are of low to moderate toxicity; however its toxicity has not been thoroughly investigated. Nd dust and salts are very irritating to the eyes and mucous membranes, and moderately irritating to the skin. Nd oxide (1313-97-9) LD50 in rat oral (> 5,000 mg/kg), mouse i.p. (86 mg/kg), and Nd2O3was investigated as a mutagen.
Pm	It is not known what human organs are affected by interaction with Pm; a possible candidate is the bone tissue. No dangers, aside from the radioactivity, have been shown.
Sm	The total amount of Sm in adults is about 50 µg, mostly in liver and kidneys, and with about 8 µg/L being dissolved in the blood. Insoluble salts of Sm are nontoxic, and the soluble ones are only slightly toxic. When ingested, only about 0.05% of Sm salts is absorbed into the bloodstream, and the remainder is excreted. From the blood, about 45% goes to the liver, and 45% is deposited on the surface of the bones, where it remains for about 10 years; the balance of 10% is excreted.
Eu	There are no clear indications that Eu is particularly toxic compared to other heavy metals. Eu chloride nitrate and oxide have been tested for toxicity: Eu chloride shows an acute i.p. LD50 toxicity of 550 mg/kg, and the acute oral LD50 toxicity is 5,000 mg/kg. Eu nitrate shows a slightly higher i.p. LD50 toxicity of 320 mg/kg, while the oral toxicity is above 5,000 mg/kg.
Gd	As a free ion, Gd is highly toxic, but magnetic resonance imaging contrast agents are chelated compounds, and are considered safe enough to be used in most persons. The toxicity depends on the strength of the chelating agent. Anaphylactoid reactions are rare, occurring in approximately 0.03-0.1%.
Tb	As with the other lanthanides, Tb compounds are of low to moderate toxicity, although their toxicity has not been investigated in detail.
Dy	Soluble dysprosium salts, such as Dy chloride and dysprosium nitrate, are mildly toxic when ingested. The insoluble salts, however, are non-toxic. Based on the toxicity of Dy chloride to mice, it is estimated that the ingestion of 500 g or more could be fatal to a human.
Ho	The element, as with other RE, appears to have a low degree of acute toxicity.
Er	Er compounds are of low to moderate toxicity, although their toxicity has not been investigated in detail.
Tm	Soluble Tm salts are regarded as slightly toxic if taken in large amounts, but the insoluble salts are non-toxic. Tm is not taken up by plant roots to any extent, and thus does not get into the human food chain.
Yb	All compounds of Yb should be treated as highly toxic, because it is known to cause irritation to the skin and eye, and some might be teratogenic.
Lu	Lu is regarded as having a low degree of toxicity: for example, Lu fluoride inhalation is dangerous and the compound irritates skin. Lu oxide powder is toxic as well if inhaled or ingested. Soluble Lu salts are mildly toxic, but insoluble ones are not.

Figure 18: Summary of toxicological information with REEs on animals and humans. Mostly referred from National Toxicology Program database search application (http://tools.niehs.nih.gov/ntp_tox/index.cfm) and material safety data sheets information in KOSHANET (http://www.kosha.or.kr/bridge?menuId=69). From (Rim et al., 2013).

Still, only little is known concerning the toxicological effects of occupational exposure to REEs. Cases of REE pneumoconiosis have been reported with high level of REEs in the bronchoalveolar fluid of workers exposed to REEs (Sulotto *et al.*, 1986). Additionally, high level of REEs were also found in the nails. Another study showed that Ce content in the blood but not in the breast milk was dependent of the environmental Ce concentrations (Höllriegl *et al.*, 2010). The analysis of the REE content in hairs of young children whose mothers live in the REE mining region of Jiangxi was also monitored. It revealed that the REE content in hairs reflected the REE body exposure. The closer to REE mining area the population lived, the higher the REE content in their body was (Wei *et al.*, 2013). It has also been argued that the long-term intake of low doses of REEs could lead to an accumulation in bones.

In vivo studies demonstrated toxicological effects of REEs at different levels. Indeed, in mice exposed to different REEs for 60 days, histopathological changes can occur in the liver, kidneys, and heart. In mice, Ce is highly accumulated in the eye, bone, testis, brain, heart, and adipose tissues (Rim *et al.*, 2013). Additionally, Ce administration increased metallothionein and glutathione (GSH) contents in the liver (Kawagoe *et al.*, 2005).

Some studies investigated the toxicological effects at a lower scale, using *in vitro* assays. For instance, in liver cells (hepatocytes), Pr and Gd decreased the activity of cytochrome P450 of hepatocytes. Dy and La blocked Ca-ATPase and Mg-ATPase, while Eu and Tb inhibited calcineurin, and more generally Ln ions could block Ca channels in human and animal cells (Palasz and Czekaj, 2000). It was therefore suggested that Ln significantly and uniquely impact cellular pathways, perturbing physiological processes (Palasz and Czekaj, 2000). Moreover, REEs can have cellular toxicity on erythrocytes (Lao *et al.*, 2006) and can also inhibit different human cancer cells *in vitro* (Rim *et al.*, 2013). A transcriptomic analysis on rats exposed to La $(NO_3)_3$ gave hints on the mode of action of this element in cellular physiology. Differentially expressed genes found in this experiment were related to cell signal and transmission, metabolism, protein translation and synthesis (Zhao *et al.*, 2004). In a similar experiment with Y, at a high exposure concentration (5,340 mg/L), differentially expressed genes were mostly related to cell receptor, signal and transmission, and ionic passage. Additionally, at lower dose (53.4 mg/L), differentially expressed genes were related to cell skeleton, movement, immunity, and DNA binding proteins (Yang *et al.*, 2006).

Most of the reported studies demonstrated the induction of both oxidative-stress and genotoxic effects in cell lines or animals after exposure to REEs (Table 12). Indeed, an increase of ROS

and lipid peroxidation together with a decrease in antioxidant capacity was observed in mice, rat hepatocytes, human lymphocytes, lung epithelial cells, and cerebral cortical neurons (Table 12). Oral et al. (2010) showed mitotic aberrations both in Ce-exposed embryos and in the offspring of Ce-pretreated sea urchin sperm (Oral *et al.*, 2010). A study on human breast cancer cells showed that exposure to La, Sm and Yb increased the mitotic activity and synthesis of DNA in those cells. The high exposure of humans to REEs around mining areas would increase the bone marrow micronucleus rate and lead to genotoxicity in bone marrow cells (Table 12) (Rim *et al.*, 2013).To sum up, the currently available data on REE toxicity are mostly limited to a dose-dependent toxicity and lack a more in depth understanding on the underlying mechanisms. Additionally, the very few studies working on the cellular and molecular mechanisms usually focus on a single REE or group of REEs, without comparing whether a uniform response can be induced by the different REEs.

Table 12: Oxidative-stress and genotoxic effects reported after REE exposure in animals and human or animal cell lines. From (Pagano *et al.*, 2015b).

REE	Test models	[REE]	Findings	References
Y	Rats	0-50 µg/rat	↑ MnSOD activity	(Marubashi *et al.*, 1998)
La	Cerebral cortical neurons	0-1 mM	↑ ROS formation; mitochondrial dysfunction	(Wu *et al.*, 2013)
	Rat liver	0-40 mg/kg BW/day	↓ SOD and CAT; ↑ GPx, GSH and malondialdehyde (MDA)	(Huang *et al.*, 2011)
Ce(IV) & La(III)	Sea urchin (*Paracentrotus lividus*)	0-10 mM	Ce(IV)-induced mitotic aberrations; no significant effect by La(III) exposure	(Oral *et al.*, 2010)
Ce	Mice	0-5 mg/kg BW	↑ ROS and lipid peroxidation; ↓ antioxidant capacity;	(Hong *et al.*, 2014)
		20 mg/kg BW	↑ Proinflammatory cytokines, cyclooxygenase-2	(Zhao *et al.*, 2011)
		20 mg/kg BW	↑ Lipid peroxidation; ↓ antioxidant capacity; ↓ SOD and CAT	(N. Li *et al.*, 2010)
	Human lung epithelial cells	0-40 mg/L	(↑) ROS, (↓) GSH and induction of OS-related genes	(Park *et al.*, 2008)
Pr(III) & Nd(III)	Mouse bone marrow cells	0-430 mg/kg BW	(↑) Chromosomal aberrations	(Jha and Singh, 1995)
Nd	Rat liver	0-40 mg/kg BW/day	↓ SOD and CAT; ↑ GPx, GSH and MDA	(Huang *et al.*, 2011)
	Mice	20 mg/kg BW	↑ Lipid peroxidation; ↓ antioxidant capacity;	(Zhao *et al.*, 2011)
		20 mg/kg BW	↓ SOD and CAT	(N. Li *et al.*, 2010)
Gd	Human lymphocytes	0-1.2 mM	↑ ROS formation	(Cho *et al.*, 2014)
	Rats	1.2 mmol/kg BW	↑ Ferritin, transferrin oversaturation; and lipid peroxidation N-acetylcysteine (NAC) protection	(Pereira *et al.*, 2012)
	Rat cortical neurons	0-20 µM	↑ ROS formation; NAC protection	(Xia *et al.*, 2011)
	Four cell lines	0-100 µM	↑ Ferritin increased iron import	(Ghio *et al.*, 2011)
Tb	Mice	0-200 µmol/kg	↓ SOD, CAT and GPx; ↑ lipid peroxidation	(Shimada, 1996)
	Human telomeric DNA	0-90 µM	htel21 Quadruplex is stabilized by low Tb(III) levels (8 µM); Tb(III) > 10 µM destabilizes quadruplex	(Galezowska *et al.*, 2007)
Yb	*Carassius auratus*	0-1 mg/L	↑↓ SOD, CAT and GPx	(Hongyan *et al.*, 2002)

V. The use of model organisms to study REE toxicity

To date, and compared to other metals such as Cd, Zn, Pb, and Hg, the knowledge on the impact of REEs on the biota is scarce, especially at the cellular and molecular level. In order to understand better the mechanisms implicated in the toxicity of a contaminant, such as trace

metal elements, model organisms have been widely used. Model organisms display many advantages. They are fast and relatively easy to grow, they are relatively easy to study and to modify genetically, thanks to the wide range of tools that are developed for their study compared to other organisms. Moreover, their genomes were the first to be entirely sequenced and annotated, and their genetic background is well described. *Saccharomyces cerevisiae* is one of the best eukaryotic organism to be characterized (Botstein *et al.*, 1997). This relatively "simple" organism is however very similar to higher eukaryotes regarding its cell structure and physiological processes. Similarly, *Arabidopsis thaliana* was defined as a plant model organism for the same purposes as mentioned above (Meinke *et al.*, 1998; Cobbett, 2003; Koornneef and Meinke, 2010). Therefore, *S. cerevisiae* and *A. thaliana* have been widely used in the analysis of cell cycle, organelle biogenesis, signaling pathways, transport mechanisms, but also at understanding metal toxicity mechanisms.

V.1. Metal transport in yeast and plant cells

REEs are non-essential elements for eukaryotes. Thus, as observed for Cd, it is probable that they enter cells through non-specific transport proteins involved in the uptake of essential elements. LREEs can enter through Ca channels. Therefore, an overview of the general transport and toxicity mechanisms of well-known metals is relevant for the understanding of REE transport processes. To illustrate the hijacking of essential element transporters by heavy metals, we describe in the following paragraphs the major way of entry and detoxification of toxic metals described in the literature.

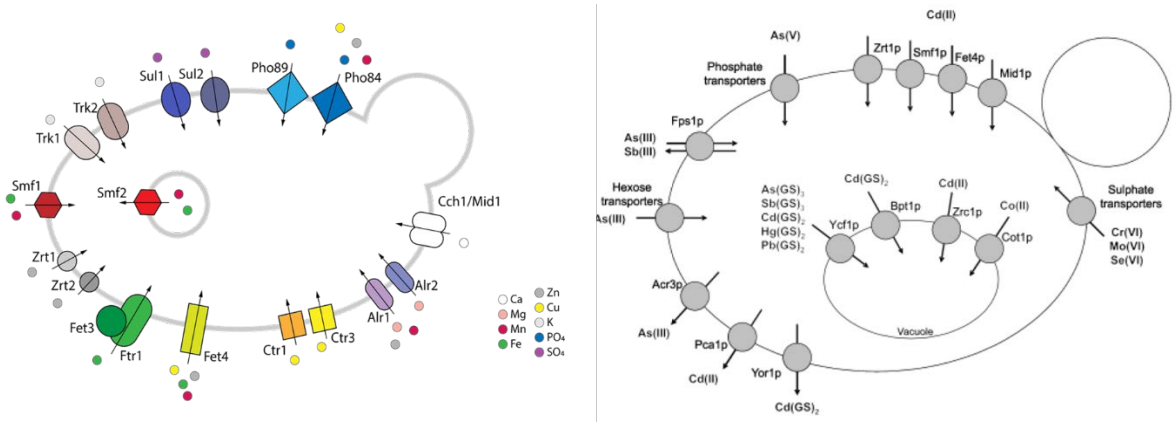

Figure 19: Ion transmembrane transporters identified in *Saccharomyces cerevisiae*. On the left, essential ion transporters. On the right, transporters mediating the uptake and detoxification of toxic metals in *Saccharomyces cerevisiae*. Adapted from (Wysocki and Tamás, 2010), and (Cyert and Philpott, 2013).

Figure 19 summarizes several of the different known ion transporters of the model organism *S. cerevisiae*. On this figure, we can notice that several ions can enter through the same plasma

membrane transporters, suggesting a non-specific action of these transporters. Therefore, they could also be an uptake system for some toxic ions. For instance, elements such as Ni^{2+} and Co^{2+} ions could enter yeast cells through the Mg transporters Alr1p and Alr2p (MacDiarmid and Gardner, 1998). Another noteworthy example is the putative uptake of arsenate through the high affinity transport system Fet3p-Ftr1p of *S. cerevisiae* (Batista-nascimento *et al.*, 2013), in addition to its uptake by phosphate and hexose transporters. Cd however, is known to cross the plasma membrane through Zrt1p (Zn transporter), Smf1p (Mn transporter), Fet4p (low specificity Fe transporter), and Mid1p (Ca channel) (Wysocki and Tamás, 2010). Lastly, sulphate transporters Sul1p and Sul2p were evidenced as ways of entry for ions such as Cr, Mo, and Se (Wysocki and Tamás, 2010). Conversely, some efflux transport systems allow cellular detoxification of toxic metals. It is the case of Pca1, that allows the efflux of Cd but also Ag and Cu out of yeast cells, and the efflux system Acre3 for As (Adle *et al.*, 2007; Wysocki and Tamás, 2010).

In the same manner as in yeast, toxic cations can also be transported in plants through several transporters of essential ions. For instance, in *A. thaliana* Cd can be transported by members of the Zn-regulated transporter (ZRT) Fe-regulated transporter (IRT)-like proteins (ZIP) (Guerinot, 2000) (e.g. the Fe transporter IRT1 (Vert *et al.*, 2002)), natural resistance-associated macrophage proteins (e.g. the Fe and Mn transporter NRAMP1 (Curie *et al.*, 2000; Thomine *et al.*, 2000; Cailliatte *et al.*, 2010)), and cation diffusion facilitator (CDF) families (Mäser *et al.*, 2001). Similarly, cyclic nucleotide-gated channels (CNGCs), a type of $Ca2^{+}$-permeable-channel have been shown to be involved in the uptake of Pb and Cd (Moon *et al.*, 2019), while As can be transported by either phosphate transporters or aquaporins (Li *et al.*, 2016).

V.2. Modes of action of metal toxicity

Following their entry inside cells, metals can interact with cellular components and induce toxicity through different phenomena. The extensive knowledge on the cellular and molecular toxicity mechanisms of heavy metals is a good baseline for the understanding of REE toxicity. These different reported mechanisms are summarized in Figure 20.

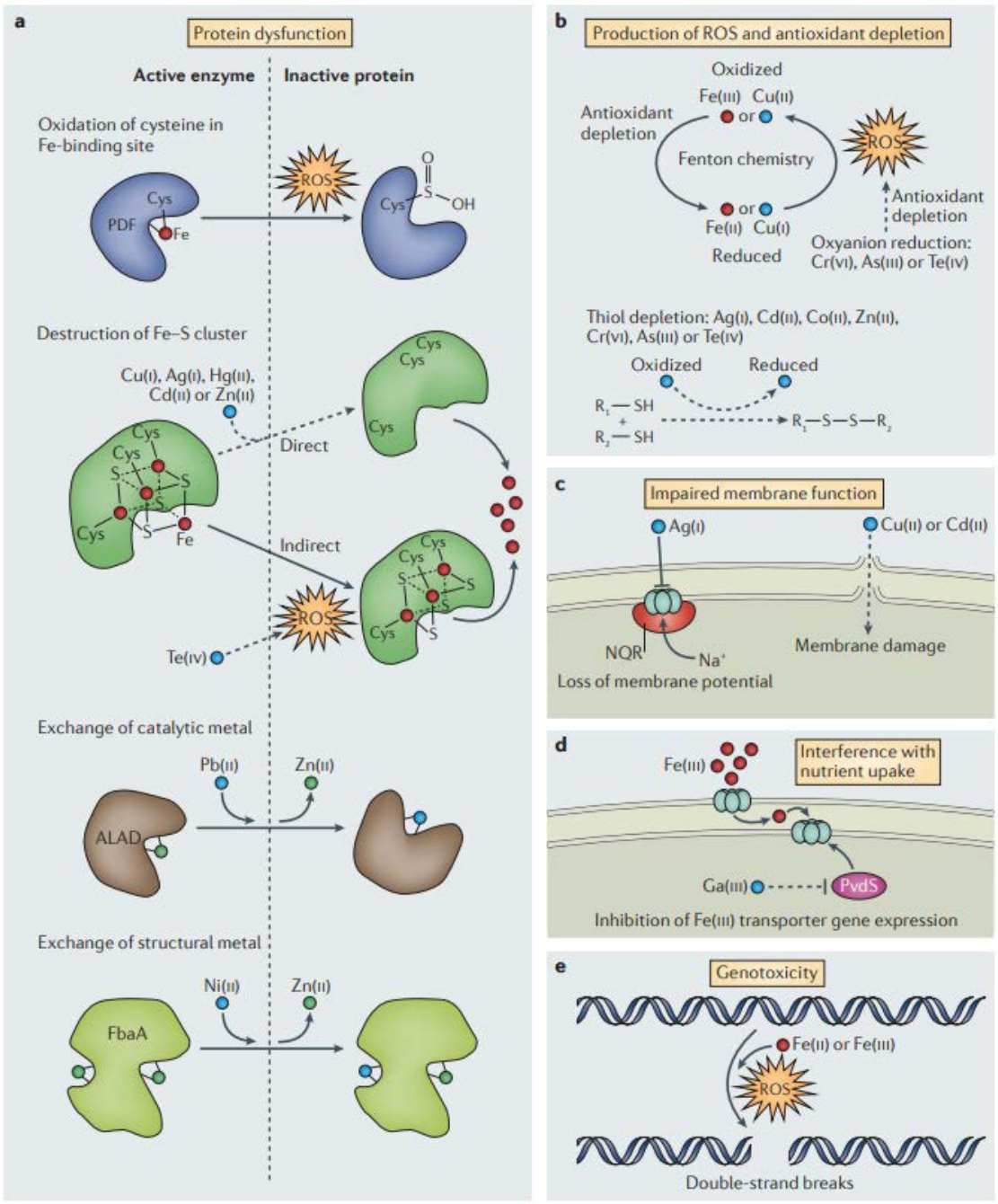

Figure 20: Mechanisms of metal toxicity. a | Metals can lead to protein dysfunction. **b** | They can also lead to the production of reactive oxygen species (ROS) and depletion of antioxidants. **c** | Certain metals have been shown to impair membrane function. **d** | Some can interfere with nutrient assimilation. **e** | They can also be genotoxic. Solid arrows represent pathways in which the underlying biochemistry has been elucidated, whereas dashed arrows represent a route of toxicity for which the underlying biochemical mechanism is unclear. ALAD, δ-aminolevulinic acid dehydratase; FbaA, fructose-1,6-bisphosphate aldolase; NQR, NADH:quinone oxidoreductase; PDF, peptide deformylase; PvdS, a σ-factor (σ24) from Pseudomonas aeruginosa. From (Lemire et al., 2013).

First, toxic metals can produce reactive oxygen species through Fenton reactions and lead consequently to an antioxidant depletion (Figure 20b). Metals can also impair membrane function, either by the loss of membrane potential (inhibition of pumps), or by producing membrane damages (Figure 20c). Another putative toxicity mechanism is the interference with

nutrient uptake by competition of toxic ions with essential ones (Figure 20d). Genotoxicity can also occur usually through the production of reactive oxygen species, which can result ultimately in DNA damages (Figure 20e). Finally, toxic metals can lead to protein dysfunction by several mechanisms (Figure 20a) such as; (i) by the oxidation of cysteine in Fe-binding site, (ii) the destruction of Fe-S clusters of proteins, (iii) or by replacing the catalytic or structural metals leading to the malfunction of proteins (Lemire *et al.*, 2013). General toxicity mechanisms (including interactions), and metal responses towards toxic metals in yeast and plants are described in Figure 21.

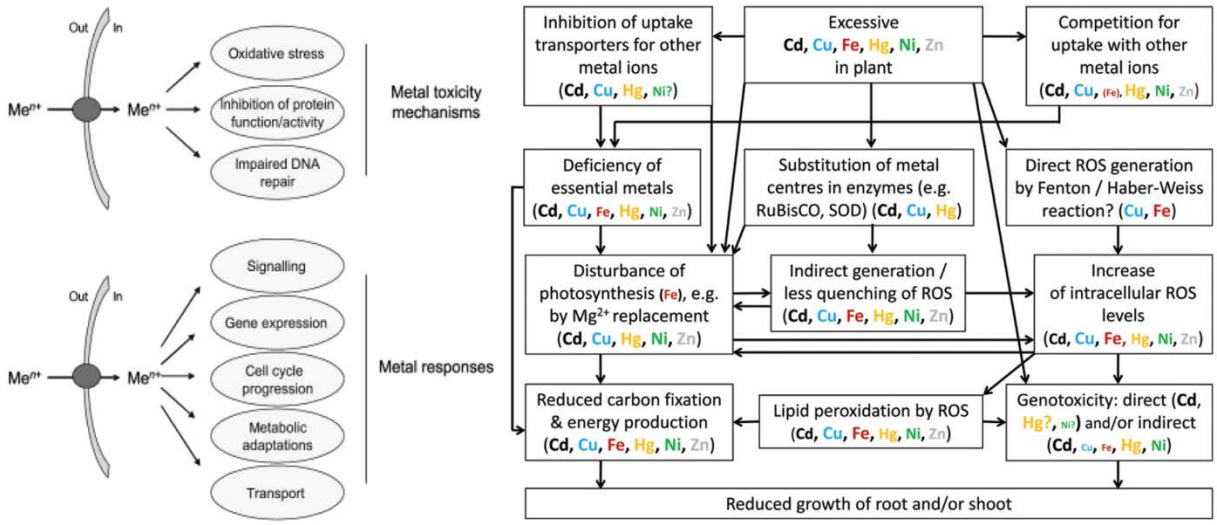

Figure 21: Metal toxicity mechanisms and metal responses in yeast (left) and plants (right). From (Wysocki and Tamás, 2010) and (Küpper and Andresen, 2016).

V.3. How organisms cope with toxic metals.

When exposed to metals at toxic concentrations, yeast cells and plants can counteract metal toxicity by several mechanisms, depending on both the toxicity mechanism of a metal, but also its physical and chemical properties (Wysocki and Tamás, 2010; Viehweger, 2014; Singh *et al.*, 2015). Low-molecular-weight cysteine-rich proteins and peptides such as glutathione (GSH), metallothioneins (MT) and phytochelatines (PC) are important contributors to metal detoxification in animals, plants, fungi, and some prokaryotes. For example, in *S. cerevisiae*, two metallothioneins, namely Cup1p, and Crs5p, can bind Cu, and Zn, but also have a minimal role in Cd tolerance. Such metallothioneins were also identified in ectomycorhizal fungi (e.g. *Paxillus involutus* (Bellion *et al.*, 2006)). PC are found in plants, and allow the chelation of metals and metalloids such as Cd, Cu, Ag, Hg, Zn, and As, but are also found in a few fungus species such as *Schizosaccharomyces pombe* (Clemens and Simm, 2003), and *Tuber melanosporum* (Bolchi *et al.*, 2011). Metal chelation can also involve GSH, for intra- and

extracellular metal chelation. Some other chelators can be involved in the detoxification process, such as nicotianamine in plants, but also organic acids. Oxidative stress defense is also triggered under certain metal toxicity, represented by a wide range of enzymatic antioxidants such as the superoxide dismutase (SOD), peroxidase (POD), catalase (CAT) and glutathione-S-transferase (GST). Along with the antioxidant defense system, protein degradation can also be modulated in order to prevent further damages made by indirect toxicity of metals (Wysocki and Tamás, 2010; Hasan *et al.*, 2017). Additionally, as mentioned earlier, some efflux transports exist to detoxify the cytoplasm from toxic metals (e.g. Pca1 for Cd, Ag, and Cu, and the efflux system Acre3 for As (Adle *et al.*, 2007; Wysocki and Tamás, 2010)). Also, the sequestration of metals or chelated metals in the vacuole is a common detoxification mechanism in eukaryotes (Ramsay and Gadd, 1997; Martinoia *et al.*, 2007; Li and Zhang, 2009; Jan and Parry, 2016; Sharma *et al.*, 2016).

The use of model organisms has shown its usefulness in understanding metal toxicity mechanisms. The increasing knowledge of toxicity mechanisms of several toxic metals is valuable to study and compare the mechanism of REE toxicity. Indeed, among the studies reported here, still little is known about REE impact on biota. Moreover, the different results were obtained using different media, therefore bioavailability and concentration of REEs used, on different organisms and not always comparing several REEs. The knowledge on REE interaction with living organisms is still scarce and disparate. There currently relatively few data on the mode of action of REE toxicity on organisms mostly focus on genotoxicity and oxidative stress generation (Pagano *et al.*, 2015b). It would be therefore interesting to compare whether REE impact organisms in the same manner as more studied toxic ions, but also on their way of entry and translocation in organisms. Altogether, it emphasizes the necessity of using well-known model organisms in order to build a strong basis on the impact of REEs on organisms.

V.4. The usefulness of 'omic' analyses to study metal homeostasis.

Large-scale 'omic' approaches have shown their pioneer role in the study of stresses, among which metal toxicity. These different omic approaches, such as deletome, transcriptome, proteome, and metabolome, have the advantage to focus on different steps of the cellular response. Therefore, combining several omic analyses is of particular interest in deciphering key cellular pathways involved either in toxicity or detoxification mechanisms of toxic metals. In addition, it allows building a strong basis for subsequent and deeper characterization of putative specific functions.

In *S. cerevisiae*, the integration of several complementary and high-throughput methods on a wide range of toxic metals helped to build comprehensive sets of metal-responsive profiles (Wysocki and Tamás, 2010). For instance, Jin et al. (2008) combined transcriptome and deletome approaches to study *S. cerevisiae* response to seven toxic metals and metalloids (Cu, Ag, Zn, Cd, Hg, Cr, As) at equi-toxic concentrations (Jin *et al.*, 2008). In the same manner, Hosiner et al. (2014) analyzed the transcriptome of yeast to ten different human health relevant metals (Ag, Al, As, Cd, Co, Hg, Mn, Ni, and V). Thanks to such meta-analysis, both studies demonstrated that cells may have developed common or convergent regulatory mechanisms to accommodate metal exposure. Nevertheless, these comparative studies highlighted the existence of some processes unique for individual metals (Wysocki and Tamás, 2010; Hosiner *et al.*, 2014).

Similar work has been done on plants (Singh *et al.*, 2016). Most of the studies currently available brought insights in the metal homeostasis in plants using transcriptomic analyses. *Arabidopsis thaliana* has been one of the major contributor, together with rice (*Oryza sativa*), into the identification of key genes, proteins and pathways that allow plants to cope with toxic elements, mostly Cd, Zn and As. Especially noteworthy, microarray analyses revealed several metal transporters (e.g. ABC, HMA) in heavy metal detoxification and root to shoot translocation processes. The usefulness of combined omic techniques for example to study As metabolism in plants even led to the use of the term 'Arsenomic' (Tripathi *et al.*, 2012). The global screenshot of metallic stress and detoxification in plants using these large-scale techniques are the first step for subsequent gene characterization.

The identification of metal specific tolerance and transport mechanisms have been pointed out by comparative transcriptomic of closely related plants that display contrasted phenotype regarding metal tolerance and/or accumulation (Verbruggen *et al.*, 2009). This was carried out for two Cd and Zn hyperaccumulating species *Arabidopsis halleri* and *Noccaea caerulescens* that were compared to *Arabidopsis thaliana* (Weber *et al.*, 2004, 2006; Halimaa *et al.*, 2014). These comparative transcriptomic studies allowed for instance the identification of a nicotinamide synthase and a putative Zn^{2+} uptake system, that would account for metal hyperaccumulation factors (Weber *et al.*, 2004). Recently again, cross-species transcriptomic analysis in different plant families of nickel hyperaccumulators have identified convergent functions that may represent major nodes in the evolution of nickel hyperaccumulating plants (Garcia de la Torre *et al.*, 2018).

The high number of studies dealing with omic analyses of metallic stress response provide insights in the basic understanding of the response of organisms to these stressors, by using well-known models, or well-adapted plants. Ultimately, it might help in identifying factors enhancing stress tolerance and be employed in breeding and engineering programs aiming at developing plants with new and desired agronomical traits. Nevertheless, such work has never been done for the REEs. It is therefore important to develop a first base for a better understanding of REE stress in eukaryotes.

CONTEXT OF THE THESIS

The boom in and fast development of new technologies, as well as the growing needs of emerging economies such as China and India, are all contributing to an ever-increasing demand for rare metal resources. Therefore, the dissemination of these elements by their various uses (technological, mining, agricultural), raises the question of the fate of these emerging pollutants and the effect on living organisms.

To meet the challenges that lie in strategic metal supply (mining, recycling) and their fate in the environment, the Laboratory of Excellence, "Strategic Metal Resources in the 21st Century - RESSOURCES21" (http://ressources21.univ-lorraine.fr/), has brought together a multidisciplinary team of researchers from the OTELo scientific center (Lorraine Earth and Environment Observatory). OTELo comprises four laboratories: LIEC (Interdisciplinary Laboratory for Continental Environments), GéoRessources, LSE (Soil and Environment Laboratory), and CRPG (Center for Petrographic and Geochemical Research). The LabEx R21 focuses on three objectives in order to better understand the biogeochemical cycle of strategic metals;

- Understanding natural and anthropogenic strategic metal cycles and the processes of metal concentration (ore deposits) or dispersion in the environment;
- Developing of innovative tools for improved ore processing and metal extraction;
- Understanding of the environmental impact of strategic metals once dispersed in the ecosystem.

This PhD work is part of the third objective of the LabEx R21, but also of the third working group of the COST (European cooperation in science and technology) NOTICE (network on technology-critical elements) Action TD1407 (https://www.costnotice.net/) (Cobelo-García *et*

al., 2015). This COST was created in 2015 with the aim of building a network of scientists interested in technology-critical elements and focus on three scientific areas (workgroup) as being (i) analytical chemistry, (ii) environmental biogeochemistry and (iii) human exposure and (eco)-toxicology.

Like the other strategic metals, REEs are undergoing a significant change in their cycle at the Earth's surface due to their increase use in a variety of technological applications. Their impact on their biogeochemical cycles and potential biological and human health threats needs to be further explored. The current diversity of results from the literature regarding their effect on biota shows a multiplicity of mechanisms associated with REEs. In addition to the biphasic response to REEs, there is currently a lack of a general basis about their toxicological effects on organisms. Despite these very few biochemical and genetic data available, especially about REE toxicity, the knowledge is still scarce and/or contradictory. Furthermore, studies mentioning mechanisms involved in absorption (e.g. membrane transport proteins), homeostasis and resistance of these emerging pollutants are also relatively rare.

OBJECTIVES

Four major questions arose after review of the current available knowledge: What are the proteins and cellular functions involved in the response to an REE stress? How are REEs transferred to organisms and what are the underlying transmembrane proteins transporting REEs? Are there different toxicity and resistance mechanisms between the REEs (LREEs *versus* HREEs)? Are REE accumulation and fractionation conserved traits in plants?

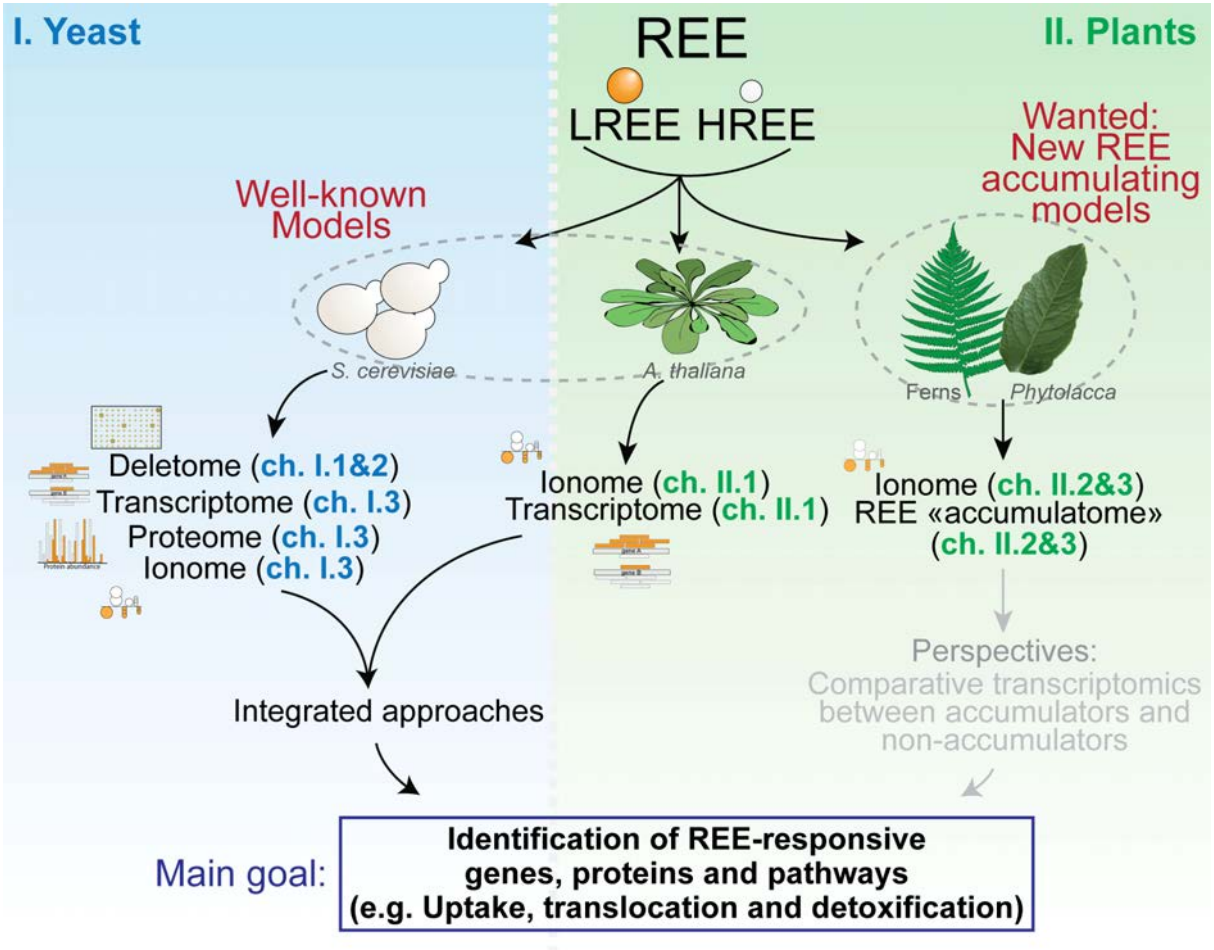

Figure 22 : General scheme of the Ph.D. work with the first part focusing on *Saccharomyces cerevisiae* and the second part on plants. The integrated approaches used to study responses to REE stress in order to identify genes, proteins, metabolites and pathways, are listed. The identification of new REE accumulating models is a first essential step for future work of comparative transcriptomics between accumulating and non-accumulating plants (grey) that is not tackled in this Ph.D. work.

To address these questions, the main objective of this thesis was to obtain a general view of REE transfer and the cellular and molecular impacts on model organisms. Therefore, we chose to study and identify the genes, proteins, and cellular pathways involved in the uptake and response to REEs by using high throughput complementary omic approaches on well-known model organisms. We also carried out a prospecting approach with REE accumulating plants

so as to identify tools that will be used for future molecular characterization of their accumulation mechanisms.

The thesis consists of two main parts, with the first analyzing REE toxicity towards the unicellular eukaryote *Saccharomyces cerevisiae* (Part 1), and the second studying REE homeostasis in plants, since they are more complex eukaryotes (Part 2). These two parts are divided into three chapters each, all contributing to the overall view of REE homeostasis in living organisms. Each chapter is presented in an article format consisting of an introduction, materials and methods, results, discussion and conclusion parts.

Part I: The use of genome-wide analyses in the eukaryotic model *Saccharomyces cerevisiae* to identify key mechanisms of REE toxicity and tolerance in eukaryotic cells (Figure 22.I).

Saccharomyces cerevisiae is one of the best eukaryotic organisms to be characterized (Botstein *et al.*, 1997); this relatively "simple" organism is, however, very similar to higher eukaryotes regarding its cell structure and physiological processes. *Saccharomyces cerevisiae* has been of particular interest in the study of cellular metal toxicity thanks to the wide range of tools and information available. Therefore, this organism was of particular interest to build a strong basis of the impact of REEs by:

I.1. Deciphering the toxicity and resistance mechanisms towards yttrium, a non-lanthanide REE using genomic phenotyping of a K.O. mutant collection of *S. cerevisiae*.

I.2. Investigating and comparing the toxicity and resistance mechanisms towards two distinct REEs belonging to the LREEs (La) and HREEs (Yb) using a genomic phenotyping of a K.O. mutant collection of *S. cerevisiae*, and complementary approaches.

I.3. Analyzing and comparing the response to LREEs (La) and HREEs (Yb) using transcriptomic and proteomic analyses. Additionally, the uptake mechanisms of REEs through the yeast plasma membrane were investigated.

Part II: Investigation of the REE toxicity, resistance and transfer mechanisms in plants, being more complex eukaryotes (Figure 22.II).

As previously mentioned, the increased demand, production, mining, and low recyclability of REEs, together with their use as fertilizer or their presence in phosphate fertilizers, has led to ecosystems becoming increasingly contaminated with REEs. In these different scenario, plants can be exposed to growing amounts of REEs, notably constituting an entry pathway for REEs in the ecosystem.

Therefore, we first used the well-known plant model *Arabidopsis thaliana*, which has been extensively used to identify metal toxicity and tolerance mechanisms in plants, to obtain the first insights into the global molecular pattern of REE transfer and impact on plants. This approach was carried out by the following methods:

II.1. Analyzing and comparing the response of *A. thaliana* to La and Yb by transcriptomic analyses, using RNA sequencing technology, and ionome analysis.

To further understand REEs' effects and homeostasis in plants, we looked for new REE-accumulating plants. The use of such plants as models in which the genes and mechanisms involved in REE specific accumulation and/or resistance is likely to become crucial in future research, which is a particularly interesting concern. These plants are good candidates to identify genes and mechanisms involved in REE transfer and tolerance through a comparative transcriptomic study of related species with contrasting phenotypes (e.g. strong REE accumulation *versus* no accumulation). This work is a post-thesis perspective, however, as a first step we screened a substantial number of plant species for their accumulation potential, and stress tolerance towards REEs, also in addition to their REE fractionation pattern. Consequently, the following chapters consist of:

II.2. Screening *Phytolacca* species to investigate whether REE accumulation and fractionation traits are conserved among the genus, and to study the effect of REEs on plant physiology (e.g. stress, root architecture, ionome).

II.3. Screening a collection of hardy ferns, belonging to different species and genera for their REE accumulation potential and REE fractionation pattern.

Part I:

The use of genome-wide analyses in the eukaryotic model ***Saccharomyces cerevisiae*** to identify key mechanisms of REE toxicity and tolerance in eukaryotic cells

Introduction

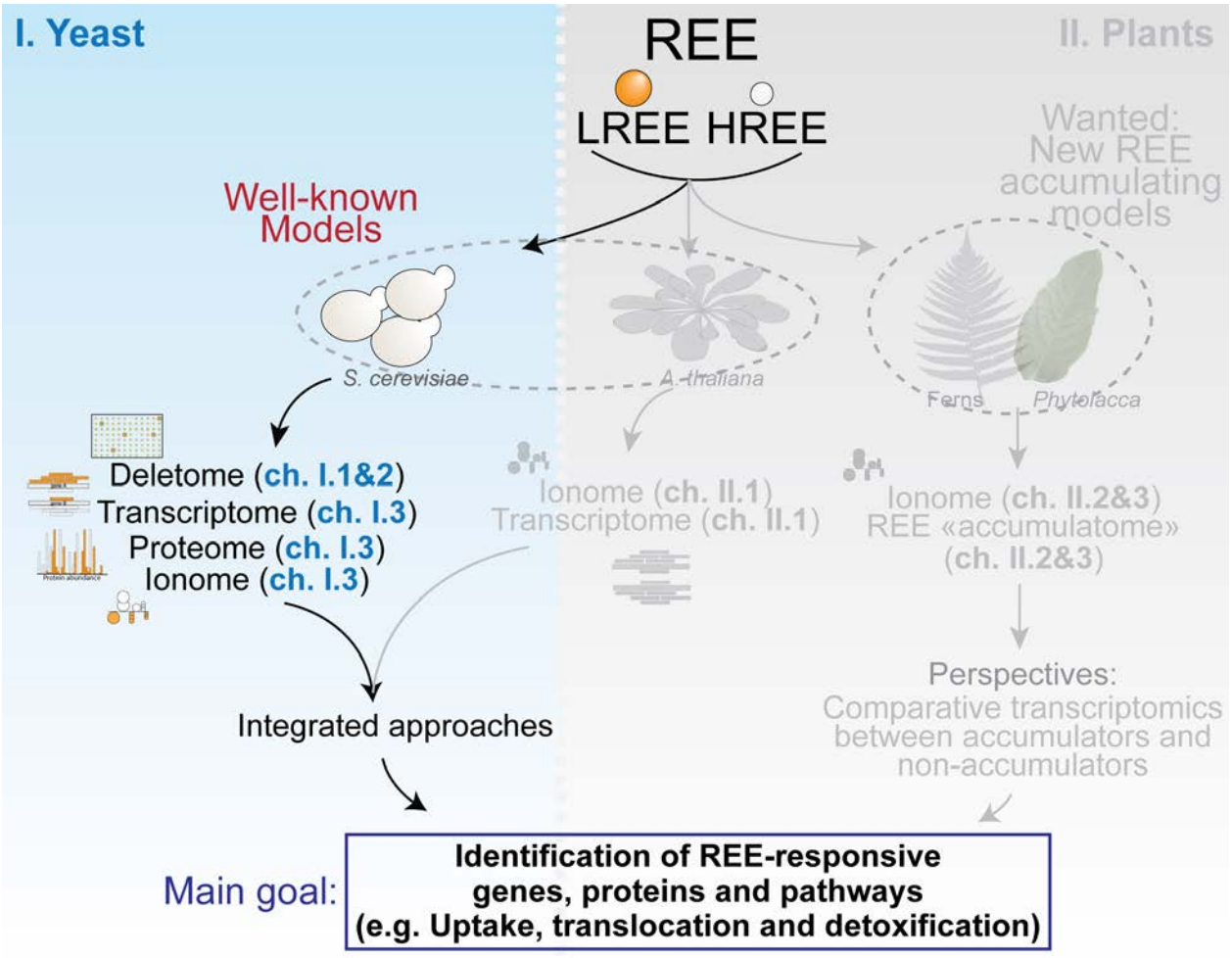

Figure 23: General scheme of the Ph.D. work with the first part focusing on Saccharomyces cerevisiae. The integrated approaches used to study the responses to REE stress in order to identify genes, proteins, metabolites and pathways, are listed.

In the first part of this study, we focused on different steps of the cellular response. To investigate this, we carried out four complementary large-scale omic methods, consisting of the screening of a genome-wide mutant collection on several REEs, transcriptional analyses (RNA-seq), in proteomic analyses (shot-gun), and the ionome profiling under REE stress. We considered the use of the well-known eukaryotic model *Saccharomyces cerevisiae* to be of particular interest for unravelling the main mechanisms affected under REE stress and in REE uptake. The first part of the study combined these different approaches for different REEs and is divided into three chapters;

Chapter I.1: We first aimed to decipher the toxicity and resistance mechanisms towards Y, one of the most produced REE and also a non-lanthanide REE. We considered the genomic phenotyping of a K.O. mutant collection of *S. cerevisiae* (a large-scale approach without prior

assumptions) to be of particular interest for the purpose of highlighting the biological functions involved in response to this element. Screening a mutant collection consists of identifying mutants for a single gene that are either more sensitive or resistant towards a sublethal concentration of a metal, here Y, compared to the wild type strain. The phenotype of the mutants gives information on the role of genes in the response to this element. A resistant mutant will indicate that the missing gene is involved in the toxicity as a result of exposure to the metal, while a sensitive mutant will inform about its important role in resistance (e.g. detoxification processes). The current lack of data concerning Y toxicity at the cellular and molecular levels made this a pioneering study for the assessment of Y toxicity towards eukaryotes, for which we used the model organism *S. cerevisiae*.

Chapter I.2: Although yttrium is considered to be a non-lanthanide element, it is usually included among the HREEs, due to its high similarity (e.g. ionic radius) to Dy and Ho. Nevertheless, only few studies have proposed that LREEs and HREEs may induce different and/or specific responses, which could be either due to their decreasing ionic radius and increased atomic mass (so-called lanthanide contraction) or, to their reactivity or chemical differences (Gonzalez *et al.*, 2014; Wang *et al.*, 2017). Consequently, we hypothesized that discrepancies could exist in the cellular response to toxic concentrations of LREEs *versus* that of HREEs. To test our hypothesis, a similar approach of genomic phenotyping of a mutant collection of *S. cerevisiae* was carried out by comparing two lanthanides. By doing so, we aimed to elucidate whether LREEs and HREEs would induce specific responses, using La and Yb as respective representatives. We expanded on the results obtained by carrying out proteomic analyses on mutants selected from the screening and a sphingolipidomic analysis in order to better describe the molecular players involved in the stress response to lanthanides.

By combining these different complementary approaches, we unravelled the toxicity and resistance mechanisms towards La and Yb. Our study allowed us to first observe that La and Yb involved different toxicity and resistance mechanisms in yeast. Additionally, we revealed that the Y toxicity pattern is similar to that of Yb, but is different from that of La.

Chapter I.3: In the first two chapters, our approach was essentially based on the genomic phenotyping of a mutant collection of *S. cerevisiae* towards different REEs. We observed that although Y, La and Yb are members of the same group of elements, discrepancies appeared in the toxicity and tolerance mechanisms involved towards these different REEs. These methods allowed us to pinpoint the major role of the cell wall and plasma membrane

organization but also that of the endocytic pathway and sphingolipid biosynthesis, in the REE response of *S. cerevisiae*.

To further understand the effects of REEs on yeast cells, we used two additional complementary large-scale omic methods, focusing on the following steps of the cellular response. Combining transcriptomic and proteomic analyses, we compared the responses to La and Yb. Unlike the use of a mutant collection, the data obtained by these two methods reflected the REE response of the wild type cells, without modification of the yeast genome. These complementary approaches reinforced the conclusions obtained previously such as the key role of the cell wall in the response to REEs. It also further enlarged our understanding of the lanthanide stress response, and emphasized the uptake mechanisms of REEs by yeast cells.

Altogether, these methods allowed us to pinpoint the major role of the cell wall and the plasma membrane organization, in addition to the endocytic pathway and sphingolipid biosynthesis, in the REE response of *S. cerevisiae*. Furthermore, we confirmed that REE uptake is mediated through non-specific plasma membrane transporters, specifically those for Ca and for the first time evidenced the involvement of Fe transporters. The unique metallic stress response triggered in this model organism by REEs, and the differences observed between LREEs and HREEs, provide a thorough foundation in the understanding of the potential impact of REEs on eukaryotic organisms at the cellular and molecular levels. The close homology of genes shared between yeast and other eukaryotes will also enable one to infer the consequences of REE dissemination in the ecosystem and further assess human health risks linked to REE toxicity.

In this part, the elemental analyses by ICP were performed by Dr. Nadia Crini (LCE, Besançon, France), the proteomic analyses by Dr. Jean Armengaud (CEA Marcoule, Bagnols-sur-Cèze, France), and the sphingolipid analyses by Dr. Josephina Casas (RUBAM, Barcelona, Spain).

Chapter I.1:

Global deletome profile of *Saccharomyces cerevisiae* exposed to the technology-critical element yttrium

frontiers in Microbiology

ORIGINAL RESEARCH
published: 04 September 2018
doi: 10.3389/fmicb.2018.02005

Global Deletome Profile of *Saccharomyces cerevisiae* Exposed to the Technology-Critical Element Yttrium

Nicolas Grosjean[1,2], Elisabeth M. Gross[2], Marie Le Jean[2†] and Damien Blaudez[1†]*

[1] Université de Lorraine, CNRS, LIEC, Nancy, France, [2] Université de Lorraine, CNRS, LIEC, Metz, France

The emergence of the technology-critical-element yttrium as a contaminant in the environment raises concern regarding its toxicological impact on living organisms. The molecular mechanisms underlying yttrium toxicity must be delineated. We considered the genomic phenotyping of a mutant collection of *Saccharomyces cerevisiae* to be of particular interest to decipher key cellular pathways involved either in yttrium toxicity or detoxification mechanisms. Among the 4733 mutants exposed to yttrium, 333 exhibited modified growth, of which 56 were sensitive and 277 were resistant. Several functions involved in yttrium toxicity mitigation emerged, primarily vacuolar acidification and retrograde transport. Conversely, functional categories overrepresented in the yttrium toxicity response included cytoskeleton organization and endocytosis, protein transport and vesicle trafficking, lipid metabolism, as well as signaling pathways. Comparison with similar studies carried out using other metals and stressors showed a response pattern similar to nickel stress. One third of the identified mutants highlighted peculiar cellular effects triggered by yttrium, specifically those affecting the pheromone-dependent signaling pathway or sphingolipid metabolic processes. Taken together, these data emphasize the role of the plasma membrane as a hotspot for yttrium toxicity. The up-to-now lack of data concerning yttrium toxicity at the cellular and molecular levels makes this pioneer study using the model *S. cerevisiae* an excellent first basis for the assessment of yttrium toxicity toward eukaryotes.

Keywords: genome-wide screening, *Saccharomyces cerevisiae*, technology critical element, yeast mutants, yttrium toxicity

OPEN ACCESS

Edited by:
Michael Benedik,
Texas A&M University, United States

Reviewed by:
Jiangxin Wang,
Shenzhen University, China
Stefan Fränzle,
Technische Universität Dresden, Germany
Darren Greetham,
University of Huddersfield, United Kingdom
Chris Vulpe,
University of Florida, United States

***Correspondence:**
Damien Blaudez
damien.blaudez@univ-lorraine.fr

† These authors have contributed equally to this work

Specialty section:
This article was submitted to Microbiotechnology, Ecotoxicology and Bioremediation, a section of the journal Frontiers in Microbiology

Received: *17 April 2018*
Accepted: *08 August 2018*
Published: *04 September 2018*

Citation:
Grosjean N, Gross EM, Le Jean M and Blaudez D (2018) Global Deletome Profile of Saccharomyces cerevisiae Exposed to the Technology-Critical Element Yttrium. Front. Microbiol. 9:2005. doi: 10.3389/fmicb.2018.02005

INTRODUCTION

Mainly mined in China, which possesses the largest deposits, and lower proportions in India, Brazil, and Malaysia, yttrium is a metallic element belonging to the group of rare earth elements (REE). Yttrium is naturally present in the earth crust with an abundance similar to cobalt, zinc, copper, chromium, or lead (Haxel et al., 2002). This element displays unique and essential properties for diverse technologies and is therefore considered a technology-critical element (TCE). The main use of yttrium is for phosphor production (54%) and, to a lesser extent, in white LED lights and ceramic production (32%) (Ciacci et al., 2015). Additional minor uses are also reported, such as additives to improve glass resistance or mechanical properties of alloys, in some lasers, as a catalyst in ethylene polymerization, or in cancer treatment using the radioactive isotope yttrium-90 (Riaz et al., 2014).

According to the expansion of these high technology-related needs, annual yttrium production is strikingly rising. It rose from 2400 t/year in 1998 (United States Geological Survey, 2000) to 8000–10,000 t/year in 2015 (United States Geological Survey, 2016). As a consequence, high residual yttrium concentrations (e.g., from 148 to 330 ppm in the A layer and from 60 to 242 ppm in the B layer in soil samples from Chinese mining sites) can be found at REE-mining sites (Wei et al., 2001). Additionally, other anthropogenic activities also contribute to the spreading of yttrium in the environment. Deposits from the combustion of coal still significantly contribute to the dissemination of yttrium worldwide, with concentrations ranging from 94 to 3540 ppm (mean 408) in coal ash and 191–259 ppm in coal fly ash (Mayfield and Lewis, 2013). Moreover, up to 110 ppm yttrium can be found in phosphate rocks (Bunus, 2000). In addition to the increasing demand and spread, another major drawback is the lack of sustainable processes for the recycling of end-use products containing this element. Taken together, these observations suggest that yttrium is an emerging contaminant for the environment (Ciacci et al., 2015).

Few studies are currently available regarding the effect of TCE on the environment or on organisms, despite its increasing abundance. To date, the scarce data concerning yttrium toxicity (Hirano et al., 1993; Li et al., 2015; Zhang et al., 2016; Trifuoggi et al., 2017; Wang Y. M. et al., 2017) mostly focus either on yttrium nanoparticles (Zhang et al., 2016; Zhou et al., 2016) or indirect effects caused by the use of the radioactive isotope yttrium-90 (Riaz et al., 2014). Although yttrium toxicity has been observed for some organisms, the associated detrimental mechanisms remain unknown (Hirano et al., 1993; Li et al., 2015; Zhang et al., 2016; Trifuoggi et al., 2017; Wang Y. M. et al., 2017). Thus, there is a strong interest in unraveling the potential toxicological effects of these elements on well-known organisms to build a general and robust knowledge.

The budding yeast *Saccharomyces cerevisiae* has been widely used as a model to uncover metal toxicity mechanisms as well as pathways that allow eukaryotes to cope with toxic metals. As an example, unprogrammed gene silencing, a major mechanism of nickel toxicity and carcinogenicity in humans, was also identified in *S. cerevisiae* (Lee et al., 1995; Broday et al., 1999; Sutherland et al., 2001; Costa et al., 2005). Those findings further support the use of *S. cerevisiae* as a model organism to elucidate metal toxicity mechanisms in humans due to the high conservation of such mechanisms between these organisms. Genomic phenotyping of knock-out (KO) mutant collections is a method of choice to decipher general functions as well as key genes involved in metal homeostasis in *S. cerevisiae*. This experimental approach has been widely applied, since the KO mutant collection release for various metals such as cadmium (Ruotolo et al., 2008; Serero et al., 2008; Thorsen et al., 2009; Wang, L. et al., 2017), nickel (Ruotolo et al., 2008; Arita et al., 2009; Bleackley et al., 2011), zinc (Pagani et al., 2007; Wang et al., 2007; Jin et al., 2008; Bleackley et al., 2011), aluminum (Kakimoto et al., 2005; Tun et al., 2014), arsenic (Haugen et al., 2004; Thorsen et al., 2006, 2009; Jin et al., 2008; Ruotolo et al., 2008; Serero et al., 2008; Johnson et al., 2016a), copper (Wang et al., 2007; Jo et al., 2008; Bleackley et al., 2011), iron (Wang et al., 2007; Jo et al., 2008; Bleackley et al., 2011), manganese (Wang et al., 2007; Bleackley et al., 2011; Chesi et al., 2012), cobalt (Bleackley et al., 2011), or chromium (Jin et al., 2008; Johnson et al., 2016b) among others. The identified mechanisms thanks to this model organism and approach have provided insights into conserved pathways in other eukaryotes (Botstein et al., 1997; Kachroo et al., 2017).

In this study, the knock-out mutant collection of the haploid strain BY4741 from EUROSCARF was screened to identify both sensitive and resistant mutants to yttrium. The yttrium-specific response was analyzed by comparisons between our set of data with those from previous phenotypic screens on other metals or stressors. The cellular compartments and functions involved in the response to yttrium exposure were investigated in detail, shedding light for the first time on molecular responses toward this emerging contaminant.

MATERIALS AND METHODS

Yeast Strains and Chemicals

The wild-type BY4741 strain of *S. cerevisiae* (MATa his3Δ1 leu2Δ0 met15Δ0 ura3Δ0) and the complete set of 4733 deletion mutants for non-essential genes used in this study were purchased from EUROSCARF (Institute of Molecular Biosciences, Frankfurt, Germany). Mutants of the *S. cerevisiae* BY4742 strain (MATα his3Δ1 leu2Δ0 lys2Δ0 ura3Δ0) were also purchased from EUROSCARF. Yttrium(III) chloride hexahydrate (99.9% purity, #211648) was from Sigma-Aldrich (St. Louis, MO, United States).

Yttrium Toxicity Screening

The wild-type strain and the deletion mutants, arrayed in 96-well master plates, were grown in 200 μL of YPD (10 $g.L^{-1}$ peptone, 20 $g.L^{-1}$ glucose, and 10 $g.L^{-1}$ yeast extract) medium until stationary phase at 28°C. A first screening for the identification of Y-resistant and Y-sensitive mutants was carried out by comparing their growth (respectively, increased or impaired) to that of the wild-type on a toxic yttrium concentration. In more detail, the strains were pin replicated using a Thermo Scientific™ Nunc™ Replication System (250520) on YPD agar plates or on the same medium supplemented with 3.75 mM yttrium chloride, allowing us to visually identify in a single step both resistant and sensitive strains. Four pin replications were performed for each mutant. Growth was recorded after 5 days at 28°C. In a second screening, the previously selected mutants were individually retested to confirm their sensitive or resistant phenotype by 10-fold serial dilution spot assays. The mutant and the wild-type strains were grown as described above, and 5 μL of stationary cultures were further diluted from 10^0 to 10^{-5} and spotted on YPD agar plates supplemented with 100% (3.75 mM) and 105% (3.90 mM) of the yttrium concentration used in the first screening. These concentrations were chosen to discriminate the different sensitivity and resistance levels, respectively, as defined below. Growth was recorded after 7 days at 28°C. Sensitivity and resistance levels were assigned to the mutant strains, according to the number of growing dilutions. Consequently, mutant strains exhibiting a reduction in

colony-forming ability at the first, second-third, or fourth-fifth dilution were classified as "high" (HS), "medium" (MS), or "low" (LS) sensitive to yttrium, respectively. Conversely, mutant strains exhibiting an increase in colony-forming ability at the second, third-fourth, or fifth-sixth dilution were classified as "low" (LR), "medium" (MR), or "high" (HR) resistant to yttrium, respectively. Finally, a set of 20 mutants, randomly chosen in the different sensitivity/resistance categories, was confirmed in the parent MATα BY4742 background.

Gene and Function Annotation

Gene descriptions corresponding to the Y-sensitive and Y-resistant mutants were retrieved from the Saccharomyces Genome Database (SGD)[1]. Biological process as well as cellular compartment analyses were performed using KEGG[2], MIPS, Gene Ontology [GO Term Finder Program (Boyle et al., 2004)] and FunSpec[3] and evaluated for statistical significance (cutoff: $P < 0.01$). The Y mutant set comparisons with other screenings were carried out by cluster analyses using Cluster 3.0 (Hoon et al., 2004) and Java Treeview 1.1.6r4[4]. Hierarchical clustering was performed with the following parameters: average linkage, uncentered correlation, and *k*-mean = 10 when stated. To achieve this analysis, data sets were retrieved from previous genomic phenotyping studies and used if a sufficient number (>50) of mutants was identified. When several independent studies performed similar screenings on the same stressor, the corresponding lists of mutants were combined. Putative Human orthologs of yeast genes and any of their associated OMIM (Hamosh et al., 2005) disease phenotypes were retrieved from the SGD YeastMine platform[5].

Functional Enrichment Analysis

The biological pathways that showed enrichment in the yttrium stress condition vs. control were identified using GSEA software v2.0 (Subramanian et al., 2005). The sensitivity and resistance of each mutant was binary encoded to −1 and +1, respectively, for gene ranking. *S. cerevisiae* GO (biological process) derived from the MSigDB format gene-sets list was downloaded from the GO2Msig (Powell, 2014) database and used as a template. The gene set sizes retrieved from GO2Msig datasets were limited to a maximum of 150 and a minimum of 15. Cytoscape v3.4 software (Shannon et al., 2003) and the Enrichment Map v2.1.0 (Merico et al., 2010) plug-in with default settings were used to visualize the GSEA results.

RESULTS

Genomic Phenotyping of Yttrium Toxicity

Phenotypic screening of the whole haploid KO mutant collection of *S. cerevisiae* strain BY4741 allowed the identification of mutants with modified growth compared with the wild-type strain when exposed to the TCE yttrium (**Figure 1**). The second screening showed that the number of false positives picked from the first screening was relatively low (10% of the total set) (data not shown). Among the 333 confirmed Y-responsive mutants, 56 were sensitive while five times as many (277) exhibited a resistant phenotype (**Figure 2**). Following the second screening, mutants were classified into six different categories by their degree of sensitivity/resistance relative to the wild-type strain [spanning from highly sensitive (HS) to highly resistant (HR) mutants] (**Figure 1**). Among the resistant mutants, 14.8%, named in **Figure 2**, were HR. The proportion was similar (16.1%) for HS mutants. The number of low (LR) and medium (MR) resistant mutants accounted for 44.0 and 41.2% of the total resistant set, respectively. Similarly, the number of low (LS) and medium (MS) sensitive mutants represented 41.1 and 42.8% of the sensitive mutants, respectively (**Figure 2**). Yttrium sensitivity or resistance phenotypes were confirmed using randomly chosen mutants, by independent serial dilution assays carried out on mutant strains of the opposite mating type (BY4742) (**Supplementary Table 1**). A total of 29 mutants for dubious proteins (8%) and 22 for uncharacterized ORFs (6%) were included in the 333 mutants (**Supplementary Table 2**).

Further examination of the details of cellular compartments related to these mutants allowed the identification of hotspots for either yttrium toxicity or detoxification. From enquiries of the MIPS subcellular localization database, the following subsequent cellular compartments were predominantly represented: endosome ($P < 1.00e{-}14$, 22 mutants out of 57), vacuole ($P = 4.07e{-}05$, 26 out of 224), Golgi apparatus ($P = 4.24e{-}04$, 16 out of 125), endoplasmic reticulum membrane ($P = 5.29e{-}03$, 14 out of 131), and Golgi-ER transport vesicles ($P = 9.10e{-}03$, 8 out of 60) (**Table 1**). For the Y-resistant mutants, endosome ($P = 4.53e{-}13$, 19 out of 57), vacuole ($P = 2.30e{-}03$, 19 out of 224), and plasma membrane ($P = 9.25e{-}03$, 15 out of 184) were clearly mostly impacted, while for sensitive mutants, vacuole ($P = 2.14e{-}03$, 7 out of 224) and Golgi ($P = 3.38e{-}03$, 5 out of 125) were emphasized (**Table 1**). Interestingly, compartments such as mitochondria and nucleus were not significantly represented (**Table 1**).

As a good eukaryotic model, the OMIM human-related diseases tool from the SGD yeastMine platform allowed the identification of human orthologs and associated disease phenotypes. One or more human orthologs were found for up to 188 of the 333 genes (56.5%) for which deletion rendered the mutant strains resistant or sensitive to yttrium. As high as 59 of these genes (17.7%) are involved in human diseases, such as cancer (**Supplementary Table 2**).

Comparison of Cellular Toxicity Signatures Between Yttrium and Other Metals

A comparison of the present Y dataset with other genome-wide deletion mutant screenings carried out on other metals (Cd, Cr, Ni, Cu, Fe, Co, Zn, Mn) and metalloid (As) is provided (**Figure 3**). Excluding Cu, few sensitive mutants (13) grouped

[1]http://www.yeastgenome.org
[2]http://www.genome.jp/kegg/
[3]http://funspec.med.utoronto.ca
[4]http://jtreeview.sourceforge.net
[5]http://yeastmine.yeastgenome.org/yeastmine/

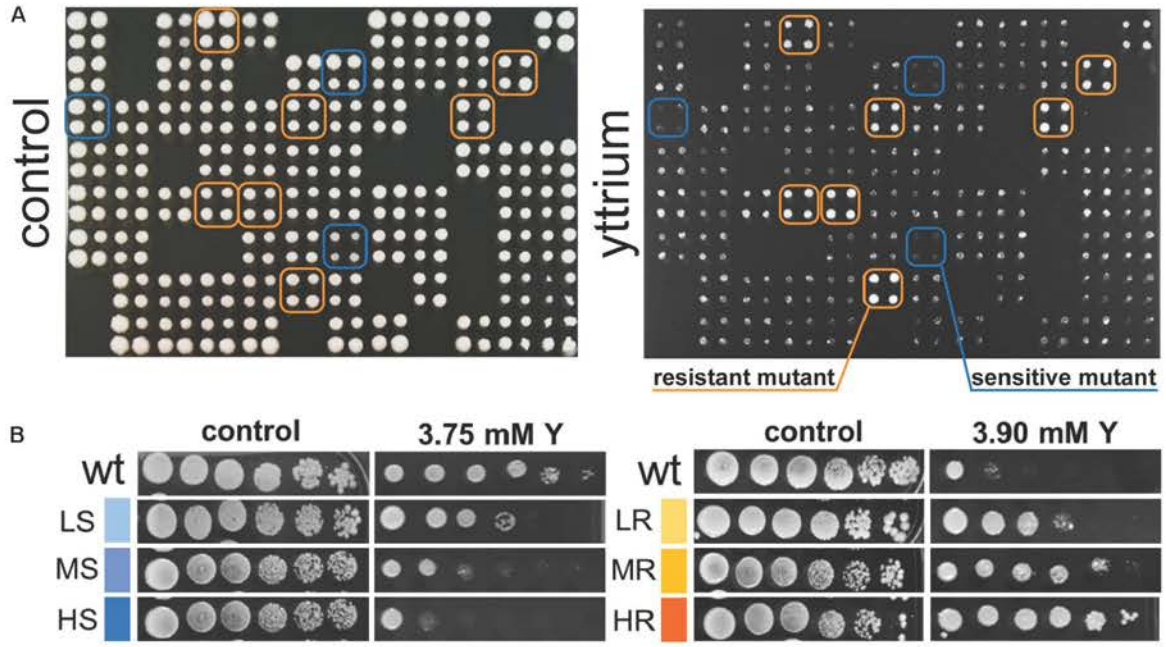

FIGURE 1 | Representative primary screen data for yttrium-responsive mutants and phenotypic confirmation of the identified mutants. **(A)** Representative 384-well format growth test for the yttrium toxicity primary screen (four pin replication of each mutant). A control plate (YPD medium) and the same plate supplemented with 3.75 mM yttrium are shown. Putative yttrium sensitive (blue) and resistant mutants (orange) are highlighted. **(B)** Phenotypic confirmation of selected sensitive and resistant mutants. Wild-type and mutant strains were grown without or with yttrium. Yttrium sensitivity was determined by 10-fold serially diluted spot assays (left to right) with saturation phase grown cells. Mutant strains exhibiting a reduction in colony-forming ability at the first, second-third or fourth-fifth dilution were classified as "high" (HS), "medium" (MS), or "low" (LS) sensitive to yttrium, respectively. Conversely, mutant strains exhibiting an increase in colony-forming ability at the second, third-fourth, or fifth-sixth dilution were classified as "low" (LR), "medium" (MR), or "high" (HR) resistant to yttrium, respectively.

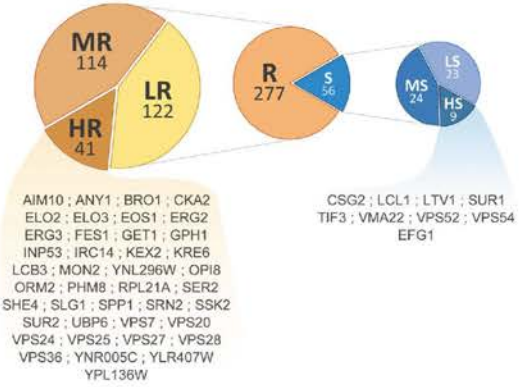

FIGURE 2 | Distribution and ranking of yttrium-responsive mutants. The middle pie chart shows the overall number of resistant (orange) and sensitive (blue) mutants. Detailed proportions of the different categories low (LR), medium (MR), high (HR) resistant mutants (left) and low (LS), medium (MS), and high (HS) sensitive mutants (right) are shown. ORF names of HR and HS mutants are mentioned.

together regardless of the metallic species tested, highlighting common response pathways (cluster C1). These shared mutants were notably involved in a global cellular response to metallic stressors such as vacuolar acidification (VMA mutants) and response to DNA damage stimulus. Cluster C3 contained 14 mutants that were sensitive to all metals but Ni, and involved in retrograde transport, Golgi to vacuole transport and glycosphingolipid process. A wide range of resistant mutants (106) were specific to yttrium stress (cluster C6) and belonged to different biological processes spanning the response to pheromone to the sphingolipid metabolic pathway (**Figure 3**).

Regarding mutants with an opposite behavior between yttrium and other metallic species, only three mutants were sensitive to yttrium but resistant toward other metals (ΔSmf2, ΔBud19, and ΔSin4), whereas 179 mutants were resistant to yttrium but sensitive to at least one other metal (clusters C4-C5-C7-C8-C9-C10). Among the latter, several biological processes were represented, mostly belonging to the lipid and fatty acid biosynthetic processes but also to the actin filament/cytoskeleton organization and endocytosis (**Figure 3**). It is noteworthy that the highest similarities were shared between yttrium and nickel (**Figure 3**). Eighty-five mutants displayed a modified phenotype toward both elements, either with the same or opposite behavior. More striking were the 39 mutants that were resistant to both nickel and yttrium (C8-C9) but sensitive to other elements. These mutants belonged mainly to the ubiquitin-dependent protein catabolic process via the multivesicular body (MVB) sorting pathway ($P < 1.00e{-}14$), including ΔStp22, ΔDoa4, ΔVps25, ΔDid4, ΔSnf7, ΔSrn2, ΔVps36, ΔVps20, ΔSnf8, and ΔVps28. The proteins encoded by these genes are involved in the ESCRT complex and in protein trafficking.

TABLE 1 | MIPS subcellular compartments involved in the yttrium stress modulation response.

		All mutants		Resistant mutants		Sensitive mutants	
Subcellular compartment	***f***	***p*-value**	***k***	***p*-value**	***k***	***p*-value**	***k***
Endosome	57	<1.00e−14	22	4.53e−13	19	NS	3
Vacuole	224	4.07e−05	26	2.30e−03	19	2.14e−03	7
Golgi	125	4.24e−04	16	NS	11	3.38e−03	5
ER membrane	131	5.29e−03	14	NS	11	NS	3
Golgi-ER transport vesicles	60	9.10e−03	8	NS	6	NS	2
Plasma membrane	184	NS	–	9.25e−03	15	NS	–
Nucleus	–	NS	–	NS	–	NS	–
Mitochondria	–	NS	–	NS	–	NS	–
Peroxisomes	–	NS	–	NS	–	NS	–

k is the number of mutants found during the present screening, and f is the number of proteins gathered under the category mentioned. NS, not significant.

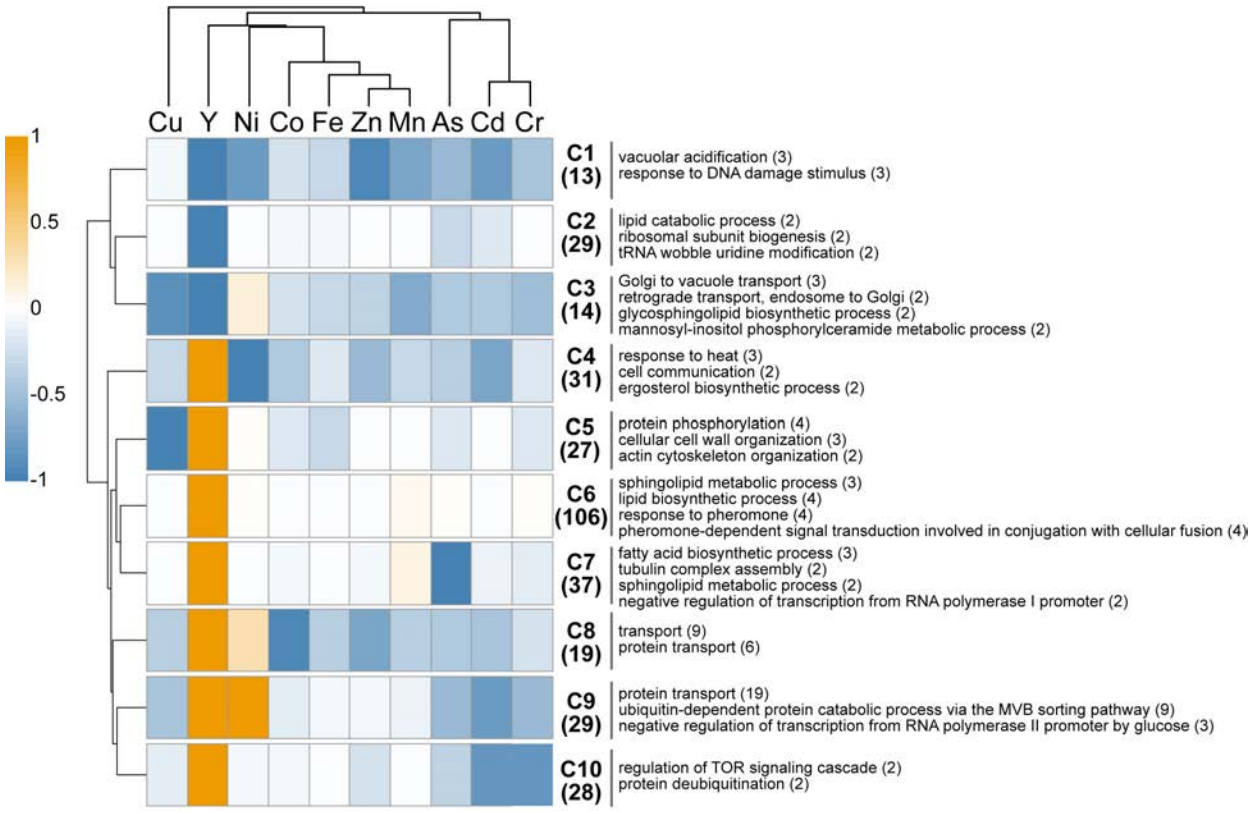

FIGURE 3 | *In silico* comparison of phenotypes of the mutants identified in this study compared with those from other metal-based screening studies. Different colors represent the mean phenotype of the clustered mutants (orange: resistant, blue: sensitive). Functions overrepresented in the clusters (C1–C10) are mentioned on the right. The number of mutants within each cluster or function is specified in brackets. Functions considered were retrieved from FunSpec (biological process GO terms, $P < 0.01$). The hierarchical clustering was done with the following parameters: average linkage, uncentered correlation, *k*-mean = 10.

Comparison of Cellular Toxicity Signatures Between Yttrium and Other Stressors

The same comparative approach was undertaken to investigate putative correlations/convergences between yttrium and gamma-rays, alkaline pH, or oxidative stress induced by a set of chemicals (Bennett et al., 2001; Chang et al., 2002; Aouida et al., 2004; Serrano et al., 2004; Thorpe et al., 2004; **Figure 4**). Interestingly, three different patterns could be observed. First, only a few mutants (40) shared a sensitive phenotype between yttrium and at least one of these other stressors. Second, 115 mutants that were sensitive to those stressors were resistant to yttrium. Third, the majority of the mutants (176) identified in this study were only responding to yttrium (**Figure 4**).

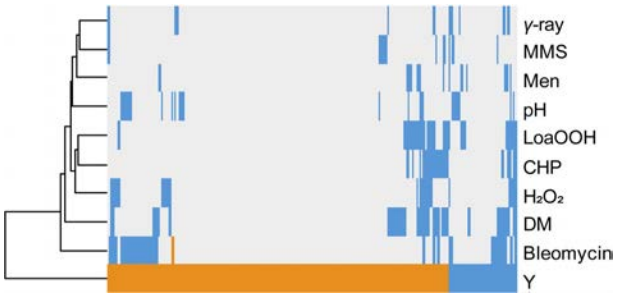

FIGURE 4 | Hierarchical clustering of yttrium sensitivity or resistance-conferring mutations with the mutant sensitivity/resistance profiles of other stressors. The *x*-axis corresponds to gene deletions, and the *y*-axis represents the different physico-chemical stressors. Mutant strains exhibiting either a higher sensitivity, a higher resistance, or no phenotype change when compared to wild-type are shown in blue, orange, and gray, respectively. Non-metal stressors were selected from previous genomic phenotyping screenings conducted on deletion mutant collections. Methyl methane sulfonate (MMS), gamma-radiation (γ-ray), alkaline pH (pH), menadione (Men), hydrogen peroxide (H_2O_2), cumene hydroperoxide (CHP), linoleic acid 13-hydroperoxide (LoaOOH), and diamide (DM). Hierarchical clustering was done with the following parameters: average linkage and uncentered correlation.

Mutations Accounting for Yttrium Sensitivity

To assess the global cell response to yttrium, functions involved in yttrium toxicity (resistant mutants) or yttrium resistance (sensitive mutants) mechanisms were revealed by functional enrichment analysis by combining both GO term finder and GSEA approaches (**Figure 5** and **Supplementary Table 3**). In this sub-section, we focus on the description of sensitive mutants, the growth of which was partially or completely inhibited by yttrium exposure. The nine mutants displaying an exacerbated sensitivity (HS mutants) (**Figure 2**) were considered to participate in either the glycosphingolipid metabolic/biosynthetic process (P = 3.82e−04) or cellular chemical homeostasis (P = 3.82e−03) (**Supplementary Table 4**).

From the entire set of mutants, two mutants (ΔSur1 and ΔCsg2) that were sensitive to yttrium were impaired in the glycosphingolipid biosynthetic process (P = 1.96e−04) (**Supplementary Table 3**). Sur1p (also known as Csg1p) is a mannosylinositol phosphorylceramide (MIPC) synthase catalytic subunit that forms a complex with the regulatory subunit Csg2p to act as an inositol phosphorylceramide mannosyltransferase complex.

Ion homeostasis consisted of only sensitive mutants (**Figure 5**). It embodied three different GO terms identified as vacuolar proton-transporting V-type ATPase complex assembly (P = 3.90e−04), vacuolar acidification (P = 1.18e−03), and ATP hydrolysis coupled proton transport (P = 8.25e−03). The only representatives of the VMA family genes were *vma21*, *vma22*, *vma7,* and *vma16* (**Supplementary Table 3**).

As high as 25% of the total sensitive mutants belonged to the transport function (P = 4.79e−03, 14 genes out of 815) (**Supplementary Table 3**). A significant proportion of sensitive mutants consisted of proteins that participate in vesicle transport from both the endosome to the trans-Golgi (P = 3.87e−04) and from the Golgi to the vacuole (P = 3.76e−05) (**Figure 6** and **Supplementary Table 3**). The GARP (Golgi Associated Retrograde Protein) complex is responsible for vesicles fusion from the endosome to the trans-Golgi (**Figure 6A**). Mutants for *VPS54*, *VPS52,* and *VPS51*, three components of the GARP complex, were particularly sensitive to yttrium (**Figure 6B**). The retrograde transport, which includes the GARP complex, allows the trafficking of extracellular molecules as well as the plasma membrane internalized by endocytosis to the trans-Golgi, thus participating in the recycling of either proteins or lipids from the membrane (**Figure 6A**). Although endocytosis (P = 4.36e−03) was also involved, it was represented by only 4 sensitive mutants ΔCdc50, ΔRcy1, ΔVps1, and ΔTlg2 (**Supplementary Table 3**). As part of the SNARE complex (Soluble NSF Attachment Protein Receptor), Tlg2p is also involved in vesicle fusion to the trans-Golgi along with the GARP complex (Burri and Lithgow, 2004; **Figure 6B**). Both Cdc50p and Rcy1p are not only involved in the polarized growth of *S. cerevisiae*, but they also play a role in recycling plasma membrane proteins internalized by endocytosis. In the same way, Vps1p, a dynamin-like GTPase, is required for actin cytoskeleton organization and endocytosis.

Linked to previously unraveled functions, 11 mutants impaired in protein transport (P = 1.97e−04) were also sensitive to yttrium. The corresponding proteins were involved at different levels in the protein transport machinery (**Supplementary Table 3**), as illustrated by the following cases. Pep3p as part of the CORVET membrane tethering complex (class C core vacuole/endosome tethering), is involved in vesicular docking fusion together with SNARE protein (Tlg2p), allowing vacuolar biogenesis. The ΔApl2 mutant was also sensitive to yttrium (**Figure 6B**). The latter protein is a subunit of the clathrin-associated protein (AP-1) complex that is involved in clathrin-dependent Golgi protein sorting. Lst4p, for its part, is required for the transport of an amino acid permease from the Golgi to the cell surface. Finally, Cog1p acts in protein trafficking by mediating the fusion of transport vesicles to Golgi compartments.

Among the group of mutants that were identified from the present screening, four mutants for protein components of nuclear and mitochondrial ribosomal subunits displayed a sensitive phenotype (**Supplementary Table 2**). Mrpl27p, a component of the mitochondrial large ribosomal subunit, Rps16ap and Rps19bp, which are part of the nuclear small ribosomal subunit, and Rpp2bp, a component of the ribosomal stalk.

Mutations Accounting for Yttrium Resistance

Many additional yttrium-resistant over sensitive mutants ensued from the screening. Mutants were considered resistant if their growth was improved compared with the wild-type strain under yttrium exposure. This phenotype indicated a key role of the deleted gene in yttrium cell toxicity since its absence allowed the yeast cells to better cope with this element. Conversely to HS mutants, the 41 HR mutants

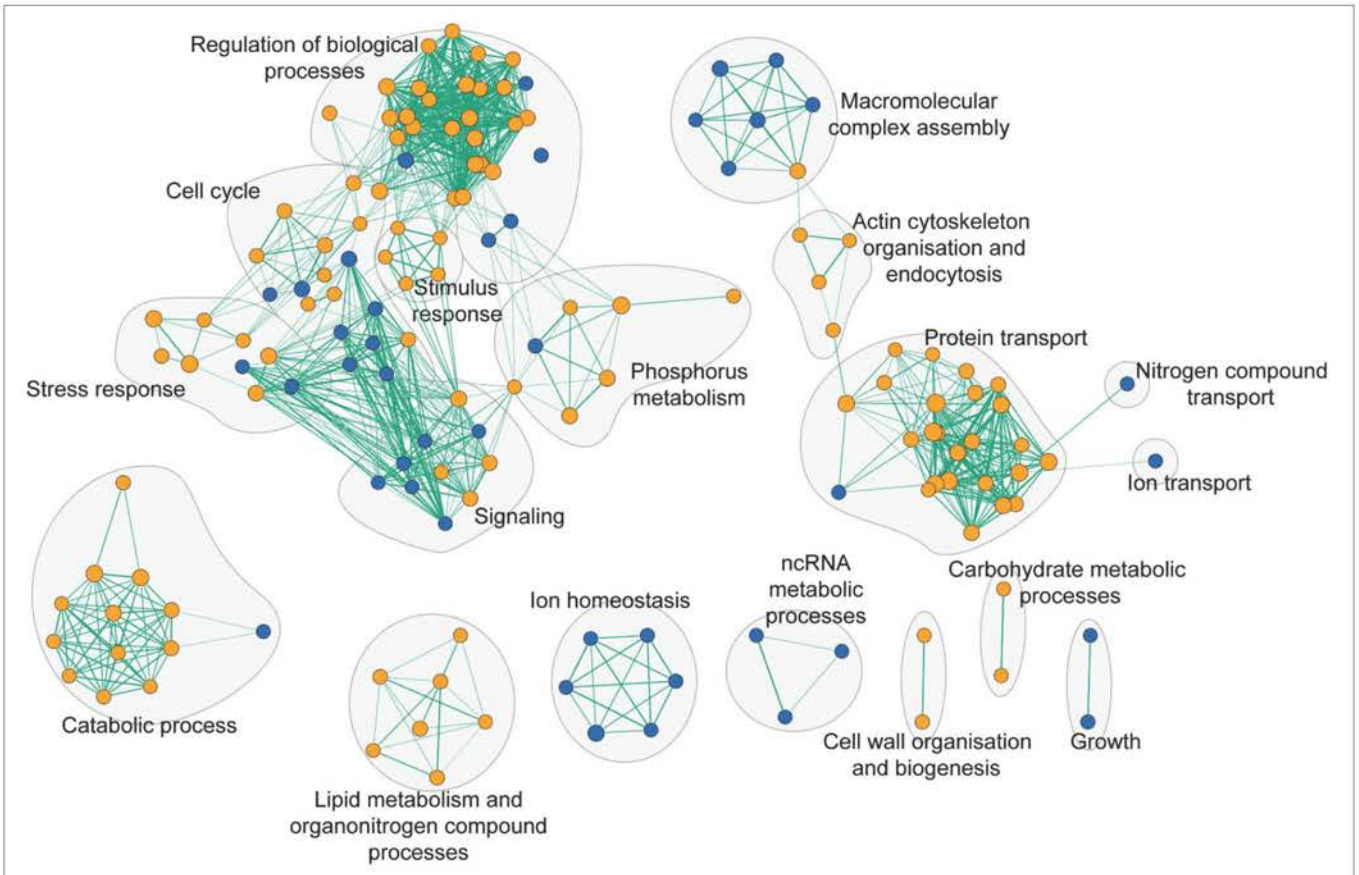

FIGURE 5 | Functional enrichment analysis network of functions that when deleted render cells either sensitive (blue nodes) or resistant (orange nodes) to yttrium. Green lines represent gene overlap between two functions, with the edge width being proportional to the number of shared genes. The enrichment map was built using GSEA and visualized by the enrichment map plugin in Cytoscape.

(**Figure 2**) were related mainly to protein transport with the ubiquitin-dependent protein catabolic process via the MVB sorting pathway (P = 1.88e−10) but also to actin cytoskeleton organization (P = 1.16e−03), and the sphingolipid biosynthetic process (P = 9.60e−05) (**Supplementary Table 4**). On a broader scale, other functions involved in yttrium toxicity were also observed in HR, MR, and LR mutants (**Figure 5** and **Supplementary Table 3**). As observed for sensitive mutants, the transport GO term was highlighted (P = 2.55e−04, 54 genes represented out of 815). Hereafter, the major functions retrieved from the analysis of the resistant mutants are detailed.

First, a group constituted predominantly by endocytosis, vesicle trafficking, and actin cytoskeleton organization, could be identified (**Figure 5**). Endocytosis is the process whereby cells recycle membranes or extracellular compounds as well as take up substances or downregulate plasma membrane transporters or receptors. Ten mutants out of 82 (12.1%) for genes involved in endocytosis (P = 1.96e−03) were resistant to yttrium (ΔDoa4, ΔYck1, ΔEnt4, ΔEnt2, ΔSla1, ΔVrp1, ΔEnd3, ΔSiw14, ΔMon2, and ΔInp53) (**Supplementary Table 2**).

Second, the functional category "protein transport" was highlighted (**Figure 5** and **Supplementary Table 3**). It included mostly functions involved in localization, transport, and catabolism of proteins (**Supplementary Table 3**). Among the 51 mutants in this category, high representation of the ESCRT complex was apparent (**Figure 6**). Indeed, excluding ΔHse1 and ΔIst1, mutants for all the sub-complexes, known as ESCRT-0 (Vps27p), ESCRT-I (Srn2p, Stp22p, Mvb12p, and Vps28p), ESCRT-II (Vps25p, Snf8p, and Vps36p), ESCRT-III (Did4p, Snf7p, Vps24p, Vps20p, and Did2p), displayed a resistant phenotype (**Figure 6B** and **Supplementary Table 2**). Moreover, the mutants of the ESCRT-associated complex Vta1p-Vps4p and complex Bro1p-Doa4p shared the same phenotype (**Supplementary Table 2**). The ESCRT complex-dependent budding of small vesicles inside the lumen of late endosomes is responsible for the formation of the MVB (**Figure 6A**). The subsequently formed MVB is targeted and fused to the vacuole where the internal vesicles are degraded. This pathway is mostly associated with ubiquitin-dependent protein catabolism. Consistently, two mutants for proteins involved in ubiquitination were resistant to yttrium (**Supplementary Table 2**). On the one hand, Doa4p is a ubiquitin hydrolase that is required for recycling ubiquitin and acts in the late endosome compartment to recover ubiquitin. On the other hand, Ubp2p is a ubiquitin-specific protease that is required for MVB sorting of membrane proteins.

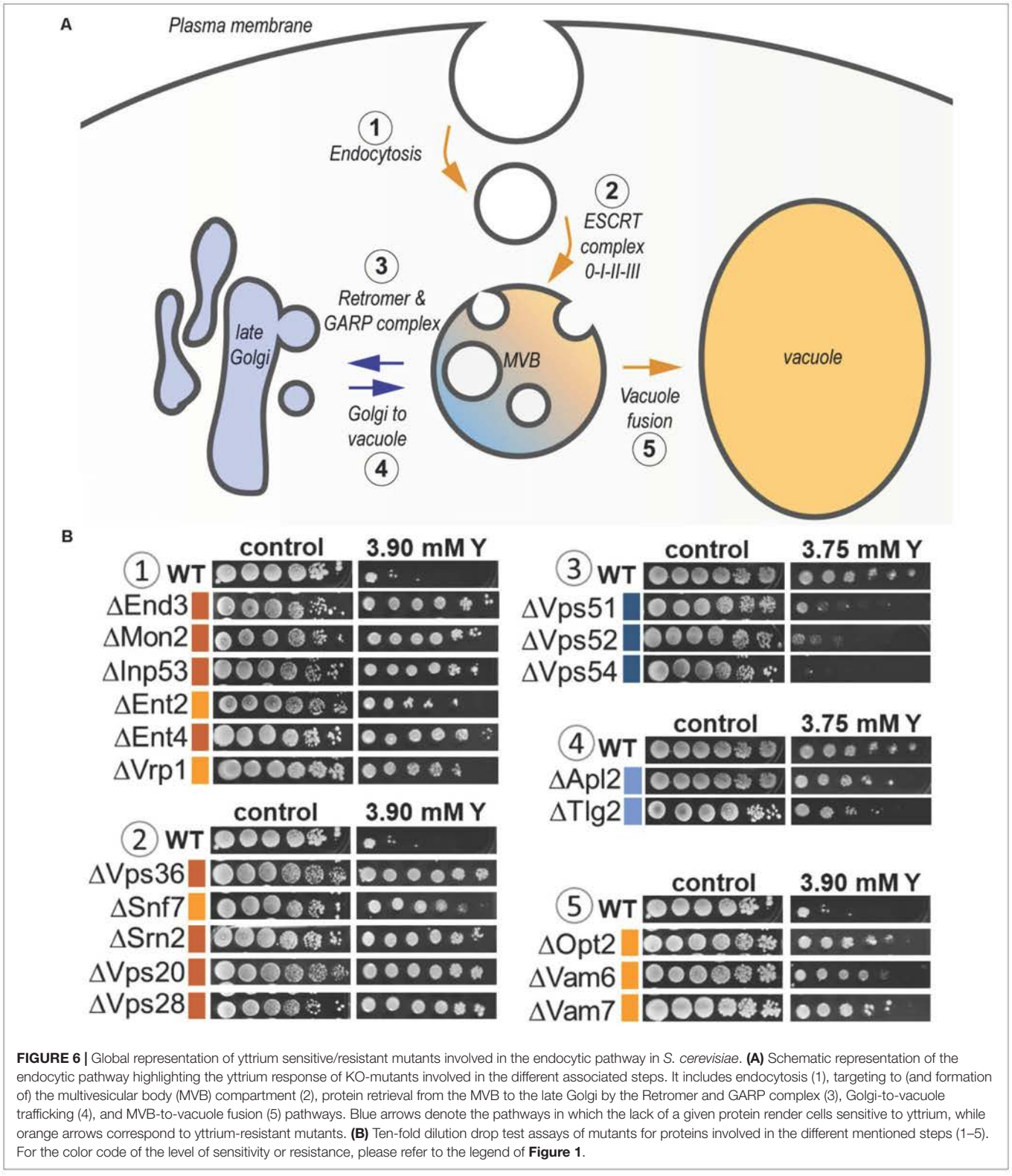

FIGURE 6 | Global representation of yttrium sensitive/resistant mutants involved in the endocytic pathway in *S. cerevisiae*. **(A)** Schematic representation of the endocytic pathway highlighting the yttrium response of KO-mutants involved in the different associated steps. It includes endocytosis (1), targeting to (and formation of) the multivesicular body (MVB) compartment (2), protein retrieval from the MVB to the late Golgi by the Retromer and GARP complex (3), Golgi-to-vacuole trafficking (4), and MVB-to-vacuole fusion (5) pathways. Blue arrows denote the pathways in which the lack of a given protein render cells sensitive to yttrium, while orange arrows correspond to yttrium-resistant mutants. **(B)** Ten-fold dilution drop test assays of mutants for proteins involved in the different mentioned steps (1–5). For the color code of the level of sensitivity or resistance, please refer to the legend of **Figure 1**.

The third group was composed of mutants with disrupted genes encoding enzymes involved in lipid metabolism (**Figure 5**). The sphingolipid metabolic process was the most significant (P = 4.46e−05). *DPL1, SUR2, SCS7, LCB3,* and *ARV1* genes are part of the sphingolipid metabolic process, and the corresponding mutants display resistance toward yttrium (**Supplementary Tables 2**, **3**). Closely related functions were also represented, such as sphingolipid biosynthetic process (*TSC3, ELO2, LCB3,*

ELO3, and *SUR1*), lipid biosynthetic process (*ELO2, SUR2, CAX4, OAR1, ERG3, ELO3, ERG2, SCS7,* and *ERG24*), and fatty acid biosynthetic process (*ELO2, SUR2, OAR1, ERG3, ELO3,* and *SCS7*) (**Supplementary Table 3**). All these mentioned mutants had impairments in enzymes involved in the modulation of sphingolipid levels, fatty acids synthesis, uptake, and elongation.

A few yttrium-resistant mutants were involved in the transcriptional regulation of RNA polymerase III ($P = 9.74e{-}03$) (**Supplementary Table 3**). Mutants for *CKB1* and *CKA2*, encoding the catalytic sub-units of casein kinase 2 (CK2), were resistant. Pheromone-dependent signal transduction involved in the conjugation to cellular fusion (*STE50, PTC1, GET3, MFA1, FAR1, STE18, ARV1,* and *STE4*) ($P = 4.41e{-}05$) and the heterotrimeric G-protein complex cycle (Ste18 and Ste4) ($P = 7.14e{-}03$) were also found (**Supplementary Table 3**). While these two latter proteins form a dimer that activates the mating signaling pathway, Ste50p acts as an adaptor that links a G protein-associated complex to the effector Ste11p to modulate signal transduction. Get3p amplifies G protein signaling and is also involved in ATP-dependent Golgi to ER trafficking. Mfa1p is the mating pheromone a-factor. Some mutants for proteins involved in the mitogen activated protein kinase signaling cascade (MAPKs) pathway were also resistant to yttrium, including ΔSte50, ΔSte7 (MAPKK), ΔSsk2 (semi-redundant MAPKKK), and a mutant lacking the phosphotyrosine phosphatase Ptp2p that has a role in the inactivation of MAPK. Ptc1p is also a 2C-type protein phosphatase that indirectly inactivates the osmosensing MAPK cascade (Chen and Thorner, 2007).

Finally, mutants for ribosomal sub-units also displayed a resistant phenotype. This category included mutants lacking the mitochondrial large ribosomal subunit components Mrpl23p, Mrpl28p, and Mrpl49p, the large nuclear ribosomal subunit proteins Rpl8bp, Rpl21ap, Rpl37bp, and Rpl40ap, a protein from the small ribosomal subunit Rps12p and Rpp1ap, a component of the ribosomal stalk (**Supplementary Table 2**).

DISCUSSION

The screening of genome-wide collections of *S. cerevisiae* haploid mutants is a good strategy to uncover essential genes/proteins or functions allowing cells to cope with metal toxicity (Haugen et al., 2004; Kakimoto et al., 2005; Thorsen et al., 2006, 2009; Pagani et al., 2007; Wang et al., 2007; Jin et al., 2008; Jo et al., 2008; Ruotolo et al., 2008; Serero et al., 2008; Arita et al., 2009; Bleackley et al., 2011; Chesi et al., 2012; Tun et al., 2014; Johnson et al., 2016a,b). As a recognized eukaryotic model, *S. cerevisiae* is relevant to better understand the hazardous effects of such contaminants on eukaryotic organisms since many genes are conserved among eukaryotic species. Identified sensitive mutants provide insights into tolerance mechanisms developed by cells, while resistant mutants may shed light on toxicity pathways (e.g., uptake or interacting molecules). In the present study, we adopted this genomic phenotyping approach under exposure to the technological critical element yttrium, an emerging contaminant (United States Geological Survey, 2000; Wei et al., 2001; Mayfield and Lewis, 2013; Ciacci et al., 2015). Strikingly, relatively few mutants (56) showed sensitivity to yttrium. Nonetheless, this number is not abnormal in comparison to other screenings (Kakimoto et al., 2005; Wang et al., 2007; Jin et al., 2008; Tun et al., 2014; Du et al., 2015; Johnson et al., 2016a). The relatively low number of sensitive mutants identified may reflect the restricted number of functions available for yeast cells to cope with yttrium toxicity. In contrast, the high number of resistant mutants is indicative of a wide range of yttrium-induced toxicity mechanisms. Furthermore, comparison of the present mutant set with available studies on other metals outlined the functions and key genes/proteins involved specifically or not in the response of yeast to yttrium stress. These major functions are discussed below.

Mutants for vacuolar membrane ATPase (VMA) family genes were sensitive to yttrium. The VMA allows pH homeostasis by acidification of the vacuolar lumen and thus creates a proton gradient across the tonoplast. As illustrated hereafter, the present set of VMA mutants lacked proteins involved in different steps ranging from assembly, translocation, to the functioning of the VMA. Vma21p and Vma22p are localized to the ER periphery and are involved in VMA assembly before its translocation, first to the Golgi and finally to the vacuolar membrane (Graham et al., 1998). Vma16p encodes the third proteolipid subunit of the VMA (Hirata et al., 1997). It is first located on the ER membrane before being pulled together with the other subunits of the VMA complex (Graham et al., 1998). Vma7p, one of the eight subunits of the V1 peripheral membrane domain of VMA, participates in the structure and activity of the whole complex (Graham et al., 1994; Forgac, 1999). It has been hypothesized that vacuolar membrane vesicles and the VMA-built proton gradient can contribute to the vacuolar uptake of nickel in *S. cerevisiae* (Nishimura et al., 1998). Indeed, the lack of the VMA and its associated proton gradient led to a defect in vacuolar sequestration of nickel and an increased cell sensitivity to this metal (Nishimura et al., 1998). Similar findings have been obtained from most of the other metals tested by genomic phenotyping (Jin et al., 2008; Ruotolo et al., 2008; Bleackley et al., 2011). Moreover, a study based on the functional characterization of VMA has also reported that acidification of the vacuole ensures an important role in ionic (e.g., calcium, manganese, zinc, and copper) homeostasis and detoxification (Ramsay and Gadd, 1997). Thus, VMA activity is likely to act as a general modulation of cellular toxicity induced by metals, including the newly studied element yttrium.

Thirteen mutants for ribosomal proteins, representing 9.5% of the 137 total ribosomal genes of *S. cerevisiae*, were also obtained from the screening, displaying either a sensitive or resistant phenotype toward yttrium exposure. This versatile response of ribosomal proteins has also been previously shown under chromium exposure (Johnson et al., 2016b). The resistant phenotype of the mutated cells could be explained by a strategy of slowing down cell growth through decreased protein synthesis. Hence, cells would mainly shift their metabolism toward toxicity

scavenging and cellular components repair. This hypothesis has recently been reinforced by Pan et al. (2017), who recorded a down-regulation of ribosomal gene expression under cadmium stress, concluding that the cellular resources could be diverted to the metal stress response rather than being consumed for the synthesis of ribosomes. Conversely, the explanation for the sensitive phenotype displayed by some ribosome-related mutants is not as straightforward. It has been further argued that chromium might impact protein translation (Johnson et al., 2016b). Altogether, this finding and the present data indicate that some of these ribosomal proteins would be essential for cells to cope with chromium and yttrium stress.

In addition to the impact of yttrium toxicity at the translational level, this study highlighted the putative role of several signaling pathways for modulation of the yttrium response. First, two mutants, ΔCkb1 and ΔCka2, showed a resistance phenotype to yttrium. CK2 is a Ser/Thr protein kinase that has many substrates, including transcription factors and all RNA polymerases. Our results suggest that this enzyme might regulate yttrium toxicity signaling. The ΔCkb1 mutant was also resistant to Cr(III) and was associated with a reduced accumulation compared with wild-type [16% less Cr(III) after 16 h], while the ΔCka2 mutant accumulated more Cr(III) (Johnson et al., 2016b). The involvement of CK2 in the response to aluminum, chromium, and arsenic toxicity underlines its key role in metal toxicity mitigation via the signaling pathway, possibly by regulating cell entry of toxic metals (Johnson et al., 2016a,b), including yttrium. Another aspect of signaling arose, since several genes involved in the pheromone-dependent signal transduction as well as in the MAPK signaling cascade conferred, when mutated, an yttrium-resistant phenotype to cells. Activation of the MAPK signaling cascade in response to different signals or stresses, such as exposure to metals, is well known in *S. cerevisiae* (Chen and Thorner, 2007). Surprisingly, discrepancies were observed for these pathways when comparing yttrium exposure to zinc, arsenic, and cadmium stresses. Indeed, these mutants, except ΔBck1, were resistant to yttrium but sensitive to the other metals (Jin et al., 2008). Among the MAPK signal transduction pathways, the pheromone response pathway was represented along with the Ste4p and Ste18p components of the heterotrimeric G-protein complex, which is associated with pheromone receptors (Chen and Thorner, 2007). It is well established that pheromone stimulation leads to cell cycle arrest. Moreover, it has been suggested that this pathway facilitates cell wall alterations required for the mating process (Chen and Thorner, 2007) and thus leads to a more susceptible cell wall. Therefore, the resistance phenotype of mutants disrupted in the pheromone-dependent signal transduction pathway could be explained by the lack of cell cycle arrest or by the reduction of cell wall alterations, allowing cells to cope with yttrium toxicity.

Comparison of the dataset of yttrium-sensitive and -resistant mutants with those from other genomic phenotyping screenings on gamma-rays, alkaline pH, or oxidative stress induced by a set of chemicals (Bennett et al., 2001; Chang et al., 2002; Aouida et al., 2004; Serrano et al., 2004; Thorpe et al., 2004), displayed limited similarities. These results do not support the hypothesis of the involvement of oxidative stress, DNA-damage or of an alkaline-pH-related response in yttrium toxicity. This hypothesis is reinforced by the observation that neither mitochondrial nor nuclear compartments were significantly impaired by yttrium (**Table 1**).

The disruption of genes related to protein transport and vesicular trafficking modified the cell response to yttrium. Notably, the whole cascade starting from membrane endocytosis to the trans-Golgi and vacuole, through endosomes and the MVB, was represented among the mutants impaired by yttrium. Interestingly, protein transport as well as recycling or catabolism via the ubiquitin-dependent catabolic process was central to the yeast response to yttrium. This phenomenon has only been previously evidenced for nickel and methyl-mercury, since the deletion of MVB sorting pathway-related proteins (ESCRT complex) rendered yeast highly resistant to these stressors (Ruotolo et al., 2008; Arita et al., 2009; Hwang et al., 2014). Our results suggest a similar conclusion for yttrium since mutants from the same pathway were also resistant to yttrium. Conversely, mutants for three components of the retrograde pathway, namely, Vps54p, Vps52p, and Vps51p, were all sensitive to yttrium, cadmium (Ruotolo et al., 2008), arsenic (Thorsen et al., 2009; Johnson et al., 2016b), and chromium (Johnson et al., 2016b), but not to nickel (Ruotolo et al., 2008). However, no straightforward explanation could be drawn. Nevertheless, the contrasting phenotypes for mutants of the ESCRT-complex vs. the retrograde pathway particularly suggest that the MVB could be a central target for yttrium toxicity modulation.

The actin cytoskeleton along with endocytosis appears to be also of high importance in yttrium homeostasis. Indeed, sub-functions related to these two categories are highly represented among yttrium-resistant mutants. The cytoskeleton and endocytosis are closely related as the latter is governed by actin (Robertson et al., 2009). Interestingly, mutants for the majority of genes involved in the connection between the cytoskeleton and endocytosis were yttrium-resistant, such as ΔVrp1, ΔEnd3, ΔSla1, ΔEnt2, and ΔEnt4. Both Vrp1p (verprolin) and End3p promote actin nucleation and cytoskeleton organization and endocytosis (Benedetti et al., 1994; Munn et al., 1995). Sla1p plays a crucial role in the cortical actin patch structure and organization. It interacts with End3p and links the actin cytoskeleton and the endocytosis machinery (Warren et al., 2002). Finally, both Ent2p and Ent4p, mammalian epsin-like proteins, possess an Epsin N-terminal homology domain that is usually found in proteins implicated in endocytosis regulation or cytoskeleton organization. It is noteworthy that endocytosis has only been previously mentioned as taking part in chromate homeostasis (Holland and Avery, 2009). Chromate accumulation and cell sensitivity were higher in endocytosis-defective mutants than in wild-type. Moreover, it has been demonstrated that chromate stress increases endocytosis in *S. cerevisiae*. Taken together, these data emphasize that actin-related endocytosis functions as a compulsory mechanism for chromate resistance, possibly through endocytic inactivation of Cr-transporting proteins. However, endocytosis mutants were yttrium-resistant, suggesting the presence of different homeostasis mechanisms between yttrium and chromate.

The toxicity of a metal might begin with the prerequisite step of its entry into cells. Thus, decreased or suppressed uptake of yttrium should lead to cellular resistance toward this element. Two hypotheses can be drawn to explain this resistance phenotype: (i) The improper recycling of a yet unidentified efflux system for yttrium would drive its accumulation at the plasma membrane. Consequently, yttrium detoxification in the cytosol would be enhanced through increased efflux of this element out of the cell. Endocytosis of metal transporters has been shown in different organisms to modulate the uptake of specific metals, rationalizing this hypothesis. For instance, the yeast membrane metal transporters Zrt1p and Ctr1p are post-translationally regulated by ubiquitination and endocytosis to be degraded in the vacuole (Ooi et al., 1996; Gitan and Eide, 2000; Liu et al., 2007). In agreement with this hypothesis, defects in these two proteins (Doa4p and Ubp2p) involved in ubiquitination induced resistance to yttrium. (ii) Alternatively, endocytic vesicles containing yttrium (either membrane-bound or in the vesicle lumen) could be involved in the non-specific uptake of yttrium. According to these two hypotheses, mutations in either of these two transport systems would result in a high intracellular content of yttrium. However, putative non-specific plasma membrane transporters mediating yttrium uptake cannot be ruled out, as suggested for nickel (Ruotolo et al., 2008). To test these hypotheses, further proteomic and ionomic (yttrium quantification) studies are needed.

The lipid biosynthetic process was identified in the present screening by fatty acid, ergosterol, and sphingolipid synthesis mutants that displayed yttrium resistance. Hence, the biosynthesis of these molecules appears to trigger yttrium toxicity, excluding in two mutants, ΔCsg2 and ΔSur1, which were highly sensitive to yttrium as well as to calcium (Beeler et al., 1994, 1997). In the latter case, a calcium-induced plasma membrane alteration would lead to sensitivity of these mutants. The complex formed by the MIPC synthase catalytic sub-unit Sur1p and the regulatory sub-unit Csg2p acts as an inositol phosphorylceramide mannosyltransferase complex (Beeler et al., 1997). Additionally, ΔCsg2 and ΔSur1 also accumulate fewer mannosylated sphingolipids along with an increase in lysophosphatidylinositol compared with the wild-type strain (Beeler et al., 1997). The calcium sensitivity of these mutants would result from the accumulation and/or mislocalization of IPC (inositol-P-ceramide) rather than a depletion of MIPC content. MIPC has been shown to be required for the proper localization of proteins to the plasma-membrane in *Schizosaccharomyces pombe* (Nakase et al., 2010). Interestingly, some other studies have proposed that this lipid might be involved in determining the activity of the plasma membrane drug transporters and/or the permeability properties of this membrane (Lisman et al., 2004). Therefore, an imbalance in plasma membrane sphingolipid composition could be responsible for the yttrium-sensitive phenotype displayed by these mutants. Moreover, several mutants mentioned earlier lack enzymes that participate either in fatty acid biosynthesis, uptake, or elongation and subsequently impact cellular sphingolipid levels. Sphingolipids are implicated in numerous pathways from temperature tolerance to the cell cycle, actin metabolism, and protein stability and localization (Montefusco et al., 2014). It has been demonstrated that several classes of lipids participate in endocytosis, and more particularly, in the clathrin-independent endocytic pathway (Kirkham and Parton, 2005). As demonstrated in Chinese hamster ovary cells, different endocytic pathways are altered by the depletion of either general sphingolipids or, more specifically, glycosphingolipids (Cheng et al., 2006). Taken together, these data emphasize the role of the plasma membrane as a hotspot for yttrium toxicity.

CONCLUSION

The present study reports the first cellular and molecular insights addressing yttrium toxicity and thus shedding light on the previously unknown impact of yttrium on eukaryotes. Both cellular toxicity and detoxification mechanisms revealed in *S. cerevisiae* provide valuable information for further potential environmental issues derived from this emerging metallic contaminant. The cellular response to yttrium appeared to exhibit peculiarities in comparison to other metals. Signaling pathways, protein translation, and the vacuolar compartment are well known for their involvement in metal toxicity modulation, while unexpected pathways such as endocytosis and sphingolipid metabolism revealed new perspectives in our understanding of metal homeostasis in eukaryotes. Based on the present findings, further investigations must be conducted in other eukaryotes, including human cells. Such studies have been performed using nickel and demonstrated a high degree of conservation of various aspects of metal toxicity between *S. cerevisiae* and mammals (Lee et al., 1995; Broday et al., 1999; Sutherland et al., 2001; Costa et al., 2005). This information will aid in deciphering whether the identified mechanisms of yttrium toxicity can be extended to all eukaryotes.

AUTHOR CONTRIBUTIONS

NG, MLJ, and DB designed the research and analyzed the data. NG performed the research. NG, MLJ, EG, and DB evaluated the data and wrote the manuscript. All authors read and approved the final manuscript.

FUNDING

This work was supported by the French National Research Agency through the National Program "Investissements d'Avenir" with the reference ANR-10-LABX-21-01/LABEX RESSOURCES21 and by the Région Grand Est.

SUPPLEMENTARY MATERIAL

The Supplementary Material for this article can be found online at: https://www.frontiersin.org/articles/10.3389/fmicb.2018.02005/full#supplementary-material

REFERENCES

Aouida, M., Pagé, N., Leduc, A., Page, N., Peter, M., and Ramotar, D. (2004). A genome-wide screen in *Saccharomyces cerevisiae* reveals altered transport as a mechanism of resistance to the anticancer drug bleomycin. *Cancer Res.* 514, 1102–1109. doi: 10.1158/0008-5472.CAN-03-2729

Arita, A., Zhou, X., Ellen, T. P., Liu, X., Bai, J., Rooney, J. P., et al. (2009). A genome-wide deletion mutant screen identifies pathways affected by nickel sulfate in *Saccharomyces cerevisiae*. *BMC Genomics* 14:524. doi: 10.1186/1471-2164-10-524

Beeler, T., Gable, K., Zhao, C., and Dunn, T. (1994). A novel protein, CSG2p, is required for Ca^{2+} regulation in *Saccharomyces cerevisiae*. *J. Biol. Chem.* 269, 7279–7284.

Beeler, T. J., Fu, D., Rivera, J., Monaghan, E., Gable, K., and Dunn, T. M. (1997). SUR1 (CSG1/BCL21), a gene necessary for growth of *Saccharomyces cerevisiae* in the presence of high Ca^{2+} concentrations at 37°C, is required for mannosylation of inositolphosphorylceramide. *Mol. Gen Genet.* 255, 570–579. doi: 10.1007/s004380050530

Benedetti, H., Raths, S., Crausaz, F., and Riezman, H. (1994). The END3 gene encodes a protein that is required for the internalization step of endocytosis and for actin cytoskeleton organization in yeast. *Mol. Biol. Cell* 5, 1023–1037. doi: 10.1091/mbc.5.9.1023

Bennett, C. B., Lewis, L. K., Karthikeyan, G., Lobachev, K. S., Jin, Y. H., Sterling, J. F., et al. (2001). Genes required for ionizing radiation resistance in yeast. *Nat. Genet.* 29, 426–434. doi: 10.1038/ng778

Bleackley, M. R., Young, B. P., Loewen, C. J. R., and Macgillivray, R. T. A. (2011). High density array screening to identify the genetic requirements for transition metal tolerance in *Saccharomyces cerevisiae*. *Metallomics* 3, 195–205. doi: 10.1039/c0mt00035c

Botstein, D., Chervitz, S. A., and Cherry, J. M. (1997). Yeast as a model organism. *Science (80-)* 277, 1259–1260. doi: 10.1126/science.277.5330.1259

Boyle, E. I., Weng, S., Gollub, J., Jin, H., Botstein, D., Cherry, J. M., et al. (2004). GO::TermFinder-open source software for accessing gene ontology information and finding significantly enriched gene ontology terms associated with a list of genes. *Bioinformatics* 20, 3710–3715. doi: 10.1093/bioinformatics/bth456.GO

Broday, L., Cai, J., and Costa, M. (1999). Nickel enhances telomeric silencing in *Saccharomyces cerevisiae*. *Mutat. Res.* 440, 121–130. doi: 10.1016/S1383-5718(99)00018-2

Bunus, F. T. (2000). Uranium and rare earth recovery from phosphate fertilizer industry by solvent extraction. *Miner. Process. Extr. Metall. Rev.* 21, 381–478. doi: 10.1080/08827500008914174

Burri, L., and Lithgow, T. (2004). A complete set of SNAREs in yeast. *Traffic* 5, 45–52. doi: 10.1046/j.1600-0854.2003.00151.x

Chang, M., Bellaoui, M., Boone, C., and Brown, G. W. (2002). A genome-wide screen for methyl methanesulfonate- sensitive mutants reveals genes required for S phase progression in the presence of DNA damage. *Proc. Natl. Acad. Sci. U.S.A.* 99, 16934–16939. doi: 10.1073/pnas.262669299

Chen, R. E., and Thorner, J. (2007). Function and regulation in MAPK signaling pathways: lessons learned from the yeast *Saccharomyces cerevisiae*. *Biochim. Biophys. Acta – Mol. Cell Res.* 1773, 1311–1340. doi: 10.1016/j.bbamcr.2007.05.003

Cheng, Z.-J., Singh, R. D., Sharma, D. K., Holicky, E. L., Hanada, K., Marks, D. L., et al. (2006). Distinct mechanisms of clathrin-independent endocytosis have unique sphingolipid requirements. *Mol. Biol. Cell* 17, 3197–3210. doi: 10.1091/mbc.e05-12-1101

Chesi, A., Kilaru, A., Fang, X., Cooper, A. A., and Gitler, A. D. (2012). The role of the Parkinson's disease gene PARK9 in essential cellular pathways and the manganese homeostasis network in yeast. *PLoS One* 7:e34178. doi: 10.1371/journal.pone.0034178

Ciacci, L., Reck, B. K., Nassar, N. T., and Graedel, T. E. (2015). Lost by design. *Environ. Sci. Technol.* 49, 9443–9451. doi: 10.1021/es505515z

Costa, M., Davidson, T. L., Chen, H., Ke, Q., Zhang, P., Yan, Y., et al. (2005). Nickel carcinogenesis: epigenetics and hypoxia signaling. *Mutat. Res.* 592, 79–88. doi: 10.1016/j.mrfmmm.2005.06.008

Du, J., Cao, C., and Jiang, L. (2015). Genome-scale genetic screen of lead ion-sensitive gene deletion mutations in *Saccharomyces cerevisiae*. *Gene* 563, 155–159. doi: 10.1016/j.gene.2015.03.018

Forgac, M. (1999). Structure and properties of the vacuolar (H+)-ATPases. *J. Biol. Chem.* 274, 12951–12954. doi: 10.1074/jbc.274.19.12951

Gitan, R. S., and Eide, D. J. (2000). Zinc-regulated ubiquitin conjugation signals endocytosis of the yeast ZRT1 zinc transporter. *Biochem. J.* 346 (Pt 2), 329–336.

Graham, L., Hill, K. J., and Stevenst, T. H. (1994). VMA7 encodes a novel 14-kDa subunit of the *Saccharomyces cerevisiae* vacuolar H+-ATPase complex. *J. Biol. Chem.* 269, 25974–25977.

Graham, L. A., Hill, K. J., and Stevens, T. H. (1998). Assembly of the yeast vacuolar H+-ATPase occcurs in the endoplasmic reticulum and requires a Vma12p/Vma22p assembly complex. *J. Cell. Biol.* 142, 39–49. doi: 10.1083/jcb.142.1.39

Hamosh, A., Scott, A. F., Amberger, J. S., Bocchini, C. A., and McKusick, V. A. (2005). Online mendelian inheritance in man (OMIM): a knowledgebase of human genes and genetic phenotypes. *Nucliec Acids Res.* 33(Suppl. 1), D514–D517. doi: 10.1093/nar/gki033

Haugen, A. C., Kelley, R., Collins, J. B., Tucker, C. J., Deng, C., Afshari, C. A., et al. (2004). Integrating phenotypic and expression profiles to map arsenic-response networks. *Genome Biol.* 5:R95. doi: 10.1186/gb-2004-5-12-r95

Haxel, G. B., Hedrick, J. B., and Orris, G. J. (2002). *Rare Earth Elements — Critical Resources for High Technology*. Reston, VA: US Geological Survey. Available at: http://pubs.usgs.gov/fs/2002/fs087-02/

Hirano, S., Kodama, N., Shibata, K., and Suzuki, K. T. (1993). Metabolism and toxicity of intravenously injected yttrium chloride in rats. *Toxicol. Appl. Pharmacol.* 121, 224–232. doi: 10.1006/taap.1993.1149

Hirata, R., Graham, L. A., Takatsuki, A., Stevens, T. H., and Anraku, Y. (1997). VMA11 and VMA16 encode second and third proteolipid subunits of the *Saccharomyces cerevisiae* vacuolar membrane H+-ATPase. *J. Biol. Chem.* 272, 4795–4803. doi: 10.1074/jbc.272.8.4795

Holland, S. L., and Avery, S. V. (2009). Actin-mediated endocytosis limits intracellular Cr accumulation and Cr toxicity during chromate stress. *Toxicol. Sci.* 111, 437–446. doi: 10.1093/toxsci/kfp170

Hoon, M. J. L., De Imoto, S., Nolan, J., and Miyano, S. (2004). Open source clustering software. *Bioinformatics* 20, 1453–1454. doi: 10.1093/bioinformatics/bth078

Hwang, G., Murai, Y., Takahashi, T., and Naganuma, A. (2014). The protein transportation pathway from Golgi to vacuoles via endosomes plays a role in enhancement of methylmercury. *Sci. Rep.* 4, 1–8. doi: 10.1038/srep05888

Jin, Y. H., Dunlap, P. E., McBride, S. J., Al-Refai, H., Bushel, P. R., and Freedman, J. H. (2008). Global transcriptome and deletome profiles of yeast exposed to transition metals. *PLoS Genet.* 4:e1000053. doi: 10.1371/journal.pgen.1000053

Jo, W. J., Loguinov, A., Chang, M., Wintz, H., Nislow, C., Arkin, A. P., et al. (2008). identification of genes involved in the toxic response of *Saccharomyces cerevisiae* against iron and copper overload by parallel analysis of deletion mutants. *Toxicol. Sci.* 101, 140–151. doi: 10.1093/toxsci/kfm226

Johnson, A. J., Veljanoski, F., O'Doherty, P. J., Zaman, M. S., Petersingham, G., Bailey, T. D., et al. (2016a). Molecular insight into arsenic toxicity via the genome-wide deletion mutant screening of *Saccharomyces cerevisiae*. *Metallomics* 8, 228–235. doi: 10.1039/c5mt00261c

Johnson, A. J., Veljanoski, F., O'Doherty, P. J., Zaman, M. S., Petersingham, G., Bailey, T. D., et al. (2016b). Revelation of molecular basis for chromium toxicity by phenotypes of *Saccharomyces cerevisiae* gene deletion mutants. *Metallomics* 8, 542–550. doi: 10.1039/C6MT00039H

Kachroo, A. H., Laurent, J. M., Yellman, C. M., Meyer, A. G., Wilke, C. O., and Marcotte, E. M. (2017). Systematic humanization of yeast genes reveals conserved functions and genetic modularity. *Science (80-)* 348, 921–925. doi: 10.1016/j.antiviral.2015.06.014.Chronic

Kakimoto, M., Kobayashi, A., Fukuda, R., Ono, Y., Ohta, A., and Yoshimura, E. (2005). Genome-wide screening of aluminum tolerance in *Saccharomyces cerevisiae*. *BioMetals* 18, 467–474. doi: 10.1007/s10534-005-4663-0

Kirkham, M., and Parton, R. G. (2005). Clathrin-independent endocytosis: new insights into caveolae and non-caveolar lipid raft carriers. *Biochim. Biophys. Acta* 1745, 273–286. doi: 10.1016/j.bbamcr.2005.06.002

Lee, Y. W., Klein, C. B., Kargacin, B., Salnikow, K., Kitahara, J., Dowjat, K., et al. (1995). Carcinogenic nickel silences gene expression by chromatin condensation and DNA methylation: a new model for epigenetic carcinogens. *Mol. Cell. Biol.* 15, 2547–2557. doi: 10.1128/MCB.15.5.2547

Li, C. X., Ma, C., Fang, H. Q., Zhi, Y., Yu, Z., Xu, H. B., et al. (2015). Neurobehavioral assessment of rats exposed to yttrium nitrate during development. *Biomed. Environ. Sci.* 28, 281–290. doi: 10.3967/bes2015.039

Lisman, Q., Pomorski, T., Vogelzangs, C., Urli-stam, D., Delwijnen, W. D. C., Van, et al. (2004). Protein sorting in the late golgi of *Saccharomyces cerevisiae* does not require mannosylated sphingolipids. *J. Biol. Chem.* 279, 1020–1029. doi: 10.1074/jbc.M306119200

Liu, J., Sitaram, A., and Burd, C. G. (2007). Regulation of copper-dependent endocytosis and vacuolar degradation of the yeast copper transporter, Ctr1p, by the Rsp5 ubiquitin ligase. *Traffic* 8, 1375–1384. doi: 10.1111/j.1600-0854.2007.00616.x

Mayfield, D. B., and Lewis, A. S. (2013). Environmental review of coal ash as a resource for rare earth and strategic elements. *World Coal Ash Conf.* 2013, 22–25.

Merico, D., Isserlin, R., Stueker, O., Emili, A., and Bader, G. D. (2010). Enrichment map: a network-based method for gene-set enrichment visualization and interpretation. *PLoS One* 5:e13984. doi: 10.1371/journal.pone.0013984

Montefusco, D. J., Matmati, N., and Hannun, Y. A. (2014). The yeast sphingolipid signaling landscape. *Chem. Phys. Lipids* 177, 26–40. doi: 10.1016/j.chemphyslip.2013.10.006

Munn, A. L., Stevenson, B. J., Geli, M. I., and Riezman, H. (1995). end5, end6, and end7: mutations that cause actin delocalization and block the internalization step of endocytosis in *Saccharomyces cerevisiae*. *Mol. Biol. Cell* 6, 1721–1742. doi: 10.1091/mbc.6.12.1721

Nakase, M., Tani, M., Morita, T., Kitamoto, H. K., Kashiwazaki, J., Nakamura, T., et al. (2010). Mannosylinositol phosphorylceramide is a major sphingolipid component and is required for proper localization of plasma-membrane proteins in *Schizosaccharomyces pombe*. *J. Cell Sci.* 123, 1578–1587. doi: 10.1242/jcs.059139

Nishimura, K. E. N., Igarashi, K., and Kakinuma, Y. (1998). Proton gradient-driven nickel uptake by vacuolar membrane vesicles of *Saccharomyces cerevisiae*. *J. Bacteriol.* 180, 1962–1964.

Ooi, C. E., Rabinovich, E., Dancis, A., Bonifacino, J. S., and Klausner, R. D. (1996). Copper-dependent degradation of the *Saccharomyces cerevisiae* plasma membrane copper transporter Ctr1p in the apparent absence of endocytosis. *EMBO J.* 15, 3515–3523.

Pagani, M. A., Casamayor, A., Serrano, R., Atrian, S., and Ariño, J. (2007). Disruption of iron homeostasis in *Saccharomyces cerevisiae* by high zinc levels: a genome-wide study. *Mol. Microbiol.* 65, 521–537. doi: 10.1111/j.1365-2958.2007.05807.x

Pan, J., Huang, X., Li, Y., Li, M., Yao, N., Zhou, Z., et al. (2017). Zinc protects against cadmium-induced toxicity by regulating oxidative stress, ions homeostasis and protein synthesis. *Chemosphere* 188, 265–273. doi: 10.1016/j.chemosphere.2017.08.106

Powell, J. A. C. (2014). GO2MSIG, an automated GO based multi-species gene set generator for gene set enrichment analysis. *BMC Bioinformatics* 15:146. doi: 10.1186/1471-2105-15-146

Ramsay, L. M., and Gadd, G. M. (1997). Mutants of *Saccharomyces cerevisiae* defective in vacuolar function confirm a role for the vacuole in toxic metal ion detoxification. *FEMS Microbiol. Lett.* 152, 293–298. doi: 10.1111/j.1574-6968.1997.tb10442.x

Riaz, A., Awais, R., and Salem, R. (2014). Side effects of yttrium-90 radioembolization. *Front. Oncol.* 4:198. doi: 10.3389/fonc.2014.00198

Robertson, A. S., Smythe, E., and Ayscough, K. R. (2009). Functions of actin in endocytosis. *Cell Mol. Life Sci.* 66, 2049–2065. doi: 10.1007/s00018-009-0001-y

Ruotolo, R., Marchini, G., and Ottonello, S. (2008). Membrane transporters and protein traffic networks differentially affecting metal tolerance: a genomic phenotyping study in yeast. *Genome Biol.* 9:R67. doi: 10.1186/gb-2008-9-4-r67

Serero, A., Lopes, J., Nicolas, A., and Boiteux, S. (2008). Yeast genes involved in cadmium tolerance: identification of DNA replication as a target of cadmium toxicity. *DNA Repair (Amst.)* 7, 1262–1275. doi: 10.1016/j.dnarep.2008.04.005

Serrano, R., Bernal, D., Simón, E., and Ariño, J. (2004). Copper and iron are the limiting factors for growth of the yeast *Saccharomyces cerevisiae* in an alkaline environment. *J. Biol. Chem.* 279, 19698–19704. doi: 10.1074/jbc.M313746200

Shannon, P., Markiel, A., Ozier, O., Baliga, N. S., Wang, J. T., Ramage, D., et al. (2003). Cytoscape: a software environment for integrated models of biomolecular interaction networks. *Genome Res.* 13, 2498–2504. doi: 10.1101/gr.1239303.metabolite

Subramanian, A., Tamayo, P., Mootha, V. K., Mukherjee, S., Ebert, B. L., Gillette, M. A., et al. (2005). Gene set enrichment analysis: a knowledge-based approach for interpreting genome-wide expression profiles. *Proc. Natl. Acad. Sci. U.S.A.* 102, 15545–15550. doi: 10.1073/pnas.0506580102

Sutherland, J. E., Peng, W., Zhang, Q. W., and Costa, M. (2001). The histone deacetylase inhibitor trichostatin A reduces nickel-induced gene silencing in yeast and mammalian cells. *Mutat. Res.* 479, 225–233. doi: 10.1016/S0027-5107(01)00163-4

Thorpe, G. W., Fong, C. S., Alic, N., Higgins, V. J., and Dawes, I. W. (2004). Cells have distinct mechanisms to maintain protection against different reactive oxygen species: oxidative-stress-response genes. *Proc. Natl. Acad. Sci. U.S.A.* 101, 6564–6569. doi: 10.1073/pnas.0305888101

Thorsen, M., Di, Y., Tängemo, C., Morillas, M., Ahmadpour, D., Van der Does, C., et al. (2006). The MAPK Hog1p modulates Fps1p-dependent arsenite uptake and tolerance in Yeast. *Mol. Biol. Cell* 17, 4400–4410. doi: 10.1091/mbc.e06-04-0315

Thorsen, M., Perrone, G. G., Kristiansson, E., Traini, M., Ye, T., Dawes, I. W., et al. (2009). Genetic basis of arsenite and cadmium tolerance in *Saccharomyces cerevisiae*. *BMC Genomics.* 15:105. doi: 10.1186/1471-2164-10-105

Trifuoggi, M., Pagano, G., Guida, M., Palumbo, A., Siciliano, A., Gravina, M., et al. (2017). Comparative toxicity of seven rare earth elements in sea urchin early life stages. *Environ. Sci. Pollut. Res.* 24, 20803–20810. doi: 10.1007/s11356-017-9658-1

Tun, N. M., O'Doherty, P. J., Chen, Z., Wu, X. Y., Bailey, T. D., Kersaitis, C., et al. (2014). Identification of aluminium transport-related genes via genome-wide phenotypic screening of of *Saccharomyces cerevisiae*. *Metallomics* 6, 1558–1564. doi: 10.1039/c4mt00116h

United States Geological Survey (2000). *Mineral Commodity Summaries*. Reston, VA: United States Geological Survey, 1–196. doi: 10.3133/70140094

United States Geological Survey (2016). *Mineral Commodity Summaries*. Reston, VA: United States Geological Survey, 1–202. doi: 10.3133/70140094

Wang, J., Wang, X., Fang, Y., and Zhou, B. (2007). Genome-wide screening of yeast metal homeostasis genes involved in mitochondrial functions. *Mol. Genet. Genom.* 277, 673–683. doi: 10.1007/s00438-007-0217-1

Wang, L., He, J., Xia, A., Cheng, M., Yang, Q., Du, C., et al. (2017). Toxic effects of environmental rare earth elements on delayed outward potassium channels and their mechanisms from a microscopic perspective. *Chemosphere* 181, 690–698. doi: 10.1016/j.chemosphere.2017.04.141

Wang, Y. M., Yu, Z., Zhao, Z. M., Jia, L., Fang, H. Q., Zhang, T. F., et al. (2017). Subchronic toxicity study of yttrium nitrate by 90-day repeated oral exposure in rats. *Regul. Toxicol. Pharmacol.* 90, 116–125. doi: 10.1016/j.yrtph.2017.08.020

Warren, D. T., Andrews, P. D., Gourlay, C. W., and Ayscough, K. R. (2002). Sla1p couples the yeast endocytic machinery to proteins regulating actin dynamics. *J. Cell. Sci.* 115, 1703–1715.

Wei, Z., Yin, M., Zhang, X., Hong, F., Li, B., Tao, Y., et al. (2001). Rare earth elements in naturally grown fern *Dicranopteris linearis* in relation to their variation in soils in South-Jiangxi region (Southern China). *Environ. Pollut.* 114, 345–355. doi: 10.1016/S0269-7491(00)00240-2

Zhang, F., Wang, Z., Wang, S., Fang, H., Chen, M., Xu, D., et al. (2016). Physicochemical properties and ecotoxicological effects of yttrium oxide nanoparticles in aquatic media: role of low molecular weight natural organic acids. *Environ. Pollut.* 212, 113–120. doi: 10.1016/j.envpol.2016.01.054

Zhou, G., Li, Y., Ma, Y., Liu, Z., Cao, L., Wang, D., et al. (2016). Size-dependent cytotoxicity of yttrium oxide nanoparticles on primary osteoblasts in vitro. *J. Nanopart. Res.* 18, 1–14. doi: 10.1007/s11051-016-3447-5

Conflict of Interest Statement: The authors declare that the research was conducted in the absence of any commercial or financial relationships that could be construed as a potential conflict of interest.

Copyright © 2018 Grosjean, Gross, Le Jean and Blaudez. This is an open-access article distributed under the terms of the Creative Commons Attribution License (CC BY). The use, distribution or reproduction in other forums is permitted, provided the original author(s) and the copyright owner(s) are credited and that the original publication in this journal is cited, in accordance with accepted academic practice. No use, distribution or reproduction is permitted which does not comply with these terms.

Chapter I.2:

A genome-wide deletion mutant screen identifies specific pathways affected by light and heavy lanthanides in *Saccharomyces cerevisiae*

A genome-wide deletion mutant screen identifies specific pathways affected by light and heavy lanthanides in *Saccharomyces cerevisiae*

A genome-wide deletion mutant screen identifies specific pathways affected by light and heavy lanthanides in *Saccharomyces cerevisiae*

(Manuscript to be submitted)

Abstract

Lanthanides (Ln) are essentials components for new-technologies, green energies, agriculture and medicine. They belong to the rare earth elements and can be split, according to their atomic mass, into light REEs (LREEs) and heavy REEs (HREEs). Their increasing production, use and current low recyclability, raise the question of their impact on the environment and human health. Yet, the few existing studies mentioning their toxicity remain elusive, pointing out the lack of data on the underlying cellular and molecular mechanisms. Through genomic phenotyping and deep proteomic analysis of *Saccharomyces cerevisiae* mutants either exposed to a LREE (La) or a HREE (Yb), we uncovered genes and pathways affecting Ln resistance and toxicity. La and Yb triggered common response pathways such as sphingolipid metabolism. In the same manner, endocytosis and vesicular trafficking were similarly involved in response to both Ln, potentially for their direct uptake or through the regulation of an efflux transporter. Conversely, discrepancies were also highlighted and we evidenced the role of the cell wall organization and pheromone signaling pathways in discriminating LREEs and HREEs. Also, the vacuole was suggested to take part into LREE detoxification specifically. In this study, we highlighted the cell wall and membranes as hotspots for Ln response. Moreover, there is a response gradient towards Ln according to their ionic radius. These results provide the first comprehensive insight in the molecular and cellular understanding of Ln toxicity, as emerging contaminants of growing concern. This work paves the way for future investigations on higher eukaryotes and for the improvement of risk assessment related to Ln release in the environment.

Introduction

The lanthanides (Ln) is a group comprising 15 chemical elements: La, Ce, Pr, Nd, Pm, Sm, Eu, Gd, Tb, Dy, Ho, Er, Tm, Yb and Lu. Among them, two subgroups are usually delineated based on both the atomic mass and the ionic radius, namely the light rare earth elements (LREE) gathering La to Eu, and the heavy REE (HREE) from Gd to Lu. These so-called technology critical elements are key elements in modern fields such as energetic transition, technology, medicine and technological military devices because of their unique magnetic, phosphorescent, and catalytic properties[1]. Ln are also used as fertilizers and food supplements for cattle, pigs, chicken, fish and rabbits in Chinese, and Swiss agriculture[2–5]. Many investigations carried out to uncover innovative processes to supply the increasing demand, which led to the rising production of Ln from 90,000 metric tons in 2000[6] to 130,000 metric tons of oxides in 2015[7]. The large production, utilization, and widespread release of Ln raise the question of their impact on the environment and human health. To date, however, the toxic effects of these elements have not been adequately evaluated.

Although Ln have very often been considered as harmless and nonessential elements[8,9], within the last few years results revealing effects of lanthanides on living organisms started to emerge, as being both essential for certain bacteria[10–12], and toxic elements for bacteria, plants and animals [13–18]. It has been shown that they have antibacterial, antifungal, and nematicidal activities[19], and can affect sea urchin embryogenesis[13,20], but also human health[21,22]. Ln-mediated oxidative stress was reported in various organisms[22,23]. Indeed, production of reactive oxygen species, lipid peroxidation, modulation of superoxide dismutase, catalase, and glutathione peroxidase in plants, fishes, rats and mice, but also in animal cell lines (including human cells) have been observed[22]. In plants, animals and animal cell lines, toxic effects were also evidenced by the presence of micronuclei as well as mitotic and chromosomal aberrations[22,24,25]. Some other toxic effects have been reported in bacteria and fungi such as membrane permeability[26,27] or exopolysaccharide overproduction[28]. However, the few existing studies mentioning toxicity remained elusive, which reflects the lack of data on cellular and molecular mechanisms causing Ln toxicity. Furthermore, since most of the existing studies deal with very unrelated organisms, a global view of the cellular and molecular pathways, involved in Ln toxicity, is particularly missing. A few studies hypothesized that LREEs and HREEs may induce different responses, which could be either due to the decreasing ionic radius and increased atomic mass (so-called Ln contraction), or to their reactivity or chemical differences[15,29].

The screening of a mutant collection of *Saccharomyces cerevisiae* has previously been shown as a relevant approach to obtain information about the role of non-essential proteins in toxicity modulation when exposed to different environmental stressors, among them many metals and metalloids[30,31]. Based on the phylogenetic relationships between *S. cerevisiae* and other eukaryotes

and a strong conservation of basic stress responses, the mechanisms revealed through this approach shed light on the pathways that may also be involved in other organisms[32,33]. To illustrate that point, several studies demonstrated that the unprogrammed gene silencing was a common toxicity mechanism of Ni in both *S. cerevisiae* and humans[34–36].

In a first step, we completed a genome-wide phenotyping screen of the entire set of 4,733 haploid *S. cerevisiae* gene deletion strains to identify gene products that modulate cellular toxicity to lanthanides. We hypothesized that LREEs and the HREEs would induce specific responses, and therefore we used lanthanum (La) and ytterbium (Yb), as representatives of the LREEs and the HREEs, respectively. In a second step, we carried out a deep proteomic analysis on selected mutant candidates in order to describe the molecular players involved in the Ln stress response.

Results and Discussion

Yeast genomic phenotyping unravel a large set of lanthanide-responsive genes

The complete set of 4733 haploid *S. cerevisiae* non-essential gene deletion mutants (BY4741 MATa) was exposed to La and to Yb. The primary screen and its subsequent validation screen revealed a total of 630 genes involved either in resistance or sensitivity to Ln, based on the modified fitness towards one or both elements when compared to the wild type (WT). They were classified into six different categories, ranging from high sensitivity (HS) to high resistance (HR) (Additional file 1: Table S1). To confirm the validity of the screen, 25 mutants were randomly picked among the sensitive, resistant and non-impacted mutants relatively to the wild type to be screened in their opposite haploid *Saccharomyces cerevisiae* gene deletion mating type (BY4742 MATα). Nearly identical responses of this subset were observed for both mating types (Additional file 2: Table S2), demonstrating the robustness of this phenotyping screen, which identified a high number of genes involved in the response of yeast cells to Ln. Notably, the number of sensitive mutants identified in the present study was in the same order of magnitude than those found from previous screens with toxic metals such as Ni and Cd[37]. These results suggest that Ln likely impact numerous cell functions and cellular compartments, some of which are detailed below.

La and Yb induce specific gene responses

Overall, 217 and 186 mutants were La-resistant and La-sensitive, respectively, whereas 135 and 7 mutants were Yb-resistant and Yb-sensitive, respectively (Fig. 1a), indicating that 84% of the whole set of mutants tested were specifically affected by one of the two Ln. This includes 84 mutants harboring extreme phenotypes, namely the highly resistant (HR) and highly sensitive (HS) mutants (Figure 1b, Additional file 3: Table S3). Interestingly, 88 and 83% of these HR and HS mutants, respectively, were specific to either La or Yb.

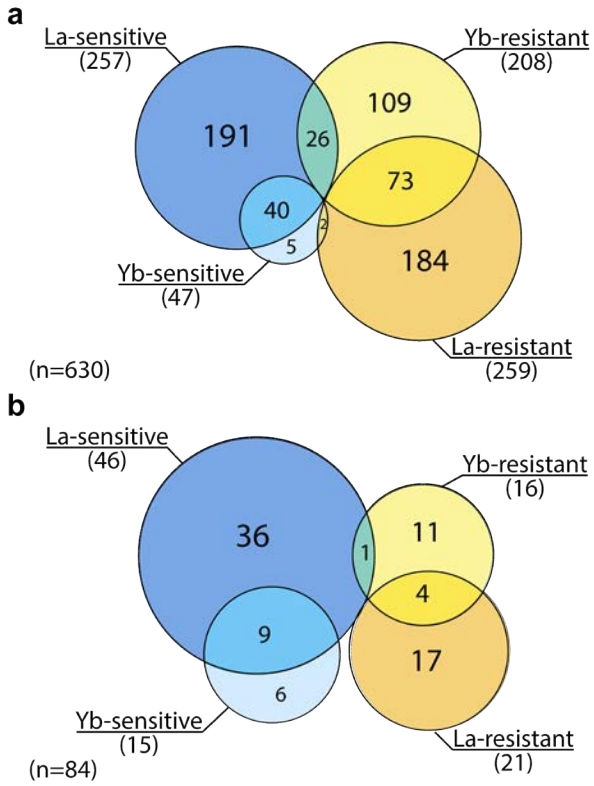

Figure 1 - Lanthanide response patterns obtained from genomic phenotyping of a whole mutant collection of *Saccharomyces cerevisiae*. (a) Venn diagram highlighting the number of mutants that are sensitive or resistant to La and/or to Yb. (b) Venn diagram highlighting the number of mutants displaying an exacerbated phenotype (highly resistant/sensitive) towards La and/or Yb.

There was 1.5 times more resistant mutants (366 mutants) to at least one Ln when compared with mutants displaying a sensitive phenotype (236 mutants). Among them, 259 and 208 genes whose deletion caused resistance to La and Yb, respectively, were found (Figure 1a). Conversely, five times more mutants were sensitive to La (257 mutants), as compared with Yb (47 mutants), suggesting the existance more resistance mechanisms towards La relatively Yb. Some mutants were resistant (73 mutants) or sensitive (40 mutants) to both Ln indicating that yeast cells respond, at least partly, to LREEs or HREEs by a common set of genes. Similarly, few sensitive mutants (13 %) were shared between the two groups of La-sensitive and Yb-sensitive mutants. Finally, a small set of mutants exhibited an opposite phenotype when exposed

to the two Ln, with 26 being both La-sensitive and Yb-resistant, while only 2 displayed a La-resistant and Yb-sensitive phenotype (Figure 1a).

Overall, the present genome-wide deletion mutant screen identifies specific genes that are affected by either LREEs or by HREEs in *S. cerevisiae*. These findings pinpoint that different cellular responses may ensue exposure to these two Ln.

Lanthanide yeast responsive genes have human counterparts

Human homologs and putative Online Mendelian Inheritance in Man (OMIM) human related diseases were retrieved from YeastMine query. At least one human homolog was found for up to 62 % (392 out of 630) of the genes, which deletion caused resistance or sensitivity to Ln. The detailed list of the mutants, including their sensitivity level, ORF accession number, gene description, human homolog(s) and putative human related disease(s) are included in the additional file S1: Table S1. Up to 37 % (23 % of the total) of them are involved in human diseases, notably cancers. Thus, the high number of Ln yeast responsive genes holding human counterparts sets a promising basis for further studies on the impact of Ln toxicity on human health.

Lanthanides affect specific functions compared to other metals

Genes and pathways identified in the present study were compared *in silico* with similar studies carried out with other metals (Cd, Co, Cr, Cu, Fe, Mn, Ni, Y and Zn) and the metalloid As (Figure 2, Additional file 4: Table S4). This cross-comparison with other metallic stressors revealed poor relationships between Ln and other metals, demonstrating the peculiar cellular effects mediated by Ln.

Mutants were classified into eleven clusters (C1-C11) based on their metal tolerance characteristics and three major patterns could be described (Figure 2). We should first emphasize that 32 % of the mutants specifically responded to La only (C6, and C8), showing for instance, sensitivity (C8) or resistance (C6), to solely Yb and Y (C3), or to La, Yb and Y (C4). These REE specific mutants, belonged to a few pathways, notably the response to pheromone-related GO Biological processes, represented by mutants of the STE family genes, as well as chromatin silencing mutants (SIR1, SIR2, and SIR3 among others). Only a few mutants were specific to Yb (C5), involved in cell wall biogenesis. Additionally, several mutants for actin-related functions were specific to Ln, as well as mutants for genes involved in the lipid metabolic processes. The identification of mutants

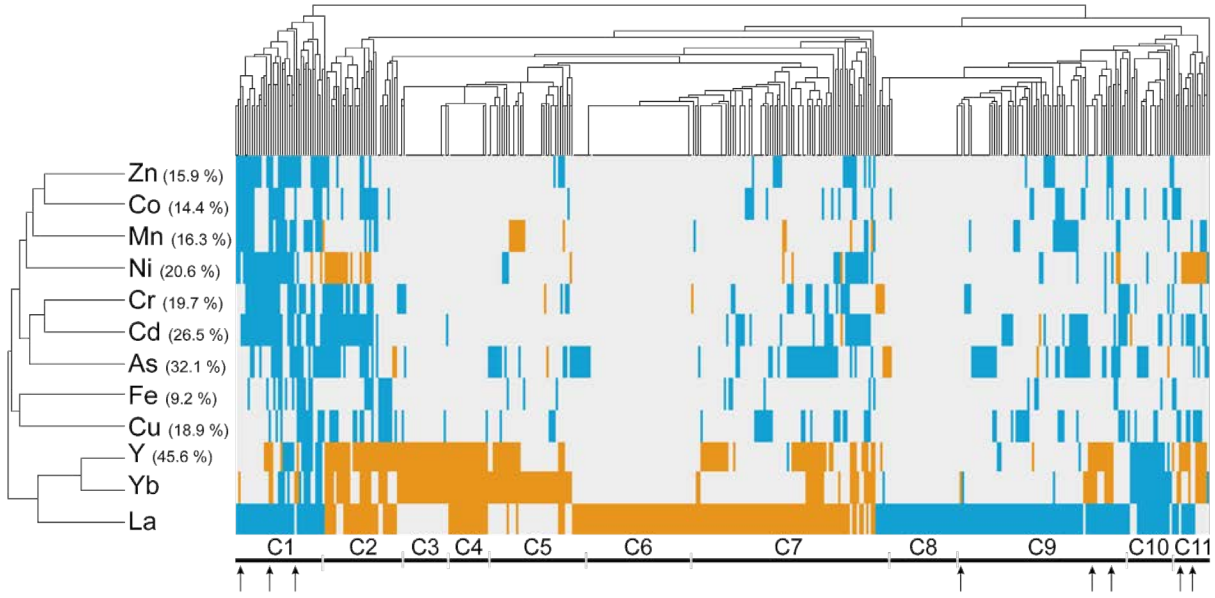

Figure 2 - Cross-comparison of mutant phenotypes to lanthanides versus other metallic stressors. Hierarchical clustering of Ln sensitivity or resistance-conferring mutations with the mutant response profiles obtained for other metallic stressors. The x-axis corresponds to gene-deleted mutants and the y-axis indicates the different stressors from previously published genomic phenotyping screens conducted on deletion mutant collections. Mutants exhibiting either an enhanced sensitivity or resistance are shown in blue and orange, respectively. Clusters of mutants are mentioned below (C1 to C11) with arrows pointing out mutants displaying an opposite phenotype between La and Yb exposure. Values into brackets after the element denote the percentage of mutants that were found common between the screening (La and Yb combined) and screenings on other elements.

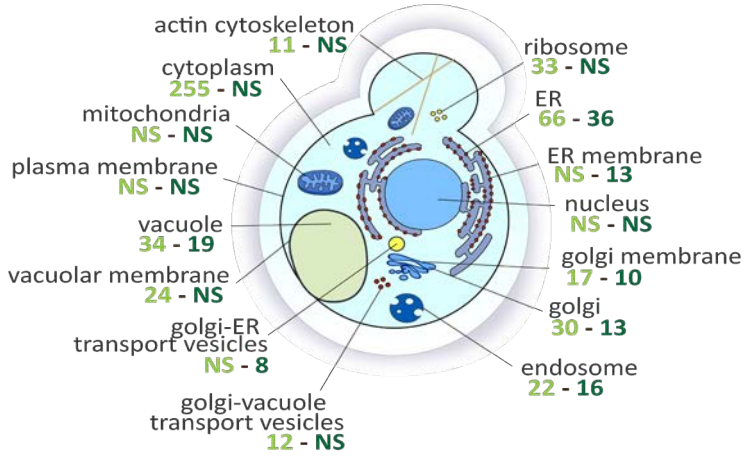

Figure 3 - Cellular compartments of *Saccharomyces cerevisiae* impacted under lanthanide stress. Values in light and dark green are the number of mutants found in the La and Yb screens, respectively, when the compartment was significantly represented ($P < 0.05$). NS: not significant.

specific to Ln in these pathways highlighted the uniqueness of the response to Ln toxicity in comparison to other well-known metals.

The mutants of the C2 cluster were specifically resistant to Ni, Y and both Ln, while sensitive to any other metal investigated. Those mutants were deleted for genes involved in the ubiquitin-dependent protein catabolic process via the multivesicular body sorting pathway (ESCRT complex). The C11 mutants were also resistant to Ni, Y and Yb but sensitive to La, corresponding to the retromer complex, a pathway linked to the ESCRT complex (VPS29, PEP8, VPS35, VPS30).

The C1, C9, and C10 mutants displayed sensitivity to numerous metals. Lacking these genes appears to be deleterious to *S. cerevisiae* when facing a metallic stress. Therefore, these genes are likely to be necessary for yeast cells to cope with metal-mediated general stress rather than for a specific Ln toxicity modulation.

Finally, there was a close relationship between Ln and Y. Indeed 46 % of the mutants identified from the present screen were also either resistant or sensitive to Y (Figure 2). More particularly, Y and Yb clustered closer than the two Ln together. Y is naturally very often found together with Ln species in rocks and soils, and all elements form trivalent cations in solution[38]. Chemically, Y and Yb have similar ionic radii (90 and 87 pm, respectively) but distant to that of La (103 pm). We could therefore hypothesize that, beyond having similar cellular effects, Y and Yb are taken up by the same transport systems across biological membranes and would differ from the transport of La that was suggested to be mediated by Ca transport systems in yeast[39]. Further experiments are however needed to identify the proteins involved in both Y and Yb transport.

Lanthanide responses differ from well-known alkaline pH and oxidative stress mediated responses

When investigating the data from the metal tolerance cross-comparison into more details, similarities between Ln and As responsive genes (32 %) and Ln and Cd responsive genes (27 %) were evidenced (Figure 2). Since Cd[40] and As[41] have been shown to induce oxidative stress in *S. cerevisiae*, we further assess whether these responses also occurred with stressors generating an oxidative stress in yeast cells. To achieve this goal, we compared our data with similar genomic phenotyping studies carried out on various chemical and physical stressors[42–46] (Additional file 5: Figure S1 and Additional file 6: Table S5). Forty-two percent of the mutants sensitive or resistant to one or both Ln were identified in at least one of these screenings. The highest similarity was found for both bleomycin and diamine with 17 %of their mutants also retrieved in our Ln screens (Additional file 5: Figure S1). A few previous studies mentioned an oxidative stress caused by Ln[22]. However, La and Yb clustered together, as an outgroup in that cross-comparison, with more than 360 mutants responding specifically to Ln and not to the other chemical or physical stressors. These results suggest that the cellular responses to Ln are not due to indirect stresses such as pH-related or oxidative stress.

The Golgi, ER, and vacuole are the major cellular compartments affected by lanthanides

To highlight the cellular hotspots of Ln responses, an analysis of the MIPS (Munich Information Center for Protein Sequences) subcellular localization was performed (Figure 3, Additional file 7: Table S6). Impairing genes linked to the Golgi and the Golgi membrane, to the vacuole or to the ER compartments, rendered cells sensitive to both Ln (Figure 3, Additional file 7: Table S6). Furthermore, endosomal proteins appeared to play a role in toxicity modulation for both Ln tested. Conversely, yeast mutants displayed a modified phenotype specifically towards La for gene products associated to the cytoplasm, the vacuolar membrane, Golgi to vacuole transport vesicles, the actin cytoskeleton and the ribosome machinery (Figure 3). Ribosomes were specifically represented in the response to La while surprisingly not to Yb.

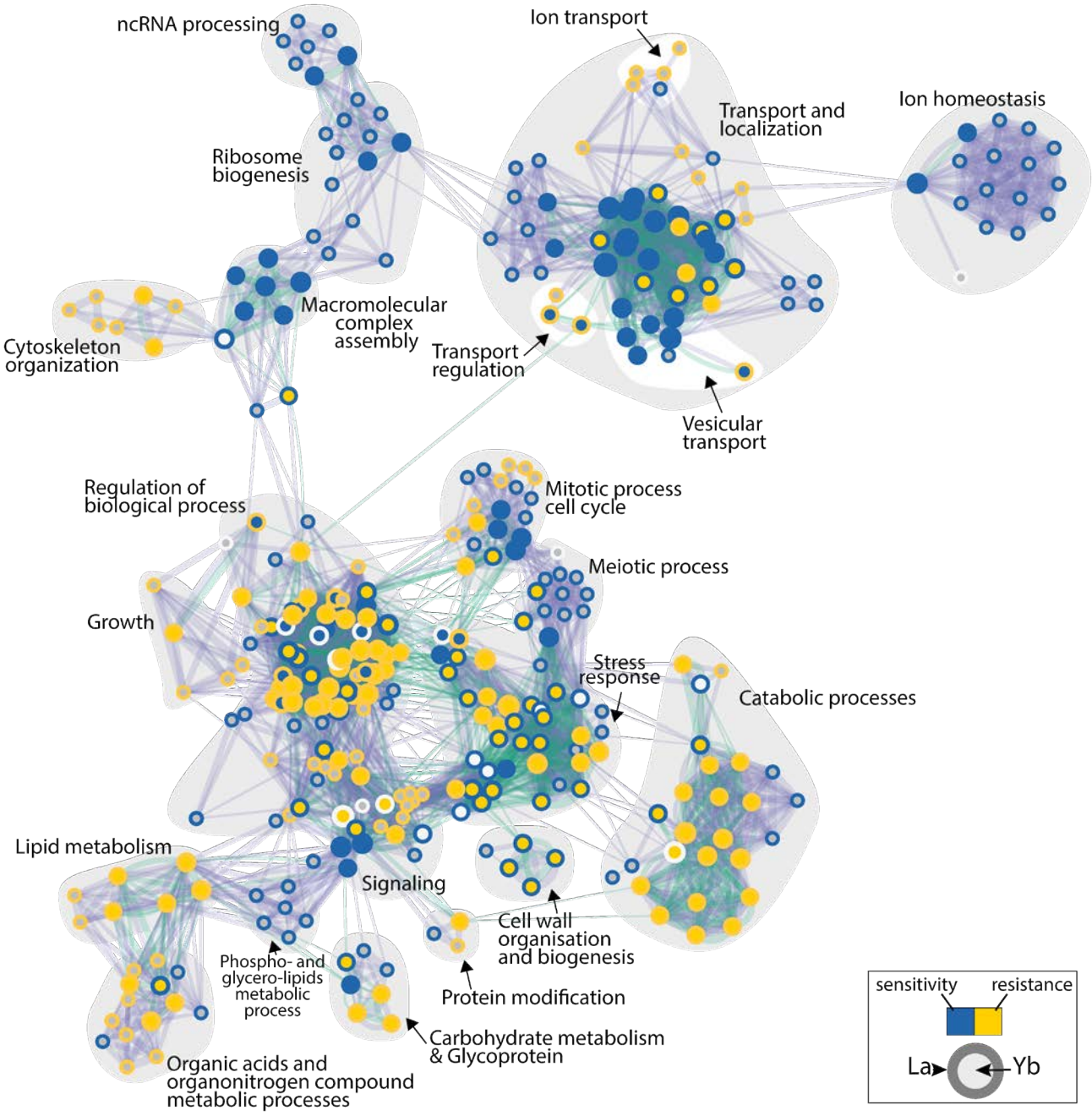

Figure 4 - Functional enrichment analysis network of functions involved in the cellular response to lanthanides. Functions whose deletion renders cells either sensitive or resistant to La (outer circle) or Yb (inner circle) are shown in blue and yellow, respectively. Inter-lines represent gene overlap between two related functions, edge width is proportional to the number of shared genes. The enrichment map was built using GSEA and visualized by the Enrichment map plugin in Cytoscape. White circles represent functions with non-significant p-values.

Lastly, mutants for proteins of the Golgi to ER transport vesicles and of the ER membrane were specifically found for Yb. Similar involvement of the vesicle transport was found for Ni and Cd[37]. The lack of representation of the nucleus, plasma membrane or mitochondria was noticeable (Figure 3). The latter observation could be related to the scarce response similarity between the Ln-mediated stress and chemical-induced oxydative stress, as evidenced in additional file 5: Figure S1.

Different lanthanides trigger different cellular functions

To go deeper into the understanding of Ln-mediated toxicity mechanisms, the identification of the cellular processes engaged in Ln toxicity response was uncovered by the analysis of biological pathways (Figure 4, Additional file 8: Table S7). Relatively contrasted enrichment maps were generated for Yb and La (Figure 4), supporting the conclusions drawn above that yeast cells trigger specific responses to the two Ln. Overall, as shown by the enrichment map (Figure 4), many biological processes are involved in the modulation of Ln toxicity. Transport and localization functions, including vacuolar transport, endocytosis and vesicle-mediated transport, but also catabolic processes and lipid metabolism were highly represented among La or Yb-responsive genes, and showed similar phenotypes for the two Ln tested (Figure 4). Some functional categories detected under La exposure such as ion homeostasis, ribosome biogenesis, ncRNA processing, were not enriched under Yb exposure (Figure 4). Some other general functions were less represented for Yb as compared with La including mitotic and meiotic processes as well as metabolic processes involving organic acids and organo-nitrogen compounds (Figure 4). More surprisingly, several functions, when mutated, caused sensitivity to La but resistance to Yb. This was the case for cell wall organisation and biogenesis, as well as stress response pathways (Figure 4), which will be further addressed below.

A wide range of mutants for proteins involved in translation was also found to be strictly sensitive to La. Indeed, cells lacking subunits of the ribosomal 60S and 40S subunit protein, RPL (Ribosomal Protein of the Large subunit) and RPS (Ribosomal Protein of the Small subunit) genes family, were sensitive to La but not Yb (Figure 4, Additional file 1: Table S1). Such a reduced translation potential might affect yeast capacity to cope with metallic stressors. Besides, autophagy, CVT pathway (cytoplasm to vacuole targeting) and vesicle fusion processes were also involved, specifically in La toxicity modulation. Although the main role of autophagy is the cellular stress response in yeast, other functions have been described such as homeostatic and biosynthetic functions[47]. This pathway is notably associated with the degradation of organelles and components of the cytoplasm in case of nutrient deprivation[47]. At last, most of the Yb-specific functions over-represented concerned mostly signaling pathways (Additional file 8: Table S7).

This analysis allowed us to assign the responsive genes to the major functions involved in the response to Ln. Once again, it highlighted that cell responses to La and Yb are made of i) a core component responsive to a general Ln stress and ii) two groups of specific pathways dedicated either to La or to Yb. We went deeper in this analysis and understanding of these shared and specific functions through the different focuses presented below.

La and Yb affect differently the cell wall and signalling

The cell wall is the first shield against extracellular stressors, including metals. Several mutants responding to Ln exposure were knocked-out for proteins involved either in the cell wall stress response and biosynthesis, or in the pheromone signaling pathways and processing (Figure 4-5, Additional file 8: Table S7). Interestingly, these mutants displayed different phenotypes following La or Yb exposure (cluster C1 & C9 Figure 2). However most of the mutants were resistant to Yb while sensitive to La as it was the case for cells mutated in cell wall integrity related proteins such as Kre1p, Kre6p (Figure 5a), Gas1p, and Chs1p (Additional file 1: Table S1). Mutants for mannosyltransferases (ΔMnn10, ΔMnn9, ΔMnn2, and ΔAnp1) involved in cell wall mannoprotein synthesis were specifically sensitive to La, while mutants for glucosyltransferases involved in glycoprotein synthesis (ΔAlg3, ΔAlg6, and ΔAlg8) were specifically resistant to Yb (Figure 5h, Additional file 1: Table S1). Kex2 and Kex1 mutants also displayed the dual phenotype (Figure 5a), and Kex2p overexpression in the WT cells displayed the opposite phenotype in response to La and Yb, relatively to the Kex2 mutant (Figure 5b). Those two proteins are both Ca-dependent serine proteases involved in the activation of proteins of the secretory pathway, but also of cell wall proteins, such as Scw4p[48–50] (Figure 5h). Accordingly, in the presence of the serine protease inhibitor tosyl phenylalanyl chloromethyl ketone (TPCK) the WT mimicked the same dual phenotype as the Kex1 and Kex2 mutants (Figure 5c). We also found that Mkc7p, an aspartyl-protease and member of the yapsin family [50] was resistant to Yb only (Figure 5h). This protease acts downstream of Kex2p for post-translational modifications of proteins, supporting the importance of cell wall maturation and composition maintenance through the activity of those enzymes.

To better understand the role of these cell wall integrity components in the contrasted response observed between the two Ln, we measured La and Yb concentrations in the wild type and the mutants by ICP-MS (Figure 5d,e).

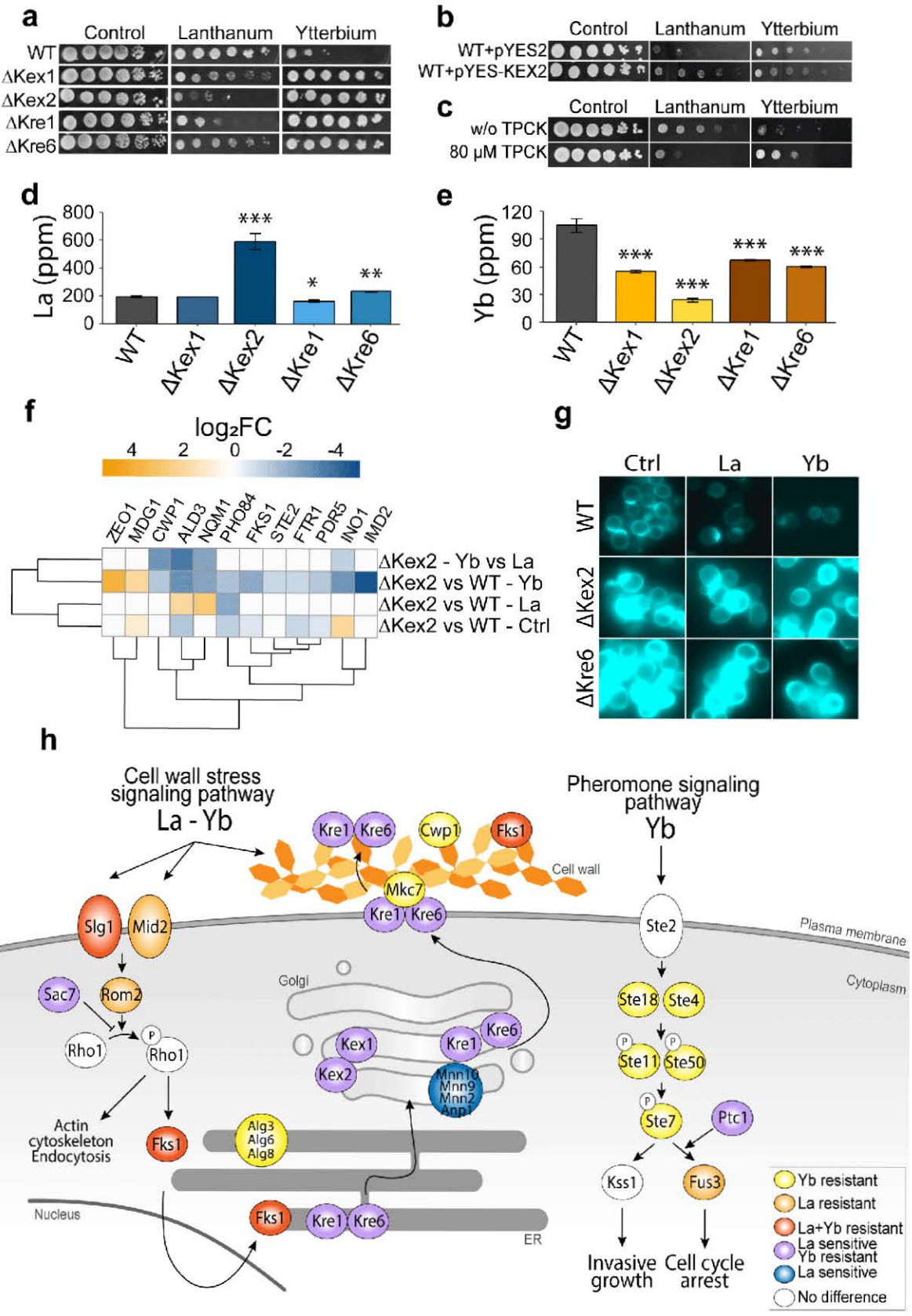
a
Control
Lanthanum
Ytterbium
WT
ΔKex1
ΔKex2
ΔKre1
ΔKre6
b
Control
Lanthanum
Ytterbium
WT+pYES2
WT+pYES-KEX2
c
Control
Lanthanum
Ytterbium
w/o TPCK
80 µM TPCK
d
La (ppm)
800
600
400
200
0
***
*
**
WT
ΔKex1
ΔKex2
ΔKre1
ΔKre6
e
Yb (ppm)
120
90
60
30
0
***
***
***
***
WT
ΔKex1
ΔKex2
ΔKre1
ΔKre6
f
log2FC
4
2
0
-2
-4
ZEO1
MDG1
CWP1
ALD3
NQM1
PHO84
FKS1
STE2
FTR1
PDR5
INO1
IMD2
ΔKex2 - Yb vs La
ΔKex2 vs WT - Yb
ΔKex2 vs WT - La
ΔKex2 vs WT - Ctrl
g
Ctrl
La
Yb
WT
ΔKex2
ΔKre6
h
Cell wall stress signaling pathway
La - Yb
Pheromone signaling pathway
Yb
Kre1
Kre6
Cwp1
Fks1
Cell wall
Mkc7
Slg1
Mid2
Ste2
Plasma membrane
Cytoplasm
Golgi
Sac7
Rom2
Rho1
P
Rho1
Kex1
Kre1
Kre6
Kex2
Mnn10
Mnn9
Mnn2
Anp1
Ste18
Ste4
P
Ste11
P
Ste50
P
Ste7
Ptc1
Actin cytoskeleton Endocytosis
Fks1
Alg3
Alg6
Alg8
Kss1
Fus3
Nucleus
Fks1
Kre1
Kre6
ER
Invasive growth
Cell cycle arrest
Yb resistant
La resistant
La+Yb resistant
La sensitive Yb resistant
La sensitive
No difference

Figure 5 - Dual involvement of the cell wall and signaling in response to lanthanides. (a) Drop-test of 10-fold serial dilutions of mutant strains displaying the opposite phenotype when exposed to La and Yb. (b) Overexpression of KEX2 confers resistance to La but sensitivity to Yb. Yeast cells were transformed with the empty pYES2 plasmid or with the same plasmid harboring Kex2. Cells were grown on YPG in the presence of La (3.8 mM), Yb (3.2 mM) or in the absence of lanthanides (Ln) (control). (c) Drop-test of 3 fold serial dilutions of the WT strain exposed to La (3.8 mM) and Yb (3.2 mM) with addition of the serine protease inhibitor tosyl phenylalanyl chloromethyl ketone (TPCK). (d-e) La and Yb contents of WT and mutant strains. Cells were grown in modified YNB and exposed to La (50 µM) or Yb (6 µM) for one hour. Data are the means (±SD) of three independent cultures, and statistically significant differences from the WT condition are indicated by asterisks (ANOVA, Tukey HSD, *<0.05, **<0.01, ***<0.001). (f) Heatmap of some differentially expressed proteins in the ΔKex2 mutant under control, La, or Yb conditions. (g) Chitin staining using calcofluor white in WT, ΔKex2, and ΔKre6, under Ln exposure. Representative pictures are given. (h) Schematic representation of the proteins involved in signaling pathways and cell wall organization in response to Ln.

Interestingly, the four mutants tested (ΔKre1, ΔKre6, ΔKex1, and ΔKex2) accumulated two to three times less Yb (Figure 5e) than the wild type, while ΔKex2 and ΔKre6 accumulated significantly more La (Figure 5d). The high concentrations of La of the ΔKex2 and ΔKre6 mutants correlated well with the sensitive phenotype whereas the reduced Yb contents of the four Kex and Kre mutants fully explain their resistance to Yb. Consequently, those proteins, and the cell wall constituents, could be involved in the differential adsorption of Ln, followed by an internalization step, or by modulating Ln uptake through ion membrane transporters.

Since out of the mutants analyzed, ΔKex2 was the most contrasted one regarding the phenotype and its Ln content, we selected this mutant to investigate its proteomic landscape modifications after Yb or La exposure (Figure 5f, Additional file 5: Figure S2 and Additional file 9: Table S8). For this, label-free high-throughput shotgun proteomics was performed on WT and mutant cells subjected to the same conditions taking into account biological triplicates. Seventy-five proteins displayed different abundance patterns in ΔKex2 between La and Yb, twelve of them being represented in figure 5f. Firstly, Nqm1p, and Ald3p were both repressed when exposed to Yb, but were more abundant under La exposure (Figure 5f, Additional file 5: Figure S2 and Additional file 9: Table S8). Nqm1p is a transaldolase

up-regulated by various stress including osmotic shock[51], while Ald3p is a stress responsive aldehyde dehydrogenase[52]. Therefore it can be hypothesized that the large influx of La in ΔKex2 (Figure 5d) could trigger an osmotic stress and thus could up-regulate Nqm1p and Ald3p, as previously reported in yeast under osmotic shocks[51]. Pdr5p was also repressed when exposed to Yb, but not to La (Figure 5f). Pdr5p is a plasma membrane ABC multidrug transporter involved in cation resistance in yeast[53] and could therefore be involved also in Yb resistance. Similarly, we noticed a lower abundance of other membrane transporters in the ΔKex2 mutant relatively to the WT. Pho84p, a high-affinity phosphate transporter and low-affinity Mn transporter, and Ftr1p, a high-affinity iron transporter (Figure 5f) were essentially less detected in this mutant. Such observation could explain the higher resistance of the ΔKex2 mutant to Yb by decreasing its putative non-specific uptake by these transporters.

Finally, cell wall glycoprotein and β-glucan synthesis enzymes were particularly repressed under Yb stress. It was the case for Cwp1p, a cell wall mannoprotein, linked to β-1,3 and β-1,6-glucans, and Fks1p, a catalytic subunit of β-1,3-D-glucan synthase (Figure 5f). Cwp1p abundance was two and a half times lower compared to the WT strain in ΔKex2 under Yb, and seven times less than in ΔKex2 under La (Figure 5f). In accordance with that observation, and as for ΔKre1 and ΔKre6, both mutants for proteins involved either in the β-glucan synthesis or assembly, ΔCwp1 and ΔFks1 were also resistant to Yb (Additional file 1: Table S1). Altogether, these observations emphasize the importance for yeast cells to modulate the amount of β-glucan and mannoprotein composition of the cell wall, in order to cope with Yb. Furthermore, it has been shown in *Candida glabrata* that disruption of Kre5 decreased the content of β-1,6-glucan and subsequently increased the chitin content in the yeast cell wall, supporting the involvement of this gene in the modulation of the cell wall composition[54].

To investigate whether the composition of yeast cell wall modulate interactions with Ln, WT, ΔKex2, and ΔKre6 cells were exposed to La or Yb and stained with calcofluor white and aniline blue to observe cell wall chitin and β-1,3-glucan, respectively. No difference was observed between the different conditions and strains used for the β-1,3-glucan staining (data not shown). However, a higher content of chitin was observed in both ΔKex2 and ΔKre6 mutants relatively to WT cells, comforting the cell wall modifications as a consequence of those mutations (Figure 5g). A previous study demonstrated the adsorption of Yb and subsequent

formation of Yb-phosphate crystals on the cell wall of *Saccharomyces cerevisiae*[55]. Several other studies mentioned the adsorption of Ln on extracellular biopolymers such as the cell wall of certain bacteria[56]. It was further argued that LREEs, such as La, preferentially bind to phosphate groups, while heavier Ln, such as Yb, would equally bind to phosphate and carboxyl groups[57]. Consequently, the modification of the cell wall content in mannoproteins (e.g. Cwp1p) could modulate the proportion of functional groups to which Ln could bind. The higher abundance of phosphate groups containing mannoproteins could favor La adsorption and toxicity. Conversely, the increase of mannoproteins would decrease the proportion of carboxyl groups, allowing a higher resistance to Yb. Thus, yeast cells might modulate their cell wall composition depending on the Ln species. To confirm the hypothesis of a selective LREE and HREE binding potential according to the cell wall properties, we evaluated growth of ΔKex2, ΔKex1, ΔKre1, and ΔKre6 mutants exposed to one of the 15 LREEs and HREEs (Additional file 5: Figure S3). We observed that ΔKex2, and to a lesser extent ΔKex1, ΔKre1, and ΔKre6 were all sensitive to the LREEs from La to Gd (Additional file 5: Figure S3). Under Tb and Dy exposure, no differences were observed between ΔKex1, ΔKre1, ΔKre6 and the WT (Additional file 5: Figure S3). Yet, for Ln from Ho to Lu, all those mutants were resistant (Additional file 5: Figure S3). These observations evidenced that the cell wall binds LREEs and HREEs differently.

This genome-wide deletion mutant screen also highlighted the cell wall as a hotspot for Ln interaction with yeast cells with mutants for genes encoding proteins responsible for signaling pathways at the cell wall level (Figures 4-5h). Again, a segregation between La and Yb was observed. The pheromone signaling pathway (p = 3.30E-02), was represented by the MAPK (p = 8.96E-03) mutants ΔSte18, ΔSte4, ΔSte11, ΔSte50, and ΔSte7, all being specifically resistant towards Yb[58] (Figure 5h, Additional file 8: Table S7). Associated to that observation, Ste2p, the pheromone receptor that contains a G-protein domain, was downregulated in the ΔKex2 mutant under Yb exposure compared to WT (Figure 5f). Altogether, these results support the involvement of the pheromone signaling pathway in Yb toxicity response specifically, involving the cell wall not only as a metal sequestration compartment but also as an active effector in response to Yb. As an additional evidence, the cell wall stress signaling pathway was also represented with the mutants ΔMid2, a plasma membrane receptor and ΔRom2, a GTP exchange factor, which were both resistant to La (Figure 5h). In agreement with ΔMid2 resistance, Zeo1p, which acts antagonistically to Mid2p in the signaling of the cell wall integrity pathway, was significantly more abundant in ΔKex2 comparatively to WT as shown by proteomics (Figure 5h). Some other mutants belonging to this signaling pathway were also resistant to both Ln, including ΔFks1 and ΔSlg1 (Figure 5h). Slg1p, a cell wall integrity sensor of *S. cerevisiae*, is also considered to play a role in actin cytoskeleton organization and to be required for mitophagy[59]. Furthermore, the mutant ΔSac7, a negative regulator of the RHO1-PKC1-MAPK cell integrity, displayed the same phenotype as observed for ΔKre and ΔKex mutants, supporting the dual role of the cell wall and its adaptation in order to respond to the different Ln (Figure 5h).

Altogether, those results support the different involvement of signaling pathways for LREEs and HREEs, allowing yeast cells to respond specifically to these two groups of metals, by modifying its cell wall composition depending on the Ln species.

The sphingolipid composition is essential in lanthanide toxicity response

Sphingolipids are a key group of molecules known to take part in several cellular pathways, such as membrane fluidity, endocytosis and signaling processes[60]. Sphingolipid biosynthetic (p = 4.00e-02 (La) & 3.85e-03 (Yb)) and metabolic (p = 4.00e-02 (La) & 3.85e-03 (Yb)) processes were two GO-terms enriched within the mutant set, along with cellular sphingolipid homeostasis (p = 8.17e-03 (La) & 3.43e-05 (Yb)) (Additional file 8: Table S7). Most of the mutants for the sphingolipid biosynthetic pathway were resistant to La and Yb, while only a few were sensitive (Figure 6a, Additional file 1: Table S1 and Additional file 8: Table S7). Interestingly, the resistant mutants, namely ΔOrm2, ΔElo2, ΔElo3, and ΔSur2, were those for proteins acting in the early steps of sphingolipid synthesis. The proteins localize in the ER and convert palmitoyl-CoA and serine into dihydrosphingosines (DHS) and ceramides (Figure 6a). Conversely, mutants for enzymes implicated in the downstream steps of complex sphingolipid synthesis, taking place in the Golgi, namely ΔSur1 and ΔCsg2, were sensitive to both Ln (Figure 6a). Since the same results were observed for La and Yb, we investigated whether this result could be extended to the whole set of Ln. Therefore, we selected the ΔOrm2, ΔElo3, and ΔCsg2 and analyzed their response to Ln. As expected, all Ln induced a resistance phenotype in ΔOrm2 and ΔElo3 and a sensitive phenotype to ΔCsg2 (Additional file 5: Figure S4). Thus, the partitioning of the sphingolipid synthesis pathway suggests the implication of the complex sphingolipids but also the early simple sphingolipid forms (long-chain base, LCB) in the response to Ln (Figure 6a). Sphingolipid synthesis was previously shown as mediating iron toxicity in *S. cerevisiae* with Orm2p playing a key role[61]. Contrary to our findings where ΔOrm2 was highly resistant to both La and Yb (Figure 6a), it displayed sensitivity to high iron concentrations[61]. Thus, Ln

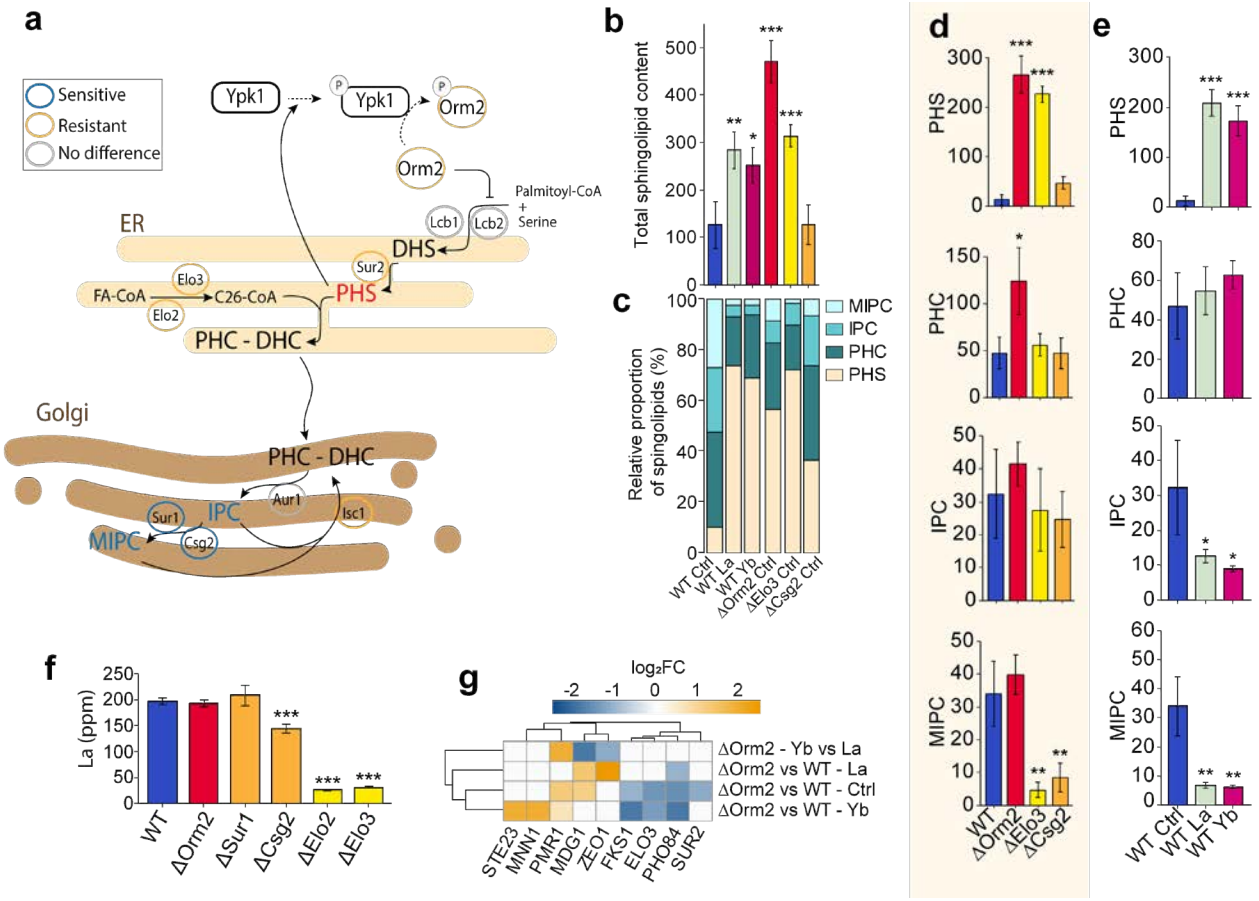

Figure 6 - Sphingolipid content regulates lanthanide (Ln) toxicity in yeast cells. (a) Yeast sphingolipid biosynthetic pathway. Mutant phenotypes under Ln exposure are indicated by colored circles. Terms in red and blue depict an increase and decrease, respectively, in sphingolipid content when exposed to Ln. Black terms indicate no difference in the sphingolipid content when exposed to Ln, relatively to the control. (b) Total sphingolipid content in yeast cells under control and Ln stress conditions. Wild-type and mutant strains were grown either on YPD medium or the same medium supplemented with LaCl3 (3.8 mM) or YbCl3 (3.0 mM), and incubated at 30°C before harvesting for sphingolipid analysis. Triplicate samples were prepared as described in Material and Methods. Sphingolipid levels are indicated as nmol-eq/A600. (c) Relative sphingolipid composition of yeast cells. (d) PHS (phytosphingosines), PHC (phytoceramides), IPC (inositol phosphoceramides), and MIPC (mannosyl-inositol phosphorylceramides) contents in WT and mutant cells not exposed to Ln. (e) Same as (d), but in WT cells exposed under control, La and Yb conditions. (f) La contents of WT and mutant strains. Cells were grown in modified YNB and exposed to La (50 µM) for one hour. Data are the means (±SD) of three independent cultures, and statistically significant differences from the wild-type condition are indicated by asterisks (ANOVA, Tukey HSD, *<0.05, **<0.01, ***<0.001). (g) Heatmap of some differentially expressed proteins in ΔOrm2 mutant under control, La, or Yb conditions.

modulate the sphingolipid-mediated response in a specific manner in comparison to Fe.

Since Orm2p is a repressor of the sphingolipid LCB synthesis, higher sphingolipid content was expected in ΔOrm2 compared to WT. As shown in figure 6b, about four times more sphingolipids were indeed found in ΔOrm2. A closer look at the sphingolipid composition evidenced an increase of 20 and 2.5 times of phytosphingosines (PHS) and phytoceramides (PHC), respectively, in ΔOrm2 compared to WT (Figure 6d). However, no difference was noticed for inositol phosphorylceramide (IPC) and mannosyl-inositol phosphorylceramide (MIPC). These observations led us to hypothesize that sphingolipid content and/or composition is modulated in response to Ln. This was confirmed by measuring the amount of the different sphingolipids in WT cells exposed to the two Ln. PHS increased dramatically (17 for La and 14 for Yb times more) while IPC and MIPC dropped by 3 to 5 times, respectively, under either La or Yb, relatively to the control (Figure 6e). From a more global point of view, it

was also noteworthy that La and Yb exposure led to a modification of the overall composition of sphingolipids in the WT. The PHS represented around 70 % of the total sphingolipids under Ln exposure, while it was below 10 % in the control condition (Figure 6c).

Downstream in the sphingolipid biosynthetic pathway, PHS and dihydrosphingosines (DHS) are complexified by the addition of very long chain fatty acids (Figure 6a). Those fatty acids are synthesized from fatty-acid CoA to C26-CoA through the activity of Elo2p and Elo3p, two fatty acid elongases[62]. Yet, it has been previously shown that Elo2 and Elo3 deletions have regulatory effects on 1,3-beta-glucan synthase[63] but also, on vacuolar ATPase[64] and on the secretory pathway[65]. While found resistant in the present study, Elo2 and Elo3 mutants were identified as Cr- and As-sensitive[66,67], supporting once again the peculiar effect of Ln (Additional file 4: Table S4). Additionally, overexpression of Elo3p in the WT rendered the cells sensitive to Yb (Additional file 5: Figure S5), which further strengthen the implication of Elo3p in the Ln response. Moreover, as observed with ΔOrm2, PHS were produced at very high level in ΔElo3 compared to WT (Figure 6d). Conversely, ΔElo3 contained a very low content of MIPC, which was not the case for both WT and ΔOrm2. Taken together, these results suggest that overproduction of PHS and/or reduction of MIPC production would be essential for Ln resistance in yeast.

At the bottom of the sphingolipid biosynthetic pathway, the glycosphingolipid (GSL) biosynthetic process and MIPC metabolic process (respective p = 7.97e-02 & 1.33e-02) also arose from our screen, involving, among others, Csg2p, Sur1p (= Csg1p) and Tlg2p (Figure 6a, Additional file 8: Table S7). These complex sphingolipids play crucial roles in signal transduction, membrane trafficking, stress adaptation and formation of lipid microdomains[68,69]. For example, MIPC is required for the proper localization of proteins to the plasma-membrane in *Schizosaccharomyces pombe*[70]. Sur1p is a MIPC synthase catalytic subunit, which forms a complex with the regulatory subunit Csg2p to act as an inositol phosphorylceramide mannosyltransferase complex. In the same manner as for La and Yb, ΔCsg2 and ΔSur1 were highly sensitive when exposed to high Ca concentrations[71,72]. The deletion of Csg2 led to a decrease of the MIPC content, similarly to ΔElo3 (Figure 6d). However, unlike ΔElo3, we did not observe an increased production of PHS. Consequently, since ΔCsg2 is sensitive, the hypothesis that MIPC reduction alone is not the key factor for Ln stress adaptation. Taken together, these results suggest that PHS are essential compounds for yeast cells to cope with a Ln stress. In response to Ln stress, WT cells would reorient their sphingolipid metabolism towards the production of PHS, at the expense of the synthesis of complex sphingolipids.

Since sphingolipids are known to be essential components of membranes[60], we hypothesize that the observed modulation of the sphingolipid composition could control the occurrence of ion transporters at the plasma membrane. Therefore, we measured Ln accumulation of WT and mutated strains when exposed to Ln (Figure 6f). No significant difference was observed in La accumulation between WT and ΔOrm2 cells, rejecting this hypothesis for these conditions. However, ΔCsg2 accumulated 25% less La than WT, while ΔElo2 and ΔElo3 contained six times less La than WT (Figure 6f). Elo3 mutant displayed a similar sphingolipid composition to that of WT exposed to Ln (Figure 6b-e). These observations support the importance of higher PHS content together with less MIPC content in yeast cells to cope with Ln, as seen in Elo3 mutant. Such membrane modifications could alter transmembrane transport. This seems to be inefficient for WT, maybe because of the time needed to achieve the response before reaching a toxic intracellular La content. However, in ΔElo3 mutant, the basal sphingolipids composition is very similar to the one in WT exposed to Ln. This could cause a constitutive membrane modification allowing the faster implementation of detoxification steps, potentially involving transmembrane transport reduction.

Thus, it was interesting to look at whether some proteins were possibly modulated, directly or indirectly, by Orm2p. We carried out a proteomic analysis of ΔOrm2 exposed to La and Yb (Figure 6g, Additional file 5: Figure S6 and Additional file 10: Table S9). Firstly, five proteins directly involved in the sphingolipid biosynthetic pathway were found. Elo3p, Sur2p and Csg2p were significantly less abundant in the mutant compared to WT, while Lcb1p and Lcb4p were more abundant (Figure 6g, Additional file 10: Table S9). Consequently, the combined modulation of these proteins would lead to production of PHS, at the expense of complex sphingolipids, and strikingly confirms the sphingolipid assays (Figure 6e). Secondly, several proteins involved either in the cell wall organization or in cell signaling were differentially produced in ΔOrm2 compared to WT (Figure 6g): Zeo1p was over-detected under La. while Mnn1p and Ste23p were more abundant under Yb. Fks1p, a catalytic subunit of 1,3-β-D-glucan synthase, and Gsc2p, redundant with Fks1p, were both less abundant under control and Yb conditions (Figure 6g, Additional file 10: Table S9). Mdg1p, a plasma membrane protein involved in G-protein mediated pheromone signaling pathway was more abundant under control and La conditions. The modulation of the abundance of these proteins supports the close relationship of the membrane composition in sphingolipids and signaling processes in response to Ln.

Moreover, it was interesting to observe a modified protein abundance of several transporters in ΔOrm2 relatively to

WT. Among them were found several metal transporters, Pho84p the high affinity phosphate and low affinity Mn transporter, Ftr1p a high affinity iron transporter, and Zrt1p a high affinity Zn transporter, all three localized at the plasma membrane, plus Pmr1p the Golgi high-affinity Ca^{2+}/Mn^{2+} ATPase transporter, and Zrt3p a Zn exporter, from the vacuolar membrane. Two other transporters as Pdr5p a multidrug ABC transporter, and Hxt2p a high-affinity glucose transporter, were found (Figure 6g, Additional file 10: Table S9). While all the other transporters were more abundant in the mutant relatively to WT, Hxt2p, Pho84p and Ftr1p were less abundant (Additional file 10: Table S9). Combining those observations, it highly supports the close relationship between sphingolipid homeostasis, cell wall organization, and transport, in response to Ln stress. Additionally, the regulation of membrane transporters could be essential to modulate the transport of Ln within the cell.

Endocytosis as a possible regulator of lanthanide uptake

A large GO biological process related to transport was strongly highlighted in the response to Ln (Figure 4). Indeed, a total of 106, and 54 mutants out of 822 genes-related proteins, were found for La and Yb screens, respectively (Additional file 8: Table S7). Interestingly, most of the mutants (65 %) were sensitive to La, whereas 39 mutants (72 %) were resistant to Yb. As a major cellular activity, vesicle mediated transport is therefore a central pathway of which many sub-functions lead to Ln resistance. Among these sub-functions, vesicle docking, regulation of the SNARE (Soluble N-ethylmaleimide-sensitive factor Attachment Protein Receptor) complex assembly, vacuole fusion (non-autophagic), vacuole organization, regulation of vacuole fusion (non-autophagic) or Golgi to vacuole transport can be mentioned (Additional file 8: Table S7). Altogether, these related functions appeared to be of high importance to allow yeast cells to cope with light and heavy Ln toxicity.

Besides, the actin-cytoskeleton and endocytosis likely play a critical role in Ln cell sensitivity. Indeed, cells mutated in genes belonging to the endocytic pathway and actin organization were resistant to both Ln tested (Figure 7a,b, Additional file 8: Table S7). Because two of the major functions filled by the actin cytoskeleton are endocytosis and vesicle trafficking[73], it could explain why several related GO terms were enriched for one or both Ln tested, such as, endocytosis (p = 3.56e-07 & 8.53e-03), actin cortical patch assembly (p = 9.48e-04 for La), actin filament organization (p = 7.12e-03 for La) and actin cytoskeleton organization (p = 2.74e-02 for La) (Additional file 8: Table S7). As shown for plant protoplasts, for which Ln were able to trigger endocytosis[74], our findings suggest an involvement of endocytosis in yeast response to Ln. Several mutants for endocytosis components were identified by our screen. Ede1p is a scaffold protein involved in the formation of early endocytic sites, Ent1p also known as Epsin-like protein and functionally redundant with Ent2p, is also involved in endocytosis and actin patch assembly. Vrp1p (=End5p, verprolin) and End3p, are known to take part in the cytoskeletal organization, cytokinesis and cell wall morphogenesis, respectively. Vrp1p also promotes actin nucleation and endocytosis. As a consequence, the subsequent disruption of either Vrp1 or End3 decreased the endocytosis activity of yeast cells[75,76]. Another clue involving actin polarization and endocytosis appeared with the resistant phenotype displayed in our screening by ΔMyo5 and ΔShe4. Myo5p is one of the two type I myosin motors needed for polarization of the actin filaments, showing a decreased endocytosis activity when disrupted[77]. She4p is required for the proper localization of the type I myosin Myo5p and F-actin [78]. Mutants for She4p showed defects of growth, endocytosis and actin cytoskeleton functionality because it has an important role in the motor-actin interaction[78]. Overall, mutants for proteins involved in each step of the CME (Clathrin Mediated Endocytosis) had an improved fitness when exposed to La or Yb (Figure 7a,b). To test the hypothesis of the involvement of endocytosis in the response to all Ln, we grew several mutants (ΔMyo5, ΔEde1, ΔVrp1, ΔEnt2, and ΔEnt1) in presence of the entire panel of Ln species. These mutants were resistant to all Ln tested (Additional file 5: Figure S7a). Thus, endocytosis is involved in the cellular response of yeast to all Ln.

In order to corroborate the results obtained with the mutants, we analyzed the effect of a chemical inhibitor of the CME on the toxicity mediated by La, chosen here as a representative Ln. The inhibitor used was chlorpromazine (CPZ), which translocates clathrin and AP2 from the cell surface to intracellular endosomes. Yeast cells exposed to high concentration of La, with the addition of CPZ demonstrated a higher survival rate compared to the absence of CPZ (Figure 7c), strengthening the importance of endocytosis in Ln response.

In a recent study, Cr was demonstrated to trigger endocytosis in *S. cerevisiae*, which was first proposed to explain the fact that endocytosis mutants were sensitive to this metal[79]. Indeed, such mutants lacking either Sac6p, Chc1p or End3p proteins, had a higher Cr content[79]. It was suggested that the endocytic inactivation of Cr transporters of the plasma membrane in an ubiquitin-dependent manner, is an essential pathway to cope with Cr toxicity[79]. However, dealing with Ln seems to rely on a different mechanism. Since endocytosis mutants were resistant to Ln, it infers that endocytosis is involved in Ln toxicity, possibly by mediating intracellular Ln uptake.

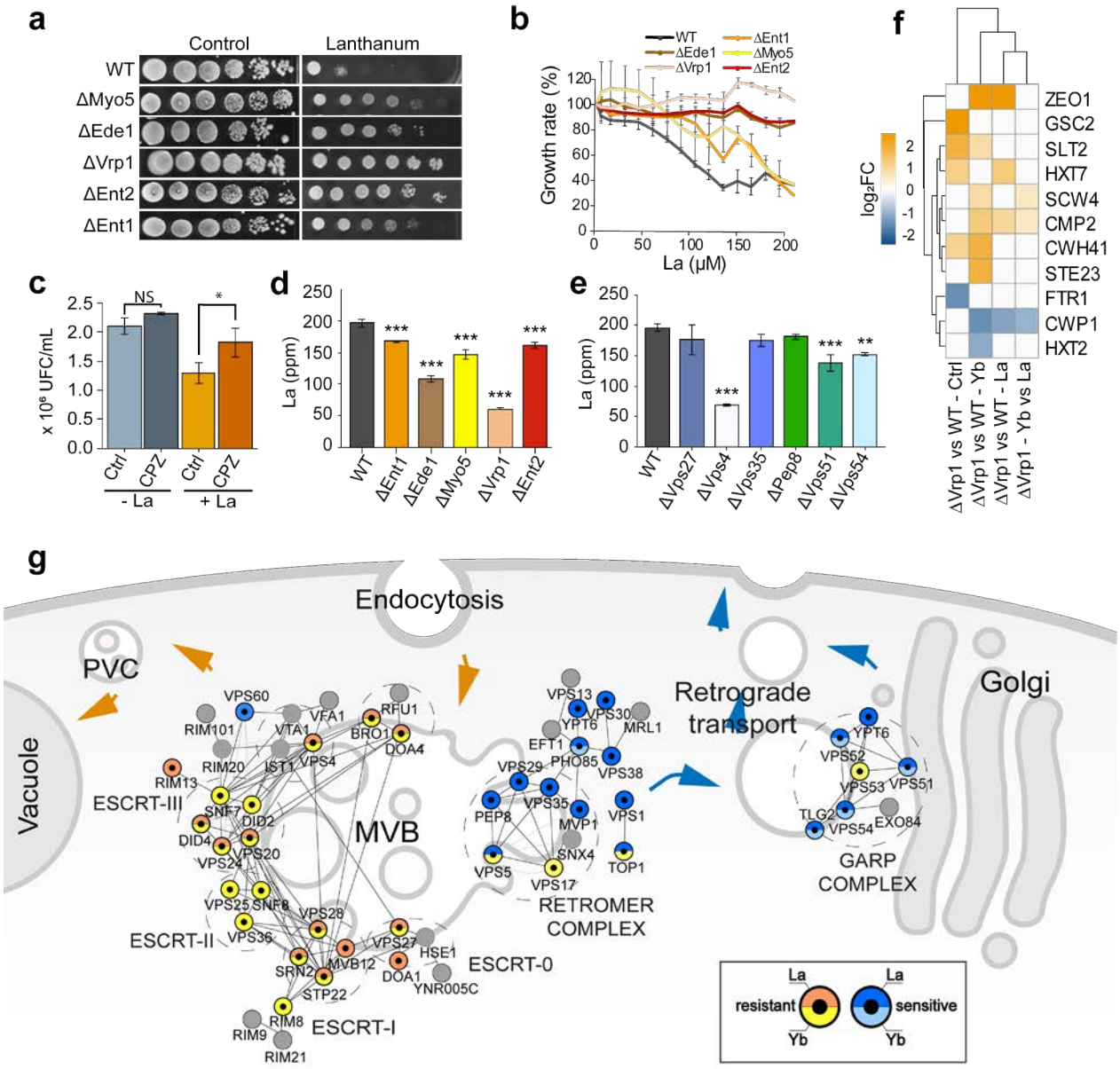

Figure 7 - Implication of the endocytic pathway in Ln-mediated stress response. (a) Drop-test of 10-fold serial dilutions of mutant strains exposed to La (4.6 mM). (b) Growth rate (relative to the control) of yeast cells as a function of La concentration. (c) Yeast survival after 1 h exposure to 350 µM La with the endocytosis inhibitor CPZ (chlorpromazine). (d-e) La contents in strains mutated for genes belonging to the endocytotic pathway (d), and to the ESCRT, Retromer and GARP complexes (e). Cells were grown in modified YNB and exposed to La (50 µM) for one hour. Data are the means (±SD) of three independent cultures, and statistically significant differences from the wild-type condition are indicated by asterisks (ANOVA, Tukey HSD, *<0.05, **<0.01, ***<0.001, NS; Not Significant). (f) Heatmap of differentially expressed proteins in ΔVrp1 mutant under control, La, and Yb conditions. (g) Schematic representation of the vesicular trafficking. Endosomes derived from membrane endocytosis are turned into a MVB (Multi Vesicular Body) by the ESCRT complex allowing the genesis of vesicles within the endosomes. The late endosome can retrieve proteins to the trans Golgi by budding via the Retromer complex. Vesicle fusion is ensured by the GARP complex to the trans Golgi. PVC: pre-vacuolar compartment. Proteins involved in these functions are shown as diagrams. The color refers to the mutant's phenotype: orange, and yellow are for La and Yb resistance, respectively, and dark blue and light blue are for La and Yb sensitivity, respectively. Orange arrows mean that the lack of this pathway renders mutants resistant to Ln while blue arrows denote that the lack of this function induces Ln sensitivity to the mutants.

To test this hypothesis, we measured whether the accumulation of La would decrease in endocytosis defective condition. In accordance with our hypothesis, all the mutants tested accumulated less La than the WT, down to two to three times less for ΔEde1 and ΔVrp1 (Figure 7d). Altogether, those observations support the hypothesis of a direct and non-specific intracellular entry of Ln through endocytosis. This hypothesis meets our above discussion concerning the role of membranes and cell walls in Ln adsorption and absorption. However, another hypothesis could be drawn. A yet unidentified efflux transporter could discard Ln from the cytoplasm. Several yeast transporters, located at the plasma membrane, are regulated by endocytosis, therefore mediating the intracellular uptake of metals. This is the case of Zrt1p and Ctr1p, respectively Zn and Cu uptake transporters that are regulated post-translationally by endocytosis to be further degraded in the vacuole[80–82]. Therefore, endocytosis inhibition would favor the accumulation of a putative Ln efflux transporter at the plasma membrane, allowing an increased efflux out of the cells of these toxic metals.

To explain the resistant phenotype of the endocytosis defective mutants, we selected the Vrp1 mutant which had the lowest La content (Figure 7d) and performed a proteomic analysis under control, La or Yb exposure conditions. (Figure 7f, Additional file 5: Figure S8 and Additional file 11: Table S10). Interestingly, several elements of the cell wall integrity pathway and organization were among the highest over-abundant proteins, as shown by an increase in Gsc2p content only in the control condition, while Zeo1p was more abundant under both La and Yb exposures (Figure 7f, Additional file 5: Figure S8 and Additional file 11: Table S10), as also observed in ΔKex2 (Figure 5f). Gsc2p is a catalytic subunit of the 1,3-β-glucan synthase and Zeo1p acts antagonistically to Mid2p in the signaling of the cell wall integrity pathway. Several other proteins involved in cell wall processes and signaling were also modulated. Slt2p, Cwh41p were more abundant under control and Yb conditions while Scw4p and Ste23p accumulated only under Yb conditions (Figure 7f, Additional file 11: Table S10). Inversely, Cwp1p, a cell wall mannoprotein was less detected, and thus its gene repressed, under La and Yb conditions (Figure 7f, Additional file 11: Table S10). Cmp2p (calcineurin), which is involved in stress signaling was more abundant in La and Yb conditions (Figure 7f, Additional file 11: Table S10). Together, those observations support our previous conclusion that the cell wall organization and signaling both play an essential role in the cellular response to Ln. We further identified plasma membrane transporters that were differentially detected in ΔVrp1, which could explain the Ln-resistant phenotype of this mutant. Two glucose transporters, Htx2p and Hxt7p, were found. Htx2p was less abundant under Yb exposure and Htx7p was more abundant under control and La conditions (Figure 7f, Additional file 11: Table S10). However, no straightforward explanation could be drawn to explain this deregulation. More interestingly, Ftr1p, the high-affinity iron permease, was three times less detected in ΔVrp1 than in WT under the control condition (Figure 7f, Additional file 5: Figure S8 and Additional file 11: Table S10). As hypothesized for the ΔKex2 mutant, lower production of Ftr1p in the endocytic mutant could, by decreasing Ln uptake, be involved in the resistant behavior of this mutant. Thus, these findings suggest that Ln uptake could be mediated by the Fe uptake system.

Two sub-parts of vesicular trafficking differentially modulate Ln toxicity

Very closely related to endocytosis, the functions of ubiquitin-dependent protein catabolic process via the MVB (Multi Vesicular Body) pathway was also over-represented in the mutant screening (Additional file 8: Table S7). Seven, and twelve mutants (out of fifteen) linked to this pathway displayed resistance to both La and Yb, respectively. The prevacuolar compartment (PVC) and MVB formations ensured by the ESCRT complex are pathways that allow recycling of misfolded membrane proteins (e.g. membrane receptors and transporters) as well as vacuolar components, or elimination of plasma membrane regions through pinocytosis[83] (Figure 7g). As shown in figure 7g and additional file 5: Figure S7b, the whole ESCRT machinery seems to be involved in Ln toxicity since almost every mutant for the proteins involved in that pathway were resistant in our screen, with ESCRT-0 (ΔVps27), ESCRT-I (ΔStp22, ΔVps28, ΔSrn2, and ΔMvb12), ESCRT-II (ΔSnf8, ΔVps25, and ΔVps36), and ESCRT-III (ΔDid4, ΔVps20, ΔVps24, ΔSnf7, and ΔDid2)[83]. The mutant for Vps4p, which catalyzes ESCRT-III disassembly and subsequent membrane release, was also resistant along with the mutant for Bro1p (Vps31p), which coordinates de-ubiquitination in the MVB pathway by recruiting Doa4p to endosomes[83]. When comparing with other metal screening studies, similar observations were made for Ni[37,84], while on the other hand, mutants lacking ESCRT proteins showed sensitivity to Cr, Cd and As (Additional file 4: Table S4). Interestingly, except for ΔVps60, mutants belonging to the ESCRT complex were sensitive to Ca chloride[37]. This finding emphasizes the segregation of Ca and Ln by yeast cells, since ESCRT mutants were resistant to Ln (Figure 7g, Additional file 5: Figure S7b).

Downstream MVB, the retrograde transport is involved in recycling of proteins and receptors of the plasma membrane or vacuolar membrane (through endosomes) to the trans-Golgi and/or back to the plasma membrane. Different mutants for this process were also significantly over-represented in our screen together with other

vesicular/endosomal transport, conferring La-sensitivity to the mutants (Figure 7g, Additional file 8: Table S7). The retrograde transport is first characterized on one side by the GARP (Golgi-associated retrograde protein) complex, which is localized on the Golgi network (Figure 7g). The GARP complex, gathering Vps51p, Vps52p, Vps53p and Vps54p[85], leads the retrograde transport of cytoplasmic vesicles from early endosomes to the late Golgi. As for Ni, Cd, and chemical stressors[37], mutants for the genes involved in this function were sensitive to the Ln tested (Figure 7g, Additional file 4: Table S4 and Additional file 6: Table S5). Secondly, this retrograde transport from the endosomal compartment to the late Golgi, also involves the retromer complex on the endosome side (Figure 7g). The latter complex counts in Vps5p, Vps17p, Vps29p, Vps35p, Mvp1p, Top1p, and Pep8p (Figure 7g). Mutants for components of the retromer complex were sensitive to La as they were for Cd (Figure 7g, Additional file 5: Figure S7b)[37]. However, some of these mutants (ΔVps5, ΔVps17, and ΔTop1) were resistant to Yb as it was also the case for Ni (Figure 7g, Additional file 4: Table S4)[37]. Additionally, reduced accumulation of La was observed in three of the six mutants tested (figure 7e).

To summarize on these results related to the ESCRT and retrograde transport, and in order to extend our observations to the whole set of Ln, several mutants were tested for their sensitivity/resistance towards the 12 other Ln. As previously demonstrated for the functions studied above, these mutants displayed the same phenotype as on La for LREE and Yb for HREE, which supports again the discrimination between LREE and HREE by this cellular process.

It has been previously hypothesized that mutants for these different pathways (ESCRT, Retrograde transport) could lead to protein missorting. Here, a deletion in the ESCRT complex, downstream of membrane endocytosis, and leading to degradation of membranes into the vacuole, renders cells more resistant to Ln. In contrast, the lack of retrograde transport of endosomes to the Golgi and/or back to the plasma membrane leads to mutant sensitivity (Figure 7g). Thus, a putative efflux system of Ln, localized in the plasma membrane, could remain at this location either by a lack of endocytosis/degradation or by its recycling back to the plasma membrane. Thus, accumulation of such a transporter would contribute to detoxify Ln ions out of the cell (Figure 7g). Another consistent hypothesis could rely on endocytosis of Ln bound to the plasma membrane or engulfed into the lumen of endosomes. In both cases, intracellular Ln exposure and their subsequent toxic effects would be reduced (Figure 7d,e). These two hypotheses fit well with the cell response to LREE and partially to that for HREE. However, other indirect associated mechanisms cannot be ruled out and will deserve further attention.

Vacuolar acidification is critical for LREE detoxification

Finally, among the functions represented under La exposure, vacuolar acidification was the most significant (p = 2.82E-08). Fourteen mutants (out of the 27 genes present in that function) were sensitive to La exposure only, while these mutants did not show any modified fitness under Yb stress (Figure 8a-c). Vacuolar acidification is related to genes involved in ion homeostasis and pH regulation. The vacuolar proton-transporting V-type ATPase complex assembly and the ATP hydrolysis coupled proton transport (both sub-functions of ATP metabolic process) are two functions that likely play an important role for cells in order to cope with La toxicity. The disrupted genes were mostly part of the VMA (Vacuolar Membrane ATPase) family, which are subunits of the VMA machinery[86] (Figure 8a). Vacuolar acidification is a critical step to ensure diverse functions played by acidic organelles such as the vacuole. The V-ATPase is the enzyme enabling the creation of a proton potential that leads to the accumulation of ions inside the vacuole, through other vacuolar transporters using the generated proto-motive force. In fungi and plant cells, the vacuole can play a similar role to lysosomes in other eukaryotic cells, but with additional functions such as storage, Ca homeostasis, osmotic control and heavy metal detoxification[86]. It has been demonstrated that VMA-gene mutants were sensitive to high Ca due to either a higher cellular Ca concentration or to a faster influx of Ca within the cells[87]. This report prompted us to investigate whether VMA mutants would also accumulate high concentration of La. Together with a high sensitivity, a very high accumulation of La was observed in the three VMA mutants we tested (ΔVma1, ΔVma5, and ΔVma13). Indeed, up to a hundred times more La was accumulated in VMA mutants compared to WT strain (Figure 8d). Increased content of Mn, Zn and Cu, while decreased content of Fe, were also measured along with La (Additional file 5: Figure S9f,g). However, the same accumulation of these micro-nutrients was also observed under Yb. Consequently, the hypersensitive phenotype of VMA mutants under La is very unlikely due to accumulation of these micro-nutrients, but to La overloading. The vacuolar H+-ATPase was shown to play an essential role in Cu, Ca, Mn and Zn detoxification[88,89]. Thus, the results obtained here suggest similar essential involvement of VMA in La detoxification. It is more likely to see here a general metal detoxification process, rather than a Ca and Ca-like ions (such as La) specific process. It is noteworthy, however, that the function ensured by the VMA machinery is not essential for cells facing an Yb stress. Yb did not cause any modified fitness of the VMA mutants, and Yb overload was not observed (Figure 8a,c).

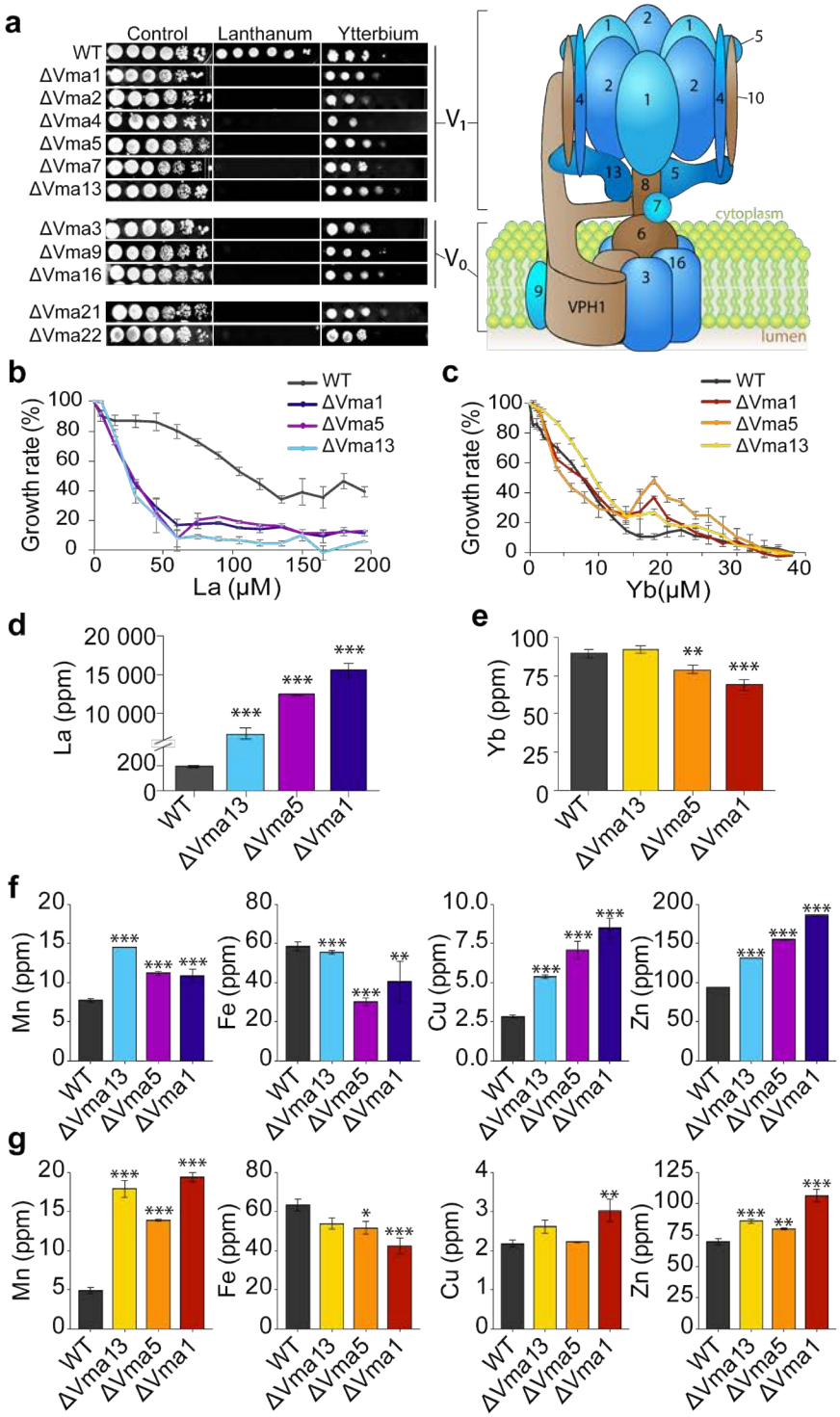

Figure 8 - Differential role of the vacuolar membrane in Ln toxicity. (a) Drop-test of 10 fold serial dilutions of mutant strains exposed to La (3.8 mM) and Yb (3.2 mM) and VMA representation. Subunits (when disrupted) leading to a sensitive phenotype towards La are depicted in blue. (b-c) Growth rate (relative to the control) of VMA mutants as a function of La (b) and Yb (c) concentrations. Data are the means (±SD) of three independent cultures. (d-e) La (d) and Yb (e) contents in VMA mutants. (f-g) Mn, Fe, Cu and Zn content in WT and VMA mutants exposed to La (f), or Yb (g). Cells were grown in modified YNB and exposed to La (50 µM) or Yb (6 µM) for one hour. Data are means (±SD) of three independent cultures, and statistically significant differences from the wild-type condition are indicated by asterisks (ANOVA, Tukey HSD, *<0.05, **<0.01, ***<0.001).

We further investigated if the lack of the VMA machinery was strictly specific to La or could be generalized to all LREE (Additional file 5: Figure S9). We observed that VMA mutants were sensitive to all LREE spanning from La to Eu (Additional file 5: Figure S9). The mutants were slightly less sensitive starting from Gd to Ho, to finally not being impacted by Ln from Er to Lu (Additional file 5: Figure S9). To support this observation, VMA mutants were slightly sensitive to Y, a non-Ln REE[90]. Y has an ionic radius between Ho et Er. It thus appears that the bigger the ionic radius, the more sensitive the VMA mutants are. This observation indicates that most of the HREE may not be detoxified by the vacuole, while it is an essential detoxifying mechanism for LREE.

Conclusions

To date, studies dealing with Ln toxicity are scarce, and thus how organisms can cope with the toxicity of these emerging contaminants is an open question. Here we investigated for the first time the molecular and cellular toxicity and detoxification mechanisms that were involved in Ln stress response. The use of *Saccharomyces cerevisiae* as a eukaryotic model organism gives valuable information about the potential impact of these emerging pollutants. We demonstrated and delineated, by combining high throughput genetic and proteomic methods, the involvement of several major pathways in Ln toxicity (Figure 9). Among them, it appeared that the different Ln modulate or trigger different response pathways in yeast cells upon their nature (Figure 9). The high reactivity of Ln to functional groups of the cell wall makes this later the first interface in the response towards those elements. We further highlighted the putative involvement of endocytosis in the uptake of Ln in the cell, directly or indirectly, but also the existence of plasma membrane transporters that could fulfil this role (Figure 9). Signaling was also important in cell response to Ln, with again a discriminant response between LREE and HREE stresses. Cell wall stress, and the pheromone signaling pathways took part in the modification of the cell wall organization but also the composition of membrane sphingolipids that play several important roles in the cell (Figure 9). Finally, some more common detoxification mechanisms were found for LREE, such as vacuolar sequestration (Figure 9). These results are a first

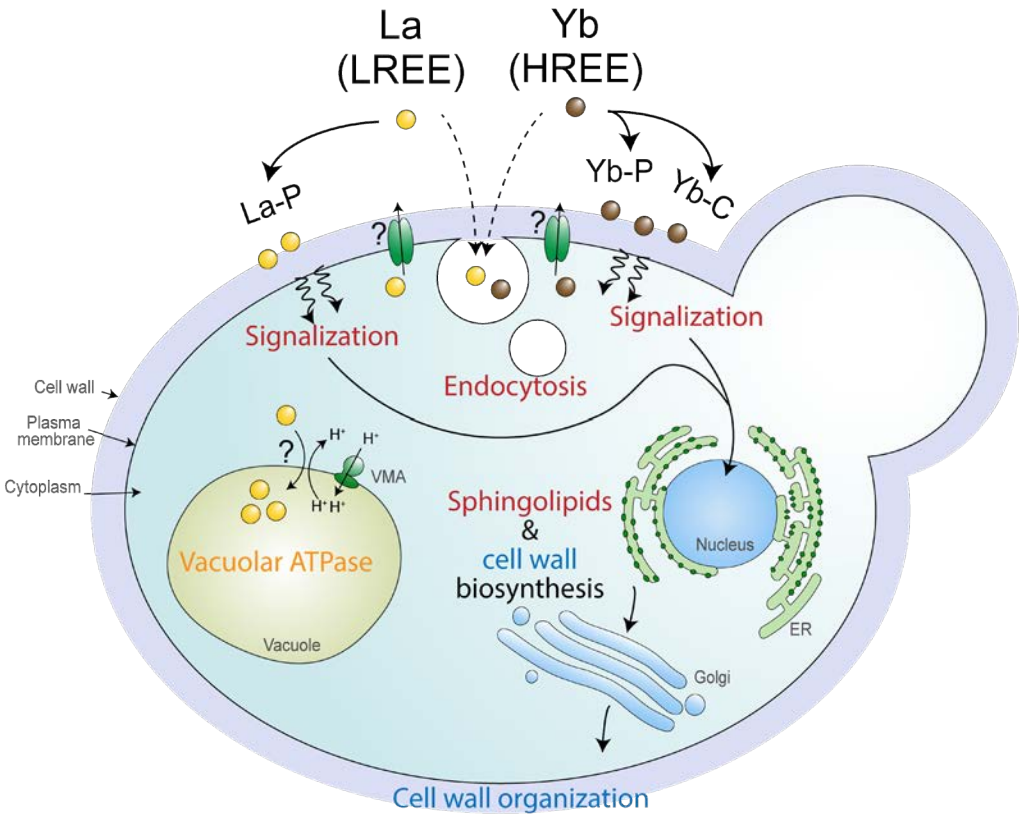

Figure 9 - Global response of *Saccharomyces cerevisiae* toward Ln stress. Schematic representation of large functions uncovered by using the screening of the mutant collection. Common functions between the two Ln are shown in red and functions showing a different behavior are shown in blue, while specific functions to La are shown in yellow. La-P and Yb-P represent Ln ions bound to phosphate groups, while Yb-C represents Ln ions bound to carboxyl groups.

step in the understanding of Ln toxicity, and future investigations can be done on more complex eukaryotes, including human cells, to improve the risk assessment towards these elements. Similar approaches have been previously done with other metals or stress agents, and showed the usefulness of such mutant screening studies. Indeed, studies on other metals such as Ni, confirmed the high degree of conservation of metal toxicity mechanisms between *S. cerevisiae* and mammals[34–36,91].

Materials and Methods

Yeast strains and chemicals

Deletion mutants as well as the wild-type of haploid *Saccharomyces cerevisiae* strains BY4741 (MATa; his3Δ1; leu2Δ0; met15Δ0; ura3Δ0) and BY4742 (MATα; his3Δ1; leu2Δ0; lys2Δ0; ura3Δ0), both isogenic to the S288C strain, were used in this study. They were purchased from EUROSCARF. The haploid deletion library consists of 4,733 non-essential genes. All Ln were purchased from Sigma-Aldrich (MO, USA) as hydrated chloride salts ($LnCl_3$, xH_2O).

Saccharomyces cerevisiae genomic phenotypic screen with lanthanides

The 4,733 mutants from the BY4741 library were used for genomic phenotyping. Two Ln were selected as La and Yb under their chloride form (respectively $LaCl_3$ and $YbCl_3$). Ln concentrations for the screening were defined by pilot experiments as 4.5 mM La and 3.8 mM Yb, allowing discrimination of either sensitive or resistant strains. Briefly, individual deleted strains were grown in 96-well master plates in 200 µL of YPD (10 g yeast extract, 20 g peptone, 20 g dextrose) at 28 °C until stationary phase. A Thermo Scientific™ Nunc™ Replication System (250520) was used to replica inoculate cells by dipping the tips in the wells three times followed by touching the surface of YPD-agar plates supplemented with either La, Yb or Ln-free. Plates were digitally recorded after 5 days of growth at 28 °C. Ln-sensitive and Ln-resistant mutants were identified when colony size under Ln exposure was decreased or increased, respectively, compared to WT and neighbouring mutants but also with the colony size on control plates lacking Ln. Four pin replications were carried out for each metal.

Genomic phenotypic validation screen

Mutant strains identified as Ln-sensitive or Ln-resistant in the primary screen were individually confirmed by serial dilution spot assays. Mutants were grown as previously until saturation in 200 µL YPD medium at 28 °C and serial ten-fold increment dilutions were performed. Five microliters of six dilutions were spotted on YPD agar plates containing Ln at 100 % and 105 % of the concentration mentioned above, in order to verify Ln-sensitive and Ln-resistant mutants, respectively. Results were observed after 7 days of growth at 28 °C. Sensitivity and resistance levels were assigned to the mutant strains, according to the number of growing dilutions. Consequently, mutant strains exhibiting a reduction in colony-forming ability at the first, second-third or fourth-fifth dilution were classified as “high” (HS), “medium” (MS) or “low” (LS) sensitivity, respectively. Conversely, mutant strains exhibiting an increase in colony-forming ability at the second, third-fourth or fifth-sixth dilution were classified as “low” (LR), “medium” (MR) or “high” (HS) resistance, respectively. Twenty-eight mutants randomly picked in the collection were assayed in the parent haploid MATα strain BY4742 in order to confirm the results.

Survival assay & lanthanide toxicity test

In order to measure Ln toxicity towards yeast strains, log-phase yeast cells (OD_{600nm} 0.15) were exposed to increasing Ln concentrations in liquid YNB-β-glycerophosphate medium (YNB w/o phosphates, 1 mM β-glycerophosphate, 2 % glucose, 2 g/L yeast synthetic drop-out medium supplement, pH 5.8) and growth was recorded for 10 h at 28°C under constant shaking (180 rpm). Cell growth rate (µ) was measured in the log-phase between 8 to 10 h, normalized to the condition without Ln, and plotted against Ln concentration.

To determine cell viability, log-phase cells (OD_{600nm} 0.15) were grown with 350 µM of the endocytosis inhibitor chlorpromazine (CPZ) for 1 h at 28 °C under constant shaking (180 rpm) followed by Ln exposure (350 µM La) for 1 h. Cells were harvested and washed twice in sterile water and diluted. Dilutions at 10^{-3} and 10^{-4} were spread on YPD agar plates and incubated at 28°C. CFUs were counted after 48 h of growth.

Chitin staining

WT and mutant cells were grown in YNB medium as above. Cultures were inoculated at an OD_{600nm} of 0.05 and grown overnight, with or without addition of 160 µM La or 8 µM Yb, corresponding to the EC_{50} of the wild type strain. Chitin was stained as described by Okada *et al.* (2010)[92]. Briefly, yeast cells were harvested at 4000 rpm, rinsed twice with deionized water, and stained with 1 mg/mL calcofluor white (Sigma-Aldrich) for 1 min. Stained cells were washed once with deionized water and resuspended into water to be visualized by fluorescence microscopy, using a DAPI filter.

Determination of lanthanide contents in yeast by inductively-coupled plasma mass spectrometry

Mutant and WT strains (BY4741) were grown in YNB medium modified with β-glycerophosphate (1 mM) as

sole phosphorus source, in order to avoid Ln precipitation, by shaking (160 rpm) at 28 °C. Cultures were inoculated at an OD_{600nm} of 0.05 and once the cultures reached an OD_{600nm} of 0.8, Ln were added at 50 µM and 6 µM of La and Yb respectively, corresponding to the EC_{10} of the wild type strain, and were exposed for 1 h. Cells were harvested at 4000 rpm for 1 min at 4 °C. Pellets were washed three times with ice-cold MES (20 mM) – EDTA (10 mM) buffer (pH 6) followed by three washings with ice-cold ultra-pure water and dried for 48 h at 70 °C. Triplicate samples were prepared. The elemental extraction was performed on aliquots (125 mg) of each sample via mineralisation with 1.75 mL HNO_3 and 0.5 mL hydrogen peroxide in closed tubes placed in a block digestion system (DigiPREP, SCP Sciences, Courtaboeuf, France). A gradual heating mode was used to achieve a final temperature of 100°C (total run of 265 min). Finally, ultrapure water was added to 12.5 mL and filtration to 1 µm was performed. Blank and reference material were processed under the same conditions as samples. Concentrations were determined in triplicate using inductively-coupled plasma mass spectrometry (ICP-MS, X Series II Model, Thermo Fischer Scientific, Courtaboeuf, France). Validity of the analytical method was checked by means of standard reference material (oriental basma tobacco leaves, INCT-OBTL-5, LGC Promochem, Molsheim, France).

Proteomics data acquisition and analysis

Mutants and wild type strains were grown in modified YNB medium as described above. Cultures were inoculated at an OD_{600nm} of 0.05 and once the cultures reached an OD_{600nm} of 0.6, Ln were added at 160 µM and 8 µM of La and Yb respectively, corresponding to the EC_{50} of the WT strain, and exposed for 4 h. Then, cells were harvested at room temperature at 4000 rpm for 1 min and pellets were washed twice with PBS (50 mM, pH 7) and snap frozen. Proteins were extracted by bead-beating with a Precellys 24 instrument (Bertin) after addition of LDS1X (Invitrogen) consisting in a solution of 106 mM Tris/HCl, 141 mM Tris base, 2 % lithium dodecyl sulfate, 10 % glycerol, 0.51 mM EDTA, 0.22 mM SERVA Blue G250, 0.175 mM phenol red, buffered at pH 8.5 that was diluted four times and supplemented with 2.5 % beta-mercaptoethanol. Proteins were then subjected to denaturing PAGE electrophoresis for 5 min onto a 4–12 % gradient 10-well NuPAGE (Invitrogen) gel as recommended by Hartmann *et al*. (2014)[93]. After trypsin proteolysis in presence of 0.01 % ProteaseMAX surfactant (Promega), peptides were subjected to tandem mass spectrometry with a Q-Exactive HF tandem mass spectrometer (Thermo) operated in data-dependent mode as described with a 90 min gradient[94]. MS/MS spectra were assigned to *S. cerevisiae* peptide sequences with the Mascot software version 2.5.1 (Matrix Science) with the following parameters: full-trypsin specificity, up to 2 missed cleavages allowed, static modification of carbamidomethylated cysteine, variable oxidation of methionine, variable deamidation of asparagine and glutamine, mass tolerance of 5 ppm on parent ions and mass tolerance on MS/MS of 0.02 Da. Peptide matches with a MASCOT peptide score below a p value of 0.05 were considered. Proteins were validated when at least two different peptides were detected. The false discovery rate (FDR) for proteins was below 1 % as estimated with the MASCOT reverse database decoy search option. Spectral counts (number of MS/MS spectra assigned per protein) were extracted for each sample without parsimony. The normalized spectral abundance factor (NSAF) for each protein was calculated as the total spectral count divided by its molecular mass in kDa and presented in percentage of the total signal. Spectral counts were compared between conditions using the T-Fold method of the PatternLab software [95]. The statistical classes were defined as: “Blue” for proteins that satisfied both, the |T-fold| ($\geq$1.5) and its associated p ($\leq$0.05), “Orange” for proteins with identifications that did not meet the fold criterion but deserved a second look because they had low p-values, “Green” for proteins that satisfied the fold criteria but, most likely, this happened by chance and “Red” for proteins that did not meet the fold and p criteria.

Sphingolipid analysis

Strains were grown either on normal YPD medium plates, 3.8 mM La or 3 mM Yb conditions, and incubated at 28 °C for 4 days before harvesting and washed once with ice-cold PBS (50 mM, pH 7). Triplicate samples were prepared and stored at -80ºC until extraction. In a round-bottom glass tube containing the sample in 150 µL of Mandala’s reagent (15 mL ethanol; 15 mL dH_2O; 5 mL ether; 1 mL pyridine; 18 µL NH_4OH), 0.5 g of glass beads and lipid standards (C17-Sphinganine, C17-SaP, C12-Ceramide, C12-Sphingomyeline, C12-Glycosylceramide, 200 pmol each) were added. The samples were vortexed vigorously for several minutes and incubated at 60 ºC for 15 min. Then, samples were sonicated twice for 20 s and incubated at 60 ºC for 15 min. Cell debris were pelleted by centrifugation at 2300 g for 10 min and the supernatant was collected and evaporated. Methanol (1ml) and chloroform (0.5 ml) were added to the residue, vortexed, incubated at 37ºC for 1 h and centrifuged at 2300g for 5 min. Supernatant was transferred to new vial, chloroform (0.5 ml) and dH_2O (0.5 ml) were added to each tube, vortexed and centrifuged at 2300g for 5 min. The lower phase was transferred to a new vial and dried. Then, methanol (0.5 ml), chloroform (0.25 ml), dH_2O (0.1 ml) and KOH in MeOH (1M, 75 µL) were added to the dried pellet, incubated for 2 h at 37ºC. Finally, acetic acid (1M, 75 µL) was added and samples were evaporated and stored at -80°C. Methanol (80 µL) was added to the samples,

vortexed, centrifuged at 9400g for 5 min and transferred into UPLC vials for their analyses.

Phytosphingolipid (phytoceramides, inositol-phosphophytoceramides, mannosyl-inositol-phosphophytoceramides) analysis was performed using an Acquity ultra-high performance liquid chromatography (UHPLC) system (Waters) connected to a Time of Flight LCT Premier XE detector. Full scan spectra from 50 to 1,800 *m/z* were acquired, and individual spectra were summed to produce data points each of 0.2 sec. Mass accuracy at a resolving power of 10,000 and reproducibility were maintained by using an independent reference spray via the LockSpray interference. Lipid extracts were injected onto an Acquity UHPLC BEH C8 column (1.7 µm particle size, 100 mm x 2.1 mm, Waters) at a flow rate of 0.3 mL/min and column temperature of 30 ºC. The mobile phases were methanol with 2 mM ammonium formate and 0.2 % formic acid (A)/ water with 2 mM ammonium formate and 0.2 % formic acid (B). A linear gradient was programmed as follows: 0.0 min: 20 % B; 3 min: 10 % B; 6 min: 10 % B; 15 min: 1 % B; 18 min: 1 % B; 20 min: 20 % B; 22 min: 20 % B. Phytosphingosine and phytosphingosine-1-phosphate were analyzed using an Acquity UHPLC system (Waters) connected to a triple quadrupole Xevo-TQ-S detector. The following transitions were used: 288.3>252.3 (C17 dihydrosphingosines), 302.3>284.4 (dihydrosphingosines), 318.3>282.4 (phytosphingosines), 382.4>284.4 (dihydrosphingosines-1-P), 398.4>182.4 (phytosphingosines-1-P). The same column and mobile phases were used. A linear gradient was programmed as follows: 0.0 min: 20 % B; 3 min: 10 % B; 6 min: 10 % B; 8 min: 1 % B; 12 min: 1 % B; 13 min: 20 % B; 15 min: 20 % B.

Data analysis

Enriched biological pathways in Ln stressed conditions vs control condition were identified using GSEA software v2.0[96,97]. To establish a gene ranking the sensitivity value difference was used. P-values for enriched gene-sets were defined by computing 1000 gene-set permutations. *Saccharomyces cerevisiae* GO (biological process) derived from MSigDB format gene-set list was downloaded from GO2Msig (http://bioinformatics.org/go2msig/) database and used as a template. From GO2Msig datasets, gene set sizes were restricted to a maximum of 300 and a minimum of 10. GSEA results were visualized using Cytoscape v3.4 software[98] and the Enrichment Map v2.1.0[99] plug-in with default settings. In computed enrichment maps, node colour corresponds to sensitivity of the mutant to Ln stress (yellow for resistant and blue for sensitive) and edge thickness represents redundancies between two gene sets.

Physical and genetic interaction networks were retrieved from GeneMANIA software[100] (http://www.genemania.org/) and visualized using the Cytoscape v3.4 software. All available interaction datasets available were used (GeneMANIA datasets as of June 2018). Input genes plus the top ten related genes were included in the networks. Nodes were manually displayed for clarity, but the overall shape of each network was preserved.

Putative Human homolog(s) of yeast gene(s) and any of their associated OMIM disease phenotypes were retrieved from the SGD YeastMine platform (http://yeastmine.yeastgenome.org/yeastmine/).

Biological process and cellular compartment (MIPS cc) analyses were performed using FunSpec (http://funspec.med.utoronto.ca) and evaluated for statistical significance (cut-off: p-value<0.01).

Clustering (heatmaps) was made using the R package pheatmap. Ln responsive mutants found in this study were compared with those from other studies carried out on *Saccharomyces cerevisiae* deletion mutant collections, on Y[90], Cd[31, 37,101,102], Ni[37,103,104], Zn[31,104–106], Al[107,108], As[31, 66, 102,109,110], Cu[31, 104, 106,111], iron[104, 106,111], Mn[104, 106,112], Co[104] or Cr[31,67] and other stressors[42–46].

For statistical analyses, one-way ANOVA and Tukey HSD post hoc test were used when normality of data (Shapiro-Wilk test) and homoscedasticity (Levene's test) conditions were respected. When at least one condition was rejected, data were subsequently analyzed using one-way non-parametric Kruskal-Wallis test followed by Wilcoxon post hoc test. All analyses were performed using R (version 3.4.1). All reported values are means ± standard deviation (SD) of triplicates (n=3).

Availability of data and materiel

The mass spectrometry proteomics data have been deposited to the ProteomeXchange Consortium via the PRIDE partner repository with the dataset identifier PXD010700 and 10.6019/PXD010700", [https://www.ebi.ac.uk/pride/archive/projects/PXD010700]. [These data can be accessed during the peer-review process of the manuscript with the Username: reviewer99428@ebi.ac.uk and Password: rnjP1qVn].

Funding

This work was supported by the French National Research Agency through the National Program "Investissements d'Avenir" with the reference ANR-10-LABX-21-01/LABEX RESSOURCES 21 and by the Region Grand Est.

References

1. Ciacci, L., Reck, B. K., Nassar, N. T., & Graedel, T. E. Lost by design. *Environ. Sci. Technol.* **49**, 9443–9451 (2015).
2. Hu, Z., Richter, H., Sparovek, G., & Schnug, E. Physiological and biochemical effects of rare earth elements on plants and their agricultural significance: A review. *J. Plant Nutr.* **27**, 183–220 (2004).
3. He, M. L. & Rambeck, W. A. Rare earth elements - A new generation of growth promoters for pigs? *Arch. Anim. Nutr.* **53**, 323–334 (2000).
4. He, M. L., Ranz, D., & Rambeck, W. A. Study on the performance enhancing effect of rare earth elements in growing and fattening pigs. *J. Anim. Physiol. Anim. Nutr. (Berl).* **85**, 263–270 (2001).
5. Panichev, A. M. Rare earth elements: review of medical and biological properties and their abundance in the rock materials and mineralized spring waters in the context of animal and human geophagia reasons evaluation. *Achiev. Life Sci.* **9**, 95–103 (2015).
6. Hedrick, J. B. *Rare Earths. Metals and minerals: U.S. Geological Survey Minerals Yearbook 2001* (2003).
7. Gambogi, J. *Rare Earths. Metals and minerals: U.S. Geological Survey Minerals Yearbook 2015* (2018).
8. Setua, S., Menon, D., Asok, A., Nair, S., & Koyakutty, M. Folate receptor targeted, rare-earth oxide nanocrystals for bi-modal fluorescence and magnetic imaging of cancer cells. *Biomaterials* **31**, 714–729 (2010).
9. Leeuw, D. & Academic, K. Inorganic yellow-red pigments without toxic metals. *Nature* **404**, 980–982 (2000).
10. Wehrmann, M., Billard, P., Martin-Meriadec, A., Zegeye, A., & Klebensberger, J. Functional role of lanthanides in enzymatic activity and transcriptional regulation of pyrroloquinoline quinone-dependent alcohol dehydrogenases in *Pseudomonas putida* KT2440. *MBio* **8**, 1–14 (2017).
11. Wehrmann, M., Berthelot, C., Billard, P., & Klebensberger, J. The PedS2/PedR2 two-component system is crucial for the rare earth element switch in *Pseudomonas putida* KT2440. *mSphere* **3**, 1–12 (2018).
12. Skovran, E. & Martinez-Gomez, N. C. Just add lanthanides. *Science* **348**, 862–863 (2015).
13. Trifuoggi, M. *et al.* Comparative toxicity of seven rare earth elements in sea urchin early life stages. *Environ. Sci. Pollut. Res.* **24**, 20803–20810 (2017).
14. Goecke, F., Vítová, M., Lukavský, J., Nedbalová, L., Řezanka, T., & Zachleder, V. Effects of rare earth elements on growth rate, lipids, fatty acids and pigments in microalgae. *Phycol. Res.* **65**, 226–234 (2017).
15. Gonzalez, V., Vignati, D. A. L., Leyval, C., & Giamberini, L. Environmental fate and ecotoxicity of lanthanides: Are they a uniform group beyond chemistry? *Environ. Int.* **71**, 148–157 (2014).
16. Joonas, E., Aruoja, V., Olli, K., Syvertsen-Wiig, G., Vija, H., & Kahru, A. Potency of (doped) rare earth oxide particles and their constituent metals to inhibit algal growth and induce direct toxic effects. *Sci. Total Environ.* **593**–**594**, 478–486 (2017).
17. Gao, J. *et al.* Determining the cytotoxicity of rare earth element nanoparticles in macrophages and the involvement of membrane damage. *Environ. Sci. Technol.* **51**, 13938–13948 (2017).
18. Romero-Freire, A. *et al.* Assessment of baseline ecotoxicity of sediments from a prospective mining area enriched in light rare earth elements. *Sci. Total Environ.* **612**, 831–839 (2018).
19. Wakabayashi, T., Ymamoto, A., Kazaana, A., Nakano, Y., Nojiri, Y., & Kashiwazaki, M. Antibacterial, antifungal and nematicidal activities of rare earth ions. *Biol. Trace Elem. Res.* **174**, 464–470 (2016).
20. Pagano, G. *et al.* Comparative toxicities of selected rare earth elements: Sea urchin embryogenesis and fertilization damage with redox and cytogenetic effects. *Environ. Res.* **147**, 453–460 (2016).
21. Wei, B., Li, Y., Li, H., Yu, J., Ye, B., & Liang, T. Rare earth elements in human hair from a mining area of China. *Ecotoxicol. Environ. Saf.* **96**, 118–123 (2013).
22. Pagano, G., Guida, M., Tommasi, F., & Oral, R. Health effects and toxicity mechanisms of rare earth elements - Knowledge gaps and research prospects. *Ecotoxicol. Environ. Saf.* **115**, 40–48 (2015).
23. Liang, C. & Wang, W. Antioxidant response of soybean seedlings to joint stress of lanthanum and acid rain. *Environ. Sci. Pollut. Res.* **20**, 8182–8191 (2013).
24. Oral, R., Bustamante, P., Warnau, M., D'Ambra, A., Guida, M., & Pagano, G. Cytogenetic and developmental toxicity of cerium and lanthanum to sea urchin embryos. *Chemosphere* **18**, 194–198 (2010).
25. Jha, A. M. & Singh, A. C. Clastogenicity of lanthanides: induction of chromosomal aberration in bone marrow cells of mice in vivo. *Mutat. Res. Toxicol.* **341**, 193–197 (1995).
26. Weiwei, H., Shihua, S., & Peidong, T. Analysis of inhibitory effect of gadolinium on *Sinorhizobium fredii*. *J. Rare Earths* **25**, 106–110 (2007).
27. Yufeng, Z., Lifen, Y., Kaoshan, C., & Liang, D. Effects of neodymium on growth, pectinase activity and mycelium permeability of *Fusarium oxysporum*. *J. Rare Earths* **25**, 100–105 (2007).
28. Fitriyanto, N. A., Nakamura, M., Muto, S., Kato, K., Yabe, T., Iwama, T., Kawai, K., & Pertiwiningrum, A. Ce^{3+}-induced exopolysaccharide production by *Bradyrhizobium* sp. MAFF211645. *J. Biosci. Bioeng.* **111**, 146–152 (2011).
29. Wang, L., He, J., Xia, A., Cheng, M., Yang, Q., Du, C., Wei, H., Huang, X., & Zhou, Q. Toxic effects of environmental rare earth elements on delayed outward potassium channels and their mechanisms from a microscopic perspective. *Chemosphere* **181**, 690–698 (2017).
30. Scherens, B. & Goffeau, A. The uses of genome-wide yeast mutant collections. *Genome Biol.* **5**, 229 (2004).
31. Jin, Y. H., Dunlap, P. E., McBride, S. J., Al-Refai, H., Bushel, P. R., & Freedman, J. H. Global transcriptome and deletome profiles of yeast exposed to transition metals. *PLoS Genet.* **4**, (2008).
32. Botstein, D., Chervitz, S. A., & Cherry, J. M. Yeast as a model organism. *Science (80-.).* **277**, 1259–1260 (1997).
33. Kachroo, A. H., Laurent, J. M., Yellman, C. M., Meyer, A. G., Wilke, C. O., & Marcotte, E. M. Systematic humanization of yeast genes reveals conserved functions and genetic modularity. *Science (80-.).* **348**, 921–925 (2017).
34. Costa, M., Davidson, T. L., Chen, H., Ke, Q., Zhang, P., Yan, Y., Huang, C., & Kluz, T. Nickel carcinogenesis: Epigenetics and hypoxia signaling. *Mutat. Res.* **592**, 79–88 (2005).
35. Sutherland, J. E., Peng, W., Zhang, Q. W., & Costa, M. The histone deacetylase inhibitor trichostatin A reduces nickel-induced gene silencing in yeast and mammalian cells. *Mutat. Res.* **479**, 225–233 (2001).
36. Broday, L., Cai, J., & Costa, M. Nickel enhances telomeric silencing in *Saccharomyces cerevisiae*. *Mutat. Res.* **440**, 121–130 (1999).
37. Ruotolo, R., Marchini, G., & Ottonello, S. Membrane transporters and protein traffic networks differentially affecting metal tolerance: a genomic phenotyping study in yeast. *Genome Biol.* **9**, R67 (2008).
38. Cotton, S. *Lanthanide and actinide chemistry*. *Lanthanide and Actinide Chemistry* (2006).
39. Ene, C. D., Ruta, L. L., Nicolau, I., Popa, C. V., Iordache, V., Neagoe, A. D., & Farcasanu, I. C. Interaction between lanthanide ions and *Saccharomyces cerevisiae* cells. *JBIC J. Biol. Inorg. Chem.* **20**, 1097–1107 (2015).
40. Brennan, R. J. & Schiestl, R. H. Cadmium is an inducer of oxidative stress in yeast. *Mutat. Res. - Fundam. Mol. Mech. Mutagen.* **356**, 171–178 (1996).

41. Litwin, I., Bocer, T., Dziadkowiec, D., & Wysocki, R. Oxidative stress and replication-independent DNA breakage induced by arsenic in *Saccharomyces cerevisiae*. *PLoS Genet.* **9**, (2013).
42. Thorpe, G. W., Fong, C. S., Alic, N., Higgins, V. J., & Dawes, I. W. Cells have distinct mechanisms to maintain protection against different reactive oxygen species: oxidative-stress-response genes. *Proc. Natl. Acad. Sci. U. S. A.* **101**, 6564–6569 (2004).
43. Chang, M., Bellaoui, M., Boone, C., & Brown, G. W. A genome-wide screen for methyl methanesulfonate- sensitive mutants reveals genes required for S phase progression in the presence of DNA damage. *Proc. Natl. Acad. Sci. USA* **99**, (2002).
44. Serrano, R., Bernal, D., Simón, E., & Ariño, J. Copper and iron are the limiting factors for growth of the yeast *Saccharomyces cerevisiae* in an alkaline environment. *J. Biol. Chem.* **279**, 19698–19704 (2004).
45. Aouida, M., Pagé, N., Leduc, A., Page, N., Peter, M., & Ramotar, D. A genome-wide screen in *Saccharomyces cerevisiae* reveals altered transport as a mechanism of resistance to the anticancer drug bleomycin. *Cancer Res.* **64**, 1102–1109 (2004).
46. Bennett, C. B., Lewis, L. K., Karthikeyan, G., Lobachev, K. S., Jin, Y. H., Sterling, J. F., Snipe, J. R., & Resnick, M. A. Genes required for ionizing radiation resistance in yeast. *Nat. Genet.* **29**, 426–434 (2001).
47. Lynch-Day, M. A. & Klionsky, D. J. The Cvt pathway as a model for selective autophagy. *FEBS Lett.* **584**, 1359–1366 (2010).
48. Lesage, G. & Bussey, H. Cell wall assembly in *Saccharomyces cerevisiae*. *Microbiol. Mol. Biol. Rev.* **70**, 317–343 (2006).
49. Fuller, R. S., Brake, A., & Thorner, J. Yeast prohormone processing enzyme (KEX2 gene product) is a Ca^{2+}-dependent serine protease. *Proc. Natl. Acad. Sci.* **86**, 1434–1438 (1989).
50. Grbavac, A., Čanak, I., Stuparević, I., Teparić, R., & Mrša, V. Proteolytic processing of the *Saccharomyces cerevisiae* cell wall protein Scw4 regulates its activity and influences its covalent binding to glucan. *Biochim. Biophys. Acta - Mol. Cell Res.* **1864**, 507–515 (2017).
51. Michel, S., Keller, M. A., Wamelink, M. M. C., & Ralser, M. A haploproficient interaction of the transaldolase paralogue NQM1 with the transcription factor VHR1 affects stationary phase survival and oxidative stress resistance. *BMC Genet.* **16**, 1–14 (2015).
52. Navarro-Aviño, J. P., Prasad, R., Miralles, V. J., Benito, R. M., & Serrano, R. A proposal for nomenclature of aldehyde dehydrogenases in *Saccharomyces cerevisiae* and characterization of the stress-inducible ALD2 and ALD3 genes. *Yeast* **15**, 829–842 (1999).
53. Miyaharan, K., Mizunuma, M., Hirata, D., Tsuchiya, E., & Miyakawa, T. The involvement of the *Saccharomyces cerevisiae* multidrug resistance transporters Pdr5p and Snq2p in cation resistance. *FEBS Lett.* **399**, 317–320 (1996).
54. Tanaka, Y., Sasaki, M., Ito, F., Aoyama, T., Sato-Okamoto, M., Takahashi-Nakaguchi, A., Chibana, H., & Shibata, N. KRE5 suppression induces cell wall stress and alternative ER stress response required for maintaining cell wall integrity in *Candida glabrata*. *PLoS One* **11**, 1–23 (2016).
55. Jiang, M. Y., Ohnuki, T., Tanaka, K., Kozai, N., Kamiishi, E., & Utsunomiya, S. Post-adsorption process of Yb phosphate nano-particle: Formation by *Saccharomyces cerevisiae*. *Geochim. Cosmochim. Acta* **93**, 30–46 (2012).
56. Moriwaki, H. & Yamamoto, H. Interactions of microorganisms with rare earth ions and their utilization for separation and environmental technology. *Appl. Microbiol. Biotechnol.* **97**, 1–8 (2013).
57. Ngwenya, B. T., Mosselmans, J. F. W., Magennis, M., Atkinson, K. D., Tourney, J., Olive, V., & Ellam, R. M. Macroscopic and spectroscopic analysis of lanthanide adsorption to bacterial cells. *Geochim. Cosmochim. Acta* **73**, 3134–3147 (2009).
58. Chen, R. E. & Thorner, J. Function and regulation in MAPK signaling pathways: Lessons learned from the yeast *Saccharomyces cerevisiae*. *Biochim. Biophys. Acta - Mol. Cell Res.* **1773**, 1311–1340 (2007).
59. Mao, K., Wang, K., Zhao, M., Xu, T., & Klionsky, D. J. Two MAPK-signaling pathways are required for mitophagy in *Saccharomyces cerevisiae*. *J. Cell Biol.* **193**, 755–767 (2011).
60. Dickson, R. C. Roles for sphingolipids in *Saccharomyces cerevisiae*. *Adv. Exp. Med. Biol.* **688**, 217–231 (2010).
61. Lee, Y. J., Huang, X., Kropat, J., Henras, A., Merchant, S. S., Dickson, R. C., & Chanfreau, G. F. Sphingolipid signaling mediates iron toxicity. *Cell Metab.* **16**, 90–96 (2012).
62. Dickson, R. C., Sumanasekera, C., & Lester, R. L. Functions and metabolism of sphingolipids in *Saccharomyces cerevisiae*. *Prog. Lipid Res.* **45**, 447–465 (2006).
63. Abe, M., Nishida, I., Minemura, M., Qadota, H., Seyama, Y., Watanabe, T., & Ohya, Y. Yeast 1,3-β-glucan synthase activity is inhibited by phytosphingosine localized to the endoplasmic reticulum. *J. Biol. Chem.* **276**, 26923–26930 (2001).
64. Chung, J. H., Lester, R. L., & Dickson, R. C. Sphingolipid requirement for generation of a functional V1 component of the vacuolar ATPase. *J. Biol. Chem.* **278**, 28872–28881 (2003).
65. David, D., Sundararabu, S., & Gerst, J. E. Involvement of long chain fatty acid elongation in the trafficking of secretory vesicles in yeast. *J. Cell Biol.* **143**, 1167–1182 (1998).
66. Johnson, A. J., Veljanoski, F., O'Doherty, P. J., Zaman, M. S., Petersingham, G., Bailey, T. D., Münch, G., Kersaitis, C., & Wu, M. J. Molecular insight into arsenic toxicity via the genome-wide deletion mutant screening of *Saccharomyces cerevisiae*. *Metallomics* **8**, 228–235 (2016).
67. Johnson, A. J., Veljanoski, F., O'Doherty, P. J., Zaman, M. S., Petersingham, G., Bailey, T. D., Münch, G., Kersaitis, C., & Wu, M. J. Revelation of molecular basis for chromium toxicity by phenotypes of *Saccharomyces cerevisiae* gene deletion mutants. *Metallomics* **8**, 542–550 (2016).
68. Morimoto, Y. & Tani, M. Synthesis of mannosylinositol phosphorylceramides is involved in maintenance of cell integrity of yeast *Saccharomyces cerevisiae*. *Mol. Microbiol.* **95**, 706–722 (2015).
69. Dickson, R. C., Sumanasekera, C., & Lester, R. L. Functions and metabolism of sphingolipids in *Saccharomyces cerevisiae*. *Prog. Lipid Res.* **45**, 447–465 (2006).
70. Nakase, M., Tani, M., Morita, T., Kitamoto, H. K., Kashiwazaki, J., Nakamura, T., Hosomi, A., Tanaka, N., & Takegawa, K. Mannosylinositol phosphorylceramide is a major sphingolipid component and is required for proper localization of plasma-membrane proteins in *Schizosaccharomyces pombe*. *J. Cell Sci.* **123**, 1578–1587 (2010).
71. Beeler, T. J., Fu, D., Rivera, J., Monaghan, E., Gable, K., & Dunn, T. M. SUR1 (CSG1/BCL21), a gene necessary for growth of *Saccharomyces cerevisiae* in the presence of high Ca^{2+} concentrations at 37°C, is required for mannosylation of inositolphosphorylceramide. *Mol. Gen. Genet.* **255**, 570–579 (1997).
72. Beeler, T., Gable, K., Zhao, C., & Dunn, T. A novel protein, CSG2p, is required for Ca^{2+} regulation in *Saccharomyces cerevisiae*. *J. Biol. Chem.* **269**, 7279–7284 (1994).
73. Mishra, M., Huang, J., & Balasubramanian, M. K. The yeast actin cytoskeleton. *FEMS Microbiol. Rev.* **38**, 213–227 (2014).
74. Wang, L. *et al.* Rare earth elements activate endocytosis in plant cells. *Proc. Natl. Acad. Sci.* **111**, 12936–12941 (2014).
75. Naqvi, S. N., Zahn, R., Mitchell, D. a, Stevenson, B. J., & Munn, A. L. The WASp homologue Las17p functions with the WIP homologue End5p/verprolin and is essential for endocytosis in yeast. *Curr. Biol.* **8**, 959–962 (1998).
76. Munn, A. L., Stevenson, B. J., Geli, M. I., & Riezman, H. end5, end6, and end7: mutations that cause actin delocalization and block

the internalization step of endocytosis in *Saccharomyces cerevisiae*. *Mol. Biol. Cell* **6**, 1721–1742 (1995).

77. Pruyne, D. & Bretscher, A. Polarization of cell growth in yeast II.The role of the cortical actin cytoskeleton. *J. Cell Sci.* **585**, 571–585 (2000).
78. Toi, H., Fujimura-Kamada, K., Irie, K., Takai, Y., Todo, S., & Tanaka, K. She4p/Dim1p Interacts with the Motor Domain of Unconventional Myosins in the Budding Yeast, *Saccharomyces cerevisiae. Mol. Biol. Cell* **14**, 2372–2384 (2003).
79. Holland, S. L. & Avery, S. V. Actin-mediated endocytosis limits intracellular Cr accumulation and Cr toxicity during chromate stress. *Toxicol. Sci.* **111**, 437–446 (2009).
80. Gitan, R. S. & Eide, D. J. Zinc-regulated ubiquitin conjugation signals endocytosis of the yeast ZRT1 zinc transporter. *Biochem. J.* **346 Pt 2**, 329–36 (2000).
81. Liu, J., Sitaram, A., & Burd, C. G. Regulation of copper-dependent endocytosis and vacuolar degradation of the yeast copper transporter, Ctr1p, by the Rsp5 ubiquitin ligase. *Traffic* **8**, 1375–1384 (2007).
82. Ooi, C. E., Rabinovich, E., Dancis, A., Bonifacino, J. S., & Klausner, R. D. Copper-dependent degradation of the *Saccharomyces cerevisiae* plasma membrane copper transporter Ctr1p in the apparent absence of endocytosis. *Embo J* **15**, 3515–3523 (1996).
83. Schmidt, O. & Teis, D. The ESCRT machinery. *Curr. Biol.* **22**, R116–R120 (2012).
84. Luo, C., Cao, C., & Jiang, L. The endosomal sorting complex required for transport (ESCRT) is required for the sensitivity of yeast cells to nickel ions in *Saccharomyces cerevisiae*. *FEMS Yeast Res.* **16**, 1–8 (2016).
85. Conibear, E. & Stevens, T. H. Vps52p, Vps53p, and Vps54p form a novel multisubunit complex required for protein sorting at the yeast late Golgi. *Mol. Biol. Cell* **11**, 305–323 (2000).
86. Kane, P. M. The where, when, and how of organelle acidification by the yeast vacuolar H^+-ATPase. *Microbiol. Mol. Biol. Rev.* **70**, 177–191 (2006).
87. Ohya, Y., Umemoto, N., Tanida, I., Ohta, A., Irda, H., & Anraku, Y. Calcium-sensitive cls mutants of *Saccharomyces cerevisiae* showing a Pet- phenotype are ascribable to defects of vacuolar membrane H^+-ATPase activity. *J. Biol. Chem.* **266**, 13971–13977 (1991).
88. Eide, D. J., Bridgham, J. T., Zhao, Z., & Mattoon, J. R. The vacuolar H^+-ATPase of *Saccharomyces cerevisiae* is required for efficient copper detoxification , mitochondrial function, and iron metabolism. *Mol. Gen. Genet.* **241**, 447–456 (1993).
89. Eide, D. J., Clark, S., Nair, T. M., Gehl, M., Gribskov, M., Guerinot, M. Lou, & Harper, J. F. Characterization of the yeast ionome: a genome-wide analysis of nutrient mineral and trace element homeostasis in *Saccharomyces cerevisiae*. *Genome Biol.* **6**, R77 (2005).
90. Grosjean, N., Gross, E. M., Le Jean, M., & Blaudez, D. Global deletome profile of *Saccharomyces cerevisiae* exposed to the technology-critical element yttrium. *Front. Microbiol.* **9**, 1–13 (2018).
91. Lee, Y. W., Klein, C. B., Kargacin, B., Salnikow, K., Kitahara, J., Dowjat, K., Zhitkovich, A., Christie, N. T., & Costa, M. Carcinogenic nickel silences gene expression by chromatin condensation and DNA methylation: a new model for epigenetic carcinogens. *Mol. Cell. Biol.* **15**, 2547–2557 (1995).
92. Okada, H., Abe, M., Asakawa-Minemura, M., Hirata, A., Qadota, H., Morishita, K., Ohnuki, S., Nogami, S., & Ohya, Y. Multiple functional domains of the yeast l,3-β-glucan synthase subunit Fks1p revealed by quantitative phenotypic analysis of temperature-sensitive mutants. *Genetics* **184**, 1013–1024 (2010).
93. Hartmann, E. M., Allain, F., Gaillard, J., Pible, O., & Armengaud, J. Taking the shortcut for high-throughput shotgun proteomic analysis of bacteria. in *Methods in Molecular Biology (Methods and Protocols)* (eds. Vergunst, A. & O'Callaghan, D.) **1197**, 275–285 (Humana Press, 2014).
94. Klein, G. *et al.* RNA-binding proteins are a major target of silica nanoparticles in cell extracts. *Nanotoxicology* **10**, 1555–1564 (2016).
95. Carvalho, P. C., Yates, J. R., & Barbosa, V. C. Improving the TFold test for differential shotgun proteomics. *Bioinformatics* **28**, 1652–1654 (2012).
96. Subramanian, A. *et al.* Gene set enrichment analysis: A knowledge-based approach for interpreting genome-wide expression profiles. *Proc. Natl. Acad. Sci.* **102**, 15545–15550 (2005).
97. Mootha, V. K. *et al.* PGC-1α-responsive genes involved in oxidative phosphorylation are coordinately downregulated in human diabetes. *Nat. Genet.* **34**, 1556–1567 (2003).
98. Shannon, P., Markiel, A., Owen Ozier, 2, Baliga, N. S., Wang, J. T., Ramage, D., Amin, N., Schwikowski, B., & Ideker, T. Cytoscape: a software environment for integrated models of biomolecular interaction networks. *Genome Res.* 2498–2504 (2003).
99. Merico, D., Isserlin, R., Stueker, O., Emili, A., & Bader, G. D. Enrichment map: A network-based method for gene-set enrichment visualization and interpretation. *PLoS One* **5**, (2010).
100. Warde-Farley, D. *et al.* The GeneMANIA prediction server: Biological network integration for gene prioritization and predicting gene function. *Nucleic Acids Res.* **38**, 214–220 (2010).
101. Serero, A., Lopes, J., Nicolas, A., & Boiteux, S. Yeast genes involved in cadmium tolerance : Identification of DNA replication as a target of cadmium toxicity. *DNA Repair (Amst).* **7**, 1262–1275 (2008).
102. Thorsen, M., Perrone, G. G., Kristiansson, E., Traini, M., Ye, T., Dawes, I. W., Nerman, O., & Tamás, M. J. Genetic basis of arsenite and cadmium tolerance in *Saccharomyces cerevisiae. BMC Genomics* **15**, 1–15 (2009).
103. Arita, A. *et al.* A genome-wide deletion mutant screen identifies pathways affected by nickel sulfate in *Saccharomyces cerevisiae*. *BMC Genomics* **14**, 1–14 (2009).
104. Bleackley, M. R., Young, B. P., Loewen, C. J. R., & Macgillivray, R. T. A. High density array screening to identify the genetic requirements for transition metal tolerance in *Saccharomyces cerevisiae*. *Metallomics* 195–205 (2011).
105. Pagani, M. A., Casamayor, A., Serrano, R., Atrian, S., & Ariño, J. Disruption of iron homeostasis in *Saccharomyces cerevisiae* by high zinc levels : a genome-wide study. *Mol. Microbiol.* **65**, 521–537 (2007).
106. Wang, J., Wang, X., Fang, Y., & Zhou, B. Genome-wide screening of yeast metal homeostasis genes involved in mitochondrial functions. *Mol. Genet. Genomics* **277**, 673–83 (2007).
107. Kakimoto, M., Kobayashi, A., Fukuda, R., Ono, Y., Ohta, A., & Yoshimura, E. Genome-wide screening of aluminum tolerance in *Saccharomyces cerevisiae*. *BioMetals* **18**, 467–474 (2005).
108. Tun, N. M., O'Doherty, P. J., Chen, Z., Wu, X., Bailey, T. D., Kersaitis, C., & Wu, M. J. Identification of aluminium transport-related genes via genome-wide phenotypic screening of. *Metallomics* 1558–1564 (2014).
109. Haugen, A. C., Kelley, R., Collins, J. B., Tucker, C. J., Deng, C., Afshari, C. A., Brown, J. M., Ideker, T., & Van Houten, B. Integrating phenotypic and expression profiles to map arsenic-response networks. *Genome Biol.* **5**, R95 (2004).
110. Thorsen, M. *et al.* The MAPK Hog1p modulates Fps1p-dependent Arsenite uptake and tolerance in Yeast. *Mol. Biol. Cell* **17**, 4400–4410 (2006).
111. Jo, W. J., Loguinov, A., Chang, M., Wintz, H., Nislow, C., Arkin, A. P., Giaever, G., & Vulpe, C. D. identification of genes involved in the toxic response of *Saccharomyces cerevisiae* against iron and copper overload by parallel analysis of deletion mutants. *Toxicol.*

Sci. **101**, 140–151 (2008).

112. Chesi, A., Kilaru, A., Fang, X., Cooper, A. A., & Gitler, A. D. The role of the Parkinson's disease gene PARK9 in essential cellular pathways and the manganese homeostasis network in yeast. *PLoS One* **7**, (2012).

ADDITIONAL FILES

https://bul.univ-lorraine.fr/index.php/s/bw9Z1eICcwtb2w5

Additional file 1: Table S1. Detailed phenotypes and related information on the genes whose disruption affects either La or Yb tolerance. Sensitivity and resistance levels were allocated to mutant strains as: Low sensitivity (LS), medium sensitivity (MS), high sensitivity (HS) and low resistance (LR), medium resistance (MR) and high resistance (HR). (XLS)

Additional file 2: Table S2. Validation screen of randomly picked mutants under the opposite mating type BY4742 for their phenotype under La and Yb exposure. (XLS)

Additional file 3: Table S3. Detailed phenotypes and related information on the genes whose disruption caused an enhanced sensitivity or resistance to either La or Yb. (XLS)

Additional file 4: Table S4. Multi-metal tolerance database of yeast mutants displaying a modified fitness under Ln exposure. Data were retrieved from previous genomic phenotyping carried out on several other metals. Sensitivity of the mutant to a metal is noted as "-1", resistance noted as "1" and "0" when no particular phenotype was reported. (XLS)

Additional file 6: Table S5. Multi-stressor tolerance database of mutants displaying a modified fitness under Ln exposure. Data were retrieved from previous genomic phenotyping carried out on several other stressors. Sensitivity of the mutant to a particular stress is noted as "-1", resistance noted as "1" and "0" when no particular phenotype was reported. (XLS)

Additional file 7: Table S6. MIPS (Munich Information Center for Protein Sequences) subcellular localization of the disrupted genes and proteins in mutant strains displaying a modified phenotype under lanthanide exposure. f is the total number of genes in each compartment and k is the number of mutants found in this study, for each compartment. NS = not significant. (XLS)

Additional file 8: Table S7. GO terms of biological pathways represented in sensitive and resistant mutants or sensitive and resistant mutants combined to either La or Yb. f is the total number of genes in each compartment, the fold enrichment corresponds to the enrichment of the GO term among the mutant set analyzed, and k is the number of mutants found in this study, for each GO term. NS = not significant. (XLS)

Additional file 9: Table S8. List of proteins and the log2FC in the ΔKex2 mutant after 4 h under control, La or Yb exposure. (XLS)

Additional file 10: Table S9. List of proteins and the log2FC in the ΔOrm2 mutant after 4 h under control, La or Yb exposure. (XLS)

Additional file 11: Table S10. List of proteins and the log2FC in the ΔVrp1 mutant after 4 h under control, La or Yb exposure. (XLS)

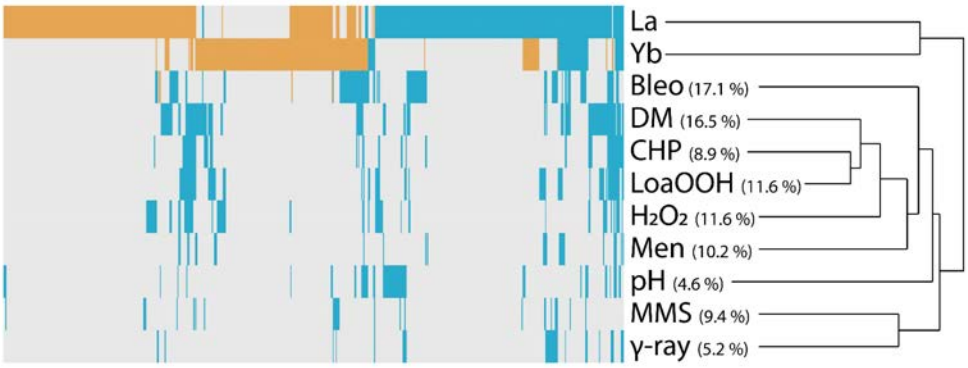

Additional file 5: Figure S1: Cross comparison of mutant phenotypes to lanthanides versus other non-metallic stressors. Hierarchical clustering of La and Yb sensitivity/tolerance-conferring mutations with the mutant sensitivity/tolerance profiles of other stressors. The x-axis corresponds to gene deletions and the y-axis indicates the different stressors from previous yeast genomic phenotyping screens conducted on deletion mutant collections; Non-metal stressors were selected: methyl methane sulfonate (MMS), γ-radiation (γ-ray), bleomycin (Bleo), alkaline pH (pH), menadione (Men), hydrogen peroxide (H_2O_2), cumene hydroperoxide (CHP), linoleic acid 13-hydroperoxide (LoaOOH), and diamide (DM). Only mutants displaying a phenotype on lanthanides were shown in this analysis. Mutant strains exhibiting either an enhanced sensitivity, a higher tolerance or no phenotype are shown in blue, orange and gray, respectively. Values into brackets after the element denote the percentage of mutants that were found common between the present screening (La and Yb) and screenings on other non-metallic stressors.

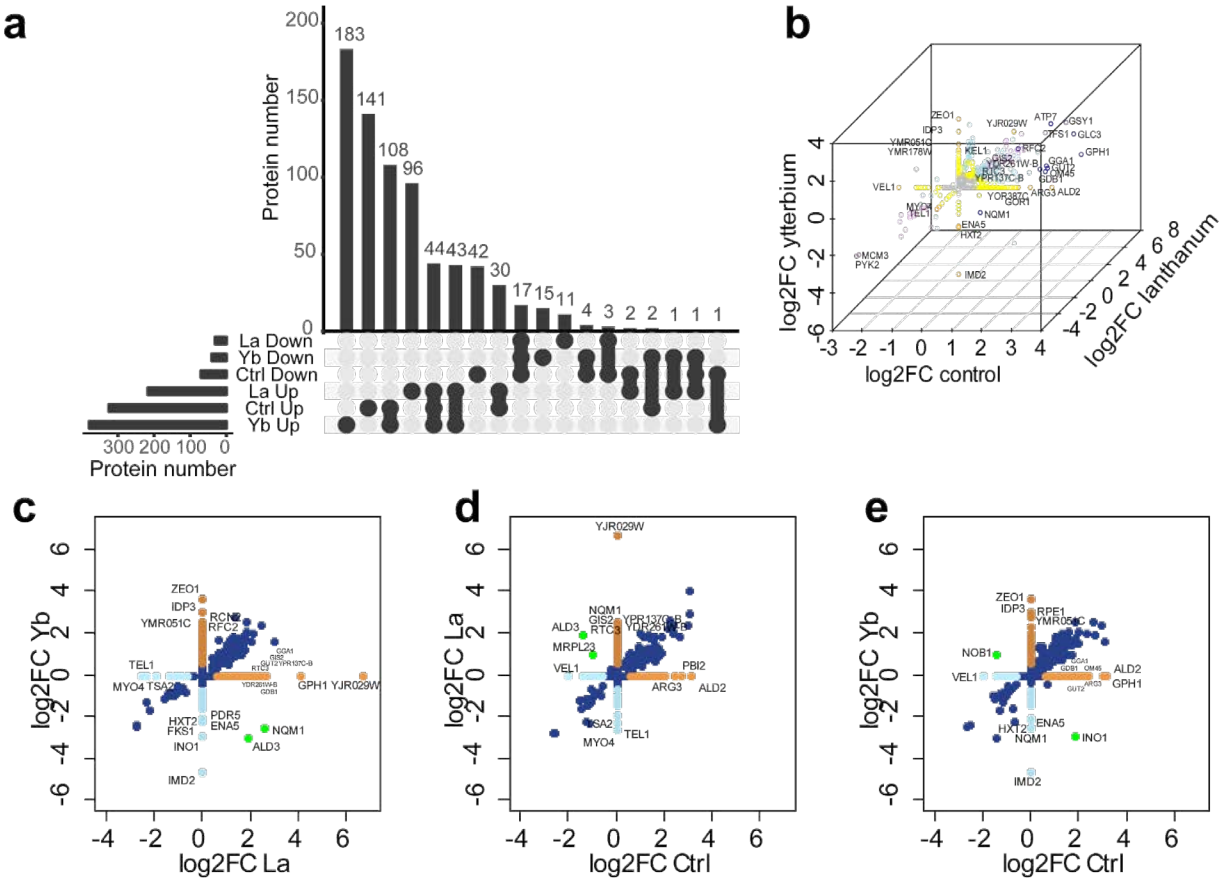

Additional file 5: Figure S2: Proteomic analysis of the Kex2 mutant under control, lanthanum, and ytterbium exposure. (a) UpSetR plot displaying the number of proteins up- and down-regulated shared between the three conditions tested. (b) 3D scatter plot of Log2 fold change (Log2FC) of proteins expressed in the mutant relatively to the WT, under control, lanthanum and ytterbium conditions. (c) Scatter plot of the Log2FC of proteins expressed in the mutant relatively to the WT, under lanthanum and ytterbium conditions. (d) Same as c, but comparing of lanthanum and control conditions. (e) Same as c, comparing ytterbium and control conditions. Green dots represent proteins whose expression is opposite in two conditions.

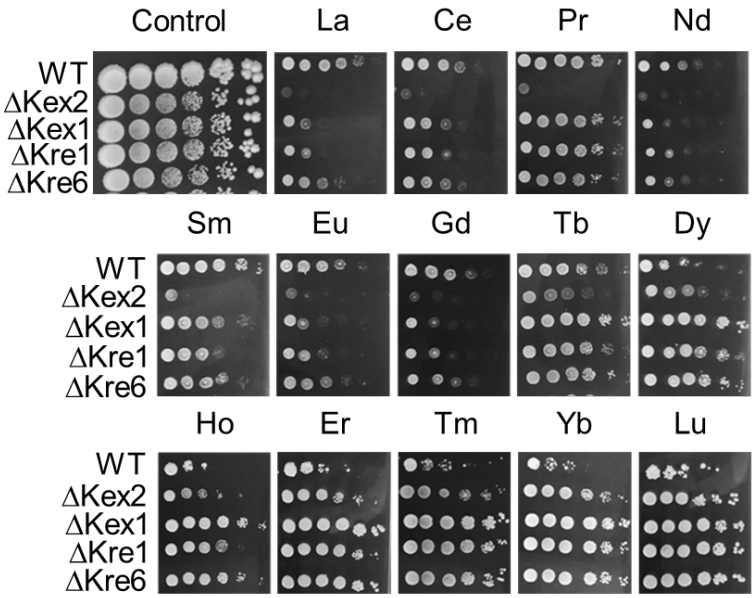

Additional file 5: Figure S3: Growth of Kex and Kre mutants in response to toxic concentrations of lanthanides. Yeast growth was assessed on YPD medium without lanthanides (control) or supplemented with 4.0 mM La, 3.8 Mm Ce, 5.8 mM Pr, 4.2 mM Nd, 3.9 mM Sm, 3.9 mM Eu, 3.8 mM Gd, 3.8 mM Tb, 3.6 mM Dy, 3.9 mM Ho, 3.9 mM Er, 3.6 mM Tm, 3.6 mM Yb, and 3.6 mM Lu, with 10 fold serial dilutions of cultures from left to right in each panel. A representative plate (out of 3 independent experiments) is shown. Plates were incubated for 5 days at 28°C.

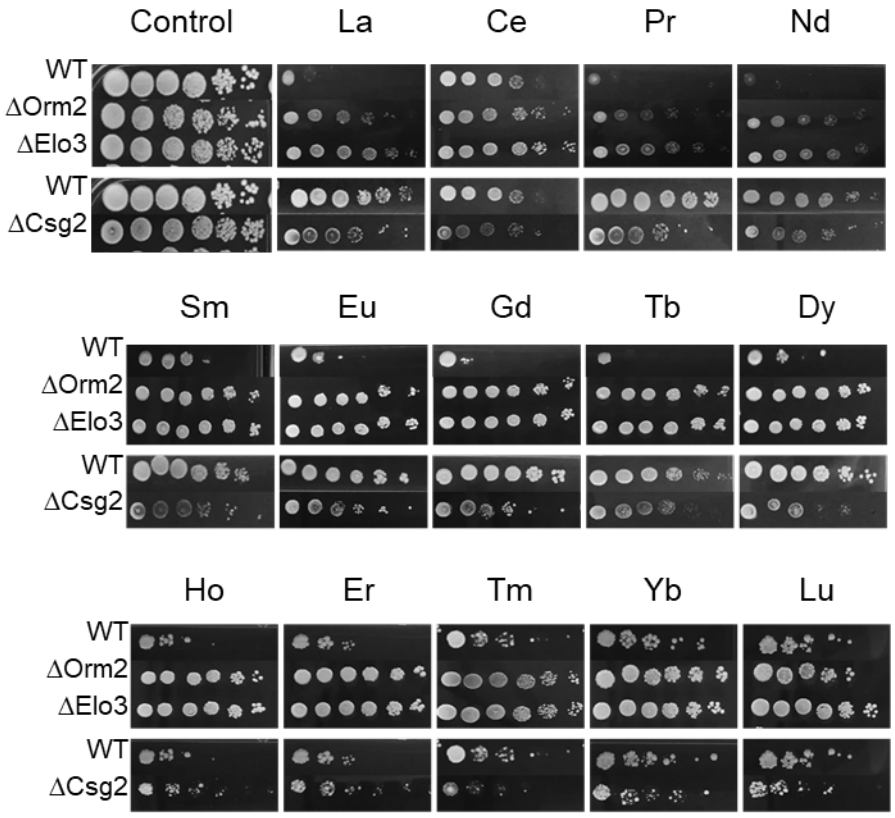

Additional file 5: Figure S4: Growth of mutants involved in the biosynthesis of sphingolipids in response to toxic concentrations of lanthanides. Yeast growth was assessed on YPD medium without lanthanides (control) or supplemented with with 4.0 mM La, 3.8 Mm Ce, 5.8 mM Pr, 4.2 mM Nd, 3.9 mM Sm, 3.9 mM Eu, 3.8 mM Gd, 3.8 mM Tb, 3.6 mM Dy, 3.9 mM Ho, 3.9 mM Er, 3.6 mM Tm, 3.6 mM Yb, and 3.6 mM Lu, with 10 fold serial dilutions of cultures from left to right in each panel. A representative plate (out of 3 independent experiments) is shown. Plates were incubated for 5 days at 28°C.



Additional file 5: Figure S5: Overexpression of Elo3 gene confers sensitivity to Yb. Yeast cells were transformed with the empty pYES2 plasmid or the same plasmid harboring Elo3. Cells were grown on YPG medium in the absence of lanthanides (control) or in the presence of lanthanum, or ytterbium.

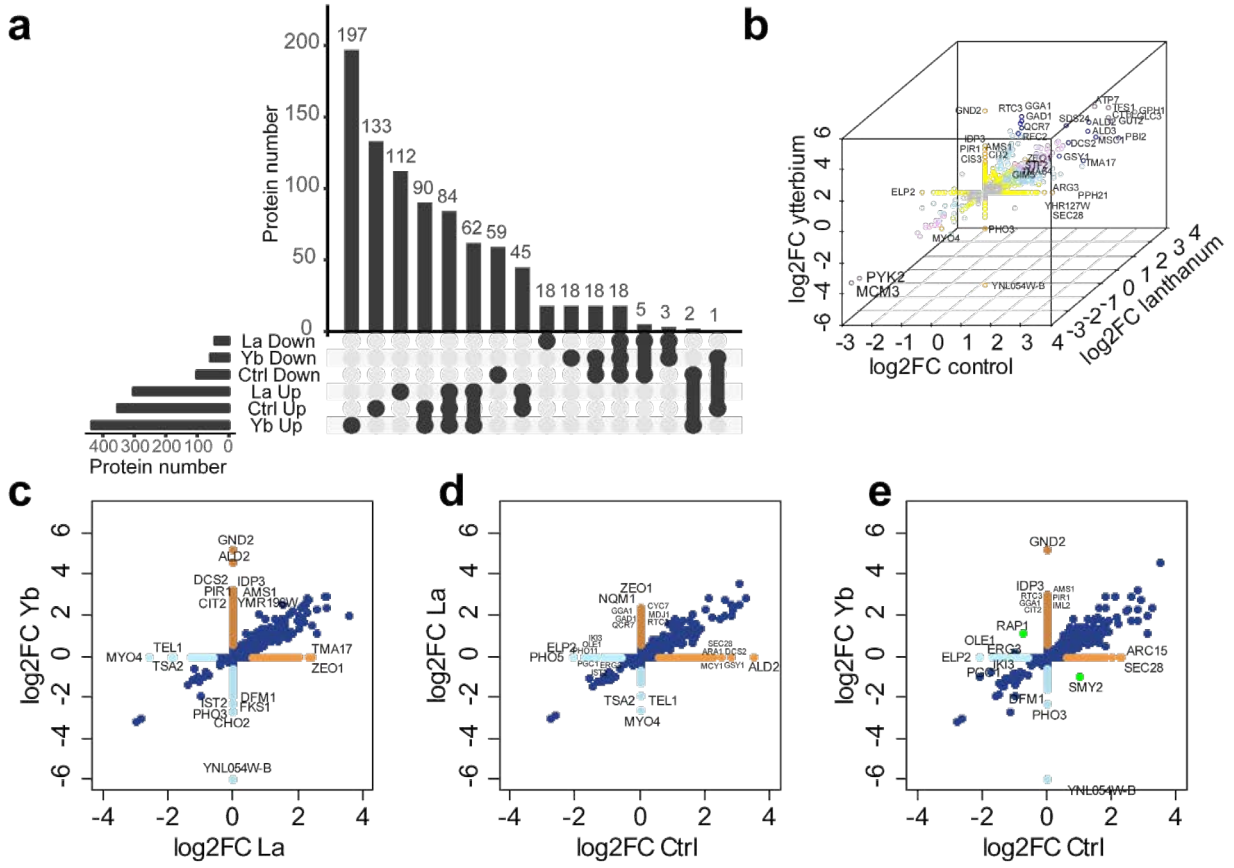

Additional file 5: Figure S6: Proteomic analysis of the Orm2 mutant under control, lanthanum, and ytterbium exposure. (a) UpSetR plot displaying the number of proteins up- and down-regulated shared between the three conditions tested. (b) 3D scatter plot of Log2 fold change (Log2FC) of proteins expressed in the mutant relatively to the WT, under control, lanthanum and ytterbium conditions. (c) Scatter plot of the Log2FC of proteins expressed in the mutant relatively to the WT, under lanthanum and ytterbium conditions. (d) Same as c, but comparing of lanthanum and control conditions. (e) Same as c, comparing ytterbium and control conditions. Green dots represent proteins whose expression is opposite in two conditions.

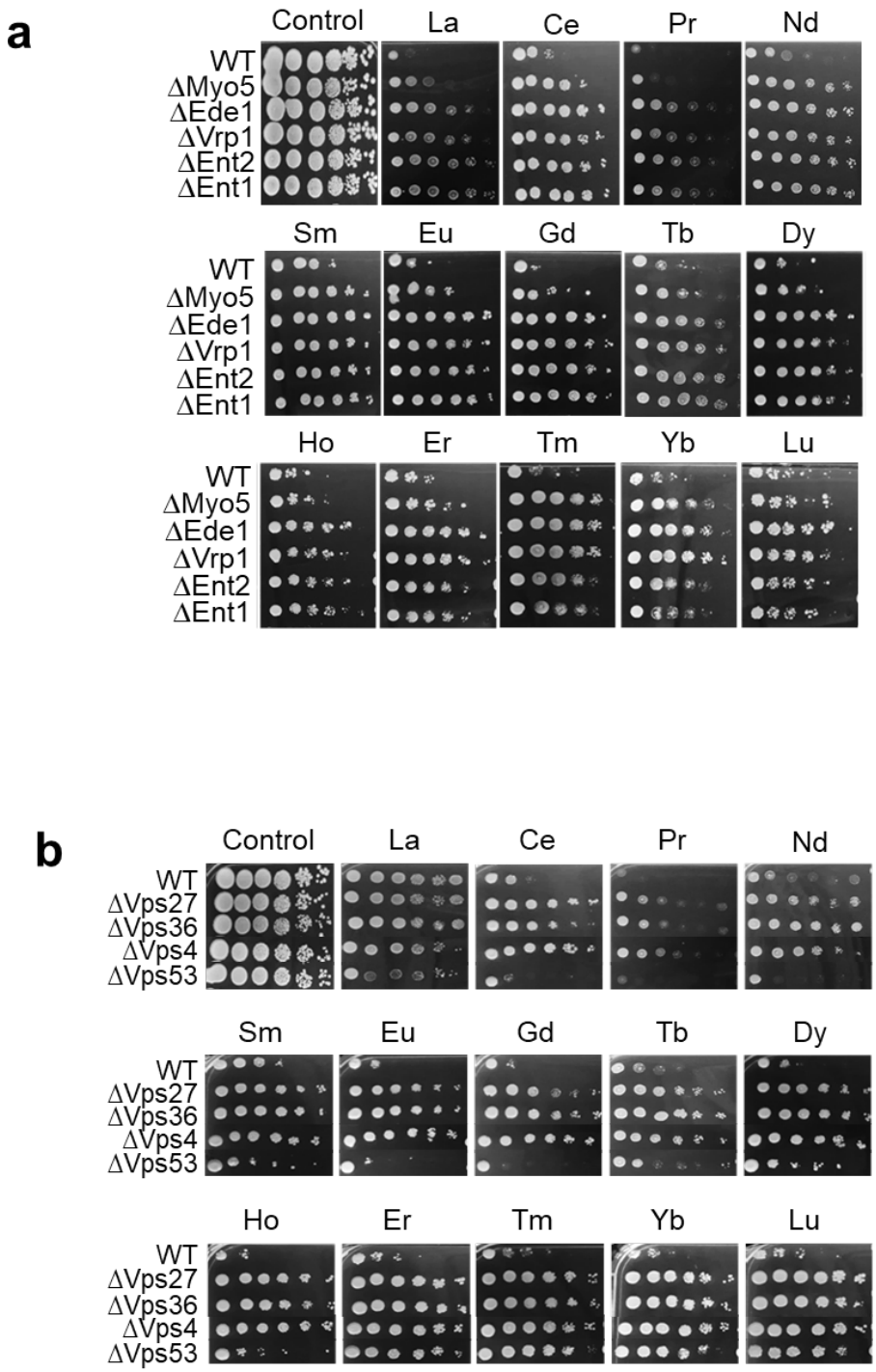

Additional file 5: Figure S7: Growth of mutants involved in the endocytosis pathway (a) and in the ESCRT/GARP/Retromer complex pathway (b) in response to toxic concentrations of lanthanides. Yeast growth was assessed on YPD medium without lanthanides (control) or supplemented with 4.2 mM La, 4.2 mM Ce, 6.7 mM Pr, 4.5 mM Nd, 4.6 mM Sm, 4.0 mM Eu, 4.0 mM Gd, 3.9 mM Tb, 3.6 mM Dy, 3.9 mM Ho, 3.9 mM Er, 3.6 mM Tm, 3.6 mM Yb, and 3.6 mM Lu, with 10 fold serial dilutions of cultures from left to right in each panel. A representative plate (out of 3 independent experiments) is shown. Plates were incubated for 5 days at 30°C.

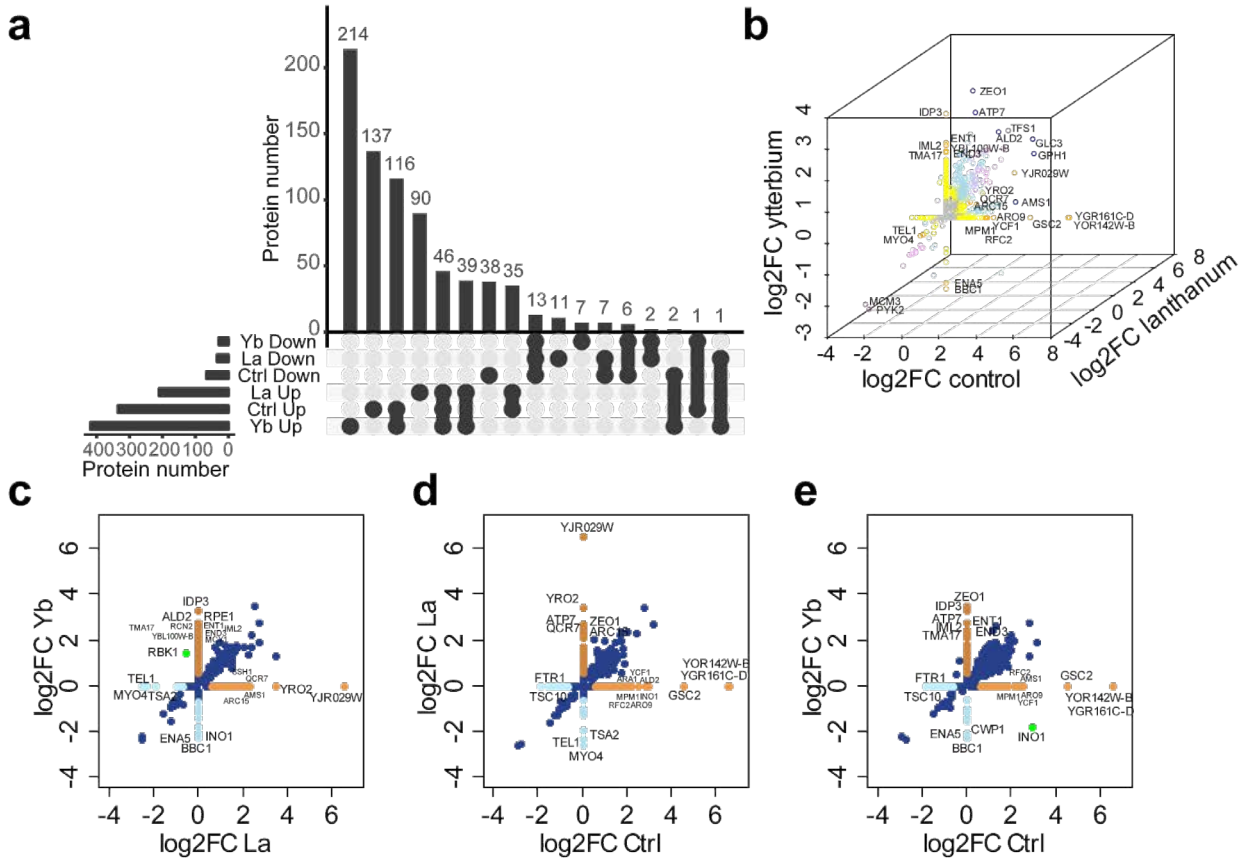

Additional file 5: Figure S8: Proteomic analysis of the Vrp1 mutant under control, lanthanum, and ytterbium exposure. (a) UpSetR plot displaying the number of proteins up- and down-regulated shared between the three conditions tested. (b) 3D scatter plot of Log2 fold change (Log2FC) of proteins expressed in the mutant relatively to the WT, under control, lanthanum and ytterbium conditions. (c) Scatter plot of the Log2FC of proteins expressed in the mutant relatively to the WT, under lanthanum and ytterbium conditions. (d) Same as c, but comparing of lanthanum and control conditions. (e) Same as c, comparing ytterbium and control conditions. Green dots represent proteins whose expression is opposite in two conditions,

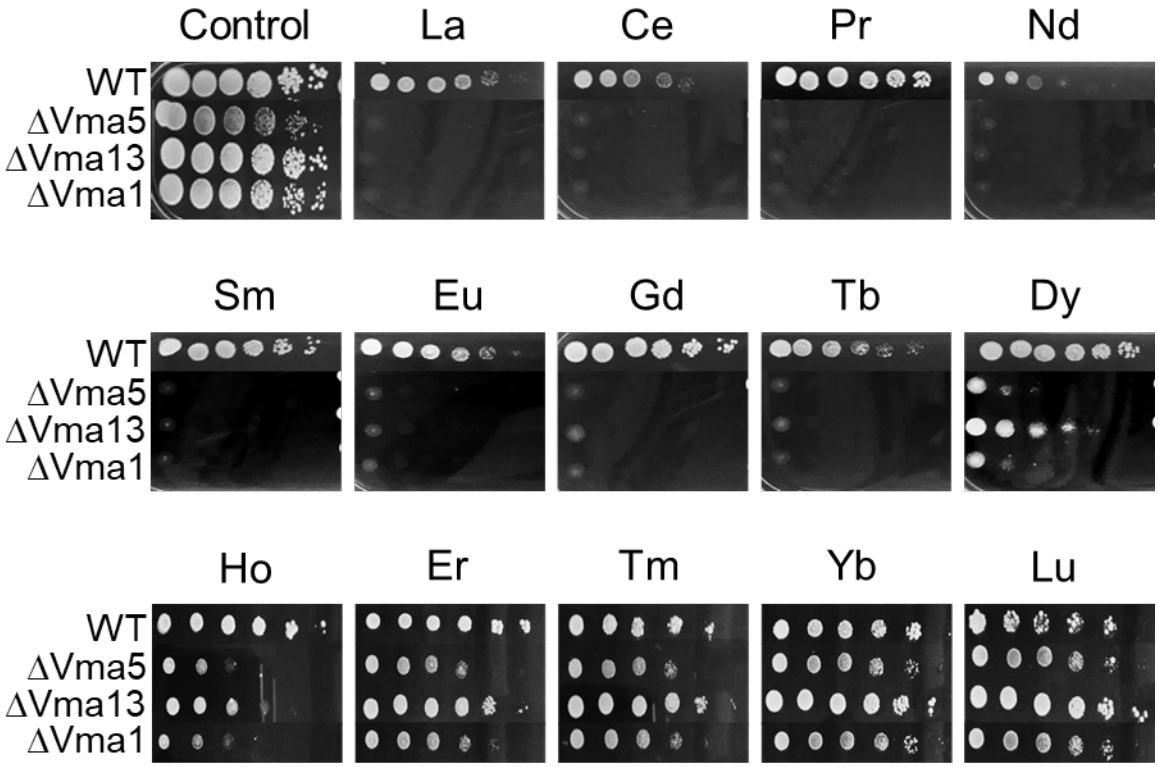

Additional file 5: Figure S9: Growth of VMA mutants in response to toxic concentrations of lanthanides. Yeast growth was assessed on YPD medium without lanthanides (control) or supplemented with 4.0 mM La, 3.8 Mm Ce, 5.8 mM Pr, 4.2 mM Nd, 3.9 mM Sm, 3.9 mM Eu, 3.8 mM Gd, 3.8 mM Tb, 3.3 mM Dy, 3.6 mM Ho, 3.6 mM Er, 3.4 mM Tm, 3.4 mM Yb, and 3.2 mM Lu, with 10 fold serial dilutions of cultures from left to right in each panel. A representative plate (out of 3 independent experiments) is shown. Plates were incubated for 5 days at 28°C.

Chapter I.3:

Omic approaches reveal response and uptake discrepancies between light and heavy rare earth elements in *Saccharomyces cerevisiae*

Omic approaches reveal response and uptake discrepancies between light and heavy rare earth elements in *Saccharomyces cerevisiae*

(Manuscript to be submitted)

Abstract

The fast development of new-technologies, green energies and medicine contribute to the increased production and use of rare earth elements (REEs), subdivided in light REEs (LREEs) and heavy REEs (HREEs). Their dissemination in the environment raises concerns about their toxicity on organisms and impact on ecosystems. Few studies reported REE toxicity but their precise underlying molecular effects and uptake mechanisms are barely known. Here, we combined transcriptomic and proteomic approaches in order to decipher the response of the model organism *Saccharomyces cerevisiae* to a LREE (La) and a HREE (Yb)). Differences were observed between the early and late response to REEs and we also highlighted oxidative-reduction processes, DNA replication, and carbohydrate metabolism as functions modulated in response to both REEs. Unlike for the response associated to the toxicity triggered by other metals, we reported here the cell wall, and the pheromone signalling pathways as being essential for yeast cells to cope with REEs. Interestingly, REEs also modified the expression of several ion transport systems, where strong discrepancies were observed between those contrasted REEs. While we confirmed the implication of the Ca channel Cch1-Mid1 in the uptake of LREEs, we identified new pathways for HREEs. For the first time, we evidenced the involvement of the Fe transport systems Ftr1-Fet3 and Fet4 in the cellular uptake of HREEs. Also, Mg and Mn transporters appeared to contribute to REE uptake. A cross gradient between LREEs and HREEs appeared for their import through the different transporters, despite a common stress-response pattern for La and Yb was found. Overall, the REE responsive pathways evidenced in this study will provide valuable tools to better understand REE toxicity on the environment and human health.

Introduction

The metal group of the Rare Earth Elements (REEs) consists of Yttrium (Y), Scandium (Sc), and 15 lanthanides, spanning from Lanthanum (La) to Lutetium (Lu). REEs can be split into two different groups known as the light REEs (LREEs), which gather La, Ce, Pr, Nd, Pm, Sm, and Eu, and the heavy REEs (HREEs) that include Gd, Tb, Dy, Y, Ho, Er, Tm, Yb, and Lu[1]. Those elements display unique physical (magnetic essentially) and chemical (catalyser) characteristics that make them essential for many up-to-date technologies (e.g. green energies, communication, screens, medicine, catalysts)[2]. REEs are also used as fertilizers and food supplements for cattle, pigs, and chicken in agriculture[3–6]. The rising production of REEs, associated to their increasing use and low recyclability proportions[2,7], spark concerns on associated environmental and toxicological impacts of these emerging contaminants.

REEs were initially considered as harmless and nonessential elements[8,9]. However, more recently, several studies mentioned the ecotoxicological effect of such elements on both aquatic and terrestrial organisms, including mammals[10–12]. REEs have been shown to display antibacterial, antifungal and nematicidal activities[13], but also to affect urchin embryogenesis[14,15] and to have consequences on human health[11,16]. More specifically, it was shown that REEs induced oxidative stress through the production of reactive oxygen species, lipid peroxidation, modulation of superoxide dismutase, catalase, and glutathione peroxidase in plants, fish, rats and mice, but also in animal cell lines (including human cells)[11,12,17]. Other effects were observed such as alteration of membrane permeability[18–20], mitotic and chromosomal aberrations[11], or the overproduction of exopolysaccharides[21] in microorganisms. Nevertheless, these aspects of REE toxicity were approached in very diverse organisms, making difficult to draw a comprehensive overview. Moreover, the precise underlying molecular mechanisms are barely described. Furthermore, only few studies hypothesized that REEs (i.e. LREEs *vs* HREEs) would induce different cellular responses, being either the result of the lanthanide contraction (a decreasing ionic radius with an increasing atomic mass) or to their reactivity and chemical differences[12,22]. Lastly, there is also a crucial lack of knowledge regarding the cellular uptake of REEs, for which the molecular transporters are barely known. The Ca channel Cch1-Mid1 was previously shown to allow the uptake of La in yeast, as well as a few other LREEs, due to the close ionic radius of LREEs with Ca[23], however, nothing is known concerning heavier lanthanides. Altogether, these few available studies support the need to elaborate a global view of the cellular and molecular mechanisms involved in the response to REEs as well as in their uptake.

In order to decipher the cellular response to new stressors and pollutants such as REEs, combining different and complementary “omic” analyses is of high interest[24]. There is a considerable amount of data regarding the

exposure of yeast cells to various toxic metals[25], but large scale "omic" methods are relatively scarce for metal stress studies[24,26,27]. Such analyses with model organisms are especially relevant as a first step to better comprehend functions involved in a newly studied stress. In our study, we selected the unicellular eukaryotic model *Saccharomyces cerevisiae*, which has been remarkably informative and extensively used as a proxy for unravelling eukaryotic cellular machinery and mechanisms[28,29]. We provide here the first study of the transcriptome associated with the proteome of *S. cerevisiae* exposed to two distinct REEs, with La belonging to the LREEs and Yb to the HREEs. The concentration used did not influenced the transcriptomic response. The proteomic profiles obtained after exposure to the two different REEs displayed discrepancies between the early and late response. Furthermore, a close relationship was found between the transcriptome (after 1 hour) and the proteome (after 4 hours) profiles, depicting the lag between gene response and protein expression. Altogether, the major functions emerging from REE exposure were cell-wall, oxidative-reduction processes, DNA replication related, as well as carbohydrate metabolism and ion-transport. Lastly, the modulation of expression of several transporters for essential elements under REE exposure, prompted us to further characterize their role and to propose new actors for REE uptake.

Materials and Methods

Yeast strains, chemicals and REE toxicity tests

The wild-type strain BY4741 of *Saccharomyces cerevisiae* (MATa; his3Δ1; leu2Δ0; met15Δ0; ura3Δ0), and isogenic single mutants were purchased from EUROSCARF. The list of used strains is shown in Table S1. Double mutants used are mentioned in Table S1. Briefly, deletion cassettes were constructed by amplifying the hygR gene from pAG32 plasmid whose hphMX expression confers selection on hygromycine B. The primers used consisted of 40 bp of genomic sequence that flanked either the 5' or 3' end of the ORF to be knocked out (directly proximal and distal from the start and stop codons, respectively), and 20 bp homologous to the hphMX cassette. Primers used for the amplification of the deletion cassettes are listed in Table S2. Deletion cassettes were generated by PCR-based homologous recombination[30,31]. The full length DNA sequence of the ORF to be overexpressed were synthesized by GeneCust (https://www.genecust.com/). Genes were cloned in the pYES2 or pESC-Leu plasmids at the *NotI* restriction site, and were expressed under the activity of the GAL1 promoter. Cloned vectors were expressed and selected in *Escherichia coli* TOP10 prior to sequence verification. For either mutation or plasmid transformation, yeast cells were transformed using the LiAc method and selected on the appropriate selection medium[30]. REEs in their trichloride form were purchased from Sigma-Aldrich (MO, USA). In order to measure REE toxicity towards yeast strains, log-phase yeast cells (OD_{600nm} 0.15) were exposed to increasing REE concentrations in modified YNB-β-glycerophosphate liquid medium (YNB medium lacking KH_2PO_4, substituted by 1 mM β-glycerophosphate, pH 5.8) and growth (OD_{600nm}) was recorded for 10 h at 28 °C under constant shaking (180 rpm). Cell growth rate (μ) was measured in the log-phase and plotted against REE concentration.

Competition assays were carried out by growth monitoring of yeast cells (WT, ΔCch1, and ΔFtr1) exposed to either La (160 µM), Yb (8 µM) or no REE (Ctrl) with the addition of essential cations (50 mM Mg, 50mM Ca, 200 µM Fe, or 500 µM Mn) for 10 h.

Mutated and overexpressing strains were individually tested for REE resistance by serial dilution spot assays. Yeast strains were grown until saturation in 200 µL YPD medium, or in SD galactose medium lacking uracil for overexpressing strains, at 28 °C, and serial tenfold increment dilutions were performed. Five microliters each of six dilutions were spotted on YPD or YPG (for overexpression studies) agar plates containing REEs. Results were observed after 7 days of growth at 28 °C.

Sample preparation for RNAseq analysis

Wild type strain BY4741 was grown in YNB-β-glycerophosphate liquid medium. Cultures were inoculated at an OD_{600nm} of 0.05 and once the cultures reached an OD_{600nm} of 0.6, REEs were added at 50 or 160 µM of lanthanum, and 6 or 8 µM of ytterbium, corresponding to their EC_{10} (concentration at which 10% of the population is inhibited) and EC_{50} (concentration at which half of the population is inhibited), respectively, and exposed for 1 h. Cells were harvested at room temperature at 4000 rpm for 1 min and snap frozen. After cell disruption by bead-beating, total RNA were column purified using the RNeasy mini kit (Qiagen), according to the manufacturer instructions, and gDNA removed using DNAse I (Sigma Aldrich). RNA integrity was further assessed using a Bioanalyzer 2100 (Agilent, CA, USA). Strand-specific cDNA libraries were prepared by Eurofins Genomics (Ebersberg, Germany) using the TruSeq-3 library kit. Sequencing was carried out on Illumina HiSeq 2500 with chemistry v4 applying the high-output run mode, using a 2x100 bp paired-end sequencing.

Analysis of the differentially expressed genes

The data obtained were analysed by the online platform Galaxy. The reads were first trimmed using the Trimmomatic v0.36.1 tool in order to remove any remaining Illumina adaptor sequences, and low-quality reads, and FastQC v0.67 was used to check reads quality

before and after the Trimmomatic step. RNAseq and sorted trimmed reads were mapped on the reference genome (S288C R64-2-1 of 2015-01-31 from https://www.yeastgenome.org/) of *S. cerevisiae* using TopHat v2.1.1. Reads that were mapped on the reference genome were quantified using HTSeq-count v0.6.1p1. Finally, differential gene expression analysis between conditions was carried out by using DESeq2 v1.14.1. Differentially expressed genes between conditions were obtained and expressed as $\log_2$-fold change with adjusted p-values calculated via a Benjamini-Hochberg test. A cut-off adjusted p-value of < 0.01 was applied.

Sample preparation for proteomics analysis.

The wild type strain was grown as mentioned above. Cultures were inoculated at an OD_{600nm} of 0.05 and once the cultures reached an OD_{600nm} of 0.6, REEs were added at the EC_{50} of the wild type strain, and exposed for 1 and 4 h. Cells were harvested at room temperature at 4000 rpm for 1 min. Cell pellets were washed twice with PBS 50 mM pH 7 and snap frozen. Proteins were extracted from frozen cells by bead-beating with a Precellys 24 instrument (Bertin) after addition of LDS1X (Invitrogen) consisting of 106 mM Tris/HCl, 141 mM Tris base, 2% lithium dodecyl sulfate, 10% glycerol, 0.51 mM EDTA, 0.22 mM SERVA Blue G250, 0.175 mM phenol red, buffered at pH 8.5 and supplemented with 2.5% ß-mercaptoethanol. Samples were heated for 5 min at 95 °C, loaded onto a denaturing 4–12% gradient 10-well NuPAGE (Invitrogen) gel (25 µL per well), and then subjected to electrophoresis for 5 min as previously recommended[32]. After quick staining with Coomassie Blue Safe (Invitrogen), polyacrylamide bands corresponding to the whole proteomes were sliced, destained with ultra-pure water, reduced with dithiothreitol, and treated with iodoacetamide, before performing proteolysis with Trypsin Gold Mass Spectrometry Grade protease (Promega) in the presence of 0.01% ProteaseMAX surfactant (Promega).

Tandem mass spectrometry.

Tryptic peptides were subjected to tandem mass spectrometry with a Q-Exactive HF tandem mass spectrometer (Thermo) incorporating an ultra-high field Orbitrap analyzer coupled in line with an Ultimate 3000 chromatography system (Thermo). The tandem mass spectrometer was operated in the data-dependent mode as described[33]. Briefly, each sample (4 µL) was injected, desalted on a reverse-phase capillary C18 PepMap TM 100 precolumn (LC-Packing) and then peptides were resolved based on their hydrophobicity on a nanoscale 500-mm C18 PepMap TM 100 (5 mm x 300 µm I.D., Thermo) column using a 90-min gradient from 2.5% to 40% of 80% CH_3CN, 20% H_20, 0.1% formic acid. Once separated, mass spectra for peptides were acquired in the full-scan range 350-1800 *m/z*, at a resolution of 60,000, and an AGC target of 3.10^6. Peptide ions with charges $^{2+}$ or $^{3+}$ were selected for fragmentation according to the Top20 method. MS/MS mass spectra were acquired with an AGC target set at 10^4, a loop count of 60 ms, an isolation window of 1.6 *m/z*, a resolution of 15,000, a dynamic exclusion of 20 s, and a scan performed over a dynamic mass range from the first mass detected up to 15-times the first mass.

Peptide-to-spectrum assignment and protein identification.

Peak lists were automatically generated from raw files with an in-house script using the Proteome Discoverer 1.4.1 (Thermo) daemon conversion function and the following options: minimum mass (400), maximum mass (5,000), grouping tolerance (0), intermediate scans (0), and threshold (1,000). MS/MS spectra from the resulting *.mgf files were assigned to *S. cerevisiae* peptide sequences with the Mascot software v2.5.1 (Matrix Science) with the following parameters: full-trypsin specificity with up to two missed cleavages allowed, static modification of carbamidomethylated cysteine, variable deamidation of asparagine and glutamine, variable oxidation of methionine, mass tolerance of 5 ppm on parent ions and mass tolerance on MS/MS of 0.02 Da. Peptide matches with a MASCOT peptide score below a p-value of 0.05 were parsed with the IRMA software[34]. Proteins were validated when at least two different peptides were detected. False discovery rate for protein identification was below 1% as estimated with the reverse database decoy MASCOT search option. Spectral counts corresponding to the number of MS/MS spectra assigned per protein were extracted for each sample without applying the parsimony rule to avoid isoform quantitation bias. The normalized spectral abundance factor (NSAF) for each protein was calculated as the total spectral count divided by its molecular mass in kDa and presented in percentage. Spectral counts were compared between conditions using the T-Fold method of the PatternLab software[35] after normalizing spectral counts. The statistical classes were defined as: “Blue” for proteins that satisfied both, the |T-fold| (≥ 1.5) and its associated p-value (≤ 0.05), “Orange” for proteins with identifications that did not meet the T-fold criterion (but they deserve a second look because they had low p-values), “Green” for proteins that satisfied the fold criteria but were most likely false positives, and “Red” for proteins that did not meet the fold and p-value criteria.

GO term enrichment analysis.

Overrepresented gene ontology (GO) terms among differentially expressed genes (DEG) and proteins (DEP), in each condition tested, were obtained using the online Database for Annotation, Visualization and Integrated

Discovery (DAVID) tool[36,37]. GO terms significantly overrepresented for biological pathways, cellular compartment, and molecular functions, were selected with a set p-value cutoff of < 0.05. Kyoto encyclopedia of genes and genomes (KEGG) analysis was also performed on DEG and DEP, via the online DAVID tool, with the same cutoff. DEG and DEP heatmaps were obtained using the R package pheatmap v1.0.10, with a complete clustering method. Euclidian clustering distance measurement was selected for both rows and columns. Venn diagrams were drawn using the R package Venneuler v1.1-0.

Determination of REE content by inductively-coupled mass spectrometry

Mutant and wild type strains were grown as mentioned above in YNB-β-glycerophosphate. Cultures were inoculated at an OD_{600nm} of 0.05 and once the cultures reached an OD_{600nm} of 0.6, REEs were added at 50 µM and 6 µM of lanthanum and ytterbium respectively. After 1 h of exposure to REEs, yeast cells were harvested at 4000 rpm for 1 min at 4 °C. Cell pellets were washed three times with ice-cold MES (20 mM) – EDTA (10 mM) buffer (pH 6) followed by three washings with ice-cold ultra-pure water, and then dried for 48 h at 70°C. Triplicate samples were prepared. Aliquots (125 mg) were mineralised with 1.75 mL HNO_3 and 0.5 mL hydrogen peroxide in closed tubes placed in a block digestion system (DigiPREP, SCP Sciences, Courtaboeuf, France). A gradual heating mode was used to achieve a final temperature of 100°C (total run of 265 min). Then, ultrapure water (Millipore Milli-Q Integral 3 system, Molsheim, France) was added for a final volume of 12.5 mL. Blank and reference material were digested in the same conditions as samples. Concentrations of elements were determined in triplicate, using inductively coupled plasma mass spectrometry (ICP-MS, X Series II Model, Thermo Fischer Scientific, Courtaboeuf, France). The validity of the analytical method was checked by standard reference material (oriental basma tobacco leaves, INCT-OBTL-5, LGC Promochem, Molsheim, France).

Results and Discussion

REE toxicity assessment.

In order to compare the cellular toxicity of two different REEs, the LREE La, and the HREE Yb we first calculated the EC_{10} and EC_{50} for both elements. *S. cerevisiae* was exposed to increasing concentrations of these two REEs. The cellular density, was then monitored every hour for nine hours (Figure 1a,c). The growth rate (µ) was further plotted against REE concentrations to allow the determination of both EC_{10} and EC_{50} (Figure 1b,d). Yb had a 20 times higher toxicity relatively to La. The EC_{10} and EC_{50} for La were 50 and 160 µM, respectively, and 6 and 8 µM for Yb, respectively (Figure 1b,d).

We also investigated the effect of La and Yb exposure on the macro and micro elemental composition of cells (Figure 1e). Surprisingly, we observed an increase of Mn (18 to 50 %), Fe (29 to 42 %), Zn (13 to 18 %) and Cu (80 to 84 %) content under both La and Yb exposure. Even more striking was the increase of Ca (10-fold) and Na (4 fold) content specifically under Yb exposure. The only decrease observed was for K (-20 %) under Yb exposure (Figure 1e). The decrease in K was very probably triggered to compensate for the increase of Ca and Na contents, to maintain the global cationic homeostasis of cells. To go deeper in the comprehension of the toxicity differences of these elements, and decipher whether the underlying mechanisms were similar, we carried out both transcriptomic and proteomic analyses (Figure 1f).

Comparative transcriptomic analysis of two REE exposure concentrations.

We first aimed at identifying the response of yeast cells to two different conditions of a high (EC_{50}) and a low (EC_{10}) toxicity concentrations. Therefore, the transcriptome of *S. cerevisiae* exposed for one hour to La and Yb at their respective EC_{10} and EC_{50} was analysed (Figure 1f, Figure 2). All combined, we identified 1924 genes that were differentially expressed (P-value <0.01) in at least one condition (REE-stressed cells *versus* control condition). The direct comparison of gene expression between EC_{50} and EC_{10}, for the two metals, displayed relatively few differentially expressed genes (DEGs), with a cut-off of a fold change (FC) ≥ 1.5 and a P-value ≤ 0.01 (Figure 2b). When exposed to La, 10 DEGs were more expressed under the EC_{10} relatively to the EC_{50}, while 14 DEGs were more expressed under the EC_{50} condition (Table S3). The same observation was made for Yb. Twenty-two DEGs were more abundant in the EC_{10} condition relatively to the EC_{50}, while it was the case for 13 DEGs in the EC_{50} condition (Figure 2b, Table S3). We extended the analysis to the entire set of genes that were significantly differentially expressed relatively to the control condition (P-value < 0.01). Again, a relatively high similarity existed between the two exposure concentrations, with low differences in the transcriptomic profiles between EC_{10} and EC_{50} conditions (Figure 2a, Table S3). In agreement with this finding, similar observations of only few differences between EC_{10} and EC_{50} exposure were made with other metals such as Zn, Cd, Cu, Cr and Ag[38]. Thus, concentrations corresponding to the EC_{50} of both La and Yb were selected for the subsequent analyses.

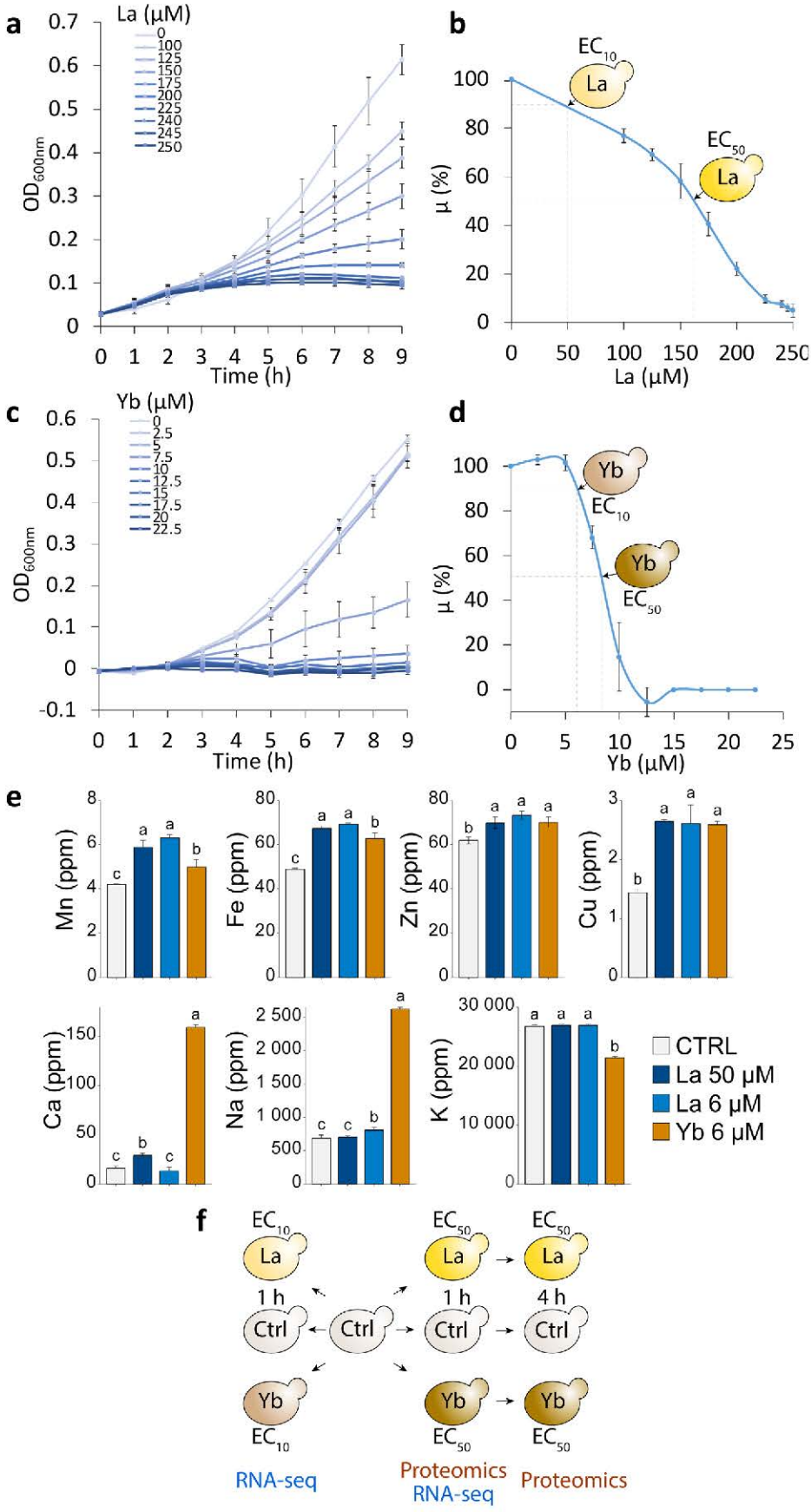
a
La (µM)
0
100
125
150
175
200
225
240
245
250
OD600nm
Time (h)
b
EC10
La
EC50
La
µ (%)
La (µM)
c
Yb (µM)
0
2.5
5
7.5
10
12.5
15
17.5
20
22.5
OD600nm
Time (h)
d
Yb
EC10
Yb
EC50
µ (%)
Yb (µM)
e
Mn (ppm)
Fe (ppm)
Zn (ppm)
Cu (ppm)
Ca (ppm)
Na (ppm)
K (ppm)
CTRL
La 50 µM
La 6 µM
Yb 6 µM
f
EC10
La
1 h
Ctrl
Ctrl
Yb
EC10
RNA-seq
EC50
La
EC50
La
1 h
Ctrl
Yb
EC50
Proteomics
RNA-seq
EC50
La
4 h
Ctrl
Yb
EC50
Proteomics

Figure 1. REE impact on *Saccharomyces cerevisiae* growth and ionome. (a) Growth monitoring of *S. cerevisiae* exposed to different La concentrations over time. (b) Growth rate (normalized with the non exposed condition) of *S. cerevisiae* exposed to increasing amounts of La allowing the identification of the EC_{10} and EC_{50}, the concentrations that inhibit 10% and 50% of the growth, respectively. (c) Growth monitoring of *S. cerevisiae* exposed to different Yb concentrations over time. (d) Growth rate (normalized with the non exposed condition) of *S. cerevisiae* exposed to increasing amounts of Yb allowing the identification of the EC_{10} and EC_{50}. (e) Ionomic analysis (Mn, Fe, Zn, Cu, Ca, Na, and K) of WT cells exposed to La at the EC_{10}, Yb at the EC_{10} and La at the same concentration as that corresponding to Yb EC_{10} (6 µM). (f) Experimental set-up of *S. cerevisiae* exposed to La and Yb using two different concentrations (EC_{10} and EC_{50}) and exposure times (1h and 4h). Yeast cells were harvested after the indicated exposure conditions and 3 independent experiments were carried out for each condition (n = 3).

Comparative proteomic analysis of two exposure times.

Temporal response analysis was also performed to investigate whether differences in cell response occurred between a short (one hour) and a long (four hours) exposure time, using a high-throughput shotgun proteomic approach (Figure 1f). Combining every condition tested and all replicates, a total of 26,785 peptides were detected, corresponding to 685,981 MS/MS recorded spectral counts. It allowed the successful identification of 2,630 proteins, among which 2,015 were certified with at least 2 peptides, when alignment querying was made against the *S. cerevisiae* S88C reference genome. Identified proteins with significant abundance change (FC ≥ 1.5 and P-value ≤ 0.05) upon REE exposure against control condition were used for the analysis. It is noteworthy that many more differentially expressed proteins (DEPs) were found under both La and Yb exposure, at one hour compared to four hours. As shown in figure 3a, 2.6 times more proteins were indeed differentially expressed at one hour

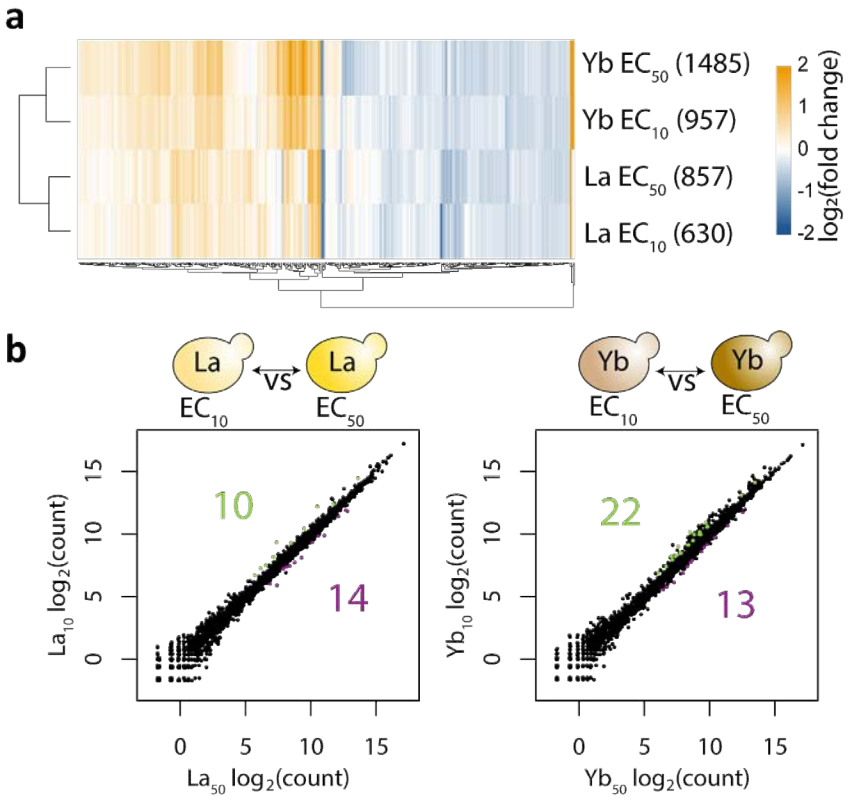

Figure 2. Comparative transcriptomic analyses of *Saccharomyces cerevisiae* exposed to La and Yb show a similar pattern between EC_{10} and EC_{50} treatments. (a) Heatmap of differentially expressed genes (DEG) (blue, downregulated and orange, upregulated) under the two different concentrations of REE (EC_{10} and EC_{50} for both La and Yb) in comparison to the control condition. The total number of DEG (P-value ≤ 0.01) is specified into brackets. (b) Scatter plots of DE transcripts under La and Yb exposure. Significantly upregulated and downregulated transcripts (FC ≥ 1.5, P-value ≤ 0.01) are shown in green and purple, respectively.

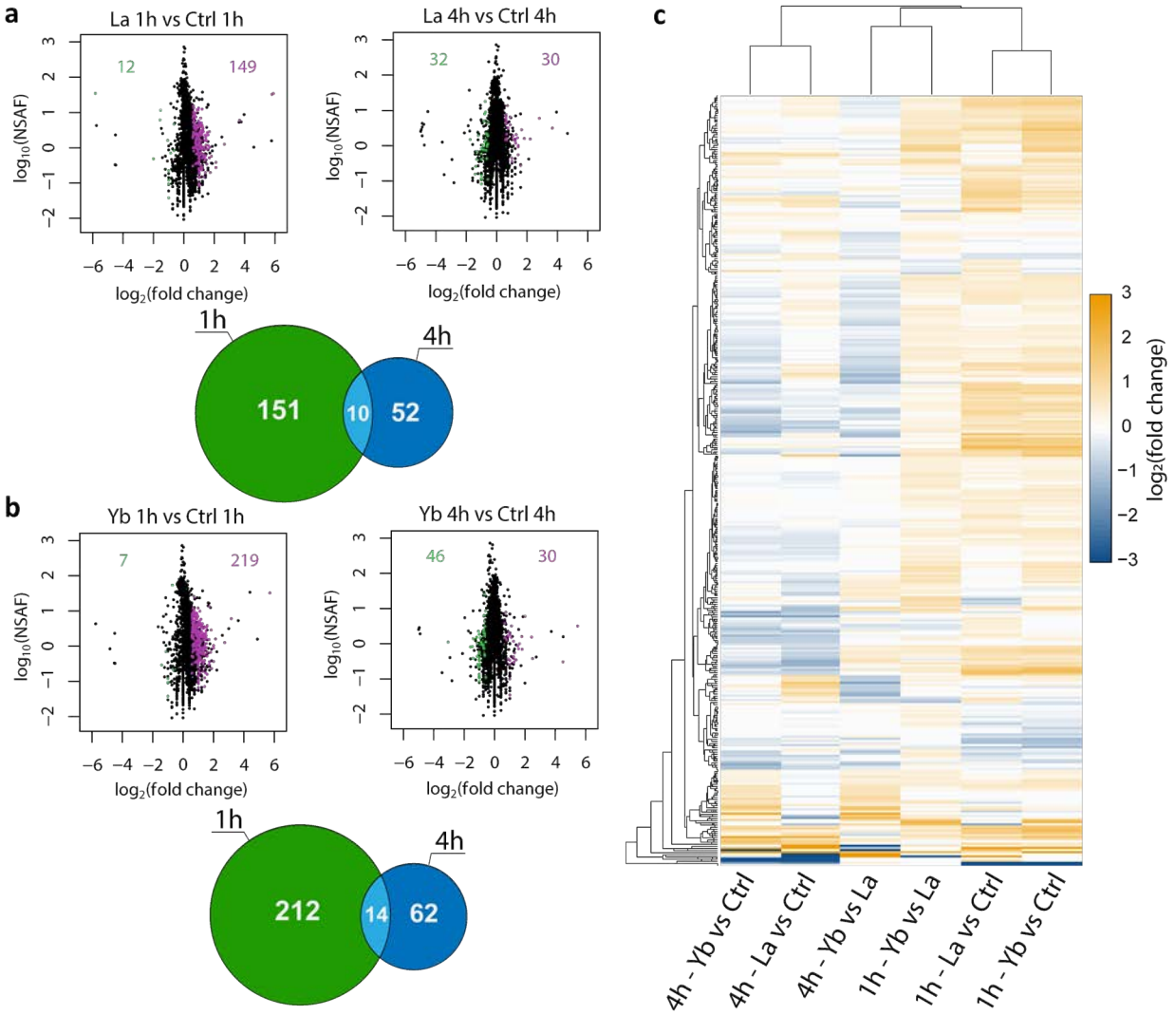

Figure 3. Comparative proteomic analyses of *S. cerevisiae* exposed to La and Yb demonstrate a differential response in time. (a) Scatter plots and Venn diagrams of differentially expressed proteins under La exposure vs control condition after 1h and 4h of exposure. Significantly upregulated and downregulated proteins (FC ≥ 1.5, P-value ≤ 0.05) are shown in green and purple, respectively. (b) Same as in (a) but under Yb exposure. (c) Heatmap of differentially expressed proteins (blue, downregulated and orange, upregulated) under the two different exposure times (1h and 4h).

compared to four hours, with a total of 161 DEP at one hour, and 62 at four hours under La stress (Table S4). Similarly, under Yb stress, 226 and 76 DEP were found after one and four hours (3 times more), respectively (Figure 3b). Surprisingly, only 10 (La) and 14 (Yb) DEPs were shared between the two exposure times, indicating a complete different response set up by yeast cells (Figure 3a-c). Those results suggest the higher and faster response during a short exposure time, relatively to a long exposure time. Congruent conclusions were drawn from the direct comparison of DEPs between one and four hours exposure for both REEs. A total of 387 and 444 DEPs were found under La and Yb exposure, respectively. Similar observations were made when *S. cerevisiae* was exposed to other metals (Ag, Cd, Hg, Zn) and the metalloid (As) while comparing the transcriptomic response under an acute stress (30 min) and a sustained stress (2 h)[27]. These authors reported that only 2.4 to 7.9% of the total DEGs were shared between an acute and a sustained stress[27]. These results further support the time-course adaptation process implemented by the cells to cope with a toxic metal.

Early proteomic response to La and Yb.

The proteome analysis of cells exposed to an acute stress of La or Yb, for one hour, allowed the identification of

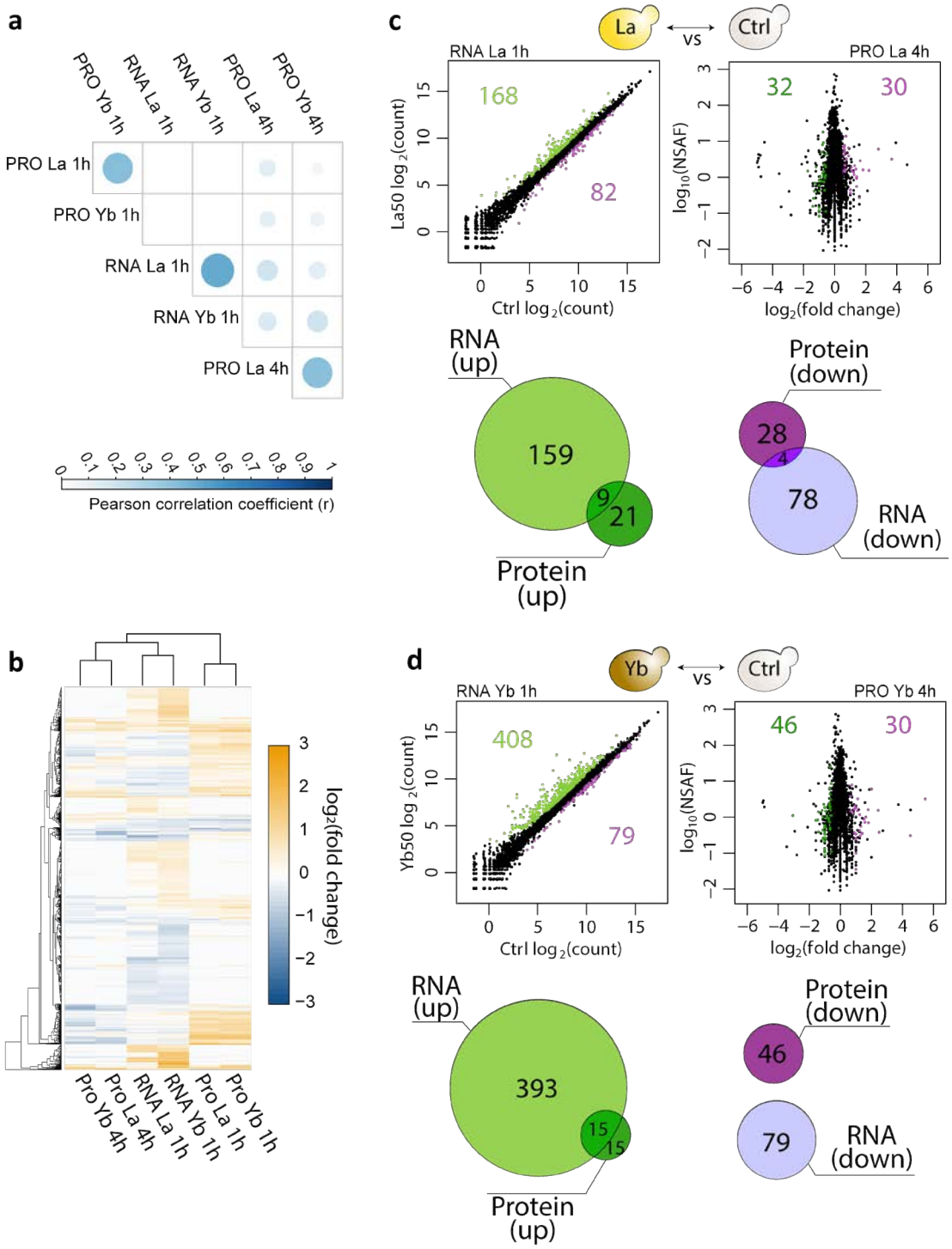

Figure 4. Comparative transcriptomic and proteomic analyses of *S. cerevisiae* exposed to REE at the EC_{50}. (a) Correlation matrix (Pearson's correlation coefficient r) of transcriptomic and proteomic data sets. (b) Heatmap of differentially expressed (DE) proteins (Pro) and DE transcripts (RNA) at the different exposure times (1h and 4h, as indicated) under La or Yb stress (blue, downregulated and orange, upregulated). (c) Scatter plots and Venn diagrams of DE proteins (after 4h) and mRNA (after 1h) under La exposure vs control condition. Significantly upregulated and downregulated proteins (FC ≥ 1.5, P-value ≤ 0.05) or transcripts (FC ≥ 1.5, P-value ≤ 0.01) are shown in green and purple, respectively. (d) Same legend as in (c) under Yb exposure.

essential genes and related pathways that cells first set up for coping with these toxic elements. It was interesting to notice the relative low number of downregulated proteins under both conditions, with 12 DEPs for La and 7 DEPs for Yb (FC ≥ 1.5 and P ≤ 0.05) (Figure 3a,b). Furthermore, these proteins were all involved in ribosome biogenesis (La; P = 2.83E-04), and rRNA processing (La; P = 1.44E-05) (Table S6, S7). If we extend our observation to all DEPs with a P-value <0.05, we can see the high representation of NOP (NucleOlar Protein), RPL (Ribosomal Protein of the Large subunit) and RPS (Ribosomal Protein of the Small subunit) family proteins (Table S4). These data further support the downregulation of ribosome biogenesis under both La and Yb stresses. Reduction in ribosome abundance was reported under different metallic stresses as being a rapid, effective, and reversible stress response against misfolded proteins[24, 27,39–41]. Guerra-Moreno *et al.* (2015)

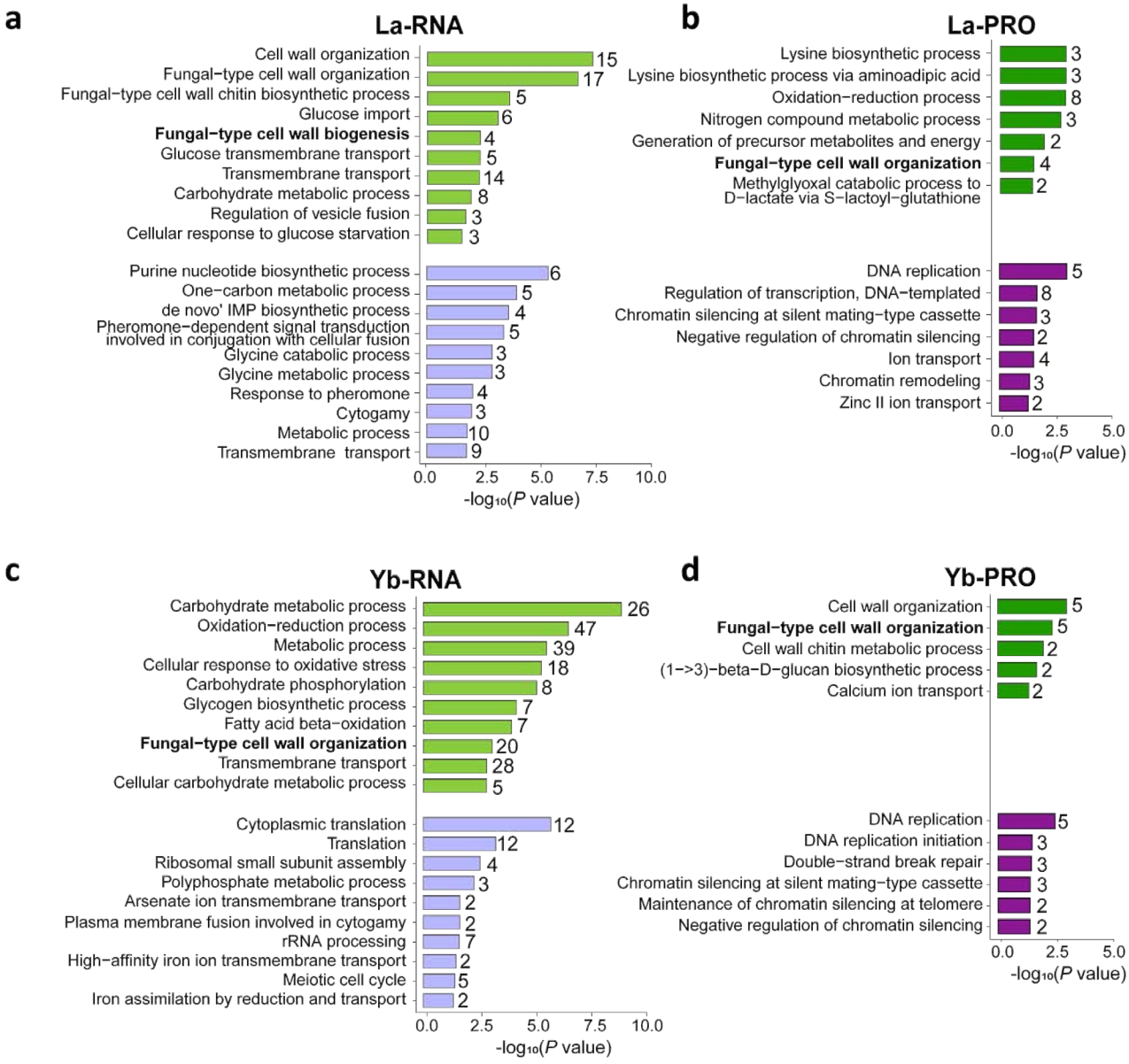

Figure 5. GO-terms Biological Pathways (BP) overrepresented in the transcriptomic and proteomic analyses of *S. cerevisiae* exposed to REEs at the EC_{50}. (a) GO-terms BP of DE transcripts under La exposure. (b) GO-terms BP of DE proteins under La exposure. (c) GO-terms BP of DE transcripts under Yb exposure. (d) GO-terms BP of DE proteins under Yb exposure. GO-terms significantly (P-value ≤ 0.05) found in upregulated and downregulated proteins or transcripts (P-value ≤ 0.01) are shown in green and purple, respectively. GO-terms found in both RNAseq and proteomic analyses are given in bold. Numbers indicate the number of proteins or mRNA of the specified BP found in our sets of data.

suggested that by reducing cellular ribosome levels, newly synthesized misfolded proteins may be limited, thus proteolysis would be more effective with existing misfolded proteins[39].

In line with this, and when looking at upregulated proteins, most of the GO terms represented in the two sets of data were proteolysis-related (P = 1.23E-02 and 8.28E-04, for La and Yb, respectively) (Table S6, S7). In the Yb treatment, upregulated proteins belonging to the ubiquitin-dependent protein catabolism were also found. Induction of proteolysis is a global cellular response to metallic stress as it was also observed at toxic concentrations of Al, Ag, Cd, Mn, Ni, Zn, Hg, and As[27,38,39]. The short exposure of yeast cells to toxic ions appears to trigger a fast detoxification process, by degrading proteins that have been damaged by this stressor. Thus, there is a need to replace those proteins, and additionally, set up new proteins and enzymes in order to adapt the cellular response toward this stressor. Under both treatments, proteins belonging to the carbohydrate metabolic process were upregulated (Table S6, S7). Furthermore, under Yb exposure only, oxidation-reduction process (P = 1.08E-03) was also upregulated, along with NADPH regeneration (P = 1.29E-02), and the cellular response to oxidative stress (P = 9.65E-03). The production of ROS under REE exposure was shown in several organisms[11,12,17], it is therefore not surprising to observe such pathway being upregulated here. Jin et al. (2008) gathered those induced biological processes under the term 'common metal responsive' genes[38]. It appears that in response to an acute stress, here after one hour of exposure, yeast cells would be more inclined to first detoxify from accumulated metals before setting up an adaptation response to a sustained stress[27].

Combining transcriptomic and proteomic analyses.

In order to combine the two -omic methods, we first tried to identify which conditions displayed the closest profiles when comparing significantly DEGs and DEPs at one and four hours for both REEs (Figure 4a,b, Table S5). Consistent with the previous observations, proteomic profiles at one and four hours were not clustered together. Conversely, the highest correlations were observed between transcriptomic profiles obtained after one hour and proteomic profiles obtained after four hours of REE exposure, rather than one hour (Figure 4a,b, Table S5).
We consequently compared mRNA levels at one hour and protein expression at four hours by overlaying the profiles obtained for each REE independently. Strikingly, there was no direct link between mRNA and the corresponding expressed proteins (Figure 4c,d). For instance, under La exposure, the expression of 21 out of 30 (70 %) upregulated proteins, as well as 28 out of 32 downregulated proteins, was not modified in the cognate mRNAs (Figure 4c). The same observation could be made under Yb exposure, with as high as 50 % of upregulated proteins and 100 % of downregulated proteins that were not found in the DEGs (Figure 4c). These statements could be explained by the relatively low number of DEPs (FC $\geq$ 1.5 and p-value $\leq$ 0.05) in comparison with the number of DEGs (FC $\geq$ 1.5 and p-value $\leq$ 0.01). A fourfold higher number of mRNAs than proteins were differentially expressed under La exposure, while it reached 6.4 times more under Yb exposure (Figure 4c,d). We thus analysed each set of data for the enriched gene ontology (GO terms), supplying complementary results, so as to identify modulated pathways and functions in response to either La and Yb (Figure 5a-d, Table S9-14).

The cell wall as the first shield to REE interaction.

While looking at La response at the transcriptomic level, upregulated genes were mainly associated with cell wall biogenesis (P = 3.94E-03) and organization (P = 3.16E-08). These functions were markedly represented by four different GO terms, associating as many as 31 different genes (Figure 5a). Accordingly, the fungal-type cell wall organization was also found upregulated in the proteins differentially expressed (P = 2.94E-02) (Figure 5b, Table S9). It was also supported by the enriched GO cellular compartments (Table S12). Comparable to La, Yb exposure upregulated 28 genes involved in fungal-type cell wall organization (P = 7.38E-04), and cell wall organization (P = 1.10E-02) (Figure 5c, 5a, Table S13). Moreover, these two functions were also found in the proteomic analysis under Yb stress. This was reinforced by the upregulation of the cell wall chitin metabolic process (P = 9.34E-03), and the 1,3-β-D-glucan biosynthetic process (P = 1.86E-02) (Figure 5d, Table S10).
Among them, Mid2p, acts as a sensor for cell wall integrity signalling and activates this pathway. Downstream the signalling pathway triggered by Mid2p, Slt2p, a serine/threonine MAP kinase involved in regulating maintenance of the cell wall integrity was also upregulated. *GSC2* (*FKS2*), known to be triggered under a cell wall stress and to encode a catalytic subunit of 1,3-ß-glucan synthase[42] was specifically upregulated under Yb stress (Figure 6a). *CWP1* and *NCW2* were upregulated under both treatments, and identified from both transcriptomic and proteomic analyses (Figure 6a). Cwp1p is a cell wall mannoprotein linked to a ß-1,3 and ß-1,6-glucan heteropolymer while Ncw2p may help in the organisation of ß-1,3-glucan structure of the cell wall, supporting the need of proper organisation of cell well constituents[43,44].
The over-representation of these cell wall-related biological pathways (BP) in all our experiments supports the role of this compartment as being the first barrier in

the interaction of yeast cells with REEs. It also gives additional clues to figure out how the different REEs interact with the cell wall. Adsorption of REEs was shown for Ce[45] and Yb[46] on the cell wall of *S. cerevisiae* and observed on the cell wall of both *Bacillus subtilis* and *Escherichia coli*, with affinity differences between LREEs and HREEs [47]. Surface complexation modelling showed that LREEs were preferentially associated with phosphate groups, while HREEs could be modelled equally well with carboxyl and phosphate groups. The use of potentiometric titration and FTIR spectroscopic analyses on *S. cerevisiae* showed the higher representation of phosphate groups (68%) on the cell surface, while amino/hydroxyl (16%) and carboxyl groups (16%) were less represented[48]. Surface of the yeast cell wall that bear such groups have been modelled to bind Ca ions, which could potentially be broadened to REEs given their similarities[48]. The higher representation of phosphate groups at the surface, and the higher affinity of LREEs for these groups, could explain the relatively lower toxicity observed for La compared to Yb (Figure 1). Thus, upregulation of cell wall related genes seems essential in response to REEs and could allow the recycling or selective remodelling of the yeast cell wall in order to cope with this stress. A modification of the exposed groups at the surface could ensue, with possible consequences on REE binding. Combined together, these results support the involvement of the cell wall as a hotspot for REE interaction with yeast cells, but also in distinguishing La from Yb-triggered effects.

Involvement of the pheromone signalling pathway

When looking at BP related to extracellular environment sensing, pheromone-related GO biological pathways surprisingly arose. Indeed, two downregulated GO biological pathways were enriched under La stress, both taking part in the pheromone signalling pathway (Figure 5a, Table S12); the pheromone-dependent signal transduction involved in conjugation with cellular fusion (P = 3.29E-04) and the response to pheromone pathway (P = 8.39E-03). Despite that these GO terms were specifically enriched under La stress, genes belonging to those pathways were also significantly downregulated

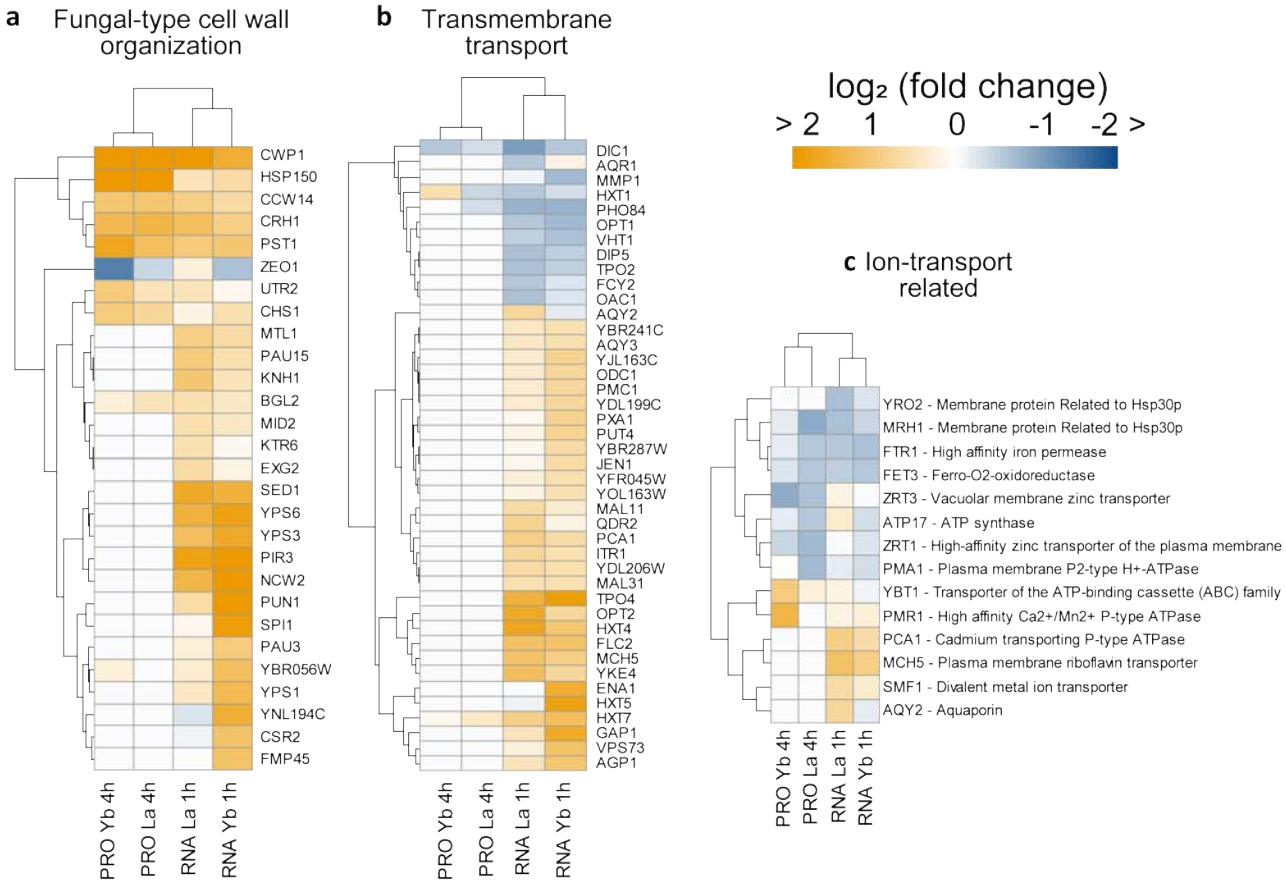

Figure 6. Expression heatmaps of GO-terms enriched in proteomic and transcriptomic analyses for both REE. (a) Fungal-type cell wall organization, (b) Transmembrane transport, (c) Oxidation-reduction process, (d) Carbohydrate metabolism, (e) DNA replication, and (f) Ion-transport related GO-terms (p-value < 0.05). Genes and proteins shown are all significantly differentially expressed.

under Yb stress, but to a lesser extent (Table S3). The GO terms included *MFA1* and *MFA2*, the two genes encoding the mating pheromone a. The alpha-factor pheromone receptor encoding gene *STE2* and its associated heterotrimeric G protein *SST2* were also both downregulated. Downstream the regulation cascade triggered by *STE2*, *FAR1* which is phosphorylated by the MAPK (Mitogen-activated serine/threonine protein kinase involved in mating) *FUS3* in response to mating pheromone were also downregulated. Among other genes modulated by the pheromone response pathways, several of them were found downregulated. It was the case for Prm1p, a pheromone-regulated multi-spanning membrane protein which is involved in membrane fusion during mating and Bar1p, an aspartyl protease secreted into the periplasmic space of mating type a cells[49]. The latter cleaves and inactivates alpha factor allowing cells to recover from alpha-factor-induced cell cycle arrest.

The modulation of the pheromone response pathway is rather surprising. However, a link can be proposed between this pathway and the REE-triggered response. It is well known that some REEs, in particular La, are Ca analogues[50], and can be absorbed through the Ca influx system Cch1-Mid1 in yeast cells[23]. It is also established that Ca influx happens during the mating process, starting with mating pheromone detection[51,52]. The response to mating pheromones notably includes the higher expression of high affinity Ca channels, Cch1p-Mid1p and Ecm7p, but also of the putative low affinity Ca channels, Fig1p[51,53]. Thus, having in mind that REEs can pass through Ca channels, downregulation of pathways involved in the transcription of these channels would reduce the amount of REEs in the cytoplasm. However, such a hypothesis therefore needs further investigations to estimate whether REE accumulation is modified in pheromone metabolism related-mutants. In response to pheromones, yeast cells can both modify their cell wall in order to allow the fusion with cells from the other mating type, but also induce the cell cycle arrest [54] and thus leads to a more susceptible cell wall. Therefore, in line with the previous observations, the downregulation of genes and proteins involved in the pheromone-dependent signal transduction pathway could reduce cell cycle arrest but also the process of cell wall alterations, allowing cells to better cope with REE toxicity.

REE impact on amino acids, carbohydrates, and DNA metabolism

Several metabolic and biosynthetic processes were altered in response to REEs at the transcriptomic and proteomic level under La stress. (Figure 5a, Table S12). First, the biosynthesis of purine nucleotides (P = 3.12E-06), through '*de novo*' IMP (P = 1.95E-04) (figure 5a) and AMP (P = 2.72E-02) biosynthetic processes, was the most significantly downregulated. Second, the one-carbon metabolic process (P = 8.55E-05), which is connected to the glycine metabolic process (P = 1.09E-03) was also downregulated (Figure 5a, Table S12). Conversely, the proteomic analysis demonstrated that under La stress, the lysine biosynthetic process was upregulated (10%, P = 9.99E-04) (Figure 5b, Table S9). It was however interesting to notice the lack of any amino acid-related GO terms under Yb stress, except three upregulated genes involved in proline transmembrane transport (P = 2.04E-02) (Figure 5c,d, Table S13).

A relatively high number of upregulated genes were associated with the carbohydrate metabolic process (P = 1.03E-02 and 9.64E-10) under both treatments with eight upregulated genes under La stress, and 28 under Yb stress (Figure 5a,c). Many related GO terms were enriched in the Yb condition, highlighting the involvement of this pathway in the response to Yb. However, the induction of carbohydrate metabolism was reported as being a common metal responsive pathway and it was also found when yeast cells were exposed under several other toxic metals[38].

The two analytical methods identified *INO1* and its encoded protein Ino1p as the most upregulated representatives under both La and Yb (Table S5). The Inositol-3-phosphate synthase Ino1p is involved in the synthesis of inositol phosphates and inositol-containing phospholipids. Under phosphate limitation, the genes implicated in the uptake and metabolism of inositol phosphate, in phosphate metabolism, and in the process of phosphorylation of metabolites were induced[24]. Interestingly, it has recently been shown that inositol-3-phosphates were involved in the proper localization of metal uptake transporters in *Arabidopsis thaliana*[55]. Thus, increase of inositol-3-phosphates through the upregulation of *INO1* could be important for membrane transporters localization in response to REEs. Another explanation would be the increase of inositol phosphates to chelate REEs, thus, decreasing their toxicity and reactivity. Indeed, all inositol phosphates are strong chelators of metal ions among which Ca, Mg, Zn, Cu, Fe, Mn and Al[56,57].

Finally, almost all the pathways downregulated at the proteomic level for both stresses were related to DNA replication and regulation (Figure 5b,d, Table S9, S10). Indeed, proteins taking part in DNA replication were downregulated under both La (P = 8.48E-04) and Yb (P = 2.93E-03) stresses together with regulation of transcription under La exposure (P = 1.96E-02). Yb stress also reduced the translation, RNA processing and ribosome small subunit assembly at the transcriptomic level (Figure 5c). It has been strongly suggested that DNA replication was a target for Cd toxicity[58]. The downregulation of DNA replication by REEs could be an evidence of REE toxicity target similarly to Cd.

Ytterbium triggers oxidative stress response

In Yb treated yeast, the best represented process was the oxidation-reduction GO biological pathway (47 genes, P = 2.48E-07) (Figure 5c Table S13). In addition, 18 genes belonging to the cellular response to oxidative stress were also upregulated (P = 4.27E-06), suggesting that Yb triggers oxidative stress (Figure 5c, Table S13). While only represented for Yb stress in our study, it was extensively shown that REEs can generate oxidative stress[11,12,17]. Interestingly, several genes involved in glutathione (GSH) homeostasis were upregulated specifically under Yb stress. GSH can act at three different levels. First GSH is able to chelate toxic metals, in order to form a complex that can be subsequently sequestrated into the vacuole. GSH can also act as a protective agent against metal-induced oxidation. Finally, protein glutathionylation can occur, resulting in a protective role against irreversible metal binding and/or oxidative damage to proteins[25,59].

Among the genes involved in GSH homeostasis and upregulated under Yb stress, we could find *GTT1* (ER) and *ECM4* (*GTO2*, cytoplasm) along with *GRX1* (cytosol) and *GRX2* (cytosol and mitochondria), but to a lesser extent (Table S3). Gtt1p and Ecm4p are glutathione-S-transferases (GSTs) while Grx1p and Grx2p are glutaredoxins that can fill the same role as GSTs[60]. GSTs catalyse the conjugation of GSH with a substrate, as for example Cd^{2+}, or isomerization of GSH to form oxidized glutathione[61]. Furthermore, the upregulation of the gene encoding the gamma-glutamyltranspeptidase *ECM38* (Table S3), a major glutathione-degrading enzyme localized into the vacuole, suggests the translocation of oxidized glutathione into the vacuole, with a subsequent need to recycle[62]. Similarly, Dug1p a metallopeptidase allow the degradation of glutathione in the cytosol[62]. Thus, along with ROS production inducing oxidative stress, Yb could be internalized through GSH-Yb complex inside the vacuole.

REEs affect plasma membrane transport

Reducing toxic ion import inside the cell is another of the mechanisms that cells can set up to cope with such stressor. Within the downregulated genes under Yb and La exposure, a set corresponded to ion transporters of the plasma membrane. Under Yb exposure, three related GO terms were enriched in the present data set; arsenate ion transmembrane transport, high-affinity Fe ion transmembrane transport and Fe assimilation by reduction and transport (Figure 5c, Table S13). Under La exposure, four downregulated proteins were involved in ion transport (P = 2.78E-02), and more specifically in Zn ion transport (2 proteins, P = 4.91E-02) (Figure 5b, Table S12). Under those GO terms, the two genes encoding the two components of the high-affinity Fe transport system Fet3p-Ftr1p, were downregulated under both La and Yb stresses (Figure 6c). Fet3p is the multiCu oxidase that oxidizes ferrous to ferric Fe, for subsequent cellular uptake by the transmembrane permease Ftr1p[63]. Some other ion-transport related genes and proteins had a modified expression, evidenced from the transcriptomic or proteomic analysis (Figure 6c). Along with Fet3-Ftr1, the high-affinity Zn transporter of the plasma membrane *ZRT1* was also downregulated in the presence of both REEs (Figure 6c). We could also observe the downregulation of the Zn transporter Zrt3p localized at the vacuolar membrane (Figure 6c, Table S5). Zrt3p allows the transport of Zn ions from vacuolar storage into the cytoplasm.

Conversely, some other genes encoding transmembrane ion transporters were upregulated. Among them, *PCA1*, encoding a Cd efflux-transporter, and *SMF1*, encoding a divalent metal transporter, were found. Thus, REE exposure appears to affect nutrient homeostasis at the ionome level, probably through the modulation of the expression of metal transporters.

The Ca channel Mid1-Cch1 is involved in LREE but not in HREE uptake

In order to understand the involvement of those ion transporters in the REE response, we investigated the phenotypic response of mutants for those proteins under REE exposure. La was extensively used as a Ca channel blocker in many studies due to the high similarity between LREEs and Ca for their ionic radius[50,64,65]. However, it has been recently shown that rather than blocking the Ca channel Cch1p-Mid1p in yeast, REEs would be taken up through this channel[23]. Ene *et al.* (2015) demonstrated that less REEs were accumulated in *CCH1* and *MID1* single mutants compared to the WT. It was especially noteworthy for La, and to a lesser extend to other LREEs[23]. This observation was confirmed in the present study by monitoring the growth of both the single *CCH1* and the double *CCH1-MID1* mutants under REE exposure. Interestingly, those mutants displayed a resistant phenotype towards La, but also to other REEs in comparison to the WT, starting from La to Tb. This result supports the findings of Ene *et al.* (2015) (Figure 7a) and suggests that Ca channels could use REEs as substrates. Thus, in order to strengthen our hypothesis, we carried out competition trials. WT cells were either grown in control conditions or exposed to REEs at their respective EC_{50} (160 µM for La and 5 µM for Yb), with the addition of Ca (50 mM), and growth was monitored for ten hours (Figure 7b). The addition of Ca had no effect on growth in the control condition. Consistently with the prior hypothesis, the addition of Ca prevented La toxicity, allowing a normal growth of the cells. However, it also reduced Yb toxicity (Figure 7b). Thus, Ca ions in this conditions, are likely to compete with REEs potentially

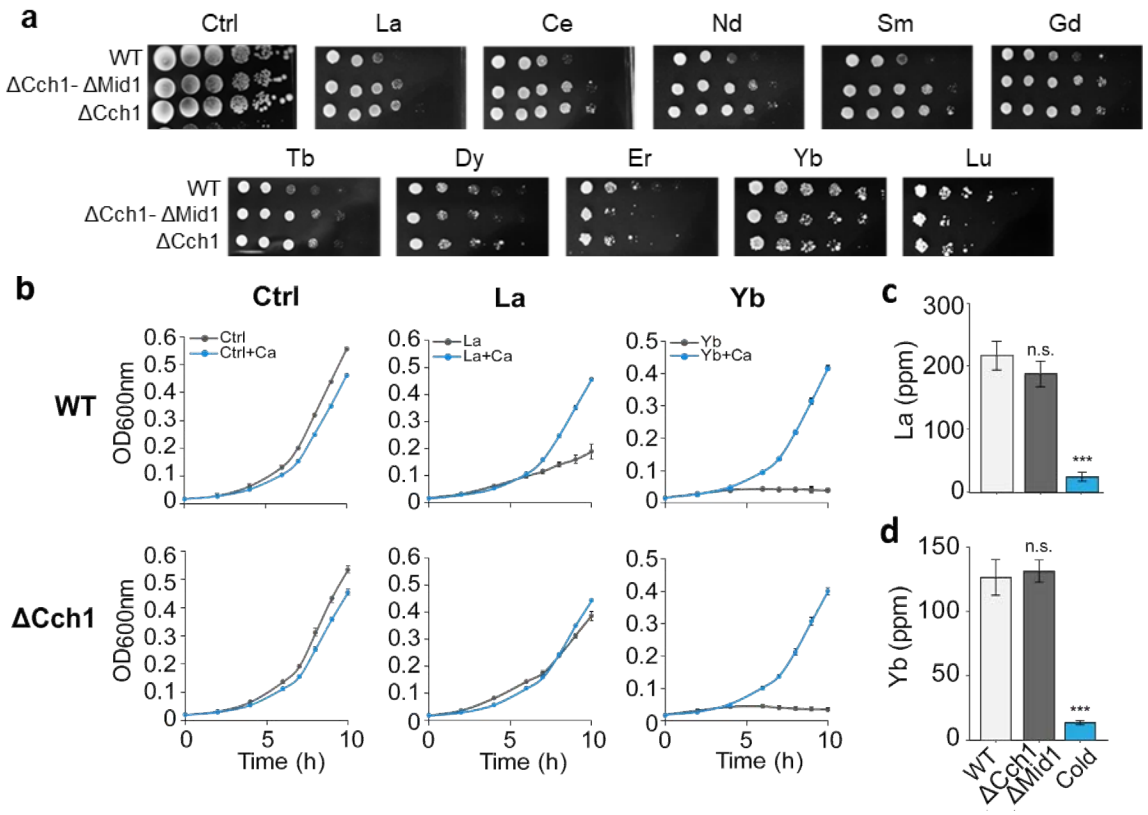

Figure 7. Calcium membrane transporters account for LREE uptake. (a) Drop-test of 10-fold serial dilutions of wild type (WT), and Ca membrane transporter mutants for their resistance towards a range of REEs, 4.0 mM La, 4.2 mM Ce, 4.5 mM Nd, 4.6 mM Sm, 4.0 mM Gd, 3.9 mM Tb, 3.6 mM Dy, 3.9 mM Er, 3.6 mM Yb, or 3.6 mM Lu. (b) Growth monitoring of yeast cells (WT, and ΔCch1) exposed to either La, Yb or no REE (Ctrl) with the addition of 50mM Ca. Representative curves out of three independent experiments are given. (c) La content in WT and mutant cells after exposure to the EC_{10} of La for one hour (50 µM). (d) Yb content in WT and mutant cells after exposure to the EC_{10} of Yb for one hour (6 µM). Cold condition corresponds to the WT exposed to La or Yb for one hour at 4 °C. Statistically significant differences from the WT are indicated by asterisks (n = 3, t-test, ***<0.001, n.s. non significant). Representative pictures of three independent experiments are given. Pictures were taken after six days of growth.

for uptake or cell wall binding, thus decreasing their toxicity[48].

The same experiment using the *CCH1* mutant was carried out (Figure 7b). In line with the results obtained for the WT, the lack of functional Ca channel allowed yeast cells to better resist to La, but not to Yb. The addition of Ca did not increase the resistance to La, supporting that the Ca channel Cch1p-Mid1p is the main route for La import into the cytoplasm (Figure 7b).

To first confirm whether the uptake of REEs is an active mechanism, WT cells were exposed to La or Yb for one hour at 4°C (Figure 7c,d). Under such conditions, ten times as less La and Yb were taken up compared to the exposure at 28 °C (Figure 7c,d). This very low accumulation of REEs supports the hypothesis of an active import of REEs into the cytosol, and not only reflecting adsorption to the cell wall. In the presence of Yb, the *CCH1-MID1* double mutant grew in a similar way to the WT (Figure 7b), which is concordant with their similar Yb uptake (Figure 7d). However, a slightly lower accumulation of La (-14 %) was observed, despite not being statistically significant, could be responsible for the higher resistance of the mutant (Figure 7c). Ene *et al.* (2015) demonstrated that the single mutation of either *CCH1* or *MID1* led to twice as less La accumulated[23]. In our case, the La content was not reduced in the *CCH1-MID1* double mutant. In order to verify these results, further experiments of La accumulation must be done using the single mutants *MID1* and *CCH1*, but also by testing longer exposure time. Nevertheless, these different phenotypic results are new evidence that support the role of Ca channels as a way of entry for LREEs but not for HREEs.

Towards new insights into REE uptake.

Previous work describing the role of both Alr1p and Alr2p, showed that the overexpression of either of those

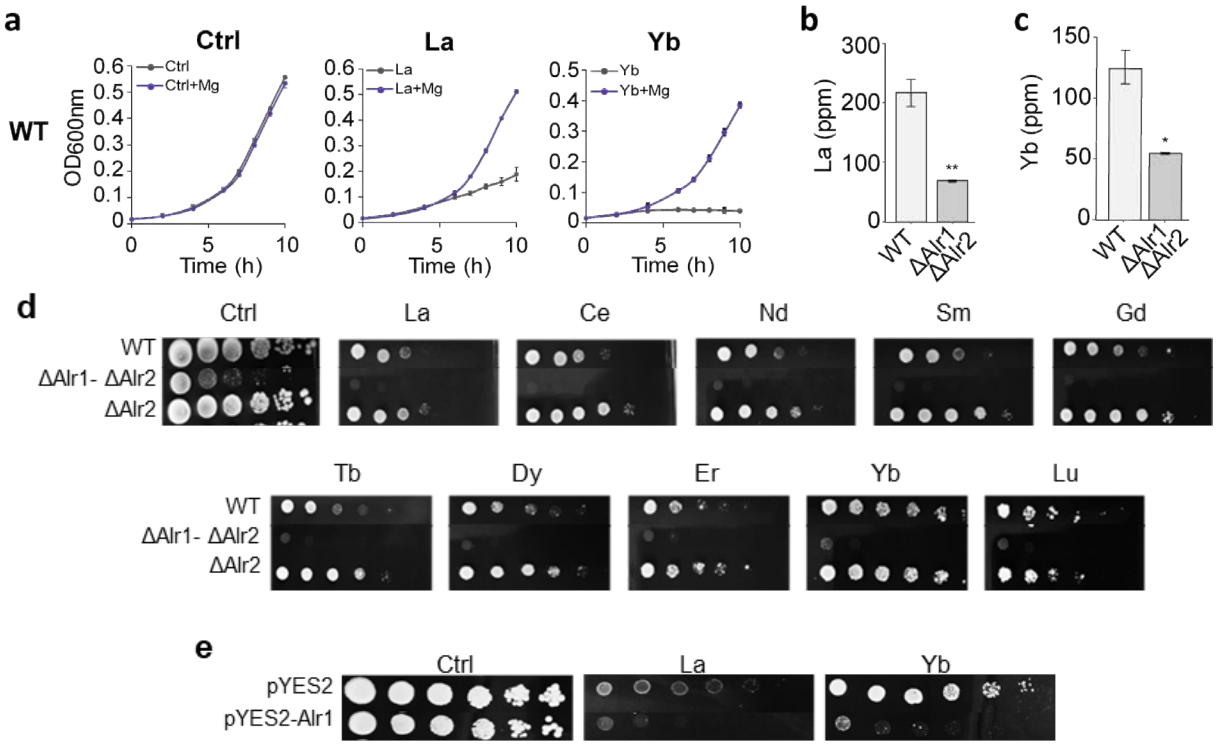

Figure 8. Magnesium membrane transporters account for REE uptake. (a) Growth monitoring of WT cells exposed to either La, Yb or no REE (Ctrl) with the addition of 50mM Mg. Representative curves out of three independent experiments are given. (b) La content in WT and mutant cells after exposure to the EC_{10} of La for one hour (50 µM). (c) Yb content in WT and mutant cells after exposure to the EC_{10} of Yb for one hour (6 µM). Statistically significant differences from the WT are indicated by asterisks (n = 3, t-test, *<0.05, **<0.01). (d) Drop-test of 10-fold serial dilutions of wild type (WT), Mg membrane transporter mutants for their sensitivity or resistance towards a range of REEs. (e) Overexpression of membrane transporters confers sensitivity to La and Yb. WT yeast cells were transformed with the empty pYES2 plasmid or with the same plasmid harboring *ALR1*. Cells were grown on YPG in the presence of La (3.8 mM), Yb (3.2 mM) or in the absence of REE (control). Representative pictures of three independent experiments are given. Pictures were taken after six days of growth.

proteins increased strain sensitivity to a range of divalent cation including La[66]. Despite not being differentially expressed in our analyses, we further explored the role of these transporters in REE absorption. To start with, the growth defect of WT cells exposed to both La and Yb was restored with the addition of Mg in the medium (Figure 8a). We hypothesized that it could either be due to a competition between Mg and REEs for cell wall binding or for Mg transporters, thus decreasing their toxicity. We therefore looked at the phenotype of *ALR2* and *ALR1-ALR2* mutants towards REEs. ALR2 mutant was slightly more resistant than the wild type on REEs ranging from La to Er (Figure 8d), in line with the sensitive phenotype of cells overexpressing Alr1p towards La (Figure 8e). Surprisingly, overexpression of Alr1p also led to Yb sensitivity, suggesting a role of this transporter not only in LREE transport but also in HREE transport. The double mutant *ALR1-ALR2* showed growth defect, as shown in Figure 8d under any condition, probably due to the lack of extra Mg amendment. However, we measured REE accumulation in the double mutant after a short exposure time of one hour. The double mutant *ALR1-ALR2* accumulated twice as less Yb and La, compared to the WT (Figure 8b,c). This result supports a possible involvement of these two transporters in the uptake of REEs. The broad range of substrate of Alr1p and Alr2p and the phenotypic evidence shown here both support its possible implication in REE uptake[66].

In the transcriptomic analysis we observed that REE induced the upregulation of *SMF1*, which encodes a plasma membrane transporter of divalent cations such as Mn (Figure 6c). This observation was concordant with the higher concentration of Mn in WT cells after treatment with La and Yb (Figure 1e). However, we did not observe any effect of Mn amendment on WT resistance to La and Yb (Figure 9a). We then looked at the effect of knocking

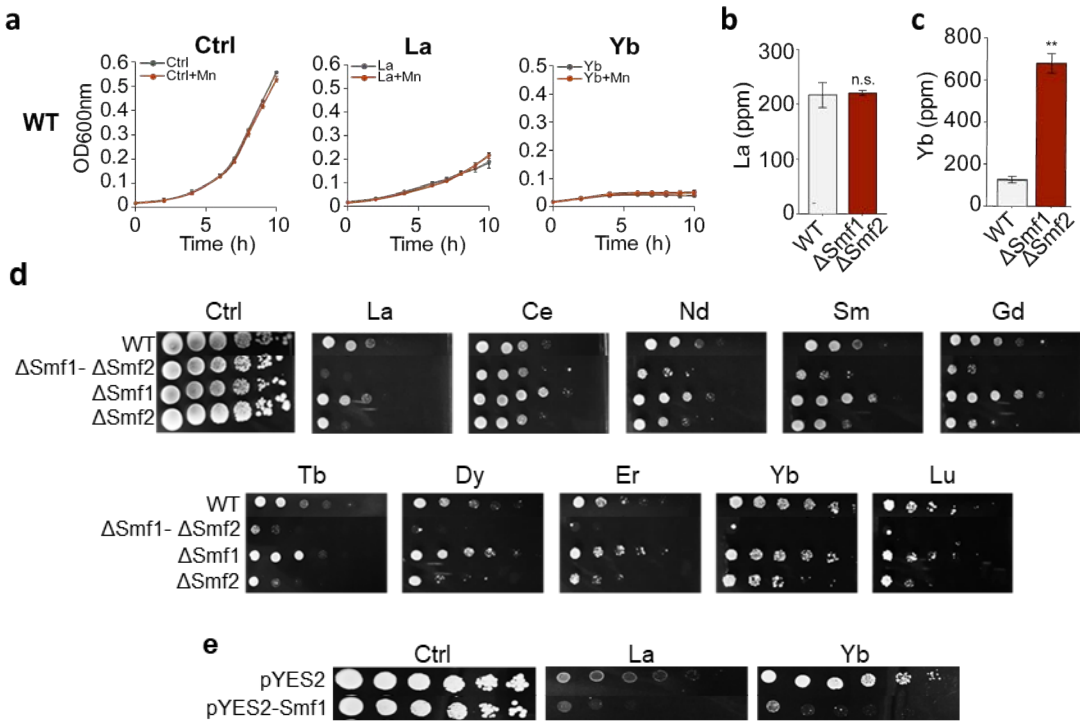

Figure 9. Manganese membrane transporters account for REE sensitivity or resistance. (a) Growth monitoring of WT cells exposed to either La, Yb or no REE (Ctrl) with the addition of 500 µM Mn. Representative curves out of three independent experiments are given. (b) La content in WT and mutant cells after exposure to the EC_{10} of La for one hour (50 µM). (c) Yb content in WT and mutant cells after exposure to the EC_{10} of Yb for one hour (6 µM). Statistically significant differences from the WT are indicated by asterisks (n = 3, t-test, **<0.01, n.s. non significant). (d) Drop-test of 10-fold serial dilutions of wild type (WT), Mn membrane transporter mutants for their sensitivity or resistance towards a range of REEs. (e) Overexpression of membrane transporters confers sensitivity to La and Yb. WT yeast cells were transformed with the empty pYES2 plasmid or with the same plasmid harboring genes encoding for membrane ion transporters. Cells were grown on YPG in the presence of La (3.8 mM), Yb (3.2 mM) or in the absence of REE (control). Representative pictures of three independent experiments are given. Pictures were taken after six days of growth.

out *SMF1* but also *SMF2* a Mn transporter localized in vesicles, on the phenotype under REE exposure (Figure 9d). The lack of *SMF1* only was slightly beneficial to yeast cells, except to La (Figure 9d), while its overexpression led to a sensitive phenotype to both La and Yb (Figure 9e). However, the lack of *SMF2*, rendered cells slightly sensitive to HREEs from Gd to Lu (Figure 9d) and the disruption of both *SMF1* and *SMF2*, however, lead to a sensitivity towards all REEs except Ce (Figure 9d), suggesting a role of this transporters in REE resistance. It was interesting to notice the higher accumulation of Yb (600 ppm against 120 ppm for the WT) in the double mutant *SMF1-SMF2*, concordant with the high sensitivity of this mutant (Figure 9c). However, it was surprising that despite its sensitive phenotype to La, the double mutant *SMF1-SMF2* did not accumulate more La (mutant and WT accumulating up to 200 ppm) (Figure 9b). No straightforward explanation was found. Yet, this could suggest the involvement of other transporter of HREEs that would be more expressed in the *SMF1-SMF2* mutant, ultimately allowing more Yb to be taken up. Further transcriptomic and proteomic analyses in this double mutant could help deciphering the mechanism set up under REE exposure.

Iron transporters as a HREE uptake pathway.

We observed in the different omic approaches the downregulation of other transporters under La and Yb stress (Figure 6c). Notably, the downregulation of the high affinity Fe uptake system *FET3-FTR1* could potentially reflect a way to prevent REE entry in the cell, thus indicating its involvement in the direct uptake of REEs. The addition of Fe in the growth medium reduced the toxicity of Yb in WT cell specifically, reflecting a competition between Fe and REE for their absorption which could suggest a role of Fe transporters in Yb uptake (Figure 10i).

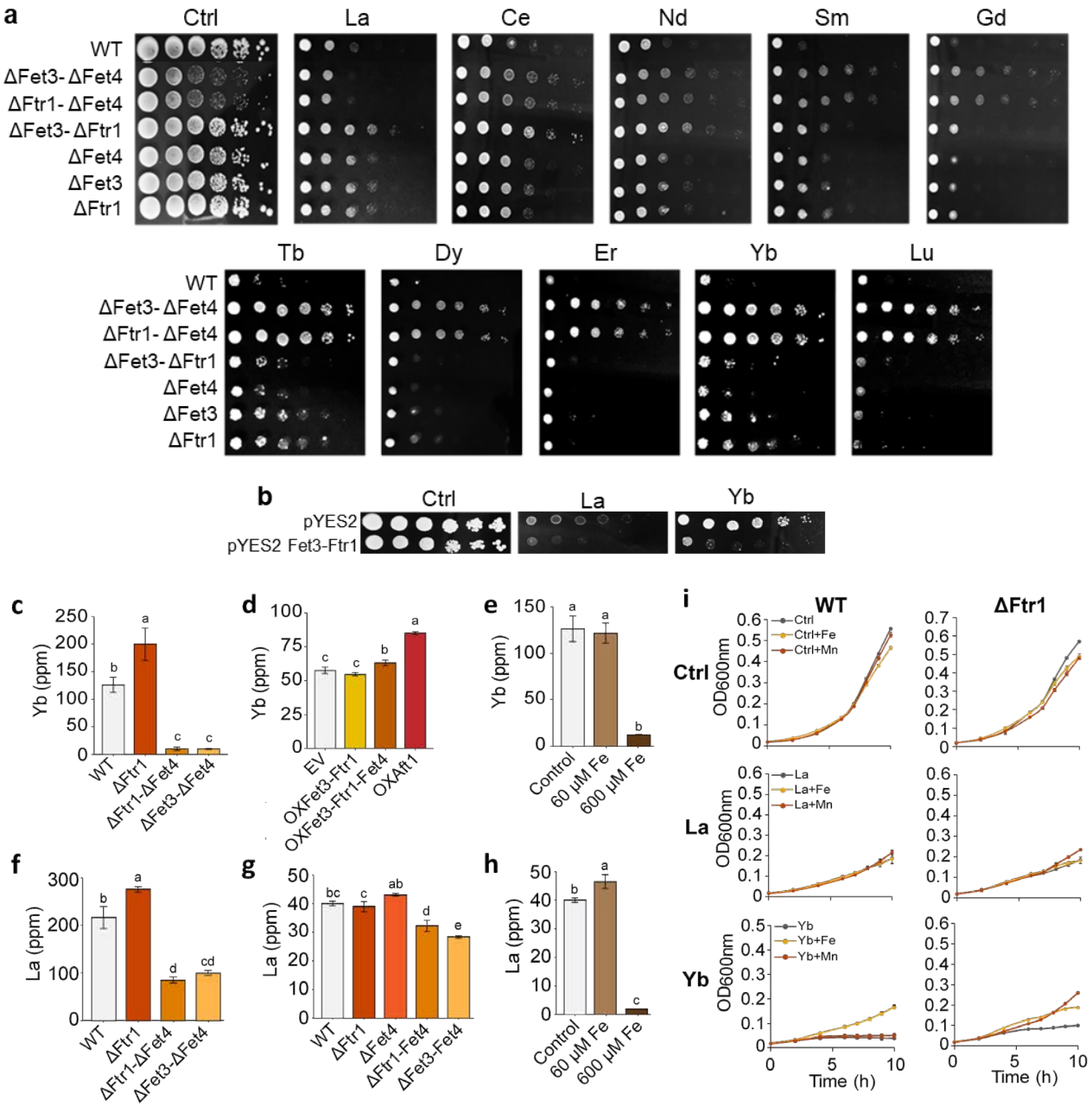

Figure 10. Iron membrane transporters involvement in HREE accumulation. (a) Drop-test of 10-fold serial dilutions of wild type (WT), and membrane transporter mutants for their sensitivity or resistance towards a range of REEs. (b) Overexpression of Fet3-Ftr1 confers sensitivity to La and Yb. WT yeast cells were transformed with the empty pYES2 plasmid or with the same plasmid harboring genes encoding for membrane ion transporters. Cells were grown on YPG in the presence of La (3.8 mM), Yb (3.2 mM) or in the absence of REE (control). Representative pictures of three independent experiments are given. Pictures were taken after six days of growth. (c-e) Yb content in WT, (c) mutants, (d) overexpressing (OX) cells, or (e) WT cells exposed to Yb with 10, and 100 more Fe added as a competitor. (f-g) La content in WT and mutants cells for Fe transporters after exposure to (f) 50 µM of La for one hour or (g,h) to 6 µM (= EC_{10} of Yb) with (h) 10, and 100 more Fe added as a competitor. Different letters account for statistically significant differences (ANOVA, Tukey HSD, P-value <0.05). (i) Growth monitoring of WT and ΔFtr1 cells exposed to either no REE (Ctrl), La, or Yb, with the addition of 200 µM Fe, 500 µM Mn, or not. Representative curves out of three independent experiments are given.

In order to confirm whether these transporters could be responsible for REE uptake through the plasma membrane, we used single and double mutants for genes involved in the Fe uptake system. Neither the lack of Ftr1p, Fet3p or the low Fe affinity transporter Fet4p separately appeared to have effect on yeast cells resistance to REEs compared to WT (Figure 10a). Interestingly, when disrupting both the high-affinity Fe transporter *FET3-FTR1* and the low-affinity Fe transporter *FET4*, a highly resistant phenotype was observed towards many REEs tested, forming a resistance gradient, ranging from no resistance (La) to high resistance (Lu) (Figure 10a). Indeed, when exposed to REEs from Tb to Lu, the double mutants *FTR1-FET4* and *FET3-FET4* were highly resistant. Exposure to lighter REEs, from Gd to Nd, decreased the resistance of the mutants, to no growth difference under La condition (Figure 10a). To comfort the observations obtained with the mutants, we overexpressed the high affinity Fe transporters *FET3-FTR1*. The overexpression of these genes rendered yeast cells more sensitive to Yb but also to La (Figure 10b). Altogether, these results support the importance of these Fe transporters in the accumulation of REEs.

To address whether the deletion of Fe transporters would reduce the uptake of REEs, as suggested by the phenotypic results obtained, we first measured the total REE concentration in yeast cells after 1h of exposure at the respective EC_{10} of La and Yb. It was first surprising to see the higher amount of Yb that was accumulated in the *FTR1* mutant (Figure 10c). However, deletion of the high-affinity Fe transporter could increase the production of the broad spectra Fe transporter Fet4p, as shown by Li and Kaplant (1998)[67]. This could be an explanation regarding the higher Yb content of the FTR1 mutant. Regarding the double mutants *FTR1-FET4* and *FET3-FET4*, and in agreement with their high resistance to Yb, these two mutants accumulated twelve times less Yb compared to the WT, further supporting the hypothesis of Yb entry through these transporters (Figure 10c). However, it was rather unexpected that more than twice as less La was also absorbed by the same double mutants (Figure 10f). In this experiment, we used an exposure concentration corresponding to the EC_{10} of each REE, representing eight times more La than Yb. Thus, we also measured the La accumulation using the same concentration as for Yb (6 µM). In this case, for the FTR1 mutant, La was accumulated as in the WT (Figure 10g). A reduced accumulation of La was observed in the double mutants but to a much lesser extent than for Yb. Around 25% less La was accumulated in the double mutants, against 50% at the previous concentration (Figure 10f,g). Despite the relatively low concentration used, the lower accumulation observed of La suggests that La could also be transported by these Fe transporters. The addition of ten times more Fe than REEs, did not decreased their absorption, which could suggest a higher affinity of these transporters for REEs or the involvement of other transporters (Figure 10e,h). However, the accumulation of both La and Yb was reduced by almost 90 % when

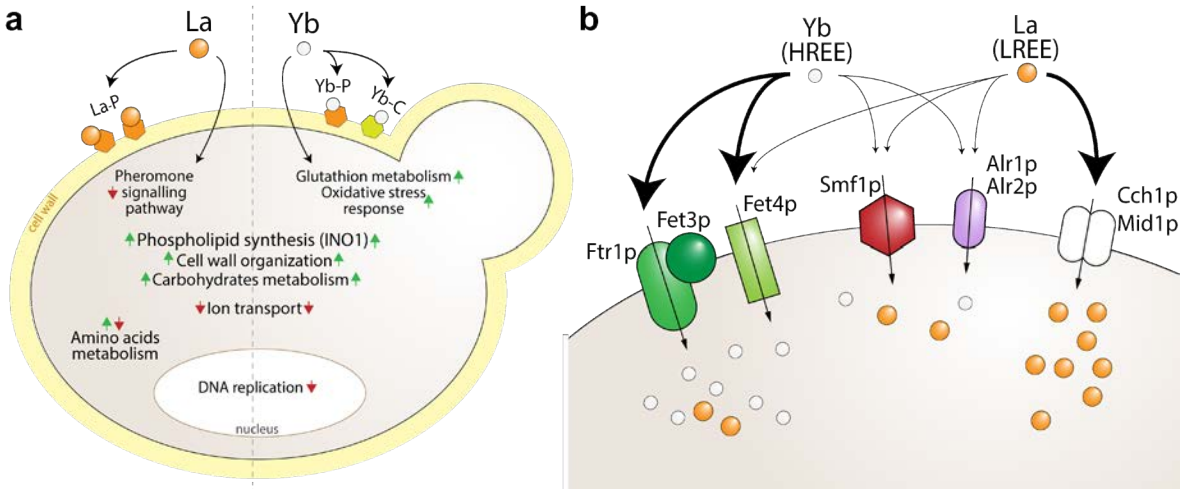

Figure 11. Schematic model of detoxification responses under acute REE stress. (a) Global response of yeast cells under REE stress. Upregulated functions are depicted with a green arrow, while downregulated functions are shown with a red arrow. La-P and Yb-P correspond to phosphate bound REE, while Yb-C corresponds to carboxylate bound REE. (b) REE import through ion transmembrane transporters. As hypothesized here, HREEs would be taken up preferentially through the Fe transporters Ftr1-Fet3 and Fet4, while LREEs through the Ca channel Cch1-Mid1. All REEs could also be taken up, in a lesser extend through the Mn and Fe transporter Smf1, but also through the Alr1-Alr2 Mg transporters.

hundred times more Fe were added during the exposure (Figure 10e,h). These lower uptakes of REEs can be either the result of Fe competing with REEs, or that in such replete conditions, Fe transporters are downregulated, again supporting the hypothesis of REE uptake through Fe transporters.

In *FTR1* mutant, the addition of either Fe or Mn did not increased the growth of the mutant under La exposure (Figure 10i). It was however interesting to notice the better growth of the mutant under Yb exposure when Fe or Mn were added (Figure 10i). The Mn transporter Smf1p is known to be non-specific Fe transporter[68]. Thus, we can hypothesise that the deletion *FTR1* together with the addition of Mn and Fe would likely prevent import of Yb, reducing the toxicity by saturating Smf1p and the low affinity transporter Fet4p. Considering this, it is plausible to say that HREEs can be taken up through Fe pathways among which Ftr1-Fet3, Fet4p, and Smf1p.

Conclusions

In conclusion, we report in this study the first cellular and molecular insights about REE toxicity response in the eukaryotic model *Saccharomyces cerevisiae*. The use of complementary methods at different level of regulation (mRNA and proteins) was of high importance. The results exposed here provide valuable knowledge to understand potential issues of these emerging metallic contaminants. Some responses were well known as being found for other toxic elements like Cd for example. Among them, we can mention proteolysis, ribosome biogenesis regulation, and oxidative stress which were specific to Yb in comparison to La. However, some other pathways and compartments appeared to be of high importance for REE toxicity modulation. Unlike for other metal toxicity, we reported here the cell wall, and the pheromone signalling pathways as being essential for yeast cells to cope with REEs (Figure 11a). Furthermore, a few differences were observed between La (LREE) and Yb (HREE), supporting the heterogeneity between the groups of the REEs. We also investigated the way of entry of REEs through the plasma membrane, and demonstrated for the first time their uptake through various transporters (Figure 11b). Fe transporters, of high or low affinity, appear to take part into the unspecific uptake of HREEs, and to a lesser extend LREEs. It was interesting to notice the cross gradient between LREEs and HREEs for their import through the different transporters. LREEs, represented by La, could be mainly taken up through the Ca channel Cch1-Mid1, explained by the high similarity with Ca ionic radius. Conversely, HREEs, represented by Yb, could be mainly taken up through different Fe transporters known as Fet3-Ftr1, Fet4p and Smf1p. Lastly, the low specificity of ALR transporters make them also good candidates for the REE uptake. The possibility of REE unspecific uptake through different transporters is not surprising considering than other toxic metals, such as Cd, can also be taken up through Zrt1p, Smf1p, Fet4p and Mid1p[25]. Altogether, these findings are valuable information in order to better assess the impact and behaviour of the REEs towards living organisms, at the cellular and molecular level.

References

1. Cotton, S. *Lanthanide and actinide chemistry*. *Lanthanide and Actinide Chemistry* (2006).
2. Ciacci, L., Reck, B. K., Nassar, N. T., & Graedel, T. E. Lost by design. *Environ. Sci. Technol.* **49**, 9443–9451 (2015).
3. Hu, Z., Richter, H., Sparovek, G., & Schnug, E. Physiological and biochemical effects of rare earth elements on plants and their agricultural significance: A review. *J. Plant Nutr.* **27**, 183–220 (2004).
4. He, M. L. & Rambeck, W. A. Rare earth elements - A new generation of growth promoters for pigs? *Arch. Anim. Nutr.* **53**, 323–334 (2000).
5. He, M. L., Ranz, D., & Rambeck, W. A. Study on the performance enhancing effect of rare earth elements in growing and fattening pigs. *J. Anim. Physiol. Anim. Nutr. (Berl).* **85**, 263–270 (2001).
6. Panichev, A. M. Rare earth elements: review of medical and biological properties and their abundance in the rock materials and mineralized spring waters in the context of animal and human geophagia reasons evaluation. *Achiev. Life Sci.* **9**, 95–103 (2015).
7. Binnemans, K., Jones, P. T., Blanpain, B., Van Gerven, T., Yang, Y., Walton, A., & Buchert, M. Recycling of rare earths: A critical review. *J. Clean. Prod.* **51**, 1–22 (2013).
8. Setua, S., Menon, D., Asok, A., Nair, S., & Koyakutty, M. Folate receptor targeted, rare-earth oxide nanocrystals for bi-modal fluorescence and magnetic imaging of cancer cells. *Biomaterials* **31**, 714–729 (2010).
9. Leeuw, D. & Academic, K. Inorganic yellow-red pigments without toxic metals. *Nature* **404**, 980–982 (2000).
10. Rim, K. T., Koo, K. H., & Park, J. S. Toxicological evaluations of rare earths and their health impacts to workers: a literature review. *Saf. Health Work* **4**, 12–26 (2013).
11. Pagano, G., Guida, M., Tommasi, F., & Oral, R. Health effects and toxicity mechanisms of rare earth elements - Knowledge gaps and research prospects. *Ecotoxicol. Environ. Saf.* **115**, 40–48 (2015).
12. Gonzalez, V., Vignati, D. A. L., Leyval, C., & Giamberini, L. Environmental fate and ecotoxicity of lanthanides: Are they a uniform group beyond chemistry? *Environ. Int.* **71**, 148–157 (2014).
13. Wakabayashi, T., Ymamoto, A., Kazaana, A., Nakano, Y., Nojiri, Y., & Kashiwazaki, M. Antibacterial, antifungal and nematicidal activities of rare earth ions. *Biol. Trace Elem. Res.* **174**, 464–470 (2016).
14. Pagano, G. *et al.* Comparative toxicities of selected rare earth elements: Sea urchin embryogenesis and fertilization damage with redox and cytogenetic effects. *Environ. Res.* **147**, 453–460 (2016).
15. Trifuoggi, M. *et al.* Comparative toxicity of seven rare earth elements in sea urchin early life stages. *Environ. Sci. Pollut. Res.* **24**, 20803–20810 (2017).
16. Wei, B., Li, Y., Li, H., Yu, J., Ye, B., & Liang, T. Rare earth elements in human hair from a mining area of China. *Ecotoxicol. Environ. Saf.* **96**, 118–123 (2013).
17. Liang, C. & Wang, W. Antioxidant response of soybean seedlings

to joint stress of lanthanum and acid rain. *Environ. Sci. Pollut. Res.* **20**, 8182–8191 (2013).

18. Gao, J. *et al.* Determining the cytotoxicity of rare earth element nanoparticles in macrophages and the involvement of membrane damage. *Environ. Sci. Technol.* **51**, 13938–13948 (2017).
19. Weiwei, H., Shihua, S., & Peidong, T. Analysis of inhibitory effect of gadolinium on *Sinorhizobium fredii*. *J. Rare Earths* **25**, 106–110 (2007).
20. Yufeng, Z., Lifen, Y., Kaoshan, C., & Liang, D. Effects of neodymium on growth, pectinase activity and mycelium permeability of *Fusarium oxysporum*. *J. Rare Earths* **25**, 100–105 (2007).
21. Fitriyanto, N. A., Nakamura, M., Muto, S., Kato, K., Yabe, T., Iwama, T., Kawai, K., & Pertiwiningrum, A. Ce^{3+}-induced exopolysaccharide production by *Bradyrhizobium* sp. MAFF211645. *J. Biosci. Bioeng.* **111**, 146–152 (2011).
22. Wang, L., He, J., Xia, A., Cheng, M., Yang, Q., Du, C., Wei, H., Huang, X., & Zhou, Q. Toxic effects of environmental rare earth elements on delayed outward potassium channels and their mechanisms from a microscopic perspective. *Chemosphere* **181**, 690–698 (2017).
23. Ene, C. D., Ruta, L. L., Nicolau, I., Popa, C. V., Iordache, V., Neagoe, A. D., & Farcasanu, I. C. Interaction between lanthanide ions and *Saccharomyces cerevisiae* cells. *JBIC J. Biol. Inorg. Chem.* **20**, 1097–1107 (2015).
24. Taymaz-Nikerel, H., Cankorur-Cetinkaya, A., & Kirdar, B. Genome-wide transcriptional response of *Saccharomyces cerevisiae* to stress-induced perturbations. *Front. Bioeng. Biotechnol.* **4**, (2016).
25. Wysocki, R. & Tamás, M. J. How *Saccharomyces cerevisiae* copes with toxic metals and metalloids. *FEMS Microbiol. Rev.* **34**, 925–951 (2010).
26. Jin, Y. H., Dunlap, P. E., McBride, S. J., Al-Refai, H., Bushel, P. R., & Freedman, J. H. Global transcriptome and deletome profiles of yeast exposed to transition metals. *PLoS Genet.* **4**, (2008).
27. Hosiner, D., Gerber, S., Lichtenberg-Fraté, H., Glaser, W., Schüller, C., & Klipp, E. Impact of acute metal stress in *Saccharomyces cerevisiae*. *PLoS One* **9**, 1–14 (2014).
28. Botstein, D., Chervitz, S. A., & Cherry, J. M. Yeast as a model organism. *Science (80-.).* **277**, 1259–1260 (1997).
29. Kachroo, A. H., Laurent, J. M., Yellman, C. M., Meyer, A. G., Wilke, C. O., & Marcotte, E. M. Systematic humanization of yeast genes reveals conserved functions and genetic modularity. *Science (80-.).* **348**, 921–925 (2017).
30. Gietz, R. D. & Schiestl, R. H. High-efficiency yeast transformation using the LiAc / SS carrier DNA / PEG method. *Nat. Protoc.* **2**, 31–35 (2008).
31. Güldener, U., Heck, S., Fiedler, T., Beinhauer, J., & Hegemann, J. H. A new efficient gene disruption cassette for repeated use in budding yeast. *Nucleic Acids Res.* **24**, 2519–2524 (1996).
32. Hartmann, E. M., Allain, F., Gaillard, J., Pible, O., & Armengaud, J. Taking the shortcut for high-throughput shotgun proteomic analysis of bacteria. in *Methods in Molecular Biology (Methods and Protocols)* (eds. Vergunst, A. & O'Callaghan, D.) **1197**, 275–285 (Humana Press, 2014).
33. Klein, G. *et al.* RNA-binding proteins are a major target of silica nanoparticles in cell extracts. *Nanotoxicology* **10**, 1555–1564 (2016).
34. Dupierris, V., Masselon, C., Court, M., Kieffer-Jaquinod, S., & Bruley, C. A toolbox for validation of mass spectrometry peptides identification and generation of database: IRMa. *Bioinformatics* **25**, 1980–1981 (2009).
35. Carvalho, P. C., Yates, J. R., & Barbosa, V. C. Improving the TFold test for differential shotgun proteomics. *Bioinformatics* **28**, 1652–1654 (2012).
36. Huang, D. W., Sherman, B. T., & Lempicki, R. A. Systematic and integrative analysis of large gene lists using DAVID bioinformatics resources. *Nat. Protoc.* **4**, (2009).
37. Huang, D. W., Sherman, B. T., & Lempicki, R. A. Bioinformatics enrichment tools : paths toward the comprehensive functional analysis of large gene lists. *Nucleic Acids Res.* **37**, 1–13 (2009).
38. Jin, Y. H., Dunlap, P. E., McBride, S. J., Al-Refai, H., Bushel, P. R., & Freedman, J. H. Global transcriptome and deletome profiles of yeast exposed to transition metals. *PLoS Genet.* **4**, (2008).
39. Guerra-Moreno, A., Isasa, M., Bhanu, M. K., Waterman, D. P., Eapen, V. V., Gygi, S. P., & Hanna, J. Proteomic analysis identifies ribosome reduction as an effective proteotoxic stress response. *J. Biol. Chem.* **290**, 29695–29706 (2015).
40. Pimentel, C., Vicente, C., Menezes, R. A., Caetano, S., Carreto, L., & Rodrigues-Pousada, C. The role of the Yap5 transcription factor in remodeling gene expression in response to Fe bioavailability. *PLoS One* **7**, 1–11 (2012).
41. White, T. J., Bruns, T., Lee, S., & Taylor, J. Amplification and direct sequencing of fungal ribosomal RNa genes for phylogenetics. in *PCR-Protocol and Applications - a Laboratory Manual* (eds. Innis, M., Gelfand, D., Sninsky, J. & White, T.) 315–322 (1990).
42. Inoue, S. B., Takewaki, N., Takasuka, T., Mio, T., Adachi, M., Fujii, Y., & Miyamoto, C. Characterization and gene cloning of 1,3-b-D-glucan synthase from *Saccharomyces cerevisiae*. *Eur. J. Biochem.* **231**, 845–854 (1995).
43. Levin, D. E. Cell Wall Integrity Signaling in *Saccharomyces cerevisiae* Cell. *Microbiol Mol Biol Rev* **69**, 262–291 (2005).
44. Lesage, G. & Bussey, H. Cell wall assembly in *Saccharomyces cerevisiae*. *Microbiol. Mol. Biol. Rev.* **70**, 317–343 (2006).
45. Jiang, M., Ohnuki, T., Kozai, N., Tanaka, K., Suzuki, Y., Sakamoto, F., Kamiishi, E., & Utsunomiya, S. Biological nano-mineralization of Ce phosphate by *Saccharomyces cerevisiae*. *Chem. Geol.* **277**, 61–69 (2010).
46. Jiang, M. Y., Ohnuki, T., Tanaka, K., Kozai, N., Kamiishi, E., & Utsunomiya, S. Post-adsorption process of Yb phosphate nano-particle: Formation by *Saccharomyces cerevisiae*. *Geochim. Cosmochim. Acta* **93**, 30–46 (2012).
47. Takahashi, Y., Yamamoto, M., Yamamoto, Y., & Tanaka, K. EXAFS study on the cause of enrichment of heavy REEs on bacterial cell surfaces. *Geochim. Cosmochim. Acta* **74**, 5443–5462 (2010).
48. Rogowska, A., Pomastowski, P., Złoch, M., Railean-Plugaru, V., Król, A., Rafińska, K., Szultka-Młyńska, M., & Buszewski, B. The influence of different pH on the electrophoretic behaviour of *Saccharomyces cerevisiae* modified by calcium ions. *Sci. Rep.* **8**, 2–11 (2018).
49. Mackay, V. L., Welch, S. K., Insley, M. Y., Manneyt, T. R., Holly, J., Saari, G. C., & Parker, M. L. The *Saccharomyces cerevisiae* BAR1 gene encodes an exported protein with homology to pepsin. *Proc. Nati. Acad. Sci. USA* **85**, 55–59 (1988).
50. Fricker, S. P. The therapeutic application of lanthanides. *Chem. Soc. Rev.* **35**, 524–533 (2006).
51. Cunningham, K. W. Acidic calcium stores of *Saccharomyces cerevisiae*. *Cell Calcium* **50**, 129–138 (2011).
52. Carbó, N., Tarkowski, N., Ipiña, E. P., Dawson, S. P., & Aguilar, P. S. Sexual pheromone modulates the frequency of cytosolic Ca^{2+}

bursts in *Saccharomyces cerevisiae*. *Mol. Biol. Cell* **28**, 1–26 (2016).

53. Muller, E. M., Mackin, N. A., Erdman, S. E., & Cunningham, K. W. Fig1p facilitates Ca^{2+} influx and cell fusion during mating of *Saccharomyces cerevisiae*. *J. Biol. Chem.* **278**, 38461–38469 (2003).
54. Chen, R. E. & Thorner, J. Function and regulation in MAPK signaling pathways: Lessons learned from the yeast *Saccharomyces cerevisiae*. *Biochim. Biophys. Acta - Mol. Cell Res.* **1773**, 1311–1340 (2007).
55. Agorio, A. *et al*. Phosphatidylinositol 3-phosphate-binding protein AtPH1 controls the localization of the metal transporter NRAMP1 in *Arabidopsis*. *Proc. Natl. Acad. Sci. U. S. A.* **114**, E3354–E3363 (2017).
56. Oh, B. C., Kim, M. H., Yun, B. S., Choi, W. C., Park, S. C., Bae, S. C., & Oh, T. K. Ca^{2+}-inositol phosphate chelation mediates the substrate specificity of β-propeller phytase. *Biochemistry* **45**, 9531–9539 (2006).
57. Balaban, N. P., Suleimanova, A. D., Valeeva, L. R., Chastukhina, I. B., & Sharipova, M. R. Inositol phosphates and their biological effects. *Biomed. Pharmacol. J.* **7**, 433–437 (2014).
58. Serero, A., Lopes, J., Nicolas, A., & Boiteux, S. Yeast genes involved in cadmium tolerance : Identification of DNA replication as a target of cadmium toxicity. *DNA Repair (Amst).* **7**, 1262–1275 (2008).
59. Deponte, M. The incomplete glutathione puzzle : Just guessing at numbers and figures ? *Antioxid. Redox Signal.* **27**, 1130–1161 (2017).
60. Morano, K. A., Grant, C. M., & Moye-Rowley, W. S. The response to heat shock and oxidative stress in *Saccharomyces cerevisiae*. *Genetics* **190**, 1157–1195 (2012).
61. Daniela, P., Adamis, B., Mannarino, S. C., Cristina, E., & Eleutherio, A. Glutathione and gamma-glutamyl transferases are involved in the formation of cadmium – glutathione complex. *FEBS Lett.* **583**, 1489–1492 (2009).
62. Cordente, A. G., Capone, D. L., & Curtin, C. D. Unravelling glutathione conjugate catabolism in *Saccharomyces cerevisiae*: the role of glutathione / dipeptide transporters and vacuolar function in the release of volatile sulfur compounds 3-mercaptohexan-1-ol and 4-mercapto-4-methylpentan-2-one. *Appl. Microbiol. Biotechnol.* (2015).
63. Stearman, R., Yuan, D. S., Yamaguchi-Iwai, Y., Klausner, R. D., & Dancis, A. A permease-oxidase complex involved in high-affinity iron uptake in yeast. *Science (80-.).* **271**, 1552–1557 (1996).
64. Friedman, H., Meir, S., Rosenberger, I., Halevy, A. H., Kaufman, P. B., & Philosoph-Hadas, S. Inhibition of the gravitropic response of snapdragon spikes by the calcium-channel blocker lanthanum chloride. *Plant Physiol.* **118**, 483–492 (2002).
65. Knight, H., Trewavas, A. J., & Knight, M. R. Calcium signalling in *Arabidopsis thaliana* responding to drought and salinity. *Plant J.* **12**, 1067–1078 (1997).
66. MacDiarmid, C. W. & Gardner, R. C. Overexpression of the Saccharomyces cerevisiae magnesium transport system confers resistance to aluminum ion. *J. Biol. Chem.* **273**, 1727–1732 (1998).
67. Li, L. & Kaplant, J. Defects in the yeast high affinity iron transport system result in increased metal sensitivity because of the increased expression of transporters with a broad transition metal specificity. *J. Biol. Chem.* **273**, 22181–22187 (1998).
68. Chen, X. Z., Peng, J. Bin, Cohen, A., Nelson, H., Nelson, N., & Hediger, M. A. Yeast SMF1 mediates H^+-coupled iron uptake with concomitant uncoupled cation currents. *J. Biol. Chem.* **274**, 35089–35094 (1999).

ADDITIONAL FILES

https://bul.univ-lorraine.fr/index.php/s/bw9Z1eICcwtb2w5

Table S1: Yeast strains used in this study

Table S2: Oligonucleotids used in this study. The primers used named Delta consisted of 40 bp of genomic sequence that flanked either the 5' or 3' end of the ORF to be knocked out (directly proximal and distal from the start and stop codons, respectively), and 20 bp homologous to the hphMX cassette of the pAG32 plasmid. The primers Sc were used to amplify the full ORF to be knocked out (start to stop codons).

Table S3: Summarized RNAseq results of yeast cells were exposed to REE for 1 h. Each condition has been compared to the non REE exposed control condition. The left table gathers differentially expressed genes with a padj < 0.01 while the right table includes the fold change values regardless the padj value.

Table S4: Summarized Proteomic results of yeast cells were exposed to REE at their respective EC50 for 1 h or 4 h as mentioned. The left table gathers differentially expressed genes with a padj < 0.05 while the right table includes the fold change values regardless the padj value.

Table S5: Summarized RNAseq and Proteomic results. Each condition has been compared to the non REE exposed control condition. Yeast cells were exposed to the REE at their respective EC50 for 1h or 4h as indicated. The left table gathers differentially expressed genes with a padj < 0.05 (PRO) and < 0.01 (RNA) while the right table includes the fold change values regardless the padj value.

Table S6: GO-Terms significantly represented in the set of DE Proteins under La vs Ctrl exposure after 1 h. Tables are separated in biological process (BP), cellular component (CC) and molecular function (MF). The

significantly represented GO terms were identified in the downregulated DE proteins (blue), upregulated (orange) or all DE proteins (grey).

Table S7: GO-Terms significantly represented in the set of DE Proteins under Yb vs Ctrl exposure after 1 h. Tables are separated in biological process (BP), cellular component (CC) and molecular function (MF). The significantly represented GO terms were identified in the downregulated DE proteins (blue), upregulated (orange) or all DE proteins (grey).

TableS8: GO-Terms significantly represented in the set of DE Proteins under Yb vs La exposure after 1 h. Tables are separated in biological process (BP), cellular component (CC) and molecular function (MF). The significantly represented GO terms were identified in the downregulated DE proteins (blue), upregulated (orange) or all DE proteins (grey).

Table S9: GO-Terms significantly represented in the set of DE Proteins under La vs Ctrl exposure after 4 h. Tables are separated in biological process (BP), cellular component (CC) and molecular function (MF). The significantly represented GO terms were identified in the downregulated DE proteins (blue), upregulated (orange) or all DE proteins (grey).

Table S10: GO-Terms significantly represented in the set of DE Proteins under Yb vs Ctrl exposure after 4 h. Tables are separated in biological process (BP), cellular component (CC) and molecular function (MF). The significantly represented GO terms were identified in the downregulated DE proteins (blue), upregulated (orange) or all DE proteins (grey).

Table S11: GO-Terms significantly represented in the set of DE Proteins under Yb vs La exposure after 4 h. Tables are separated in biological process (BP), cellular component (CC) and molecular function (MF). The significantly represented GO terms were identified in the downregulated DE proteins (blue), upregulated (orange) or all DE proteins (grey).

Table S12: GO-Terms significantly represented in the set of DE genes under La vs Ctrl exposure after 1 h. Tables are separated in biological process (BP), cellular component (CC) and molecular function (MF). The significantly represented GO terms were identified in the downregulated DE genes (blue), upregulated (orange) or all DE genes (grey).

Table S13: GO-Terms significantly represented in the set of DE genes under Yb vs Ctrl exposure after 1 h. Tables are separated in biological process (BP), cellular component (CC) and molecular function (MF). The significantly represented GO terms were identified in the downregulated DE genes (blue), upregulated (orange) or all DE genes (grey).

Table S14: GO-Terms significantly represented in the set of DE genes under La vs Yb exposure after 1 h. Tables are separated in biological process (BP), cellular component (CC) and molecular function (MF). The significantly represented GO terms were identified in the downregulated DE genes (blue), upregulated (orange) or all DE genes (grey).

Part II:

Investigation of REE toxicity, resistance and transfer mechanisms in plants

Introduction

By employing the extensively used eukaryotic model *S. cerevisiae* in the first part of this study, we demonstrated that discrepancies existed between the LREEs and HREEs. Those results further supported the necessity to not consider REEs as a single and homogenous group of elements.

In this second part, we studied REE toxicity, transfer and detoxification mechanisms in plants as more complex eukaryotes and because they represent a significant mode of entry of REEs to the biota in contaminated areas or in an agricultural context. As previously mentioned, the increased demand, production, mining, and the low recyclability, together with their use as fertilizer or phosphate fertilizers has led to an increase contamination of ecosystems with REEs. Especially noteworthy are the high concentrations of REEs measured in Chinese mining areas, which can reach up to more than 2,000 mg/kg. Those concentrations are greater than ten-times higher than the average concentration naturally found in some regions (Zhenggui *et al.*, 2001; Liang *et al.*, 2014; Liu *et al.*, 2018; Yuan *et al.*, 2018). Previous studies of REE transfer to plants have provided clues about REE absorption preferences in plants, their transfer to the above ground parts, possible transport correlation with other nutrients, and even their accumulation potential in a few species. Although beneficial or detrimental effects of REEs have been described for several end-point parameters (e.g. yield, photosynthesis, root-growth disturbance) in crops or model plants, there is still a lack of data on the molecular and cellular toxicity and detoxification mechanisms of REEs in plants. To address this, the second part of this thesis combined two approaches. The first approach is the molecular analyses on the model plant *Arabidopsis thaliana*, to identify the main biological functions responding to REEs. The second approach consists in the screening of REE accumulating plants was used to discover new biological models for unravelling the molecular mechanisms of REE transfer. These different approaches are divided into the following three chapters (Figure 1);

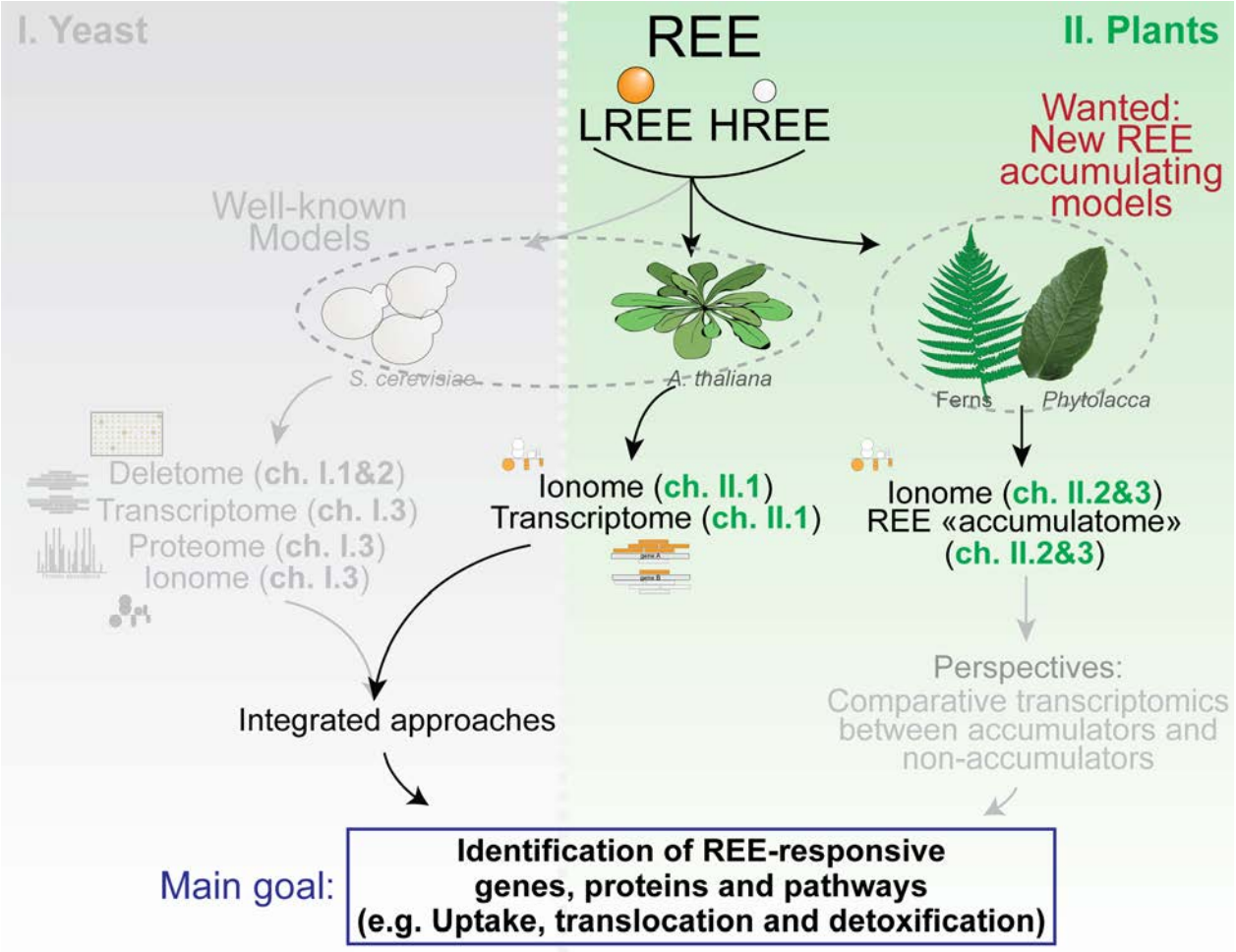

Figure 1: General scheme of the Ph.D. work with the second part focusing on plants. The integrated approaches used to study plant responses to REE stress in order to identify genes, proteins, metabolites and pathways, are listed. The identification of new REE accumulating models is a first essential step for future work of comparative transcriptomics between accumulating and non-accumulating plants, that is not tackled in this Ph.D. work.

Chapter II.1: To obtain a global view of the molecular response to REE exposure in the widely used plant model *Arabidopsis thaliana*, a transcriptomic analysis (RNA-seq) was undertaken. Such an approach has been useful in the understanding of plant responses to trace metal elements (Weber *et al.*, 2006; Kumari *et al.*, 2008; Gomez-Sagasti *et al.*, 2016; Singh *et al.*, 2016; Landa *et al.*, 2017). By analysing the response to La (LREE) and Yb (HREE) in the roots and shoots of Arabidopsis, we unravelled the global toxicity mechanisms involved in the REE stress response in plants. It clearly appeared that these contrasting REEs induced specific responses (e.g. Ca transporter modulation) in the plant but also shared common modes of action, notably responsible for the modification of root architecture, auxin signalling and oxidative stress response.

Additionally, we proposed putative uptake and detoxification mechanisms developed by Arabidopsis to cope with such toxic elements. Importantly, the present study allowed us to highlight a link between REEs and iron homeostasis that has not been previously reported.

Following the analysis of the *Arabidopsis* responses to REE exposure using a transcriptomic approach, we aimed to identify new REE-accumulating plant species. Some plants are indeed known to (hyper)accumulate certain metals in their tissues. They have developed specific accumulation, translocation and resistance mechanisms for these metals. To date, nothing is known regarding the underlying mechanisms of REE accumulating plants. REE accumulating species could be used as new and interesting models for the comprehension of these exacerbated mechanisms. For future work, a comparative transcriptomic analysis of an REE-accumulating species and a non-accumulating close relative would be particularly suitable for this purpose. A similar approach has been carried out for several hyperaccumulating plants compared to non-accumulating plants, such as the comparative transcriptomic analyses of *Arabidopsis halleri* and *Noccaea caerulescens*, two Cd and Zn hyperaccumulators with the related non-accumulator related *Arabidopsis thaliana* (Weber *et al.*, 2004, 2006; Halimaa *et al.*, 2014). Similarly cross-species transcriptomic analysis in different plant families of nickel hyperaccumulators has identified convergent functions that may represent major nodes in the evolution of nickel-hyperaccumulating plants (Garcia de la Torre *et al.*, 2018).

Chapter II.2: To identify underlying mechanisms of REE accumulation, the first step is to identify phylogenetically related plants that displayed contrasting phenotypes regarding REE accumulation. After reviewing the literature, we found that one species of *Phytolacca*, *P. americana*, accumulates REEs (Yuan *et al.*, 2017). Notably, this species was found at an REE mining site in south Jiangxi Province in China, with an average REE concentration of approximately 250 mg/kg in leaves, reaching a maximum of 1,040 mg/kg (Yuan *et al.*, 2018). Additionally, two *Phytolacca* species (*P. americana* and *P. acinosa*) were previously known to hyperaccumulate manganese (Min *et al.*, 2007; Xu *et al.*, 2009). *Phytolacca americana* is one of the few angiosperm species shown to accumulate REEs. The other angiosperm REE accumulating species all belong to the *Carya* genus (Wood and Grauke, 2011; Liu *et al.*, 2017), demonstrating that such trait can be shared among a single genus. However, in the case of *Phytolacca*, none of

the other species have been studied for their REE accumulation abilities. Therefore, we phenotypically investigated whether the REE accumulation trait was conserved in this genus or if discrepancies arose. For this purpose, we hydroponically screened five species of *Phytolacca*, namely *P. americana*, *P. acinosa*, *P. bogotensis*, *P. clavigera*, and *P. icosandra* for their REE accumulation potential and their REE fractionation pattern. In order to analyse the effect of REE exposure on physiological parameters, we carried out additional analyses on the plant growth, root morphology, pigment parameters, and ionome.

In the five species tested, we observed comparable REE accumulation and fractionation patterns (HREEs enrichment in the leaves), which suggest the conservation of this REE accumulation trait. This conserved trait within a plant genus could be highly interesting for phytoremediation purposes. Indeed, different species can become adapted, or may already have specific adaptations to certain growth conditions. Appropriate species should be used depending on the location, climate, and soil characteristics of the contaminated area. However, the conserved REE-accumulation trait shared by all of the tested *Phytolacca* species makes them unsuitable for a strategy of comparative transcriptomics. Indeed, this approach aims to compare two phylogenetically close species that have contrasting phenotypes regarding metal accumulation to identify the underlying specific mechanisms of transfer and tolerance. Since this condition was not found among the different Phytolacca species, we needed to identify new REE-accumulating plant models.

Chapter II.3: In the literature, apart from the very few angiosperms known to accumulate REEs, most of the reported REE accumulating species are found among the tropical ferns (Liu *et al.*, 2017). The highest accumulating species reported are *Dicranopteris dichotoma* (Zhenggui *et al.*, 2001; Shan *et al.*, 2003) and *Pronephrium simplex* (Lai *et al.*, 2005, 2006) with up to 3,300 mg/kg and 1,200 mg/kg dry weight found in their fronds, respectively (Liu *et al.*, 2017). Together with the relatively small number of other ferns reported to accumulate REEs, all of these species were discovered either in China or Japan. Therefore, the identification of other fern species that accumulate REEs is of high interest. Consequently, we undertook the screening of hardy ferns, adapted to various climates and soil conditions, to identify new REE-accumulating fern species. To this end, we screened forty-nine hardy fern species, belonging to fifteen different genera, in soil contaminated with six representative REEs (La, Ce, Sm, Gd, Yb and Y) at equal concentrations.

By doing so, we identified new fern species that can accumulate REEs. When comparing the different species and/or genera, we measured different accumulation patterns. Interestingly, among all fern species, the LREEs and HREEs were not uniformly transferred, with an enrichment of LREEs over HREEs in the fronds. This result suggests the presence of different translocation modes for the two groups of REEs into shoots. We also report here the close relationship between REE accumulation and the homeostasis of essential elements in ferns, supporting common uptake pathways. Notably, all of the species tested from several genera were able to accumulate REEs (e.g. *Athyrium*, *Blechnum*). This result raises the hypothesis of a putative shared REE-accumulation trait among these genera. However, in the *Dryopteris* genus, we measured discrepancies in the REE-accumulation potential. This finding will be useful for future comparative transcriptomic analyses in order to identify key mechanisms for REE accumulation and tolerance.

In this part, the elemental analyses by ICP were performed by Dr. Nadia Crini (LCE, Besançon, France).

Chapter II.1:

Transcriptomic identification of rare earth element responsive genes in *Arabidopsis thaliana*: the root architecture and ion homeostasis at stake

Transcriptomic identification of rare earth element responsive genes in *Arabidopsis thaliana*: the root architecture and ion homeostasis at stake

Transcriptomic identification of rare earth element responsive genes in *Arabidopsis thaliana*: the root architecture and ion homeostasis at stake

(Manuscript to be submitted)

Abstract

Rare earth elements (REEs) are crucial elements for many technological applications and green energy advances but are also used as fertilizers. They are subdivided in light REEs (LREEs) and heavy REEs (HREES). Their increasing use associated to their low recyclability raise the question of their impact on living organisms. Yet, little is known regarding the cellular and molecular effects of REEs in plants. Such information is of great interest for risk assessment, crop safety and phytoremediation. Here, we analyzed the transcriptomic response and ionome of *Arabidopsis thaliana* hydroponically exposed to a LREE (La) and a HREE (Yb). We confirmed by transcriptomic analyses that root toxicity was related to the expression of ROS-detoxifying genes, auxin redistribution, but also of a putative involvement of aquaporins, all contributing to a modified root architecture. Interestingly, we found evidence of a perturbation of Fe homeostasis by REEs in both roots and leaves of *Arabidopsis*, suggesting a competition or an interaction between REEs and Fe, which has never been reported previously. Effort must be done to deepen and confirm the observations made through the transcriptomic analysis regarding REE toxicity mechanisms and putative ways of entry of REEs inside cells. Notably, several candidates belonging to Fe or Mg transporters, aquaporins, and ABC transporters were proposed here. Furthermore, several genes involved in *Arabidopsis* response belong to organic acid transporters and are known as Al-responsive genes, paving the way for further investigations between Al and REE toxicity. Overall, we provide here the first global insights into the pathways involved in the REE uptake and toxicity response in *Arabidopsis thaliana*, and propose hypotheses for deciphering the environmental impact of these elements.

Introduction

Rare earth elements (REEs) are found in the Earth's crust and soils at concentrations similar to those of Ni, Zn, Cu, and Mo[1]. Among the REEs, two subgroups of lanthanides are usually considered based on both the atomic mass and the ionic radius, namely the light rare earth elements (LREEs) gathering La to Eu, and the heavy REEs (HREEs) from Gd to Lu.

They have been extensively used as crop fertilizers since the 1970s. The use of REEs in agriculture has been justified by several studies regarding their physiological role and effect at low concentrations, exemplifying their ability to promote growth, yield and resistance to biotic and abiotic stresses of many crop plants (i.e. wheat, rice, corn, and soybean)[2,3]. Among the presumed mechanisms involved, REEs seem to modulate the antioxidant pool, mineral nutrient uptake, photosynthetic activity, and affect phytohormone homeostasis[4]. These properties could be related to certain characteristics of REEs similar to other micronutrients. For example, some REEs were able to replace Ca of the hemoenzyme peroxidase in horseradish, without modification of the protein structure and enzymatic activity[5]. REEs could also replace other macro-elements such as Mg in chlorophyll, stimulating photosynthetic efficiency in plants[6].

However, REE concentrations in soils are increasing due to their extensive mining to fulfil the increasing demand due to their essential properties for many high technology fields[7,8]. They are also released in the environment in agriculture intentionally[2] or unintentionally through the use of phosphate fertilizers naturally enriched in REEs[5,9]. Consequently, accumulation of REEs in mining areas[10,11] and in agricultural soils raise the question of their toxicity to plants.

In contrast to the positive effects reported at low concentrations and the use of REEs as beneficial elements for crop production, higher concentrations of REEs can induce toxic effects. While low concentrations of Ce stimulated primary root elongation, chlorophyll content and rosette diameter of *Arabidopsis thaliana*, higher concentrations had the opposite effects[12]. In root cells, Ce was taken up intracellularly, destroyed the ultrastructure and disturbed the intrinsic balance of nutrient elements[12]. In wheat seedlings, root elongation was inhibited by La and Ce, and root and shoot dry weights decreased as well as contents of Ca, Mg, K, Cu, and Zn[13]. Since the 2010s, many studies on different plants revealed that REE response was partly marked by oxidative stress[14]. REEs (Y, La, Ce, Nd, Gd, Tb, and Yb) induced reactive oxygen species (ROS) formation, and lipid peroxidation in *Glycine max* and *Oryza sativa*[15]. Furthermore, they could also mainly decrease the activity of antioxidants such as

superoxide dismutase (SOD), catalase (CAT), and glutathione peroxidase (GPx)[14].

To date, only a few studies started to investigate the molecular mechanisms underlying the toxicological effects of REEs on plants, using the model *Arabidopsis thaliana*. Kobayashi *et al*. (2007) observed that La tolerance of root growth was not correlated with tolerance to either Al or Cu, but with tolerance towards verapamil, a well-known Ca channel blocker. Thus, they hypothesized that the major mechanism of La toxicity on root growth may involve its action as a Ca channel antagonist[16]. Conversely, La and Gd indirectly induced low-P adaptive responses by inducing P deficiency through phosphate precipitation[17], likely due to the high reactivity of REE ions with phosphates. Such response was characterized by the inhibition of the primary root growth together with an increased development of root hairs and lateral roots[17]. This low-P phenotype was also confirmed by the increased expression of the phosphate transporters AtPT1 and AtPT2 in roots exposed to Gd[17]. The reduction of cell proliferation was caused by the reduction of the number of meristematic cells and mitotic activity. Furthermore, in response to Gd, the involvement of auxin signaling in the modulation of lateral root formation was demonstrated by the increased expression of the auxin-responsive gene marker DR5[17]. Under La exposure, the inhibition of the primary root growth in *A. thaliana* was caused by the lower abundance of auxin carriers (AtAUX1, and AtPIN1/2/4/7) in the primary root tip. Such observation lead to the hypothesis that the La-mediated primary root growth inhibition was caused by a cell death increase at the root tip leading to a loss of meristematic cell division potential[18]. The same study showed a La-induced ROS over-accumulation in the root tip, possibly causing cell death, auxin redistribution and ultimately remodeling the root system architecture[18]. Additionally, two other studies showed the involvement of another plant hormone, abscisic acid (ABA), in REE response[19,20].

Despite these recent advancements on the understanding of root growth inhibition in response to REEs, there is still a lack of knowledge on the overall REE toxicity and detoxification mechanisms in plants. Therefore, a global view of the molecular response to REE exposure in both the roots and shoots using a transcriptomic analysis would allow deciphering the underlying mechanisms. Such approach has proven its efficiency in the understanding of plant responses to other trace metal elements[21–25]. Furthermore, no study so far has undertaken a comparative analysis of cell response triggered by two distinct REEs, such as La (LREE) and Yb (HREE). Here, we unravel the molecular toxicity mechanisms involved in REE stress response, notably responsible for the root architecture modification. We also propose putative uptake pathways and detoxification mechanisms developed by *A. thaliana* to cope with such elements. Finally, we demonstrate for the first time a close link between REEs and Fe homeostasis.

Materials and methods

Plant growth conditions

Arabidopsis thaliana Col-0 were grown hydroponically according to the protocol of Conn et al. (2013)[26]. Seeds were sown on lids of black micro-centrifuge tubes containing agar germination medium (GM), dipping in liquid GM (0.75 mM $CaCl_2$, 1 mM KCl, 0.25 mM $Ca(NO_3)_2{\cdot}4H_2O$, 1 mM $MgSO_4{\cdot}7H_2O$, 0.2 mM KH_2PO_4, 50 µM NaFe(III)-EDTA, 50 µM H_3BO_3, 5 µM $MnCl_2{\cdot}4H_2O$, 10 µM $ZnSO_4{\cdot}7H_2O$, 0.5 µM $CuSO_4{\cdot}5H2O$, 0.1 µM Na_2MoO_3, pH 5.6, 0.7% (m/v) agar). Seeds were then vernalized at 4°C for three days in the dark and further transferred in a growth chamber (18/23°C, 16/8 h dark/light cycles (260 µmol/m^2/s)). After 10 days of growth, seedlings were transferred into BNS medium (2 mM NH_4NO_3, 3 mM KNO_3, 2 mM KCl, 2 mM $Ca(NO_3)_2{\cdot}4H_2O$, 2 mM $MgSO_4{\cdot}7H_2O$, 1.5 mM NaCl, 600 µM KH_2PO_4, 100 µM $CaCl_2$, 50 µM NaFe(III)-EDTA, 50 µM H_3BO_3, 5 µM $MnCl_2{\cdot}4H_2O$, 10 µM $ZnSO_4{\cdot}7H_2O$, 0.5 µM $CuSO_4{\cdot}5H_2O$, 0.1 µM Na_2MoO_3, pH 5.6)[26]. Three week-old seedlings were subsequently transferred individually into bottomless 50 mL centrifuge tubes, so that roots could dip into 10 L BNS medium in a black container. The solution was continuously aerated. Six week-old *Arabidopsis* plants were then exposed to 5 µM of either La or Yb (provided as $LaCl_3$ and $YbCl_3$, respectively) or not exposed (control condition), into 2 L black containers of BNS medium lacking phosphate, for 72 h before harvesting. Seven independently grown batches of three plants each were established per treatment. *Arabidopsis* plants were harvested and roots rinsed three times in deionized water. Roots and shoots were then separated, and snapped frozen. The three plants of each replicates were pooled and ground into powder with liquid nitrogen using a mortar and a pestle, and kept at -80°C for subsequent analyses.

Root growth analysis

Six week-old plants (n=3) were transferred in a "rhizoponics" setup made of glued square Petri dishes (120x120x20 mm) cut open on the top. Plants were placed in polystyrene floats on BNS medium lacking P, and exposed to different concentrations (5, 10, and 20 µM) of either La or Yb, or not exposed. Root growth was documented using a camera after 7 days of exposure.

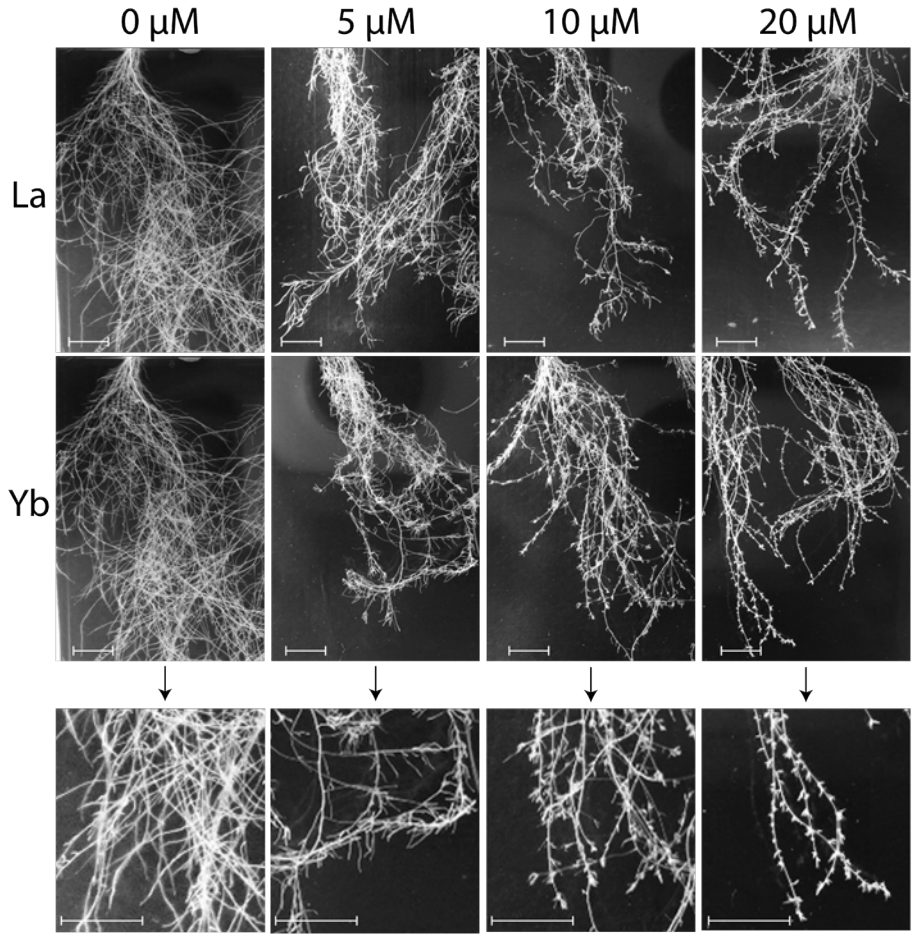

Figure 1. REE effect on *Arabidopsis thaliana* root system. *Arabidopsis thaliana* Col-0 were exposed to 5, 10, or 20 µM of either La or Yb, or without REE for 7 days. Plants were exposed hydroponically in BNS medium lacking phosphate to prevent REE precipitation. Bottom pictures are zoom on control and Yb-treated roots. Representative pictures are given. Bars = 1 cm.

Elemental analysis

Elemental analysis was carried out on ground tissues that had been dried for 48 h at 70°C. Four replicates of each three plants were prepared. The elemental extraction was performed on 250 mg dry weight samples and mineralized with 3.5 mL HNO_3 (65%, analytical grade, Optima) and 1 mL H_2O_2 (30 %) in closed tubes placed in a block digestion system (DigiPREP, SCP Sciences, Courtaboeuf, France). Gradual heating was carried out until a final temperature of 100°C for a total run of 265 min. Ultrapure water (Millipore Milli-Q Integral 3 system, Molsheim, France) was added to a final volume of 25 mL, and further filtrated to 1 µm. Elemental analyses were performed using either inductively-coupled plasma (ICP)-MS (La, Yb, Fe, Zn, Mn, and Cu) (X Series II Model, Thermo Fischer Scientific, Courtaboeuf, France), or ICP-AES (Na, P, K, S, Ca, Mg, and B) (Radial ICAP 6500 Model, Thermo Fischer Scientific, Courtaboeuf, France). Validity of the analytical method was checked by means of standard reference material (oriental basma tobacco leaves, INCT-OBTL-5, LGC Promochem, Molsheim, France). Statistical analyses were performed using R studio by Student's t-test.

RNA sequencing

Plants of three independently grown batches exposed to either La or Yb or not exposed were used for the transcriptomic analysis. Total RNAs were extracted and purified from the roots and the shoots using the RNeasy Plant Mini Kit (Qiagen), following the manufacturer's instructions. Genomic DNA was removed using DNAse I (Sigma Aldrich). Total RNAs were quantified spectrophotometrically using a Nanodrop ND-1000 (NanoDrop Technologies), and RNA integrity assessed using a Bioanalyzer 2100 (Agilent, CA, USA). RNA sequencing was performed by Eurofins Genomics (Ebersberg, Germany). Stranded cDNA libraries

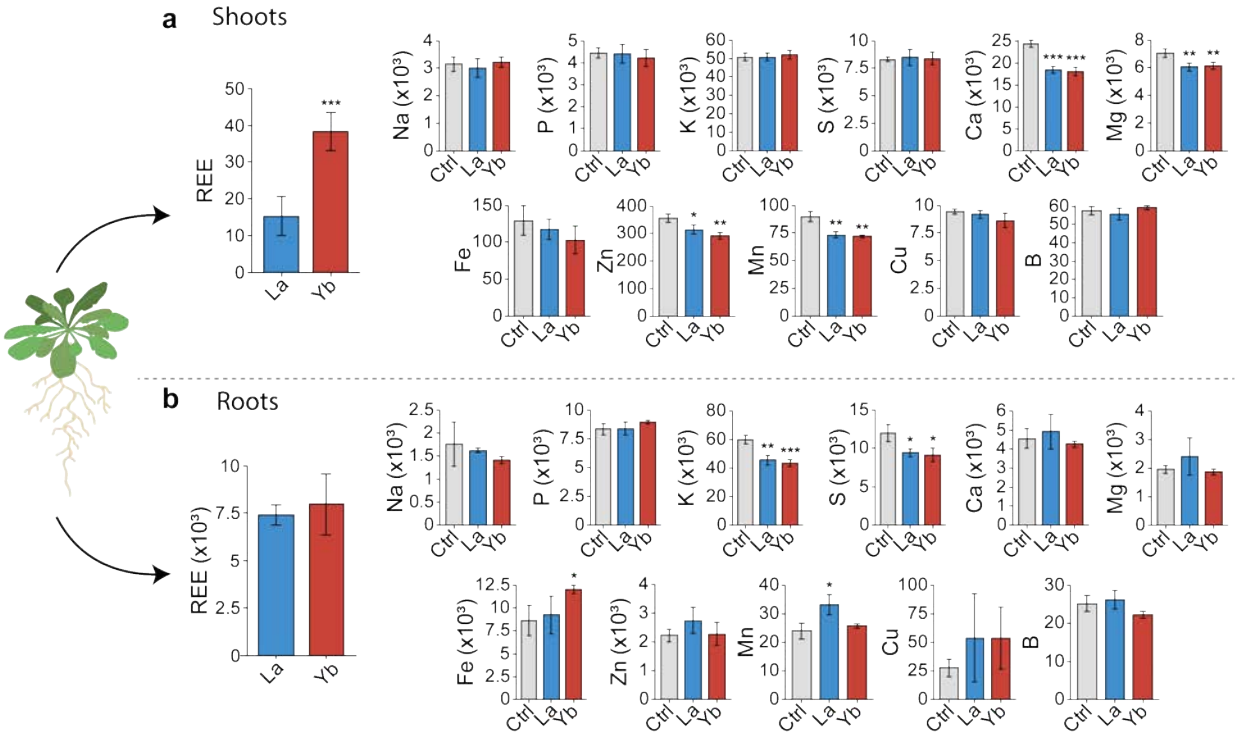

Figure 2. REE impact on *Arabidopsis thaliana* ionome. (a) REE accumulation (La and Yb), and ionomic analysis of macro- and micro-elements of shoots of *Arabidopsis thaliana* exposed to 5 µM of La, Yb, or without REE for 72 h. (b) Same as (a), but in the roots. Data are expressed in µg/g DW, and are the means (±SD) of four composite samples of three plants each, and statistically significant differences from the control condition are indicated by asterisks (t-test, Benjamini-Hochberg, *<0.05, **<0.01, ***<0.001).

(TruSeq-3 library kit) were made using at least 2 µg RNA, and RNA selection using polyA selection. RNA-sequencing was performed using an Illumina HiSeq 2500 instrument, with 2x 125 bp paired-end sequencing.

Data analysis

Raw data sequences were trimmed for their adaptor (TruSeq3) using Trimmomatic v0.36.1. Sorted reads were mapped to the *Arabidopsis thaliana* Col-0 genome (version TAIR10) using TopHat v2.1.1. Reads mapped to multiple locations were discarded. Numbers of reads in genes were counted by the HTSeq-count v0.6.1p1 tool using corresponding *Arabidopsis thaliana* gene annotations (available from https://www.arabidopsis.org/). For pairwise comparisons, significantly differentially expressed genes (DEGs) were identified by analyzing the number of reads aligned to genes with DEseq2 v1.14.1. The thresholds for the null hypothesis for differential expression were adjusted to p-values of <0.01 for the leaves and <0.001 for the roots (Benjamini-Hochberg test). GO-term analysis of the different datasets was performed using the Cluster Profiler R package[27].

Results

Root growth analysis

Root elongation impairment and architecture modifications after REE exposure have been reported by several authors[19,28], pointing a link between the observed phenotype and REE induced P-deficiency. However, these experiments did not fully explain if the root phenotype was a direct consequence of REE toxicity or a side effect caused by phosphate precipitation with REEs. To investigate this issue, we decided to expose *Arabidopsis thaliana* plants to REEs in a medium lacking phosphate for both control and REE conditions. Furthermore, to highlight the potential plant response specificity to a LREE *versus* a HREE, we selected La and Yb as contrasted lanthanides. Several concentrations of La and Yb were tested in order to determine a concentration inducing observable effects on root growth. After 7 days of exposure to La or Yb, primary and lateral root growth was inhibited (Figure 1). However, increased lateral root number and density were observed in those treatments. Five micromolar of either La or Yb were enough to alter *A. thaliana* root architecture (Figure 1) in a stronger manner than the control medium deprived of phosphorus. Higher concentrations (10 or 20 µM)

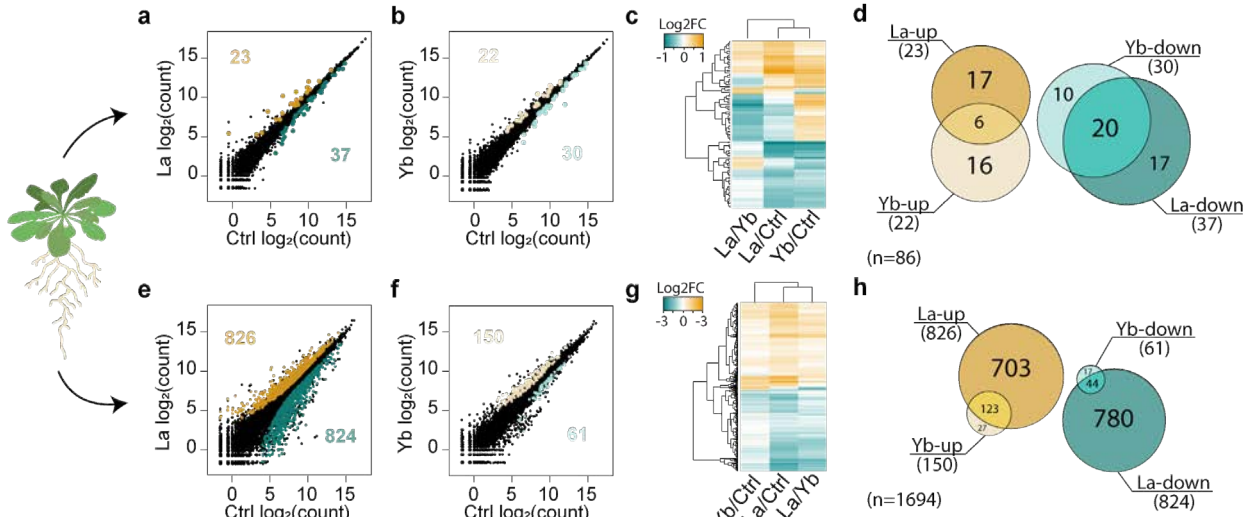

Figure 3. Differentially expressed genes in *Arabidopsis thaliana* exposed to La and Yb. Statistically significant genes that were differentially expressed compared to the control condition (no REE) in the shoots (a-d) and roots (e-h) of *A. thaliana* exposed to either La (a,e), or Yb (b,f) for 72 h. RNA-seq data are from three independent experiments gathering three plants each. For the shoots (a-d), all DEGs with a p-value < 0.01 were selected, while for the roots (e-h), genes with a fold change (FC) > 1.5 and a p-value < 0.001 were selected.

reduced the growth of both primary and lateral roots (Figure 1). Consequently, we selected 5 µM of both La and Yb for investigating the mechanistic effects of these two REEs on *A. thaliana*.

Ionome of *Arabidopsis thaliana* under REE exposure

To investigate whether a similar uptake of both REEs occurs in *A. thaliana*, we measured by ICP-MS their concentrations in *A. thaliana* exposed to 5µM La or Yb (Figure 2). La and Yb were found in similar concentrations in roots. However, more than twice as much Yb was accumulated in the shoots compared to La (38 and 15 ppm, respectively; Figure 2).

We then investigated whether La and Yb impacted the macro and micro elemental composition of shoots and roots of *Arabidopsis* (Figure 2). In the leaves, no differences in the ionome between La- and Yb-exposed plants were found (Figure 2a). However lower concentrations of Ca (-24 and -26%), Mg (-14 and -12%), Zn (-12 and -18%) and Mn (-19 and -20%) were found under exposure to La and Yb, respectively. A slight decrease in Fe (-9% and -20%) concentration was also observed but it was not statistically significant ($p = 0.380$ and $p = 0.107$, for La and Yb, respectively) (Figure 2a). In roots, we observed a decrease of K (-24 and -27%) and S (-21 and -24%) concentrations when exposed to both La and Yb, respectively (Figure 2b). However, La and Yb triggered different effects on Fe and Mn concentrations. A 39% higher concentration of Fe was specifically found under Yb exposure, while a 38% higher concentration of Mn was only found under La exposure (Figure 2b).

REE effects on gene expression and metabolic functions

To identify genes and functions that are modulated in response to REE exposure, we performed a transcriptomic analysis with shoots and roots of *A. thaliana* under La and Yb. For each condition, three replicates were sequenced by Illumina HiSeq 2500, with an average of 38 million reads of raw sequences per sample.

Out of the 24115 retrieved genes in the present dataset, 86 (0.36%) differentially expressed genes (DEGs) ($p < 0.01$) were found in the shoots exposed to REEs compared to the control condition (Figure 3a-d, Table supp. 1). Among them, 23 and 22 DEGs were upregulated and 37 and 30 DEGs were downregulated under La and Yb exposure, respectively (Figures 3a,b,d). While only 6 (15%) DEGs were upregulated under both REEs, 20 DEGs (42%) were downregulated by both metals (Figure 3d). A specific response to La and Yb in leaves was highlighted by 17 up- and 17 downregulated genes for La, and 16 up- and 10 downregulated genes for Yb (Figure 3d).

In roots, 1696 DEGs were found (FC>1.5, $p < 0.001$) out of the 24919 genes retrieved (6.80 %) (Figure 3e-h, Table supp. 2). However, strong discrepancies were observed between La and Yb. 826 upregulated and 824 downregulated DEGs were found for La, while only 150 upregulated and 61 downregulated DEGs were found for Yb (Figure 3e,f). Up to 82% of the Yb upregulated DEGs (123 DEGs) and 72% of the Yb downregulated DEGs (44 DEGs) were also found under La treatment (Figure 3h).

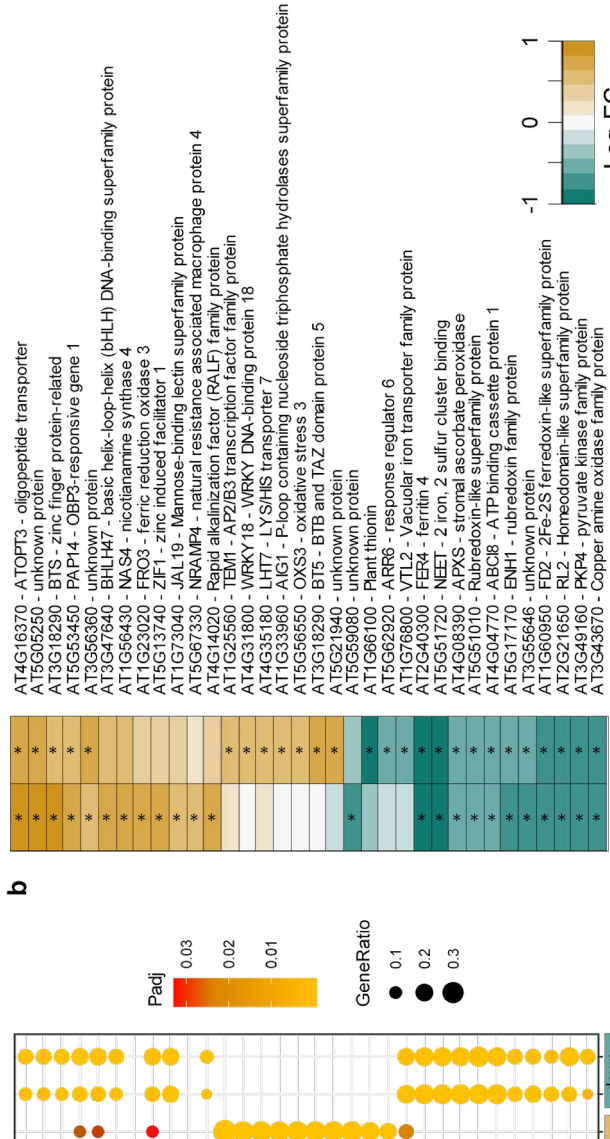

Figure 4. Major functions over-represented and genes differentially expressed under La and Yb exposure in leaves of *A. thaliana*. (a) Most significant functions enriched under La or Yb exposure. Associated differentially expressed genes (DEGs) were classified as upregulated (up) and downregulated (down). The number of DEGs is indicated in brackets. Gene ratio corresponds to the ratio of DEGs represented in a specific function on the total DEGs number. (b) Top DEGs under La and Yb exposure. Asteriks denote significant modulations of gene expression under La or Yb exposure compared to the control condition (Benjamini-Hochberg test, $p < 0.01$).

Overall, while a similar number of La- and Yb-DEGs was encountered in shoots, the number of DEGs in roots was higher in plants treated with La compared to that obtained from plants treated with Yb despite a similar global expression pattern was found between both REEs (figure 3g).

To gain insights into the biological processes that were affected following a REE stress, we analyzed the enriched GO-terms within the DEGs (Figure 4a, Table supp. 3).

Several functions were enriched among the 86 DEGs from the shoots exposed to REEs compared to the control condition ($p < 0.05$) (Figure 4a, Table supp. 3). Congruent with the high proportion of downregulated DEGs shared between La and Yb, we observed that identical functions were downregulated by both metals. Among them, there were several GO-terms related to nicotinamide and pyridine nucleotide metabolic processes, and in a minor proportion to photosynthesis. Regarding the upregulated genes, we observed that under Yb exposure, they were linked to GO-terms related to the response to salicylic acid (Figure 4a, Table supp. 3). Nevertheless, the largest group of GO-terms enriched that were both up and downregulated under both REEs, was related to cation homeostasis, and more specifically Fe homeostasis (Figure 4a, Table supp. 3).

Iron starvation genes are induced under REE exposure in leaves

Under both La and Yb exposure, several genes involved in Fe homeostasis and storage were significantly downregulated (Figure 4b, Table supp. 1). This was the case for the genes NEET (At5g51720), FD2 (At1g60950), ABCI8 (At4g04770), and FER4 (At2g40300). NEET encodes a 2Fe-2S cluster binding protein involved in Fe metabolism[29] and FD2[30] encodes a major ferredoxin (2Fe-2S cluster binding protein) in leaves involved in plastid electron transport and stress response[31]. ABCI8 encodes a Fe-stimulated ATPase and is an ABC transporter. It is involved in Fe-S cluster assembly and regulation of Fe homeostasis[32]. FER4 encodes a ferritin, which binds ferric Fe and is used as Fe storage in chloroplasts[33]. Another ferritin encoding gene, FER1 (At5g01600), was specifically downregulated by Yb. That was also the case of the VTL2 gene (At1g76800) which encodes a vacuolar Fe transporter that catalyze Fe import and storage in vacuoles.

Regarding upregulated DEGs, different GO-terms were enriched depending on the REE (Figure 4b, Table supp. 1). Under La exposure, most of the GO-terms represented for upregulated DEGs were also associated to Fe homeostasis and response to Fe starvation. Among these GO-terms associated genes, OPT3 (At4g16370), NRAMP4 (At5g67330), ZIF1 (At5g13740), FRO3 (At1g23020), bHLH47 (At3g47640), bHLH38 (At3g56970) and NAS4 (At1g56430) were found. NRAMP4 encodes for a vacuolar transporter that retrieves Fe and Mn from the vacuole under Fe deficiency, which works antagonistically to the VIT protein[34]. The upregulated zinc-induced facilitator 1 (ZIF1) gene, encodes a vacuolar membrane transporter involved in Zn sequestration by mediating the efflux of Zn-ligand complexes such as Zn-NA (nicotianamine) into vacuoles[35]. NAS4, which encodes a nicotianamine synthase[36,37], was also upregulated under La exposure. Lastly, we observed the upregulation of FRO3, which encodes a ferric chelate reductase whose transcription is regulated by FIT1[36,37]. Two basic helix-loop-helix (bHLH) transcription factors were also upregulated under La. POPEYE (PYE)-bHLH47 is involved in the response to Fe deficiency[36,37] and ORG2-bHLH38 is usually induced by Fe deficiency[36,37] in roots and leaves, as well as by Ni, high Zn or Cu treatments. Additionally, two genes were upregulated by both La and Yb. OPT3 was one of the most upregulated genes under both REEs. It encodes for a phloem-specific Fe transporter that is essential for systemic Fe signaling and redistribution of Fe and Cd[38]. It loads Fe into the phloem, facilitates Fe recirculation from the xylem to the phloem, and regulates both shoot-to-root Fe signaling and Fe redistribution from mature to developing tissues. The BRUTUS-BTS (At3g18290) gene, involved in cellular response to Fe starvation and negatively regulating the response to Fe deficiency under Fe replete condition[36,37], was also upregulated by La and Yb.

Iron starvation genes are also induced under REE exposure in roots

Up to 1696 DEGs were found in the roots under REE exposure (Figure 3h, Table supp. 2). Despite the apparently similar root toxicity of the two REEs tested, we observed different GO-terms enriched between La and Yb treatments (Figure 5a, Table supp. 4).

Similar to the results obtained from the transcriptomic analysis in leaves, the expression of several Fe homeostasis related genes were modulated in roots in the presence of REEs (Figure 5b, Table supp. 2). Indeed, a few DEGs were involved in the "cellular response to Fe ion starvation" (Figure 5a, Table supp. 4). We counted 15 and 2 of them for La and Yb, respectively. Most of these DEGs encode Fe-dependent or heme-binding proteins. We observed a higher expression of bHLH100 (At2g41240), and bHLH39 (ORG3 - At3g56980) among the genes upregulated under both La and Yb exposure (Figure 5b, Table supp. 2). Furthermore, specifically under La exposure we observed the upregulation of several other transcription factors, i.e. bHLH38 (ORG2), bHLH101 (At5g04150), and bHLH47 (POPEYE) (Figure 5b, Table supp. 2).

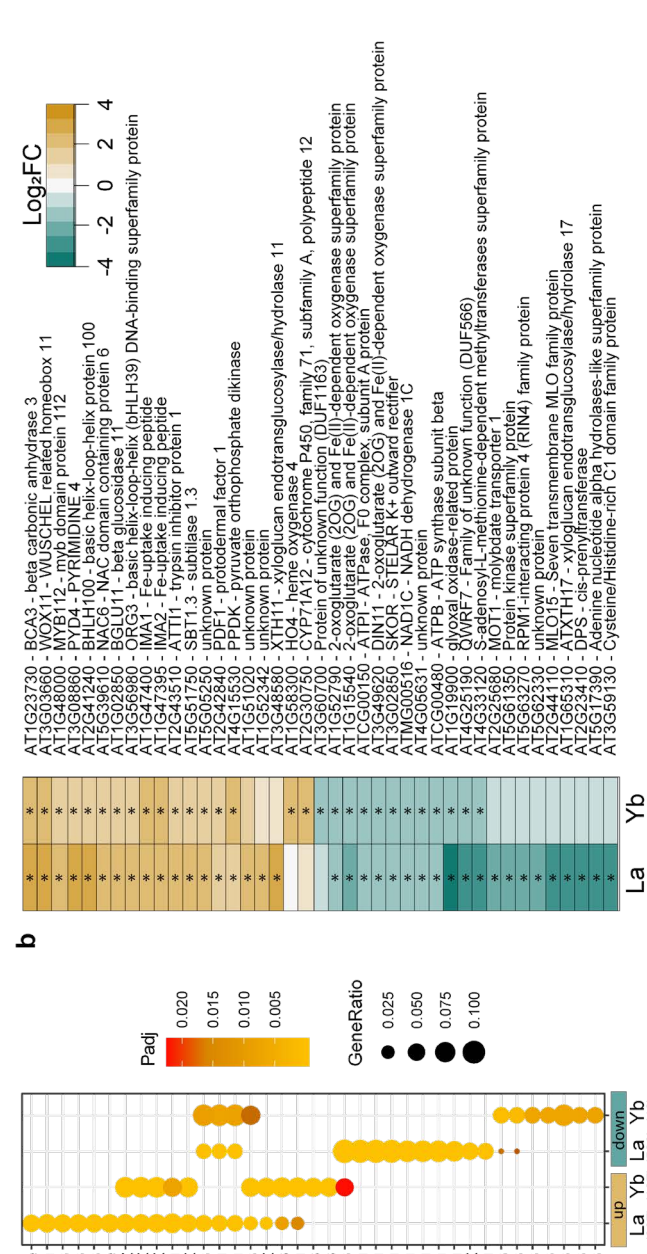

Figure 5. Major functions over-represented and genes differentially expressed under La and Yb exposure in roots of *A. thaliana*. (a) Most significant functions enriched under La or Yb exposure. Associated differentially expressed genes (DEGs) were classified as upregulated (up) and downregulated (down) in the two conditions. The number of DEGs is indicated in brackets. Gene ratio corresponds to the ratio of DEGs represented in a specific function on the total DEGs number. (b) Top DEGs under La and Yb exposure. Asteriks denote significant modulations of gene expression under La or Yb exposure compared to the control condition (Benjamini-Hochberg test, $p < 0.01$).

Additionally, the gene encoding for the transcription factor WRKY45 (At3g01970), activated under Zn deficiency[39] was upregulated under La and Yb exposure. FRO2 and FRO3, two ferric chelate reductases were also upregulated[36,37]. The cation transporters, NRAMP4 and IRT1, were significantly more expressed in the roots of *Arabidopsis* exposed to La compared to the control. At1g47400, At1g47395 and At5g05250 were highly upregulated under both REEs. The two first genes respectively encodes for IRONMAN1 (IMA1) and 2 (IMA2)[40], peptides involved in Fe transport control, while the last one encodes for an unknown protein likely involved in Fe homeostasis[41]. Additionally, YSL2 (At5g24380) was more expressed under La exposure. YSL2 encodes a transporter of NA-ion complexes which is usually downregulated under Fe and Zn starvation[42]. Among the most upregulated genes under La and both REEs were NAC019 (At1g52890) and NAC6 (At5g39610), respectively, that both encode for NAC transcription factors that are induced by salt stress and abscisic acid[43]. Lastly, we observed the upregulation of GLP5 (At1g09560) under La exposure. GLP5 was previously shown to be up-regulated under Fe deficiency[44,45].

Other metal-related genes are induced under REE exposure in roots

MRS2-8 (At5g09720), a gene encoding for a Mg transporter from the CorA-like superfamily[46], was specifically upregulated under Yb exposure. The same observation was made for At2g16660, a major facilitator protein that showed a significantly higher expression level in roots of *A. halleri* relatively to *A. thaliana*[47]. Another major facilitator protein, At4g34950, was however also upregulated under La.

Also of high interest was the over-representation of heavy metal-associated isoprenylated plant proteins (HIPP) (Table supp. 2). These proteins are metallochaperones that allow the transport of ions through the cell[48]. They are soluble intracellular proteins that strongly bind metallic ions (e.g. Cu and Cd) and thus prevent putative deleterious reactions. Some genes encoding these HIPP were upregulated (HIPP14, HIPP33, HIPP24, HIPP04, and HIPP45) while some others were downregulated (HIPP09, HIPP16, HIPP43 and HIPP25). Especially noteworthy were two genes encoding proteins from the Cu transport protein family At5g52670 and At5g52680. These two genes were both downregulated under La exposure while upregulated under Yb exposure. We observed also the upregulation of the two metallothioneins MT3 and MT5, as well as HMA5, which is known to allow the detoxification of Cu by extruding Cu outside of the cytosol (Table supp. 2). MTP8 (At3g58060), belonging to the cation diffusion facilitator (CDF) family, was highly upregulated by both REEs. Its role in the sequestration of excess Mn from the cytoplasm into vacuoles to maintain Mn homeostasis, notably under Fe deprivation, was previously reported[49]. A second CDF, MTP9 (At1g79520), was slightly upregulated under La only.

Root architecture and cell walls are modified under REE exposure

Under La exposure, several GO-terms over-represented in both up and downregulated DEGs were linked to root morphogenesis (Figure 5a, Table supp. 4). Among these genes, we first observed the upregulation of the transcription factors WOX11 (At3g03660), WOX12 (At5g17810), and LRP1 (At5g12330) (Figure 5b, Table supp. 2). WOX11 and LRP1 intervene in lateral root initiation, notably under Pi deficiency in the case of LRP1[50]. Also, NAC6 (At5g3910), a transcription activator involved in the promotion of lateral root development was also upregulated under both REEs (Figure 5b, Table supp. 2). Some other genes involved in root architecture and morphogenesis were downregulated. Among them we found three genes, bHLH82 (At5g58010), bHLH83 (At1g66470), and bHLH85 (At4g33880), that encode for helix-loop-helix transcription factors. They are all involved in root hair development[51].

Effects on root structure are evidenced by the downregulation of cell wall related genes. The GO-term “plant-type cell wall organization” was particularly significant under La exposure (Figure 5a, Table supp. 4) and several genes encoding for expansins were downregulated under La, such as EXPB1 (At2g20750), EXPA11 (At1g20190), EXPA14 (At5g56320), and EXPA9 (At5g02260). Expansins loosen the cell wall at cellulose-xyloglucan junctions, allowing for slippage of the cellulose microfibrils and thus to cell wall extension[52]. XTH proteins are involved in the cell wall loosening[53] and some of them ((XTH21 (At2g18800), XTH12 (At5g57530), XTH17 (At1g65310), and XTH33 (At1g10550)) were repressed under La exposure as expansins-encoding genes.

REE modify the expression of auxin-homeostasis genes in roots

The three related GO-terms “regulation of hormone levels”, “hormone metabolic process”, and “hormone biosynthetic process” were highlighted among the downregulated genes (Table supp. 4) Conversely, “auxin transport”, “response to auxin”, “auxin polar transport”, and “hormone transport” were found among the upregulated DEGs (Table supp. 4). Several auxin-responsive genes were upregulated (Figure 5b, Table supp. 2). IAA7 (At3g23050), which encodes a transcription regulator inhibiting auxin-inducible gene

expression, was downregulated. YUC5 (At5g43890), and YUC3 (At1g04610) were downregulated under La exposure, while YUC9 (At1g04180) was upregulated. These genes involved in YUC-mediated *de novo* auxin synthesis play a role in root organogenesis[54].

We also observed a modulated expression of genes encoding proteins involved in auxin transport. PIN2 and PILS5, encoding for auxin efflux carriers[55], were both downregulated under La exposure, but genes encoding the auxin efflux transmembrane transporters PIN7 and ABCB4 (At2g47000), were upregulated. ABCB4 functions in the basipetal redirection of auxin from the root tip, and is involved in root hair elongation, while PIN7 has a preferential role in terminating radial root expansion[56].

The expression of numerous transporters is modulated under REE exposure in roots

Twenty-two genes encoding for ABC transporters were found to be either up- or downregulated under La exposure (Table supp. 2). Both the highest (ABCB4 (At2g47000), ABCB2 (At4g25960), and ABCB11 (At1g02520)) and lowest (ABCB5 (At4g01830), and ABCB17 (At3g28380)) expressed representatives of the ABCB sub-family genes take part in the auxin transport, reinforcing the effect of REE exposure in altering auxin homeostasis. Some other ABC transporters from the ABCG sub-family that are involved in suberin and wax transport were all upregulated, such as ABCG6 (At5g13580), ABCG10 (At1g53270), ABCG2 (At2g37360), ABCG32 (At2g26910), ABCG1 (At2g39350), and ABCG12 (At1g51500).

Additionally, several PDR transporters, also members of the ABCG transporters sub-family that can transport different substances including ions, were affected by REEs. The gene encoding PDR11 (At1g66950) was upregulated by both REEs. PDR4 (At2g26910), PDR10 (At3g30842), and PDR5 (At2g37280) were more expressed under La exposure, but also under Yb exposure despite being not significant ($p = 0.0014$).

Apart from effects on ABC transporters, REE exposure modulated the expression of several other transporters, among them Ca channels (Table supp. 2). CNGC14 was downregulated by La, but remained unchanged under Yb. The same holds for GLR genes, encoding for glutamate receptors involved in Ca homeostasis[57,58] were found. This was the case of GLR1.3, GLR2.3, GLR2.4, GLR2.5, GLR2.6 and GLR3.5 that were all upregulated under La exposure. The gene encoding CAX3 (At3g51860), a Ca^{2+}/H^{+} transporter, was also upregulated by La.

The expression of several genes encoding for proteins that transport organic acids, metal ions and amine compounds was modulated (Figure 5a,b, Table supp. 2,4). ALMT1 (At1g08430) which encodes an Al-activated malate efflux transporter[59] was upregulated. The genes DTX42 (At1g51340), DTX14 (At1g71140), DTX40 (At3g21690), were also upregulated. They encode MATE (multi antimicrobial extrusion) efflux transporters. Especially noteworthy is DTX42, a root citrate efflux transporter, together with ALMT1 are the primary mechanisms of Al tolerance. Two other genes, namely DTX7 (At1g64820), DTX36 (At1g11670), and ALMT3 (At1g18420) an aluminum activated malate transporter, were however downregulated.

Finally, eleven aquaporins-encoding genes, namely TIP4;1 (At2g25810), TIP1;2 (At3g26520), TIP2;1 (At3g16240), TIP2;3 (At5g47450), PIP2;7 (At4g35100), PIP2;3 (At2g37180), PIP2B (At2g37170), PIP1;1 (At3g61430), PIP1;5 (At4g23400), PIP2;4 (At5g60660), and NIP1;1 (At4g19030), were downregulated by La treatment (Table supp. 2). Aquaporins are membrane pore proteins that conduct water molecules and metal ions in and out of plant cells[60].

REEs induce genes involved in oxidative stress response and ROS scavenging in roots

The expression of several genes encoding for proteins involved in the detoxification of ROS in cells was modulated under REE exposure. The GO-terms “response to oxidative stress” and “detoxification” were also over-represented among the upregulated genes (Table supp. 4). Eighteen glutathione-S-transferase genes were upregulated under La exposure (GSTU1, GSTU2, GSTU4, GSTU7, GSTU8, GSTU10, GSTU14, GSTU19, GSTU20, GSTU22, GSTU24, GSTU25, GSTU26, GSTU28, GSTL1, GSTL3, GSTF6, and GSTZ1). GSTF6 and GSTU10 were the only GST being upregulated under Yb exposure (Table supp. 2).

We could also observe the upregulation under La treatment of the Fe superoxide dismutase FSD1 (At4g25100), the glutathione peroxidase GPX6 (At4g11600), the catalases CAT1 (At1g20630) and CAT3 (At1g20620), and the alpha-dioxygenase DOX1 (At3g01420). The peroxidases PER11 (At1g68850), PER15 (At2g18150), PER20 (At2g35380), PER34 (At3g49120), PER38 (At4g08780), and At5g14130 were more expressed under La exposure, while the peroxidases PER49 (At4g36430), PER54 (At5g06730), and PER62 (At5g39580), were more expressed under both REEs. These peroxidases are mostly expressed in the upper part of roots, and to a lesser extent in the apex. Conversely, the genes encoding for the peroxidases PER16 (At2g18980), PER24 (At2g39040), PER35 (At3g49960), PER45 (At4g30170), PER60 (At5g22410), and PER61 (At5g24070) were all downregulated under La. These peroxidases are mostly expressed in the root apex.

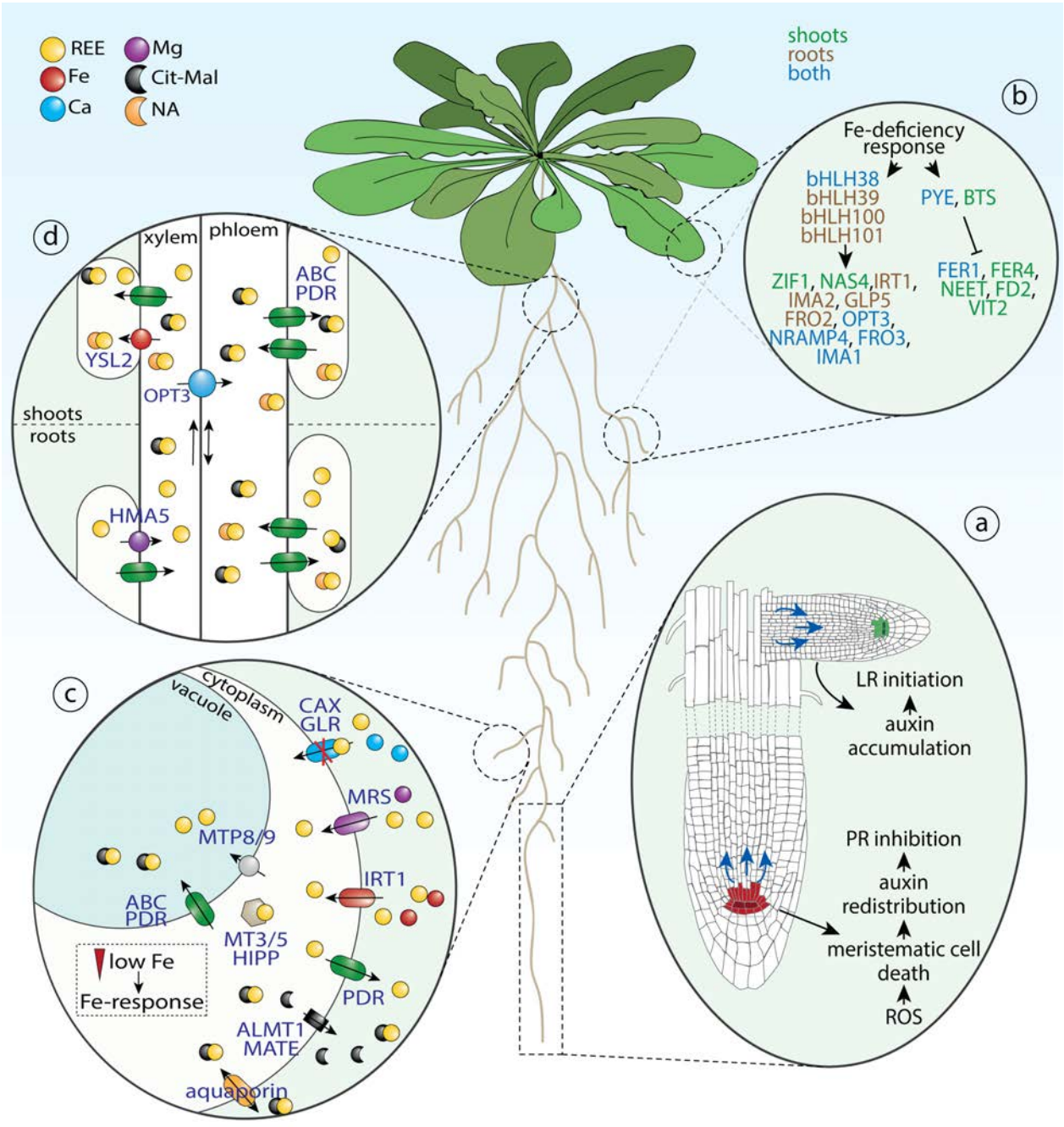

Figure 6. Proposed model of the effects of REEs and their homeostasis in *Arabidopsis thaliana*. (a) REEs modify root architecture by inhibiting primary root growth and inducing auxin redistribution leading to root branching. (b) Fe-deficiency response triggered by REEs in both roots and shoots possibly due to uptake competition between REEs and Fe at the root level. (c) Proposed mechanisms of REE root uptake, chelation to organic acids or other chelators, sequestration in the vacuole, and efflux of REEs or organic acids in the rhizosphere. (d) REE translocation in the shoots through the xylem, and redistribution in the plant via the phloem under complex forms of REEs. LR: Lateral roots, PR: primary root, Cit: citrate, Mal: malate, NA: nicotianamine.

The thioredoxin-dependent peroxidase TPX2 (At1g65970) was downregulated under Yb exposure (Table supp. 2).

Discussion

The modified root architecture is the result of ROS production by REEs and auxin redistribution in roots

We present in this paper a molecular study of the effects of toxic exposure to REEs, which revealed yet unknown pathways regarding REE toxicity response in plants. We exposed *Arabidopsis* plants to REEs in a medium lacking phosphates in order to avoid the precipitation of REEs with phosphates, which allowed a higher bioavailability and reactivity of REEs to plants. Consequently, the previously reported root toxicity of REEs consisting of a root architecture modification and the primary root length inhibition was visible at 5 µM instead of 50 µM in a P containing medium[17]. Interestingly, twenty times more DEGs were found in roots compared to shoots. The number of DEGs in shoots and roots was however in the same order of magnitude than what was found after exposure of *Arabidopsis* to other metals[22,61]. The large difference observed in the response between roots and shoots could be explained by the high rhizotoxicity induced by REEs and their low translocation.

The modulation of the expression of genes taking part in the plant-type cell wall organization in the roots supports the high interaction of REEs with roots. Several genes downregulated under La exposure such as expansins as well as XTH-encoding genes, are involved in cell wall loosening during cell wall extension. This result is consistent with the inhibition of root elongation under REE exposure, where root development and consequently cell wall extension was inhibited.

Concomitant to the inhibition of primary root growth, the increased density and growth inhibition of lateral roots have been observed. Confirming the phenotype observed, we noticed the upregulation of several genes involved in lateral root initiation. Among them were the four transcription factors WOX11, WOX12, NAC6, and LRP1. Some others that take part into hair root development were downregulated such as bHLH82, bHLH83, and bHLH85. Altogether, these data highly support the impact of REEs on root architecture in *Arabidopsis*. A similar phenotype was reported in response to Ni and Co stress[62], but also under P deficiency[63]. This phenotype was previously shown and studied in response to REEs (La, Gd) in *Arabidopsis*[17,18]. Under Gd, a modified root architecture had been induced by a P-deficiency response due to the precipitation of REEs with phosphates[17]. Nevertheless, we observed here a difference in root architecture between the control condition under P deficiency and REE exposure (Figure 1). Therefore, the observed modified root architecture was not only the result of P deprivation, but the result of a REE toxicity effect.

It has been shown in *A. thaliana* that primary root growth inhibition caused by La exposure was due to an increased cell death in the tip and subsequent loss of meristematic cell division potential[18]. In the same study, Liu and coworkers demonstrated that La induced ROS over-accumulation in the tip, possibly causing cell death, and ultimately remodeling the root system architecture by auxin redistribution[18]. Therefore, the role of auxin in the modification of the root system architecture in response to REEs is essential. Expression of AtPIN2 and AtPIN7 has been previously demonstrated to be modified under La exposure[55], which is concordant with our results where AtPIN7, AtPILS5 and ABCB4 were upregulated, and AtPIN2 downregulated. Liu *et al*. (2017) demonstrated that the inhibition of the primary root by La in *A. thaliana* was caused by the lower auxin carrier abundance in the primary root tip (AtAUX1 and AtPIN1/2/4/7). Therefore, impairment of auxin distribution in roots, by the modification of transporter localization, was responsible for the modified root architecture[55]. Here, we observed several other auxin-related genes that were differentially expressed under REE exposure. We identified the downregulation of AtYUC3 and AtYUC5. It was previously shown that AtYUC3 was upregulated under La exposure but by only 1.2 fold[18]. AtIAA7 was also repressed, which would also allow increased auxin levels, supporting the necessity of auxin production in roots exposed to REEs. The upregulation of ARF5, an auxin response factor further supports the effect of REEs on roots, since ARF (auxin response factors) genes mediate the development and emergence of lateral roots, giving rise to a branched root system[64]. Altogether, these results highlight the impact of REEs on auxin signaling and homeostasis, and its strong effects on root architecture (Figure 6a).

In the transcriptome of the roots of *Arabidopsis* exposed to either La or Yb, we observed the upregulation of several genes involved in the response to oxidative stress. This might be an attempt of the plant to cope with oxidative stress. REEs trigger the increased expression of genes encoding for enzymes involved in ROS scavenging, notably represented by superoxide dismutase, glutathione peroxidase, catalases, alpha-dioxygenase, and peroxidases. This result supports the toxicological studies that reported the induction of an oxidative stress in plants (*Nymphoides peltata*[65], soybean[66], rice[67], and horseradish[68]) as a result of REE exposure. Furthermore, the upregulation of twelve GSTs found in the roots confirm the oxidative stress induced by REEs. Those GSTs could be involved in the binding of REEs for their detoxification, as it is the case for Cd

sequestration[69], but other explanations cannot be excluded.

REE perturbs ion homeostasis in the plant

The exposition of *Arabidopsis* to REEs led to a changed composition of its ionome. In leaves, we observed a lower concentration of of Ca, Mg, Zn, and Mn. However, in roots Fe concentration was higher under Yb exposure, as well as Mn concentration under La exposure, while lower concenrations of S and K were found under both REEs. Such an effect has been previously reported for La and Ce[13], the latter destroyed the ultrastructure of cells and disturbed the intrinsic balance of nutrient elements[12]. The application of Ce to the culture medium of wheat seedlings had negative effects; elongation of the primary root was inhibited, together with lower concentrations of Ca, Mg, K, Cu and Zn[13]. Our observations are therefore consistent with those previous results, reinforcing the hypothesis that REEs may interfere with nutrient transport and homeostasis.

Ca homeostasis is perturbed under REE exposure

Glutamate receptor-like (GLR) proteins are involved in the intracellular flux of Ca, and thus take part in the signaling process in response to numerous stressors. Ca and GLR proteins have been implicated in light and C:N signaling, abscisic acid (ABA) metabolism, stress responses, and general ion transport, but also root growth, and lateral root initiation[70,71]. The modulated expression of several Ca channels and GLR proteins under La exposure can be interpreted by three hypotheses. Firstly, GLR proteins could take part in the signaling process of an REE stress in roots. Secondly, their modulated expression could be involved in the root architecture modification in response to REEs. Lastly, La has been extensively used as a non-specific Ca channel blocker for studying Ca signaling in plants[72,73]. Therefore, the inhibition of Ca channels by lanthanides could induce a response, such as Ca starvation, in which Ca channels would be modulated in different root parts (Figure 6c). This hypothesis is supported by first the downregulation of the (Ca^{2+}/H^{+}) antiporter CAX3 under La exposure but also by the lower concentration of Ca in the aerial parts of *Arabidopsis* exposed to REEs.

REE uptake, efflux and detoxification could be performed by Fe, Mg and ABC transporters

Despite the modification of root architecture was not typical of an Fe deficiency response[62], we observed the upregulation of genes related to Fe retrieval (FRO2, FRO3, NAS4, OPT3, YSL2, IMA1, IMA2), together with the downregulation of genes related to Fe storage (FER4, FER1, NEET, VTL2) (Figure 6b). In the same manner as reporter here, Fe starvation response was induced by several metals (Cd, Zn, Co, Ni, Mn)[62]. However, studies on U, also performed under P-deficient conditions, demonstrated an opposite response. U exposure downregulated the Fe-uptake response notably by the downregulation of FIT1, FRO2, IRT1, AHA2 and AHA7[74]. Also, FIT1 was downregulated in tobacco roots exposed to Th[75]. Despite the close chemical relationship between lanthanides and actinides, it appears that they trigger a complete different response in *Arabidopsis*. Nevertheless, among the genes involved in this response, we observed the modulation of the transcription factors involved in the control of Fe homeostasis bHLH038, bHLH039, bHLH100 and bHLH101 that were highly upregulated in roots. In leaves we observed the same upregulation of the transcription factors PYE, ORG2, and BTS. The higher expression of these transcription factors related to Fe-deficiency, supports that REEs induce Fe deficiency in both roots and leaves.

The subsequent increased expression of the Fe transporters NRAMP4 and IRT1 in roots supports the need of Fe for the plant under REE exposure (Figure 6b). Cd flux to the cytosol can be mediated by these two Fe transporters[76], thus other toxic elements such as REEs could follow this path. We can hypothesize that REEs compete with Fe for root uptake via IRT1, which ultimately would lead to Fe deficiency in shoots. Although there is no difference in Fe concentration in the roots, the long distance signaling from the shoots to the roots of the Fe-deficiency response would be responsible for the increased expression of these transporters (e.g. IRT1)[77] (Figure 6b,c).

Three other transporters were upregulated either under La or Yb exposure. Among them, MRS2-8 which encode a Mg transporter. MRS2-8p has been shown to transport also Ni ions[46,78], while MRS2-10 have been shown to allow the uptake of Al^{3+}[79]. Therefore, the hypothesis of REEs competing with Mg for this transporter is also possible (Figure 6c). This observation would be in line with the lower concentration of Mg in leaves under REE exposure, triggering an Mg deficiency response by increasing Mg transporter expression. The two other transporters At2g16660 and At4g34950 are two major facilitator proteins that were also more expressed in roots. Hence, it would be interesting to use mutants for all of these transporters in order to look at their implications in REE uptake.

We also observed that the expression of several ABC transporters were induced by either La or Yb, that could be involved in the detoxification process of REEs (Figure 6c). Transporters related to the ABC family, among which PDR transporters, can transport different substances, but also heavy metals. For instance, PDR12 and PDR8 are involved in Pb and Cd tolerance[80]. Notably, it has been demonstrated that the latter was a Cd extrusion pump conferring heavy metal resistance[81]. The yeast

Pdr5p is a plasma membrane ABC multidrug transporter involved in cation resistance[82]. Also, it was shown that the ABC transporter ALS3 was involved in the transport of Al^{3+} in *Arabidopsis*[83]. Therefore, it is plausible that the upregulation of ABC transporters under REE exposure, such as PDR11, PDR4, PDR10, and PDR5, would be a way to get rid of REE ions out of the cytosol (Figure 6c). Thanks to the high diversity of roles of ABC transporters, they could possibly have implication in the vacuolar sequestration, root-to-shoot translocation, but also in redistribution of REEs (Figure 6c,d).

Additionally, we noticed the upregulation of the two cation efflux transporters MTP8 and MTP9 and the heavy-metal ATPase HMA5. MTP8 is localized on the vacuolar membrane and allows the movement of Mn from the cytosol to the vacuole under Fe deficiency, in order to cope with Mn toxicity[49,84]. On the other hand, HMA5 was shown to be a mechanism of Cu detoxification under excess of Cu[85]. In our case, these transporters could allow the detoxification of REEs from the cytosol, and would therefore be important leads into the detoxification mechanisms of REEs (Figure 6c,d). The upregulation of HIPP metallochaperones that allow the transport of ions through the cell, could also be part of the detoxification process set up by plants. These proteins are able to strongly bind metallic ions, such as Cu and Cd, thus prevent putative deleterious reactions[48]. Additionally, the higher expression of the metallothioneins MT3 and MT5, suggest their putative involvement in the chelation of REEs, to reduce their interactions with cellular components (Figure 6c). Metallothioneins have been shown to take part into heavy metal tolerance by chelating Cu and Cd in plants[86,87].

Organic acids could play a pivotal role in REE scavenging and tolerance

We further looked at the possible transfer of REEs from roots to leaves by measuring their concentration in both compartments. While looking at the translocation of REEs from roots to leaves, we observed different concentrations between La and Yb in leaves. This result suggests a difference of uptake ability for the different REEs tested, but also that there would be a differential translocation. Similar observations were reported when plants were hydroponically grown and exposed at equimolar concentrations of the whole set of the 16 REEs. Indeed, HREEs (i.e. Yb) were preferentially translocated to leaves comparatively to LREEs (i.e. La) in wheat (*Triticum aestivum*)[88,89] and soybean (*Glycine max*)[90]. The same conclusions were found in the REE hyperaccumulator *Phytolacca americana*[91]. The specific enrichment of HREEs in the shoots is thought to be due to the better transport and stability of complexed HREEs with organic acids compared to LREE free ions. Among the organic acids potentially involved in this mechanism, malate and citrate were reported[88–93]. It is noteworthy that in our transcriptomic analysis, genes encoding the proteins ALMT1, and DTX42 were highly upregulated under La exposure in roots, together with other MATE efflux transporters. ALMT1, an Al-activated malate efflux transporter and the root citrate efflux transporter DTX42 could play a role in REE binding (Figure 6c). Malate and citrate have been shown to bind REEs and be responsible of REE transfer in wheat[89]. This mechanism of detoxification was previously suggested for other rhizotoxic trivalent elements such as Al[59], and could therefore be a mechanism of detoxification for REEs. Indeed, as shown for Al, the efflux of malate would convert free REE ions in metal-malate complexes that are less toxic[59], and therefore be excreted or translocated (Figure 6c,d). Such a hypothesis seems plausible since ALMT1 also showed enhanced response to trivalent cations such as Al and several REEs (La, Gd, Er, Yb)[94].

The downregulation of several aquaporins was observed under La exposure in roots. Under metal stress, aquaporins might have several roles. First, it has been previously shown that aquaporins were inhibited by Au, Ag, and Hg via covalent modification of cysteine residues[95–97]. Indeed, under Au exposure, several aquaporin encoding genes were downregulated[96]. Secondly, it is known that aquaporins are involved in lateral root development, allowing the development of lateral roots after auxin-induced downregulation of aquaporins[98]. Therefore, the lower expression of these aquaporins could take part in the modified root architecture caused by REE toxicity, in response to auxin redistribution in roots as shown above. Lastly, it has previously been demonstrated that several metals and metalloids can be taken up via aquaporins. Moreover, NIP3;1 and NIP1;2 are able to transport As[99] and Al-malate[100], respectively. Despite that NIP1;2 is specifically upregulated under Al exposure to allow the uptake of Al-malate and for its further translocation in shoots, one can hypothesize that the downregulation of a REE-transporting aquaporin would be a way of preventing REE uptake and toxicity (Figure 6c,d). Therefore, it seems important to further investigate the role of aquaporins in the root response to REE exposure.

Conclusion

The molecular mechanisms of REE toxicity in plants have been yet relatively poorly investigated. The few studies reporting the effects of REEs on plants have highlighted the mechanisms underlying primary root growth inhibition and lateral root initiation. Here, we confirm by a transcriptomic analysis that root toxicity was mainly the result of the loss of meristematic cell division potential by ROS, and therefore auxin redistribution contributing to a modified root architecture

(Figure 6a). We also provide here new putative actors involved in the modified root architecture with several aquaporins. Interestingly, we found indications for the perturbation of Fe homeostasis by REEs in both roots and leaves of *Arabidopsis* (Figure 6b) even though levels of Fe did not differ significantly in leaves or were even enhanced by La in roots. The Fe deficiency-like response suggests a competition between REEs and Fe (Figure 6c), which has never been reported previously. Effort must be done to deepen and confirm the observations made through the transcriptomic analysis regarding REE toxicity mechanisms and putative ways of entry of REEs inside cells, among which the best candidates could belong to Fe or Mg transporters, aquaporins, and ABC transporters (PDR). Furthermore, several DEGs were also found in common to previous studies on trivalent Al. As suggested for other plant species, the importance of organic acids such as malate and citrate in the tolerance mechanisms in response to REEs needs further investigations in *Arabidopsis*. In order to explore the above hypotheses and deepen the comprehension of the molecular toxicity of REEs in plants, future investigations should be carried out with for instance mutants for genes that are transcriptionally regulated by REEs, together with more targeted physiological experiments.

References

1. Survey U.S. Geological. Rare Earth Elements—Critical Resources for High Technology. (2002).
2. Hu, Z., Richter, H., Sparovek, G., & Schnug, E. Physiological and biochemical effects of rare earth elements on plants and their agricultural significance: A review. J. Plant Nutr. 27, 183–220 (2004).
3. Wang, L. et al. Rare earth elements activate endocytosis in plant cells. Proc. Natl. Acad. Sci. 111, 12936–12941 (2014).
4. Redling, K. Rare earth elements in agriculture with emphasis on animal husbandry. (Ludwig-Maximilians-Universität München, 2006).
5. Tyler, G. Rare earth elements in soil and plant systems - A review. Plant Soil 267, 191–206 (2004).
6. Tao, Y., Zhao, G., Yang, J., Ikeda, S., Jiang, J., Hu, T., Chen, W., Wei, Z., & Hong, F. Determination of double decker sandwich structured La-substituted chlorophyll a by EXAFS. J. Synchrotron Radiat. 8, 996–997 (2001).
7. Ciacci, L., Reck, B. K., Nassar, N. T., & Graedel, T. E. Lost by design. Environ. Sci. Technol. 49, 9443–9451 (2015).
8. Long, K. R., Van Gosen, B. S., Foley, N. K., & Cordier, D. The principal rare earth elements deposits of the United States: A summary of domestic deposits and a global perspective. U.S. Geological Survey Scientific Investigations Report 2010-5220 (2010).
9. Ramos, S. J., Dinali, G. S., Oliveira, C., Martins, G. C., Moreira, C. G., Siqueira, J. O., & Guilherme, L. R. G. Rare earth elements in the soil environment. 28–50 (2016).
10. Liang, T., Li, K., & Wang, L. State of rare earth elements in different environmental components in mining areas of China. Environ. Monit. Assess. 186, 1499–1513 (2014).
11. Zhenggui, W., Ming, Y., Xun, Z., Fashui, H., Bing, L., Ye, T., Guiwen, Z., & Chunhua, Y. Rare earth elements in naturally grown fern *Dicranopteris linearis* in relation to their variation in soils in South-Jiangxi region (Southern China). Environ. Pollut. 114, 345–355 (2001).
12. Wang, X., Lin, Y., Liu, D., Xu, H., Liu, T., & Zhao, F. Cerium toxicity, uptake and translocation in *Arabidopsis thaliana* seedlings. J. Rare Earths 30, 579–585 (2011).
13. Hu, X., Ding, Z., Chen, Y., Wang, X., & Dai, L. Bioaccumulation of lanthanum and cerium and their effects on the growth of wheat (*Triticum aestivum* L .) seedlings. Chemosphere 48, 621–629 (2002).
14. Pagano, G., Guida, M., Tommasi, F., & Oral, R. Health effects and toxicity mechanisms of rare earth elements - Knowledge gaps and research prospects. Ecotoxicol. Environ. Saf. 115, 40–48 (2015).
15. Pagano, G., Guida, M., Tommasi, F., & Oral, R. Health effects and toxicity mechanisms of rare earth elements—Knowledge gaps and research prospects. Ecotoxicol. Environ. Saf. 115, 40–48 (2015).
16. Kobayashi, Y., Ikka, T., Kimura, K., & Yasuda, O. Characterisation of lanthanum toxicity for root growth of *Arabidopsis thaliana* from the aspect of natural genetic variation. Funct. Plant Biol. 34, 984–994 (2007).
17. Ruiz-Herrera, L. F., Sanchez-Calderon, L., Herrera-Estrella, L., & Lopez-Bucio, J. Rare earth elements lanthanum and gadolinium induce phosphate-deficiency responses in *Arabidopsis thaliana* seedlings. Plant Soil 353, 231–247 (2012).
18. Liu, Y. Y., Wang, R. L., Zhang, P., Sun, L. L., & Xu, J. Involvement of reactive oxygen species in lanthanum-induced inhibition of primary root growth. J. Exp. Bot. 67, 6149–6159 (2016).
19. Wang, J., Wang, L., Hu, T., Li, W., & Xue, S. Effects of lanthanum on abscisic acid regulation of root growth in *Arabidopsis*. J. Rare Earths 32, 78–82 (2014).
20. Liu, M., Kilaru, A., & Hasenstein, K. H. Abscisic acid response of corn (*Zea mays* L.) roots and protoplasts to lanthanum. J. Plant Growth Regul. 27, 19–25 (2007).
21. Kumari, M., Taylor, G. J., & Deyholos, M. K. Transcriptomic responses to aluminum stress in roots of *Arabidopsis thaliana*. Mol. Genet. Genomics 279, 339–357 (2008).
22. Landa, P., Dytrych, P., Prerostova, S., Petrova, S., Vankova, R., & Vanek, T. Transcriptomic response of *Arabidopsis thaliana* exposed to CuO nanoparticles, bulk material, and ionic copper. Environ. Sci. Technol. 10814−10824 (2017).
23. Gomez-Sagasti, M. T., Barrutia, O., Ribas, G., Garbisub, C., & Becerril, J. M. Early transcriptomic response of *Arabidopsis thaliana* to polymetallic contamination : implications for the identification of potential biomarkers of metal exposure. Metallomics 8, 518–531 (2016).
24. Singh, S., Parihar, P., Singh, R., Singh, V. P., Prasad, S. M., & Antonio, C. Heavy metal tolerance in plants: Role of transcriptomics, proteomics, metabolomics, and ionomics. Front. Plant Sci. 6, 1–36 (2016).
25. Weber, M., Trampczynska, A., & Clemens, S. Comparative transcriptome analysis of toxic metal responses in *Arabidopsis thaliana* and the Cd^{2+}-hypertolerant facultative metallophyte *Arabidopsis halleri*. Plant. Cell Environ. 29, 950–963 (2006).
26. Conn, S. J. et al. Protocol: optimising hydroponic growth systems for nutritional and physiological analysis of *Arabidopsis thaliana* and other plants. Plant Methods 9, 4 (2013).
27. Yu, G., Wang, L.-G., Han, Y., & He, Q.-Y. clusterProfiler : an R Package for comparing biological. Omi. A J. Integr. Biol. 16, 284–

287 (2012).

28. Liu, Y., Sun, L., Zhang, P., Wan, J., & Wang, R. Lanthanum inhibits primary root growth by repressing auxin carrier abundances in *Arabidopsis*. Front. Plant Sci. 8, 1–9 (2017).
29. Nechushtai, R. et al. Characterization of *Arabidopsis* NEET reveals an ancient role for NEET proteins in iron metabolism. Plant Cell 24, 2139–2154 (2012).
30. Hanke, G. T., Kimata-ariga, Y., Taniguchi, I., & Hase, T. A post genomic characterization of ferredoxins. Plant Physiol. 134, 255–264 (2004).
31. Wang, M. et al. The major leaf ferredoxin Fd2 regulates plant innate immunity in *Arabidopsis*. Mol. Plant Pathol. 19, 1377–1390 (2018).
32. Ming Xu, X., Adams, S., Chua, N. H., & Møller, S. G. AtNAP1 represents an atypical SufB protein in *Arabidopsis* plastids. J. Biol. Chem. 280, 6648–6654 (2005).
33. Petit, J. M., Briat, J. F., & Lobréaux, S. Structure and differential expression of the four members of the *Arabidopsis thaliana* ferritin gene family. Biochem. J. 359, 575–82 (2001).
34. Oomen, R. J. F. J., Wu, J., Lelièvre, F., Blanchet, S., Richaud, P., Barbier-brygoo, H., Aarts, M. G. M., & Thomine, S. Functional characterization of NRAMP3 and NRAMP4 from the metal hyperaccumulator *Thlaspi caerulescens*. New Phytol. 637–650 (2009).
35. Haydon, M. J., Kawachi, M., Wirtz, M., Hillmer, S., Hell, R., & Krämer, U. Vacuolar nicotianamine has critical and distinct roles under iron deficiency and for zinc sequestration in *Arabidopsis*. Plant Cell 24, 724–37 (2012).
36. Brumbarova, T., Bauer, P., & Ivanov, R. Molecular mechanisms governing *Arabidopsis* iron uptake. Trends Plant Sci. 20, 124–133 (2015).
37. Tissot, N. et al. Transcriptional integration of the responses to iron availability in *Arabidopsis* by the bHLH factor ILR3. New Phytol. (2019).
38. Zhai, Z. et al. OPT3 is a phloem-specific iron transporter that is essential for systemic iron signaling and redistribution of iron and cadmium in *Arabidopsis*. Plant Cell 26, 2249–2264 (2014).
39. van de Mortel, J. E. et al. Large expression differences in genes for iron and zinc homeostasis, stress response, and lignin biosynthesis distinguish roots of *Arabidopsis thaliana* and the related metal Hyperaccumulator *Thlaspi caerulescens*. Plant Physiol. 142, 1127–1147 (2006).
40. Grillet, L., Lan, P., Li, W., Mokkapati, G., & Schmidt, W. IRON MAN is a ubiquitous family of peptides that control iron transport in plants. Nat. Plants 4, 953–963 (2018).
41. Waters, B. M., McInturf, S. A., & Stein, R. J. Rosette iron deficiency transcript and microRNA profiling methylation and chromatin patterning reveals links between copper and iron homeostasis in *Arabidopsis thaliana*. J. Exp. Bot. 63, 695–709 (2012).
42. Jr, R. J. D., Roberts, L. A., Sanderson, T., Eisley, R. B., & Walker, E. L. *Arabidopsis* Yellow Stripe-Like2 (YSL2): a metal-regulated gene encoding a plasma membrane transporter of nicotianamine-metal complexes. Plant J. 2, 403–414 (2004).
43. Tran, L. P. et al. Isolation and functional analysis of *Arabidopsis* stress-inducible NAC transcription factors that bind to a drought-responsive cis-element in the early responsive to dehydration stress 1 promoter. Plant Cell 16, 2481–2498 (2004).
44. Schmidt, W. & Buckhout, T. J. A hitchhiker's guide to the *Arabidopsis* ferrome. Plant Physiol. Biochem. 49, 462–470 (2011).
45. Buckhout, T. J., Yang, T. J. W., & Schmidt, W. Early iron-deficiency-induced transcriptional changes in *Arabidopsis* roots as revealed by microarray analyses. 16, 1–16 (2009).
46. Schindl, R., Weghuber, J., Romanin, C., & Schweyen, R. J. Mrs2p forms a high conductance Mg^{2+} selective channel in mitochondria. Biophys. J. 93, 3872–3883 (2007).
47. Weber, M., Harada, E., Vess, C., Roepenack-lahaye, E., & Ã, S. C. Comparative microarray analysis of *Arabidopsis thaliana* and *Arabidopsis halleri* roots identifies nicotianamine synthase, a ZIP transporter and other genes as potential metal hyperaccumulation factors. Plant J. 37, 269–281 (2004).
48. Abreu-neto, B. De, Turchetto-zolet, A. C., Felipe, L., & Oliveira, V. De. Heavy metal-associated isoprenylated plant protein (HIPP): characterization of a family of proteins exclusive to plants. FEBS J. 280, 1604–1616 (2013).
49. Eroglu, S., Meier, B., Wirén, N. Von, & Peiter, E. The vacuolar manganese transporter MTP8 determines tolerance to iron deficiency-induced chlorosis in *Arabidopsis*. Plant Physiol. 170, 1030–1045 (2016).
50. Liu, J., Sheng, L., Xu, Y., Li, J., Yang, Z., Huang, H., & Xu, L. WOX11 and 12 are involved in the first-step cell fate transition during de novo root organogenesis in *Arabidopsis*. Plant Cell 26, 1081–1093 (2014).
51. Lin, Q., Ohashi, Y., Kato, M., Tsuge, T., Gu, H., Qu, L.-J., & Aoyama, T. GLABRA2 directly suppresses basic helix-loop-helix transcription factor genes with diverse functions in root hair development. Plant Cell 27, tpc.15.00607 (2015).
52. Che, J., Yamaji, N., Shen, R. F., & Ma, J. F. An Al-inducible expansin gene, OsEXPA10 is involved in root cell elongation of rice. Plant J. 88, 132–142 (2016).
53. Sharples, S. C., Nguyen-Phan, T. C., & Fry, S. C. Xyloglucan endotransglucosylase/hydrolases (XTHs) are inactivated by binding to glass and cellulosic surfaces, and released in active form by a heat-stable polymer from cauliflower florets. J. Plant Physiol. 218, 135–143 (2017).
54. Chen, L., Tong, J., Xiao, L., Ruan, Y., Liu, J., Zeng, M., Huang, H., Wang, J. W., & Xu, L. YUCCA-mediated auxin biogenesis is required for cell fate transition occurring during de novo root organogenesis in *Arabidopsis*. J. Exp. Bot. 67, 4273–4284 (2016).
55. Liu, Y., Sun, L., Zhang, P., Wan, J., Wang, R., & Xu, J. Lanthanum inhibits primary root growth by repressing auxin carrier abundances in *Arabidopsis*. Front. Plant Sci. 8, 1–9 (2017).
56. Rosquete, M. R., Waidmann, S., & Kleine-Vehn, J. PIN7 auxin carrier has a preferential role in terminating radial root expansion in *Arabidopsis thaliana*. Int. J. Mol. Sci. 19, 1–11 (2018).
57. Weiland, M., Mancuso, S., & Baluska, F. Signalling via glutamate and GLRs in *Arabidopsis thaliana*. Functional Plant Biology 43, 1–25 (2016).
58. Swarbreck, S. M., Colaco, R., & Davies, J. M. Plant calcium-permeable channels. PLANT Physiol. 163, 514–522 (2013).
59. Kobayashi, Y., Kobayashi, Y., Sugimoto, M., Lakshmanan, V., Iuchi, S., Kobayashi, M., Bais, H. P., & Koyama, H. Characterization of the complex regulation of AtALMT1 expression in response to phytohormones and other inducers. Plant Physiol. 162, 732–40 (2013).
60. Afzal, Z., Howton, T., Sun, Y., & Mukhtar, M. The roles of aquaporins in plant stress responses. J. Dev. Biol. 4, 9 (2016).
61. Sawaki, K., Sawaki, Y., Zhao, C. R., Kobayashi, Y., & Koyama, H. Specific transcriptomic response in the shoots of *Arabidopsis thaliana* after exposure to Al rhizotoxicity: - potential gene expression biomarkers for evaluating Al toxicity in soils. Plant Soil 409, 131–142 (2016).

62. Lešková, A., Giehl, R. F. H., Hartmann, A., Fargašová, A., & von Wirén, N. Heavy metals induce iron deficiency responses at different hierarchic and regulatory levels. Plant Physiol. 174, 1648–1668 (2017).

63. Gruber, B. D., Giehl, R. F. H., Friedel, S., & von Wiren, N. Plasticity of the *Arabidopsis* root system under nutrient deficiencies. PLANT Physiol. 163, 161–179 (2013).

64. Vermeer, J. E. M. & Geldner, N. Lateral root initiation in *Arabidopsis thaliana*: a force awakens. F1000Prime Rep. 7, 1–7 (2015).

65. Fu, Y., Li, F., Xu, T., Cai, S., Chu, W., Qiu, H., Sha, S., Cheng, G., & Xu, Q. Bioaccumulation, subcellular, and molecular localization and damage to physiology and ultrastructure in *Nymphoides peltata* (Gmel.) O. Kuntze exposed to yttrium. Environ. Sci. Pollut. Res. 21, 2935–2942 (2014).

66. Liang, C. & Wang, W. Antioxidant response of soybean seedlings to joint stress of lanthanum and acid rain. Environ. Sci. Pollut. Res. 20, 8182–8191 (2013).

67. Rico, C. M. et al. Cerium oxide nanoparticles modify the antioxidative stress enzyme activities and macromolecule composition in rice seedlings. Environ. Sci. Technol. 47, 14110–14118 (2013).

68. Jiang, N., Wang, L., Lu, T., & Huang, X. Toxic effect of terbium ion on horseradish cell. Biol. Trace Elem. Res. 143, 1722–1728 (2011).

69. Mendoza-Cózatl, D. G., Jobe, T. O., Hauser, F., & Schroeder, J. I. Long-distance transport, vacuolar sequestration, tolerance, and transcriptional responses induced by cadmium and arsenic. Current Opinion in Plant Biology 14, 554–562 (2011).

70. Gilliham, M., Campbell, M., Dubos, C., Becker, D., & Davenport, R. The *Arabidopsis thaliana* glutamate-like receptor family (AtGLR). in Communication in Plants (ed. F. Baluška, S. Mancuso, D. V. (Eds. .) 187–204 (2006).

71. Vincill, E. D., Clarin, A. E., Molenda, J. N., & Spalding, E. P. Interacting glutamate receptor-like proteins in phloem regulate lateral root initiation in *Arabidopsis*. Plant Cell 25, 1304–1313 (2013).

72. Lewis, B. D. & Spalding, E. P. Nonselective block by La^{3+} of *Arabidopsis* ion channels involved in signal transduction. J. Membr. Biol. 162, 81–90 (1998).

73. Lansman, J. B. Blockade of current through single calcium channels by trivalent lanthanide cations. Effect of ionic radius on the rates of ion entry and exit. J. Gen. Physiol. 95, 679–696 (1990).

74. Doustaly, F., Combes, F., Fie, J. B., Berthet, S., Bastien, O., Leonhardt, N., Rivasseau, C., & Vavasseur, A. Uranium perturbs signaling and iron uptake response in *Arabidopsis thaliana* roots. Metallomics 6, 809–821 (2014).

75. Mazari, K., Landa, P., Přerostová, S., Müller, K., Vaňková, R., Soudek, P., & Vaněk, T. Thorium impact on tobacco root transcriptome. J. Hazard. Mater. 325, 163–169 (2017).

76. He, X. L., Fan, S. K., Zhu, J., Guan, M. Y., Liu, X. X., Zhang, Y. S., & Jin, C. W. Iron supply prevents Cd uptake in *Arabidopsis* by inhibiting IRT1 expression and favoring competition between Fe and Cd uptake. Plant Soil 416, 453–462 (2017).

77. Vert, G. A., Briat, JF, C. Dual regulation of the *Arabidopsis* high-affinity root iron uptake system by local and long-distance signals. Plant Physiol. 132, 796–804 (2003).

78. Gebert, M., Meschenmoser, K., Svidova, S., Weghuber, J., Schweyen, R., Eifler, K., Lenz, H., Weyand, K., & Knoop, V. A root-expressed magnesium transporter of the MRS2/MGT gene family in *Arabidopsis thaliana* allows for growth in low-Mg^{2+} environments. Plant Cell 21, 4018–4030 (2009).

79. Ishijima, S., Manabe, Y., Shinkawa, Y., Hotta, A., Tokumasu, A., Ida, M., & Sagami, I. The homologous *Arabidopsis* MRS2/MGT/CorA-type Mg^{2+} channels, AtMRS2-10 and AtMRS2-1 exhibit different aluminum transport activity. Biochim. Biophys. Acta - Biomembr. 1860, 2184–2191 (2018).

80. Lee, M., Lee, K., Lee, J., Noh, E. W., & Lee, Y. AtPDR12 contributes to lead resistance in *Arabidopsis*. Plant Physiol. 138, 827–836 (2005).

81. Kim, D. Y., Bovet, L., Maeshima, M., Martinoia, E., & Lee, Y. The ABC transporter AtPDR8 is a cadmium extrusion pump conferring heavy metal resistance. Plant J. 50, 207–218 (2007).

82. Miyaharan, K., Mizunuma, M., Hirata, D., Tsuchiya, E., & Miyakawa, T. The involvement of the *Saccharomyces cerevisiae* multidrug resistance transporters Pdr5p and Snq2p in cation resistance. FEBS Lett. 399, 317–320 (1996).

83. Dong, J., Piñeros, M. A., Li, X., Yang, H., Liu, Y., Murphy, A. S., Kochian, L. V, & Liu, D. An *Arabidopsis* ABC transporter mediates phosphate deficiency-induced remodeling of root architecture by modulating iron homeostasis in roots. Mol. Plant 10, 244–259 (2017).

84. Chu, H. H., Car, S., Socha, A. L., Hindt, M. N., Punshon, T., & Guerinot, M. Lou. The *Arabidopsis* MTP8 transporter determines the localization of manganese and iron in seeds. Sci. Rep. 7, 1–10 (2017).

85. Andres-Colas, N., Sancenon, V., Rodrigues-Navarro, S., Mayo, S., Thiele, D. J., Ecker, J. R., Puig, S., & Penarrubia, L. The *Arabidopsis* heavy metal P-type ATPase HMA5 interacts with metallochaperones and functions in copper detoxification of roots. Plant J. 45, 225–236 (2006).

86. Guo, W. J., Bundithya, W., & Goldsbrough, P. B. Characterization of the *Arabidopsis* metallothionein gene family: Tissue-specific expression and induction during senescence and in response to copper. New Phytol. 159, 369–381 (2003).

87. Guo, W.-J., Meetam, M., & Goldsbrough, P. B. Examining the specific contributions of individual *Arabidopsis* metallothioneins to copper distribution and metal tolerance. Plant Physiol. 146, 1697–1706 (2008).

88. Ding, S., Liang, T., Zhang, C., Huang, Z., Xie, Y., & Chen, T. Fractionation mechanisms of rare earth elements (REEs) in hydroponic wheat : an application for metal accumulation by plants. Environ. Sci. Technol. 40, 2686–2691 (2006).

89. Ding, S. M., Liang, T., Zhang, C. S., Yan, J. C., & Zhang, Z. L. Accumulation and fractionation of rare earth elements (REEs) in wheat: Controlled by phosphate precipitation, cell wall absorption and solution complexation. J. Exp. Bot. 56, 2765–2775 (2005).

90. Ding, S. M., Liang, T., Yan, J. C., Zhang, Z. L., Huang, Z. C., & Xie, Y. N. Fractionations of rare earth elements in plants and their conceptive model. Sci. China, Ser. C Life Sci. 50, 47–55 (2007).

91. Yuan, M. et al. The accumulation and fractionation of rare earth elements in hydroponically grown *Phytolacca americana* L. Plant Soil 421, 67–82 (2017).

92. Wu, J., Chen, A., Peng, S., Wei, Z., & Liu, G. Identification and application of amino acids as chelators in phytoremediation of rare earth elements lanthanum and yttrium. Plant Soil 373, 329–338 (2013).

93. Wu, J. L., Wei, Z. G., Zhao, H. Y., Li, H. X., & Hu, F. The role of amino acids in the long-distance transport of La and Y in the xylem sap of tomato. Biol. Trace Elem. Res. 129, 239–250 (2009).

94. Sasaki, T., Tsuchiya, Y., Ariyoshi, M., Ryan, P. R., & Yamamoto, Y. A chimeric protein of aluminum-activated malate transporter

generated from wheat and Arabidopsis shows enhanced response to trivalent cations. Biochim. Biophys. Acta 1858, 1427–1435 (2016).

95. Preston, G. M., Sup JungS, J., Gugginoll, W. B., & Agre, P. The Mercury-sensitive Residue at Cysteine 189 in the CHIP28 water channel. J. Biol. Chem. 268, 17–20 (1993).
96. Taylor, A. F., Rylott, E. L., Anderson, C. W. N., & Bruce, N. C. Investigating the toxicity, uptake, nanoparticle formation and genetic response of plants to gold. PLoS One 9, (2014).
97. Christa, M. N. & Tyerman, S. D. New potent inhibitors of aquaporins : silver and gold compounds inhibit aquaporins of plant and human origin. FEBS Lett. 531, 443–447 (2002).
98. Péret, B. et al. Auxin regulates aquaporin function to facilitate lateral root emergence. Nat. Cell Biol. 14, 1–9 (2012).
99. Xu, W. et al. Arabidopsis NIP3;1 plays an important role in arsenic uptake and root-to-shoot translocation under arsenite stress conditions. Mol. Plant 8, 722–733 (2015).
100. Wang, Y. et al. NIP1;2 is a plasma membrane-localized transporter mediating aluminum uptake, translocation, and tolerance in *Arabidopsis*. Proc. Nati. Acad. Sci. USA 114, 5047–5052 (2017).

ADDITIONAL FILES

https://bul.univ-lorraine.fr/index.php/s/bw9Z1eICcwtb2w5

Table S1: DEG in shoots of Arabidopsis exposed to REE. Padj in grey represent non-significant genes (padj<0.01).

Table S2: DEG in roots of Arabidopsis exposed to REE. Padj in grey represent non-significant genes (padj<0.001).

Table S3: GO BP enriched in leaves of Arabidopsis exposed to REE (p-val<0.05). f is the total number of genes in each category and the counts is the number of DEG allocated in each category.

Table S4: GO BP enriched in roots of Arabidopsis exposed to REE (p-val<0.05). f is the total number of genes in each category and the counts is the number of DEG allocated in each category.

Chapter II.2:

Heavy for the shoots: rare earth element accumulation and fractionation are conserved traits in the *Phytolacca* genus

Heavy for the shoots: rare earth element accumulation and fractionation are conserved traits in the *Phytolacca* genus

(Manuscript submitted for publication)

Nicolas Grosjean[1,2], Marie Le Jean[2], Charlotte Berthelot[1,3], Michel Chalot[4,5], Elisabeth Maria Gross[2], Damien Blaudez[1*]

[1]Université de Lorraine, CNRS, LIEC, F-54000 Nancy, France. [2]Université de Lorraine, CNRS, LIEC, F-57000 Metz, France. [3]CTIFL, ZI Belle Etoile, F-44483 Carquefou, France. [4]Université de Bourgogne Franche-Comté, UMR CNRS 6249 Laboratoire Chrono-environnement, F-25211, Montbéliard, France. [5]Université de Lorraine, F-54000 Nancy, France.

Abstract

Rare earth elements (REEs) are now considered emerging pollutants in the environment. *Phytolacca americana*, a REE hyperaccumulating plant, has been proposed for the remediation of REE-contaminated soils. However, there is no REE-related information for other *Phytolacca* species. Here, we considered five species (*P. americana*, *P. acinosa*, *P. clavigera*, *P. bogotensis,* and *P. icosandra*) for their response to REEs. REE accumulation and fractionation traits were both in the same order of magnitude among the five species. Heavy REEs were preferentially transferred to leaves relatively to light REEs. Regardless of the species, lateral root length and chlorophyll content decreased under REE exposure and lateral roots and foliar anthocyanins increased. However, plants were poorly subjected to oxidative stress. Finally, REE exposure strongly modulated the ionome of roots, and to a lesser extent that of leaves with a negative correlation between REE and Mn contents. In conclusion, our study brings new data on the response of several *Phytolacca* species to REEs. Moreover, we highlighted that the REE accumulation trait was conserved among the *Phytolacca* species. Thus, it represents a valuable information for phytoremediation of REE-contaminated sites since the most appropriate *Phytolacca* species could be selected depending on the climatic/pedological area to be remediated.

Keywords: lanthanides, *Phytolacca*, ionome, rare earth elements, hyperaccumulating plant, rare earth fractionation

Introduction

The Rare Earth Elements (REEs) are a group of 17 metallic elements gathering the 15 lanthanides plus yttrium and scandium. REEs can be further split into two groups known as the light REEs (LREEs, spanning from lanthanum (La) to europium (Eu), plus scandium (Sc)) and the heavy REEs (HREEs, spanning from gadolinium (Gd) to lutetium (Lu), plus yttrium (Y)). REEs are widely found in the Earth's crust. Cerium (Ce), La, neodymium (Nd) and Y are the most abundant REEs and can be found at concentrations similar to those of Zn, Cu, Ni and Mo among others[1]. A fast increase in the demand and subsequent production of REEs has been observed over the past decades because of their diverse uses in new technologies, green energies and medical devices[2]. Moreover, the very low recyclability for these elements[3], their use as food additives for livestock and poultry[4], their spreading as fertilizers in agriculture[1] or as eutrophication regulators[5], along with the high soil concentrations found in mining areas[6,7] lead REEs to be considered as emerging pollutants.

Although these elements are not essential to plants, REEs can be detected at moderate concentrations under non-contaminated conditions in plant tissues. REE concentrations in leaves ranged from 0.0011 (Lu) to 0.33 mg/kg DW (Ce)[8] and even up to 5 mg REE/kg DW[9]. However, as reported for other metals, several plant species, mainly ferns, are able to accumulate REEs. Two fern species displayed the highest REE accumulation potential. *Dicranopteris dichotoma* (syn. *D. linearis*), accumulated up to 0.7% DW of LREEs[6,10] and *Pronephrium simplex* accumulated 1.2 g REE/kg DW[11,12]. To a lesser extent, other ferns could also accumulate REEs, such as *Dryopteris erythrosora*[9], *Blechnum orientale*[13,14] or *Athyrium yokoscense*[15]. Even though ferns are highly represented, a few Angiosperms are also known to accumulate REEs. *Carya tomentosa* (mockernut) accumulated REEs up to 859 mg/kg in a non-contaminated environment[14,16]. *Phytolacca americana* (pokeweed), first identified as a Mn hyperaccumulator[17–19], with a Mn accumulation up to 2000 mg REE/kg DW on non-contaminated soils[17],was further reported as a REE accumulator[15,20].

In comparison to other REE-accumulating species, *P. americana* is a fast growing and high-biomass producing plant that can reach 3 m height. This ubiquitous weed of roadsides and disturbed areas in its native range of the southeastern United States is now distributed worldwide[17]. Notably, this species was found at a REE mining site in south Jiangxi Province in China, with an average REE concentration of around 250 mg/kg

in leaves, reaching up to 1,040 mg/kg[7]. Recently, several studies investigated the translocation and fractionation of REEs in *P. americana*. Yuan et al. (2017, 2018) observed a higher translocation of HREEs in the leaves compared to LREEs, while more LREEs accumulated in the roots and stems. Organic or amino acids have been suggested for complexing REEs and participating in the long-distance transport of these elements in *P. americana*[20,21]. Combined, these features would be of great interest for phytoremediation of REE contaminated soils. In addition, REEs extracted from plant could be further purified[22] or used for ecocatalysis[23].

Combining ecological and genetic analyses on *P. americana*, no genetic differentiation could be detected between populations from Mn-contaminated and uncontaminated sites[24], suggesting that phenotypic plasticity is probably the major contributor to the successful colonization of marginal lands, such as metal-contaminated soils. The related species *P. acinosa*[25,26] is also a Mn hyperaccumulator, showing that the Mn hyperaccumulation trait is found in different species of *Phytolacca*. Similar findings were reported concerning the Ni hyperaccumulation trait in several species of *Alyssum* and *Cochlearia*[27]. Likewise, several *Carya*

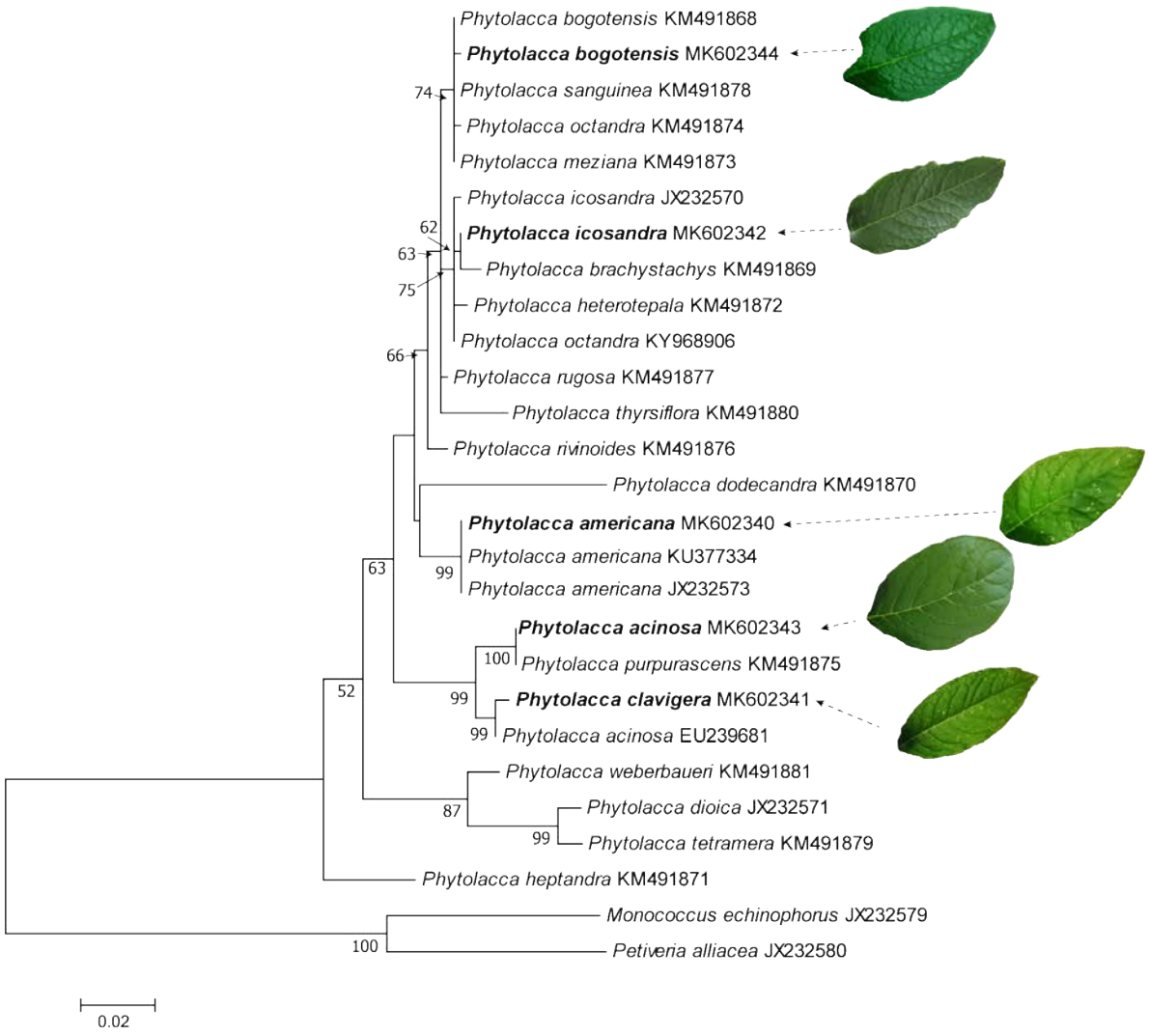

Figure 1. Maximum likelihood phylogram for the identification of *Phytolacca* species used based on ITS1-5.8S-ITS2 sequences. Aligned sequences using ClustalW were used to build a Maximum likelihood tree based on the Kimura 2-parameter method. Bootstrap values over 50% (1000 replicates) are indicated below the branches. Analyses were conducted in MEGA7[54]. ITS sequences of the *Phytolacca* species used in this study are indicated in bold and compared with other *Phytolacca* species available in GeneBank. *Monococcus echinophorus* and *Petiveria alliacea* were used as outgroups. Leaf morphology of the tested species is shown.

species accumulated similar REE concentrations in leaves[16], therefore highlighting that the REE accumulation trait could be conserved throughout the *Carya* genus. However, the conservation of this REE accumulation potential has not yet been investigated for *Phytolacca* species other than *P. americana*.

Consequently, we propose the hypothesis of a monophyletic REE accumulation trait within the *Phytolacca* genus. Therefore, we analysed the REE accumulation potential as well as the REE fractionation pattern of five *Phytolacca* species (*P. americana, P. acinosa, P. bogotensis, P. clavigera* and *P. icosandra*). Our analyses aimed to reveal also how REE accumulation in these species of *Phytolacca* modified the elemental composition of roots and shoots. In addition, analyses were performed to study the effects of REEs on a set of biomarkers related to modification of root architecture, leaf pigment composition and oxidative stress.

Results & Discussion

Molecular confirmation of the *Phytolacca* species

Seeds from five species of Phytolacca were obtained from commercial or institutional origins as described in the material and methods section, and identified as *P. americana*, *P. acinosa, P. bogotensis*, *P. clavigera*, and *P. icosandra*. The identification of these species was based on morphological traits. However, due to the ambiguous taxonomy within the *Phytolacca* genus[28], we performed a molecular investigation to confirm that the species tested were different. To this purpose, the ITS region was amplified, sequenced and compared with ITS sequences of *Phytolacca* species retrieved from GeneBank. For most species there was a single ITS sequence available in the database, and even none for *P. clavigera* (Fig. 1). For *P. bogotensis*, *P. icosandra* and *P. americana*, our data matched to the previously published ITS sequences for these species. However, it was less straightforward for *P. acinosa* and *P. clavigera*, where a mis-identification might have been made. Facing this problem, we analysed a second seed batch of *P. acinosa* obtained from a different supplier. Both plant morphology and ITS sequences were identical for the two batches suggesting a correct identification of *P. acinosa*. Noteworthy, different leaf morphologies were observed between *P. acinosa* and *P. clavigera* (Fig. 1), which shared the highest identity (97%). Leaves of *P. acinosa* were obovate whereas the four other species had oval shaped leaves. In conclusion, the molecular analyses confirm that the five species tested were different. Sequence data were deposited in GenBank under the following accession numbers: MK602340 (*P. americana*), MK602343 (*P. acinosa*), MK602344 (*P. bogotensis*), MK602341 (*P. clavigera*), and MK602342 (*P. icosandra*).

The REE accumulation trait was shared among *Phytolacca* species

We first investigated the potential of the different *Phytolacca* species to accumulate REEs in their tissues. To this aim, *Phytolacca* seedlings were grown hydroponically and exposed to a mixture of 16 REEs, supplied at equimolar concentrations. We used two different REE concentrations, a low and a high concentration (10 and 100 µM), pre-determined from preliminary experiments (data not shown), for which biomass was either not affected or reduced. Indeed, at the concentration of 10 µM REEs in the nutrient solution (REE10), no negative effect was observed for root, shoot and total plant biomass for any species (Fig. 2). A significant positive effect on shoot biomass of *P. icosandra* and root biomass of *P. americana* was even

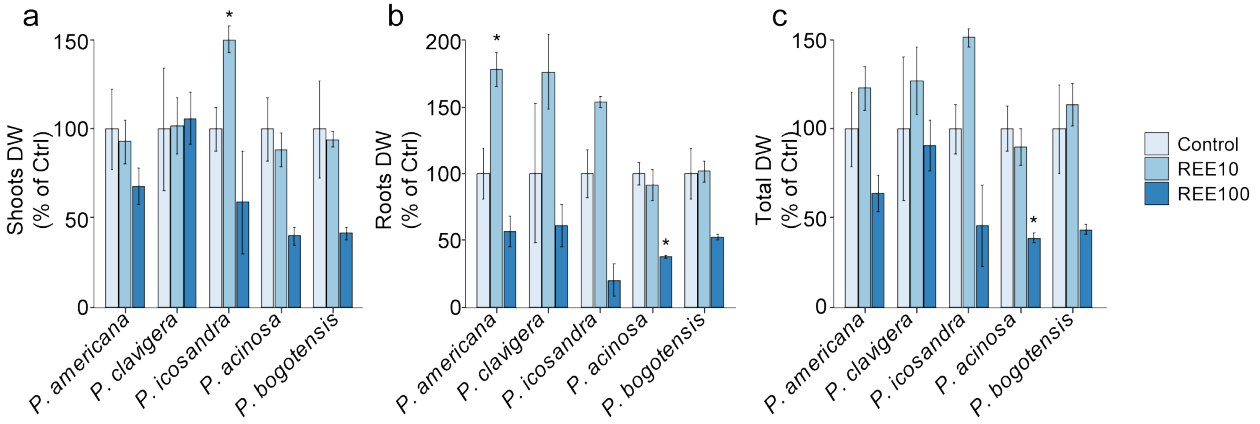

Figure 2. Effect of REEs on the biomass of *Phytolacca* species. Biomass (DW) is expressed as percentage of that of the control (no REE) in shoots (a), roots (b) and total plant (c) exposed to 10 µM or 100 µM REEs (REE10 and REE100, respectively). The data are the means (± SE) of n=3 (control, REE10) or n=4 (REE100) plants. Significant differences from the control condition are indicated by asterisks (P<0.05, t-test).

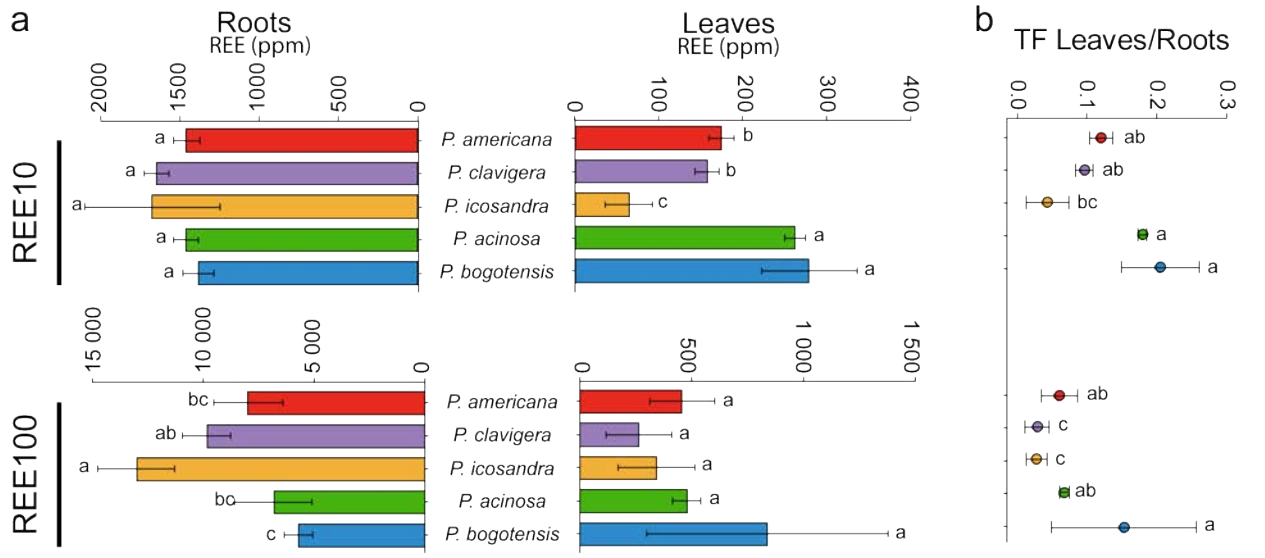

Figure 3. REE accumulation by five *Phytolacca* species. Plants were exposed to a mixture of 10 µM or 100 µM REEs (REE10 and REE100, respectively). (a) REE concentrations in roots and leaves of *Phytolacca* species. (b) Translocation factor (TF) of REEs from the roots to the leaves. The data are the means (± SD) of n=3 (REE10) or n=4 (REE100). Within a given treatment, values with the same letter are not significantly different (P<0.05, ANOVA, Tukey HSD).

observed at this lowest concentration. Conversely, at 100 µM REEs (REE100), biomass tended to decrease by about 50% for most species, despite not being always significant (Fig. 2). These results suggest a similar REE tolerance level of the five *Phytolacca* species.

Then, REE accumulation was determined by ICP-MS and results are given in Figure 3. At REE10, the five species accumulated approximately 1500 mg/kg REEs in the roots and no significant difference was observed between the species (Fig. 3a). However, at REE100, an overall higher accumulation was found and differences between species could be noted (Fig. 3a). *Phytolacca icosandra* displayed the highest concentration, of about 13,000 mg/kg REEs, while *P. acinosa* and *P. bogotensis* accumulated 2.4 and 2.3 times less REEs, respectively (Fig. 3a). *P. clavigera* and *P. americana* had intermediate concentrations in their roots.

In leaves, the patterns of REE accumulation differed from those of roots. At REE10, *P. bogotensis* and *P. acinosa* were the two species accumulating the highest concentrations of REEs, with respectively 279 and 261 mg/kg. *Phytolacca americana* and *Phytolacca clavigera* accumulated slightly less, with 174 and 157 mg/kg, respectively, while the lowest concentration was recorded for *P. icosandra*, with less than 100 mg/kg (Fig. 3a). However, those variations were not observed at REE100. Despite a mean accumulation value ranging from 265 mg/kg (*P. clavigera*) to 837 mg/kg (*P. bogotensis*), the differences were indeed not significantly different (Fig. 3a). Our results with *P. americana* are consistent with those from a previous study, carried out with the same species also grown hydroponically, where a similar REE accumulation capacity was reported[21]. As a comparison, *P. americana* accumulated in the leaves around 300 and 500 mg/kg REEs when exposed to 10 and 100 µM REEs, respectively[21].

For each species, the translocation factor (TF) of REEs from roots to leaves was further calculated (Fig. 3b). Under both REE concentrations, *P. acinosa* and *P. bogotensis* had the highest TFs, whereas *P. clavigera* and *P. icosandra* had the lowest TFs. However, TF values were in the same range and relatively low differences were found between the species (Fig. 3b). Moreover, our data are in agreement with those described by Yuan *et al.* (2017) for *P. americana*, where a TF of approximately 0.1 was reported[21].

Overall, our results suggest that the accumulation of REEs in the leaves and their translocation from roots to shoots are of the same order of magnitude in the five *Phytolacca* species.

HREEs were preferentially translocated to leaves in the five *Phytolacca* species

We further investigated whether various REE fractionation patterns (LREEs *vs* HREEs) could be mediated by the different *Phytolacca* species. Therefore, we analysed the fractionation pattern of the whole set of REEs in both roots and shoots of the five species. To compare the fractionation process for various REE species mediated by different plant species, we took profit of our hydroponic system to meet equimolar concentrations of all REE species in the nutritive medium. The data of REE fractionation are given in Fig.

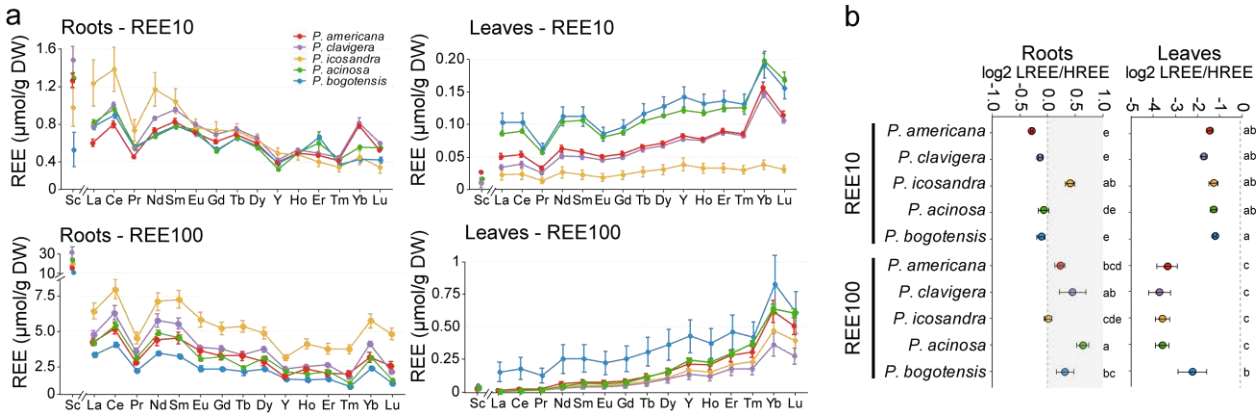

Figure 4. REE fractionation in roots and leaves of *Phytolacca* species. Plants were exposed to a mixture of 10 µM or 100 µM REEs (REE10 and REE100, respectively). (a) REE concentration patterns in roots and leaves of *Phytolacca* species (the linkage of data points does not indicate dependence). (b) Concentration ratios of LREEs (Sc, La to Eu) over HREEs (Gd to Lu, Y) among the species tested and exposed either to 10 µM or 100 µM as indicated. The data are the means (± SD) of n=3 (REE10) or n=4 (REE100). Within a given treatment, values with the same letter are not significantly different (P<0.05, ANOVA, Tukey HSD).

4a. REEs are ordered by decreasing ionic radius at their trivalent oxidation state. The non-lanthanide Y, generally included in the HREEs, thus ranged between Dy and Ho. Interestingly, the five *Phytolacca* species displayed very similar REE accumulation patterns. In roots, REE concentration decreased from La to Lu (Fig. 4a). Conversely, in leaves, REE concentration increased from La to Lu (Fig. 4a). These conclusions were true regardless of the *Phytolacca* species and the REE concentration (REE10, REE100). The only exceptions were praseodynium (Pr) and ytterbium (Yb) for which anomalies could be evidenced. However, these anomalies were similar in the five *Phytolacca* species.

We further analysed the accumulation ratios between LREEs and HREEs (Fig. 4b). At REE10, there was no particular enrichment of LREEs *versus* HREEs in roots. At REE100, and except *P. icosandra*, a slight LREE enrichment in roots was found for the different *Phytolacca* species. Conversely, leaves were highly enriched in HREEs whatever the *Phytolacca* species considered. At REE10, HREE concentration was indeed between 2 to 4 times higher than that of LREEs. This enrichment was more pronounced at REE100, where HREEs were from 5 (*P. bogotensis*) to 13 (*P. clavigera*) times more abundant than LREEs (Fig. 4b). Altogether, the data indicated a preferential root-to-leaf translocation of HREEs *vs* LREEs, a trait that was conserved in the five *Phytolacca* species.

The preferential translocation of HREEs to shoots had already been observed for *P. americana* grown either under hydroponic conditions or naturally in REE-mining areas[7,21]. In non-accumulator species, a higher transfer of HREEs *vs* LREEs had also been reported in several Angiosperms, notably wheat[29,30], soybean[31] and rice[32]. Conversely, LREE enrichment in shoots has been reported in fern species accumulating REE. Likewise, non-accumulating ferns also had a higher content of LREEs than HREEs (Grosjean N., personal communication). Therefore, the different fractionation patterns described above are very unlikely related to the REE accumulation trait. More probably, Angiosperms and Pteridophytes, which are evolutionary very distant, might not share the same mechanisms underlying REE translocation from roots to shoots. Such different fractionation processes could be explained by the production of specific compounds with distinct REE-chelating properties. This hypothesis was supported by previous works which reported that the REE-accumulating fern *D. dichotoma* produces a specific LREE-binding peptide[33] and that HREE enrichment in the shoots of *P. americana* was associated to the long-distance transport of HREE-organic acid complexes, such as HREE-citrate[21]. However, to test this hypothesis, further studies investigating the ligands associated to REEs in the xylem sap of a panel of Angiosperms and Pteridophytes would be needed.

REEs impacted the root architecture

It has already been reported that high concentrations of La can inhibit root elongation and induce lateral root development in *Arabidopsis thaliana*[34]. This mechanism was explained by the accumulation of reactive oxygen species (ROS) in the root tip, leading to the death of cells from the primary root tips and reorientation of auxin to lateral roots[34,35]. Thus, in order to verify whether root elongation and branching were also affected by a mixture of REEs, the root

Table 1. Total Antioxidant Capacity (TAC) and Malondialdehyde (MDA) contents in leaves and roots of plants exposed to REEs. *Phytolacca* species were exposed to a mixture of 10 µM (REE10) (n=3) or 100 µM REEs (REE100) (n=4). Values are means ± SD. Within a given species, significant differences between treatments are indicated by different letters (P<0.05, ANOVA Tukey HSD).

		Treatment	*P. americana*	*P. clavigera*	*P. icosandra*	*P. acinosa*	*P. bogotensis*
Leaves	TAC (nmol/ mg FW)	Control	5.06 ± 0.43 a	4.40 ± 0.67 b	4.66 ± 1.42 a	3.50 ± 1.98 a	2.92 ± 0.08 a
		REE - 10	6.82 ± 1.23 a	5.53 ± 0.09 a	6.94 ± 0.63 a	3.73 ± 0.72 a	2.65 ± 0.13 a
		REE - 100	6.05 ± 0.69 a	3.35 ± 0.30 c	6.53 ± 1.63 a	4.04 ± 1.10 a	2.62 ± 0.60 a
	MDA (nmol/ mg FW)	Control	1.04 ± 0.06 a	0.81 ± 0.05 a	0.66 ± 0.18 b	0.98 ± 0.13 a	1.16 ± 0.14 a
		REE - 10	1.09 ± 0.18 a	1.35 ± 0.71 a	1.08 ± 0.16 a	0.42 ± 0.05 b	0.47 ± 0.12 b
		REE - 100	0.86 ± 0.15 a	0.85 ± 0.07 a	0.94 ± 0.09 ab	0.84 ± 0.16 a	1.20 ± 0.12 a

		Treatment	*P. americana*	*P. clavigera*	*P. icosandra*	*P. acinosa*	*P. bogotensis*
Roots	TAC (nmol/ mg FW)	Control	0.55 ± 0.07 a	0.60 ± 0.12 ab	0.47 ± 0.03 a	0.64 ± 0.06 b	0.48 ± 0.30 a
		REE - 10	0.63 ± 0.20 a	0.70 ± 0.15 a	0.46 ± 0.07 a	1.00 ± 0.05 a	0.41 ± 0.05 a
		REE - 100	0.99 ± 0.49 a	0.38 ± 0.05 b	0.33 ± 0.29 a	0.70 ± 0.11 b	0.62 ± 0.20 a
	MDA (nmol/ mg FW)	Control	0.16 ± 0.02 a	0.20 ± 0.09 a	0.09 ± 0.02 a	0.16 ± 0.03 a	0.17 ± 0.01 a
		REE - 10	0.30 ± 0.20 a	0.34 ± 0.13 a	0.11 ± 0.02 a	0.15 ± 0.05 a	0.09 ± 0.03 a
		REE - 100	0.18 ± 0.04 a	0.19 ± 0.02 a	0.14 ± 0.02 a	0.23 ± 0.10 a	0.22 ± 0.05 a

architecture of the five *Phytolacca* species was analysed after exposure to 10 and 100 µM REEs and compared to control plants (Fig. 5). The overall root architecture of the different species was relatively similar under the control condition (Fig. 5a). The addition of REEs triggered modifications in the root architecture that was characterized by shorter lateral roots compared to the control condition (Fig. 5a). At REE10, morphological differences were noticed for *P. clavigera*, *P. icosandra*, and *P. acinosa* when compared to non-exposed plants. These differences were much less obvious for *P. bogotensis* and *P. americana*. However, at REE100, the root architecture of all species was more impacted even if *P. americana* was the less affected species (Fig. 5a). The quantification of both the density and length of lateral roots confirmed the visual observations (Fig. 5b-c). The number of lateral roots indeed increased under REE exposure. However, for both *P. americana* and *P. bogotensis*, the values were only significantly different when comparing the control and REE100 conditions (Fig. 5b). Similarly, with increasing REE concentrations, the lateral root length decreased, with the exception of *P. americana* that was not affected at REE10 when compared to the control (Fig. 5c). In conclusion, analysis of the root architecture of the different species allowed us to show that, despite a similar REE accumulation rate for the species tested, *P. americana* was the one least affected by REEs.

Phytolacca species were poorly subjected to oxidative stress under REE exposure

We further selected two markers related to oxidative stress, namely the malondialdehyde (MDA) concentration and the total antioxidant capacity (TAC), to investigate the effect of REE exposure in the five species (Table 1).

TAC represents the non-enzymatic antioxidant capacity, and is indicative of the ability to counteract oxidative stress-induced damage in cells. In both roots and leaves of the different species, only few differences were found among the different treatments (Table 1). Indeed, REE exposure only impacted the TAC (1.3 fold compared to the control) in leaves of *P. clavigera*. Similarly, in roots of *P. acinosa*, the TAC content increased by 1.6 fold at REE10 when compared to the control (Table 1).

The quantification of MDA, one of the end products of the chain reaction of lipid peroxidation, allows to estimate the potential oxidative damages. No significant change was observed in roots under REE exposure, whatever the species considered. In leaves of *P. acinosa* and *P. bogotensis* MDA concentration decreased by 2.5 fold at REE10, and to a lesser extent (1.3 fold) in *P. acinosa* at REE100. Conversely, it slightly increased (1.6 fold) in leaves of *P. icosandra* at REE10 (Table 1).

Combined, MDA and TAC analyses suggest that *Phytolacca* species were not or only slightly affected by oxidative stress when exposed to REEs. Conversely, several studies have demonstrated the generation of REE-induced oxidative stress in plant species that are not REE

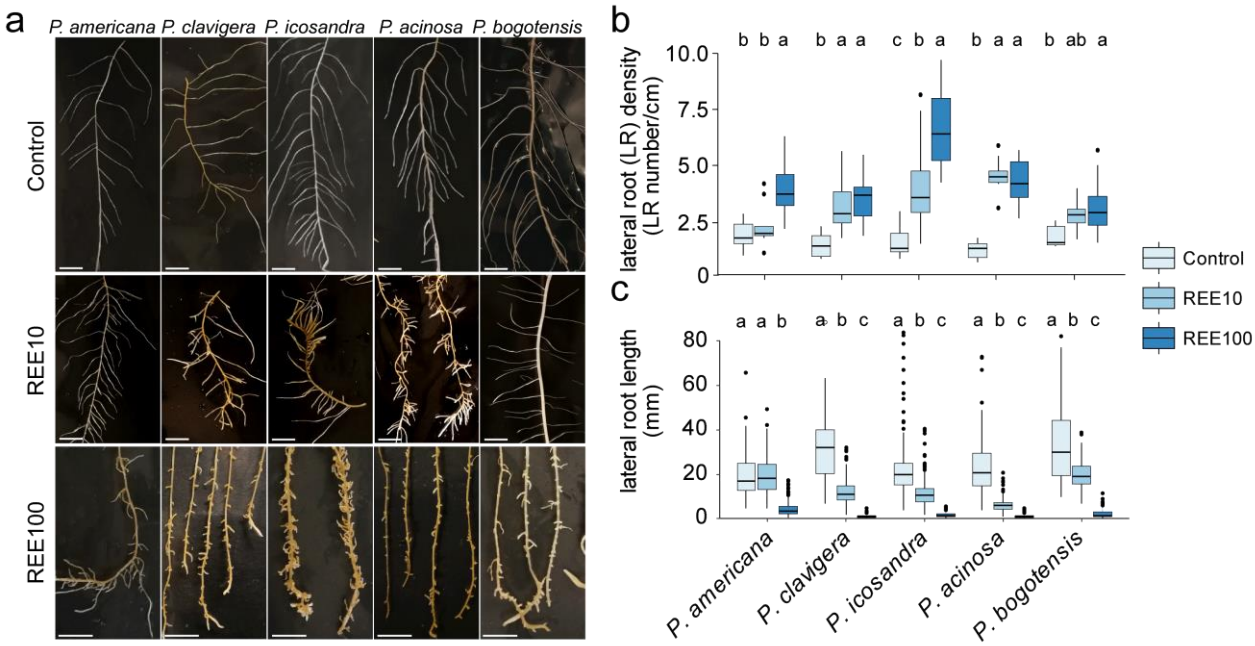

Figure 5. Effect of REEs on the root architecture of *Phytolacca* species. (a) Architecture of representative roots (scale bars = 1 cm), (b) lateral root branching (expressed as the number of lateral roots per cm of primary root) and (c) lateral roots length of the different *Phytolacca* species exposed to a mixture of 10 µM or 100 µM REEs (REE10 and REE100 respectively) or not exposed (control). Root systems of three (control, REE10) or four (REE100) plants per species and per treatment were analysed. Within a given species, significant differences between treatments are indicated by different letters (P<0.05, Kruskal-Wallis).

accumulators (e.g. *Nymphoides peltata* and *Hydrilla verticillata*), with, for example, a progressive increase in the concentration of MDA with increasing REE concentrations[36–38]. Therefore, our data suggest that the five *Phytolacca* species were probably highly tolerant to REEs. However, additional studies will be needed to compare the REE tolerance levels of different *Phytolacca* species.

REEs impacted the pigment contents and nitrogen balance index

Given the high REE accumulation in leaves, we investigated its impact on the content of different pigments (chlorophyll, flavonoids, and anthocyanins) and on the nitrogen balance index (NBI). Differences between the treatments but also between the species were recorded (Fig. 6). Regardless of the species, the chlorophyll index moderately decreased at REE100 when compared to the control. Indeed, the chlorophyll content was reduced from 1.1 to 1.6 times in *P. bogotensis* and *P. icosandra*, respectively (Fig. 6a). The lower chlorophyll content under REE exposure, could either be due to a reduction of Mg supply[38], or to chlorophyll degradation caused by lipid peroxidation[37]. Since MDA concentration did not increase at REE100 in the different *Phytolacca* species, this second hypothesis is very unlikely. It was however noteworthy that the chlorophyll content increased for *P. icosandra* and *P. americana* at REE10 (Fig. 6a). Such result could suggest a stimulation of photosynthesis. Several studies reported indeed a growth stimulation in rice[39], tobacco[40] and soybean[41] at low REE concentrations.

Compared to chlorophylls, the flavonoid content was poorly affected by REE exposure (Fig. 6b). When compared to the control, it slightly increased at REE10 by 1.1 and 1.2 times in *P. icosandra* and *P. acinosa*, respectively. Conversely, it decreased in *P. americana* and *P. bogotensis* at either REE10 or REE100. The anthocyanin index, usually indicative of a plant stress[42], was also analysed and is reported in Fig. 6c. A similar pattern was found for the different species, where all species showed a significant increase in anthocyanins at REE100 when compared to the control (Fig. 6c). These data suggest that this high dose of REEs, associated to a subsequent high REE accumulation in leaves (Fig. 3a), could lead to a modification of anthocyanin biosynthesis. In addition, the increase in anthocyanin content could be caused by an increased limitation of phosphate content in the plant, due to the high reactivity of REEs with phosphates. Surprisingly, at REE10, *P. americana* was the only species for which there was a decrease of anthocyanins (Fig. 6c), suggesting that at this low REE exposure the leaf stress was less important to *P. americana* than to its close relatives. The different

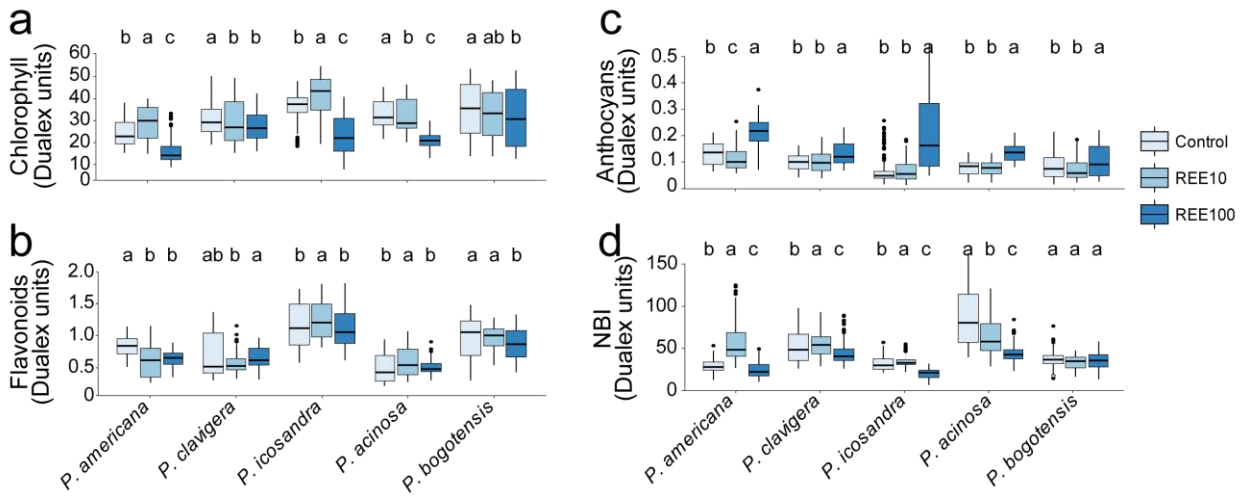

Figure 6. Pigment contents and nitrogen balance index of *Phytolacca* species exposed to REE. (a) Chlorophyll, (b) flavonoid, (c) anthocyanin, and (d) nitrogen balance (NBI) indexes were measured in the leaves of *Phytolacca* species exposed to a mixture of 10 µM or 100 µM REEs (REE10 and REE100, respectively). Twenty measurements on three (control, REE10) or four (REE100) plants per species and per treatment were performed. Within a given species, significant differences between treatments are indicated by different letters (P<0.05, Kruskal-Wallis, Wilcoxon post-hoc test).

pigment indexes measured can provide indications on the health or stress status of plants under tested conditions. It has been demonstrated in *Arabidopsis thaliana* that an increase of anthocyanins combined with a decrease of the chlorophyll content was triggered in response to metallic stress[43]. Indeed, anthocyanins can play a major protection role against metal stresses by acting as antioxidants[43]. However, since no difference was obtained from the MDA and TCA measurements, strong oxidative stress is unlikely and a higher anthocyanin index of all the five species measured at the highest REE concentration might reflect phosphorus deficiency, as suggested above and as previously reported[44].

We also analysed the NBI in plants exposed or not to REEs. NBI is a marker that corresponds to the ratio of chlorophyll content to that of flavonoids and gives an indication on the nitrogen status of plants[45]. While no difference was noticed for *P. bogotensis*, the NBI slightly increased at REE10 for *P. americana*, *P. clavigera*, and *P. icosandra* (Fig. 6d). Except for *P. bogotensis*, the NBI decreased at REE100 in the four other species.

The relative lower root branching, the increase of the chlorophyll content, along with the increased NBI for *P. americana* at REE10, could suggest that *P. americana* is slightly more tolerant to the low REE exposure compared to the other species tested (Fig. 5, Fig. 6). However, since the growth of other *Phytolacca* species was no more affected by REEs than that of *P. americana* for both REE10 and REE100 (Fig. 2), REE tolerance levels of the different species should be similar. Further dose-response studies would however be needed to shed more light on the tolerance level of the different *Phytolacca* species.

REEs modulate the ionome of *Phytolacca* species

Finally, the ionome of the different species under the three different exposure conditions was established (Supplementary Table S1, Supplementary Table S2). The two different compartments, leaves (Supplementary Table S1a, Supplementary Table S2a) and roots (Supplementary Table S1b, Supplementary Table S2b), were treated separately. Regarding the accumulation and fractionation of REEs, no differences were observed between the five species tested. Consequently, a global analysis was carried out using the ionomes of the different *Phytolacca* species in order to identify putative correlations between REE accumulation and essential element composition (Fig. 7). Two principal component analyses (PCA) (Fig. 7a-b) and correlation matrices were generated for both leaves and roots (Fig. 7c-d).

In the PCA for the leaves, the two first principal components accounted for 78.4% of the observed variations, with the first principal component accounting for 54.6% (Fig. 7a). The different conditions tested (control, REE10, and REE100) were well distinguished in the PCA. As expected, all the REEs were positively correlated together (Fig. 7a). Interestingly, in the second principal component, we observed that LREEs and HREEs were grouped separately (Fig. 7a). This is in agreement with the HREE enrichment relatively to LREEs observed in leaves (Fig. 4a). The first axis of the PCA was mostly structured by REEs, contributing for

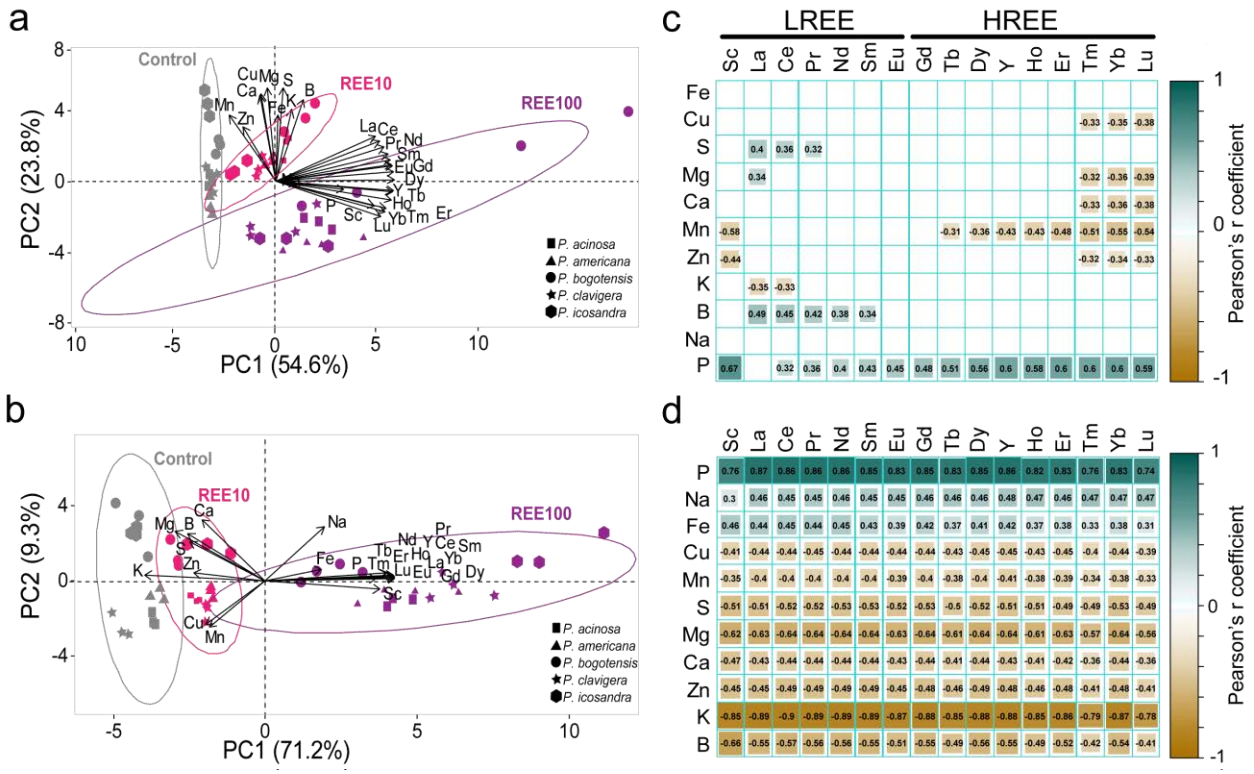

Figure 7. Principal component analysis and Pearson correlation matrices of REE, micro- and macro-elemental composition of leaves (a,c), and roots (b,d) of *Phytolacca* species. Plants were exposed to a mixture of 10 µM or 100 µM REEs (REE10 and REE100, respectively) or left unexposed (control). REE, macro- and micro-element concentrations were used as quantitative variables. For the Pearson correlation matrices, only significant correlations are shown (P<0.05, BH adjustment).

more than 82% each, but also by P with 57%, and Mn for 40%. In the second axis, S and Mg were the most structuring variables with 91% of explained inertia, followed by Cu (85%), Ca (84%), B (80%), K (70%), Fe and Mn (65%). The segregation of REEs (first axis) from the other elements (second axis) on the PCA (Fig. 7a) is supported by the Pearson correlation matrix (Fig. 7c). Indeed, relatively few correlations were found between REE accumulation and the concentration of essential elements. Whereas no significant correlation was found between any of the REEs and Fe or Na, negative correlations were found between the heaviest REEs (Tm to Lu) and Cu, Ca, Mg, and Zn (Fig. 7c). A similar negative correlation was observed for Mn with HREEs (Gd excepted) (Fig. 7c). Conversely, positive correlations were found between P and all REEs except La. Similar positive correlations were also found between some LREEs and B and S (Fig. 7c). Interestingly, the Pearson's r coefficient increased (P only) or decreased (the other elements), with the atomic number of REEs (Fig. 7c). Again, Sc did not follow the global rule observed for the other REEs, supporting its difference compared to the lanthanides and Y.

Correlations were more abundant and stronger between macro- or micronutrient elements and REEs in the root compartment (Fig. 7b-d). In the PCA, the two first principal components accounted for 80.5% of the observed variations, with the first principal component accounting for 71.2% (Fig. 7b). The first axis of the PCA was mostly structured by REEs, K, and P contributing for more than 84% each, and Mg with 68%. In the second axis, Ca was the most structuring variable with 74% of explained inertia, followed by Na (65%), Mg (59%), B (56%), and S (47%). REEs covariated together and were also positively correlated to phosphorus in both roots and leaves. However, since (i) the nutritive solution was lacking P during the exposure phase with REEs and (ii) growth at REE100 was reduced compared to the control, it was expected that P concentration in the biomass would be subjected to a dilution effect in the control treatment compared to REE-exposed treatments. The observations reported in Supplementary Table S1 and Fig. 7c-d are in agreement with this hypothesis. While no correlation was found in the leaves with Fe or Na and REEs, positive correlations were observed in the roots (Fig. 7b-d). The other elements, namely Cu, Mn, S, Mg, Ca, Zn, K, and B, were all negatively correlated with REEs. These

correlations were highly influenced by the highest exposure condition (REE100) (Fig. 7b-d, Supplementary Table S1, Supplementary Table S2).

REEs have a similar ionic radius to that of Ca. Because of this characteristic REEs have been used as Ca-channel blockers[46,47], and later on, it was suggested that La and Eu could enter into plant cells through Ca-channels[48]. Therefore, the negative correlation found between Ca and REEs is not unexpected. Such antagonistic effects between Ca and La have been previously reported in plants[39,49]. Yuan *et al.* (2017) also demonstrated that increasing concentrations of Ca inhibited REE accumulation in *P. americana*[21]. Along with Ca, Mg also had a negative correlation with REE content. Such deprivation had already been reported for *P. americana* exposed to REEs[21], but also in *Brassica napus* exposed to Ce[50]. Mg is necessary for chlorophyll synthesis and functioning, thus, the decrease in chlorophyll content could be related to the Mg reduction due to REE exposure. A negative correlation between REE and Mn was also found in leaves and roots (Fig. 7). *Phytolacca americana*[17–19] and *P. acinosa*[25,26] are two known Mn hyperaccumulators. It is interesting to notice the reduced Mn content concomitantly to the accumulation of REEs. This might suggest a competitive uptake between these elements in *Phytolacca* species as in *P. acinosa* between Mn and Cd[51].

Conclusions

Phytolacca species are fast growing and high-biomass producing plants. *P. americana* was the first species of the genus to be demonstrated as a REE accumulator. By testing five *Phytolacca* species on two different REE concentrations, this study therefore brings new information on the effect of REEs on the physiology and ionome of the REE-accumulating *Phytolacca* species. It is interesting to note that the REE accumulating trait is conserved within the *Phytolacca* genus, as reported for the *Carya* genus[16]. Such information is very useful for phytoremediation of REE-contaminated sites. Indeed, the different *Phytolacca* species tested here are originating from different locations. For example, *P. bogotensis* is native from Colombia, *P. icosandra* from Mexico, and *P. acinosa* from Tibet[28]. Therefore, the conserved REE accumulation trait among these different species can be used to choose the most appropriate species according to climatic and/or pedological context of the area to be remediated. Finally, in order to better understand the molecular and genetic mechanisms that underlie this particular trait, further work is needed.

Material and Methods

Plant growth and REE treatments

Five *Phytolacca* species were used in the present study, including *P. acinosa* Roxb., *P. americana* L., *P. bogotensis* Kunth, *P. icosandra* L. and *P. clavigera* W.W. Smith. Seeds were obtained from Chiltern seeds (Wallingford, UK), the VanDusen Botanical Garden (Vancouver, Canada) and the Jean-Marie Pelt Botanical Garden (Villers-lès-Nancy, France). They were treated with 37% H_2SO_4 for 5 min and rinsed 5 times in sterile deionized water. Seeds were subsequently sown in Petri dishes on half-strength Murashige & Skoog agar medium. Four week-old seedlings were transferred into a modified quarter-strength Hoagland nutrient solution (2 mM NH_4NO_3, 3 mM KNO_3, 2 mM KCl, 2 mM $Ca(NO_3)_2{\cdot}4H_2O$, 2 mM $MgSO_4{\cdot}7H_2O$, 1.5 mM NaCl, 600 µM KH_2PO_4, 100 µM $CaCl_2$, 50 µM NaFe(III)-EDTA, 50 µM H_3BO_3, 5 µM $MnCl_2{\cdot}4H_2O$, 10 µM $ZnSO_4{\cdot}7H_2O$, 0.5 µM $CuSO_4{\cdot}5H_2O$, 0.1 µM Na_2MoO_3, pH 5.6)[52]. Two-liter black containers were filled with nutritive solution that was continuously aerated. Six week-old seedlings were subsequently transferred to the same nutritive solution containing REEs or not (control medium), and lacking KH_2PO_4 in order to avoid REE precipitation with phosphates. Promethium was omitted since it is only available under its radioactive form. Two different total concentrations (10 and 100 µM) of a mixture of 16 REEs were used. All REEs were therefore brought at equimolar concentrations (625 nM or 6.25 µM). REE tri-chloride salts were used (Sc, Y, La, Ce, Pr, Nd, Sm, Eu, Gd, Tb, Dy, Ho, Er, Tm, Yb and Lu) and were purchased from Sigma-Aldrich (Saint-Quentin-Fallavier, France). Three or four plants (control and 10 µM REE treatments, n = 3; 100 µM REE treatments, n= 4) per species and per treatment were grown individually in hydroponic containers in a growth chamber under controlled conditions: 18/23°C, 12/12 h dark/light cycles (light intensity 260 µmol photons /m^2/s), respectively.

After 21 days of exposure, plants were harvested. Roots were first rinsed in water, followed by a 15 min incubation in 5 mM ice-cold $CaCl_2$, washed twice in deionized water and finally blotted dry carefully with tissue paper. Root architecture and leaf pigments were analysed (see below). Subsequently, plants were separated into roots, stems and leaves and weighed. Lastly, the samples were ground into thin powder using liquid nitrogen and stored at -80°C until use. Aliquots of powder samples were also dried at 70 °C for 2 days, weighed and further used for elemental analysis (see below).

Species identification

Cellular extracts from the different *Phytolacca* species were obtained by using the REDextract-N-Amp™ Plant PCR kit (Sigma-Aldrich) according to the manufacturer's protocol. The internal transcribed spacer (ITS) region was amplified using the primers ITS1 and ITS4[53]. Twenty microliters of a mixture containing 0.2 µM of each primer, 4 µl of plant extract, 5.6 µl of H_2O and 10 µl of REDExtract-N-Amp PCR ready mix were used for PCR amplification. The following PCR program was used: 3 min at 94°C, followed by 40 cycles of 94°C for 1 min, 55°C for 1 min and 72°C for 1 min, and 10 min at 72°C. PCR products were cloned into the pGEM-T® Easy vector system I (Promega, Charbonnières-les-Bains, France), and the corresponding plasmids were sequenced. Related *Phytolacca* sequences were retrieved from the GenBank database using the NCBI BLAST program and ClustalW was used to align sequences. The maximum likelihood tree was drawn with the kimura 2-parameter model using MEGA 7[54]. Bootstrap analysis was performed with 1,000 replications.

Analysis of biomarkers

A series of biomarkers were used to assess potential toxic effects of REEs on *Phytolacca* species. First, leaf pigments (chlorophylls, flavonoids and anthocyanins) as well as the nitrogen balance index (NBI) were quantified using a DUALEX® SCIENTIFIC+ apparatus (Force-A, Orsay, France) before harvesting. Forty technical replicates were carried out per plant. Second, root architecture was analysed. Root systems were pictured at harvest. The analyses of lateral root length and lateral root density (number of lateral roots per cm of primary root) were carried out using the RootNav software[55]. Finally, leaf and root contents of malondialdehyde (MDA) and total antioxidant compounds (TAC) were assayed from 50 mg of frozen powder, using commercial kits (MAK085 and MAK187, Sigma-Aldrich, France) according to the manufacturer's protocols. Two technical replicates were done per sample.

Elemental analysis

The quantification of elements was performed using 250 mg of dried plant powder. Mineralization was carried out using 3.5 mL nitric acid (HNO3, 65%, analytical grade, Optima) and 1 mL hydrogen peroxide and samples were incubated in a heating block digestion system (DigiPREP, SCP Sciences, Courtaboeuf, France). A gradual heating mode is used to achieve a final temperature of 100°C (total run of 265 min). Then, ultrapure water (18.2 MΩ/cm^2, Millipore Milli-Q Integral 3 system, Molsheim, France) was added to a final volume of 25 mL and samples were filtrated to 1 µm. Elemental concentrations were determined by ICP-AES (Radial ICAP 6500 Model, Thermo Fischer Scientific, Courtaboeuf, France) or ICP-MS (X Series II Model, Thermo Fischer Scientific, Courtaboeuf, France) for REEs. Oriental basma tobacco leaves (INCT-OBTL-5, LGC Promochem, Molsheim, France) was used as certified reference material.

Statistical analyses

One-way ANOVA and Tukey HSD post hoc test were used when normality of data (Shapiro-Wilk test) and homoscedasticity (Levene's test) conditions were respected. When at least one condition was rejected, data were subsequently analysed using one-way non-parametric Kruskal-Wallis test followed by Wilcoxon post hoc test. The rejection level was set at $\alpha = 0.05$ in all analyses. Percentage values were *arcsin*-transformed before statistical analyses. All analyses were performed using R software (version 3.4.1).

Acknowledgements

This work has been supported by the French National Research Agency through the national program "Investissements d'avenir" with the reference ANR-10-LABX-21-01/LABEX RESSOURCES21 and by the Région Grand-Est. We acknowledge Dr. Nadia Morin-Crini for the ICP-MS analyses and the Conservatoire et Jardins Botaniques de Nancy for providing the *Phytolacca* seeds.

Author Contributions Statement

The authors' responsibilities were as follows: NG, MLJ, MC and DB designed the research; NG, CB, MLJ, and DB performed the research; NG and CB analysed the data; NG, MLJ, MC, EMG, and DB evaluated the data; NG, MLJ, CB, MC, EMG, and DB wrote the manuscript. All authors read and approved the final manuscript.

Competing interests

The author(s) declare no competing interests

References

1. Tyler, G. Rare earth elements in soil and plant systems - A review. *Plant Soil* **267**, 191–206 (2004).
2. Long, K. R., Van Gosen, B. S., Foley, N. K., & Cordier, D. *The principal rare earth elements deposits of the United States: A summary of domestic deposits and a global perspective*. *U.S. Geological Survey Scientific Investigations Report 2010-5220* (2010).
3. Ciacci, L., Reck, B. K., Nassar, N. T., & Graedel, T. E. Lost by design. *Environ. Sci. Technol.* **49**, 9443–9451 (2015).
4. Redling, K. Rare earth elements in agriculture with emphasis on animal husbandry. (Ludwig-Maximilians-Universität München, 2006).
5. Lürling, M. & van Oosterhout, F. Controlling eutrophication by combined bloom precipitation and sediment phosphorus inactivation. *Water Res.* **7**, 6527–6537 (2013).
6. Zhenggui, W., Ming, Y., Xun, Z., Fashui, H., Bing, L., Ye, T., Guiwen, Z., & Chunhua, Y. Rare earth elements in naturally grown

fern *Dicranopteris linearis* in relation to their variation in soils in South-Jiangxi region (Southern China). *Environ. Pollut.* **114**, 345–355 (2001).

7. Yuan, M., Liu, C., Liu, W.-S., Guo, M.-N., Morel, J. L., Huot, H., Yu, H.-J., Tang, Y.-T., & Qiu, R.-L. Accumulation and fractionation of rare earth elements (REEs) in the naturally grown *Phytolacca americana* L. in southern China. *Int. J. Phytoremediation* **20**, 415–423 (2018).
8. Djingova, R., Ivanova, J., Wagner, G., Korhammer, S., & Markert, B. Distribution of lanthanoids , Be , Bi , Ga , Te , Tl , Th and U on the territory of Bulgaria using *Populus nigra* ' Italica ' as an indicator. (2001).
9. Ozaki, T., Enomoto, S., Minai, Y., Ambe, S., Ambe, F., & Tominaga, T. Determination of lanthanides and other trace elements in ferns by instrumental neutron activation analysis. *J. Radioanal. Nucl. Chem.* **217**, 117–124 (1997).
10. Shan, X., Wang, H., Zhang, S., Zhou, H., Zheng, Y., Yu, H., & Wen, B. Accumulation and uptake of light rare earth elements in a hyperaccumulator *Dicropteris dichotoma*. *Plant Sci.* **165**, 1343–1353 (2003).
11. Lai, Y., Wang, Q. Q., Yan, W. W., Yang, L. M., & Huang, B. L. Preliminary study of the enrichment and fractionation of REEs in a newly discovered REE hyperaccumulator *Pronephrium simplex* by SEC-ICP-MS and MALDI-TOF/ESI-MS. *J. Anal. At. Spectrom.* **20**, 751–753 (2005).
12. Lai, Y., Wang, Q., Yang, L., & Huang, B. Subcellular distribution of rare earth elements and characterization of their binding species in a newly discovered hyperaccumulator *Pronephrium simplex*. *Talanta* **70**, 26–31 (2006).
13. Zhang, Z. Y., Wang, Y. Q., Li, F. L., Xiao, H. Q., & Chai, Z. F. Distribution characteristics of rare earth elements in plants from a rare earth ore area. *J. Radioanal. Nucl. Chem.* **252**, 461–465 (2002).
14. Liang, T., Li, K., & Wang, L. State of rare earth elements in different environmental components in mining areas of China. *Environ. Monit. Assess.* **186**, 1499–1513 (2014).
15. Ichihashi, H., Morita, H., & Tatsukawa, R. Rare earth elements (REEs) in naturally grown plants in relation to their variation in soils. *Environ. Pollut.* **76**, 157–162 (1991).
16. Wood, B. W. & Grauke, L. J. The rare-earth metallome of pecan and other *Carya*. *J. Am. Soc. Hortic. Sci.* **136**, 389–398 (2011).
17. Pollard, A. J., Stewart, H. L., & Roberson, C. B. Manganese Hyperaccumulation in *Phytolacca americana* L. from the Southeastern United States. *Northeast. Nat.* **16**, 155–162 (2009).
18. Dou, C., Fu, X., Chen, X., Shi, J., & Chen, Y. Accumulation and detoxification of manganese in hyperaccumulator *Phytolacca americana*. *Plant Biol.* **11**, 664–670 (2009).
19. Min, Y., boqing, T., Meizhen, T., & Aoyama, I. Accumulation and uptake of manganese in a hyperaccumulator *Phytolacca americana*. *Miner. Eng.* **20**, 188–190 (2007).
20. Wu, J., Chen, A., Peng, S., Wei, Z., & Liu, G. Identification and application of amino acids as chelators in phytoremediation of rare earth elements lanthanum and yttrium. *Plant Soil* **373**, 329–338 (2013).
21. Yuan, M. *et al.* The accumulation and fractionation of rare earth elements in hydroponically grown *Phytolacca americana* L. *Plant Soil* **421**, 67–82 (2017).
22. Chour, Z., Laubie, B., Morel, J. L., Tang, Y., Qiu, R., Simonnot, M.-O., & Muhr, L. Recovery of rare earth elements from *Dicranopteris dichotoma* by an enhanced ion exchange leaching process. *Chem. Eng. Process. - Process Intensif.* **130**, 208–213 (2018).
23. Grison, C. Combining phytoextraction and ecocatalysis: a novel concept for greener chemistry, an opportunity for remediation. *Environ. Sci. Pollut. Res. Int.* **22**, 5589–5591 (2015).
24. Chen, C., Zhang, H., Wang, A., Lu, M., Shen, Z., & Lian, C. Phenotypic plasticity accounts for most of the variation in leaf manganese concentrations in *Phytolacca americana* growing in manganese- contaminated environments. *Plant Soil* (2015).
25. Xu, X., Shi, J., Chen, X., Chen, Y., & Hu, T. Chemical forms of manganese in the leaves of manganese hyperaccumulator *Phytolacca acinosa* Roxb. (Phytolaccaceae). *Plant Soil* **318**, 197–204 (2009).
26. Xue, S., Wang, J., Zhou, X., Liu, H., & Chen, Y. A critical reappraisal of *Phytolacca acinosa* Roxb. (Phytolaccaceae) – A manganese-hyperaccumulating plant. *Acta Ecol. Sin.* **30**, 335–338 (2010).
27. Krämer, U. Metal hyperaccumulation in plants. *Annu. Rev. Plant Biol.* **61**, 517–534 (2010).
28. Ajmal Ali, M., Lee, J., Kim, S. Y., Park, S. H., & Al-Hemaid, F. M. A. Molecular phylogenetic analyses of internal transcribed spacer (ITS) sequences of nuclear ribosomal DNA indicate monophyly of the genus Phytolacca L. (Phytolaccaceae). *Bangladesh J. Plant Taxon.* **22**, 1–8 (2015).
29. Ding, S., Liang, T., Zhang, C., Huang, Z., Xie, Y., & Chen, T. Fractionation mechanisms of rare earth elements (REEs) in hydroponic wheat : an application for metal accumulation by plants. *Environ. Sci. Technol.* **40**, 2686–2691 (2006).
30. Ding, S. M., Liang, T., Zhang, C. S., Yan, J. C., & Zhang, Z. L. Accumulation and fractionation of rare earth elements (REEs) in wheat: Controlled by phosphate precipitation, cell wall absorption and solution complexation. *J. Exp. Bot.* **56**, 2765–2775 (2005).
31. Ding, S. M., Liang, T., Yan, J. C., Zhang, Z. L., Huang, Z. C., & Xie, Y. N. Fractionations of rare earth elements in plants and their conceptive model. *Sci. China, Ser. C Life Sci.* **50**, 47–55 (2007).
32. Liang, T., Ding, S., Song, W., Chong, Z., Zhang, C., & Li, H. A review of fractionations of rare earth elements in plants. *J. Rare Earths* **26**, 7–15 (2008).
33. Wang, H., Shan, X.-Q., Zhang, S., & Wen, B. Preliminary characterization of a light-rare-earth-element-binding peptide of a natural perennial fern *Dicranopteris dichotoma*. *Anal. Bioanal. Chem.* **376**, 49–52 (2003).
34. Liu, Y. Y., Wang, R. L., Zhang, P., Sun, L. L., & Xu, J. Involvement of reactive oxygen species in lanthanum-induced inhibition of primary root growth. *J. Exp. Bot.* **67**, 6149–6159 (2016).
35. Liu, Y., Sun, L., Zhang, P., Wan, J., Wang, R., & Xu, J. Lanthanum inhibits primary root growth by repressing auxin carrier abundances in *Arabidopsis*. *Front. Plant Sci.* **8**, 1–9 (2017).
36. Pagano, G., Guida, M., Tommasi, F., & Oral, R. Health effects and toxicity mechanisms of rare earth elements - Knowledge gaps and research prospects. *Ecotoxicol. Environ. Saf.* **115**, 40–48 (2015).
37. Wang, X., Shi, G. X., Xu, Q. S., Xu, B. J., & Zhao, J. Lanthanum- and cerium-induced oxidative stress in submerged *Hydrilla verticillata* plants. *Russ. J. Plant Physiol.* **54**, 693–697 (2007).
38. Xu, Q., Fu, Y., Min, H., Cai, S., Sha, S., & Cheng, G. Laboratory assessment of uptake and toxicity of lanthanum (La) in the leaves of *Hydrocharis dubia* (Bl.) Backer. *Environ. Sci. Pollut. Res.* **19**, 3950–3958 (2012).
39. Liu, D., Wang, X., Chen, X., Lin, Y., Chen, Z., & Xu, H. Effects of lanthanum on the change of calcium level in the root cells of rice. *Commun. Soil Sci. Plant Anal.* **43**, 1994–2003 (2012).
40. Chen, W. J., Tao, Y., Gu, Y. H., & Zhao, G. W. Effect of lanthanide chloride on photosynthesis and dry matter accumulation in tobacco seedlings. *Biol. Trace Elem. Res.* **79**, 169–176 (2001).
41. de Oliveira, C. *et al.* Bioaccumulation and effects of lanthanum on growth and mitotic index in soybean plants. *Ecotoxicol. Environ. Saf.* **122**, 136–144 (2015).
42. Chalker-scott, L. Environmental significance of anthocyanins in plant stress responses. *Photochem. Photobiol.* **70**, 1–9 (1999).
43. Baek, S. A., Han, T., Ahn, S. K., Kang, H., Cho, M. R., Lee, S. C., & Im, K. H. Effects of heavy metals on plant growths and pigment contents in *Arabidopsis thaliana*. *Plant Pathol. J.* **28**, 446–452 (2012).

44. Hernández, I. & Munné-Bosch, S. Linking phosphorus availability with photo-oxidative stress in plants. *J. Exp. Bot.* **66**, 2889–2900 (2015).
45. Cartelat, A., Cerovic, Z. G., Goulas, Y., Meyer, S., Lelarge, C., & Prioul, J. Optically assessed contents of leaf polyphenolics and chlorophyll as indicators of nitrogen deficiency in wheat (*Triticum aestivum* L.). *F. Crop. Res.* **91**, 35–49 (2005).
46. Lewis, B. D. & Spalding, E. P. Nonselective block by La^{3+} of *Arabidopsis* ion channels involved in signal transduction. *J. Membr. Biol.* **162**, 81–90 (1998).
47. Lansman, J. B. Blockade of current through single calcium channels by trivalent lanthanide cations. Effect of ionic radius on the rates of ion entry and exit. *J. Gen. Physiol.* **95**, 679–696 (1990).
48. Gao, Y., Zeng, F., Yi, A., Ping, S., & Jing, L. Research of the entry of rare earth elements Eu^{3+} and La^{3+} into plant cell. *Biol. Trace Elem. Res.* **91**, 253–265 (2003).
49. Han, F., Shan, X. Q., Zhang, J., Xie, Y. N., Pei, Z. G., Zhang, S. Z., Zhu, Y. G., & Wen, B. Organic acids promote the uptake of lanthanum by barley roots. *New Phytol.* **165**, 481–492 (2005).
50. Pošćić, F., Schat, H., & Marchiol, L. Cerium negatively impacts the nutritional status in rapeseed. *Sci. Total Environ.* **593–594**, 735–744 (2017).
51. Liu, H., Zhang, Y., Chai, T., Tan, J., & Wang, J. Plant physiology and biochemistry manganese-mitigation of cadmium toxicity to seedling growth of *Phytolacca acinosa* Roxb . is controlled by the manganese / cadmium molar ratio under hydroponic conditions. *Plant Physiol. Biochem.* **73**, 144–153 (2013).
52. Conn, S. J. *et al.* Protocol: optimising hydroponic growth systems for nutritional and physiological analysis of *Arabidopsis thaliana* and other plants. *Plant Methods* **9**, 4 (2013).
53. White, T. J., Bruns, T., Lee, S., & Taylor, J. Amplification and direct sequencing of fungal ribosomal RNA genes for phylogenetics. in *PCR-Protocol and Applications - a Laboratory Manual* (eds. Innis, M., Gelfand, D., Sninsky, J. & White, T.) 315–322 (1990).
54. Kumar, S., Stecher, G., & Tamura, K. MEGA7: Molecular Evolutionary Genetics Analysis Version 7.0 for Bigger Datasets. *Mol. Biol. Evol.* **33**, 1870–1874 (2016).
55. Pound, M. P., French, A. P., Atkinson, J. A., Wells, D. M., Bennett, M. J., & Pridmore, T. RootNav: Navigating images of complex toot architectures. *Plant Physiol.* **162**, 1802–1814 (2013).

Supplementary Table S1. Macroelement composition (mg/g DW) of leaves (a) and roots (b) of *Phytolacca* species exposed to REEs. *Phytolacca* species were exposed to a mixture of 10 µM or 100 µM REEs (REE10 and REE100, respectively). Values are means ± SD (n=3 or n=4). Within a given species, significant differences between treatments are indicated by different letters (P<0.05, ANOVA Tukey's HSD).

a

	Treatment	*P. americana*	*P. clavigera*	*P. icosandra*	*P. acinosa*	*P. bogotensis*
K	Control	40.2 ± 0.99 b	51.5 ± 5.09 ab	57.3 ± 4.22 a	59.0 ± 13.8 a	63.6 ± 3.83 a
	REE - 10	53.1 ± 4.91 a	55.3 ± 3.41 a	35.3 ± 2.52 b	45.1 ± 5.81 b	62.3 ± 11.3 a
	REE - 100	35.4 ± 3.07 b	41.5 ± 7.42 b	37.2 ± 3.23 b	47.6 ± 5.68 ab	60.7 ± 6.38 a
S	Control	1.32 ± 0.10 b	2.39 ± 0.47 a	4.38 ± 0.19 a	2.08 ± 0.15 b	3.44 ± 0.29 a
	REE - 10	2.32 ± 0.18 a	2.55 ± 0.22 a	3.22 ± 0.32 b	2.51 ± 0.22 a	3.87 ± 0.18 a
	REE - 100	1.24 ± 0.10 b	1.35 ± 0.20 b	1.47 ± 0.02 c	1.31 ± 0.08 c	3.34 ± 0.53 a
P	Control	0.42 ± 0.05 b	0.69 ± 0.09 b	1.03 ± 0.01 a	0.81 ± 0.16 b	1.12 ± 0.22 b
	REE - 10	0.73 ± 0.09 a	0.95 ± 0.03 b	1.08 ± 0.02 a	0.70 ± 0.06 b	1.09 ± 0.03 b
	REE - 100	0.90 ± 0.07 a	1.49 ± 0.20 a	1.13 ± 0.07 a	1.77 ± 0.17 a	2.13 ± 0.22 a
Mg	Control	4.01 ± 0.51 b	4.33 ± 0.59 a	7.33 ± 0.61 a	4.75 ± 0.22 b	6.19 ± 0.85 a
	REE - 10	6.90 ± 0.73 a	5.19 ± 0.45 a	5.96 ± 0.71 a	6.82 ± 0.41 a	6.29 ± 0.77 a
	REE - 100	3.16 ± 0.35 b	2.65 ± 0.64 b	2.24 ± 0.31 b	3.50 ± 0.35 c	4.66 ± 1.37 a
Ca	Control	3.74 ± 0.46 b	3.67 ± 0.62 ab	8.39 ± 0.62 a	3.49 ± 0.22 b	5.02 ± 0.91 ab
	REE - 10	6.34 ± 0.62 a	4.22 ± 0.47 a	6.15 ± 0.29 b	6.20 ± 0.25 a	6.04 ± 0.48 a
	REE - 100	3.46 ± 0.30 b	2.54 ± 0.71 b	2.41 ± 0.33 c	2.82 ± 0.18 c	3.87 ± 0.91 b
Na	Control	0.50 ± 0.08 a	0.41 ± 0.23 a	0.08 ± 0.06 a	0.13 ± 0.05 a	0.10 ± 0.02 a
	REE - 10	1.39 ± 0.58 a	0.38 ± 0.10 a	0.05 ± 0.01 a	0.24 ± 0.14 a	0.10 ± 0.08 a
	REE - 100	0.59 ± 0.07 a	0.26 ± 0.16 a	0.08 ± 0.03 a	0.11 ± 0.04 a	0.30 ± 0.40 a

b

	Treatment	*P. americana*	*P. clavigera*	*P. icosandra*	*P. acinosa*	*P. bogotensis*
K	Control	62.0 ± 6.75 a	78.1 ± 1.36 a	67.4 ± 2.93 a	64.8 ± 2.89 a	64.5 ± 15.9 ab
	REE - 10	58.7 ± 2.80 a	61.6 ± 1.78 b	52.4 ± 14.3 a	50.1 ± 2.66 b	72.9 ± 10.3 a
	REE - 100	26.8 ± 3.38 b	22.7 ± 1.75 c	21.0 ± 4.11 b	22.5 ± 0.24 c	46.6 ± 6.01 b
S	Control	2.42 ± 0.13 a	3.12 ± 0.11 a	3.74 ± 0.41 a	2.84 ± 0.09 b	4.14 ± 0.82 a
	REE - 10	2.36 ± 0.12 ab	3.11 ± 0.09 a	3.34 ± 0.44 a	3.71 ± 0.22 a	4.40 ± 0.70 a
	REE - 100	2.11 ± 0.15 b	2.52 ± 0.39 a	2.04 ± 0.12 b	2.18 ± 0.09 c	3.57 ± 0.82 a
P	Control	1.05 ± 0.07 c	1.49 ± 0.30 c	1.19 ± 0.04 b	1.63 ± 0.13 b	1.46 ± 0.53 b
	REE - 10	1.34 ± 0.04 b	2.11 ± 0.18 b	2.43 ± 0.97 ab	1.58 ± 0.07 b	1.37 ± 0.26 b
	REE - 100	2.61 ± 0.16 a	3.15 ± 0.22 a	3.13 ± 0.32 a	2.75 ± 0.11 a	2.83 ± 0.37 a
Mg	Control	3.23 ± 0.17 a	4.27 ± 0.48 a	7.30 ± 0.82 a	2.44 ± 0.08 b	6.25 ± 1.82 a
	REE - 10	3.06 ± 0.56 a	2.60 ± 0.06 b	4.44 ± 0.78 b	3.58 ± 0.49 a	3.57 ± 0.57 b
	REE - 100	2.21 ± 0.65 a	1.47 ± 0.36 c	1.58 ± 0.20 c	1.37 ± 0.08 c	3.34 ± 0.48 b
Ca	Control	6.57 ± 1.20 a	6.23 ± 1.23 a	12.2 ± 0.97 a	5.12 ± 0.69 a	13.7 ± 0.99 a
	REE - 10	3.72 ± 0.08 b	4.46 ± 0.73 ab	9.39 ± 3.57 ab	5.99 ± 0.31 a	9.81 ± 0.85 b
	REE - 100	3.71 ± 0.26 b	3.90 ± 0.52 b	6.33 ± 0.88 b	3.98 ± 0.10 b	5.04 ± 0.84 c
Na	Control	2.69 ± 0.13 ab	1.00 ± 0.41 b	4.29 ± 0.40 a	1.54 ± 0.07 b	2.83 ± 1.59 a
	REE - 10	3.14 ± 0.44 a	1.01 ± 0.25 b	4.08 ± 0.50 a	1.40 ± 0.20 b	1.52 ± 0.25 a
	REE - 100	2.46 ± 0.04 b	3.15 ± 0.49 a	5.38 ± 0.79 a	2.57 ± 0.35 a	3.46 ± 1.39 a

Supplementary Table S2. Microelement composition (µg/g DW) of leaves (a) and roots (b) of *Phytolacca* species exposed to REEs. *Phytolacca* species were exposed to a mixture of 10 µM or 100 µM REEs (REE10 and REE100, respectively). Values are means ± SD (n=3 or n=4). Within a given species, significant differences between treatments are indicated by different letters (P<0.05, ANOVA Tukey's HSD).

a

	Treatment	*P. americana*	*P. clavigera*	*P. icosandra*	*P. acinosa*	*P. bogotensis*
B	Control	16.8 ± 1.36 b	31.5 ± 8.71 ab	46.4 ± 1.19 a	24.9 ± 0.67 b	46.7 ± 7.51 a
	REE - 10	41.9 ± 4.79 a	50.4 ± 9.18 a	41.2 ± 6.39 a	42.8 ± 8.48 a	56.6 ± 4.73 a
	REE - 100	19.6 ± 1.55 b	31.3 ± 7.55 b	20.8 ± 4.03 b	31.6 ± 5.36 ab	46.5 ± 8.77 a
Cu	Control	8.85 ± 1.68 a	7.12 ± 1.41 a	17.8 ± 5.42 a	9.46 ± 0.67 a	11.0 ± 2.13 ab
	REE - 10	11.2 ± 0.68 a	6.19 ± 0.32 a	6.64 ± 0.40 b	10.9 ± 2.17 a	13.6 ± 1.08 a
	REE - 100	2.90 ± 0.90 b	5.04 ± 0.76 a	4.16 ± 0.56 b	5.37 ± 0.71 b	9.17 ± 1.92 b
Fe	Control	44.4 ± 6.13 a	53.9 ± 17.2 a	130 ± 41.3 a	41.8 ± 6.02 ab	129 ± 22.3 a
	REE - 10	56.5 ± 4.47 a	55.5 ± 8.25 a	83.1 ± 3.55 ab	60.4 ± 12.3 a	148 ± 25.2 a
	REE - 100	63.3 ± 23.9 a	65.1 ± 12.2 a	47.4 ± 21.9 b	38.1 ± 1.71 b	82.0 ± 6.95 b
Mn	Control	92.9 ± 18.2 a	154 ± 23.2 a	152 ± 14.1 a	153 ± 12.7 a	111 ± 8.84 a
	REE - 10	90.1 ± 24.1 a	137 ± 10.3 a	81.1 ± 6.66 b	136 ± 10.5 a	113 ± 19.9 a
	REE - 100	21.8 ± 7.91 b	69.5 ± 11.6 a	36.1 ± 11.4 c	107 ± 7.13 b	63.7 ± 15.9 b
Zn	Control	63.0 ± 9.29 a	167 ± 26.5 a	215 ± 20.7 a	134 ± 28.0 a	85.9 ± 6.40 a
	REE - 10	71.1 ± 2.96 a	120 ± 4.69 ab	111 ± 16.6 b	150 ± 9.75 a	90.3 ± 12.5 a
	REE - 100	32.6 ± 5.88 b	103 ± 21.6 b	88.2 ± 7.82 b	124 ± 13.5 a	75.9 ± 30.0 a

b

	Treatment	*P. americana*	*P. clavigera*	*P. icosandra*	*P. acinosa*	*P. bogotensis*
B	Control	13.4 ± 0.66 ab	14.3 ± 1.07 a	17.1 ± 1.13 ab	14.4 ± 0.65 a	18.6 ± 5.88 a
	REE - 10	14.1 ± 1.95 a	14.3 ± 0.98 a	20.1 ± 3.02 a	13.0 ± 0.39 b	19.0 ± 2.36 a
	REE - 100	11.3 ± 0.26 b	10.1 ± 3.84 a	12.4 ± 2.98 b	8.91 ± 0.29 c	9.81 ± 0.78 b
Cu	Control	40.3 ± 12.1 a	79.0 ± 13.0 a	33.6 ± 9.48 a	50.9 ± 6.87 a	13.5 ± 2.99 c
	REE - 10	29.4 ± 3.63 a	68.2 ± 15.8 a	48.6 ± 31.1 a	45.9 ± 8.42 a	28.4 ± 1.43 a
	REE - 100	26.8 ± 2.95 a	22.2 ± 4.71 b	19.4 ± 6.75 a	26.9 ± 2.70 b	22.0 ± 2.29 b
Fe	Control	156 ± 39.2 b	117 ± 34.7 a	227 ± 86.0 a	130 ± 32.6 c	151 ± 53.2 a
	REE - 10	170 ± 9.46 b	301 ± 22.7 a	865 ± 580 a	242 ± 6.51 b	170 ± 3.12 a
	REE - 100	380 ± 57.8 a	554 ± 264 a	424 ± 59.5 a	452 ± 32.7 a	188 ± 38.7 a
Mn	Control	57.8 ± 16.5 a	282 ± 18.3 a	60.2 ± 0.29 a	171 ± 17.6 a	20.6 ± 2.63 c
	REE - 10	41.0 ± 3.94 a	54.7 ± 7.63 b	55.0 ± 13.2 ab	121 ± 27.5 b	26.7 ± 2.84 b
	REE - 100	52.8 ± 19.2 a	33.6 ± 5.50 b	35.0 ± 4.25 b	30.6 ± 1.29 c	34.2 ± 2.06 a
Zn	Control	287 ± 124 a	676 ± 405 a	254 ± 59.1 a	276 ± 101 a	414 ± 112 a
	REE - 10	139 ± 33.0 ab	161 ± 10.5 a	345 ± 57.3 a	193 ± 29.2 ab	252 ± 47.4 ab
	REE - 100	89.4 ± 12.7 b	94.7 ± 9.12 a	174 ± 62.0 a	55.1 ± 3.89 b	199 ± 27.2 b

Chapter II.3:
Searching for new hardy ferns accumulating rare earth elements

Searching for new hardy ferns accumulating rare earth elements

Searching for new hardy ferns accumulating rare earth elements

(Manuscript submitted for publication)

Nicolas Grosjean[1,2], Damien Blaudez[1], Michel Chalot[3,4], Elisabeth Maria Gross[2], Marie Le Jean[2]

[1]Université de Lorraine, CNRS, LIEC, F-54000 Nancy, France. [2]Université de Lorraine, CNRS, LIEC, F-57000 Metz, France. [3]Université de Bourgogne Franche-Comté, UMR CNRS 6249 Laboratoire Chrono-environnement, F-25211, Montbéliard, France. [4]Université de Lorraine, F-54000 Nancy, France.

Abstract

The increasing demand for rare earth elements (REEs) mainly driven by new-technologies, together with their current low recyclability, allow to consider them as emerging contaminants. The REE group includes the lanthanides, plus yttrium and scandium, and can be split, according to their atomic mass, into light REEs (LREEs) and heavy REEs (HREEs). Although broadly present at moderate levels in the Earth crust and in soils (approximatively 100 ppm), REEs can reach higher concentrations. Indeed, soils around REE mining sites in China can bear up to 2,000 mg/kg REEs. The identification of new REE accumulators, could bring out candidates for environmental friendly remediation techniques or agromining. To that end, a collection of forty-nine hardy fern species was screened, including the REE accumulating species *Dryopteris erythrosora*. It highlighted contrasted behaviors between several genera, but also evidenced the conservation of this REE accumulation trait in others. Interestingly, LREEs and HREEs were not uniformly transferred to the fronds, suggesting either a different bioavailability of LREEs vs HREEs or different specific transfer systems for the two groups of REEs. We also reported here a correlation between REE accumulation and essential element content in ferns, supporting either common uptake pathways and/or behaviours in soils. Altogether, these results are of great interest for phytoremediation purposes since appropriate species can be chosen according to the area to be remediated, but also for more in depth characterization of the underlying REE accumulation mechanisms.

Introduction

Land pollution by metals has been widely reported and considered a major environmental problem. The rare earth elements (REEs) are a group of 17 metals sharing similar chemical and geochemical properties. It contains 15 lanthanides, as well as yttrium and scandium. The light REEs (LREEs, lanthanum to europium) and the heavy REEs (HREEs, gadolinium to lutetium) can be distinguished within the 15 lanthanides according to their atomic mass and ionic radius [1]. The demand for REE and the associated extraction of these elements have increased significantly because of their essential properties for green energies, new technologies, as well as for medical applications [2,3]. Overall, the production of lanthanides increased from 90,000 metric tons in 2000 [4] to 130,000 metric tons of oxides in 2015 [5]. These elements are also commonly used as crop fertilizers to stimulate growth and production, but also as dietary supplement for cattle [6]. Furthermore, high concentrations of REEs can be found in soils, especially around mining areas where concentrations reach more than 2,000 mg/kg, which is more than 10 times the average soil concentration in the world [7]. Associated to their mining and use, a crucial lack of recyclability for these elements currently exists [2,8]. Together, the recent substantial production, use and widespread of REEs has begun to raise concerns about their impact on human and environmental health [9,10]. REE transfer throughout the ecosystem is now recognized as a potential problem, because many studies have shown toxic effects on bacteria, fungi, plants or animals [11–14]. These observations are strong arguments for considering REEs as emerging pollutants.

Environmentally friendly phytoremediation solutions (*i.e.* phytoextraction) could help reduce high levels of REE in soils through the use of REE-accumulating plants [15,16]. In general, the REE content in plants was 0.0011 (Lu), 0.33 ppm (Ce) [17] or up to 5 ppm [18]. Although REEs are not considered essential for plants, it has been widely shown that they can be taken up and transferred to the aboveground parts of plants at moderate concentrations. In the same way as for other metals, a few plant species were reported to accumulate REEs. The REE concentrations in *Phytolacca americana* (pokeweed) and *Carya tomentosa* (mockernut), can reach 1,040 and 859 ppm respectively [19,20]. In addition to these two angiosperms, the majority of REE-accumulating plants belongs to pteridophytes [16]. Two species of fern that with the greatest capacity for REE accumulation are particularly interesting. *Pronephrium simplex* can accumulate up to 1,200 ppm [21,22], while *Dicranopteris dichotoma* contains up to 3,300 ppm [18,23,24]. It has been suggested that high concentrations of REEs in ferns may help these species to adapt better to changing environments [16]. Some other fern species have also been

mentioned as REE accumulators. Such species included *Dryopteris erythrosora* [18], *Blechnum orientale* [25,26] and *Athyrium yokoscense* [27] and their accumulation trait was identified from plants growing in non-contaminated environments. However, the number of REE-accumulating plants is limited to a relatively small number of species and the potential of REE accumulation by ferns in contaminated or enriched-environment has been little studied so far.

The identification of new species of ferns accumulating REE is of great interest to allow the selection of appropriate species adapted to a prospected area (soil, climatic conditions) for their use in environmental restoration, and for the purpose of phytoextraction. Screening of plants for new metal-accumulating species has already been done for several metals, including Cr [28], As [29], Pb [30], and Cd [31]. In order to identify new species that accumulate REE, but also to determine if this trait is conserved among certain genera, we have carried out a screening of fern species to determine their potential for REE accumulation. Unlike previous studies carried out under non-contaminated conditions [18,27], in the present study, an extensive set of forty-nine fern species, belonging to fifteen different genera, were screened on a soil enriched with REEs. This approach allowed us to identify new species of ferns accumulating REE. In addition, unlike plants harvested in mine areas contaminated with LREE, our experiment was aimed at providing equimolar concentrations of a group of LREEs (La, Ce, Sm) and HREEs (Gd, Yb, and Y), so that the fractionation patterns in plant tissue could be compared. We show here that all fern species preferentially accumulated LREEs, and particularly La and Ce, regardless of their accumulating status. In addition, the ionome analysis of the different fern species indicated a positive correlation between REEs and both Al and Ca, suggesting either common uptake pathways, or similar behaviour of these elements in the soil.

Materials and Methods

Plant species, substrate preparation and growth conditions

Forty-nine fern species, belonging to fifteen different genera, were used in the present study. The plants were purchased from a nursery specialized into hardy ferns and were all grown with the same substrate at the nursery. Plants were first removed from their substrate and subsequently grown on a REE-spiked loam (peat and perlite mixture, pH 5.7, Gramoflor GmbH & Co, Germany).

The loam was spiked with a total of 2,000 ppm REEs (333 ppm of La, Ce, Sm, Gd, Yb, and Y). Hexahydrate salts of $LaCl_3$, $CeCl_3$, $SmCl_3$, $GdCl_3$, $YbCl_3$, and YCl_3 (Sigma Aldrich, Saint-Quentin-Fallavier, France) were used. The REE solution was sprayed on a thin layer of loam (1 cm) prior to thorough hand mixing to ensure proper homogenization of the contamination. Five hundred grams (DW) of REE-spiked loam were then disposed into 3.4 L plastic pots (20 x 15 x 15 cm). This REE spiked loam was used for both the first and confirmation screens. In a third experiment, *Dryopteris erythrosora* was also exposed to 333 or 2,000 ppm of either La or Yb, or to a mix of the six REEs as mentioned above.

Plants were grown under controlled conditions in a phytotronic chamber (18/23°C, 12/12 h dark/light cycles (260 µmol/m^2/s), respectively) and watered twice a week. After 6 months of exposure, the aboveground biomass was harvested. Fronds were thoroughly rinsed with deionized water in order to remove potential soil contamination. Samples were dried at 70 °C for two days and used for subsequent elemental analyses.

Elemental analysis

The quantification of elements was performed from 250 mg of dried plant powder. Mineralization was carried out using 3.5 mL nitric acid and 1 mL hydrogen peroxide and samples were incubated in a heating block digestion system (DigiPREP, SCP Sciences, Courtaboeuf, France). A gradual heating mode was used to achieve a final temperature of 100°C (total run of 265 min). Then, ultrapure water (Millipore Milli-Q Integral 3 system, Molsheim, France) was added to a final volume of 25 mL and samples were filtrated to 1 µm. Elemental concentrations were determined by ICP-AES (Radial ICAP 6500 Model, Thermo Fischer Scientific, Courtaboeuf, France) or ICP-MS (X Series II Model, Thermo Fischer Scientific, Courtaboeuf, France) for REEs. Oriental basma tobacco leaves (INCT-OBTL-5, LGC Promochem, Molsheim, France) was used as certified reference material.

Statistical analyses

One-way ANOVA and Tukey HSD post hoc test were used when normality of data (Shapiro-Wilk test) and homoscedasticity (Levene's test) conditions were respected. When at least one condition was rejected, data were subsequently analysed using one-way nonparametric Kruskal-Wallis test followed by Dunntest. The rejection level was set at 5% in all analyses. Correlation analyses were performed using the R package Corrplot. All analyses were performed using R software (version 3.4.1). All reported values are means ± standard deviation (SD).

Results

Identification of new REE-accumulating ferns

Ferns were grown for six months and REE concentrations in fronds were analysed by ICP-MS. Of the 49 species tested, three main REE accumulation patterns were observed. REE concentrations were very low (<10 ppm) in ten species, twenty-four accumulated moderately between 10 and 100 ppm REEs, and 15 species accumulated more than 100 ppm REEs in their fronds (Figure 1). Of the ferns accumulating over 100 ppm, only three reached more than 200 ppm (Figure 1). This was the case of *Athyrium filix-femina* var. Victoriae, *A. othophorum,* and *Onoclea sensibilis*. At the genus level, three REE accumulation patterns were observed. REE concentrations were very low (<10 ppm) in all *Polypodium* species, whereas all *Athyrium* species highly accumulated REEs (ranging from 130 to 220 ppm) (Figure 1). The REE accumulation level was more variable among the different species of the other genera. In *Dryopteris* large disparities were measured between species (Figure 1). Two species accumulated less than 10 ppm (*D. carthusiana* and *D. filix-mas*), while the other species accumulated between 23 (*D. cycadina*) and 100 (*D. marginalis*) ppm REEs. The known REE-

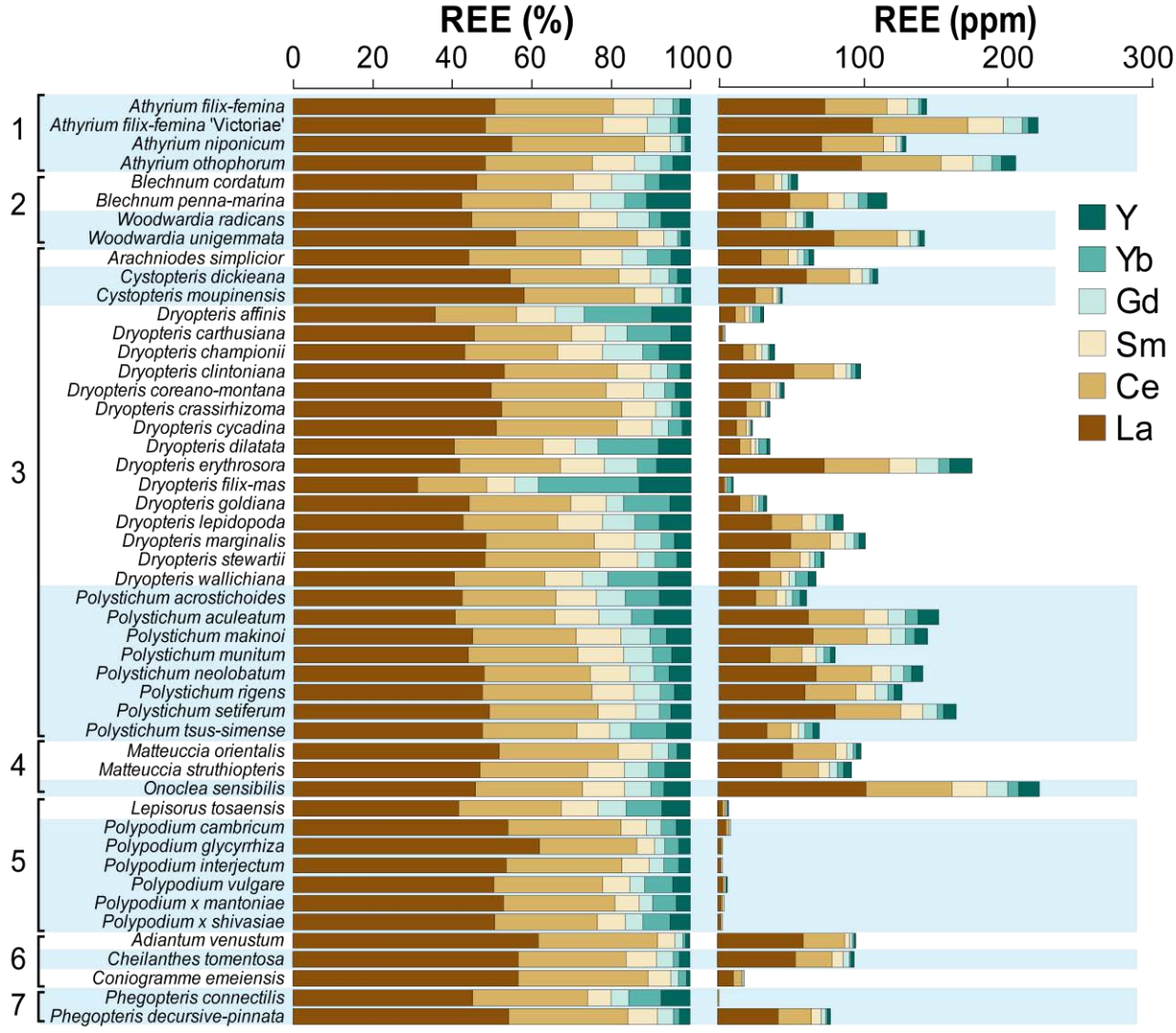

Figure 1: Screening for REE accumulation potential among fern species. On the left, the accumulation pattern of REEs in the fronds of forty-nine species of ferns is expressed as a percentage of the various REEs (La, Ce, Sm, Gd, Yb, and Y) on the total REEs accumulated. Species are gathered by family, as; (1) *Athyriaceae*, (2) *Blechnaceae*, (3) *Dryopteridaceae*, (4) *Onocleaceae*, (5) *Polypodiaceae*, (6) *Pteridaceae*, and (7) *Thelypteridaceae*. On the right, REE accumulation by fern species is expressed as ppm (mg/kg) of DW of the above ground biomass. For the first screen, a single plant was tested for each species.

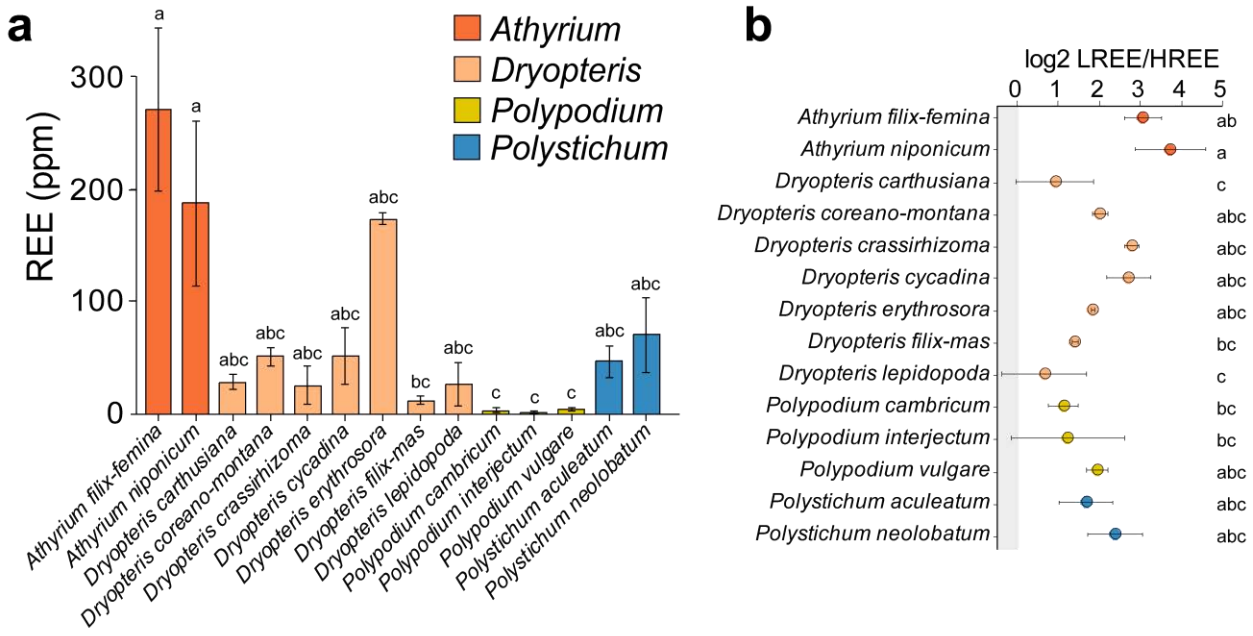

Figure 2: REE concentrations and fractionation in aboveground parts of ferns at the second screening. (a) Total REE concentrations in fern species harvested at the second screening (n = 3, mean ± SD). (b) REE fractionation process in fern pinnae. Log2 ratio of LREEs (La, Ce, Sm) to HREEs (Gd, Yb, Y) are given (n = 3, mean ± SD). Bars topped by the same letter do not differ significantly between species ($p<0.05$, ANOVA followed by Tukey HSD or Kruskal followed by Dunn test).

accumulating species *D. erythrosora* accumulated up to 175 ppm. Similar to *Dryopteris*, but to a lesser extent, *Blechnum*, *Woodwardia*, *Cystopteris*, and *Polystichum*, showed varying levels of REE accumulation.

In the primary screening, we tested 49 species of hardy ferns. The species tested belonged to seven families, namely Athyriaceae, Blechnaceae, Dryopteridaceae, Thelypteridaceae, in which species accumulating REE were already described in the literature[16], as well as Onocleaceae, Polypodiaceae, and Pteridaceae, (Figure 1). However, none of the species in this group have been previously tested for their REE-accumulation capacity, with the exception of *Dryopteris erythrosora*, which has been reported as a REE-accumulating species [32]. The second screening consisted in 14 species, representing 28 % of the ferns tested in the first screening. This second screening was carried out in triplicate in order to confirm the results obtained from the first screening. We focused our attention on 4 genera (*Athyrium*, *Dryopteris*, *Polypodium*, and *Polystichum*) representing different accumulating patterns (Figure 2a). This second dataset confirmed the first screening, with *Athyrium filix-femina* and *A. niponicum* being strong accumulating species of REEs, whereas the *Polypodium* species proved to be poor REE-accumulators. Finally, a significant variation in REE concentrations was again observed among *Dryopteris* species (Figure 2a).

Preferential accumulation of LREEs

In order to investigate whether a preferential accumulation of different REEs in the fronds of these ferns occurred, we investigated the fractionation pattern of REEs in different species. Interestingly, similar behavior was observed among all fern species studied in the first and second screenings (Figure 1, Figure 3). LREEs were more accumulated than HREEs and accounted for between 70% and 90% of the total REE content (Figure 1, Figure 3), with the exception of *Dryopteris filix-mas* and *D. affinis,* which accumulated a little less LREEs (Figure 1). This general LREE enrichment in ferns was confirmed during the second screening with LREE/HREE ratios (Figure 2b). The two *Athyrium* species accumulated 8 times more LREEs than HREEs, while in *Polystichum* and *Polypodium* species this ratio was respectively 4 and 2 (Figure 2b). In *Dryopteris* species, LREE/HREE ratio ranged from 2 (*D. lepidopoda*) to 8 (*D. crassirhizoma*). The highest REE-accumulating species of *Dryopteris* (*D. erythrosora*) had a ratio of 4 (Figure 2b). In general, higher concentrations of La were found in all species, followed by Ce, Sm, Gd, Y, and Yb (Figure 3). However, in *Polypodium* species, Yb was more abundant than Gd and Sm, as it was in some *Dryopteris* species (Figure 1, Figure 3c,d).

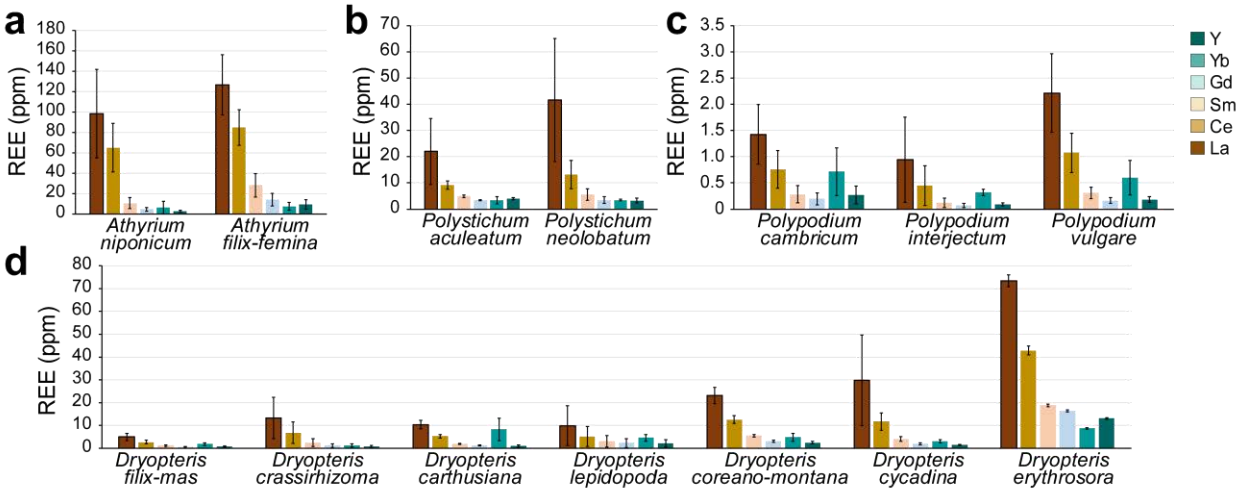

Figure 3: Detailed REE concentrations in selected ferns at the second screening. REE concentrations in (a) *Athyrium*, (b) *Polystichum*, (c) *Polypodium,* and (d) *Dryopteris* species. Plants were harvested after 6 months of growth on a REE-contaminated loam (n = 3, mean ± SD).

Macro- and micro-element composition under REE exposure

Principal component analysis (PCA) and Pearson correlation matrix of REE, micro and macro elements were derived from species belonging to the four genera used in the second screening (Figure 4, Table S1). This was done to identify the putative correlations between macro-, microelements, and REE accumulation in this set of ferns. The first two principal components of the PCA accounted for 48.3 % of the observed changes, with the first principal component accounting for 30.7 % (Figure 4a). REEs clustered, while among all REEs, Yb showed a slightly lower correlation with other REEs (Figure 4a). In the first principal component, several macro- and micro-elements clustered with REEs, such as Ca, Ni, Mg, Al, B, Fe, Na, and Mn (Figure 4a), while Mo was negatively correlated with REEs (Figure 4a). When analysing the correlation matrix, several macro- and micro-elements exhibited a significant positive correlation with REEs. This observation was true for Ca, Al, and to a lesser extent for Na (Figure 4b). A significant negative correlation was found only between Mo and La (Figure 4b). Yb was positively correlated with Ni and Mg (Figure 4b).

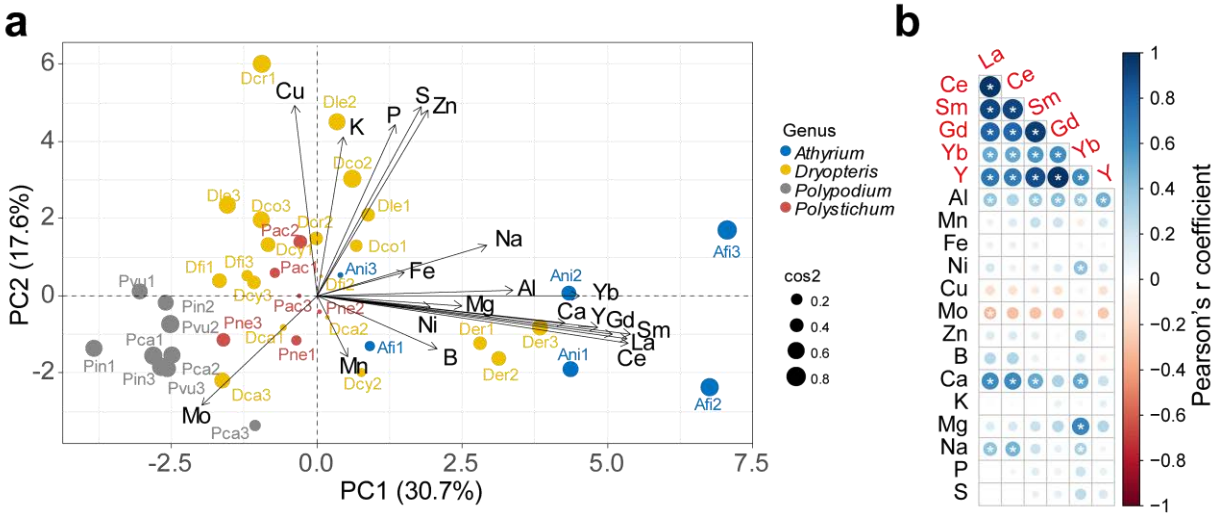

Figure 4: Correlation between REE and nutrient concentrations in fronds. (a) Principal component analysis of ferns exposed to 2000 ppm REEs. Ferns are color-coded depending on their genera. Cos2 indicates the contribution of the component for the PCA. (b) Pearson correlation matrix. White asterisks refer to significant p-values (< 0.05). REE, macro- and micro- elements were used as quantitative variables.

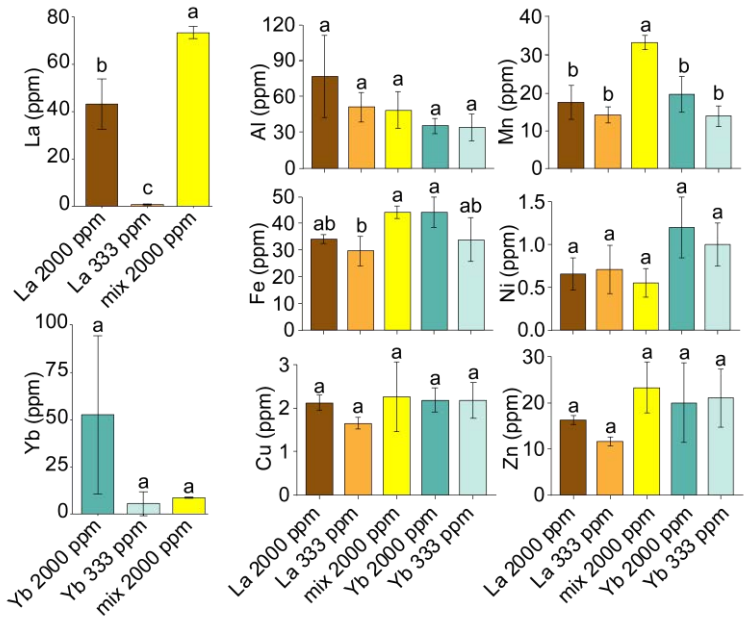

Figure 5: Selective accumulation of REEs by *Dryopteris erythrosora* and impact on elemental composition. Accumulation of La (a), Yb (b) and different microelements (c) by *D. erythrosora* under La or Yb exposure only (333 or 2000ppm), or under a mixture (mix) of the 6 REEs (La, Ce, Sm, Gd, Yb, and Y, 333 ppm each) (n = 3, mean ± SD). Bars topped by the same letter do not differ significantly between treatments ($p < 0.05$, ANOVA, Tukey HSD).

Increased La uptake under REE mixture treatment

Finally, we sought to determine whether there was a competition between light and heavy REEs by focusing on the REE-accumulator *D. erythrosora*. (Figure 5). Therefore, we exposed *D. erythrosora* to either 333 or 2000 ppm of either La or Yb only, or to a mixture of 6 REEs at 333 ppm each (2000 ppm total) as reported in both previous screenings. As expected, La and Yb concentrations were higher in fronds of the 2,000 ppm single REE treatment compared to the 333 ppm treatment (Figure 5a-b). Interestingly, more La accumulated in plants grown in the REE mixture treatment compared to those exposed to the 333 and 2000 ppm La only-exposed plants (Figure 5a). This finding was not true for Yb, where similar concentrations of this REE were found in plants exposed to mixed and single elements (Figure 5b). Apart from their REE content, plants exposed to the different treatments had similar ionomes (Figure 5c). Significant differences were observed only for Mn and Fe. Notably, fronds of *D. erythrosora* exposed to a mixture of the six REEs contained twice as much Mn compared to pure La and Yb treatments at different concentrations.

Discussion

The increasing use of REEs worldwide along with environmental contamination, especially around mining areas, raises the question of remediation of these sites. Plant-based remediation techniques could help to reduce high REE contents in soils through the use of REE-accumulating plants [15,16,33]. Relatively few plant species accumulating REEs are currently known and most of the species are fern [18, 21,22, 24–27,34]. Thus it is of interest to study ferns in order to identify new REE-accumulating species. For that purpose, we screened a large panel of forty-nine fern species, all hardy and ornamental ferns, on a loam spiked with six REEs (La, Ce, Sm, Gd, Yb, and Y). The screening of hardy and ornamental plants displays several advantages [31]. Indeed, the use of non-edible plants restricts their entry in the food chain [31,35,36]. Moreover, associated to their hardiness, these plants can be grown over several seasons and in diverse environments and climates. Furthermore, high cultivation skills and knowledge for such plants have been developed, which help in their application in phytoremediation [31,35,36].

Unlike previous studies [18], the present work is the first screening of ferns grown on a REE-contaminated substrate for their ability to accumulate REE. Using this screening strategy, we identified new REE-accumulating species. Of these, the species that accumulated the most (>200 ppm) were *Onoclea sensibilis*, followed by two species of *Athyrium*, namely *A. othophorum* var *okanum*, and *A. filix-femina* 'Victoriae'. The already known REE-accumulating species *D. erythrosora* ranked fourth with more than 175 ppm accumulated in its fronds. *Athyrium yokoscense* [27] has been previously mentioned as a REE-accumulating fern, thus it was noteworthy to note that other *Athyrium* species were also able to accumulate REEs. Similarly, two *Blechnum* species were able to accumulate moderate amounts of REEs in our study (55 ppm and 115 ppm for *B. cordatum*, and *B. penna-marina*, respectively); so far only a single species, *B. orientale* was reported in the literature [25,26]. In addition, we identified here for the first time new REE accumulators belonging to other fern genera. This is the case of several *Polystichum* species, along with *Onoclea sensibilis (Onocleaceae)*, and *Woodwardia unigemmata*

(Blechnaceae), which accumulate all more than 100 ppm REEs in their fronds.

In several cases, different species of the same genus have a similar accumulation potential. This was particularly the case of *Athyrium* species, which accumulated high REE contents, in contrast to *Polypodium* species that had very low REE contents. A possible explanation could be a conserved mechanism of REE uptake and/or translocation in *Athyrium*, which would be lacking in *Polypodium* species. Such a conserved trait of metal accumulation has been reported for *Carya* species that all accumulated REEs in their shoots [19], but also for Ni hyperaccumulation in several species of *Alyssum* and *Cochlearia* [37]. Conversely, it was interesting to note the differences in REE-accumulation between different species of a given genus. That was notably the case for *Dryopteris* comprising *D. erythrosora,* the highest accumulator in this genera and *D. filix-mas,* the lowest. This variation in REE-accumulation capacities between *Dryopteris* species could be correlated with the presence of specific mechanisms of REE absorption and/or translocation, which are not common to all *Dryopteris* species. The possible involvement of the different ploidy levels, as it has been demonstrated for *Carya* species [19] can be ruled out because of the higher ploidy level of *D. filix-mas* (tetraploid)[38] compared to *D. erythrosora* (triploid)[39]. Therefore, it supposes another explanation for the difference in the REE-accumulation ability.

A preferential accumulation of LREEs has been previously reported in REE-accumulating ferns [23,40,41]. However, those studies were based on samples taken from ferns grown naturally in mining areas that were highly enriched in LREEs. Indeed, in these areas, LREEs were usually 3 to 60 times more abundant than HREEs, which resulted in an obvious bias when comparing the accumulation pattern of LREEs *versus* that of HREEs. To circumvent this bias in the present study, we exposed ferns to equal amounts of each REE species. Nevertheless, we observed a preferential accumulation of LREEs (La, Ce, Sm) in fronds compared to HREEs (Gd, Yb, Y), ranging from 2 to 8 times more LREEs than HREEs. More specifically, REE accumulation increased with the increase of ionic radii of REE species (La > Ce > Sm > Gd > Y > Yb). These distinct/selective uptake preferences were also confirmed in *D. erythrosora* that accumulated more La when a mixture of six different REEs were provided, compared to only La, while no difference was observed for Yb only *versus* the mixture of REEs. It could be hypothesized that in the REE mixture, the HREEs that bind to chemical groups either in the roots or into the xylem, could leave more LREEs in their free ionic form, then be transferred into the shoots. Consequently, the addition of a mixture of LREEs and HREEs seems to favor an LREE enrichment. In species other than ferns, under equal amounts of each REE, the opposite pattern was observed, with a preferential accumulation of HREEs, as shown in pokeweed (*Phytolacca america)* [42], wheat (*Triticum aestivum*) [43,44] and soybean (*Glycine max*) [45].

The difference in REE fractionation between pteridophytes and angiosperms suggests various mechanisms of root-to-shoot transfer and selective enrichment. It has been shown that in wheat and soybean grown in hydroponic culture, the HREE enrichment observed in the leaves was mostly due to the larger transfer of HREEs complexed with organic ligands, compared to free LREE ions. Indeed, it has appeared an increase in the stability of organic acid-REE complexes with increasing atomic number. Thus, free LREE ions would be more likely to be adsorbed to cell walls or precipitated (e.g. with phosphate) in the xylem. In *P. americana*, it has been suggested that asparagine, glutamate, and histidine could be involved in the transfer of La and Y through the xylem [46]. Similarly, Yuan *et al*. (2017) showed the important role of citrate in REE translocation in the same plant [42]. In tomato, glutamate is playing this role [46,47], whereas in wheat transfer is assured by citrate, malate, and oxalate in the xylem sap [43,44]. Overall, these data suggest the importance of several amino and organic acids in REE translocation in plants. However, future studies using transgenic lines with modulated amino or organic acid synthesis or transport would be needed to fully validate these hypotheses.

In fern species a different mechanism could be involved in the LREE enrichment observed in fronds. In *Dicranopteris dichotoma*, Wang *et al.* (2003) identified a low molecular weight LREE-binding peptide [48]. Similarly, Lai *et al.* (2006) found another peptide specifically binding LREEs in the REE-hyperaccumulator fern *Pronephrium simplex* [22]. These peptides may be involved in reducing LREE toxicity in plants. They may be ubiquitous in fern species that accumulate REEs, and therefore explain the LREE enrichment observed in pteridophytes. However, we cannot rule out a lower content of organic acids in fern species than in angiosperms, precluding a relative HREE enrichment in fronds. In addition, angiosperms possess a xylem consisting of well-developed vessels and tracheids, while pteridophytes only have a tracheid-based xylem [49]. Such differences in the water-conducting tissues, and in particular in their structural composition (cell wall, organic ligands), could be a possible explanation for the enrichment of LREEs *versus* HREEs in the shoots of different plant lineages.

The ionome analysis showed that a higher content in several macro- and micro-elements were found in REE accumulating plants. Indeed, the REE content was found to be positively correlated with most elements analysed except for Mo and Cu. This positive correlation

with Fe, but also Al, Mg, K, and P has also been reported in beech, spruce, and oak [50]. In *D. erythrosora*, we also observed an increase in Mn content and REE accumulation. Similar results have been obtained in other accumulating plants, such as *Melastoma malabathricum* [51], an Al-accumulating plant. Furthermore, putative shared entry pathways in the roots between REEs and Ca but also Al ions have been suggested in *P. americana* [42]. These observations support the existence of common uptake pathways for REEs and essential elements.

Additionally, the availability of elements in soils is highly pH dependent. The availability of elements such as Al, Fe, Zn, Cu, B, and Mn, but also REEs, increases at low pH values, while the availability of elements such as Mo decreases at lower pH values [52]. The modified availability of these elements due to the soil pH could explain the correlations observed between REEs and essential elements. Wiche et al. (2016) observed an increase in Fe, Mn, and P content, as well as REEs in barley and white lupine [53]. The authors suggested that these elements could come from dissolution of REE-phosphates, carbonates and Fe-Mn oxyhydroxides under the influence of root exudates [53]. This hypothesis was confirmed by Shan, Lian & Wen (2002), who demonstrated that the bioavailability of REEs in soil is affected by soil pH, but also by low molecular weight organic acids [54]. In addition, they highlighted the involvement of organic matter, Fe-, Mn- and Al-oxides, on the adsorption and desorption behavior of REEs. Therefore, local acidification, as well as release of root exudates by the plants into the rhizosphere could contribute to the increased availability and subsequent uptake of essential elements, together with REEs, by plants. A similar REE concentration pattern has also been observed between that of roots of *D. dichotoma* and that of soluble REEs in the soil [23]. This underlines that soil-soluble REEs can be closely inter-related with REE uptake by plants [16].

Conclusion

In this study, we identified new fern species that can accumulate REEs in their fronds. The high REE-accumulation capacity identified in many species suggests a common putative trait of REE-accumulation in ferns, similar to the angiosperm genus *Carya*. Further analyses of root exudates, REE speciation, and molecular determinants, will lead to the identification of the specific mechanisms underlying the REE-accumulation trait. It is particularly interesting to decipher the underlying genetic and physiological determinants for LREE enrichment in pteridophytes *versus* HREE enrichment in angiosperms. We also report here the close relationship between REE accumulation and homeostasis of essential elements in ferns, supporting either common uptake pathways and/or behaviours in soils. Finally, the trait of REE accumulation conserved among these different species is of great interest for phytoremediation purposes since appropriate species can be chosen according to the area to be remediated. To go further, as has already been done for other metal accumulating plants [55], the isolation of rhizospheric and endophytic microorganisms (bacteria, fungi) will enable the establishment of microorganism-assisted phytoremediation. The inoculation of REE-accumulating plants with such organisms could improve the accessibility of nutrient to plants [56], and at the same time increase the efficiency of REE phytoextraction.

Acknowledgements

This work has been supported by the French National Research Agency through the national program "Investissements d'avenir" with the reference ANR-10-LABX-21-01/LABEX RESSOURCES21 and by the Région Grand-Est. We acknowledge Dr. Nadia Morin-Crini for the ICP-MS analyses, Christine Friry and Sarah Guinchard for technical support with plant growth and harvest.

References

1. Cotton, S. *Lanthanide and actinide chemistry*. *Lanthanide and Actinide Chemistry* (2006).
2. Ciacci, L., Reck, B. K., Nassar, N. T., & Graedel, T. E. Lost by design. *Environ. Sci. Technol.* **49**, 9443–9451 (2015).
3. Long, K. R., Van Gosen, B. S., Foley, N. K., & Cordier, D. *The principal rare earth elements deposits of the United States: A summary of domestic deposits and a global perspective*. *U.S. Geological Survey Scientific Investigations Report 2010-5220* (2010).
4. Hedrick, J. B. *Rare Earths*. *Metals and minerals: U.S. Geological Survey Minerals Yearbook 2001* (2003).
5. Gambogi, J. *Rare Earths*. *Metals and minerals: U.S. Geological Survey Minerals Yearbook 2015* (2018).
6. Tyler, G. Rare earth elements in soil and plant systems – A review. *Plant Soil* **267**, 191–206 (2004).
7. Ramos, S. J., Dinali, G. S., de Carvalho, T. S., Chaves, L. C., Siqueira, J. O., & Guilherme, L. R. G. Rare earth elements in raw materials and products of the phosphate fertilizer industry in South America: Content, signature, and crystalline phases. *J. Geochemical Explor.* **168**, 177–186 (2016).
8. Binnemans, K., Jones, P. T., Blanpain, B., Van Gerven, T., Yang, Y., Walton, A., & Buchert, M. Recycling of rare earths: A critical review. *J. Clean. Prod.* **51**, 1–22 (2013).
9. Zhuang, M. *et al.* Health risk assessment of rare earth elements in cereals from mining area in Shandong, China. *Sci. Rep.* **168**, 578–582 (2017).
10. Gonzalez, V., Vignati, D. A. L., Leyval, C., & Giamberini, L. Environmental fate and ecotoxicity of lanthanides: Are they a uniform group beyond chemistry? *Environ. Int.* **71**, 148–157 (2014).
11. Ikhlayel, M. Evaluation of the environmental impacts of rare earth elements production. *Int. J. Environ. Stud.* **74**, 939–957 (2017).
12. Rim, K. T., Koo, K. H., & Park, J. S. Toxicological evaluations of rare earths and their health impacts to workers: a literature review. *Saf. Health Work* **4**, 12–26 (2013).
13. Pagano, G., Guida, M., Tommasi, F., & Oral, R. Health effects and

toxicity mechanisms of rare earth elements - Knowledge gaps and research prospects. *Ecotoxicol. Environ. Saf.* **115**, 40–48 (2015).

14. Wakabayashi, T., Ymamoto, A., Kazaana, A., Nakano, Y., Nojiri, Y., & Kashiwazaki, M. Antibacterial, antifungal and nematicidal activities of rare earth ions. *Biol. Trace Elem. Res.* **174**, 464–470 (2016).
15. Padmavathiamma, P. K. & Li, L. Y. Phytoremediation technology: Hyper-accumulation metals in plants. *Water. Air. Soil Pollut.* **184**, 105–126 (2007).
16. Liu, C. *et al.* Element case studies: Rare earth elements. in *Agromining: Farming for metals. mineral resource reviews* (eds. Van der Ent, A., Echevarria, G., Baker, A. & Morel, J.-L.) (Springer, Cham, 2017).
17. Djingova, R., Ivanova, J., Wagner, G., Korhammer, S., & Markert, B. Distribution of lanthanoids, Be, Bi, Ga, Te, Tl, Th and U on the territory of Bulgaria using *Populus nigra* ' Italica ' as an indicator. (2001).
18. Ozaki, T., Enomoto, S., Minai, Y., Ambe, S., Ambe, F., & Tominaga, T. Determination of lanthanides and other trace elements in ferns by instrumental neutron activation analysis. *J. Radioanal. Nucl. Chem.* **217**, 117–124 (1997).
19. Wood, B. W. & Grauke, L. J. The rare-earth metallome of pecan and other *Carya*. *J. Am. Soc. Hortic. Sci.* **136**, 389–398 (2011).
20. Yuan, M., Liu, C., Liu, W.-S., Guo, M.-N., Morel, J. L., Huot, H., Yu, H.-J., Tang, Y.-T., & Qiu, R.-L. Accumulation and fractionation of rare earth elements (REEs) in the naturally grown *Phytolacca americana* L. in southern China. *Int. J. Phytoremediation* **20**, 415–423 (2018).
21. Lai, Y., Wang, Q. Q., Yan, W. W., Yang, L. M., & Huang, B. L. Preliminary study of the enrichment and fractionation of REEs in a newly discovered REE hyperaccumulator *Pronephrium simplex* by SEC-ICP-MS and MALDI-TOF/ESI-MS. *J. Anal. At. Spectrom.* **20**, 751–753 (2005).
22. Lai, Y., Wang, Q., Yang, L., & Huang, B. Subcellular distribution of rare earth elements and characterization of their binding species in a newly discovered hyperaccumulator *Pronephrium simplex*. *Talanta* **70**, 26–31 (2006).
23. Zhenggui, W., Ming, Y., Xun, Z., Fashui, H., Bing, L., Ye, T., Guiwen, Z., & Chunhua, Y. Rare earth elements in naturally grown fern *Dicranopteris linearis* in relation to their variation in soils in South-Jiangxi region (Southern China). *Environ. Pollut.* **114**, 345–355 (2001).
24. Shan, X., Wang, H., Zhang, S., Zhou, H., Zheng, Y., Yu, H., & Wen, B. Accumulation and uptake of light rare earth elements in a hyperaccumulator *Dicropteris dichotoma*. *Plant Sci.* **165**, 1343–1353 (2003).
25. Zhang, Z. Y., Wang, Y. Q., Li, F. L., Xiao, H. Q., & Chai, Z. F. Distribution characteristics of rare earth elements in plants from a rare earth ore area. *J. Radioanal. Nucl. Chem.* **252**, 461–465 (2002).
26. Liang, T., Li, K., & Wang, L. State of rare earth elements in different environmental components in mining areas of China. *Environ. Monit. Assess.* **186**, 1499–1513 (2014).
27. Ichihashi, H., Morita, H., & Tatsukawa, R. Rare earth elements (REEs) in naturally grown plants in relation to their variation in soils. *Environ. Pollut.* **76**, 157–162 (1991).
28. Shahandeh, H. & Hossner, L. R. Plant screening for chromium phytoremediation. *Int. J. Phytoremediation* **2**, 31–51 (2000).
29. Zhang, Z., Sugawara, K., Hatayama, M., Huang, Y., & Inoue, C. Screening of As-accumulating plants using a foliar application and a native accumulation of As. *Int. J. Phytoremediation* **16**, 257–266 (2014).
30. Salazar, M. J. & Pignata, M. L. Lead accumulation in plants grown in polluted soils. Screening of native species for phytoremediation. *J. Geochemical Explor.* **137**, 29–36 (2014).
31. Wu, M., Luo, Q., Liu, S., Zhao, Y., Long, Y., & Pan, Y. Screening ornamental plants to identify potential Cd hyperaccumulators for bioremediation. *Ecotoxicol. Environ. Saf.* **162**, 35–41 (2018).
32. Ozaki, T., Enomoto, S., Minai, Y., Ambe, S., Ambe, F., & Makide, Y. Beneficial effect of rare earth elements on the growth of *Dryopteris Erythrosora*. *J. Plant Physiol.* **156**, 330–334 (2000).
33. Chaney, R. L., Malik, M., Li, Y. M., Brown, S. L., Brewer, E. P., Angle, J. S., & Baker, A. J. Phytoremediation of soil metals. *Curr. Opin. Biotechnol.* **8**, 279–284 (1997).
34. Zhenggui, W. Rare earth elements in naturally grown fern *Dicranopteris linearis* in relation to their variation in soils in South-Jiangxi region (Southern China). *Environ. Pollut.* **114**, 345–355 (2001).
35. Liu, J. nv, Zhou, Q. xing, Sun, T., Ma, L. Q., & Wang, S. Growth responses of three ornamental plants to Cd and Cd-Pb stress and their metal accumulation characteristics. *J. Hazard. Mater.* **151**, 261–267 (2008).
36. Jelusic, M. & Lestan, D. Remediation and reclamation of soils heavily contaminated with toxic metals as a substrate for greening with ornamental plants and grasses. *Chemosphere* **138**, 1001–1007 (2015).
37. Krämer, U. Metal hyperaccumulation in plants. *Annu. Rev. Plant Biol.* **61**, 517–534 (2010).
38. Sessa, E. B., Zimmer, E. A., & Givnish, T. J. Unraveling reticulate evolution in North American *Dryopteris* (Dryopteridaceae). *BMC Evol. Biol.* **12**, (2012).
39. Hori, K., Watano, Y., & Murakami, N. Hybrid origin of the apogamous fern *Dryopteris hondoensis* (Dryopteridaceae). *Acta Phytotaxon. Geobot.* **67**, 133–146 (2016).
40. Wang, L. F., Ji, H. B., Bai, K. Z., Li, L. B., & Kuang, T. Y. Photosynthetic characterization of the plant *Dicranopteris dichotoma* Bernh. in a rare earth elements mine. *J. Integr. Plant Biol.* **47**, 1092–1100 (2005).
41. Ozaki, T., Enomoto, S., Minai, Y., Ambe, S., Ambe, F., & Tominaga, T. Determination of lanthanides and other trace elements in ferns by instrumental neutron activation analysis. *J. Radioanal. Nucl. Chem.* **217**, 117–124 (1997).
42. Yuan, M. *et al.* The accumulation and fractionation of rare earth elements in hydroponically grown *Phytolacca americana* L. *Plant Soil* **421**, 67–82 (2017).
43. Ding, S., Liang, T., Zhang, C., Huang, Z., Xie, Y., & Chen, T. Fractionation mechanisms of rare earth elements (REEs) in hydroponic wheat : an application for metal accumulation by plants. *Environ. Sci. Technol.* **40**, 2686–2691 (2006).
44. Ding, S. M., Liang, T., Zhang, C. S., Yan, J. C., & Zhang, Z. L. Accumulation and fractionation of rare earth elements (REEs) in wheat: Controlled by phosphate precipitation, cell wall absorption and solution complexation. *J. Exp. Bot.* **56**, 2765–2775 (2005).
45. Ding, S. M., Liang, T., Yan, J. C., Zhang, Z. L., Huang, Z. C., & Xie, Y. N. Fractionations of rare earth elements in plants and their conceptive model. *Sci. China, Ser. C Life Sci.* **50**, 47–55 (2007).
46. Wu, J., Chen, A., Peng, S., Wei, Z., & Liu, G. Identification and application of amino acids as chelators in phytoremediation of rare earth elements lanthanum and yttrium. *Plant Soil* **373**, 329–338 (2013).
47. Wu, J. L., Wei, Z. G., Zhao, H. Y., Li, H. X., & Hu, F. The role of amino acids in the long-distance transport of La and Y in the xylem sap of tomato. *Biol. Trace Elem. Res.* **129**, 239–250 (2009).
48. Wang, H., Shan, X.-Q., Zhang, S., & Wen, B. Preliminary characterization of a light-rare-earth-element-binding peptide of a natural perennial fern *Dicranopteris dichotoma*. *Anal. Bioanal. Chem.* **376**, 49–52 (2003).
49. Pittermann, J., Limm, E., Rico, C., & Christman, M. A. Structure-function constraints of tracheid-based xylem: A comparison of conifers and ferns. *New Phytol.* **192**, 449–461 (2011).
50. Brioschi, L., Steinmann, M., Lucot, E., Pierret, M. C., Stille, P., Prunier, J., & Badot, P. M. Transfer of rare earth elements (REE) from natural soil to plant systems: implications for the

environmental availability of anthropogenic REE. *Plant Soil* **366**, 143–163 (2013).

51. Khairil, M. & Burslem, D. F. R. P. Controls on foliar aluminium accumulation among populations of the tropical shrub *Melastoma malabathricum* L. (Melastomataceae). *Tree Physiol.* **38**, 1752–1760 (2018).
52. Fageria, N. K., Baligar, V. C., & Clark, R. B. *Micronutrients in Crop Production*. *Advances in Agronomy* **77**, (Elsevier Inc., 2004).
53. Wiche, O., Kummer, N. A., & Heilmeier, H. Interspecific root interactions between white lupin and barley enhance the uptake of rare earth elements (REEs) and nutrients in shoots of barley. *Plant Soil* **402**, 235–245 (2016).
54. Shan, X. quan, Lian, J., & Wen, B. Effect of organic acids on adsorption and desorption of rare earth elements. *Chemosphere* **47**, 701–710 (2002).
55. Visioli, G., D'Egidio, S., & Sanangelantoni, A. M. The bacterial rhizobiome of hyperaccumulators: future perspectives based on omics analysis and advanced microscopy. *Front. Plant Sci.* **5**, (2015).
56. Rengel, Z. & Marschner, P. Nutrient availability and management in the rhizosphere: Exploiting genotypic differences. *New Phytol.* **168**, 305–312 (2005).

Table S1: REE concentrations (mg/kg dry weight) in the fronds of ferns exposed to 2000 ppm REEs and grown for 6 months for the second screening (mean ± SD, n= 3).

Genus	*species*	Sample	REE	La	Ce	Sm	Gd	Yb	Y
Polypodium	*cambricum*	Pca	3.63 ± 1.80	1.47 ± 0.57	0.77 ± 0.38	0.30 ± 0.17	0.17 ± 0.12	0.70 ± 0.44	0.30 ± 0.17
Polypodium	*interjectum*	Pin	2.00 ± 1.31	0.93 ± 0.81	0.47 ± 0.40	0.10 ± 0.10	0.07 ± 0.06	0.33 ± 0.06	0.10 ± 0.00
Polypodium	*vulgare*	Pvu	4.57 ± 1.63	2.23 ± 0.71	1.07 ± 0.40	0.27 ± 0.12	0.13 ± 0.06	0.60 ± 0.35	0.23 ± 0.06
Polystichum	*aculeatum*	Pac	46.80 ± 13.65	21.97 ± 12.50	9.17 ± 1.53	4.97 ± 0.50	3.33 ± 0.21	3.37 ± 1.37	4.00 ± 0.46
Polystichum	*neolobatum*	Pne	70.53 ± 32.84	41.60 ± 23.44	13.10 ± 5.41	5.57 ± 2.17	3.50 ± 1.23	3.47 ± 0.25	3.30 ± 0.89
Athyrium	*niponicum*	Ani	187.17 ± 72.86	98.23 ± 43.11	64.77 ± 23.81	10.53 ± 5.28	4.50 ± 1.87	6.33 ± 6.06	2.80 ± 1.06
Athyrium	*filix-femina*	Afi	270.13 ± 72.46	126.70 ± 29.49	84.67 ± 17.52	28.10 ± 11.59	14.03 ± 6.12	7.47 ± 3.83	9.20 ± 4.50
Dryopteris	*crassirhizoma*	Dcr	25.85 ± 17.47	13.30 ± 9.05	6.85 ± 4.74	2.50 ± 1.70	1.15 ± 0.78	1.20 ± 0.71	0.75 ± 0.49
Dryopteris	*coreano-montana*	Dco	51.63 ± 8.30	23.17 ± 3.58	12.53 ± 1.71	5.57 ± 0.61	3.03 ± 0.47	4.87 ± 1.72	2.47 ± 0.51
Dryopteris	*cycadina*	Dcy	52.00 ± 25.36	29.83 ± 19.79	11.73 ± 3.78	4.10 ± 1.00	1.93 ± 0.47	3.03 ± 0.72	1.43 ± 0.29
Dryopteris	*filix-mas*	Dfi	12.13 ± 3.59	4.97 ± 1.62	2.70 ± 0.82	1.17 ± 0.31	0.67 ± 0.12	1.87 ± 0.64	0.80 ± 0.17
Dryopteris	*lepidopoda*	Dle	27.27 ± 19.00	9.97 ± 8.62	5.20 ± 4.37	3.07 ± 2.61	2.30 ± 1.97	4.60 ± 1.50	2.17 ± 1.63
Dryopteris	*carthusiana*	Dca	28.27 ± 6.63	10.40 ± 1.78	5.30 ± 0.82	2.00 ± 0.26	1.17 ± 0.25	8.33 ± 4.94	1.07 ± 0.40
Dryopteris	*erythrosora*	Der	173.27 ± 5.50	73.47 ± 2.65	42.83 ± 1.90	18.80 ± 0.53	16.27 ± 0.42	8.78 ± 0.34	13.09 ± 0.29

Table S2: Ionome (macro and micro elements, mg/kg dry weight) of the fronds of ferns exposed to 2000 ppm REEs and grown for 6 months for the second screening (mean ± SD, n= 3).

Genus	*species*	Sample	Al	Fe	Mn	Ni	Mo	Zn	B
Polypodium	*cambricum*	Pca	19.9 ± 24.7	60.67 ± 27.87	0.39 ± 0.17	2.56 ± 0.17	4.83 ± 3.35	16.1 ± 1.6	48.3 ± 20.5
Polypodium	*interjectum*	Pin	3.9 ± 6.8	35.03 ± 10.50	0.09 ± 0.00	2.61 ± 0.42	1.20 ± 0.66	16.1 ± 4.2	35.1 ± 16.9
Polypodium	*vulgare*	Pvu	0.0 ± 0.0	39.80 ± 8.23	0.00 ± 0.00	3.67 ± 0.72	4.67 ± 1.67	24.0 ± 9.2	43.2 ± 9.2
Polystichum	*aculeatum*	Pac	36.7 ± 7.0	53.70 ± 6.96	0.63 ± 0.05	4.86 ± 1.01	0.10 ± 0.00	32.0 ± 6.9	30.6 ± 1.3
Polystichum	*neolobatum*	Pne	47.3 ± 15.8	39.70 ± 6.54	0.73 ± 0.18	3.47 ± 0.35	0.70 ± 0.20	32.5 ± 4.8	36.6 ± 2.7
Athyrium	*niponicum*	Ani	35.7 ± 12.2	55.80 ± 4.44	0.50 ± 0.10	2.94 ± 0.45	0.37 ± 0.38	35.7 ± 5.5	68.6 ± 14.5
Athyrium	*filix-femina*	Afi	31.0 ± 13.6	55.43 ± 14.71	0.23 ± 0.15	4.00 ± 1.55	0.53 ± 0.23	37.7 ± 17.9	44.7 ± 10.3
Dryopteris	*crassirhizoma*	Dcr	16.3 ± 8.8	65.35 ± 5.03	0.25 ± 0.07	8.88 ± 3.02	0.10 ± 0.00	56.5 ± 8.6	34.5 ± 4.2
Dryopteris	*coreano-montana*	Dco	35.3 ± 6.2	62.23 ± 10.52	0.43 ± 0.21	5.17 ± 1.70	0.63 ± 0.15	33.9 ± 3.7	35.5 ± 3.1
Dryopteris	*cycadina*	Dcy	35.0 ± 14.0	61.23 ± 9.07	0.50 ± 0.20	3.93 ± 0.34	0.90 ± 0.62	32.6 ± 10.5	57.6 ± 6.9
Dryopteris	*filix-mas*	Dfi	52.2 ± 21.6	69.63 ± 11.96	0.72 ± 0.16	3.27 ± 0.51	0.40 ± 0.10	35.3 ± 3.7	51.4 ± 20.2
Dryopteris	*lepidopoda*	Dle	27.8 ± 19.4	42.07 ± 3.66	0.38 ± 0.24	5.63 ± 1.02	0.33 ± 0.25	40.2 ± 16.8	40.6 ± 13.2
Dryopteris	*carthusiana*	Dca	15.4 ± 3.6	53.70 ± 9.26	0.54 ± 0.50	4.17 ± 0.79	4.47 ± 0.93	32.5 ± 7.8	47.4 ± 1.0
Dryopteris	*erythrosora*	Der	48.5 ± 15.3	44.17 ± 2.91	0.56 ± 0.13	3.24 ± 0.91	1.23 ± 0.12	23.3 ± 5.6	34.5 ± 2.9

Genus	*species*	Sample	Ca	K	Mg	Na	P	S
Polypodium	*cambricum*	Pca	14721 ± 4548	19747 ± 7569	4246 ± 311	5546 ± 2906	1643 ± 252	1443 ± 212
Polypodium	*interjectum*	Pin	8622 ± 3786	14211 ± 6243	2718 ± 984	3583 ± 510	2690 ± 1183	1498 ± 309
Polypodium	*vulgare*	Pvu	11450 ± 2127	18393 ± 9751	3343 ± 301	5421 ± 1088	2652 ± 341	1954 ± 139
Polystichum	*aculeatum*	Pac	13254 ± 1674	12217 ± 3384	3241 ± 233	4105 ± 1709	2918 ± 408	3059 ± 236
Polystichum	*neolobatum*	Pne	13680 ± 1608	12649 ± 2815	3081 ± 171	1022 ± 155	1660 ± 544	1899 ± 306
Athyrium	*niponicum*	Ani	28068 ± 10929	24748 ± 15318	4552 ± 1627	15445 ± 6736	2181 ± 660	2258 ± 562
Athyrium	*filix-femina*	Afi	25200 ± 12104	17366 ± 7040	3959 ± 1808	8609 ± 6889	3505 ± 1271	2384 ± 1412
Dryopteris	*crassirhizoma*	Dcr	9818 ± 3236	35355 ± 16203	3624 ± 191	7007 ± 1078	3717 ± 915	3510 ± 773
Dryopteris	*coreano-montana*	Dco	16183 ± 2761	24716 ± 5434	4019 ± 621	5291 ± 2346	2948 ± 509	4324 ± 782
Dryopteris	*cycadina*	Dcy	17420 ± 4176	17105 ± 8917	3218 ± 515	5299 ± 1942	2444 ± 655	2404 ± 686
Dryopteris	*filix-mas*	Dfi	14284 ± 3373	19733 ± 4419	3972 ± 546	3620 ± 1217	1780 ± 126	3324 ± 295
Dryopteris	*lepidopoda*	Dle	15773 ± 3916	32046 ± 3587	4817 ± 1357	7124 ± 4405	4996 ± 1020	3663 ± 907
Dryopteris	*carthusiana*	Dca	16668 ± 2966	7024 ± 2072	7501 ± 892	2558 ± 1496	2330 ± 596	1769 ± 405
Dryopteris	*erythrosora*	Der	9484 ± 3302	28470 ± 3956	5751 ± 1489	3783 ± 1674	2168 ± 199	2650 ± 377

Discussions, perspectives and conclusion

The present work is part of the Laboratoire d'Excellence Ressources 21 (LabEx R21) that gathers multidisciplinary actors together to better understand the biogeochemical cycles and potential environmental and human health threats of strategic metals from the 21st century, among which are REEs. The current diversity of results from the literature regarding their effect on biota shows a multiplicity of mechanisms associated with REE exposure. There is a paucity of available biochemical and genetic data, especially regarding REE toxicity, and related knowledge is scarce and/or contradictory. Furthermore, studies mentioning mechanisms involved in REE absorption (e.g., membrane transport proteins), homeostasis and tolerance are also relatively rare. After reviewing the current literature, four major questions arose: What are the proteins and cellular functions involved in the response to REE stress? How are REEs transferred to organisms and what are the underlying transmembrane systems and mechanisms? Are there different toxicity and tolerance mechanisms between the REEs (LREEs vs HREEs)? Are REE accumulation and fractionation conserved traits in plants?

To address these questions, we aimed to build a comprehensive basis for understanding through the study and identification of genes, proteins, and cellular pathways involved in the response to REEs. The use of **high-throughput complementary omic** approaches in **model organisms** was our best option for this purpose. The different questions are addressed in the different chapters of this thesis, which is separated into two main parts. The first part **analysed REE toxicity in the unicellular eukaryote *Saccharomyces cerevisiae* (Part 1)**, while the second part **studied the effects of REEs in plants, as more complex eukaryotes (Part 2)**. These two parts are sub-divided into three chapters each, and they all contributing to the overall understanding of the effects of REEs in yeast and plants.

Part I - The use of genome-wide analyses in the eukaryotic model *Saccharomyces cerevisiae* to identify key mechanisms of REE toxicity and tolerance in eukaryotic cells

In the first part of this study, we provide new insights into the global cellular and molecular response of *S. cerevisiae*, a eukaryotic model organism, to different REEs. We combined several complementary large scale 'omic' approaches, each focusing on different steps of the cellular response (e.g., genes, RNA, proteins, cation homeostasis) to identify key genes, proteins, pathways and compartments involved in the response to REE exposure and uptake mechanisms (Figure 1).

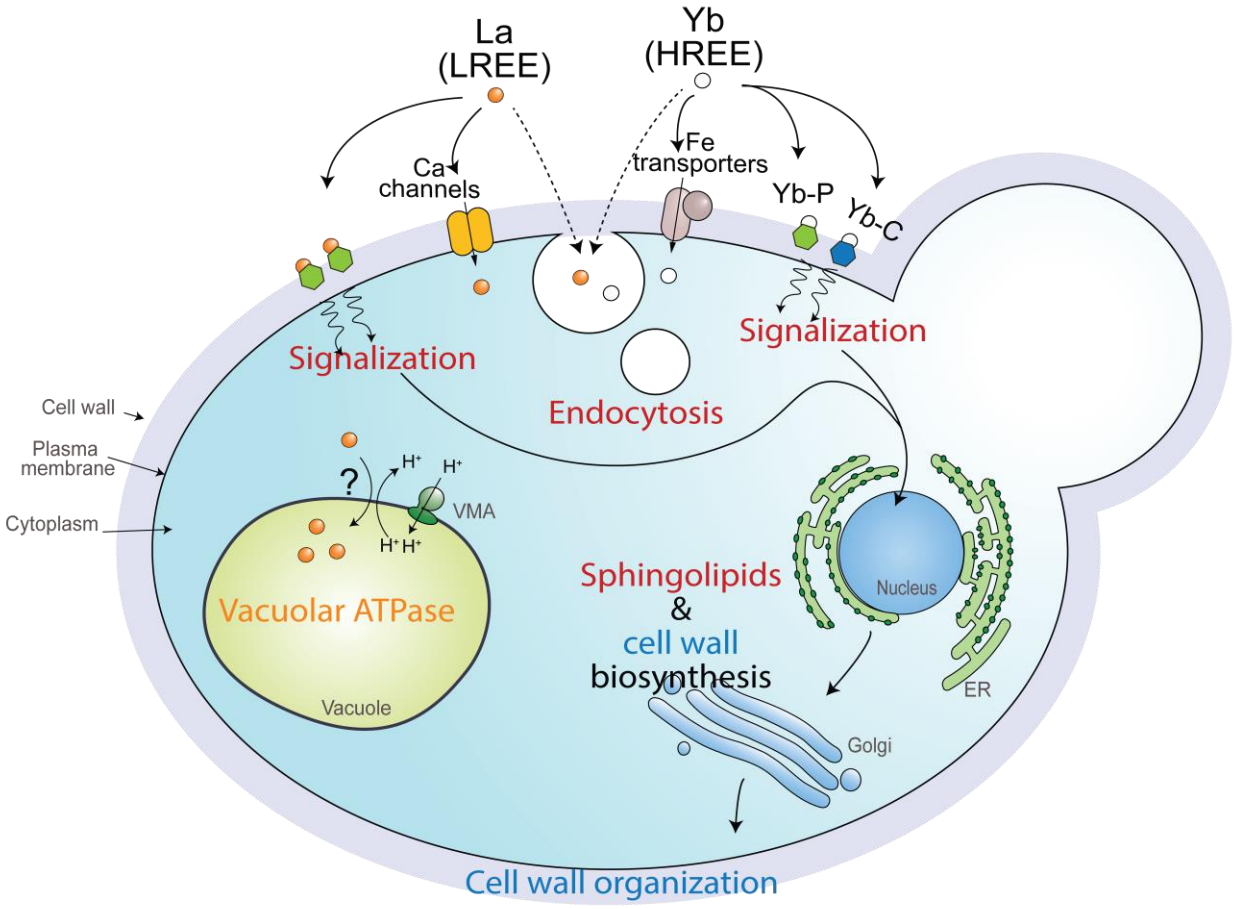

Figure 1: Global scheme of REE toxicity and tolerance mechanisms in *Saccharomyces cerevisiae* identified by complementary large-scale omic approaches.

First, in the initial two chapters (I.1 and I.2), we used the non-lanthanide HREE yttrium (Y), the LREE lanthanum (La) and the HREE ytterbium (Yb). Y displayed a very similar response pattern to that of Yb. However, many differences were observed between the HREEs (e.g., Yb and Y) and La. The results highlight discrepancies in the toxicity and tolerance mechanisms between

LREEs and HREEs. For instance, when screening the yeast mutant collection on La, Yb, and Y, we observed the clustering of Yb and Y (Figure 2a). However, in chapters I.2 and I.3, we further demonstrate that the differences between the LREEs and HREEs were not dichotomic, but they are progressive with the atomic number/ionic radius of REEs. This tendency can also be observed on the Pearson correlation table (Figure 2b), where Y is more similar to La (r of 0.35) than Yb is to La (r of 0.25), with Y and Yb being the most highly correlated (r of 0.59).

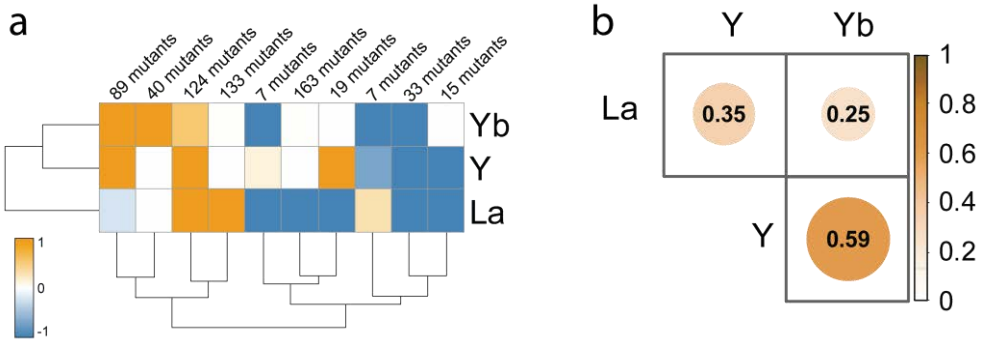

Figure 2: REE response patterns obtained from the genomic phenotyping of a whole mutant collection of *Saccharomyces cerevisiae* for La, Y and Yb. (a) Heatmap of mutant phenotypes to REEs. Different colours represent the mean phenotype of the clustered mutants (orange: resistant, blue: sensitive). The number of mutants within each cluster is specified. The hierarchical clustering was performed with the following parameters: average linkage, uncentred correlation, k-mean = 10. (b) Pearson correlation matrix with mutants used as quantitative values where significant r values are indicated (p-values < 0.05).

Second, the complementarity of the different approaches enabled us to identify, at a yet unreached level, the pathways, cellular compartments, genes and proteins that play a central role in the cellular response to REEs (Figure 1). We observed that REEs displayed specific responses and mechanisms in *S. cerevisiae* compared to other toxic metals, metalloids, and other stressors. We demonstrated the importance of endocytosis as a direct way of either uptake for these elements or the regulation of REE-transporting proteins. We also showed that the sphingolipid composition of yeast cells, which was modulated under REE exposure, was crucial for REE tolerance, either due to their involvement in membrane fluidity or in signalling. The pheromone-signalling pathway was highly over-represented in several of the omic approaches used, which underlines its essential role in yeast response to REE exposure. Discrepancies in the role of the vacuole in REE resistance also arose. It appeared through the implication of the VMA machinery, that the vacuole would be a detoxification compartment for LREEs, as it is for other toxic metals, but not for HREEs. Finally, we also demonstrated the importance of the cell wall as the first barrier in the interaction of yeast cells with these elements. Although REEs can interact with the cell wall, differences in adsorption

exist between the different REEs. The cell wall composition (phosphate versus carboxyl groups) seems to be critical for interactions with REEs, and this supports its essential role as a first shield against REE toxicity, together with a role in the yeast selective responses to LREEs and HREEs.

Finally, we provide here new insights into the uptake mechanisms of REEs in yeast cells. Despite historical knowledge about the similarity between the La and Ca ions, it was only quite recently shown that La could be taken up through Ca channels in yeast cells (Ene *et al.*, 2015). Here, by combining transcriptomic, proteomic and mutant analyses, we confirmed the role of the Ca channel Cch1-Mid1 in the uptake of LREEs. We also provide the first evidence that heavier REEs can be taken up through other essential ion transporters, specifically the Fe transport systems Fet3-Ftr1 and Fet4. To our knowledge, this is the first study reporting the close relationship between REEs and Fe homeostasis. Additionally, a possible role of Mg (Alr1-Alr2) and Mn (Smf1-Smf2) transporters in the uptake of REEs was also highlighted.

A complementary experiment of evolutionary engineering under both La and Yb stress was also carried out as part of a master's student internship (Ory, 2018). This approach consisted of exposing *S. cerevisiae* to increasing concentrations of either La or Yb in order to select evolved strains that were highly resistant to REEs. We observed that the acquired La resistance was extended to all LREEs, while that of Yb was extended to HREEs. By whole-genome sequencing of the evolved strains, we observed that the highly resistant strains towards La had mutations in the *CCH1* gene, encoding for the main transmembrane Ca channel in *S. cerevisiae*. Some other genes were also mutated, and their implication in REE stress resistance is under characterization. However, the first results of this evolutionary engineering experiment were congruent with those obtained previously, notably reinforcing the role of the Ca channel in LREE uptake.

In summary, these three chapters are closely intertwined and provide a solid basis to better understand the impact of REEs on eukaryotic cells. The present view of the yeast response to REEs provides a premise for complementary studies by focusing on the key pathways, compartments, genes and proteins involved. Among these, we can recommend the following:

- The interaction of REEs with signalling pathways needs further investigation. Effort should be made to decipher whether signal induction is the result of a direct interaction of REEs with receptors or is an indirect response (e.g., cell wall interactions, osmosis).

- Additional work might be done on sphingolipid interactions with REEs to ascertain whether sphingolipids are essential for membrane properties in response to REEs or whether they are essential regarding the signalling process, as was demonstrated for Fe.
- We demonstrated the involvement of endocytosis in REE uptake, and REEs have been shown to trigger endocytosis in plant protoplasts (Wang *et al.*, 2014). Therefore, the study of the regulation of transporters by endocytosis under REE stress would be essential to better understand the regulation of the uptake and detoxification of REEs. The occurrence of such a regulation mechanism for membrane transporters has been shown with other metallic stressors (Ooi *et al.*, 1996; Gitan and Eide, 2000; Liu *et al.*, 2007; Barberon *et al.*, 2011; Zelazny and Vert, 2015).
- Additionally, we hypothesized the existence of an REE efflux transporter. Further work should be done to identify such transporter and also to identify other possible detoxification mechanisms (e.g., vacuolar transporters).
- The uptake of REEs through essential ions transporters, especially Cch1-Mid1 for LREEs and Fet3-Ftr1/Fet4 for HREEs, should be further characterized. Kinetic uptake of REEs and Fe, or Ca could be accomplished with various concentrations of the different ions. The use of radioactive REE isotopes should also be considered.
- Electrophysiological analyses using the patch-clamp technique, or the apoaequorin cDNA expression system (Ene *et al.*, 2015) (a Ca^{2+}-induced photoprotein, allowing monitoring of intracellular Ca) on wild-type, mutants and yeast strains overexpressing these different transporters could help to validate/confirm the REE uptake through those transporters.
- Mutants for homologous transporters in other model fungi (e.g., *Neurospora crassa*, *Podospora anserina*, *Schizosaccharomyces pombe*) should be tested for their uptake and resistance towards REEs to support and extend our hypotheses on the uptake of REEs through essential ion transporters.

Part II - Investigation of the REE toxicity, resistance and transfer mechanisms in plants, being more complex eukaryotes

Until know, the studies available on this topic mostly dealt with the transfer of REEs from soil to plants and their translocation within the plant, without identifying the underlying mechanisms. The few studies focusing on cellular and molecular effects were on root growth inhibition triggered by REE toxicity. Therefore, there was a clear lack of molecular and cellular data concerning REE impacts and translocation. Therefore, in the second part of this thesis, we investigated global REE toxicity and transfer mechanisms in plants through molecular analyses (chapter II.1) and through the screening of different plants for their ability to accumulate REEs (chapter II.2 and II.3). The objective of chapters II.2 and II.3 was to identify phylogenetically related plants that displayed contrasting REE accumulation phenotypes. These new models would help to decipher the underlying mechanisms of REE accumulation and resistance by using comparative transcriptomic analyses.

We primarily used the well-known plant model *Arabidopsis thaliana* to investigate the response to toxic concentrations of REEs and the putative uptake and detoxification pathways. A transcriptomic analysis by RNA-seq was carried out on both roots and shoots exposed to either La or Yb. This approach evidenced unexpected pathways involved in the plant's response to REEs and new insights regarding the effects, uptake, translocation and detoxification of REEs in *Arabidopsis*.

Through this transcriptomic analysis, we confirmed and deepened the understanding of REEs' impacts on root architecture, which is likely to be the result of ROS production, meristematic cell death, and auxin redistribution. Unexpectedly, we found that REEs disturbed Fe homeostasis. Indeed, a Fe deficiency-like response was observed with exposure to either La or Yb. A possible explanation for this is competition between Fe and REE uptake through Fe transporters, which leads to a Fe-deficiency response. REEs might also trigger the Fe deficiency response at another level (e.g., regulatory), uncoupling REE effects from Fe competition at the transport step. Furthermore, we observed the modulated expression of genes encoding various transporters. Among them were several aquaporins, ABC and Mg transporters.

To deepen and confirm the observations made through the transcriptomic analysis, several more in-depth experiments must be carried out:

- Competition experiments between REEs and essential ions such as Ca, Mg, Mn, and especially Fe, to investigate uptake and toxicity would provide further evidence that REEs could enter plant cells through essential ions transporters and give information on their affinity for REEs. Such competition uptake experiments, combined with the use of radioactive isotope of REEs, could also confirm the hypotheses.
- The use of mutants of transporters suspected of participating in either the uptake or detoxification processes of REEs is also essential. For instance, IRT1 mutant lines would help to discriminate between the two hypotheses of Fe-REE competition for transport or the upstream effect of REEs on Fe deficiency signalling. If taken up by IRT1, REEs would less enter into root cells, thereby increasing plant tolerance to REEs in the mutant.
- To confirm the Fe-deficiency response induced by REEs, ferric-chelate reductase (FCR) activity could be analysed under REE exposure. Higher FCR activities would be expected in response to REEs, as was shown under Zn, Ni, Co, and Mn exposure (Lešková *et al.*, 2017). Additionally, monitoring the coumarin exudation by REE-exposed roots would also reinforce our understanding of Fe homeostasis modulation under REE stress (Lešková *et al.*, 2017).
- Since no Fe shortage was measured in the leaves or roots of REE-treated plants, proper Fe localization in these tissues needs to be assessed. A delimited mislocalization of Fe could also potentially trigger deficiency responses, notably leading to the higher Fe content observed in Yb-treated roots. Such Fe localization could be performed using the Perl's DAB method (Roschzttardtz *et al.*, 2009).

Notably, several genes related to the Al detoxification process were found, among which were organic acid transporters (e.g., malate, citrate).

- REE tolerance and uptake assays with or without the addition of organic acids in the growth medium must be tested to confirm the important chelating and detoxifying role of these molecules.
- The use of mutants for organic acid (malate or citrate) production or transport would also highlight the importance of these molecules in REE detoxification or translocation.

Mutants for the malate efflux transporter ALMT1, the citrate efflux transporter DTX42, or the citrate transporter FRD3 could be good candidates for testing.

We also observed a higher uptake of Yb compared to La when exposed to similar concentrations, suggesting a preferential accumulation of HREES. Altogether, according to these first insights in REE uptake, toxicity and detoxification, several complementary studies must be carried out to strengthen our findings and confirm our hypotheses.

- We need to characterize the role of unknown transporters that were modulated under REE exposure in REE homeostasis (e.g., the two major facilitator proteins At2g16660 and At4g34950, which were expressed at higher levels in the roots).
- The use of a transcriptomic approach investigating a shorter exposure time and different exposure concentrations could be performed to evaluate the plasticity and time-course of the plant response towards REE.
- A comparative analysis of REEs and other trivalent ions (e.g., Al, Ga, In, Cr, actinides) could help to identify specific markers of each ion exposure rather than a global response to trivalent ions.
- We performed RNA-seq on *Arabidopsis* using paired-end sequencing of 125 bp amplicons. The paired-end sequencing allowed us to carry out transcriptome profiling to identify transcript isoforms and splicing differences. It would be highly interesting to search for additional isoforms and differences in the data we obtained. Alternative splicing has been shown to be important for plants to adapt to environmental stress (Staiger and Brown, 2013; Filichkin *et al.*, 2015) and to maintain mineral nutrient homeostasis (Dong *et al.*, 2018). More specifically, it has been shown to be an important in response to Cd stress (Shen *et al.*, 2015) and for Zn tolerance. For example, Remy *et al*. (2014) investigated the vacuolar Zn transporter ZIF2 (zinc-induced facilitator 2). The authors demonstrated that high Zn levels favour the production of the longer ZIF2.2 transcript, which compared to ZIF2.1 confers greater Zn tolerance to transgenic plants by promoting higher Zn immobilization (Remy *et al.*, 2014). Only a few studies have investigated alternative splicing in *Arabidopsis*.

Following the transcriptomic approach carried out on the plant model *Arabidopsis thaliana*, we screened several plant species for their REE accumulation abilities. In this second approach, we aimed to find phylogenetically related plants that displayed different phenotypes regarding REE accumulation. Ultimately, a comparative transcriptomic analysis of such plants will be performed to identify putative specific mechanisms of REE accumulation and/or tolerance. This approach has been carried out on several hyperaccumulating plants. For example, comparative transcriptomics of two Cd and Zn hyperaccumulators, *Arabidopsis halleri* and *Noccaea caerulescens*, with the non-accumulator related species *Arabidopsis thaliana*, identified key pathways responsible for their hyperaccumulation trait (Weber *et al.*, 2004, 2006; Halimaa *et al.*, 2014). Additionally, a recent cross-species transcriptomic analysis in different plant families of nickel hyperaccumulators identified convergent functions that may represent major nodes in the evolution of nickel hyperaccumulating plants (Garcia de la Torre *et al.*, 2018).

In the angiosperm *Phytolacca*, this screening first established that the REE accumulation trait is likely shared and conserved between different *Phytolacca* species. Indeed, *P. americana* was the only REE-accumulating angiosperm species reported in the literature (Yuan *et al.*, 2017). Here, we demonstrated that this ability was extended to four other *Phytolacca* species, and they had a similar efficiency. The conservation of this trait was also observed in the genus *Carya*, in which all the species tested were able to accumulate REEs (Wood and Grauke, 2011). A similar procedure could be performed with a screening of hardy fern species. Interestingly, for *Phytolacca*, it is likely that the REE accumulation trait is shared among the species of several genera (*Athyrium*, *Blechnum*, and *Polystichum*). In *P. americana*, a known Mn-hyperaccumulator, no genetic differentiation could be detected between populations from Mn-contaminated and uncontaminated sites (Chen *et al.*, 2015), which classifies *Phytolacca* as a facultative accumulator (Pollard *et al.*, 2014). This suggests the not pollution-related evolution (van der Ent *et al.*, 2016) of Mn and REE-accumulation traits, but rather these species share a common ancestor possessing the REE accumulation trait. Despite the relatively limited number of species tested (less than ten per genus), these findings further strengthen the hypothesis that the REE accumulation trait evolved early on in the genus drift. Also notable is that the REE accumulation trait is polyphyletic, as exemplified by the repartition of REE-accumulating species in fern phylogeny (Figure 3). Nevertheless, little is known regarding the evolution of metal hyperaccumulation in plants. Most of the available data are about Ni hyperaccumulation and the particularly high occurrence of metal hyperaccumulation in the

Brassicaceae family (Krämer, 2010). These data highlight the broad distribution of hyperaccumulators across the angiosperm phylogeny is likely the consequence of multiple independent evolutionary events (Goolsby and Mason, 2015), as in our case for the REE-accumulation trait. Future work in this area would be valuable.

It would be interesting to study the conserved mechanisms underlying this shared accumulation and fractionation trait in, for example, *Phytolacca* and *Athyrium*, more in-depth. Since no accumulator/non-accumulator pair could be found among these genera, it will be necessary for comparative transcriptomics to identify a non-accumulating plant from a closely related genus (e.g., *Monococcus* or *Petiveria* for *Phytolacca*)) despite being a more complicated method or to screen the species of these genera more exhaustively. The more phylogenetically distant the species, the more difficult it is to compare their sequences, therefore implying more complicated bioinformatics processing. An alternative option would be to perform a gain of function approach in a heterologous system (e.g., *S. cerevisiae*) with cDNA libraries obtained from total mRNA of REE-accumulating plants. Screening for either a higher resistance (e.g., due to intracellular detoxification or efflux) or sensitivity (higher REE accumulation) will enable candidate genes to be selected.

Interestingly, we identified contrasting REE-accumulation trait phenotypes when screening ferns of the *Dryopteris* genus. The ploidy level of the *Carya* species was shown to be related to the accumulation of REEs (Wood and Grauke, 2011). Species with a higher ploidy level accumulated more REEs in their shoots. Consequently, the ploidy level should be considered for the fern species to verify whether a similar rule exists that could explain these discrepancies (e.g., more copies of a particularly important gene). As previously mentioned, we identified species that take up REEs (e.g., *Dryopteris erythrosora*) and species that do not (e.g., *Dryopteris filix-mas*). However, the higher ploidy level of *D. filix-mas* (tetraploid) (Sessa *et al.*, 2012) compared to *D. erythrosora* (triploid) (Hori *et al.*, 2016) implied the explanation for the difference in the REE-accumulation ability. Such a couple is particularly suitable for comparative transcriptomics, which will be performed to identify specific mechanisms of REE transfer and tolerance developed by REE-accumulating plants (EC2CO project RAREFERN, project leader M. Le Jean, collaboration LIEC-I2BC).

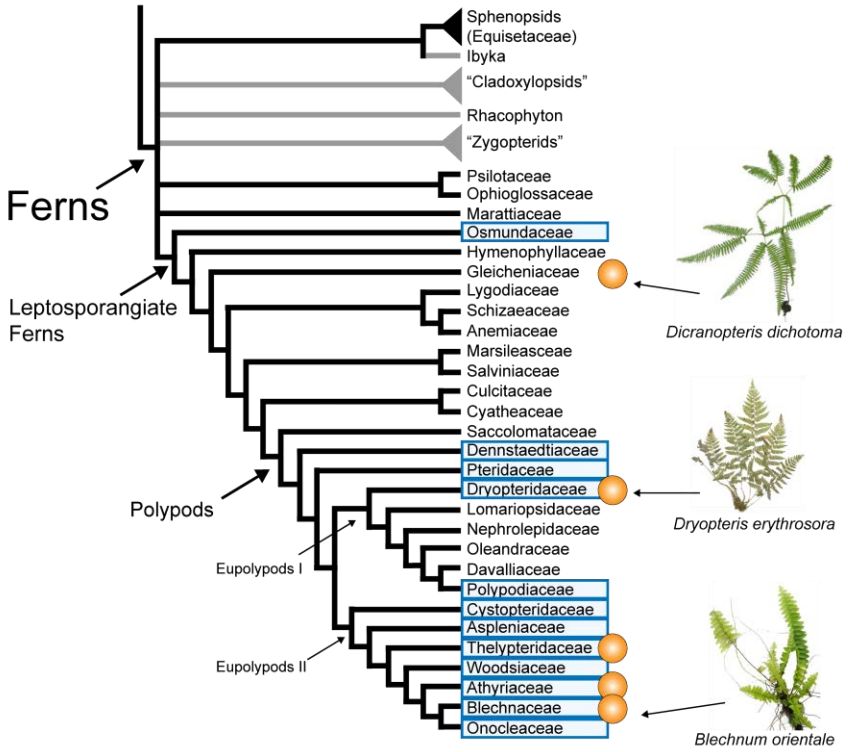

Figure 3: Fern phylogeny; the families of reported REE-accumulating species are indicated by orange circles. Families tested in our REE accumulation screening are indicated by blue boxes.

When studying the fractionation of REEs in plants, we observed an enrichment of HREEs translocated to the aerial part of *Phytolacca* species when exposed at equimolar concentrations of each REE, in the same manner as was observed in *Arabidopsis* (Figure 4). Conversely, unlike what was observed in these two angiosperms, ferns preferentially took up LREEs (Figure 4). The different REE fractionation between the two divisions suggests diverse root-to-shoot mechanisms and selective enrichments. HREEs have been suggested to be transferred through organic complexes, while LREEs could be transferred as free ions (Liang *et al.*, 2008). Therefore, free LREEs would likely interact more with cell walls or precipitate in the vascular system. Conversely, the higher enrichment of LREEs could be due to either a lower production of organic ligands (carboxylates) compared to angiosperms, the result of the different vascular system compositions, or the result of specific interacting molecules in ferns. In *Dicranopteris dichotoma*, Wang *et al.* (2003) identified a low molecular weight LREE-binding peptide (Wang *et al.*, 2003). Similarly, Lai *et al.* (2006) found another LREE-binding peptide in the REE hyperaccumulator fern

Pronephrium simplex (Lai *et al.*, 2006). Each of them is a good candidate to explain the observed LREE enrichment in ferns.

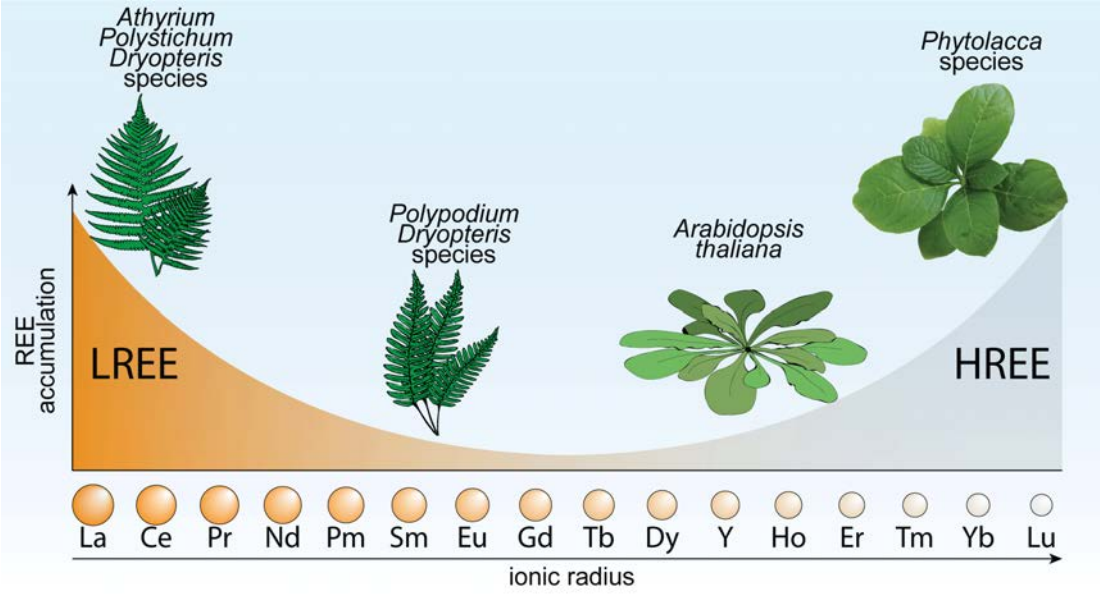

Figure 4: Preferential accumulation of LREES versus HREES in ferns and angiosperms.

A series of µXRF experiments at P.06 (PETRA III synchrotron, Hamburg) and LUCIA (SOLEIL synchrotron, Saint-Aubin) assessed the localization of REEs in plant leaves. REEs could be successfully distinguished, providing an elemental distribution in frond parts (pinnae, pinnule and rachis) of *D. erythrosora* and revealed that REEs were mostly located in the vascular system of the rachis and pinnae (personal communication). The occurrence of REEs in the vascular system of the aerial parts illustrates their effective translocation from roots to shoots. However, since they were mostly found in the vascular system, there might be a limitation in their discharge from parenchymatic cells. A few hypotheses can be drawn from this observation. The transport of REEs from the roots to the shoots can be achieved by organic acids (e.g., oxalate, citrate, malate) that would allow their transport in the roots through the symplastic route to pass the Casparian strip. Their translocation to the shoots could, however, encounter differential reactivity, where REEs could interact and bind to cell wall constituents, limiting their discharge. Additionally, the absence of a transporter involved in their discharge cannot be ruled out.

- More in-depth studies of the different tissues of ferns using synchrotron facilities will give insights about the different REE-specific absorption, transfer and fractionation

processes in different plants (fern *versus* angiosperm and accumulating *versus* non-accumulating) and under different growth and exposure conditions.

- The analysis of the sap metabolome of accumulating species would help to identify key molecules involved in the tolerance and transfer of REEs (e.g., organic acids).
- A comparative analysis (e.g., metabolome under REE exposure) of angiosperms (e.g., *Phytolacca*, *Arabidopsis*) *versus* ferns in the preferential uptake of HREEs and LREEs, respectively, would help to clarify this dichotomy in REE fractionation and accumulation.

General discussion

The present thesis aimed to unravel the REE-responsive genes in model organisms. To fill this knowledge gap and build a general framework regarding their toxicological effects on organisms, we focused our study on the genes, proteins, and cellular pathways involved in the response to REEs using well-known model organisms, *S. cerevisiae* and *A. thaliana*. We also investigated REE toxicity and transfer in plants by identifying REE-accumulating plant models to ultimately study REE-specific accumulation and tolerance mechanisms. Taken together, these results help to build a global knowledge basis on the effects of REEs on organisms and to apprehend their toxicity in the environment. In the two different model organisms, *S. cerevisiae* and *A. thaliana*, we observed mechanisms that were (1) in common with the response to other well-known elements, (2) specific to REEs, (3) different between LREEs and HREEs, and (4) new putative transport mechanisms of REEs.

1. REEs trigger mechanisms in common with other elements

Jin *et al*. (2008) carried out a global transcriptome and deletome profiling of yeast exposed to transition metals. The authors observed that several pathways were affected by every metal tested, and they identified the genes involved, terming them common metal responsive genes (Jin *et al.*, 2008). In the different studies carried out in our work, we also found that some mechanisms in common with other toxic metals were induced in response to REE stress. Several articles refer to the oxidative stress induced by REEs, mainly in plants and animals (Pagano *et al.*, 2015). In both *S. cerevisiae* and *A. thaliana*, an oxidative stress response occurred at the transcriptional level. Hence, part of REE toxicity might be explained by the production of oxidative stress. Another effect of REEs is their toxicity (mutants for this pathway are resistant) through the ubiquitin-dependent protein catabolic process via the multivesicular body sorting pathway (ESCRT complex), as was shown for nickel (Ruotolo *et al.*, 2008), which therefore cannot be considered as REE-specific. Finally, the vacuole is an essential cellular compartment for the detoxification of toxic metals (e.g., Cd, Zn, Cu, Mn) in many organisms. Here, we identified its importance as a detoxification compartment for LREEs in *S. cerevisiae*, where VMA-lacking mutants were sensitive to LREEs but not to HREEs, and potentially in *A. thaliana* with the upregulation of transporters involved in vacuolar sequestration, such as MTP8, MTP9, ZIF1 and ABC/PDR family transporters, following REE exposure.

2. REEs cause specific cellular reactions

In this study, we have reported several indications of REE-specific mechanisms and pathways, notably in *S. cerevisiae*. We identified that endocytosis was involved in the REE response given that mutants for this pathway were resistant to REEs in our screening. The opposite phenomenon seemed to occur with Cr, with mutants for endocytosis showing sensitivity to Cr (Holland and Avery, 2009). Since endocytosis mutants were resistant to REEs, this inferred that endocytosis is involved in REE toxicity, possibly by mediating intracellular Ln uptake. Therefore, we hypothesize that endocytosis could either be involved in the direct uptake of REEs in cells or in mediating the removal of plasma membrane transporters (efflux system). Since REEs also trigger endocytosis in plant protoplasts, thereby allowing their entry into the cells (Wang *et al.*, 2014), it would be interesting to further study the implications of this process in REE homeostasis.

In addition, the sphingolipid composition, which is essential in the REE toxicity response, also appeared to be specific. In the genomic phenotyping of the *S. cerevisiae* mutant collection, we observed results that were opposite to those obtained for Fe (Lee *et al.*, 2012). Through several experiments in *S. cerevisiae*, we found a close relationship between sphingolipid homeostasis, cell wall organization, and transport, in response to REE stress. Additionally, the regulation of transporters by plasma membrane microdomains (Grossmann *et al.*, 2008) could be essential in modulating the transport of REEs within the cell.

3. LREEs and HREEs interact differently with cells

A few studies have suggested that LREEs and HREEs may induce different responses, which could be due to either the decreasing ionic radius and increased atomic mass (so-called Ln contraction), to their reactivity or to other chemical differences (Gonzalez *et al.*, 2014; Wang *et al.*, 2017). In all of the different studies carried out in this work, we confirmed and further characterized these discrepancies in the responses to the different REEs. In each of the omic analyses comparing the La and Yb response in *S. cerevisiae*, we showed the importance of the cell wall in the REE stress response. Indeed, in both proteomic and transcriptomic analyses, we observed the upregulation of genes involved in cell wall organization. In the mutant collection screening, *S. cerevisiae* mutants with a modified cell wall composition displayed different phenotypes depending on the REE species. Therefore, we hypothesize that the preferential reactivity of REEs with either phosphate (LREEs) or carboxyl (HREEs) groups was the main driver for the observed

differences. The discrepancies between the LREE and HREE effects were not dichotomic, but were progressive with the atomic number and ionic radius of REEs, as shown in the phenotypic characterization of cell wall mutants (Chapter I.2). Previous studies have demonstrated the selective adsorption of REEs by biological membranes (Texier *et al.*, 2002, 2010; Andrès *et al.*, 2003). The cell wall is the first compartment to sort the REEs, and its composition is essential for REE interaction.

Discrepancies in REE detoxification mechanisms were also observed. As previously mentioned, in *S. cerevisiae* the vacuole was a detoxification compartment for LREEs, as it is for other toxic metals but was not for HREEs. The putative dissimilarity for the vacuole role in plants for detoxifying the different REEs has yet to be delineated. In yeast, we hypothesize that the differential involvement of the vacuole in REE detoxification leads to differential vacuolar REE accumulation; however, this needs to be analysed. Differences in the vacuole LREE and HREE sequestration could be due to the specificity (LREEs *versus* HREEs) of a yet unidentified tonoplast transporter (e.g., the Cd transporter Zrt1p or the Co transporter Cot1p).

4. New putative transport mechanisms for REEs

To date, relatively few studies are available regarding the transport mechanisms (both uptake and translocation) of REEs in living organisms. However, the present work reveals new molecular evidence, reinforcing the current hypothesis of the involvement of organic acids, putative REE transport through ion transporters and channels, and provides new insights into the effects of REEs on Fe homeostasis.

- ***Organic acids are involved in REE transport***

In plants, similar to metals and metalloids (Anjum *et al.*, 2015), organic acids have been suggested to be differentially involved in REE translocation from roots to shoots. A higher affinity of organic acids for HREEs could explain a specific enrichment in the shoots, as suggested by the involvement of citrate in HREE accumulation in *Phytolacca* (Yuan *et al.*, 2017). Consistently, the transcriptomic analysis in *Arabidopsis thaliana* showed an upregulation of organic acid transporters (ALMT3, DTX2), supporting the involvement of organic acids in the response to REEs. Therefore, the analysis for a modified REE transfer or tolerance in mutant lines would help to confirm this hypothesis.

- ***REEs are transported though Ca channels***

The available examples and comparisons with other toxic metal (e.g., Cd) transport support the putative nonspecific entry of REEs through essential cation transporters, with different transport systems responsible for LREE and HREE entry. Uptake through Ca channels has been primarily supported by the similarity between the ionic radius of lanthanides (notably La), as well as the use of La as a Ca channel inhibitor (Lansman, 1990; Lewis and Spalding, 1998). A few years later, it was demonstrated that lanthanides could indeed be taken up through the Ca channels. La and Eu where shown to enter into plant cells through an artificial Ca channel (Gao *et al.*, 2003). In yeast, La and to a lesser extend Gd, were taken up by Cch1-Mid1 (Ene *et al.*, 2015). In our work with *S. cerevisiae* and *A. thaliana*, we established a better understanding of REE uptake through transmembrane cation transporters. Notably, we confirmed phenotypically (chapter I.3) the involvement of the Ca channel Cch1-Mid1 in the uptake of REEs and revealed its specificity for the lighter species (from La to Tb) in *S. cerevisiae*. In *Arabidopsis thaliana*, exposure to La impaired Ca homeostasis, again supporting the close link between LREEs and Ca transport. Further functional characterization of LREEs *versus* HREEs transport through plant Ca channels will allow us to confirm the hypothesis of a possibly conserved mode of transport for LREEs through Ca channels.

- ***Mg transporters take part in REE transport***

Macdiarmid and Gardner (1998) showed that the overexpression of ALR1 and ALR2, encoding Mg uptake transporters in *S. cerevisiae*, led to La sensitivity (MacDiarmid and Gardner, 1998). Accordingly, we observed that the ALR2 mutant was resistant to most of the LREEs. Furthermore, in the transcriptomic analysis of *Arabidopsis* exposed to REEs, we noticed increased expression of the Mg transporter MRS2-8 in the roots. Therefore, we hypothesize that REEs could also partly accumulate in organisms through Mg transporters.

- ***A close link exists between REE and Mn transport***

Combining all the results from our experiments on yeast and plants identifies a close relationship between REEs and Mn. First, we observed that the mutation of SMF1-SMF2 (Mn transporters) in *S. cerevisiae* led to a sensitive phenotype to all REEs. This sensitive phenotype was associated with

a higher Yb accumulation, which could suggest the involvement of other transporters of HREEs. These other transporters would be more highly expressed in the SMF1-SMF2 mutant, such as Fe transporters, which ultimately allow more Yb to be taken up. However, this hypothesis must be verified. Second, we observed that less Mn was accumulated in *Arabidopsis* leaves under both La and Yb stress, together with a modified expression for MTP8, a Mn tonoplastic transporter. Moreover, our data confirmed the negative correlation between Mn and HREEs in both the leaves and roots of *Phytolacca* species, among which were *P. americana* and *P. acinosa*, which are known as Mn hyperaccumulators (Min *et al.*, 2007; Dou *et al.*, 2009; Xu *et al.*, 2009). These convergent observations lead to the questions of why and how there is a close link between the metabolism of Mn and REEs. A first hint is regarding the Mn hyperaccumulation by *Phytolacca* species. It was speculated that Mn accumulation was the result of high carboxylate (e.g., oxalate) concentration and proton release (Lambers *et al.*, 2015). The pH, redox potential, and carboxylate production combined enable the dissolution of Fe-Mn oxyhydroxides and metal-phosphate complexes from soil, which then can release REEs and Mn (Hu *et al.*, 2006; Lambers *et al.*, 2015); this could explain the similarities observed for REEs and Mn. Further evidence of effective REE transport in plants and yeast through the proposed candidates is, however, needed to unravel the precise interplay between these elements.

- ***Fe homeostasis disruption by REEs***

In the different chapters, we highlighted the yet unreported disruption of Fe homeostasis by REEs. Indeed, the Fe-starvation response was predominant in *Arabidopsis*, with several Fe-related differentially expressed genes, despite no effect on the global Fe content in shoots after 3 days of REE treatment. This Fe deficient-like expression pattern could be due to a mislocalization of Fe under REE stress instead of a lower global content. However, three days of exposure may have been too short to modify the Fe content, and a longer experiment (seven days) is currently being performed. Alternatively, the Fe-status signalling could be impaired without direct effects on Fe transport/uptake, as exemplified by the consequences of other metals on Fe homeostasis at different steps of its regulation or transport (Lešková *et al.*, 2017). Additionally, since we observed a higher expression level of IRT1 under La and Yb exposure, a competition of REEs and Fe for this transporter could be suggested, therefore proposing IRT1 as a mode of entry of REEs into root cells. This hypothesis is currently being tested using IRT1-mutated plants.

Additionally, in *S. cerevisiae*, we showed that mutants for the Fe transporters (FTR1-FET3 and FET4) were more resistant to and accumulated less HREEs. In the same way, the proteomic analysis showed a lower expression level of FTR1-FET3 under Yb exposure, which could reflect a protective mechanism against REE entry or an REE-induced perturbation of Fe homeostasis. Taken together, our results demonstrate for the first time that Fe transporters could be a mode of entry for HREEs in yeast. The transcriptomic response of plants exposed to REEs also strongly suggests the transport of REEs through the Fe pathway. Differences in REE specificity arise from comparisons of the yeast and *Arabidopsis* experiments regarding Fe homeostasis. HREE specificity was found for yeast regarding the Fe uptake system, while the Fe-deficient response was triggered by both La and Yb in *Arabidopsis*.

Outcomes of the thesis

Overall, the different approaches presented here will help establish general knowledge of the cellular and molecular metabolism of REEs in living organisms. We reported the relevant pathways, proteins and genes for REE toxicity and began investigating the putative transport mechanisms. Beyond the theoretical knowledge obtained in this work, further fundamental research studies will ensue, together with novel biotechnological applications (Figure 5).

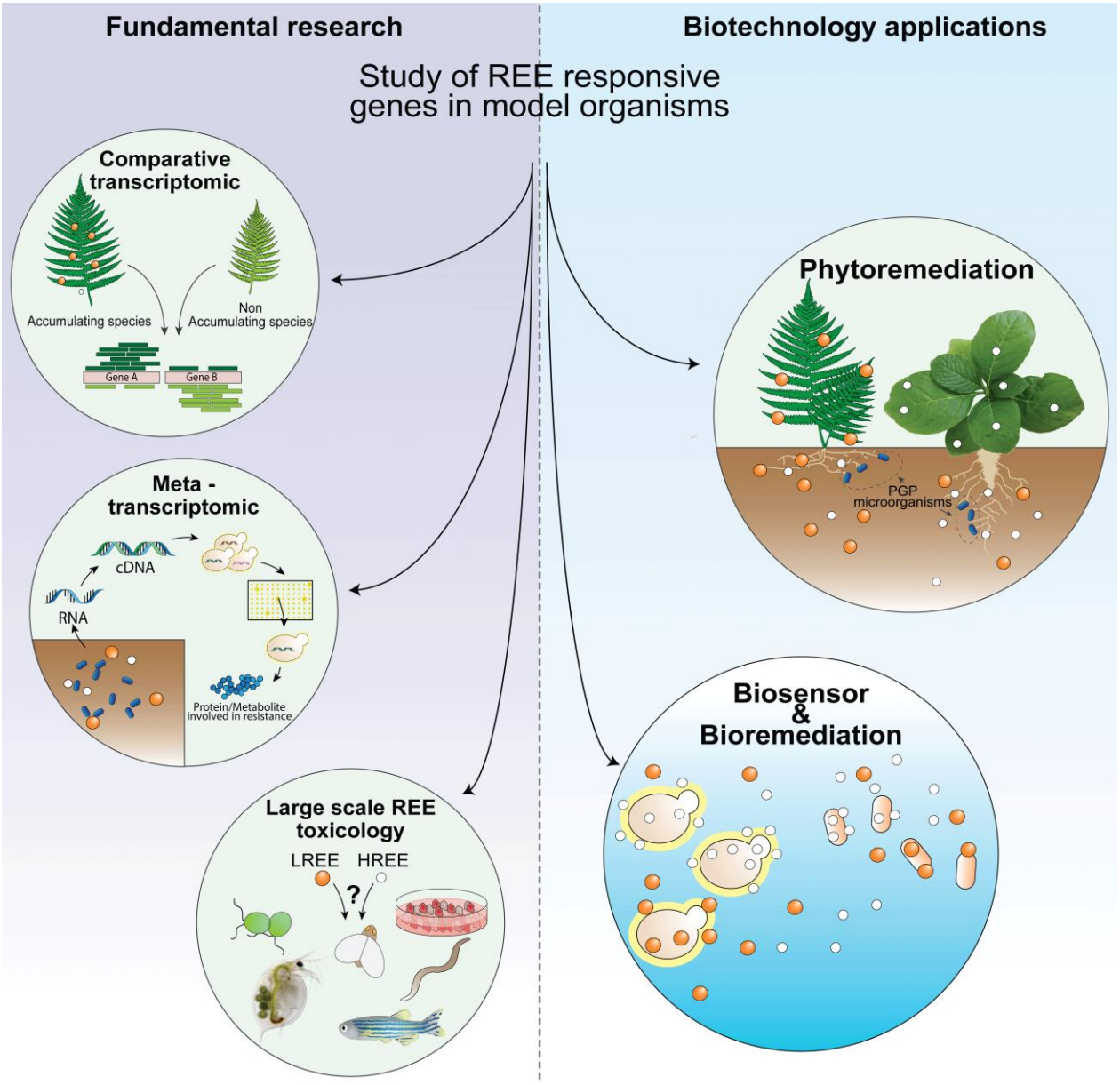

Figure 5: Future fundamental research and biotechnology applications that can emerge from the present thesis work.

- **Further identifying REE-specific targets and their applications**

In the present work, we demonstrated that REEs trigger the expression of specific genes or proteins in exposed organisms such as yeast. A broader scale meta-analysis on yeast mutant collection screenings for metal toxicity could find new selective responses to a specific element. Here, we carried out the screening with Y, La, and Yb. Combining the currently published results with new screenings of other elements (e.g., platinum group elements, Co, Ga, In, Nb, Li, Ta, Sn) would be valuable. The ultimate goal would be to place all yeast genes and their corresponding products on a functional network in the context of metal homeostasis. Specific genes, proteins and pathways for each element could be identified and could serve in the future as specific biomarkers.

Complementary work could be carried out to identify specific REE-interacting molecules. For example, such molecules could be isolated on a metal chelate affinity chromatography system with an REE-bound matrix. The use of such REE-bound matrices has been demonstrated, using trivalent lanthanide ions for phosphopeptide enrichment (Mirza *et al.*, 2013). The results obtained from such studies should lead to novel biotechnological applications. Indeed, several works have identified REE-binding molecules in order to recover REEs from solid waste and water. It was argued that by using engineered bacteria with lanthanide-binding tag-proteins (Park *et al.*, 2016, 2017) or fixed-bed *Pseudomonas aeruginosa* for lanthanides (La, Eu, Yb), they could be removed from aqueous solutions (Texier *et al.*, 2002). To go further, the sorting of the different REEs would be even more interesting. Here, we demonstrated that the cell wall characteristics of *S. cerevisiae* were REE-dependent (LREEs and HREEs for phosphate and carboxyl groups, respectively). Therefore, engineered microorganisms that differ in their cell wall composition could be developed for specific REE recovery (Figure 5).

Another useful application for identified genes that specifically respond to REE stress would be the engineering of microorganisms that can selectively recognize and respond to REEs for their use as biosensors. For example, the *Salmonella* PmrA/PmrB two-component system that usually uses an Fe(III)-binding motif has been engineered by replacing the Fe(III)-binding motif with a lanthanide-binding peptide sequence that selectively recognizes trivalent lanthanide ions. This was the first known lanthanide-based sensing and response mechanism in live cells, and it could be used in the remediation or sequestration of lanthanides (Liang *et al.*, 2013). Researchers

from our laboratory (P. Billard) in collaboration with a German team identified a two-component system named PedS2/PedR2 that is crucial for the REE switch in *Pseudomonas putida* KT2440 (Wehrmann *et al.*, 2018). Such useful work could also lead to the use of these microorganisms as biosensors. In the current study, we demonstrated that some genes responded specifically to either LREEs or HREEs. Therefore, genes that respond differently to different REEs could be used as biosensors to decipher specific REE enrichment and bioavailability in certain matrices (Figure 5). Despite not being well-developed yet, one advantage of using yeast cells as biosensors is that they are eukaryotic and could be used to give information that is more directly applicable to plant, animal and human cells compared to bacteria (Baronian, 2004; Adeniran *et al.*, 2015; Gutiérrez *et al.*, 2015).

- **From a phytoremediation perspective**

The data presented here provide new candidates for phytoremediation purposes. We demonstrated that the REE accumulation trait is shared among several species of the *Phytolacca* genus. Additionally, we showed similar results in two fern genera, namely, *Athyrium* and *Polystichum*. We observed a preferential accumulation related to the phylogeny, where ferns accumulated more LREEs, while *Phytolacca* accumulated more HREEs. The different REE accumulation profiles identified could be used to select the most appropriate species depending on the climatic and/or pedological context in the area to be remediated (Figure 5). As described earlier, there is also a need to determine the underlying genetic mechanisms of REE uptake and tolerance in REE-accumulating plants, for example by comparative transcriptomics (Figure 5). It would not only be essential to obtain a better understanding of REE homeostasis in such plants, but it would also have potential uses in biotechnology. The genes, proteins, and mechanisms identified could be used for plant breeding or engineering. Such plants could be selected for their high organic acid production, for their higher synthesis of uptake transporters, or their detoxification mechanisms (Eapen and Souza, 2005; Jan and Parray, 2016). They could be used for agromining, which aims to farm plants not for food crops but for metals recovery (Liu *et al.*, 2017). They could also be used for their eco-catalysis processes (Grison, 2015), which is the direct use of metals derived from plants as support catalysts in organic chemistry.

We have also found a putative involvement of essential nutrient transporters in the uptake of REEs. Organisms tend to increase their expression of these transporters under nutrient

starvation. Thus, in an REE-contaminated environment, plants with drastic nutritional deficiencies (e.g., Ca, Fe, Mg) would ultimately be more sensitive to REEs. Our results can help to apprehend such unexpected effects, where a balance between nutrient uptake and REE toxicity regulation could be reached (e.g., for phytoremediation). Furthermore, undertaking the isolation of microorganisms that could either stimulate plant growth or enhance REE accumulation by these plants would help to optimize REE phytoremediation (Figure 5). Plant growth-promoting (PGP) traits are widely known and range from phytohormone (e.g., auxin) production and siderophore synthesis to the solubilization of phosphate, which is often limiting for plant growth. Associated with these PGP properties is the ability of certain microorganisms to solubilize phosphate complexes, which could therefore enhance REE solubility in the soil solution, ultimately leading to increased REE uptake by the associated plants. The search for PGP microorganisms (rhizospheric bacteria, mycorrhizal fungi, endophytes) has been successfully investigated for the remediation of trace metal elements (e.g., Cd, Zn, Cu, Ni) (Ma *et al.*, 2011; Tak *et al.*, 2013).

- **Search for REE responsive genes in the environment**

The cellular and molecular mechanisms identified in our study concern model organisms. However, few studies have been carried out on metal (i.e., REE) resistance in soil organisms. Thus, it is likely that there are still many unknown genes that take part in REE resistance in eukaryotes, bacteria and archaea. A metatranscriptomic investigation of REE-contaminated soils would be a good way to identify such genes (Figure 5). For instance, environmental eukaryotic cDNA libraries could be established and used to transform REE-sensitive yeast mutant strains (e.g., VMA mutant for LREEs) that could be screened on REE-containing medium. The resistant clones would likely carry a gene involved in REE resistance, which could then be characterized. Such an approach has previously been executed for several trace metal elements (Zn, Cu and Cd) (Fraissinet-Tachet *et al.*, 2013; Mukherjee *et al.*, 2019).

Further, the insights provided in this work will help to extend the knowledge of the impact of REEs on the environment. Here, we aimed to elucidate REE-mediated stress mechanisms using *S. cerevisiae* and *A. thaliana* as model organisms. To further extend the knowledge regarding REE responses, it will be important to carry out similar approaches in other model organisms (e.g., *Escherichia coli*, *Chlamydomonas reinhardtii, Daphnia magna, Coenorabditis elegans, Drosophila melanogaster, Danio rerio)* and in animal cell lines (Figure 5). Such cross comparisons,

together with a global database, would be useful for deciphering shared REE toxicity mechanisms that could be used as biomarkers of REE toxicity. Environmental REE contamination occurs primarily as a multicontamination of several REEs. We therefore selected widely used representatives from the lanthanides and non-lanthanides, and from LREEs and HREEs. Indeed, after building this large database on the toxicity of single elements in organisms, it will be interesting to investigate multicontaminations of these metals in more detail.

- **Improvement of legislation regarding REE toxicity**

Ultimately, the identification of conserved REE toxicity mechanisms could help to improve the **legislation regarding REE toxicity**. Indeed, the close homology of shared genes between yeast and humans will aid further research on the health risk assessment of REEs. To illustrate this point, several studies have demonstrated that unprogrammed gene silencing is a common toxicity mechanism of Ni in both *S. cerevisiae* and humans (Broday *et al.*, 1999; Sutherland *et al.*, 2001; Costa *et al.*, 2005). The best current example is regarding Gd, which is widely used in gadolinium-based contrast agents for magnetic resonance imaging (Ramalho *et al.*, 2016; Rogosnitzky and Branch, 2016). Studies showed the accumulation and toxicity of Gd-containing molecules in the kidneys. New policies then emerged regarding the dose of these Gd-based contrast agents, because nephrogenic systemic fibrosis was observed in patients with renal insufficiency. However, Gd can also accumulate and reach toxic concentrations in the liver, bones, and brain of patients without renal failure, supporting the necessity of new studies to investigate Gd toxicity (Rogosnitzky and Branch, 2016). Therefore, one should consider the allelomorphism between different individuals as an important factor to consider in the risk assessments of REE toxicity. In short, an individual with a mutant/allelic gene might be more sensitive to REE toxicity, as we showed for some yeast mutants. For example, VPS33 knockout yeast were sensitive to REEs. Mutations in the gene VPS33B in humans is responsible for arthrogryposis, renal dysfunction, and cholestasis-1 (ARCS1) (Gissen *et al.*, 2004). Individuals who have a mutation in the VPS33B locus with renal dysfunction could, therefore, be more sensitive to REEs, and more specifically Gd. Such examples indicate that more attention should be given to the selective toxicity of REEs in sensitive persons.

General conclusion

In conclusion, by using large-scale and complementary approaches in model organisms, we unravelled unique metallic stress responses triggered by REEs. Furthermore, we demonstrated that discrepancies exist in the response towards different REEs (e.g., cell wall, vacuolar sequestration, level of accumulation in shoots and roots). Taken together, the results obtained here establish a principal groundwork for understanding the potential uptake (e.g., Ca and Fe transporters, organic acids) and impact of REEs on two eukaryotic model organisms at the cellular and molecular levels. This work provides new insights for short- and long-term perspectives for either more in-depth targeted fundamental research or novel biotechnology applications and is complementary to the different projects investigating the effects of REEs on the environment (biota) that are part of the LabEx R21 (e.g., ecotoxicology, essential effects of REEs). Through this work, we have highlighted the importance of large-scale omic approaches to better under the response of organisms to emerging contaminants. The integration of similar data collected from studies on metal toxicity in model organisms should be carried out to identify specific markers that could ultimately be used as biomarkers.

References

A

Abdel-Haleem, A. S. et al. (2001) Heavy metals and rare earth elements in phosphate fertilizer components using instrumental neutron activation analysis, *Appl Radiat Isot*, 55, pp. 569–573.

Adeniran, A., Sherer, M. and Tyo, K. E. J. (2015) Yeast-based biosensors: Design and applications, *FEMS Yeast Research*, 15(1), pp. 1–15.

Adle, D. J., Sinani, D., Kim, H., *et al.* (2007) A cadmium-transporting P1B -type ATPase in yeast *Saccharomyces cerevisiae*, *J. Biol. Chem.*, 282(2), pp. 947–955.

Ahmad, Z. (2003) The properties and application of scandium-reinforced aluminium, *JOM*, 55, pp. 35–39.

Al-Thyabat, S. and Zhang, P. (2015) REE extraction from phosphoric acid, phosphoric acid sludge, and phosphogypsum, *Miner. Process. Extr. Metall.*, pp. 1–8.

Alonso, E., Wallington, T., Sherman, A., *et al.* (2012) An assessment of the rare earth element content of conventional and electric vehicles, *SAE International Journal of Materials and Manufacturing*, 5(2), pp. 473–477.

Álvarez-fernández, A., Díaz-benito, P., Abadía, A., *et al.* (2014) Metal species involved in long distance metal transport in plants, *Frontiers in Plant Science*, 5, pp. 1–20.

Andrès, Y., Texier, A. C. and Le Cloirec, P. (2003) Rare earth elements removal by microbial biosorption : A review, *Environmental Technology2*, 24(11), pp. 1367–1375.

Anjum, N. A., Hasanuzzaman, M., Hossain, M. A., *et al.* (2015) Jacks of metal/metalloid chelation trade in plants - an overview, *Frontiers in Plant Science*, 6, pp. 1–17.

B

Bandara, H. M. D., Field, K. D. and Emmert, M. H. (2016) Rare earth recovery from end-of-life motors employing green chemistry design principles, *Green Chemistry*. 18(3), pp. 753–759.

Barberon, M., Zelazny, E., Robert, S., *et al.* (2011) Monoubiquitin-dependent endocytosis of the transporter controls iron uptake in plants, *Proceedings of the National Academy of Sciences of the United States of America*, 108, pp. e450–e458.

Baronian, K. H. R. (2004) The use of yeast and moulds as sensing elements in biosensors, *Biosensors and Bioelectronics*, 19(9), pp. 953–962.

Batista-nascimento, L., Toledano, M. B., Thiele, D. J., *et al.* (2013) Yeast protective response to arsenate involves the repression of the high af fi nity iron uptake system, *Biochimica et Biophysica Acta*. 1833(5), pp. 997–1005.

Bellion, M., Courbot, M., Jacob, C., *et al.* (2006) Extracellular and cellular mechanisms sustaining metal tolerance in ectomycorrhizal fungi, *FEMS Microbiology Letters*, 254(2), pp. 173–181.

Bian, Y., Guo, S., Jiang, L., *et al.* (2016) Recovery of rare earth elements from NdFeB magnet by VIM-HMS method, *ACS Sustainable Chemistry & Engineering*. 4(3), pp. 810–818.

Böhme, H., Fleckenstein, J., Hu, Z., *et al.* (2002) Bilanzversuche zum Einsatz von Seltenen Erden in der Schweinemast 114, in *VDLUFA-Kongress in Leipzig*, p. 20.

Bolchi, A., Ruotolo, R., Marchini, G., *et al.* (2011) Genome-wide inventory of metal homeostasis-related gene products including a functional phytochelatin synthase in the hypogeous mycorrhizal fungus *Tuber melanosporum*, *Fungal Genetics and Biology*. 48(6), pp. 573–584.

Bontemps, C., Toussaint, M., Revol, P., *et al.* (2013) Taxonomic and functional diversity of *Streptomyces* in a forest soil, *FEMS Microbiology Letters*, 342, pp. 157–167.

Borger, C. (2003) *Alternative methoden in der schweinemast*. lmu.

Botstein, D., Chervitz, S. A. and Cherry, J. M. (1997) Yeast as a model organism, *Science*, 277(5330), pp. 1259–1260.

Brioschi, L., Steinmann, M., Lucot, E., *et al.* (2013) Transfer of rare earth elements (REE) from natural soil to plant systems: implications for the environmental availability of anthropogenic REE, *Plant and Soil*, 366(1–2), pp. 143–163.

Broday, L., Cai, J. and Costa, M. (1999) Nickel enhances telomeric silencing in *Saccharomyces cerevisiae*, *Mutation Research*, 440(2), pp. 121–130.

C

Cailliatte, R., Schikora, A., Briat, J. F., *et al.* (2010) High-affinity manganese uptake by the metal transporter NRAMP1 is essential for *Arabidopsis* growth in low manganese conditions, *The Plant Cell*, 22(3), pp. 904–917.

Caspari, T. et al. (2006) Geochemical investigation of soils developed in different lithologies in Bhutan, *Eastern Himalayas Geoderma*, 136, pp. 436–458.

Chen, C., Zhang, H., Wang, A., *et al.* (2015) Phenotypic plasticity accounts for most of the variation in leaf manganese concentrations in *Phytolacca americana* growing in manganese- contaminated environments, *Plant Soil*.

Chen, H. F. (1997) Influence of rare earth compounds on the growth of pigs, *Journal of the Chinese Rare Earth Society*, 15, pp. 441–443.

Cheng, H., Fanghua, H., Ouyang, W., *et al.* (2012) Vertical distribution of rare earth elements in a wetland soil core from the Sanjiang Plain in China, *Journal of Rare Earths*. 30(7), pp. 731–738.

Cho, S., Lee, Y., Lee, S., *et al.* (2014) Enhanced cytotoxic and genotoxic effects of gadolinium following ELF-EMF irradiation in human lymphocytes, *Drug and chemical toxicology*. 37(4), pp. 440–447.

Chojnicki, J. (2000) Rare earth elements in alluvial soils of central Vistula valley and Zulawy, *ROCZNIKI GLEBOZNAWCZE TOM LI*, pp. 57–65.

Ciacci, L., Reck, B. K., Nassar, N. T., *et al.* (2015) Lost by design, *Environmental Science & Technology*. 49(16), pp. 9443–9451.

Clemens, S. and Simm, C. (2003) *Schizosaccharomyces pombe* as a model for metal homeostasis in plant cells: The phytochelatin-dependent pathway is the main cadmium detoxification mechanism, *New Phytologist*, 159(2), pp. 323–330.

Cobbett, C. S. (2003) Heavy metals and plants – model systems and hyperaccumulators, *New Phytologist*, 159, pp. 289–293.

Cobelo-García, A., Filella, M., Croot, P., *et al.* (2015) COST action TD1407: network on technology-critical elements (NOTICE)—from environmental processes to human health threats, *Environmental Science and Pollution Research*, 22(19), pp. 15188–15194.

Copetti, D., Finsterle, K., Marziali, L., *et al.* (2016) Eutrophication management in surface waters using lanthanum modified bentonite : A review, *Water research*, 97, pp. 162–174.

COST (2016) *ReCreew - European network for innovative recovery strategies of rare earth and other Critical metals from electrical and electronic waste*.

Costa, M., Davidson, T. L., Chen, H., *et al.* (2005) Nickel carcinogenesis: Epigenetics and hypoxia signaling, *Mutation Research*, 592(1–2), pp. 79–88.

Cotton, S. (2006) *Lanthanide and actinide chemistry*. John Wiley, *Lanthanide and Actinide Chemistry*. John Wiley.

Curie, C., Alonso, J. M., Jean, M. L. E., *et al.* (2000) Involvement of NRAMP1 from *Arabidopsis thaliana* in iron transport Catherine, *Biochem. J.*, 347, pp. 749–755.

Cyert, M. S. and Philpott, C. C. (2013) Regulation of cation balance in *Saccharomyces cerevisiae*, *Genetics*, 193(3), pp. 677–713.

D

d'Aquino, L., Morgana, M., Carboni, M. a., *et al.* (2009) Effect of some rare earth elements on the growth and lanthanide accumulation in different *Trichoderma* strains, *Soil Biology and Biochemistry*. 41(12), pp. 2406–2413.

Diatloff, E., Asher, C. J. and Smith, F. W. (1996) Concentrations of rare earth elements in some Australian soils, *Soil Research*. 34(5), pp. 735–747.

Diatloff, E., Smith, F. W. and Asher, C. J. (1995) Rare earth elements and plant growth: II. Responses of corn and mungbean to low concentrations of cerium in dilute, continuously flowing nutrient solutions., *Journal of Plant Nutrition*, 18(10), pp. 1977–1989.

Dinali, G. S. (2014) *Elementos terras raras em materiais derivados da indústria de fosfatos no Brasil. 2014. 107 f.* Dissertação (Mestrado em Ciência do Solo)--Universidade Federal de Lavras.

Ding, S., Liang, T., Zhang, C., *et al.* (2005) Role of ligands in accumulation and fractionation of rare earth elements in plants, *Biological trace element research*, 107(1), pp. 73–86.

Ding, S., Liang, T., Zhang, C., *et al.* (2006) Fractionation mechanisms of rare earth elements (REEs) in hydroponic wheat: an application for metal accumulation by plants, *Environmental Science & Technology*, 40(8), pp. 2686–2691.

Ding, S. M., Liang, T., Zhang, C. S., *et al.* (2005) Accumulation and fractionation of rare earth elements (REEs) in wheat: Controlled by phosphate precipitation, cell wall absorption and solution complexation, *Journal of Experimental Botany*, 56(420), pp. 2765–2775.

Djingova, R., Ivanova, J., Wagner, G., *et al.* (2001) Distribution of lanthanoids, Be, Bi, Ga, Te, Tl, Th and U on the territory of Bulgaria using *Populus nigra* 'Italica' as an indicator, *Science of the Total Environment*, 280(1–3), pp. 85–91.

Djinovic-Carugo, K. and Carugo, O. (2015) Structural biology of the lanthanides—mining rare earths in the Protein Data Bank, *Journal of Inorganic Biochemistry*. 143, pp. 69–76.

Dong, C., He, F., Berkowitz, O., *et al.* (2018) Alternative splicing plays a critical role in maintaining mineral nutrient homeostasis in rice (*Oryza sativa*), *The Plant Cell*, 30(10), pp. 2267–2285.

Dou, C., Fu, X., Chen, X., *et al.* (2009) Accumulation and detoxification of manganese in hyperaccumulator *Phytolacca americana, Plant Biology*, 11, pp. 664–670.

Dressler, L., Golbik, R. and Ulbrich-hofmann, R. (2014) Lanthanides as substitutes for calcium ions in the activation of plant α -type phospholipase D, 395, pp. 791–799.

Duclos, L., Svecova, L., Laforest, V., *et al.* (2016) Process development and optimization for platinum recovery from PEM fuel cell catalyst, *Hydrometallurgy*. 160, pp. 79–89.

Dupont, D. and Binnemans, K. (2015) Rare-earth recycling using a functionalized ionic liquid for the selective dissolution and revalorization of Y_2O_3:Eu^{3+} from lamp phosphor waste, *Green Chemistry*. 17(2), pp. 856–868.

Dutta, T., Kim, K., Uchimiya, M., *et al.* (2016) Global demand for rare earth resources and strategies for green mining, *Environmental Research*. 150, pp. 182–190.

E - F

Eapen, S. and Souza, S. F. D. (2005) Prospects of genetic engineering of plants for phytoremediation of toxic metals, *Biotechnology Advances*, 23, pp. 97–114.

Eisele, N. (2003) *Untersuchungen zum einsatz seltener erden als leistungsfoerderer beim schwein*. lmu.

El-Ramady, H. (2010) *Ecotoxicology of rare earth elements: ecotoxicology of rare earth elements within soil and plant environments*. VDM Publis.

El-Ramady, H. R. (2008) *A contribution on the bio-actions of rare earth elements in the soil/plant environment*.

Emmanuel, E. C., Ananthi, T., Anandkumar, B., *et al.* (2012) Accumulation of rare earth elements by siderophore-forming *Arthrobacter luteolus* isolated from rare earth environment of Chavara, India, *Journal of Biosciences*, 37(1), pp. 25–31.

Ene, C. D., Ruta, L. L., Nicolau, I., *et al.* (2015a) Interaction between lanthanide ions and *Saccharomyces cerevisiae* cells, *JBIC Journal of Biological Inorganic Chemistry*, 20(7), pp. 1097–1107.

van der Ent, A., Baker, A. J. M., Reeves, R. D., *et al.* (2016) Commentary: Toward a more physiologically and evolutionarily relevant definition of metal hyperaccumulation in plants, *Frontiers in Plant Science*, 6, pp. 2014–2016.

Ferella, F., Innocenzi, V. and Maggiore, F. (2016) Oil refining spent catalysts: a review of possible recycling technologies, *Resources, Conservation and Recycling*. 108, pp. 10–20.

Filichkin, S., Priest, H. D., Megraw, M., *et al.* (2015) Alternative splicing in plants: Directing traffic at the crossroads of adaptation and environmental stress, *Current Opinion in Plant Biology*. 24, pp. 125–135.

Fitriyanto, N. A., Fushimi, M., Matsunaga, M., *et al.* (2011) Molecular structure and gene analysis of Ce^{3+} -induced methanol dehydrogenase of *Bradyrhizobium* sp. MAFF211645., *Journal of bioscience and bioengineering*. 111(6), pp. 613–7.

Fraissinet-Tachet, L., Richaud, P., Baude, J., *et al.* (2013) Soil metatranscriptomics for mining eukaryotic heavy metal resistance genes, *Environmental Microbiology*, 15(10), pp. 2829–2840.

Franklin, S. J. (2001) Lanthanide-mediated DNA hydrolysis, *Current Opinion in Chemical Biology*, pp. 201–208.

Fu, Y., Li, F., Xu, T., *et al.* (2014) Bioaccumulation, subcellular, and molecular localization and damage to physiology and ultrastructure in *Nymphoides peltata* (Gmel.) O. Kuntze exposed to yttrium, *Environmental Science and Pollution Research*, 21(4), pp. 2935–2942.

G

Galezowska, E., Gluszynska, A. and Juskowiak, B. (2007) Luminescence study of G-quadruplex formation in the presence of Tb^{3+} ion, *Journal of inorganic biochemistry*. 101(4), pp. 678–685.

Gambogi, J. (2018) *Rare Earths*, *Metals and minerals: U.S. Geological Survey Minerals Yearbook 2015*.

Gao, X. J., Zhang, S. and Wang, L. J. (2001) Environmental chemistry of rare earth elements (REEs) in the cultivated soil of typical REE mine in the Southern Jiangxi, *Soil and Environmental science*, 10, pp. 11–13.

Gao, Y., Zeng, F., Yi, A., *et al.* (2003) Research of the entry of rare earth elements Eu^{3+} and La^{3+} into plant cell, *Biological Trace Element Research*, 91(3), pp. 253–265.

Garcia de la Torre, V. S., Majorel-Loulergue, C., Gonzalez, Dubiel A. Soubigou-Taconnat, L., *et al.* (2018) Wide cross-species RNA-Seq comparison reveals a highly conserved role for Ferroportins in nickel hyperaccumulation in plants, *bioRxiv*.

Ghio, A. J., Soukup, J. M., Dailey, L. A., *et al.* (2011) Gadolinium exposure disrupts iron homeostasis in cultured cells, *JBIC Journal of Biological Inorganic Chemistry*. 16(4), pp. 567–575.

Gissen, P., Johnson, C. A., Morgan, N. V., *et al.* (2004) Mutations in VPS33B, encoding a regulator of SNARE-dependent membrane fusion, cause arthrogryposis-renal dysfunction-cholestasis (ARC) syndrome, *Nature Genetics*, 36(4), pp. 400–404.

Gitan, R. S. and Eide, D. J. (2000) Zinc-regulated ubiquitin conjugation signals endocytosis of the yeast ZRT1 zinc transporter., *The Biochemical journal*. 346 Pt 2(Pt 2), pp. 329–36.

Gomez-Sagasti, M. T., Barrutia, O., Ribas, G., *et al.* (2016) Early transcriptomic response of *Arabidopsis thaliana* to polymetallic contamination : implications for the identification of potential biomarkers of metal exposure, *Metallomics*, 8, pp. 518–531.

Gonzalez, V., Vignati, D. A. L., Leyval, C., *et al.* (2014) Environmental fate and ecotoxicity of lanthanides: Are they a uniform group beyond chemistry?, *Environment International*. 71, pp. 148–157.

Goolsby, E. W. and Mason, C. M. (2015) Toward a more physiologically and evolutionarily relevant definition of metal hyperaccumulation in plants, *Frontiers in Plant Science*, 6, pp. 1–4.

Grison, C. (2015) Combining phytoextraction and ecocatalysis: a novel concept for greener chemistry, an opportunity for remediation, *Environmental science and pollution research international*, 22(8), pp. 5589–5591.

Grossmann, G., Malinsky, J., Stahlschmidt, W., *et al.* (2008) Plasma membrane microdomains regulate turnover of transport proteins in yeast, *Journal of Cell Biology*, 183(6), pp. 1075–1088.

Guerinot, M. Lou (2000) The ZIP family of metal transporters, *Biochimica et Biophysica Acta - Biomembranes*, 1465(1–2), pp. 190–198.

Gutiérrez, J. C., Amaro, F. and Martín-González, A. (2015) Heavy metal whole-cell biosensors using eukaryotic microorganisms: An updated critical review, *Frontiers in Microbiology*, 6, pp. 1–8.

H

Halimaa, P., Blande, D., Aarts, M. G. M., *et al.* (2014) Comparative transcriptome analysis of the metal hyperaccumulator *Noccaea caerulescens*, *Frontiers in Plant Science*, 5, pp. 1–7.

Halle, I., Fleckenstein, J., Hu, Z. Y., *et al.* (2002) Untersuchungen zum einfluss von seltenen erden auf das wachstum und die schlachtleistung von broilern 114, in *VDLUFA-Kongress in Leipzig*, p. 20.

Haque, M. U. F., Kalidass, B., Bandow, N., *et al.* (2015) Cerium regulates expression of alternative methanol dehydrogenases in *Methylosinus trichosporium* OB3b, *Applied and Envrionmental Microbiology*, 81(21), pp. 7546–7552.

Haque, N., Hughes, A., Lim, S., *et al.* (2014) Rare earth elements: overview of mining, mineralogy, uses, sustainability and environmental impact, *Resources*, 3(4), pp. 614–635.

Hasan, M. K., Cheng, Y., Kanwar, M. K., *et al.* (2017) Responses of plant proteins to heavy metal stress - A review, *Frontiers in Plant Science*, 8, pp. 1–16.

Hayat, S., Faraz, A. and Faizan, M. (2017) Root exudates: composition and impact on plant-microbe interaction chemical composition of root exudates and their significance root exudates in mediating plant-microbe interaction in rhizosphere (negative and positive interactions), *Biofilms in Plant and Soil Health*. First Edit. Edited by J. W. & S. Ltd. John Wiley & Sons Ltd, (C), pp. 179–193.

He, M. L. and Rambeck, W. A. (2000) Rare earth elements - A new generation of growth promoters for pigs?, *Archives of Animal Nutrition*, 53(4), pp. 323–334.

He, M. L., Ranz, D. and Rambeck, W. A. (2001) Study on the performance enhancing effect of rare earth elements in growing and fattening pigs, *Journal of Animal Physiology and Animal Nutrition*, 85(7–8), pp. 263–270.

He, R. and Xia, Z. (1998) Effects of rare earth elements on growing and fattening of pigs, *Guangxi Agric Sci*, 5, pp. 243–245.

He, Y. and Loh, C. (2000) Cerium and lanthanum promote floral initiation and reproductive growth of *Arabidopsis thaliana*, *Plant science : an international journal of experimental plant biology*, 159(1), pp. 117–124.

Hibi, Y., Asai, K., Arafuka, H., *et al.* (2011) Molecular structure of La^{3+}-induced methanol dehydrogenase-like protein in *Methylobacterium radiotolerans*. *Journal of bioscience and bioengineering*. 111(5), pp. 547–9.

Hirano, S. and Suzuki, K. T. (1996) Exposure, metabolism, and toxicity of rare earths and related compounds, *Environmental Health Perspectives*, 104(15), pp. 85–95.

Holland, S. L. and Avery, S. V. (2009) Actin-mediated endocytosis limits intracellular Cr accumulation and Cr toxicity during chromate stress, *Toxicological Sciences*, 111(2), pp. 437–446.

Höllriegl, V., González-Estecha, M Trasobares, E., Giussani, A., *et al.* (2010) Measurement of cerium in human breast milk and blood samples, *Journal of Trace Elements in Medicine and Biology*, 24, pp. 193–9.

Hong, J., Yu, X., Pan, X., *et al.* (2014) Pulmonary toxicity in mice following exposure to cerium chloride, *Biological trace element research*. 159(1–3), pp. 269–277.

Hongyan, G., Liang, C., Xiaorong, W., *et al.* (2002) Physiological responses of *Carassius auratus* to ytterbium exposure, *Ecotoxicology and environmental safety*. 53(2), pp. 312–316.

Hori, K., Watano, Y. and Murakami, N. (2016) Hybrid origin of the apogamous fern *Dryopteris hondoensis* (Dryopteridaceae), *Acta phytotaxonomica et geobotanica*, 67(3), pp. 133–146.

Horiike, T. and Yamashita, M. (2015) A new fungal isolate, *Penidiella* sp. strain T9, accumulates the rare earth element dysprosium., *Applied and environmental microbiology*, 81(9), pp. 3062–8.

Hosiner, D., Gerber, S., Lichtenberg-Fraté, H., *et al.* (2014) Impact of acute metal stress in *Saccharomyces cerevisiae*, *PLoS ONE*, 9(1), pp. 1–14.

Hu, X., Ding, Z., Wang, X., *et al.* (2002) Effects of lanthanum and cerium on the vegetable growth of wheat (*Triticum aestivum* L.) seedlings, *Bulletin of Environmental Contamination and Toxicology*, 69(5), pp. 727–733.

Hu, Z., Wang, J., Yang, Y., *et al.* (1999) Effect of REE on the nutrients digestibility for growing pigs, *Feed World*, 11(1), pp. 29–31.

Hu, Z., Richter, H., Sparovek, G., *et al.* (2004) Physiological and biochemical effects of rare earth elements on plants and their agricultural significance: A review, *Journal of Plant Nutrition*, 27(1), pp. 183–220.

Hu, Z., Haneklaus, S., Sparovek, G., *et al.* (2006) Rare earth elements in soils, *Communications in Soil Science and Plant Analysis*, 37, pp. 1381–1420.

Huang, P., Li, J., Zhang, S., *et al.* (2011) Effects of lanthanum, cerium, and neodymium on the nuclei and mitochondria of hepatocytes: accumulation and oxidative damage, *Environmental toxicology and pharmacology*. 31(1), pp. 25–32.

Huang, S. F., Li, Z. Y., Fu, M. L., *et al.* (2007) Detection of genotoxicity of 6 kinds of rare earth nitrates using orthogonal experimental design, *Journal of Agro-Environment Science*, 1, pp. 351–356.

Hughes, A. E. (1995) Interfacial phenomena in Y_2O_3-ZrO_2-based ceramics: A surface science perspective, *Materials Science Monographs*, 81, pp. 183–238.

Humphries, M. (2012) *Rare earth elements: the global supply chain*. Library of Congress, Congressional Research Service, 2012.

Hurst, C. (2010) *China's rare earth elements industry: What can the west learn?* Institute for the Analysis of Global Security: Fort Leavenworth, KS, USA.

I - J - K

Ichihashi, H., Morita, H. and Tatsukawa, R. (1991) Rare earth elements (REEs) in naturally grown plants in relation to their variation in soils., *Environmental pollution (Barking, Essex : 1987)*, 76(2), pp. 157–162.

Ichihashi, H., Morita, H. and Tatsukawa, R. (1992) Rare earth elements (REEs) in naturally grown plants in relation to their variation in soils, *Environmental Pollution*. 76(2), pp. 157–162.

Inaoka, T. and Ochi, K. (2012) Undecaprenyl pyrophosphate involvement in susceptibility of *Bacillus subtilis* to rare earth elements., *Journal of Bacteriology*, 194(20), pp. 5632–7.

Jan, S. and Parry, J. A. (2016) Heavy metal uptake in plants, in *Approaches to Heavy Metal Tolerance in Plants*. Springer S. Singapore, pp. 1–110.

Jha, A. M. and Singh, A. C. (1994) Clastogenicity of lanthanides induction of micronuclei in root tips of *Vicia faba*, *Mutation Research/Genetic Toxicology*. 322(3), pp. 169–172.

Jha, A. M. and Singh, A. C. (1995) Clastogenicity of lanthanides: induction of chromosomal aberration in bone marrow cells of mice in vivo, *Mutation Research/Genetic Toxicology*. 341(3), pp. 193–197.

Jiang, M., Ohnuki, T., Kozai, N., *et al.* (2010) Biological nano-mineralization of Ce phosphate by *Saccharomyces cerevisiae*, *Chemical Geology*. 277(1–2), pp. 61–69.

Jiang, M. Y., Ohnuki, T., Tanaka, K., *et al.* (2012) Post-adsorption process of Yb phosphate nano-particle: Formation by *Saccharomyces cerevisiae*, *Geochimica et Cosmochimica Acta*. 93, pp. 30–46.

Jiang, N., Wang, L., Lu, T., *et al.* (2011) Toxic effect of terbium ion on horseradish cell, *Biological trace element research*. 143(3), pp. 1722–1728.

Jin, Y. H., Dunlap, P. E., McBride, S. J., *et al.* (2008) Global transcriptome and deletome profiles of yeast exposed to transition metals., *PLoS genetics*, 4(4).

Jorjani, E. and Shahbazi, M. (2016) The production of rare earth elements group via tributyl phosphate extraction and precipitation stripping using oxalic acid, *Arabian journal of chemistry*. 9, pp. S1532--S1539.

Kamijo, M., Suzuki, T., Kawai, K., *et al.* (1998) Accumulation of yttrium by *Variovorax paradoxus*, *Journal of Fermentation and Bioengineering*, 86(6), pp. 564–568.

Kamijo, M., Suzuki, T., Kawai, K., *et al.* (1999) Ytterbium-decreasing *Streptomyces* sp. and its naphthoquinone-pigment production in the presence of rare-earth elements, *Journal of Bioscience and Bioengineering*, 87(3), pp. 340–343.

Kawagoe, M., Hirasawa, F., Cun Wang, S., *et al.* (2005) Orally administrated rare earth element cerium induces metallothionein synthesis and increases glutathione in the mouse liver, *Life Science*, 77, pp. 922–37.

Kawai, K., Wang, G., Okamoto, S., *et al.* (2007) The rare earth, scandium, causes antibiotic overproduction in *Streptomyces* spp., *FEMS Microbiology Letters*, 274(2), pp. 311–315.

Kessler, J. (2004) Lanthanoide –Wachstumsförder mit Zukunft., in *Schweinehaltung*, p. 255.

Klusenerl, B., Boheim, G., Lift, H., *et al.* (1995) Gadolinium-sensitive, voltage-dependent calcium release channels in tje endoplasmic reticulum of a higher plant mechanoreceptor organ, *The EMBO Journal*, 14(12), pp. 2708–2714.

Kobayashi, Y., Ikka, T., Kimura, K., *et al.* (2007) Characterisation of lanthanum toxicity for root growth of *Arabidopsis thaliana* from the aspect of natural genetic variation, *Functional Plant Biology*, 34, pp. 984–994.

Kobayashi, Y., Kobayashi, Y., Sugimoto, M., *et al.* (2013) Characterization of the complex regulation of AtALMT1 expression in response to phytohormones and other inducers., *Plant physiology*, 162(2), pp. 732–40.

Koornneef, M. and Meinke, D. (2010) The development of *Arabidopsis* as a model plant, *The Plant Journal*, 61, pp. 909–921.

Koschinski, A., Wengler, G., Wengler, G., *et al.* (2005) Rare earth ions block the ion pores generated by the class II fusion proteins of alphaviruses and allow analysis of the biological functions of these pores, *Journal of General Virology*, 86(12), pp. 3311–3320.

Koyama, M., Shirakawa, M., Takada, J., *et al.* (1987) Trace elements in land plants: concentration ranges and accumulators of rare earths, Ba, Ra, Mn, Fe, Co and heavy halogens, *Journal of Radioanalytical and Nuclear Chemistry*. Springer, 112(2), pp. 489–506.

Krämer, U. (2010) Metal hyperaccumulation in plants, *Annual Review of Plant Biology*, 61(1), pp. 517–534.

Kumari, M., Taylor, G. J. and Deyholos, M. K. (2008) Transcriptomic responses to aluminum stress in roots of *Arabidopsis thaliana*, *Molecular Genetics and Genomics*, 279, pp. 339–357.

Küpper, H. and Andresen, E. (2016) Mechanisms of metal toxicity in plants, *Metallomics*, 8, pp. 269–285.

L

Lai, Y., Wang, Q. Q., Yan, W. W., *et al.* (2005) Preliminary study of the enrichment and fractionation of REEs in a newly discovered REE hyperaccumulator *Pronephrium simplex* by SEC-ICP-MS and MALDI-TOF/ESI-MS, *Journal of Analytical Atomic Spectrometry*, 20(8), pp. 751–753.

Lai, Y., Wang, Q., Yang, L., *et al.* (2006) Subcellular distribution of rare earth elements and characterization of their binding species in a newly discovered hyperaccumulator *Pronephrium simplex*, *Talanta*, 70(1), pp. 26–31.

Lambers, H., Hayes, P. E., Laliberté, E., *et al.* (2015) Leaf manganese accumulation and phosphorus-acquisition efficiency, *Trends in Plant Science*, 20(2), pp. 83–90.

Landa, P., Dytrych, P., Prerostova, S., *et al.* (2017) Transcriptomic response of *Arabidopsis thaliana* exposed to CuO nanoparticles, bulk material, and ionic copper, *Environ. Sci. Technol.*, p. 10814−10824.

Lansman, J. B. (1990) Blockade of current through single calcium channels by trivalent lanthanide cations. Effect of ionic radius on the rates of ion entry and exit, *The Journal of General Physiology*, 95(4), pp. 679–696.

Lao, F., Li, R. and Wang, K. (2006) Study on the hemolysis of human erythrocytes induced by rare earth ion Ln^{3+} and their complex ion $[Ln(Cit)_2]_3$, *Beijing Da Xue Xue Bao*, 34(163–6).

Laul, J. C., Weimer, W. C. and Rancitelli, L. A. (1979) Biogeochemical distribution of rare earths and other trace elements in plants and soils, *Physics and Chemistry of the Earth*. 11, pp. 819–827.

Lee, Y. J., Huang, X., Kropat, J., *et al.* (2012) Sphingolipid signaling mediates iron toxicity, *Cell Metabolism*. 16(1), pp. 90–96.

Lemire, J. A., Harrison, J. J. and Turner, R. J. (2013) Antimicrobial activity of metals: mechanisms, molecular targets and applications, *Nature reviews. Microbiology*. 11(6), pp. 371–384.

Leonardo, L. et al. (2014) Lichen specie *Canoparmelia texana* as bioindicator of environmental impact from the phosphate fertilizer industry of Sao Paulo, *Brazil J Radioanal Nucl Chem*, 299, pp. 1935–1941.

Lešková, A., Giehl, R. F. H., Hartmann, A., *et al.* (2017) Heavy metals induce iron deficiency responses at different hierarchic and regulatory levels, *Plant Physiology*, 174(3), pp. 1648–1668.

Lewis, B. D. and Spalding, E. P. (1998) Nonselective block by La^{3+} of *Arabidopsis* ion channels involved in signal transduction, *Journal of Membrane Biology*, 162(1), pp. 81–90.

Li, H. and Zhang, X. (2009) The yeast lysosome-like vacuole: Endpoint and crossroads, *Biochim Biophys Acta*, 1793(4), pp. 650–663.

Li, N., Wang, S., Liu, J., *et al.* (2010) The oxidative damage in lung of mice caused by lanthanoide, *Biological trace element research*. 134(1), pp. 68–78.

Li, N., Wang, J. and Song, W. Y. (2016) Arsenic uptake and translocation in plants, *Plant and Cell Physiology*, 57(1), pp. 4–13.

Li, X., Chen, Z., Chen, Z., *et al.* (2013) A human health risk assessment of rare earth elements in soil and vegetables from a mining area in Fujian Province, Southeast China, *Chemosphere*. 93(6), pp. 1240–1246.

Li, Y. X., Zhang, L. and Zhou, X. M. (2010) Resource and environment protected exploitation model for ion-type rare earth deposit in southern of China, *China Rare Earths*, 31, pp. 80–85.

Liang, C. and Wang, W. (2013) Antioxidant response of soybean seedlings to joint stress of lanthanum and acid rain, *Environmental Science and Pollution Research*. 20(11), pp. 8182–8191.

Liang, H., Deng, X., Bosscher, M., *et al.* (2013) Engineering bacterial two-component system PmrA/PmrB to sense lanthanide ions, *Journal of the American Chemical Society*, 135(6), pp. 2037–2039.

Liang, T., Ding, S., Song, W., *et al.* (2008) A review of fractionations of rare earth elements in plants, *Journal of Rare Earths*, 26(1), pp. 7–15.

Liang, T., Li, K. and Wang, L. (2014) State of rare earth elements in different environmental components in mining areas of China, *Environmental Monitoring and Assessment*, 186(3), pp. 1499–1513.

Liu, C., Yuan, M., Liu, W., *et al.* (2017) Element case studies: Rare earth elements, in Van der Ent, A. et al. (eds) *Agromining: Farming for metals. mineral resource reviews*. Springer, Cham.

Liu, J., Sitaram, A. and Burd, C. G. (2007) Regulation of copper-dependent endocytosis and vacuolar degradation of the yeast copper transporter, Ctr1p, by the Rsp5 ubiquitin ligase, *Traffic*, 8(10), pp. 1375–1384.

Liu, M., Kilaru, A. and Hasenstein, K. H. (2007) Abscisic acid response of corn (*Zea mays* L.) roots and protoplasts to lanthanum, *Journal of Plant Growth Regulation*, 27(1), pp. 19–25.

Liu, W., Guo, M., Liu, C., *et al.* (2018) Water , sediment and agricultural soil contamination from an ion- adsorption rare earth mining area, *Chemosphere*. 10(109), pp. 75–83.

Liu, Y., Sun, L., Zhang, P., *et al.* (2017) Lanthanum inhibits primary root growth by repressing auxin carrier abundances in *Arabidopsis*, *Frontiers in Plant Science*, 8, pp. 1–9.

Liu, Y. Y., Wang, R. L., Zhang, P., *et al.* (2016) Involvement of reactive oxygen species in lanthanum-induced inhibition of primary root growth, *Journal of Experimental Botany*, 67(21), pp. 6149–6159.

Loell, M., Reiher, W. and Felix-Henningsen, P. (2011) Contents and bioavailability of rare earth elements in agricultural soils in Hesse (Germany), *Journal of Plant Nutrition and Soil Science*. 174(4), pp. 644–654.

Long, K. R., Van Gosen, B. S., Foley, N. K., *et al.* (2010) *The principal rare earth elements deposits of the United States: A summary of domestic deposits and a global perspective*, *U.S. Geological Survey Scientific Investigations Report 2010-5220*.

M - N

Ma, Y., Prasad, M. N. V, Rajkumar, M., *et al.* (2011) Plant growth promoting rhizobacteria and endophytes accelerate phytoremediation of metalliferous soils Phytoremediation Bioremediation Rhizoremediation, *Biotechnology Advances*, 29, pp. 248–258.

MacDiarmid, C. W. and Gardner, R. C. (1998) Overexpression of the *Saccharomyces cerevisiae* magnesium transport system confers resistance to

aluminum ion, *Journal of Biological Chemistry*, 273(3), pp. 1727–1732.

Markert, B. (1987) The pattern of distribution of lanthanide elements in soils and plants, *Phytochemistry*. 26(12), pp. 3167–3170.

Markert, B. and De Li, Z. (1991) Natural background concentrations of rare-earth elements in a forest ecosystem, *Science of the total environment*. 103(1), pp. 27–35.

Marques, R., Prudêncio, M. I., Rocha, F., *et al.* (2012) REE and other trace and major elements in the topsoil layer of Santiago island, Cape Verde, *Journal of African Earth Sciences*. 64, pp. 20–33.

Martinoia, E., Maeshima, M. and Neuhaus, H. E. (2007) Vacuolar transporters and their essential role in plant metabolism, *Journal of Experimental Botany*, 58(1), pp. 83–102.

Marubashi, K., Hirano, S. and Suzuki, K. T. (1998) Effects of intratracheal pretreatment with yttrium chloride (YCl_3) on inflammatory responses of the rat lung following intratracheal instillation of YCl_3, *Toxicology letters*. Elsevier, 99(1), pp. 43–51.

Mäser, P., Thomine, S., Schroeder, J. I., *et al.* (2001) Phylogenetic relationships within cation transporter families of Arabidopsis, *Plant Physiology*, 126(4), pp. 1646–1667.

Meinke, D. W., Cherry, J. M., Dean, C., *et al.* (1998) *Arabidopsis thaliana*: A model plant for genome analysis, *Science*, p. 662.

Meshram, P., Pandey, B. D. and Mankhand, T. R. (2016) Process optimization and kinetics for leaching of rare earth metals from the spent Ni-metal hydride batteries, *Waste Management*. 51, pp. 196–203.

Miao, L., Xu, R., Ma, Y., *et al.* (2008) Geochemistry and biogeochemistry of rare earth elements in a surface environment (soil and plant) in South China, *Environmental geology*. 56(2), pp. 225–235.

Min, Y., boqing, T., Meizhen, T., *et al.* (2007) Accumulation and uptake of manganese in a hyperaccumulator *Phytolacca americana*, *Minerals Engineering*, 20(2), pp. 188–190.

Mirza, M. R., Rainer, M., Messner, C. B., *et al.* (2013) A new type of metal chelate affinity chromatography using trivalent lanthanide ions for phosphopeptide enrichment, *Analyst*, 138, pp. 2995–3004.

Moon, J. Y., Belloeil, C., Ianna, M. L., *et al.* (2019) Arabidopsis CNGC family members contribute to heavy metal ion uptake in plants, *International Journal of Molecular Sciences*, 20(2).

Moreira, H., Marques, A. P. G. C., Rangel, A. O. S. S., *et al.* (2011) Heavy metal accumulation in plant species indigenous to a contaminated Portuguese site: Prospects for phytoremediation, *Water, Air, and Soil Pollution*, 221(1–4), pp. 377–389.

Moriwaki, H. and Yamamoto, H. (2013) Interactions of microorganisms with rare earth ions and their utilization for separation and environmental technology, *Applied Microbiology and Biotechnology*, 97(1), pp. 1–8.

Mukherjee, A., Yadav, R., Marmeisse, R., *et al.* (2019) Heavy metal hypertolerant eukaryotic aldehyde dehydrogenase isolated from metal contaminated soil by metatranscriptomics approach, *Biochimie*. Société Française de Biochimie et Biologie Moléculaire (SFBBM).

Nagahashi, G., Thomson, W. W. and Leonard, R. T. (1974) The casparian strip as a barrier to the movement of lanthanum in corn roots, *Science*, 183(4125), pp. 670–671.

Nakagawa, T., Mitsui, R., Tani, A., *et al.* (2012) A catalytic role of XoxF1 as La^{3+}-dependent methanol dehydrogenase in *Methylobacterium extorquens* strain AM1, *PLoS ONE*, 7(11), p. e50480.

Ngwenya, B. T., Mosselmans, J. F. W., Magennis, M., *et al.* (2009) Macroscopic and spectroscopic analysis of lanthanide adsorption to bacterial cells, *Geochimica et Cosmochimica Acta*. 73(11), pp. 3134–3147.

O - P - Q

Ochi, K. (1987) Metabolic initiation of differentiation and secondary metabolism by *Streptomyces griseus*: significance of the stringent response (ppGpp) and GTP content in relation to A factor., *Journal of bacteriology*, 169(8), pp. 3608–16.

Ochi, K., Tanaka, Y. and Tojo, S. (2014) Activating the expression of bacterial cryptic genes by rpoB mutations in RNA polymerase or by rare earth elements, *Journal of Industrial Microbiology & Biotechnology*, 41(2), pp. 403–414.

Öhlander, B., Land, M., Ingri, J., *et al.* (1996) Mobility of rare earth elements during weathering of till in northern Sweden, *Applied Geochemistry*. 11(1–2), pp. 93–99.

Oliveira, K. A. P., Menezes, M., Von Sperling, E., *et al.* (2012) Transfer factor of rare earth elements from phosphogypsum amended Brazilian tropical soils to lettuce, corn and soybean, *The Journal of Solid Waste Technology and Management*. 38(3), pp. 202–210.

Ooi, C. E., Rabinovich, E., Dancis, A., *et al.* (1996) Copper-dependent degradation of the *Saccharomyces cerevisiae* plasma membrane copper transporter Ctr1p in the apparent absence of endocytosis, *Embo J*, 15(14), pp. 3515–3523.

Oral, R., Bustamante, P., Warnau, M., *et al.* (2010) Cytogenetic and developmental toxicity of cerium and lanthanum to sea urchin embryos, *Chemosphere*. 18, pp. 194–198.

Ory, J. (2018) *Caractérisation de mutants de Saccharomyces cerevisiae résistants au lanthane et à l'ytterbium obtenus par ingénierie évolutive*. Université de Lorraine, Vandoeuvre-lès-Nancy, France.

Otero, N., Vitòria, L., Soler, A., *et al.* (2005) Fertiliser characterisation: Major, trace and rare earth elements, *Applied Geochemistry*. 20(8), pp. 1473–1488.

Ozaki, T., Enomoto, S., Minai, Y., *et al.* (1997) Determination of lanthanides and other trace elements in ferns by instrumental neutron activation analysis, *Journal of Radioanalytical and Nuclear Chemistry*, 217(1), pp. 117–124.

Ozaki, T., Enomoto, S., Minai, Y., *et al.* (2000) A survey of trace elements in Pteridophytes, *Biological Trace Element Research*, 74, pp. 259–273.

Pagano, G., Guida, M., Tommasi, F., *et al.* (2015b) Health effects and toxicity mechanisms of rare earth elements - Knowledge gaps and research prospects, *Ecotoxicology and Environmental Safety*. 115, pp. 40–48.

Palasz, A. and Czekaj, P. (2000) Toxicological and cytophysiological aspects of lanthanides action, *Acta Biochimica Polonica*, 47, pp. 1107–14.

Park, D. M., Reed, D. W., Mimi, C., *et al.* (2016) Bioadsorption of rare earth elements through cell surface display of lanthanide binding tags, *Environmental science & technology*, 50(5), pp. 2735–2742.

Park, D. M., Brewer, A., Reed, D. W., *et al.* (2017) Recovery of rare earth elements from low-grade feedstock leachates using engineered bacteria, *Environmental Science and Technology*, 51(22), pp. 13471–13480.

Park, E.-J., Choi, J., Park, Y.-K., *et al.* (2008) Oxidative stress induced by cerium oxide nanoparticles in cultured BEAS-2B cells, *Toxicology*. 245(1–2), pp. 90–100.

Peng, K., Luo, C., You, W., *et al.* (2008) Manganese uptake and interactions with cadmium in the hyperaccumulator - *Phytolacca americana* L., *Journal of Hazardous Materials*, 154(1–3), pp. 674–681.

Pereira, L. V. B., Shimizu, M. H. M., Rodrigues, L. P. M. R., *et al.* (2012) N-acetylcysteine protects rats with chronic renal failure from gadolinium-chelate nephrotoxicity, *PLoS One*. 7(7), p. e39528.

Pol, A., Barends, T. R. M., Dietl, A., *et al.* (2014) Rare earth metals are essential for methanotrophic life in volcanic mudpots, *Environmental Microbiology*, 16(1), pp. 255–264.

Pollard, A. J., Reeves, R. D. and Baker, A. J. M. (2014) Facultative hyperaccumulation of heavy metals and metalloids, *Plant Science*. 217–218, pp. 8–17.

Qu, A., Wang, C. R. and Bo, J. (2004) Research on the cytotoxic and genotoxic effects of rare-earth element holmium to *Vicia faba*, *Yi chuan= Hereditas*, 26(2), pp. 195–201.

R

Ramalho, J., Semelka, R. C., Ramalho, M., *et al.* (2016) Gadolinium-based contrast agent accumulation and toxicity: An update, *American Journal of Neuroradiology*, 37(7), pp. 1192–1198.

Rambeck, W. A., He, M. L., Chang, J., *et al.* (2000) Possible role of rare earth elements as growth promoters, in *Proceedings of the Society of Nutrition Physiology (Germany)*.

Rambeck, W. A. and Wehr, U. (2005) Rare earth elements as alternative growth promoters in pig production, *Pig News and Information*, 26(2), pp. 41–47.

Ramos, S. J., Dinali, G. S., de Carvalho, T. S., *et al.* (2016) Rare earth elements in raw materials and products of the phosphate fertilizer industry in South America: Content, signature, and crystalline phases, *Journal of Geochemical Exploration*. 168, pp. 177–186.

Ramos, S. J., Dinali, G. S., Oliveira, C., *et al.* (2016) Rare earth elements in the soil environment, pp. 28–50.

Ramsay, L. M. and Gadd, G. M. (1997) Mutants of *Saccharomyces cerevisiae* defective in vacuolar function confirm a role for the vacuole in toxic metal ion detoxification, *FEMS Microbiology Letters*, 152, pp. 293–298.

Reisman, D., Weber, R., McKernan, J., *et al.* (2013) *Rare earth elements : A review of productionp, processing, recycling, and associated environmental issues*, *U.S. Environmental Protection Agency, Washington, DC*. Washington, DC.

Remy, E., Cabrito, T. R., Batista, R. A., *et al.* (2014) Intron retention in the 5′UTR of the novel ZIF2 transporter enhances translation to promote zinc tolerance in *Arabidopsis*, *PLoS Genetics*, 10(5), pp. 15–19.

Rico, C. M., Morales, M. I., McCreary, R., *et al.* (2013) Cerium oxide nanoparticles modify the antioxidative stress enzyme activities and macromolecule composition in rice seedlings, *Environmental science & technology*. 47(24), pp. 14110–14118.

Rim, K. T., Koo, K. H. and Park, J. S. (2013) Toxicological evaluations of rare earths and their health impacts to workers: a literature review, *Safety and Health at Work*. 4(1), pp. 12–26.

Robinson, W. O. (1943) The occurrence of rare earths in plants and soils, *Soil Science*. 56(1), pp. 1–6.

Rogosnitzky, M. and Branch, S. (2016) Gadolinium-based contrast agent toxicity: a review of known and proposed mechanisms, *BioMetals*. 29(3), pp. 365–376.

Roschzttardtz, H., Conejero, G., Curie, C., *et al.* (2009) Identification of the endodermal vacuole as the iron storage compartment in the *Arabidopsis* embryo, *Plant Physiology*, 151(3), pp. 1329–1338.

Roy, K., Sinha, P. and Lahiri, S. (2008) Immobilization of long-lived radionuclides ^{152,154}Eu by selective bioaccumulation in *Saccharomyces cerevisiae* from a synthetic mixture of ^{152,154}Eu, ^{137}Cs and ^{60}Co, *Biochemical Engineering Journal*, 40(2), pp. 363–367.

Ruiz-Herrera, L. F., Sanchez-Calderon, L., Herrera-Estrella, L., *et al.* (2012) Rare earth elements lanthanum and gadolinium induce phosphate-deficiency responses in *Arabidopsis thaliana* seedlings, *Plant and Soil*, 353(1–2), pp. 231–247.

Ruotolo, R., Marchini, G. and Ottonello, S. (2008) Membrane transporters and protein traffic networks differentially affecting metal tolerance: A genomic phenotyping study in yeast, *Genome Biology*, 9(4), pp. 4–6.

S

Sadeghi, M., Morris, G. A., Carranza, E. J. M., *et al.* (2013) Rare earth element distribution and mineralization in Sweden: An application of principal component analysis to FOREGS soil geochemistry, *Journal of geochemical exploration*. 133, pp. 160–175.

Salminen, R. B. et al. (2005) *FOREGS Geochimical Atlas of Europe, part 1: background information, methodology and maps*. Espoo: Geol. Surv. Finland.

Schuller, S., Borger, C., He, M. L., *et al.* (2002) Untersuchungen zur wirkung seltener erden als mögliche alternative zu leistungsförderern bei schweinen und geflügel.

Sessa, E. B., Zimmer, E. A. and Givnish, T. J. (2012) Unraveling reticulate evolution in North American *Dryopteris* (Dryopteridaceae), *BMC Evolutionary Biology*, 12(104).

Shan, X., Wang, H., Zhang, S., *et al.* (2003) Accumulation and uptake of light rare earth elements in a hyperaccumulator *Dicropteris dichotoma*, *Plant Science*, 165(6), pp. 1343–1353.

Sharma, S. S., Dietz, K. and Mimura, T. (2016) Vacuolar compartmentalization as indispensable component of heavy metal detoxification in plants, *Plant, Cell & Environment*, 39, pp. 1112–1126.

Shen, Q. (1991) Application of rare earth elements on animal production, *Feed Ind.*, 12, pp. 21–22.

Shen, Z., Zheng, L., Liu, Q., *et al.* (2015) RNA-seq analysis of rice roots reveals the involvement of post-transcriptional regulation in response to cadmium stress, *Frontiers in Plant Science*, 6, pp. 1–16.

Shimada, H. (1996) Pulmonary toxicity of systemic terbium chloride in mice, *Journal of Toxicology and Environmental Health Part A*. 48(1), pp. 81–92.

Singh, M., Kumar, J., Singh, S., *et al.* (2015) Adaptation strategies of plants against heavy metal toxicity: A short review, *Biochemistry & Pharmacology: Open Access*, 04(02).

Singh, S., Parihar, P., Singh, R., *et al.* (2016) Heavy metal tolerance in plants: Role of transcriptomics, proteomics, metabolomics, and ionomics, *Frontiers in Plant Science*, 6(1143), pp. 1–36.

Sinha, S., Meshram, P., Pandey, B. D., *et al.* (2016) Metallurgical processes for the recovery and recycling of lanthanum from various resources: a review, *Hydrometallurgy*. 160, pp. 47–59.

Skovran, E. and Martinez-Gomez, N. C. (2015) Just add lanthanides, *Science (New York, N.Y.)*, 348, pp. 862–863.

Smidt, G. A. et al. (2011) Heavy metal concentrations in soils in the vicinity of a fertilizer factory in Southern Brazil, *Agriculture and Forestry Research*, 61, pp. 353–364.

Smith, B., Rawlins, B. G., Cordeiro, M., *et al.* (2000) The bioaccessibility of essential and potentially toxic trace elements in tropical soils from Mukono District, Uganda, *Journal of the Geological Society*. 157(4), pp. 885–891.

Spears, B. M., Lürling, M., Yasseri, S., *et al.* (2013) Lake responses following lanthanum-modified bentonite clay (Phoslock®) application: An analysis of water column lanthanum data from 16 case study lakes, *Water Research*, 47(15), pp. 5930–5942.

Staiger, D. and Brown, J. W. S. (2013) Alternative splicing at the intersection of biological timing, development, and stress responses, *The Plant Cell*, 25(10), pp. 3640–3656.

Sulotto, F., Romano, C., Berra, A., *et al.* (1986) Rare-earth pneumoconiosis: a new case, *American Journal of Industrial Medecine*, 9, pp. 567–75.

Sun, Z., Xiao, Y., Agterhuis, H., *et al.* (2016) Recycling of metals from urban mines-a strategic evaluation, *Journal of cleaner production*. 112, pp. 2977–2987.

Sutherland, J. E., Peng, W., Zhang, Q. W., *et al.* (2001) The histone deacetylase inhibitor trichostatin A reduces nickel-induced gene silencing in yeast and mammalian cells, *Mutation Research*, 479(1–2), pp. 225–233.

T

Tak, H. I., Ahmad, F. and Babalola, O. O. (2013) Advances in the application of plant growth-promoting rhizobacteria in phytoremediation of heavy metals, in *Reviews of environmental contamination and toxicology*. New York: Springer Science+Business Media New, pp. 33–52.

Takahashi, Y., Yamamoto, M., Yamamoto, Y., *et al.* (2010) EXAFS study on the cause of enrichment of heavy REEs on bacterial cell surfaces, *Geochimica et Cosmochimica Acta*. 74(19), pp. 5443–5462.

Takeda, A., Kimura, K. and Yamasaki, S. (2004) Analysis of 57 elements in Japanese soils, with special reference to soil group and agricultural use, *Geoderma*. 119(3–4), pp. 291–307.

Tan, Q., Deng, C. and Li, J. (2016) Innovative application of mechanical activation for rare earth elements recovering: process optimization and mechanism exploration, *Scientific reports*. 6, p. 19961.

Tanaka, Y., Hosaka, T. and Ochi, K. (2010) Rare earth elements activate the secondary metabolite-biosynthetic gene clusters in *Streptomyces coelicolor* A3(2)., *The Journal of Antibiotics*. 63(8), pp. 477–81.

Tao, Y., Zhao, G., Yang, J., *et al.* (2001) Determination of double decker sandwich structured La-substituted chlorophyll a by EXAFS, *Journal of Synchrotron Radiation*, 8(2), pp. 996–997.

Texier, A. C., Andrès, Y., Faur-Brasquet, C., *et al.* (2002) Fixed-bed study for lanthanide (La, Eu, Yb) ions removal from aqueous solutions by immobilized Pseudomonas aeruginosa : experimental data and modelization, *Chemosphere*, 47, pp. 333–342.

Texier, A. C., Andrès, Y. and Cloirec, P. L. (2010) Selective biosorption of lanthanide (La, Eu) ions by *Mycobacterium smegmatis*, *Environmental Technology*, 18(8), pp. 835–841.

Thomas, W. A. (1975) Accumulation of rare earths and circulation of cerium by mockernut hickory trees, *Canadian Journal of Botany*. 53(12), pp. 1159–1165.

Thomine, S., Wang, R., Ward, J. M., *et al.* (2000) Cadmium and iron transport by members of a plant metal transporter family in *Arabidopsis* with homology to Nramp genes., *Proceedings of the National Academy of Sciences of the United States of America*, 97(9), pp. 4991–6.

Todorovsky, D. S. et al. (1997) Effect of the application of superphosphate on rare earths content in the soil, *Sci Total Environ*, 203, pp. 13–16.

Tripathi, R. D., Tripathi, P., Dwivedi, S., *et al.* (2012) Arsenomics : omics of arsenic metabolism in plants, *Frontiers in Plant Science*, 3, pp. 1–14.

Tsuruta, T. (2006) Selective accumulation of light or heavy rare earth elements using gram-positive bacteria, *Colloids and Surfaces B: Biointerfaces*, 52(2), pp. 117–122.

Tsuruta, T. (2007) Accumulation of rare earth elements in various microorganisms, *Journal of Rare Earths*, 25(5), pp. 526–532.

Tunsu, C., Petranikova, M., Gergorić, M., *et al.* (2015) Reclaiming rare earth elements from end-of-life products: a review of the perspectives for urban mining using hydrometallurgical unit operations, *Hydrometallurgy*. 156, pp. 239–258.

Turra, C. et al. (2011) Evaluation on rare earth elements of Brazilian agricultural supplies, *J Environ Chem Ecotoxicol*, 3, pp. 86–92.

Tyler, G. (2004a) Rare earth elements in soil and plant systems - A review, *Plant and Soil*, 267(1–2), pp. 191–206.

Tyler, G. and Olsson, T. (2002) Conditions related to solubility of rare and minor elements in forest soils, *Journal of Plant Nutrition and Soil Science*. 165(5), pp. 594–601.

U - V - W

Uchida, S., Tagami, K. and Hirai, I. (2007) Soil-to-plant transfer factors of stable elements and naturally occurring radionuclides (1) upland field crops collected in Japan, *Journal of Nuclear Science and Technology*. 44(4), pp. 628–640.

United States Geological Survey (2016) Mineral commodity summaries 2016, *U.S. Geological Survey*, pp. 1–202.

Verbruggen, N., Hermans, C. and Schat, H. (2009) Molecular mechanisms of metal hyperaccumulation in plants, *New Phytologist*, 181, pp. 759–776.

Vert, G., Grotz, N., Dédaldéchamp, F., *et al.* (2002) IRT1, an *Arabidopsis* transporter essential for iron uptake from the soil and for plant growth, *The Plant Cell*, 14, pp. 1223–1233.

Viehweger, K. (2014) How plants cope with heavy metals, *Botanical Studies*, 55(35), p. 12.

Voncken, J. H. L. (2016) The ore minerals and major ore deposits of the rare earths, in *The Rare Earth Elements*. p. X, 127.

Voßenkaul, D. D., Stoltz, N. B., Meyer, F. M., *et al.* (2013) Extraction of rare earth elements from non-Chinese ion adsorption clays, *Proceedings of EMC 2013*, pp. 1–11.

Waheed, S. et al. (2011) Rare earths elements in phosphorite and granulated single super-phosphate fertilizers of Pakistan, a study using instrumental neutron activation analysis, *J Radioanal Nucl Chem*, 289, pp. 521–528.

Wakabayashi, T., Ymamoto, A., Kazaana, A., *et al.* (2016) Antibacterial, antifungal and nematicidal activities of rare earth ions, *Biological Trace Element Research*. 174(2), pp. 464–470.

Walter, A., Lusty, P. and Hill, A. (2011) *Mineral profile: Rare Earth Elements*.

Wang, H., Shan, X.-Q., Zhang, S., *et al.* (2003) Preliminary characterization of a light-rare-earth-element-binding peptide of a natural perennial fern *Dicranopteris dichotoma*. *Analytical and bioanalytical chemistry*, 376(1), pp. 49–52.

Wang, J., Wang, L., Hu, T., *et al.* (2014) Effects of lanthanum on abscisic acid regulation of root growth in *Arabidopsis*, *Journal of Rare Earths*. 32(1), pp. 78–82.

Wang, L., Liang, T., Zhang, S., *et al.* (2004) Biogeochemical cycle and residue of extraneous rare earth elements in agricultural ecosystem, *Journal of the Chinese Rare Earth Society*, 22, pp. 701–6.

Wang, L., Li, J., Zhou, Q., *et al.* (2014) Rare earth elements activate endocytosis in plant cells, *Proceedings of the National Academy of Sciences*, 111(35), pp. 12936–12941.

Wang, L., He, J., Xia, A., *et al.* (2017) Toxic effects of environmental rare earth elements on delayed outward potassium channels and their mechanisms from a microscopic perspective, *Chemosphere*. 181, pp. 690–698.

Wang, L., Zhou, Q. and Huang, X. (2014) Direct interaction between terbium ion and peroxidase in horseradish at different pH values, *Biological Trace Element Research*, 157(2), pp. 183–188.

Wang, M. and Xu, Z. (2003) Effect of supplemental lanthanum on growth performance of pigs and its security as a feed additive, *Chinese Journal of Veterinary Science*, 23(1), pp. 88–90.

Wang, X., Lin, Y., Liu, D., *et al.* (2011) Cerium toxicity, uptake and translocation in *Arabidopsis thaliana* seedlings, *Journal of Rare Earths*. 30(6), pp. 579–585.

Wang, Y. Q., Sun, J. X., Chen, H. M., *et al.* (1997) Determination of the contents and distribution characteristics of REE in natural plants by NAA, *Journal of Radioanalytical and Nuclear Chemistry*, 219(1), pp. 99–103.

Wang, Z. G., Yu, X. Y. and Zhao, Z. H. (1989) *The geochemistry of rare earth elements*. Beijing: Science Press.

Weber, M., Harada, E., Vess, C., *et al.* (2004) Comparative microarray analysis of *Arabidopsis thaliana* and *Arabidopsis halleri* roots identifies nicotianamine synthase, a ZIP transporter and other genes as potential metal hyperaccumulation factors, *Plant Journal*, 37(2), pp. 269–281.

Weber, M., Trampczynska, A. and Clemens, S. (2006) Comparative transcriptome analysis of toxic metal responses in *Arabidopsis thaliana* and the Cd^{2+}-hypertolerant facultative metallophyte *Arabidopsis halleri*, *Plant, Cell & Environment*, 29, pp. 950–963.

Wehrmann, M., Billard, P., Martin-Meriadec, A., *et al.* (2017) Functional role of lanthanides in enzymatic activity and transcriptional regulation of pyrroloquinoline quinone-dependent alcohol dehydrogenases in *Pseudomonas putida* KT2440, *mBio*, 8(3), pp. 1–14.

Wehrmann, M., Berthelot, C., Billard, P., *et al.* (2018) The PedS2/PedR2 two-component system is crucial for the rare earth element switch in *Pseudomonas putida* KT2440, *mSphere*, 3(4), pp. 1–12.

Wei, B., Li, Y., Li, H., *et al.* (2013) Rare earth elements in human hair from a mining area of China, *Ecotoxicology and Environmental Safety*. 96, pp. 118–123.

Wei F. S. Zheng C. J., C. J. S. W. Y. Y. (1991) Study on the background contents on 61 elements of soils in China, *Chinese Journal of Environmental Science*, 12, pp. 12–20.

Wenhua, L., Ruming, Z., Zhixiong, X., *et al.* (2003) Effects of La^{3+} on growth, transformation, and gene expression of *Escherichia coli*, *Biological Trace Element Research*, 94(2), pp. 167–177.

Wood, B. W. and Grauke, L. J. (2011) The rare-earth metallome of pecan and other *Carya*, *Journal of the American Society for Horticultural Science*, 136(6), pp. 389–398.

Wu, J., Chen, A., Peng, S., *et al.* (2013) Identification and application of amino acids as chelators in phytoremediation of rare earth elements lanthanum and yttrium, *Plant and Soil*, 373(1–2), pp. 329–338.

Wu, J., Yang, J., Liu, Q., *et al.* (2013) Lanthanum induced primary neuronal apoptosis through mitochondrial dysfunction modulated by Ca^{2+} and Bcl-2 family, *Biological trace element research*. 152(1), pp. 125–134.

Wu, J. L., Wei, Z. G., Zhao, H. Y., *et al.* (2009) The role of amino acids in the long-distance transport of La and Y in the xylem sap of tomato, *Biological Trace Element Research*, 129(1–3), pp. 239–250.

Wu, J., Wang, C. and Mei, X. (2001) Stimulation of taxol production and excretion in *Taxus* spp cell cultures by rare earth chemical lanthanum, *Journal of Biotechnology*, 85(1), pp. 67–73.

Wu, J., Zhang, Z. and Yan, J. (1994) An initial study on effect of adding rare earth element on productivity of egg laying breeder hens, *NingXia Science and Technology of Farming and Forestry*, 4, pp. 36–38.

Wysocki, R. and Tamás, M. J. (2010) How *Saccharomyces cerevisiae* copes with toxic metals and metalloids., *FEMS microbiology reviews*, 34(6), pp. 925–951.

X - Y

Xia, Q., Feng, X., Huang, H., *et al.* (2011) Gadolinium-induced oxidative stress triggers endoplasmic reticulum stress in rat cortical neurons, *Journal of neurochemistry*. 117(1), pp. 38–47.

Xia, Z. and He, R. (1997) A review of applying REE in agriculture production, *Chinese, unpublished*.

Xiao, H., Zhang, Z., Li, F., *et al.* (2003) Study on contents and distribution characteristics of REE in fern by NAA, *Nuclear Techniques*, 26(6), pp. 420–424.

Xie, J. and Wang, Z. (1998) The effect of organic rare-earth compounds on production performance of chicken, in *2nd International Symposium on Trace Elements and Food Chain*, p. 1998.

Xiuqin, Z. and Wenji, Z. (2006) Lanthanum to pathogenic fungi and its morphological characteristics, *Journal of Rare Earths*, 24, pp. 607–612.

Xu, X., Zhu, W., Wang, Z., *et al.* (2002) Distributions of rare earths and heavy metals in field-grown maize after application of rare earth-containing fertilizer, *Science of the Total Environment*. 293(1–3), pp. 97–105.

Xu, X., Shi, J., Chen, X., *et al.* (2009) Chemical forms of manganese in the leaves of manganese hyperaccumulator *Phytolacca acinosa* Roxb. (Phytolaccaceae), *Plant and Soil*, 318(1–2), pp. 197–204.

Xu, Z., Wang, M. and Chen, L. (1999) Growth response of pigs fed supplemental lanthanum and approach of mechanism, *Journal of the Chinese Rare Earth Society*, 17, pp. 53–59.

Xue, S., Wang, J., Zhou, X., *et al.* (2010) A critical reappraisal of *Phytolacca acinosa* Roxb. (Phytolaccaceae) – A manganese-hyperaccumulating plant, *Acta Ecologica Sinica*. 30(6), pp. 335–338.

Xue, Y. (2009) *Studies of the hyperaccumulation ability of Pronephrium simplex and Pronephrium triphyllum to rare earth elements and their binding peptides*. Xiamen University.

Yang, Q., Wang, L., He, J., *et al.* (2016) Vitronectin-like protein is a first line of defense against lanthanum (III) stress in *Arabidopsis* leaf cells, *Environmental and Experimental Botany*. 130, pp. 86–94.

Yang, W., Zhang, P., Liu, J., *et al.* (2006) Effect of long-term intake of Y^{3+} in drinking water on gene expression in brains of rats, *Journal of Rare Earths*, 24, pp. 369–73.

Yoshida, S., Muramatsu, Y., Tagami, K., *et al.* (1998) Concentrations of lanthanide elements, Th, and U in 77 Japanese surface soils, *Environment International*. 24(3), pp. 275–286.

Yu, J., Huang, Z. Y. and Chen, T. (2009) Determination of rare-earth elements (REEs) in orange-growing soils and navel oranges around rare-earth mining area in southern Jiangxi, *Food Science*, 30, pp. 309–313.

Yuan, F. (1994) Research group of apply ion type REE in agriculture, *Hunan Agriculture Science*, 2, pp. 41–42.

Yuan, M., Guo, M. N., Liu, W. S., *et al.* (2017) The accumulation and fractionation of rare earth elements in hydroponically grown *Phytolacca americana* L, *Plant and Soil*. 421(1–2), pp. 67–82.

Yuan, M., Liu, C., Liu, W.-S., *et al.* (2018) Accumulation and fractionation of rare earth elements (REEs) in the naturally grown *Phytolacca americana* L. in southern China, *International Journal of Phytoremediation*. 20(5), pp. 415–423.

Z

Zelazny, E. and Vert, G. (2015) Regulation of iron uptake by IRT1: Endocytosis pulls the trigger, *Molecular Plant*, 8(7), pp. 977–979.

Zepf, V. (2013) A new approach to the nexus of supply, demand and use: Exemplified along the use of neodymium in permanent magnets, in *Rare Earth Elements*. Springer T. Springer-Verlag Berlin Heidelberg, p. XIV, 157.

Zhang, B. and Shao, L. (1995) Effect of inorganic REE on growth performance of broilers, *Chinese Journal of Husbandry*, 31(3), pp. 38–39.

Zhang, C., Li, Q., Zhang, M., *et al.* (2013) Effects of rare earth elements on growth and metabolism of medicinal plants, *Acta Pharmaceutica Sinica B*. 3(1), pp. 20–24.

Zhang, Q. H., Tong, L. G., Cheng, L., *et al.* (2012) Characteristics of REE distribution in the surface soil of the farmland in wastewater irrigation area, *Acta Agriculturae Universitatis Jiangxiensis.*, 34, pp. 614–618.

Zhang, Q., Lei, T. and Zhao, J. (2008) Estimation of the detachment rate in eroding rills in flume experiments using an REE tracing method, *Geoderma*. 147(1–2), pp. 8–15.

Zhang, Z. Y., Wang, Y. Q., Li, F. L., *et al.* (2002) Distribution characteristics of rare earth elements in plants from a rare earth ore area, *Journal of Radioanalytical and Nuclear Chemistry*, 252(3), pp. 461–465.

Zhao, H., Hao, W., Xu, H., *et al.* (2004) Gene expression profiles of hepatocytes treated with $La(NO_3)_3$ of rare earth in rats. *World Journal of Gastroenterology*, 10, pp. 1625–9.

Zhao, H., Cheng, Z., Hu, R., *et al.* (2011) Oxidative injury in the brain of mice caused by lanthanid, *Biological trace element research*. 142(2), pp. 174–189.

Zhenggui, W., Ming, Y., Xun, Z., *et al.* (2001) Rare earth elements in naturally grown fern *Dicranopteris linearis* in relation to their variation in soils in South-Jiangxi region (Southern China), *Environmental Pollution*, 114(3), pp. 345–355.

Zhou, B., Li, Z. and Chen, C. (2017) Global potential of rare earth resources and rare earth demand from clean technologies, *Minerals*, 7(11), p. 203.

Zhu, J. H., Yuan, Z. K., Wang, X. Y., *et al.* (2002) Investigation on the contents of rare earth elements in environment of rare earth ore area in Jiangxi, *Environmental Health*, 19, pp. 443–448.

Extended Abstract – Résumé étendu

Les terres rares : des métaux stratégiques en plein essor

Le groupe des terres rares (REEs – rare earth elements) regroupe 17 éléments (Y, Sc et les 15 lanthanides) ayant des caractéristiques chimiques et physiques proches. Parmi les REEs, deux groupes peuvent être distingués, en fonction de leur rayon ionique. Les REEs légères (LREEs – light REEs) comprennent les éléments du La à l'Eu, tandis que les REEs lourdes (HREEs – heavy REEs) regroupent les éléments allant du Gd au Lu, comprenant également l'élément non lanthanide (Ln) Y (Cotton, 2006).

Contrairement à leur dénomination, les REEs ne sont pas rares dans la croûte terrestre et dans les sols. Comparativement à d'autres éléments bien connus, leur teneur dans la croûte terrestre est aussi élevée que l'Au, le Cr, le Cu, le Ni, le Mo, le Sn ou encore le Pb (https://pubs.usgs.gov/fs/2002/fs087-02/). Les concentrations en REEs dans les sols peuvent varier de 34 ppm à plus de 200 ppm, avec une moyenne relative en REEs de 155 ppm (Ramos *et al.*, 2016). Cependant, comme pour de nombreux métaux, des concentrations beaucoup plus élevées peuvent être trouvées dans les sols de zones minières. Plusieurs études ont reporté des concentrations pouvant être jusqu'à dix fois supérieures, de 542 ppm à 2 373 ppm allant même jusqu'à 27 000 ppm en Chine (Zhenggui *et al.*, 2001; Liang *et al.*, 2014). Des concentrations aussi élevées dans les sols peuvent donc avoir un impact important sur l'écosystème, et les interactions entre REEs et biota nécessitent donc d'être mieux élucidées.

Les REEs sont des éléments clés dans les récents progrès technologiques. Ce sont des métaux stratégiques du XXIe siècle dont la demande croissante résulte de leurs propriétés essentielles, notamment dans les domaines des énergies renouvelables, de la médecine et des nouvelles technologies (Reisman *et al.*, 2013; Haque *et al.*, 2014). Outre leurs principales utilisations pour leurs propriétés physiques, elles ont été également utilisées en tant qu'engrais dans l'agriculture. En plus de cette dissémination des REEs via l'agriculture, le recyclage des REEs est actuellement très faible, voire inexistant pour des REEs tels que pour l'Ho et l'Er (Ciacci *et al.*, 2015).

Effets des REEs sur les organismes vivants

Bien que parfois considérées comme inerte vis-à-vis des organismes, des travaux démontrent que les REEs peuvent influencer leur physiologie. Le transfert et les effets des REEs chez de nombreux organismes tels que les plantes et les microorganismes a notamment été démontré.

En conditions de laboratoire, leur transfert via les canaux calciques, Cch1-Mid1 chez *Saccharomyces cerevisiae* (Ene *et al.*, 2015a), a pu être mis en évidence. De plus, certaines bactéries ont une croissance stimulée en présence de REEs qui jouent le rôle de cofacteurs d'alcool déshydrogénases (Pol *et al.*, 2014). D'autres bactéries du genre *Streptomyces* et *Bacillus* ont une synthèse accrue de métabolites secondaires induite par ces éléments (Ochi, 1987; Kamijo *et al.*, 1999; Kawai *et al.*, 2007; Tanaka *et al.*, 2010; Inaoka and Ochi, 2011; Ochi *et al.*, 2014). A l'inverse, différents travaux exposent que la présence de ces REEs peut également induire un stress et avoir un effet antibactérien et antifongique (Wakabayashi *et al.*, 2016)

Chez les plantes, les REEs sont accumulées en quantité restreinte (moins de 10 ppm) en conditions de non contamination. A l'inverse et comme pour de nombreux éléments (Zn, Cd, As, Ni, etc.), quelques plantes, notamment des fougères, ont la capacité d'hyperaccumuler les REEs : *Dicranopteris dichotoma* (Zhenggui, 2001; Shan *et al.*, 2003), *Pronephrium simplex* (Lai *et al.*, 2005, 2006), ainsi que *Dryopteris erythrosora* (Ozaki *et al.*, 1997)*, Blechnum orientale* (Zhang *et al.*, 2002) ou encore *Athyrium yokoscense* (Ichihashi *et al.*, 1991). Une surreprésentation des fougères comme plantes accumulatrices de ces éléments est actuellement observée. Cependant quelques angiospermes démontrent une accumulation importante de REEs. On peut notamment citer *Carya tomentosa* (noix de pécan) (Wood and Grauke, 2011) et *Phytolacca americana* (raisin d'Amérique) (Wu *et al.*, 2013; Yuan *et al.*, 2017).

De nombreuses études ont démontré la présence de REEs dans la partie racinaire de plantes et leur transfert vers la partie aérienne. Aussi, différents effets des REEs ont pu être observés. Chez la fougère *Dicranopteris dichotoma*, le Mg de la chlorophylle serait substitué par du Ce entrainant une augmentation de croissance, de la concentration en chlorophylles et de l'efficacité photosynthétique (Tao *et al.*, 2001). De plus, la stimulation de la croissance cellulaire à faible concentration et des dommages cellulaires (taille, structure) à forte concentration ont été montrés. Différentes études révèlent que la toxicité des REEs est en partie marquée par un stress oxydatif

(Pagano *et al.*, 2015). Des effets génotoxiques ont pu également être observés (Pagano *et al.*, 2015). Plus étonnant encore, il a été mis en évidence l'activation de l'endocytose par les REEs (La et Tb) de protoplastes de cellules foliaires d'*Armoracia rusticana* (Wang *et al.*, 2014).

Cette grande diversité de résultats montre la multiplicité de mécanismes associés aux REEs ainsi que l'existence d'un effet toxique de ces éléments. Cependant, il subsiste un cruel manque de données au niveau cellulaire et moléculaire pour expliquer les mécanismes de toxicité et de résistance des organismes aux REEs.

Objectifs de la thèse

Afin d'identifier les mécanismes de toxicité et de résistance à des métaux tels que le Ni et le Cd, de nombreuses études ont utilisé des approches sans *a priori* et à haut débit (approches omiques). Pour combler le manque de connaissances et construire une base générale des effets toxiques des REEs cette étude s'est focalisée sur l'identification des gènes, protéines et voies cellulaires impliqués dans la réponse aux REEs chez des organismes modèles par l'utilisation d'approches omiques. Nous avons premièrement étudié la réponse, ainsi que l'absorption des REEs chez le modèle eucaryote *Saccharomyces cerevisiae*. Les délétome, transcriptome, protéome et ionome de la levure ont été analysés et approfondis via des analyses physiologiques ciblées complémentaires. Deuxièmement, nous avons exploré les effets des REEs sur le transcriptome et le ionome du modèle végétal *Arabidopsis thaliana*. De plus, afin d'identifier de nouvelles plantes modèles accumulant les REEs, un panel d'espèces de *Phytolacca* et de fougères ont été criblées. Les plantes accumulatrices de REEs identifiées représenteront de nouveaux modèles pertinents pour décrypter les mécanismes d'accumulation et de tolérance aux REEs.

Résultats

En synthétisant l'ensemble des résultats obtenus avec les deux organismes modèles, *S. cerevisiae* et *A. thaliana*, ainsi que par le criblage de plantes pour leur capacité d'accumulation des REEs, nous avons observé des mécanismes de réponse (i) communs à d'autres éléments bien connus, (ii) spécifiques aux REEs, (iii) différents entre les LREEs et les HREEs, ainsi que (iv) de nouveaux mécanismes de transport présumés des REEs.

i. Mécanismes de réponse communs avec d'autres éléments métalliques

Dans les différentes études menées dans ce travail, nous avons mis en évidence que certains mécanismes communs avec d'autres métaux étaient induits en réponse à une exposition aux REEs. Plusieurs articles font mention d'un stress oxydatif induit par les REEs, principalement chez les plantes et les animaux (Jin *et al.*, 2008). Chez *S. cerevisiae* et *A. thaliana*, la réponse à un stress oxydatif a été observée au niveau du transcriptome. Par conséquent, une partie de la toxicité des REEs pourrait effectivement être expliquée par la production d'un stress oxydatif. Par ailleurs, notre étude montre que le catabolisme de protéines dépendant de l'ubiquitine via la voie ESCRT, est également impliqué dans la toxicité des REEs (les mutants de levure de cette voie sont résistants), comme il a été démontré pour le Ni (Ruotolo *et al.*, 2008). Enfin, la vacuole est un compartiment cellulaire essentiel à la détoxification de métaux (par exemple Cd, Zn, Cu, Mn) dans de nombreux organismes. Nous avons souligné ici son importance en tant que possible compartiment de détoxification pour les LREEs chez *S. cerevisiae* et potentiellement chez *A. thaliana*.

ii. Mécanismes spécifiques des REEs

Dans cette thèse, les mécanismes de réponse spécifiques aux REEs, ont été mis en lumière, notamment chez *S. cerevisiae*. Nous avons identifié que l'endocytose était impliquée dans la réponse aux REEs, grâce à des mutants de cette voie qui sont résistants aux REEs. L'endocytose pourrait donc être impliquée dans la toxicité des REEs en régulant leur absorption intracellulaire, soit de manière directe, soit via la régulation de transporteurs de la membrane plasmique (système d'efflux).

Une autre composante importante de la réponse aux REEs est liée à la composition cellulaire en sphingolipides. À travers les différentes approches omiques utilisées chez la levure, nous avons démontré la relation étroite existant entre l'homéostasie des sphingolipides, l'organisation de la paroi cellulaire et le transport de ces éléments, en réponse à un stress REEs. Ainsi, la régulation des transporteurs membranaires pourrait être essentielle pour moduler le transport des REEs dans la cellule.

iii. Mécanismes de réponse : différences entre LREEs et HREEs

Quelques travaux ont suggéré que les LREEs et les HREEs pourraient induire des réponses différentes, en lien avec la diminution du rayon ionique et avec l'augmentation de la masse

atomique (appelée contraction des lanthanides), à leur réactivité ou à d'autres différences chimiques (Gonzalez *et al.*, 2014; Wang *et al.*, 2017). Il a également été observé au cours de cette thèse des différences dans la réponse aux REEs pour certains des mécanismes identifiés, indiquant que ce groupe d'éléments n'est pas homogène et qu'il est possible d'identifier des voies de réponse spécifiques à chacun.

Nous avons utilisé l'Y comme REE non-lanthanide, le La comme LREE et l'Yb comme HREE pour cribler une banque de mutants de levures. Globalement, la réponse de *S. cerevisiae* à l'Y est très similaire à celle de l'Yb. Cependant, de nombreux mutants montraient un phénotype similaire suite à une exposition à l'Yb et à l'Y, mais qui était différent du phénotype observé en présence de La. Ces résultats montrent qu'il existe des divergences dans les mécanismes de toxicité et de tolérance en réponse aux LREEs et HREEs. Cependant, ces différences d'effets entre les LREEs et les HREEs ne sont pas dichotomiques, mais progressives avec le nombre atomique - rayon ionique des REEs.

Dans chacune des analyses -omiques comparant les réponses de *S. cerevisiae* au La et à l'Yb, l'importance de la paroi cellulaire vis-à-vis du stress induit par les REEs a été souligné. Nous avons émis l'hypothèse que la réactivité préférentielle des REEs avec des groupes phosphates (LREEs) ou carboxyles (HREEs) serait le principal facteur expliquant les différents résultats observés. A nouveau, les différences entre les LREEs et les HREEs ne sont pas dichotomiques, mais progressives avec le numéro atomique / rayon ionique des REEs, comme le montre la caractérisation phénotypique des mutants de la paroi cellulaire. La paroi cellulaire est par conséquent le premier compartiment permettant de discriminer les REEs et sa composition est essentielle pour les interactions des REEs avec la cellule.

Des divergences dans la détoxication cellulaire des REEs ont également été observées. Comme mentionné précédemment, la vacuole constituerait un compartiment de détoxication pour les LREEs, tout comme pour d'autres métaux, ce qui ne serait pas le cas pour les HREEs chez *S. cerevisiae*. La raison de cette différence entre la séquestration des LREEs et des HREEs dans la vacuole pourrait être due à la spécificité d'un transporteur localisé au niveau de la membrane vacuolaire. De plus, dans les différentes expériences menées lors de cette thèse, des différences ont été mises en évidence concernant l'absorption cellulaire et la translocation des LREEs et des HREEs chez *S. cerevisiae* et les plantes. Ces différences pourraient être liées au rayon ionique inégal parmi les REEs.

iv. Nouveaux mécanismes de transport potentiels pour les REEs.

À ce jour, relativement peu de données sont disponibles concernant les mécanismes de transport (à la fois pour l'absorption et la translocation) des REEs dans les organismes vivants.

Premièrement, chez les plantes et comme pour d'autres métaux et métalloïdes (Anjum *et al.*, 2015), il a été suggéré que les acides organiques étaient impliqués différentiellement dans la translocation de REEs des racines aux parties aériennes. Une affinité plus importante des acides organiques pour les HREEs pourrait expliquer un enrichissement spécifique dans les parties aériennes, tel que le citrate, dans l'accumulation des HREEs chez *Phytolacca* (Yuan *et al.*, 2017). Aussi, chez *A. thaliana*, plusieurs aquaporines, et transporteurs ABC ont été identifiés, dont plusieurs gènes liés au processus de détoxication de l'Al tels que des transporteurs d'acides organiques (par exemple malate et citrate).

Deuxièmement, la comparaison avec d'autres métaux toxiques (par exemple Cd) met en évidence une entrée potentielle non spécifique des REEs par le biais de transporteurs de cations essentiels. La similitude entre le rayon ionique des REEs (notamment La) et du Ca présentait un grand intérêt pour des études de physiologie et de biochimie chez les plantes en utilisant le La comme inhibiteur de canaux calciques (Lansman, 1990; Lewis and Spalding, 1998). Il a été ensuite établi que les REEs pouvaient être transportées par ces canaux calciques. Dans les différents organismes modèles testés, *S. cerevisiae* et *A. thaliana*, nous avons montré que l'absorption de REEs était effectivement médiée par des transporteurs transmembranaires de cations. Nous avons confirmé phénotypiquement l'implication du canal calcique CCH1-MID1, dans l'absorption de LREEs (du La au Tb) chez *S. cerevisiae*, comme précédemment démontré par Ene *et al.* (2015). Cependant, d'autres transporteurs semblent être impliqués dans le transport des REEs.

Des auteurs ont montré que la surexpression de ALR1 et ALR2, codant pour des transporteurs de Mg chez *S. cerevisiae*, entraînait une sensibilité au La (MacDiarmid and Gardner, 1998). Dans le même sens, nous avons observé que le mutant ALR2 était résistant à la plupart des REEs. De plus, lors de l'analyse transcriptomique d'*Arabidopsis* exposé aux REEs, nous avons constaté une expression plus élevée du transporteur de Mg MRS2-8 dans les racines. Par conséquent, nous émettons l'hypothèse que les REEs pourraient également être accumulées dans les organismes par le biais de transporteurs de Mg.

En prenant en compte l'ensemble de nos résultats, une relation étroite entre les REEs et le Mn peut également être remarquée. Tout d'abord, nous avons observé que la mutation de SMF1-SMF2 (transporteurs de Mn) chez *S. cerevisiae* entraînait un phénotype sensible à toutes les REEs. Deuxièmement, nous avons observé que moins de Mn était absorbé dans les feuilles d'*Arabidopsis* exposés au La et à l'Yb. De même, une corrélation négative entre le Mn et les HREEs a été constatée à la fois dans les feuilles et les racines de *Phytolacca*, parmi lesquelles *P. americana* et *P. acinosa*, deux espèces hyperaccumulatrices de Mn (Min *et al.*, 2007; Dou *et al.*, 2009; Xu *et al.*, 2009). Ces observations convergentes mènent à se demander pourquoi et comment l'homéostasie du Mn et des REEs sont étroitement liées.

Dans les différents chapitres, nous avons mis en évidence la perturbation de l'homéostasie du Fe par les REEs. En effet, la réponse à une carence en Fe était prépondérante chez *Arabidopsis*, avec plusieurs gènes liés à l'homéostasie du Fe différentiellement exprimés. Nous avons observé une expression plus élevée d'IRT1 lors de l'exposition au La et à l'Yb, qui pourrait suggérer une compétition entre les REEs et le Fe pour ce transporteur et, par conséquent, IRT1 pourrait représenter une entrée privilégiée des REEs dans les cellules racinaires. De plus, chez *S. cerevisiae*, nous avons montré que les mutants des transporteurs de Fe (FTR1-FET3 et FET4) étaient plus résistants et accumulaient moins de REEs. De la même manière, l'analyse protéomique a montré une expression plus faible de FTR1-FET3 en présence d'Yb.

Conclusion

L'utilisation d'approches complémentaires et à haut débit sur des organismes modèles, a mis en évidence les réponses spécifiques à un stress REEs. De plus, des divergences ont été observées dans la réponse aux différentes REEs (par exemple ; la paroi cellulaire, la détoxification vacuolaire, les acides organiques, l'accumulation et le fractionnement des REEs dans les parties aériennes et les racines), en fonction de leur rayon ionique. Dans l'ensemble, les résultats obtenus ici instaurent des bases sur la compréhension de l'absorption potentielle (par exemple ; transporteurs de Ca et de Fe, et d'acides organiques) et l'impact des REEs sur les organismes eucaryotes aux niveaux cellulaire et moléculaire. Ce travail fournit de nouvelles informations sur les perspectives à court et à long terme pour la recherche fondamentale ou des applications biotechnologiques. Cette thèse s'inscrit dans le LabEx R21 au sein duquel d'autres projets étudient les interactions entre REEs et organismes vivants, tels que l'écotoxicologie des REEs à l'interface

eau-sédiments ou encore le rôle essentiel des REEs chez certaines bactéries. Ces différents projets ainsi que les données obtenues lors de cette thèse sont complémentaires et permettent d'appréhender l'impact, à différentes échelles du vivant, des REEs une fois disséminées dans l'écosystème. De plus, dans le cadre de ce travail, nous avons souligné l'importance des approches -omiques à grande échelle pour améliorer la compréhension de la réponse des organismes à ces contaminants émergents. Ainsi, la méta-analyse de larges données -omiques sur la toxicité des métaux sur des organismes modèles devrait être réalisée. Cela permettrait d'identifier des marqueurs moléculaires spécifiques qui pourraient finalement être utilisés comme biomarqueurs, tel que des gènes rapporteurs dont l'expression serait régulée spécifiquement par un groupe ou toutes les REEs.

Etude des gènes de réponse aux terres rares chez des organismes modèles

Les terres rares (TRs) sont des métaux stratégiques du XXIe siècle dont la demande croissante résulte de leurs propriétés essentielles, notamment dans les domaines des énergies renouvelables, de la médecine et des hautes technologies. Ils sont classés en TR lourdes (HTRs), terres légères légères (LTRs) et non-lanthanides. Leur dissémination dans l'environnement, associée à une faible recyclabilité, fait des TRs des contaminants émergents pour lesquels les études de toxicité sont jusqu'à présent très disparates.

Afin d'établir une base générale de la réponse cellulaire et moléculaire à un stress TRs, nous avons premièrement utilisé des stratégies complémentaires et à haut débit pour étudier la réponse, ainsi que l'absorption des TRs chez le modèle eucaryote *Saccharomyces cerevisiae*. Les deletome, transcriptome, protéome et ionome de la levure ont été analysés et approfondis par des analyses physiologiques ciblées. Bien que des réponses communes aux TRs et à d'autres métaux aient été mises en évidence, les réponses spécifiques aux TRs étaient prédominantes. La composition de la paroi cellulaire, la biosynthèse des sphingolipides, la voie ESCRT et l'endocytose sont des éléments clés de la réponse aux TRs.

Deuxièmement, nous avons exploré les effets des TRs sur le transcriptome et le ionome du modèle végétal *Arabidopsis thaliana*. L'exposition des TRs a négativement impacté l'architecture racinaire, comme l'a révélé la modulation de gènes liés à l'auxine. De plus, le ionome a été modifié et les gènes liés à une carence en Fe largement représentés parmi les gènes les plus différentiellement exprimés. Afin d'identifier de nouvelles plantes modèles accumulant des TRs, des espèces de *Phytolacca* et de fougères ont été criblées. Malgré un trait d'accumulation des TRs conservé chez quelques genres de fougères et *Phytolacca*, un enrichissement en HTRs chez *Phytolacca* et en LTRs chez les fougères a été observé. Cependant, plusieurs espèces de *Dryopteris* présentent des teneurs contrastées en TRs dans les frondes et représentent de nouveaux modèles pertinents pour décrypter les mécanismes d'accumulation et de tolérance aux TRs.

Globalement, des divergences ont été mises en évidence dans la réponse aux différentes TRs, en fonction de leur rayon ionique. La composition de la paroi cellulaire, la détoxification vacuolaire, mais aussi l'accumulation et le fractionnement des TRs ont souligné ces différences. Nous avons confirmé que les LTRs empruntaient les canaux calciques, tandis que de nouvelles preuves ont été données sur le rôle des transporteurs de Fe dans l'accumulation de HTRs. En conclusion, nous apportons ici de nouveaux éléments sur la toxicité et les spécificités des TRs, ainsi que des explications moléculaires pour certains effets déjà connus. Ce travail constitue un premier travail de base complet et multi-approches pour de futures études afin d'approfondir la compréhension de la toxicité des TRs chez les organismes vivants.

Mots-clés: Terres rares, *Saccharomyces cerevisiae*, *Arabidopsis thaliana,* criblage de plantes, multi-omics, accumulation de terres rares

---

Study of rare earth element responsive genes in model organisms

Rare earth elements (REEs) are strategic metals whose demand in the 21st century is increasing as a result of their essential properties useful to the fields of renewable energies, medicine, and high-technologies. They are classified as heavy REEs (HREEs), light REEs (LREEs) and non-lanthanides. Their dissemination in the environment, together with poor recyclability, leads REEs to be considered emerging contaminants, for which toxicity studies are currently very fragmented.

To build a strong general foundation on the cellular and molecular response to REEs, we first adopted high-throughput and complementary strategies to study the REE stress response and their uptake in the unicellular eukaryotic model *Saccharomyces cerevisiae.* The deletome, transcriptome, proteome and ionome of yeast were analysed together with in-depth physiological experiments. Although common responses between REEs and other metals were highlighted, REE-specific responses were predominant. Cell wall composition, sphingolipid biosynthesis, the ESCRT pathway and endocytosis were emphasized as key elements in the cellular response to REEs.

Second, we explored how REEs affect the transcriptome and ionome of the plant model *Arabidopsis thaliana.* REE exposure negatively affected the root architecture, as revealed by the modulation of auxin-related genes. REEs impaired the ionome, and Fe deficiency-related genes were largely represented among the most differentially expressed genes in both roots and leaves. Additionally, to identify new REE-accumulating plant models, collections of ferns and *Phytolacca* species were screened. Despite a conserved REE accumulation trait for *Phytolacca* and a few fern genera, HREE enrichment was observed in *Phytolacca*, while LREEs were preferentially transferred into the fronds of all fern species. However, several *Dryopteris* species harboured contrasting REE contents in the fronds. The latter species will be of great importance in deciphering the mechanisms of REE accumulation and tolerance.

Overall, the response towards REEs differed according to their ionic radius. The cell wall composition, vacuolar detoxification, and the accumulation and fractionation of REEs notably accounted for these differences. Our findings support LREE-mediated entry through calcium channels, while new evidence was provided for the role of Fe transporters in the accumulation of HREEs. In conclusion, we have provided new insights into REE toxicity and specificities, together with the molecular elucidation of REE effects that have not previously been mechanistically explained. This work is a first multi-approach comprehensive groundwork that will be used for future studies to deepen the understanding and assessment of REE toxicity in organisms.

Keywords: Rare earth elements, *Saccharomyces cerevisiae*, *Arabidopsis thaliana,* plant screening, multi-omics, REE accumulation.